

307218

49/1998

# Acta Biologica Hungarica

18,

VOLUME 49, NUMBER 1, 1998

EDITOR

**J. SALÁNKI**

EDITORIAL BOARD

V. CSÁNYI, D. DUDITS, K. ELEKES, L. FERENCZY, E. FISCHER,  
B. FLERKÓ, K. GULYA, F. HAJÓS, J. HÁMORI, L. HESZKY, P. KÁSA,  
J. KOVÁCS, J. NEMCSÓK, P. PÉCZELY, M. SIPICZKY, **G. SZABÓ**,  
J. SZEBERÉNYI, GY. SZÉKELY, A. TIGYI



**Akadémiai Kiadó, Budapest**

ACTA BIOL. HUNG. ABAHAU 49 (1) 1-164 (1998) HU ISSN 0236-5383



# ACTA BIOLOGICA HUNGARICA

A QUARTERLY OF THE HUNGARIAN  
ACADEMY OF SCIENCES

---

*Acta Biologica Hungarica* publishes original papers on experimental biology.

*Acta Biologica Hungarica* published in yearly volumes of four issues by

AKADÉMIAI KIADÓ  
H-1117 Budapest, Prielle K. u. 19–35

Manuscript and editorial correspondence should be addressed to

*Acta Biologica Hungarica*  
H-8237 Tihany, Hungary  
Phone: (36-87) 448-244  
Fax: (36-87) 448-006  
E-mail: [salanki@tres.blki.hu](mailto:salanki@tres.blki.hu)

## *Subscription information*

Orders should be addressed to

AKADÉMIAI KIADÓ  
H-1519 Budapest, P.O. Box 245

Subscription price for Volume 49 (1998) in 4 issues USS 136.00, including normal postage, airmail delivery USS 20.00.

“This periodical is included in the document delivery program THE GENUINE ARTICLE of the Institute of Scientific Information, Philadelphia. The articles published in the periodical are available through *The Genuine Article* at the Institute for Scientific Information, 3501 Market Street, Philadelphia PA 19104.”

---

*Acta Biologica Hungarica* is abstracted/indexed in Biological Abstracts, chemical Abstracts, Current Contents–Agriculture, Biology and Environmental Sciences, database (EMBASE), Index Medicus, International Abstracts of Biological Sciences

---

49  
1998

307218

## CONTENTS

Editorial. J. SALÁNKI .....	1
Reflections. P. KÁSA .....	3
Biological activities of amyloid precursor protein. K. GULYA .....	7
The olfactory bulb in Alzheimer's disease. I. KOVÁCS, I. TÖRÖK, J. ZOMBORI, H. YAMAGUCHI .....	29
Effects of beta-amyloid on cholinergic, cholinceptive and GABAergic neurons. MAGDOLNA PÁKÁSKI, HENRIETTA PAPP, MÓNICA FORGON, P. KÁSA JR., B. PENKE .....	43
Cholinesterase in Alzheimer's disease and cholinesterase inhibitors in Alzheimer therapy. Z. RAKONCZAY, I. KOVÁCS .....	55
Aged synthetic human amyloid $\beta$ -peptide 1-42 and related fragments induce direct acetylcholine release from rat basal forebrain tissue slices. MÓNICA FORGON, Z. FARKAS, MAGDOLNA PÁKÁSKI, MÁRTA ZARÁNDI, B. PENKE .....	71
Investigation of 2,6-dimethoxy-benzoquinone in eight tree species grown in Hungary. RITA TÖMÖSKÖZI FARKAS, M. HIDVÉGI, R. LÁSZTITY .....	79
DNA technology and its application in forensic medicine. A. LÁSZIK, A. FALUS, L. KERESZTURY, P. SOMOGYI .....	89
RAS-dependence of nerve growth factor-induced inhibition of proliferation of PC12 cells. KATALIN KISS, B. BARTEK, NÓRA NUSSE, J. SZEBERÉNYI .....	97
Evaluation of genotoxic, mutagenic and antitumor properties of 2-amino-2-thiazoline, L-thioprolin and 2-amino-2-thiazoline $\epsilon$ -formylaminocaproate. VITALIJA ŠIMKEVIČIENĖ, J. STRAUKAS, LARISA CHAUSTOVA .....	103
Growth hormone inhibits the interleukine-6 induced junB protooncogene and fibrinogen expression in HepG2 human hepatoma cells. P. IGÁZ, BEÁTA DÉRFALVI, SÁRA TÓTH, A. FALUS .....	113
Homoplasmic A12,753G mitochondrial DNA mutation in a Hungarian family. ANDREA KIS, A. MATOLCSY, L. VÉCSEI, G. KOSZTOLÁNYI, K. MÉHESE, B. MELEGH .....	119
Colormapping: a non-matemathical procedure for genetic mapping. G. B. KISS, A. KERESZT, P. KISS, GABRIELLA ENDRE .....	125
Effects of administration of cyproterone acetate on seminal vesicle and testicular activity, and serum testosterone and estradiol-17 $\beta$ levels in the catfish <i>Clarias batrachus</i> . M. S. SINGH, K. P. JOY.....	143
Body perception and conciousness. Contributions of interoception research. R. HÖLZL, A. MÖLTNER, C. NEDIG .....	155



MAGYAR  
TUDOMÁNYOS AKADÉMIA  
KÖNYVTÁRA

## EDITORIAL

The present issue of *Acta Biologica Hungarica* is partly devoted to the honor and celebration of Professor Péter Kása, head of the Alzheimer's Disease Research Centre of the Albert Szent-Györgyi Medical University in Szeged, at the occasion of 25 years activity of this specialised, unique laboratory. Some of the papers presented here are original research communications while others bear a review character, and together with the "Reflections" written by Prof. Kása they not only demonstrate the recent activity and earlier achievements of this group, but also give a comprehensive outlook on present knowledge concerning mostly the possible role of cholinergic mechanisms in Alzheimer's disease.

Independent research laboratories are not common at Medical Universities in Hungary, even research groups maintained and supported by the Academy of Sciences belong usually to ordinary Departments. To develop an originally technical unit equipped with individual hightech instruments for the service of the University into a research unit with its own scientific program requires a leading person of strong character with definite scientific ideas, able to recruit, inspire and direct young fellows successfully in order to achieve new and original results in the chosen topic. During the past 25 years Professor Kása proved to be such a personality. He combined luckily his earlier, mainly morphological experiences with new methodical approaches to study Alzheimer's disease and could stimulate a group of colleagues to join, follow, support and develop further his research initiatives.

With publishing these papers in one issue we join to the jubilee commemoration, and congratulate to the Laboratory and its Founder, member of our Editorial Board, wishing further successes in their internationally recognized research activity.

JÁNOS SALÁNKI  
Editor





## REFLECTIONS

Péter KÁSA

Alzheimer's Disease Research Centre, Albert Szent-Györgyi Medical University,  
Szeged, Hungary



It is not an easy task to look over a quarter of a century (1973–1998), a period which has included both hard times and pleasures, but I hope it has not been a failure. It is now 25 years since I was appointed head of the Central Research Laboratory (CRL) at the Medical University, in Szeged. Clearly, if someone is attempting to recall the various events, the subjective elements in his memory will always be mixed in with the objective facts. I will therefore strive to attempt to remain with the facts, rather than focus on my subjective feelings.

In 1959 I started to work at the Department of Anatomy, Histology and Embryology, Medical University, Szeged, where Professor B. Csillik guided my first steps in the research work. It was 1973 when I took over the leadership of a small unit, the CRL, from Professor F. Guba, then Dean of the Medical University. This laboratory had been created in 1958 by the Ministry of Health with the primary goals of helping the University research workers with the instruments available in the laboratory, teaching students and carrying out independent research work. However, it was not an easy task to satisfy these requirements. The research staff numbered only 3 and the instruments were very out of date (some of them were 15 years old). The number of scientific publications achieved by the CRL from 1958 up to 1973 was 3.

As a relatively young leader (at that time I was 38 years old), my background was based most firmly on the 2 years of research work I had done abroad as a Wellcome Re-



search Fellow (in Cambridge, England) and 4 papers I had published in *Nature* (England) on the cholinergic system (*Nature* 208, 695–696, 1965; *Nature* 218, 1265–1267, 1968; *Nature* 226, 812–814, 1970; *Nature* 226, 814–816, 1970).

As head of the CRL, I thought that my main programme should be:

- a) to attract talented young research workers into a well-planned multidisciplinary research laboratory,
- b) to set up a laboratory with the most important and newly-developed research equipment, and
- c) to start work on a scientific problem which was equally of importance for basic science (cholinergic system) and from a clinical aspect (a neurodegenerative disorder, Alzheimer's disease), and to be accepted internationally by other laboratories. Overall, with the help of my staff and the University leadership, I wanted to transform the small unit into an internationally accepted research laboratory.

I knew that the attainment of this goal was dependent on numerous objective and subjective factors. The objective elements were only partially under my control, while the subjective ones (optimism, enthusiasm, determination, desire, persistence and commitment) depended largely on myself and my colleagues. At the beginning of the organization of the laboratory, I was full of doubts as to how I could accomplish this task. I have to admit, however, that I received tremendous help from my colleagues in our University, from friends in Hungary and from a good number of scientist abroad.

Ad a) Fortunately, at the beginning of my leadership I was granted a possibility to increase the number of the research staff. Young and enthusiastic, well-qualified postgraduates joined me (among them D. Budai, K. Gulya, M. Pákáski, Z. Rakonczay and P. Szerdahelyi). I am delighted that Károly Gulya is now professor and head of the Department of Zoology and Cell Biology at József Attila University in Szeged, and Dénes Budai has been appointed head of the Juhász Gyula Teacher Training College Department of Biology. Later on, it was possible for these young researchers to go abroad (especially to the USA), where they worked for several years in various high-level research laboratories. My co-workers have spent altogether 27 years abroad (23 years in the USA and 4 years in Germany, Italy or Finland). In consequence of the scientific connections with different laboratories, we have had opportunities to cooperate with well-known scientists in 10 different countries (Australia, Czechoslovakia, England, Germany, Finland, France, Israel, Japan, Norway and the USA), and within these countries with 25 different laboratories and departments. Members of the CRL have been trained by and enjoyed long collaboration with, among others, S. Appel (Houston, USA), S. Duckles (Irvine, USA), A. Fisher (Ness-Ziona, Israel), C. Geula (Boston, USA), E. Giacobini (Minnesota, USA), I. Hanin (Chicago, USA), C. O. Hebb (Cambridge, England), A. Lajtha (New York, USA), M. B. Lees (Boston, USA), A. Silver (Cambridge, England), P. Riekkinen (Turku, Finland), H. Yamaguchi (Gunma, Japan), H. Yamamura (Tucson, USA) and J. R. Wolff (Göttingen, Germany).

Ad b) During my leadership, I have set up a number of laboratories with different functions (a neurochemical laboratory, a tissue culture laboratory, a human neuropa-

thological laboratory, an electrophysiological laboratory, a neuropharmacological laboratory, a laboratory for trace element research and an isotopic laboratory). These laboratories were fitted out with important research equipment such as a scanning electron microscope equipped with the EDAX analytical system, light microscopes equipped with a video recorder, computerized gas chromatograph, ultracentrifuges, different spectrophotometers, an atomic absorption spectrophotometer, a radio isotopic counter and various microwave equipment. This research equipment became the basis of our scientific work.

Ad c) After spending 2 years at the Department of Physiology in Cambridge (England), my research interest became focussed on study of the distribution of cholinergic neurons and their axon terminals, and particularly their function in the central nervous system. The main achievement of my work in Cambridge was the development of a histochemical technique for the demonstration of cholineacetyltransferase activity in cholinergic neurons and cholinergic axon terminals. Although this technique suffered from some degree of non-specificity, this was the very first method for the visualization of cholinergic neurons and cholinergic axon terminals at the light-microscopical and electron-microscopical levels (*Nature* 226, 812–814, 1970; *Nature* 226, 814–816, 1970). On returning to Szeged and becoming head of the CRL, I decided to change the life and the function of the laboratory. As regards the function, my purpose was not only to help the university research workers with the available equipment, but also to involve the laboratory staff very actively in the scientific life and to stimulate them to do their own research work as well. At the beginning, our main research task was to map the cholinergic neurons in the brain of different species (Prog. Neurobiol., 1986), and in human (Prog. Neurobiol., 1996) and to study their functions in health and disease (concentrating our studies on Alzheimer's disease). During the 25 years under my leadership, we have published 197 papers in different scientific journals, with a cumulative impact factor of 581.011. According to the Science Citation Index (SCI), our papers have been cited 2527 times. Six of the laboratory staff have received the Ph.D. degree and 3 the D.Sc. degree. Most recently, 3 have been awarded Széchenyi Professorships and 1 a Bólyai Stipendium.

In 1994, the local university politics changed radically. The CRL was wound up; luckily, however, with the financial help of the World Bank (350,000 USD), an Alzheimer's Disease Research Centre was created instead, and I became head of this research laboratory. Other activities:

Since our scientific interest concentrated on Alzheimer's disease in 1991, we have organized the First Hungarian Conference on Alzheimer's Disease (Szeged, 1991), and have also taken part in the organization of a conference, Research on Alzheimer's Disease in Hungary (Debrecen, 1994). With our involvement, the 3rd Hungarian Congress on Alzheimer's Disease was organized in Budapest (1996) and the 4th Hungarian Conference on Alzheimer's Disease and Related Disorders will be held in Szeged this year (1998).

It is a great honour for us that the main organizers of the International Conferences of Alzheimer's Disease and Related Disorders (1996: Osaka, Japan; and 1998: Amsterdam, The Netherlands) have invited us to be among the members of the International Scientific Committee.



These are some of our main achievements during the past 25 years. I leave it to the reader to judge the level of our achievements.

Overall, I am a little proud that, during my leadership, the CRL and nowadays the Alzheimer's Disease Research Centre have grown out of a small unknown laboratory into a reasonably internationally accepted site of Alzheimer's disease research, which plays a role in Hungarian work on Alzheimer's disease.

I know that without my many helpers this result could not have been achieved. I would therefore like to thank all of my co-workers, both those still with me and those who have left the laboratory, my colleagues and friends both abroad and in Hungary, for all their enormous help during my leadership. It is a wonderful feeling to know that during the past 25 years there have been so many participants who have been able to share in our results and our joy, and I wish to express my most sincere thanks to so many who have played a part in the development of our laboratory.

## BIOLOGICAL ACTIVITIES OF AMYLOID PRECURSOR PROTEIN\*

K. GULYA

Department of Zoology and Cell Biology, University of Szeged, Szeged, Hungary

Received: 1998-06-12; accepted: 1998-06-26)

Amyloid precursor protein (APP), a transmembrane glycoprotein, is the source of amyloidogenic  $\beta$ -amyloid peptide ( $\beta$ AP), the major constituent of the peptides deposited in senile plaques. Normally-cleaved forms of APP exert potent neuroprotective action. Accumulating data suggest that an altered expression and/or post-translational processing of APP is responsible for the neuropathological changes observed in Alzheimer's disease and related disorders. This review discusses the metabolism and secretion of APP, the biological activities of the various APP forms, and the physiological, pathophysiological and experimental circumstances that affect the APP metabolism.

*Keywords:* Alzheimer's disease – amyloid – precursor – protein – physiology

### INTRODUCTION

A variety of pathological changes, including senile plaque formation, the presence of neurofibrillary tangles, neuronal cell loss, gliosis and a reduced level of the neurotransmitter acetylcholine have been described so far as hallmarks of Alzheimer's disease (AD). Whereas most of these abnormalities are frequently to be found in other neuropathological disorders, high densities of senile plaques in the extracellular space of the brain tissue are detected almost exclusively in patients with AD. The major component of the senile plaques is a group of peptides composed of 38–43 amino acid residues, called  $\beta$ -amyloid peptides ( $\beta$ AP) [35, 51, 68], proteolytic products of amyloid precursor protein (APP).

\*Dedicated to Professor Peter Kasa on the occasion of the 25th anniversary of his appointment as Head of the Central Research Laboratory and the Alzheimer's Disease Research Centre.

Send offprint requests to: Prof. K. Gulya, Department of Zoology and Cell Biology, University of Szeged, H-6722 Szeged, Egyetem u. 2, P.O. Box 659; e-mail: gulyak@bio.u-szeged.hu.

## ALTERNATIVE PROCESSING OF APP

APP, a membrane-spanning 695–770 amino acid glycoprotein, encoded on chromosome 21, is the source of  $\beta$ AP [54]. APP is a type-1 transmembrane protein [26] with a small C-terminal cytoplasmic domain with three phosphorylation sites, one transmembrane domain and a large N-terminal extracellular domain with two glycosylation sites [127].  $\beta$ AP generally consists of a 40–42 amino acid segment of APP that resides in part in the extracellular space and in part within the cell membrane. Thus, the  $\beta$ AP domain is partially embedded, as part of the transmembrane domain of APP, within the phospholipid bilayer of the plasma membrane, protecting it from proteolytic cleavage.

Several forms of the precursor peptide for  $\beta$ AP exist, including one form lacking (APP695) and two forms containing (APP751 and APP770) a Kunitz protease inhibitor domain in the amino terminal region [26, 87, 123]. A number of alternative pathways of the APP metabolism have been identified so far that result in different end-products secreted from the cell. However, the identities and the regulatory elements of the proteases involved in the process, known as  $\alpha$ -,  $\beta$ - and  $\gamma$ -secretases, are unclear. Two constitutive enzymatic cleavages occur near the cell surface [27, 111] that liberate secreted forms of APP (secAPP). Cleavage through one secretory pathway occurs within the  $\beta$ AP sequence by the as yet unidentified enzyme  $\alpha$ -secretase, generating secAPP and non-amyloidogenic peptide fragments, and also resulting in a membrane-bound 10 kDa C-terminal fragment [88]. Cleavage by  $\alpha$ -secretase occurs at position 17 of the  $\beta$ AP domain, thereby preventing amyloid formation [27]. In a recent study, Chen [20] proposed that  $\alpha$ -secretase could be a calcium-dependent protease. Moreover, there is evidence which indicates that this pathway is regulated by protein kinase C (PKC)-mediated events [67]. An additional trafficking pathway, involving reinternalization of the uncleaved precursor and targeting to endosomes and lysosomes, was demonstrated by Haass et al. [43] and Yamazaki et al. [129]; this pathway has also been claimed to be involved in the generation of  $\beta$ AP [40, 60]. Although the identity of  $\alpha$ -secretase is unknown, recent evidence suggests that the enzyme is probably closely related to zinc metalloproteases, such as the angiotensin converting enzyme secretase [94]. Gelatinase A (matrix metalloproteinase 2, a 72 kDa type IV collagenase), however, probably does not play an essential role in the generation and release of soluble derivatives of APP under physiological conditions [50], since mice devoid of gelatinase A activity in consequence of gene targeting or fibroblasts without the enzyme activity secreted APP that was cleaved within the  $\beta$ AP region. Interestingly, a recent study by Haass et al. [39] raised the possibility that proteases from the coagulation cascade may contribute to APP proteolysis since factor Xa was found to cleave APP after Arg 102, 268, 510, 573 and 601 (APP695 numeration), and generated six potentially amyloidogenic fragments.

An alternative cleavage, presumably within the endosomal-lysosomal pathway [36, 40], results in the generation of intact  $\beta$ AP by  $\beta$ -secretase at the amino terminal of the  $\beta$ AP sequence. This cleavage generates an intact  $\beta$ AP as part of a potentially amyloidogenic COOH-terminal fragment of APP remaining in the cell membrane. The  $\beta$ -secretase cleavage occurs in a late endosomal compartment in SY5Y cells [95]. A recent study by Chyung et al. [21] demonstrated a novel  $\beta$ -secretase cleavage of APP in the endoplasmic



reticulum/intermediate compartment of NT2N neurons derived from a human embryonal carcinoma cell line (NT2). These cells constitutively process APP to  $\beta$ AP; the amino-terminal fragment of APP generated by  $\beta$ -secretase cleavage was not abolished by trypsin digestion of the intact cells at 4 °C. The intracellular production of  $\beta$ -secretase-cleaved APP was characteristic of postmitotic neurons and was not detected in several non-neuronal cell lines. As senile plaques contain lysosomal enzymes, and the production of some of the amyloidogenic intermediates is inhibited by lysosomotropic agents, it has also been suggested that cathepsins are involved in amyloidogenesis. In accordance with this notion, Austen and Stephens [9] demonstrated that a synthetic 31-residue peptide overlapping the  $\beta$ -secretase cleavage site was found to be digested at two mutually exclusive sites, one and three residues on the N-terminal side of the N-terminal Asp residue of  $\beta$ AP. Coupled with the action of amidopeptidases, lysosomal and endosomal cathepsin D could therefore be responsible for the generation of N-terminal  $\beta$ AP in vivo.

Since it has been suggested that acetylcholinesterase (AChE) possesses both putative proteolytic activity against APP, and a capacity to accelerate the assembly of  $\beta$ AP into fibrils, purified AChE from bovine brain was studied to establish whether the enzyme does display these characteristics. It was found that, although brain AChE did promote  $\beta$ AP aggregation, it did not hydrolyze APP in vitro [18]. Cholinesterase inhibitors were also tested as regards their effects on the secretion of secAPP in cell cultures [61, 62]. Treatment of neuroblastoma, pheochromocytoma, HeLa cells and fibroblast cells with a high dose of either 3,4-diaminopyridine, metrifonate, or physostigmine did not inhibit the secretion of secAPP. Treatment of these cells with tacrine, however, reduced the release of secAPP. Interestingly, treatment of glioblastoma cells with either 3,4-diaminopyridine or metrifonate led to an increased secretion of secAPP. Although the difference in action of these inhibitors was independent of their anticholinesterase activities, the noncatalytic functions of cholinesterase inhibitors can alter the metabolism of APP [61, 62].

The third, still hypothetical, enzyme involved in the generation of  $\beta$ AP is  $\gamma$ -secretase [45]. This enzyme generates the C-terminal of  $\beta$ AP, and cleaves within the transmembrane domain of APP, preferentially after  $\beta$ AP residue 40 ( $\beta$ AP40), but also after residue 42 ( $\beta$ AP42).  $\beta$ AP42 is the major constituent of the plaques in AD. According to data obtained on SY5Y cells,  $\gamma$ -secretase cleavage occurs in early endosomes [95]. This is in harmony with data indicating that increased neuronal endocytosis and protease delivery to early endosomes in AD constitutes a potential mechanism by which the genesis of  $\beta$ AP may become accelerated [19]. Since the position of  $\gamma$ -secretase cleavage is crucial for an understanding of the pathogenic pathway, Lichtenthaler et al. [65] investigated the different point mutations at Thr43 on  $\gamma$ -secretase specificity. They concluded that the mutations altered  $\gamma$ -secretase specificity, but that different  $\beta$ AP and other fragments can be generated by the enzyme's cleavage activities with a similar enzymatic mechanism. The release of non-transmembrane full-length APP from the luminal surface of chromaffin granule membranes was recently demonstrated by Tezapsidis and coworkers [120]. Full-length APP within the granules was shown to exist as three different populations: 1. transmembrane, 2. membrane-associated/non-transmembrane, and 3. soluble. The existence of non-transmembrane populations suggested that putative  $\gamma$ -secretase cleavage



sites of APP, assumed to be buried within the lipid bilayer, could be accessible to proteolysis in a soluble intravesicular environment.

Interestingly, a facilitated reduction of APP by synthetic oligonucleotides in COS-7 cells expressing a hammerhead ribozyme targeted to bases APP mRNA 133–148 has been demonstrated [24]. The results implied that deoxyoligonucleotides targeted immediately upstream from a ribozyme binding site of APP mRNA could work cooperatively in vivo.

Because of its similarity to the systems of mammalian cells, the yeast secretory system has recently provided important clues concerning the possible secretory pathways of APP. For example, when expressed in *Saccharomyces cerevisiae*, APP is processed by enzymes that possess the specificity of the  $\alpha$ -secretases of multicellular organisms [131]. Two yeast aspartyl proteases, Yap3 and Mkc7, are  $\alpha$ -secretases which act on APP in the late Golgi. Deletions of genes encoding these enzymes resulted in a decreased proteolytic activity, suggesting that these aspartyl proteases may be involved in the processing of APP in mammalian tissues.

APP is subject to N- and O-glycosylation and potential Tyr sulfation, following protein synthesis. The cleavage of APP by secretases occurs after O-glycosylation of APP in the protein secretory pathway during these post-translational modifications [122]. APP is cleaved by the secretases in a step(s) during the transport of APP through the Golgi complex, where O-glycosylation occurs, or in compartments subsequent to the trans-Golgi of the APP secretory pathway. Sulfated glycoconjugates attached to APP might also play a role in the substrate specificity of APP for proteases [69].

Apart from APP, there are two, similarly highly conserved transmembrane glycoproteins: the amyloid precursor-like proteins (APLP1 and APLP2), which complement the superfamily of APPs, and whose functions are unknown. In a recent study, Lyckman et al. [66] shed light on the post-translational processing and turnover kinetics of presynaptically targeted amyloid precursor superfamily proteins in the central nervous system. Five post-translationally modified, full-length species of APP and at least one APP-like protein (APLP2) are transported by fast axonal transport to the mature presynaptic terminal, where they are subsequently rapidly cleared [66]. The mean half-life of these proteins is about 3.5 h. The turnover of the most rapidly arriving APP species is accompanied by a delayed accumulation of a 120 kDa APP fragment lacking the C-terminal, consistent with presynaptic APP turnover via constitutive proteolysis. A single 150 kDa APLP2 species containing the Kunitz protease inhibitor domain was the major amyloid precursor superfamily protein transported to the presynaptic terminal. Presynaptic APP and APLP2 are sialylated and N- and O-glycosylated, and some also carry chondroitin sulfate glycosaminoglycan and/or dermatan sulfate glycosaminoglycan. As pointed out by Lyckman et al. [66], the rapid kinetics for the turnover of presynaptic APP and APP-like protein predicts a sensitive balance of synthesis, transport and elimination rates that may be critical for normal neuronal functions and metabolic fates of these proteins. In the nerve terminals of the cholinergic neurons from the electric ray electric organ, the cDNA of APP was isolated [47]. This peptide form consisted of 699 amino acids, and the cytoplasmic domain contained three phosphorylation sites, similarly to the form found in humans. Its  $\beta$ AP domain exhibited 80.7% similarity with the human APP695 isoform, and a completely preserved cytoplasmic domain. APP 699 in the presynaptic terminal existed exclusively in



the mature form. The phosphorylated form of mature APP699 was found in the nerve terminals as well as in cell bodies. The immature APP699 was not subject to phosphorylation [47].

In a recent study, Ikezu et al. [48] presented both biochemical and histochemical evidence that the caveolae, e.g. plasma membrane invaginations, where key signaling elements are concentrated, are necessary for the release of  $\alpha$ -secretase-mediated APP. Caveolin-1, a principal component of the caveolae, was found to be physically associated with APP, and the cytoplasmic domain of APP participates in this binding directly. The characteristic C-terminal fragment that results from APP processing by  $\alpha$ -secretase was also localized within these caveolae. Further analysis by cell surface biotinylation revealed that this cleavage event occurred at the cell surface. Recombinant overexpression of caveolin in intact cells resulted in enhanced  $\alpha$ -secretase processing, but caveolin depletion using antisense oligonucleotides effectively prevented this cleavage event. In another study, however, Parkin et al. [93] could not demonstrate the presence of APP in caveolae-like, detergent-insoluble membrane microdomains prepared from either the mouse cerebellum or the human neuroblastoma cell line SH-SY5Y, and concluded that APP is not normally present in these membrane microdomains.

A characterization of the compositions of soluble and membrane-bound isoform populations of APP in the porcine brain has established at least three types of secAPPs and membrane-bound APP with molecular masses ranging from 86 kDa to 116 kDa [23]. In that study, CD and infrared spectroscopy were used to determine the overall secondary-structure content of APP. The infrared spectra of soluble and membrane-bound AAP suggested that their overall secondary structures were roughly identical, while the CD spectra indicated the presence of  $\alpha$ -helix structures in both forms of APP.

Alternative processing, presumably in an acidic intracellular compartment, of full-length APP or C-terminal fragments can result in the liberation of intact  $\beta$ AP in low amounts from neurons, glia or other cells [44, 114].  $\beta$ AP circulates in minute quantities in the cerebrospinal fluid and blood under physiological conditions. Moreover, through use of a novel antiserum, human APLP1, a 650 amino acid glycoprotein with both N- and O-linked glycans, was identified in human cerebrospinal fluid [92]. It is believed that mutation, an altered APP gene expression and/or the processing of  $\beta$ AP occurs in AD and related disorders, such as Down's syndrome, leading to an increased liberation of  $\beta$ AP from the cells [70, 81, 110], and that this could result in neuronal degeneration by compromising a normal neuroprotective function of APPs.

## MUTATIONS OF APP, TRANSGENIC MODELS OF AD

Mutations are found in some families, with familial AD mapped to the APP gene. These mutations are localized in a very characteristic pattern close to the cleavage sites of all three secretases [38]. In a Swedish family, a double mutation was found at the N-terminal of the  $\beta$ AP domain, exactly at the  $\beta$ -secretase site [79], resulting in a 3- to 6-fold overproduction of  $\beta$ AP. Another mutation was mapped to the middle of the  $\beta$ AP domain, very close to the  $\alpha$ -secretase cleavage site [46]. This mutation inhibited the secretase activity,



thereby resulting in a modest increase in the amount of  $\beta$ AP and in the generation of N-terminal-truncated  $\beta$ AP-like peptides [42]. A third set of those mutations is localized close to the  $\gamma$ -secretase site [81]. These three types of familial AD mutations directly influence the formation of  $\beta$ AP, either by causing an enhanced production of  $\beta$ AP or by increasing the rate of aggregation of the peptides [38].

McPhie et al. [74] screened five different AD mutations of APP that were expressed in neurons via recombinant herpes simplex virus vectors, and the levels of APP metabolites were quantified. The neuronal expression of these proteins caused the intracellular accumulation of a potentially amyloidogenic and neurotoxic C-terminal fragment containing both the  $\beta$ AP and cytoplasmic domains.

In recent years, transgenic animals have started to emerge as animal models of AD [80]. When human APP751 containing these mutations was expressed in the brains of transgenic mice, a 2-fold overexpression of APP with the Swedish double mutation at positions 670/671, combined with the V717I mutation, caused  $\beta$ AP accumulation in the neocortex and the hippocampus of 18-month-old transgenic mice [119]. In mice with a 7-fold overexpression of human APP harboring the Swedish mutation alone, typical plaques appeared at 6 months, and increased with age. The plaques formed were positive for Congo-red, accompanied by neuritic plaques and dystrophic cholinergic fibers. The plaques were also immunopositive for hyperphosphorylated tau-protein. In general, these mice displayed major features resembling those of AD pathology, strongly suggesting a central role of  $\beta$ AP in the pathogenesis of the disease. Transgenic mice were also used to examine the spatial and temporal regulation of the APP gene promoter region in vivo [28]. A 2.9 kb DNA fragment encompassing the APP gene promoter was fused to a reporter gene or a partial cDNA encoding the potentially amyloidogenic C-terminal 100 amino acid region of APP. Expressions of these transgenes occurred primarily, but not exclusively, in the brain and testis in multiple independent lineages of transgenic mice. The temporal expression of the reporter gene during development paralleled that found for the endogenous APP gene. This study suggested that a central nervous system-responsive cis-acting element may exist in the promoter/5'-flanking region of the APP gene [28]. Ischemic brain damage was found in transgenic mice overexpressing the Swedish-type mutation of APP695 [130]. The effect probably involved a  $\beta$ AP-induced disturbance in endothelium-dependent vascular reactivity that led to more severe ischemia. Aging mice transgenic for the C-terminal of APP underwent an age-dependent neuronal and synaptic degeneration [89]. A 100 amino acid-long C-terminal sequence of APP was expressed in these mice. The animals (18–28 months old) exhibited a profound degeneration of the neurons and synapses in Ammon's horn and the dentate gyrus of the hippocampal formation. The numerous degenerating axonal profiles contained increased numbers of neurofilaments and accumulations of debris resembling secondary lysosomes near the cell body.

Missense mutations in two related genes, termed presenilin 1 (PS1) and presenilin 2 (PS2), cause dementia in a subset of early-onset familial AD. Familial AD-linked presenilin variants influence the processing of APP, leading to elevated levels of  $\beta$ AP1-42 preferentially deposited in the brains of AD patients. It was recently shown that the profiles of APP and PS2-like proteins are correlated during development in the hypothalamus of the mouse [3]. An overexpression of wild-type PS1 in transfected cultured cells, how-



ever, increased  $\beta$ AP secretion [2]. By contrast, familial AD-linked mutants of PS1 triggered an increased secretion of both  $\beta$ AP1–40 and  $\beta$ AP1–42, but clearly favored the production of the latter species in the same study. It was also demonstrated that an overexpression of the wild-type PS1 augmented the  $\alpha$ -secretase-derived C-terminally truncated fragment of APP recovery, whereas transfectants expressing mutated PS1 secreted drastically lower amounts of APP as compared with cells expressing wild-type PS1 [2]. These data indicated that PS1 mutations linked to familial AD not only triggered an increased ratio of  $\beta$ AP1–42 over total  $\beta$ AP secretion, but concomitantly down-regulated the production of APP cleaved by  $\alpha$ -secretase.

Transgenic animals that coexpress a familial AD-linked human PS1 variant and a chimeric mouse/human APP harboring mutations linked to Swedish familial AD kindred (APPswe) developed numerous amyloid deposits much earlier than age-matched mice expressing APPswe and wild-type human PS1 or APPswe alone [15]. The fact that amyloid deposition is accelerated in the brains of transgenic mice coexpressing mutant PS1 and APP provided new evidence that one pathogenic mechanism by which familial AD-linked mutant PS1 causes AD is via acceleration of the rate of  $\beta$ AP deposition in the brain. This notion was confirmed when PS1 was shown to bind directly to APP in two-hybrid interaction assays between these proteins in yeast cells [126].

## PHYSIOLOGICAL FUNCTIONS OF APP

Several putative functions have been ascribed to the membrane-associated and secreted forms of APP in non-neuronal cells. For example, APP751 is identical to protease nexin II [87, 123], a potent inhibitor of serine proteases. This peptide can also function as a growth factor for fibroblasts [102, 104], as an inhibitor of blood coagulation factor XIa [116], or as a substrate for factor Xa [39], at least under in vitro circumstances. Secreted forms of APP regulate cell proliferation in non-neuronal cells [104, 107]. Furthermore, APPs are suspected of participating in signal-transduction processes as well, since membrane-associated APP molecules have been shown to form complexes with a member of the G-protein family,  $G_o$  [83], and may function as cell surface receptors [54]; in harmony with this notion, high-affinity binding sites for [ $^{125}$ I]secAPP751 were found on intact fibroblast cells [52]. Moreover, there are data showing that both membrane-associated and secreted APPs may participate in cell-cell and cell-substrate adhesion [108]. For example, a down-regulation of APP synthesis by antisense oligonucleotides was demonstrated to reduce neuronal adhesion to specific substrates [22]. APP probably mediates a substrate-specific interaction between neurons and extracellular matrix components collagen type I, laminin and heparan sulfate proteoglycan, but not fibronectin or poly-L-lysine [22]. It remains to be established whether this effect is a direct result of APP-matrix interactions, or whether an intermediate pathway is involved. In primary cultured rat cells, the colocalization of APP with integrins was reported by Yamazaki et al. [128]. APP was colocalized with  $\alpha 1\beta 1$  and  $\alpha 5\beta 1$  integrin heterodimers in rat hippocampal primary neurons. In rat cortical astrocytes, however, both cell surface APP and  $\beta 1$  integrin were located at the cell periphery in the spreading stage shortly after plating. In flattened



astrocytes cultured for several days, APP was found in punctate deposits called point contacts [128]. In these sites, APP was colocalized with  $\alpha 1\beta 1$ , but not with  $\alpha 5\beta 1$  integrin heterodimers. In both neurons and astrocytes examined after shearing, clathrin and  $\alpha$ -adaptin were colocalized with APP on the surface in direct contact with the substrate. Thus, APP either interacts with selected integrins or shares similar cellular machinery to promote cell adhesion.

Secreted APPs protect neurons from glucose deprivation and glutamate toxicity in cultured rat hippocampal and septal neurons, and in human cortical neurons [73]. For example, APP695 and APP751 protect neurons against hypoglycemic damage, and the neuroprotection is abolished by antibodies to a specific region common to the two peptide forms. These APPs cause a rapid and prolonged reduction in intracellular free  $\text{Ca}^{2+}$  content ( $[\text{Ca}^{2+}]_i$ ) that mediates hypoglycemic damage [73]; the secreted forms of APPs are also effective in protecting neurons against glutamate neurotoxicity, effectively raising the excitotoxic threshold and stabilizing  $[\text{Ca}^{2+}]_i$  [72]. SecAPP modulates calcium responses to glutamate in cultured embryonic hippocampal neurons [71]. Recent data suggest that secAPPs mediate the  $[\text{Ca}^{2+}]_i$ -lowering effects on cultured hippocampal neurons through increases in cGMP levels [11]. However, inhibition of the formation of nitric oxide or carbon monoxide does not affect the ability of secAPPs to lower intraneuronal  $\text{Ca}^{2+}$  levels rapidly or elevate cGMP, suggesting that secAPPs do not activate a soluble (cytosolic) guanylyl cyclase [13]. In this study, a dose-dependent stimulation of cGMP formation by secAPP was observed in brain membrane preparations, and the stimulation was also dependent on the presence of ATP. These data indicate that secAPP activates a membrane-associated guanylyl cyclase. Moreover, Furukawa and Mattson [33] reported that secAPP selectively suppressed N-methyl-D-aspartate (NMDA) currents in cultured embryonic rat hippocampal neurons. Whole-cell patch-clamp data confirmed that the rapid and reversible suppression of the NMDA current by secAPP was mediated by cGMP. Moreover,  $\text{K}^+$  channel activation and suppression of neuronal activity by secAPP were verified in cultured hippocampal neurons [32]. Whole-cell perforated patch and single-channel patch-clamp analysis of hippocampal neurons was used to demonstrate that secAPPs suppress action potentials and hyperpolarize these neurons by activating high-conductance, charybdotoxin-sensitive  $\text{K}^+$  channels. Activation of  $\text{K}^+$  channels by secAPP695 was mimicked by a cGMP analog and sodium nitroprusside and blocked by an antagonist of cGMP-dependent kinase and a phosphatase inhibitor. These data suggested that the effect was mediated by cGMP and protein dephosphorylation. Calcium imaging studies confirmed that the activation of  $\text{K}^+$  channels mediated the ability of secAPPs to decrease  $[\text{Ca}^{2+}]_i$  levels. As pointed out by Furukawa et al. [32], this sort of neuronal excitability could be a major mechanism by which APP regulates developmental and synaptic plasticity in the nervous system.

Further evidence for an excitoprotective role for APP has been provided by Schubert and Behl [106], who demonstrated that a clonal neuron-like cell line transfected with APP was more resistant to glutamate neurotoxicity than was the parent cell line lacking expressed APPs. In a recent report, Tominaga et al. [121] demonstrated that the human APP holoprotein gene introduced into cultured rat hippocampal neurons by an adenoviral vector enhanced the responsiveness of the neurons to applied glutamate as compared with the

non-expressing control neurons, and speculated that one function of APP may be the regulation of glutamate receptors in APP-expressing neurons.

The secreted APP forms promote neuronal survival in cultured cerebral cortical neurons [4, 73] and neuritic outgrowth [71, 76]. For example, membrane-bound APP was shown to enhance neuron viability, axogenesis and arborization and modulate neuronal polarity, while the secreted forms of APP modulated axon growth, dendrite branching and numbers in hippocampal neuronal cultures [96]. Highly purified human APP751 induced the outgrowth of neurites in PC12 cells [124]. The neurotropic activity was inhibited by an antibody that was directed to the C-terminal portion of secAPP, but not by an antibody directed to the Kunitz protease inhibitor domain. This neurotropic activity of APP was independent of the TrkA nerve growth factor (NGF) receptor because neither phospholipase C $\gamma$ 1 nor TrkA exhibited tyrosine phosphorylation on APP treatment. The  $\alpha$ -secretase-derived secAPP forms increased the number of neurites per cell and enhanced the level of tyrosine phosphorylation [77]. The secreted forms of APP were also shown to induce the activation of the signaling pathways through a stimulation of the phosphoinositide-PKC cascade. For example, secAPP695 activated PKC and phospholipase C $\gamma$ 1 in cultured embryonic rat neocortical cells, where a dose- and time-dependent phosphorylation of endogenous substrates was demonstrated by Ishiguro et al. [49]. Microglial activation by secAPP has also been reported [12]. Both amyloidogenic and non-amyloidogenic forms of secAPPs induced inflammatory reactions in microglia that enhanced their production of neurotoxins. Microglia activation was blocked by prior incubation with apolipoprotein E3. Thus, increased amyloidogenic processing could adversely affect the balance of secAPP activities that determine neuronal viability. SecAPP was even proposed to act as an autocrine growth factor mediating the proliferative effect of thyrotropin on neighboring thyroid epithelial cells [97].

Not surprisingly, secAPP functions in synaptogenesis. For example, Morimoto et al. [78] demonstrated that, as more and more neurons formed synapses with each other in a hippocampal neuronal culture, increasing numbers of neuronal cells displayed synchronized spontaneous oscillations in  $[Ca^{2+}]_i$ . The number of such neurons was significantly lower when culturing was performed in the presence of monoclonal antibody against the N-terminal portion of APP. Moreover, incubation with excess amounts of either the secAPP form or the N-terminal fragment of APP also inhibited the increase in number of neurons with synchronized spontaneous oscillations of  $[Ca^{2+}]_i$ .

Recently, APP (and some of its amyloidogenic metabolites) have been shown to alter cellular ionic activity and movements, either through interaction with existing channels or by de novo channel formation [5–8, 29, 32]. Intracellular application of APP770 to *Xenopus* oocytes activated a smooth, non-selective ionic current with full recovery, and probably without  $Ca^{2+}$  involvement [30].



## (PATHO)PHYSIOLOGICAL AND EXPERIMENTAL CONDITIONS THAT AFFECT APP LEVELS

Since the glucose metabolism and consequential ATP production are depressed in AD, a number of studies have investigated the possible role of a hypometabolism in the pathogenesis of AD, using animal models [98] or cell cultures [34, 112]. A reduction in cerebral energy metabolism by occlusion of the carotid and vertebral arteries altered the formation of APP due to cerebral hypoperfusion in the rat cerebral cortex and hippocampus [98]. Rat primary cortical astroglial cells, incubated for 2 h to 4 days in a medium deprived of 95% of its glucose, demonstrated an enhanced expression of APP mRNA. Hypoglycemia caused a time-dependent increase in APP mRNA that peaked at 24 h of hypoglycemia. It was noteworthy that hypoglycemia favored the alternative splicing that includes the exon 7 segment encoding a Kunitz-type serine protease inhibitor domain. Thus, hypoglycemia in AD might contribute to an increased APP mRNA expression and the processing of APP mRNA to a form that might deposit in the brains of AD patients. An energy shortage and energy-related metabolic (oxidative) stress were linked to the amyloid metabolism in COS cells [34]. Glucose deprivation of the cells by incubation of 2-deoxy-D-glucose in glucose-free medium reduced APP secretion. Similarly, inhibition by sodium azide of cytochrome c oxidase, a member of the mitochondrial electron transfer chain, decreased secAPP; treatment of COS cells with the antioxidant glutathione fully antagonized the inhibitory effect of azide and consequently elicited secAPP release over the basal level [34]. In spite of the seemingly contradictory data emerging from these studies, a clear connection between energy metabolism and APP processing could be established.

There is mounting evidence that the activation of PKC regulates the processing and catabolism of APP into its soluble forms and  $\beta$ AP [25, 31, 75]. In many cell lines and rodent primary neuron cultures, phorbol ester activation of PKC increased the secretion of a large N-terminal fragment of APP and decreased  $\beta$ AP release. For example, the microbial alkaloid toxin staurosporine, a PKC inhibitor widely used in signal-transduction research, blocked the increase in APP in rat pheochromocytoma PC12 sympathetic neuron cultures [31]. In partial harmony with these results, the activation of PKC in human primary neurons increased the rate of secAPP release and the production of APP C-terminal fragments, but it also increased the release of the 4 kDa form of  $\beta$ AP [63]. Since species- and cell type-specific regulation of the APP metabolism cannot be ruled out, this result might curtail the potential use of PKC activators in controlling human  $\beta$ AP levels. Normally, the turnover rate of APP is high [105]. When an excess amount of  $\beta$ AP is expressed in mice, an intracortical injection of phorbol ester, 6 h after treatment, effectively reduces the amounts of  $\beta$ AP and some N-terminal APP fragments [105]. Thus, an elevation of the PKC activity for the reduction of  $\beta$ AP may be useful for therapeutic purposes. However, only sporadic data are available as concerns the intermediate steps between PKC activation and the modulation of APP metabolism. The stimulation of PKC by phorbol ester rapidly induced secAPP secretion through a mechanism involving activation of the mitogen-activated protein (MAP) kinase cascade in various cell lines [25]. In PC12-M1 cells, activation of MAP kinase by NGF was associated with the stimulation of secAPP release.



Conversely, M1 muscarinic receptor stimulation, which is known to act partly through a PKC-independent pathway, increased secAPP secretion in this experimental setup mainly through a MAP-kinase-independent pathway. A MAP inhibitor (PD 98059) antagonized the NGF stimulation of both APP production and extracellular signal-regulated protein kinase (ERK) activation. Moreover, PD 98059 inhibited the phorbol ester stimulation of APP production and the activation of ERK in both human kidney cells and cortical neurons. The overexpression of a kinase-inactive MAP mutant inhibited the phorbol ester stimulation of APP secretion and the activation of ERK in human embryonic kidney cell lines [75]. Thus, MAP and ERK may be involved in the PKC and NGF regulation of APP processing, and the MAP-activated protein kinase cascade could provide a novel target for altering the catabolic processing of APP.

APP secretion, via  $\alpha$ -secretase activity, was stimulated by epidermal growth factor receptors, this being partly dependent upon the PKC activity [115]. These receptors possess intrinsic tyrosine kinase activity, and are known to be coupled to a variety of effectors, including phosphoinositide-specific phospholipase C $\gamma$ . In A431 cells, epidermal growth factor caused time- and dose-dependent increases in the formation of inositol phosphates in cultures pretreated with myo-<sup>3</sup>H-inositol, and in the release of APP into the cell culture medium. A specific PKC antagonist decreased the effect of epidermal growth factor that also abolished the stimulation of APP. In a recent study, Benussi et al. [14] presented evidence that PKC $\alpha$  is the only PKC isoform involved in controlling the secretion of secAPP in human skin fibroblasts. The specific PKC $\alpha$  inhibitor Go-6976 reduced basal APP secretion and completely abolished the effect of phorbol ester-mediated PKC stimulation on secAPP release.

Heparin oligosaccharides that pass the blood-brain barrier were shown to inhibit APP secretion and heparin binding to a short form of  $\beta$ AP [64]. Chemically depolymerized low-molecular-weight (LMW) heparin did not have a significant effect on APP secretion. However, LMW heparin fragments, especially heparin disaccharides, efficiently inhibited the stimulatory effect of heparin on APP secretion. LMW heparin derivatives also inhibited the binding of heparin to the  $\beta$ AP1-28 peptide in that study. Since LMW heparin fragments pass through the blood-brain barrier, their derivatives or analogs might be effective as therapeutic agents for AD.

Increases in APP levels were demonstrated after injury to the brain, even in the early stage of the damage [55]. APP-like immunoreactivity was upregulated during olfactory nerve regeneration in adult rats [118]; in that study, subcutaneous diethyldithiocarbamate was used to lesion the olfactory epithelium reversibly and it was found that the APP-like immunoreactivity significantly decreased after the lesion, then increased, reaching almost 5 times the normal levels 6 weeks after the treatment. Immunocytochemical techniques identified APP immunoreactive perikarya and fibers in and around the glomeruli 3–7 days after the lesion, and upregulation of the immunoreactivity in the mitral cells and dendrites at 5 weeks [118].

APP accumulated within axonal swellings in human brain lesions [86], in experimentally induced diffuse axonal injury in rats [16], or in the ibotenic acid-lesioned rat hippocampus after injection [82]. A selective induction of APP mRNA was demonstrated after persistent focal ischemia in the rat cerebral cortex [1]. After transient ischemia, however,



the mRNAs of the Kunitz protease inhibitor-bearing isoforms were increased, whereas that of APP695, which lacks this domain, was decreased in the rat cerebral cortex [57]. In a rabbit spinal cord ischemia model, the effects of reversible (15-min) and irreversible (60-min) ischemia were tested on the endogenous levels of APP at both mRNA and protein levels [58]. A transiently increased APP level, without an increase in APP mRNA level, was observed after 15 min of reversible ischemia. The APP level was normal after 60 min. The increased levels of APPs, and particularly the soluble form, could support the possibility that APPs may play a neuroprotective role as stress-induced proteins in this type of ischemia model. In contrast, failure to maintain the increased APP levels or to increase the mRNA, as seen in the 60-min ischemia samples, could be one of the causal factors that induce necrosis and neuronal death, leading to an irreversible neurological impairment [58]. Since the APP gene promoter region contains a heat-shock element, an abnormal APP heat-shock response could increase the accumulation of  $\beta$ AP. Moreover,  $\beta$ AP production is affected by PS1 mutations. Johnston et al. [53] tested this hypothesis and found that heat-shock influenced APP mRNA synthesis in lymphoblastoid cell lines bearing PS1 mutations. However, the increase in mRNA content was not influenced by the PS1 mutations of the cells [53].

APP immunoreactivity was observed in damaged axons and reactive glial cells in the rat brain shortly after a needle stab injury [90]. Molecules normally participating in the cell-cell signaling processes, such as NGF [108], basic fibroblast growth factor [108] and interleukin-1 [37], were demonstrated to increase APP levels. Moreover, APP expression is upregulated in response to growth factors and cytokines [99, 101], as additional evidence of a role for APPs in the response of the brain to injury. Interestingly, Quon et al. [99] detected the effects of fibroblast growth factors on the induction of APP mRNA synthesis only in glial, but not in neuronal cells.

The functions of secAPP in neurons under normal or physiological conditions are largely unknown. However, one possible role for synaptic proteins is involvement in neuronal plasticity. Indeed, after exposure to an enriched environment as compared with impoverished conditions, rats exhibited a superior cognitive capacity and expressed up to 4-fold amounts of APP isoforms (APP695 and APP751/770) in cortical and subcortical tissues, as detected by immunocytochemical techniques [10]. Full-length APPs undergo fast anterograde axonal transport to the terminals [59], where they may be released, suggesting a possible function in synaptic transmission [109]. For example, Nitsch et al. [84, 85] reported that APP and its derivatives can be released from presynaptic terminals either by activation of muscarinic acetylcholine receptors or by electrical depolarization. Moreover, both the muscarinic and nicotinic cholinergic systems are involved in the regulation of APP metabolism. Alterations in the mainly M1 muscarinic receptor population of the rat neocortex by saporin-induced partial immunoablation of the cortical cholinergic system affected the amount of secAPP [103]. While the total APP levels in cortical homogenates were unaffected by cholinergic deafferentation, a significant reduction in secAPP and concomitant increases in membrane-bound forms were also demonstrated. The changes were reversed in immunoablated rats subsequently transplanted with NGF-producing fibroblasts. Additionally, a transient decrease was found in the ratio of cortical APP transcripts containing the Kunitz protease inhibitor domain (APP770 and APP751) versus



APP695 in rats with cholinergic hypoactivity. Nicotine enhanced the release of secAPP from PC12 cells [56], implying that nicotinic receptor agonists might be beneficial in the treatment of AD, not only by supplementing the deficient nicotinic cholinergic neurotransmission, but also by stimulating the release of beneficial secAPP forms.

Another example of receptor-mediated secAPP release was the demonstration of bradykinin-induced APP secretion [100]. The mechanism by which APP was released from human skin fibroblasts was via bradykinin 2 receptors and was found to be PKC-independent. APP secretion after bradykinin treatment in fibroblasts from patients with sporadic AD, however, did not differ from that from control cells and was paralleled by equivalent levels of inositol trisphosphate production. Melatonin also altered the metabolism of APP in the neuroendocrine cell line PC12 [117]. Normal levels of secretion of secAPP into conditioned media were severely inhibited by treatment of the cells with melatonin, an effect that could be reversed by washing-out of the agent. Melatonin also decreased the amounts of mRNA encoding APP,  $\beta$ -actin and glyceraldehyde-3-phosphate dehydrogenase in PC12 cells, whereas the treatment did not have any effect on these transcripts in human neuroblastoma cells. Melatonin potentiated the NGF-mediated differentiation in PC12 cells. Overall, this study demonstrated that melatonin regulated the metabolism of APP and other housekeeping genes in a cell-type specific manner, and that melatonin accelerated the early process of neuronal differentiation [117].

APP potentiates the neurotrophic activity of suboptimal concentrations of NGF on PC12 cells [124]. APP stimulated the tyrosine phosphorylation of a number of proteins, including the insulin receptor substrate-1 (IRS-1). It was found that incubation of native cells with antisense oligonucleotides to IRS-1 mRNA resulted in dramatic reductions in IRS-1 levels and inhibition of APP-stimulated neurite outgrowth. Additionally, phosphatidylinositol 3-kinase became associated with IRS-1 and was activated upon APP stimulation [125]. ERK 1 and ERK 2 phosphorylation was also detected. The potentiation of NGF activity was reflected in a correspondingly synergistic elevation of tyrosine phosphorylated ERK. The pattern of signal transduction targets indicated that APP potentiated the neurotrophic effects of NGF via activation of the IRS-1 signaling pathway [125].

The distribution of APP was investigated after kainic acid-induced seizures in the rat cortex [113]. Seizures were associated with a decrease in neuronal, but an increase in glial APP-like immunoreactivity. The increase in glial APP-like immunoreactivity was far more extensive in adult than in young rats, and the anatomical distribution of this immunoreactivity was grossly correlated with concomitant c-fos-like immunoreactivity.

Mild acidosis was sufficient to alter the neuronal processing of APP into potentially amyloidogenic forms and increased certain fragments bound to the substrate in embryonic rat hippocampal neurons [17]. Lactic acid-elicited acidosis increased cellular  $\beta$ AP immunoreactivity and the amounts of some membrane-bound, N- and C-terminal forms but did not affect the secretion of  $\beta$ AP or its derivatives into the medium. APP production was slightly reduced by acidosis, without an effect on the maturation or proteolytic processing. Similar acidotic processes that may stimulate an extracellular deposition of amyloids in aging brain cannot be ruled out.

The possible role of aluminum (Al) in the pathogenesis of AD was much discussed in the past. Two novel pathologically critical processes that Al influences, protein turnover

and aggregation, were recently implicated in the disease [91]. In that study, A1 was shown to induce secondary structure alterations into APP. APP consequently became resistant to proteases such as trypsin,  $\alpha$ -chymotrypsin and calpain, possibly promoting protein aggregation.

## CONCLUSION

APP is certainly best known as the source of  $\beta$ AP that accumulates in neuritic plaques in AD and related age-associated dementias and other disorders. However, various beneficial roles have been ascribed to AP and its numerous proteolytic forms in normal brain functioning. A proteolytic processing alternative to that which generates  $\beta$ AP liberates most of the extracellular portion of the protein. This soluble APP exerts numerous beneficial effects on a wide variety of cell physiological phenomena, including the ionic homeostasis, the enhancement of mitogenesis, or the neurite outgrowth and survival, the synapse formation and synaptic plasticity in the nervous tissue. At least some of these effects result from cell signaling processes that include receptor-activated signal-transduction mechanisms. Moreover, APP synthesis, processing and metabolism are all closely related to the cell's general physiological status which, when changed, can modulate the effects of APP and its metabolites in numerous (patho)physiological conditions.

## REFERENCES

1. Abe, K., Tanzi, R. E., Kogure, K. (1991) Selective induction of Kunitz-type inhibitor domain-containing amyloid precursor protein mRNA after persistent focal ischemia in rat cerebral cortex. *Neurosci. Lett.* 125, 172–174.
2. Ancolio, K., Marambaud, P., Dauch, P., Checler, F. (1997) Alpha-secretase-derived product of beta-amyloid precursor protein is decreased by presenilin 1 mutations linked to familial Alzheimer's disease. *J. Neurochem.* 69, 2494–2499.
3. Apert, C., Czech, C., Faivre-Bauman, A., Loudes, C., Pradier, L., Epelbaum, J. (1998) Profiles of amyloid precursor and presenilin 2-like proteins are correlated during development of the mouse hypothalamus. *J. Neuroendocrinol.* 10, 101–109.
4. Araki, W., Kitaguch, N., Tokushima, Y., Ishii, K., Aratake, H., Shimohama, S., Nakamura, S., Kimura, J. (1992) Trophic effect of  $\beta$ -amyloid precursor protein on cerebral cortical neurons in culture. *Biochem. Biophys. Res. Commun.* 181, 265–271.
5. Arispe, N., Pollard, H. B., Rojas, E. (1993)  $\text{Zn}^{2+}$  interaction with Alzheimer amyloid  $\beta$  protein calcium channels. *Proc. Natl. Acad. Sci. USA* 93, 1710–1715.
6. Arispe, N., Pollard, H. B., Rojas, E. (1994)  $\beta$ -amyloid  $\text{Ca}^{2+}$ -channel hypothesis for neuronal death in Alzheimer's disease. *Mol. Cell. Biochem.* 140, 119–125.
7. Arispe, N., Pollard, H. B., Rojas, E. (1994) The ability of amyloid  $\beta$ -protein [ $\text{A}\beta$  (1–40)] to form  $\text{Ca}^{2+}$  channels provides a mechanism for neuronal death in Alzheimer's disease. *Ann. N. Y. Acad. Sci.* 747, 256–266.
8. Arispe, N., Rojas, E., Pollard, H. B. (1993) Alzheimer's disease amyloid  $\beta$ -protein forms calcium channels in bilayer membranes: blockade by tromethamine and aluminum. *Proc. Natl. Acad. Sci. USA* 90, 567–571.
9. Austen, B. M., Stephens, D. J. (1995) Cleavage of a beta-amyloid precursor sequence by cathepsin D. *Biomed. Pept. Prot. Nucl. Acids* 1, 243–246.
10. Bailly, H. G., Bailly, Y., Martin, J. R., Mariani, J., Brugg, B. (1997) Synaptic beta-amyloid precursor proteins increase with learning capacity in rats. *Neuroscience* 80, 313–320.



11. Barger, S. W., Fiscus, R. R., Ruth, P., Hofmann, F., Mattson, M. P. (1995) Role of cyclic GMP in the regulation of neuronal calcium and survival by secreted forms of  $\beta$ -amyloid precursor. *J. Neurochem.* 64, 2087–2096.
12. Barger, S. W., Harmon, A. D. (1997) Microglial activation by Alzheimer amyloid precursor protein and modulation by apolipoprotein E. *Nature* 388, 878–881.
13. Barger, S. W., Mattson, M. P. (1995) The secreted form of the Alzheimer's  $\beta$ -amyloid precursor protein stimulates a membrane-associated guanylate cyclase. *Biochem. J.* 311, 45–47.
14. Benussi, L., Govoni, S., Gasparini, L., Binetti, G., Trabucchi, M., Bianchetti, A., Racchi, M. (1998) Specific role for protein kinase C  $\alpha$  in the constitutive and regulated secretion of amyloid precursor protein in human skin fibroblasts. *Neurosci. Lett.* 240, 97–101.
15. Borchelt, D. R., Ratovitski, T., van Lare, J., Lee, M. K., Gonzales, V., Jenkins, N. A., Copeland, N. G., Price, D. L., Sisodia, S. S. (1997) Accelerated amyloid deposition in the brains of transgenic mice coexpressing mutant presenilin 1 and amyloid precursor proteins. *Neuron* 19, 939–945.
16. Bramlett, H. M., Kraydieh, S., Green, E. J., Dietrich, W. D. (1997) Temporal and regional patterns of axonal damage following traumatic brain injury: a beta-amyloid precursor protein immunocytochemical study in rats. *J. Neuropathol. Exp. Neurol.* 56, 1132–1141.
17. Brewer, G. J. (1997) Effects of acidosis on the distribution of processing of the beta-amyloid precursor protein in cultured hippocampal neurons. *Mol. Chem. Neuropathol.* 31, 171–186.
18. Campos, E. O., Alvarez, A., Inestrosa, N. C. (1998) Brain acetylcholinesterase promotes amyloid-beta-peptide aggregation but does not hydrolyze amyloid precursor protein peptides. *Neurochem. Res.* 23, 135–140.
19. Cataldo, A. M., Barnett, J. L., Pieroni, C., Nixon, R. A. (1997) Increased neuronal endocytosis and protease delivery to early endosomes in sporadic Alzheimer's disease: neuropathologic evidence for a mechanism of increased  $\beta$ -amyloidogenesis. *J. Neurosci.* 17, 6142–6151.
20. Chen, M. (1997) Alzheimer's alpha-secretase may be a calcium-dependent protease. *FEBS Lett.* 417, 163–167.
21. Chyung, A. S. C., Greenberg, B. D., Cook, D. G., Doms, R. W., Lee, V. M. (1997) Novel beta-secretase cleavage of beta-amyloid precursor protein in the endoplasmic reticulum/intermediate compartment of NT2N cells. *J. Cell Biol.* 138, 671–680.
22. Coulson, E. J., Barrett, G. L., Storey, E., Bartlett, P. F., Beyreuther, K., Masters, C. L. (1997) Down-regulation of the amyloid protein precursor of Alzheimer's disease by antisense oligonucleotides reduces neuronal adhesion to specific substrata. *Brain Res.* 770, 72–80.
23. de la Fourniere-Bessueille, L., Grange, D., Buchet, R. (1997) Purification and spectroscopic characterization of beta-amyloid precursor protein from porcine brains. *Eur. J. Biochem.* 250, 705–711.
24. Denman, R. B., Smedman, M., Abraham, M., Chen-Hwang, M. C., Currie, J. R. (1997) Facilitated reduction of beta-amyloid peptide precursor by synthetic oligonucleotides in COS-7 cells expressing a hammerhead ribozyme. *Arch. Biochem. Biophys.* 348, 82–90.
25. Desdouits-Magnen, J., Desdouits, F., Takeda, S., Syu, L. J., Saltiel, A. R., Buxbaum, J. D., Czernik, A. J., Nairn, A. C., Greengard, P. (1998) Regulation of secretion of Alzheimer amyloid precursor protein by the mitogen-activated protein kinase cascade. *J. Neurochem.* 70, 524–530.
26. Dyrks, T., Weidemann, A., Multhaup, G., Salbaum, J. M., Lemaire, H.-G., Kang, J., Muller-Hill, B., Masters, C. L., Beyreuther, K. (1988) Identification, transmembrane orientation and biogenesis of the A4 precursor of Alzheimer's disease. *EMBO J.* 7, 949–957.
27. Esch, F. S., Keim, P. S., Beattie, E. C., Blacher, R. W., Culwell, A. R., Oltersdorf, T., McClure, D., Ward, P. J. (1990) Cleavage of amyloid  $\beta$ -peptide during constitutive processing of its precursor. *Science* 248, 1122–1124.
28. Fox, N. W., Johnstone, E. M., Ward, K. E., Schrementi, J., Little, S. P. (1997) APP gene promoter constructs are preferentially expressed in the CNS and testis of transgenic mice. *Biochem. Biophys. Res. Commun.* 240, 759–762.
29. Fraser, S. P., Suh, Y.-H., Djamgoz, M. B. A. (1997) Ionic effects of the Alzheimer's disease  $\beta$ -amyloid precursor protein and its metabolic fragments. *Trends Neurosci.* 20, 67–72.

30. Fraser, S. P., Suh, Y. H., Chong, Y. H., Djamgoz, M. B. (1996) Membrane currents induced in *Xenopus* oocytes by the C-terminal fragment of the beta-amyloid precursor protein. *J. Neurochem.* 66, 2034–2040.
31. Friedman, L. M., Matsuda, Y., Lazarovici, P. (1997) The microbial alkaloid toxin staurosporine blocks the phorbol ester-induced increase in beta-amyloid precursor protein in PC12 cells. *Nat. Toxins* 5, 173–179.
32. Furukawa, K., Barger, S. W., Blalock, E. M., Mattson, M. P. (1996) Activation of K<sup>+</sup> channels and suppression of neuronal activity by secreted  $\beta$ -amyloid precursor protein. *Nature* 379, 74–78.
33. Furukawa, K., Mattson, M. P. (1998) Secreted amyloid precursor protein alpha selectively suppresses N-methyl-D-aspartate currents in hippocampal neurons: involvement of cyclic GMP. *Neuroscience* 83, 429–438.
34. Gasparini, L., Racchi, M., Benussi, L., Curti, D., Binetti, G., Bianchetti, A., Trabucchi, M., Govoni, S. (1997) Effect of energy shortage and oxidative stress on amyloid precursor protein metabolism in COS cells. *Neurosci. Lett.* 231, 113–117.
35. Glenner, G. G., Wong, C. W. (1984) Alzheimer's disease: initial report of the purification and characterization of a novel cerebrovascular and amyloid protein. *Biochem. Biophys. Res. Commun.* 120, 885–890.
36. Golde, T. E., Estus, S., Younkin, L. H., Selkoe, D. J., Younkin, S. G. (1992) Processing of the amyloid protein precursor to potentially amyloidogenic derivatives. *Science* 255, 728–730.
37. Goldgaber, D., Harris, H. W., Hla, T., Maciag, T., Donnelly, R. J., Jacobsen, J. S., Vitek, M. P., Gajdusek, D. C. (1989) Interleukin 1 regulates synthesis of amyloid  $\beta$ -protein precursor mRNA in human endothelial cells. *Proc. Natl. Acad. Sci. USA* 86, 7606–7610.
38. Haass, C. (1996) The molecular significance of amyloid  $\beta$ -peptide for Alzheimer's disease. *Eur. Arch. Psychiatry Clin. Neurosci.* 246, 118–123.
39. Haass, C., Aldudo, J., Cazorla, P., Bullido, M. J., de Miguel, C., Vazquez, J., Valdivieso, F. (1997) Proteolysis of Alzheimer's disease beta-amyloid precursor protein by factor Xa. *Biochim. Biophys. Acta* 1343, 85–94.
40. Haass, C., Hung, A. Y., Schlossmacher, M. G., Teplow, D. B., Selkoe, D. J. (1993)  $\beta$ -amyloid peptide and a 3-kDa fragment are derived by distinct cellular mechanisms. *J. Biol. Chem.* 268, 3021–3024.
41. Haass, C., Hung, A. Y., Selkoe, D. J. (1991) Processing of  $\beta$ -amyloid precursor protein in microglia and astrocytes favors an internal localization over constitutive secretion. *J. Neurosci.* 11, 3738–3793.
42. Haass, C., Hung, A. Y., Selkoe, D. J., Teplow, D. B. (1994) Mutations associated with a locus for familial Alzheimer's disease result in alternative processing of amyloid  $\beta$ -protein precursor. *J. Biol. Chem.* 269, 17741–17748.
43. Haass, C., Koo, E. H., Mellon, A., Hung, A. Y., Selkoe, D. J. (1992) Targeting of cell-surface  $\beta$ -amyloid precursor protein to lysosomes: alternative processing into amyloid-bearing fragments. *Nature* 357, 500–503.
44. Haass, C., Schlossmacher, M. G., Hung, A. Y., Vigo-Pelfrey, C., Mellon, A., Ostaszewski, B., Lieberburg, I., Koo, E. H., Schenk, D., Teplow, D. B., Selkoe, S. J. (1992) Amyloid  $\beta$ -peptide is produced by cultured cells during normal metabolism. *Nature* 359, 322–325.
45. Haass, C., Selkoe, D. J. (1993) Cellular processing of  $\beta$ -amyloid precursor protein and the genesis of amyloid  $\beta$ -peptide. *Cell* 75, 1039–1042.
46. Hendriks, L., van Duijn, C. M., Cras, P., Cruts, M., Van Hul, W., van Harskamp, F., Warren, A., McInnis, M. G., Antonarakis, S. E., Martin, J. J., Hofman, A., Van Broeckhoven, C. (1992) Presenile dementia and cerebral haemorrhage linked to a mutation at codon 692 of the  $\beta$ -amyloid precursor gene. *Nature Genet.* 1, 218–221.
47. Iijima, K., Lee, D. S., Okutsu, J., Tomita, S., Hirashima, N., Kirino, Y., Suzuki, T. (1998) cDNA isolation of Alzheimer's amyloid precursor protein from cholinergic nerve terminals of the electric organ of the electric ray. *Biochem. J.* 330, 29–33.
48. Ikezu, T., Trapp, B. D., Song, K. S., Schlegel, A., Lisanti, M. P., Okamoto, T. (1998) Caveolae, plasma membrane microdomains for alpha-secretase-mediated processing of the amyloid precursor protein. *J. Biol. Chem.* 273, 10485–10495.



49. Ishiguro, M., Ohsawa, I., Takamura, C., Morimoro, T., Kohsaka, S. (1998) Secreted form of beta-amyloid precursor protein activates protein kinase C and phospholipase C $\gamma$ 1 in cultured embryonic rat neocortical cells. *Mol. Brain Res.* 53, 24–32.
50. Itoh, T., Ikeda, T., Gomi, H., Nakao, S., Suzuki, T., Itohara, S. (1997) Unaltered secretion of beta-amyloid precursor protein in gelatinase A (matrix metalloproteinase 2)-deficient mice. *J. biol. Chem.* 272, 22389–22392.
51. Joachim, C. L., Duffy, L. K., Selkoe, D. (1988) Protein chemical and immunochemical studies of meningeovascular  $\beta$ -amyloid protein in Alzheimer's disease and normal aging. *Brain Res.* 474, 100–111.
52. Johnson-Wood, K. L., Henriksson, T., Seubert, P., Oltersdorf, T., Lieberburg, I., Schenk, D. B. (1990) Identification of specific binding sites for  $^{125}$ I secreted APP751 on intact fibroblast cells. *Neurobiol. Aging* 11, 306.
53. Johnston, J. A., Lannfelt, L., Wichager, B., O'Neill, C., Cowburn, R. F. (1997) Amyloid precursor protein heat shock response in lymphoblastoid cell lines bearing presenilin-1 mutations. *Biochem. Biophys. Acta* 1362, 183–192.
54. Kang, J., Lemaire, H., Unterbeck, A., Salbaum, J. M., Masters, C. L., Grzeschik, K.-H., Multhaup, G., Bexreuther, K., Muller-Hill, B. (1987) The precursor of Alzheimer's disease amyloid A $\beta$ -protein resembles a cell-surface receptor. *Nature* 325, 733–736.
55. Kawarabayashi, T., Shoji, M., Harigaya, Y., Yamaguchi, H., Hirai, S. (1991) Expression of APP in the early stage of brain damage. *Brain Res.* 563, 334–338.
56. Kim, H. S., Kim, Y. K., Jeong, S. J., Haass, C., Kim, Y. H., Suh, Y. H. (1997) Enhanced release of secreted form of Alzheimer's amyloid precursor protein from PC12 cells by nicotine. *Mol. Pharmacol.* 52, 430–436.
57. Kim, H. S., Lee, S. H., Kim, S. S., Kim, Y. K., Jeong, S. J., Ma, J., Han, D. H., Cho, B. K., Suh, Y. H. (1998) Post-ischemic changes in the expression of Alzheimer's APP isoforms in rat cerebral cortex. *Neuroreport* 9, 533–537.
58. Komori, N., Kittel, A., Kang, D., Shackelford, D., Masliah, E., Zivin, J. A., Saitoh, T. (1997) Reversible ischemia increases levels of Alzheimer amyloid precursor without increasing levels of mRNA in the rabbit spinal cord. *Mol. Brain Res.* 49, 103–112.
59. Koo, E. H., Sisodia, S. S., Archer, D. A., Martin, L. J., Weidemann, A., Beyreuther, K., Masters, C. L., Fisher, P., Price, D. L. (1990) Precursor of amyloid protein in Alzheimer's disease undergoes fast anterograde axonal transport. *Proc. Natl. Acad. Sci. USA* 87, 1561–1565.
60. Koo, E. H., Squazzo, S. (1994) Evidence that production and release of amyloid  $\beta$ -protein involves the endocytic pathway. *J. biol. Chem.* 269, 17386–17389.
61. Lahiri, D. K., Farlow, M. R., Nurnberger, J. I., Greig, N. H. (1997a) Effects of cholinesterase inhibitors on the secretion of beta-amyloid precursor protein in cell cultures. *Ann. N. Y. Acad. Sci.* 826, 416–421.
62. Lahiri, D. K., Farlow, M. R., Sambamurti, K., Nall, C. (1997b) The effect of tacrine and leupeptin on the secretion of the beta-amyloid precursor protein in HeLa cells. *Life Sci.* 61, 1985–1992.
63. LeBlanc, A. C., Koutroumanis, M., Goodyer, C. G. (1998) Protein kinase C activation increases release of secreted amyloid precursor protein without decreasing A $\beta$  production in human primary neuron cultures. *J. Neurosci.* 18, 2907–2913.
64. Leveugle, B., Ding, W., Laurence, F., Dehouck, M. P., Scanameo, A., Cecchelli, R., Fillit, H. (1998) Heparin oligosaccharides that pass the blood-brain barrier inhibit beta-amyloid precursor protein secretion and heparin binding to beta-amyloid peptide. *J. Neurochem.* 70, 736–744.
65. Lichtenthaler, S. F., Ida, N., Multhaup, G., Masters, C. L., Beyreuther, K. (1997) Mutations in the transmembrane domain of APP altering gamma-secretase specificity. *Biochemistry* 36, 15396–15403.
66. Lyckman, A. W., Confaloni, A. M., Thinakaran, G., Sisodia, S. S., Moya, K. L. (1998) Post-translational processing and turnover kinetics of presynaptically targeted amyloid precursor superfamily proteins in the central nervous system. *J. biol. Chem.* 273, 11100–11106.
67. Marambaud, P., Lopez-Perez, E., Wilk, S., Checler, F. (1997) Constitutive and protein kinase C-regulated secretory cleavage of Alzheimer's beta-amyloid precursor protein: different control of early and late events by the proteasome. *J. Neurochem.* 69, 2500–2505.



68. Masters, C. L., Simms, G., Weinman, N. A., Multhaup, G., McDonald, B. L., Beyreuther, K. (1985) Amyloid plaque core protein in Alzheimer's disease and Down syndrome. *Proc. Natl. Acad. Sci. USA* 82, 4245–4249.
69. Matsumoto, A., Matsumoto, R., Enomoto, T., Itoh, K. (1998) A human brain proteolytic activity capable of cleaving natural beta-amyloid precursor protein is affected by its substrate glycoconjugates. *Neurosci. Lett.* 242, 109–113.
70. Mattson, M. P. (1994) Calcium and neuronal injury in Alzheimer's disease. Contributions of  $\beta$ -amyloid precursor protein mismetabolism, free radicals, and metabolic compromise. *Ann. N.Y. Acad. Sci.* 747, 50–76.
71. Mattson, M. P. (1994) Secreted forms of  $\beta$ -amyloid precursor protein modulate dendrite outgrowth and calcium responses to glutamate in cultured embryonic hippocampal neurons. *J. Neurobiol.* 25, 439–450.
72. Mattson, M. P., Barger, S. W., Cheng, B., Lieberburg, I., Smith-Swintosky, V. L., Rydel, R. E. (1993a)  $\beta$ -amyloid precursor protein metabolites and loss of neuronal  $\text{Ca}^{2+}$  homeostasis in Alzheimer's disease. *Trends Neurosci.* 16, 409–414.
73. Mattson, M. P., Cheng, B., Culwell, A. R., Esch, F. S., Lieberburg, I., Rydel, R. E. (1993b) Evidence for excitoprotective and intraneuronal calcium-regulating roles for secreted forms of the  $\beta$ -amyloid precursor protein. *Neuron* 10, 243–254.
74. McPhie, D. L., Lee, R. K. K., Eckman, C. B., Olstein, D. H., Durham, S. P., Yager, D., Younkin, S. G., Wurtman, R. J., Neve, R. L. (1997) Neuronal expression of beta-amyloid precursor protein Alzheimer mutations causes intracellular accumulation of a C-terminal fragment containing both the amyloid beta and cytoplasmic domains. *J. Biol. Chem.* 272, 24743–24746.
75. Mills, J., Laurent Charest, D., Lam, F., Beyreuther, K., Ida, N., Pelech, S. L., Reiner, P. B. (1997) Regulation of amyloid precursor protein catabolism involves the mitogen-activated protein kinase signal transduction pathway. *J. Neurosci.* 17, 9415–9422.
76. Milward, E. A., Papadopoulos, R., Fuller, S. J., Moir, R. D., Small, D., Beyreuther, K., Masters, C. L. (1992) The amyloid protein precursor of Alzheimer's disease is a mediator of the effects of nerve growth factor on neurite outgrowth. *Neuron* 9, 129–137.
77. Mook-Jung, I., Saitoh, T. (1997) Amyloid precursor protein activates phosphotyrosine pathway. *Neurosci. Lett.* 235, 1–4.
78. Morimoto, T., Ohsawa, I., Takamura, C., Ishiguro, M., Kohsaka, S. (1998) Involvement of amyloid precursor protein in functional synapse formation in cultured hippocampal neurons. *J. Neurosci. Res.* 51, 185–195.
79. Mullan, M., Crawford, F., Axelman, K., Houlden, H., Lilius, L., Winblad, B., Lannfelt, L. (1992) A pathogenic mutation for probable Alzheimer's disease in the APP gene at the N-terminus of  $\beta$ -amyloid. *Nature Genet.* 1, 345–347.
80. Murai, H., Pierce, J. E., Raghupathi, R., Smith, D. H., Saatman, K. E., Trojanowski, J. Q., Lee, V. M., Loring, J. F., Eckman, C., Younkin, S., McIntosh, T. K. (1998) Twofold overexpression of human beta-amyloid precursor proteins in transgenic mice does not affect the neuromotor, cognitive, or neurodegenerative sequelae following experimental brain injury. *J. comp. Neurol.* 392, 428–438.
81. Murrel, J., Farlow, M., Ghetti, B., Benson, M. D. (1991) A mutation in the amyloid precursor protein associated with hereditary Alzheimer's disease. *Science* 254, 97–99.
82. Nakamura, Y., Takeda, M., Niigawa, H., Hariguchi, S., Nishimura, T. (1992) Amyloid  $\beta$ -protein precursor deposition in rat hippocampus lesioned by ibotenic acid injection. *Neurosci. Lett.* 136, 95–98.
83. Nishimoto, I., Okamoto, T., Matsuura, Y., Takahashi, S., Okamoto, T., Murayama, Y., Ogata, E. (1993) Alzheimer amyloid protein precursor complexes with brain GTP-binding protein  $G_o$ . *Nature* 362, 75–79.
84. Nitsch, R. M., Slack, B. E., Growdon, J. H., Wurtman, R. J. (1993) Release amyloid  $\beta$ -protein precursor derivatives by electrical depolarization of rat hippocampal slices. *Proc. Natl. Acad. Sci. USA* 90, 5090–5093.
85. Nitsch, R. M., Slack, B. E., Wurtman, R. J., Growdon, J. H. (1992) Release of Alzheimer amyloid precursor derivatives stimulated by the activation of muscarinic acetylcholine receptors. *Science* 258, 304–307.

86. Ohgami, T., Kitamoto, T., Tateishi, J. (1992) Alzheimer's amyloid precursor protein accumulates within axonal swellings in human brain lesions. *Neurosci. Lett.* 136, 75–78.
87. Oltersdorf, T., Fritz, L. C., Schenk, D. B., Lieberburg, I., Johnson-Wood, K. L., Beattie, E. C., Ward, P. J., Blacher, R. W., Dovey, H. F., Sinha, S. (1989) The secreted form of Alzheimer's amyloid precursor protein with the Kunitz domain is protease nexin II. *Nature* 347, 144–147.
88. Oltersdorf, T., Ward, P., Henriksson, T., Beattie, E., Neve, R., Lieberburg, I., Fitz, I. (1990) The Alzheimer amyloid precursor protein. Identification of a stable intermediate in the biosynthetic/degradative pathway. *J. biol. Chem.* 265, 4492–4497.
89. Oster-Granite, M. L., McPhie, D. L., Greenan, J., Neve, R. L. (1996) Age-dependent neuronal and synaptic degeneration in mice transgenic for the C terminus of the amyloid precursor protein. *J. Neurosci.* 16, 6732–6741.
90. Otsuka, N., Tomonaga, M., Ikeda, K. (1991) Rapid appearance of  $\beta$ -amyloid precursor protein immunoreactivity in damaged axons and reactive glial cells in rat brain following needle stab injury. *Brain Res.* 568, 335–338.
91. Paik, S. R., Lee, J. H., Kim, D. H., Chang, C. S., Kim, J. (1997) Aluminum-induced structural alterations of the precursor of the non-A beta component of Alzheimer's disease amyloid. *Arch. Biochem. Biophys.* 344, 325–334.
92. Paliga, K., Peraus, G., Kreger, S., Durrwang, U., Hesse, L., Multhaup, G., Masters, C. L., Beyreuther, K., Weidemann, A. (1997) Human amyloid precursor-like protein 1-cDNA cloning, ectopic expression in COS-7 cells and identification of soluble forms in the cerebrospinal fluid. *Eur. J. Biochem.* 250, 354–363.
93. Parkin, E. T., Hussain, I., Turner, A. J., Hooper, N. M. (1997) The amyloid precursor protein is not enriched in caveolae-like, detergent-insoluble membrane microdomains. *J. Neurochem.* 69, 2179–2188.
94. Parvathy, S., Hussain, I., Karran, E. H., Turner, A. J., Hooper, N. M. (1998) Alzheimer's amyloid precursor protein alpha-secretase is inhibited by hydroxamic acid-based zinc metalloprotease inhibitors: similarities to the angiotensin converting enzyme secretase. *Biochemistry* 37, 1680–1685.
95. Peraus, G. C., Masters, C. L., Beyreuther, K. (1997) Late compartments of amyloid precursor protein transport in SY5Y cells are involved in  $\beta$ -amyloid secretion. *J. Neurosci.* 17, 7714–7724.
96. Perez, R. G., Yheng, H., Van der Ploeg, L. H. T., Koo, E. H. (1997) The  $\beta$ -amyloid precursor protein of Alzheimer's disease enhances neuron viability and modulates neuronal polarity. *J. Neurosci.* 17, 9407–9414.
97. Pietrzik, C. U., Hoffmann, J., Stober, K., Chen, C. Y., Bauer, C., Otero, D. A., Roch, J. M., Herzog, V. (1998) From differentiation to proliferation: the secretory amyloid precursor protein as a local mediator of growth in thyroid epithelial cells. *Proc. Natl. Acad. Sci. USA* 95, 1770–1775.
98. Plaschke, K., Ranneberg, T., Bauer, J., Weigand, M., Hoyer, S., Bardenheuer, H. J. (1997) The effect of stepwise cerebral hypoperfusion on energy metabolism and amyloid precursor protein (APP) in cerebral cortex and hippocampus in the adult rat. *Ann. N. Y. Acad. Sci.* 826, 502–506.
99. Quon, D., Catalano, R., Cordell, B. (1990) Fibroblast growth factor induces beta-amyloid precursor mRNA in glial but not neuronal cultured cells. *Biochem. Biophys. Res. Commun.* 167, 96–102.
100. Racchi, M., Ianna, P., Binetti, G., Trabucchi, M., Govoni, S. (1998) Bradykinin-induced amyloid precursor protein secretion: a protein kinase C-independent mechanism that is not altered in fibroblasts from patients with sporadic Alzheimer's disease. *Biochem. J.* 330, 1271–1275.
101. Refolo, L. M., Salton, S. R. J., Anderson, J. P., Mehta, P., Robakis, N. K. (1989) Nerve and epidermal growth factors induce the release of the Alzheimer amyloid precursor from PC12 cell cultures. *Biochem. Biophys. Res. Commun.* 164, 664–670.
102. Roch, J.-M., Shapiro, I. P., Sundsmo, M. P., Otero, D. A. C., Refolo, L. M., Robakis, N. K., Saitoh, T. (1992) Bacterial expression, purification and functional mapping of the amyloid  $\beta$ /A4 protein precursor. *J. biol. Chem.* 267, 2214–2221.
103. Rossner, S., Ueberham, U., Yu, J., Kirazov, L., Schliebs, R., Perez-Polo, J. R., Bigl, V. (1997) In vivo regulation of amyloid precursor protein secretion in rat neocortex by cholinergic activity. *Eur. J. Neurosci.* 9, 2125–2134.



104. Saitoh, T., Sundsmo, M., Roch, J.-M., Kimura, N., Cole, G., Schubert, D., Oltersdorf, T., Schenk, D. B. (1989) Sected form of amyloid  $\beta$  protein precursor is involved in the growth regulation of fibroblasts. *Cell* 58, 615–622.
105. Savage, M. J., Trusko, S. P., Howland, D. S., Pinsker, L. R., Mistretta, S., Reaume, A. G., Grenberg, B. D., Siman, R., Scott, R. W. (1998) Turnover of amyloid beta-protein in mouse brain and acute reduction of its level by phorbol ester. *J. Neurosci.* 18, 1743–1752.
106. Schubert, D., Behl, C. (1993) The expression of amyloid beta protein precursor protects nerve cells from  $\beta$ -amyloid and glutamate toxicity and alters their interaction with the extracellular matrix. *Brain Res.* 629, 275–282.
107. Schubert, D., Cole, G., Saitoh, T., Oltersdorf, T. (1989) Amyloid beta protein precursor is a mitogen. *Biochem. Biophys. Res. Commun.* 162, 83–88.
108. Schubert, D., Jin, L.-W., Saitoh, T., Cole, G. (1989) The regulation of amyloid  $\beta$  protein precursor secretion and its modulatory role in cell adhesion. *Neuron* 3, 689–694.
109. Schubert, W., Prior, R., Weidemann, A., Dirksen, H., Multhaup, G., Masters, C. L., Beyreuther, K. (1991) Localization of Alzheimer  $\beta$ A4 amyloid precursor protein at cell and peripheral synaptic sites. *Brain Res.* 563, 184–194.
110. Selkoe, D. J. (1993) Physiological production of the  $\beta$ -amyloid protein and the mechanism of Alzheimer's disease. *Trends Neurosci.* 16, 403–409.
111. Seubert, P., Oltersdorf, T., Lee, M. G., Barbour, R., Blomquist, C., Davis, D. L., Bryant, K., Fritz, L. C., Galasko, D., Thal, L. J., Lieberburg, I., Schenk, D. B. (1993) Secretion of  $\beta$ -amyloid precursor protein cleaved at the amino terminus of the  $\beta$ -amyloid peptide. *Nature* 361, 260–263.
112. Shi, J., Xiang, Y., Simpkins, J. W. (1997) Hypoglycemia enhances the expression of mRNA encoding beta-amyloid precursor protein in rat primary cortical astroglial cells. *Brain Res.* 772, 247–251.
113. Shoham, S., Ebstein, R. P. (1997) The distribution of beta-amyloid precursor protein in rat cortex after systemic kainate-induced seizures. *Exp. Neurol.* 147, 361–376.
114. Shoji, M., Golde, T. E., Ghiso, J., Cheung, T. T., Estus, S., Shaffer, L. M., Cai, S.-D., McKay, D. M., Tintner, R., Frangione, B., Younkin, S. G. (1992) Production of the Alzheimer amyloid  $\beta$  protein by normal proteolytic processing. *Science* 258, 126–129.
115. Slack, B. E., Breu, J., Muchnicki, L., Wurtman, R. J. (1997) Rapid stimulation of amyloid precursor protein release by epidermal growth factor: role of protein kinase C. *Biochem. J.* 327, 245–249.
116. Smith, R. P., Higuchi, D. A., Broze, G. J. (1990) Platelet coagulation factor XIa-inhibitor, a form of Alzheimer amyloid precursor protein. *Science* 248, 1126–1128.
117. Song, W., Lahiri, D. K. (1997) Melatonin alters the metabolism of the beta-amyloid precursor protein in the neuroendocrine cell line PC12. *J. Mol. Neurosci.* 9, 75–92.
118. Struble, R. G., Dhanraj, D. N., Mei, Y., Wilson, M., Wang, R., Ramkumar, V. (1998) Beta-amyloid precursor protein-like immunoreactivity is upregulated during olfactory nerve regeneration in adult rats. *Brain Res.* 780, 129–137.
119. Sturchler-Pierrat, C., Abramowski, D., Duke, M., Wiederhold, K. H., Mistl, C., Rothacher, S., Ledermann, B., Burki, K., Frey, P., Paganetti, P. A., Waridel, C., Calhoun, M. E., Jucker, M., Probst, A., Staufenbiel, M., Sommer, B. (1997) Two amyloid precursor protein transgenic mouse models with Alzheimer disease-like pathology. *Proc. Natl. Acad. Sci. USA* 94, 13287–13292.
120. Tezapsidis, N., Li, H. C., Ripellino, J. A., Efthimiopoulos, S., Vassilacopoulou, D., Sambamurti, K., Toneff, T., Yasothornsrikul, S., Hook, V. Y., Robakis, N. K. (1998) Release of nontransmembrane full-length Alzheimer's amyloid precursor protein from the lumenar surface of chromaffin granule membranes. *Biochemistry* 37, 1274–1282.
121. Tominaga, K., Uetsuki, T., Ogura, A., Yoshikawa, K. (1997) Glutamate responsiveness enhanced by neurones expressing amyloid precursor protein. *Neuroreport* 8, 2067–2072.
122. Tomita, S., Kirino, Y., Suzuki, T. (1998) Cleavage of Alzheimer's amyloid precursor protein (APP) by secretases occurs after O-glycosylation of APP in the protein secretory pathway. Identification of intracellular compartments in which APP cleavage occurs without using toxic agents that interfere with protein metabolism. *J. Biol. Chem.* 273, 6277–6284.

123. Van Nostrand, W. E., Wagner, S. L., Suzuki, M., Choi, B. H., Farrow, J. S., Geddes, J. W., Cotman, C. W. (1989) Protease nexin II, a potent antichymotrypsin, shows identity to amyloid beta-protein precursor. *Nature* 341, 546–549.
124. Wallace, W. C., Akar, C. A., Lyons, W. E. (1997) Amyloid precursor protein potentiates the neurotrophic activity of NGF. *Mol. Brain Res.* 52, 201–212.
125. Wallace, W. C., Akar, C. A., Lyons, W. E., Kole, H. K., Egan, J. M., Wolozin, B. (1997) Amyloid precursor protein requires the insulin signaling pathway for neurotrophic activity. *Mol. Brain Res.* 52, 213–227.
126. Waragai, M., Imafuku, I., Takeuchi, S., Kanazawa, I., Oyama, F., Udagawa, Y., Kawabata, M., Ozazawa, H. (1997) Presenilin 1 binds to amyloid precursor protein directly. *Biochem. Biophys. Res. Commun.* 239, 480–482.
127. Weidemann, A., König, G., Bunke, D., Fischer, P., Masters, C. L., Beyreuther, K. (1989) Identification, biogenesis and localization of precursors of Alzheimer's disease A4 amyloid protein. *Cell* 57, 115–126.
128. Yamazaki, T., Koo, E. H., Selkoe, D. J. (1997) Cell surface amyloid  $\beta$ -protein precursor colocalizes with  $\beta$ 1 integrins at substrate contact sites in neural cells. *J. Neurosci.* 17, 1004–1010.
129. Yamazaki, T., Selkoe, D. J., Koo, E. H. (1995) Trafficking of cell-surface  $\beta$ -amyloid precursor protein: retrograde and transcytotic transport in cultured neurons. *J. Cell Biol.* 129, 431–442.
130. Zhang, F., Eckman, C., Younkin, S., Hsiao, K. K., Iadecola, C. (1997a) Increased susceptibility to ischemic brain damage in transgenic mice overexpressing the amyloid precursor protein. *J. Neurosci.* 17, 7655–7661.
131. Zhang, W., Espinoza, D., Hines, V., Innis, M., Mehta, P., Miller, D. L. (1997b) Characterization of beta-amyloid peptide precursor processing by the yeast Yap3 and Mkc7 proteases. *Biochim. Biophys. Acta* 1359, 110–122.





# THE OLFACTORY BULB IN ALZHEIMER'S DISEASE\*

I. KOVÁCS<sup>1</sup>, I. TÖRÖK<sup>2</sup>, J. ZOMBORI<sup>2</sup> and H. YAMAGUCHI<sup>3</sup>

<sup>1</sup>Alzheimer's Disease Research Centre, Albert Szent-Györgyi Medical University, Szeged,

<sup>2</sup>Erzsébet Hospital, Hódmezővásárhely, Hungary,

<sup>3</sup>Gunma University School of Health Sciences, Gunma, Japan

(Received: 1998-06-12; accepted: 1998-06-26)

This report describes the laminar distribution of acetylcholinesterase-positive structures in the human olfactory bulb of control and Alzheimer's disease brain samples. Light microscopic histochemistry revealed the enzyme-positive neurons and nerve fibres. No acetylcholinesterase staining was present in the olfactory nerve layer, the glomerular layer or the external granule cell layer. A few enzyme-positive (cholinergic) nerve fibres were detected in the external plexiform layer and the white matter. A large number of cholinergic axons were present in the internal plexiform layer and the internal granule cell layer. Acetylcholinesterase-positive nerve fibres and cells were present in the mitral/tufted cell layer and the anterior olfactory nucleus. In Alzheimer's disease brain samples, a weak and patchy acetylcholinesterase staining appeared in the internal plexiform layer and the internal granule cell layer. In the anterior olfactory nucleus, enzyme-positive neurofibrillary tangles and senile plaques were found. The neuropathological changes were studied with silver impregnation techniques and immunohistochemistry revealed a diffuse amyloid staining in the olfactory nerve layer and in the external plexiform layer, and large numbers of senile plaques in the glomerular layer and the anterior olfactory nucleus. The presence of amyloid positivity in the olfactory nerve layer and in a number of glomeruli suggests that no correlation exists between the cholinergic structures and the neuropathologic alterations in the human olfactory bulb in Alzheimer's disease.

**Keywords:** Alzheimer's disease – olfactory bulb – acetylcholinesterase – cholinergic structures – amyloid

## INTRODUCTION

### *Neuropathological changes in Alzheimer's disease*

The characteristic neuropathological alterations in Alzheimer's disease (AD) brain samples are the neurofibrillary tangles (NFTs), the senile plaques (SPs) and the extensive reduction in the number of cholinergic neurons. The main component of the NFTs is the

\*Dedicated to Professor Péter Kása on the occasion of the 25th anniversary of his appointment as Head of the Central Research Laboratory and the Alzheimer's Disease Research Centre.

Send offprint requests to: Imre Kovács M.D., Alzheimer's Disease Research Centre, Albert Szent-Györgyi Medical University, H-6720 Szeged, Somogyi u. 4, Hungary. E-mail: kimre@comser.szote.u-szeged.hu.



hyperphosphorylated tau protein, while in the SPs among others it is the amyloid beta protein (A $\beta$ ).

### *Alzheimer's disease and cholinergic system*

The pathomechanism of AD is still not known. There are several hypotheses as concerns the aetiologic factors (Table 1), but none of them is sufficient. The diagnosis of AD is generally established clinically, with a variable degree of uncertainty, by excluding other causes of dementia. The diagnosis is generally confirmed by the pathological findings at autopsy, including atrophy of the brain, the presence of NFTs, (neuritic) SPs [1], the presence of A $\beta$  deposits and the loss of cholinergic elements [12]. Damage to the cholinergic system in AD is a complex process [31]: the acetylcholine (ACh) level [57] and synthesis [62] and the high-affinity choline uptake [59] are decreased. Nevertheless, the number of cholinergic receptors (AChRs) such as the muscarinic and nicotinic AChRs, decrease or may decrease [23, 38], while the activities of cholinergic enzymes either synthesizing ACh, e.g. choline acetyltransferase [12] (ChAT) or hydrolysing ACh, e.g. acetylcholinesterase (AChE) are significantly reduced in the different parts of AD brain [53]. The severe damage to the cholinergic system in AD led to the development of the principle known as "cholinergic hypothesis" [6, 9, 12]. Since this hypothesis proved insufficient [25, 45] to answer certain key problems, other hypotheses have evolved (Table 1). Although the cholinergic system is not the aetiologic factor responsible for the development of AD, the role of the cholinergic system in the development of AD is indisputable.

*Table 1*  
Some of the possible aetiologic or risk factors which may cause AD

Aetiologic/risk factor	References
Chronic exposure to aluminium	[10]
Cytoskeletal protein pathology	[71]
Signal transduction abnormalities	[63]
The "cholinergic hypothesis"	[12]
Overactivation of the calcium and/or inositol pathways	[42]
Glutamate toxicity	[22]
Constitutive cleavage of amyloid precursor protein	[15]
Inflammatory and immune processes	[44]
Mitochondrial DNA mutation	[51]
Amyloid cascade hypothesis	[24]
Apolipoprotein E4 genotype	[64]
Infection of spirochetes	[47]
Acetylcholinesterase hypothesis	[60]
Mutation of presenilin 1 gene	[11]

*The olfactory bulb in Alzheimer's disease*

It is well known that in AD the olfactory function decreases much more than during normal aging [14, 56]. Nevertheless, the brain regions connected with the olfactory system, such as the hippocampal formation [4], the entorhinal area [5], the amygdaloid nuclei [27, 29], the anterior olfactory nuclei [2, 16, 61, 74], the prepiriform cortex [55] and the basal forebrain [70], are the most affected sites in AD. The early and severe damage to the olfactory system and olfactory bulb (OB) (Table 2) in AD, together with findings in animals of the active transport mechanisms of viruses along the olfactory pathways [3] and the absent blood-brain barrier between the nose and the brain [69], suggested that the olfactory pathways may be the site of initial involvement in the disease [39, 40, 52]. Roberts has proposed that AD may begin in the olfactory system, with toxins entering sensory neurons of the nose and spreading transneuronally to the olfactory-related areas of the brain [58].

*Objectives*

Despite the fact that AD is one of the most studied topics in modern neurobiology, results from previous studies on neuropathological alterations in OB in AD seemed contradictory. The main objective of our work was therefore to study the cholinergic system as concerns the neuropathological alterations in the human OB, as in order to clarify whether the extensive damage to the cholinergic system is connected or not with the classical neuropathological changes of AD. To detect the cholinergic elements and AD-related neuropathology, we applied histochemical, enzyme histochemical methods and highly specific immunohistochemical methods. The application of immunohistochemistry may be special interest, because this method has not been used extensively to date in studies of the human OB in AD.

Table 2  
Neuropathological changes in the OB in AD

Neuropathological changes	References
Cell loss, SPs, NFTs in the AON, the OB and the olfactory tract (OT)	[2]
Cell loss, NFTs in the AON	[16]
SPs in the AON, NFTs and NTs in the AON and all layers except the ONL	[50]
SPs and NFTs in the OB, but it is less affected than the amygdala or hippocampus	[40]
Mitral cell degeneration without NFTs, periglomerular A $\beta$ -like immunoreactivity	[65]
Cell loss, SPs, NFTs in the AON	[67]
All the alterations listed above and diffuse amyloid in the ONL, GL, EPL	[36]



## MATERIALS AND METHODS

### *Samples*

Seventeen OBs were taken from AD patients (mean age: 75.4 yr.  $\pm$  3.6 SEM, range: 48–98 yr.) at autopsy, selected in accordance with clinical and neuropathological criteria [28, 32]. The 17 control OBs were also taken at autopsy from sex-matched cases of similar age (mean age: 76.1 yr.  $\pm$  4.1 SEM, range: 20–90 yr.) in whom there had been no history of neurological or psychiatric disorders. The post-mortem delay ranged from 3 to 24 h.

### *Methods*

#### Tissue processing

OBs obtained from autopsy were fixed by immersion in 4% paraformaldehyde (Merck) in a 0.01 M phosphate buffer (pH 7.4) containing 0.9% NaCl. For cryoprotection, all OBs were immersed in a 30% sucrose solution overnight at 4 °C. After this, 24- $\mu$ m thick frontal or horizontal consecutive sections were cut on a freezing microtome (Reichert-Jung).

#### Cresyl violet staining

Free-floating sections were immersed for 2 min in a solution containing 200 ml of 0.2 M acetic acid (Reanal), 133 ml of 0.2 mM sodium acetate (Merck) and 67 ml of 0.1% cresyl violet acetate (Sigma). The sections then were mounted, and dehydrated in an ethyl alcohol series and cleared in Histo-clear II (National Diagnostics). The tissue was subsequently coverslipped, using Histomount mountant medium (National Diagnostics).

#### Acetylcholinesterase histochemistry

For light microscopy, a specific and sensitive method [66] was used.

#### Silver impregnation techniques

For the demonstration of A $\beta$ -containing diffuse SPs, a methenamine-silver stain [73] was applied. To detect the neuropathological alterations in the various layers in the human control (non-AD) and AD OB samples, the Gallyas silver impregnation method [18] was used for the demonstration of primary SPs and mainly NFTs, a physical developer solution being applied [19].

## Immunohistochemistry

Free-floating sections were immunostained with antibodies to a synthetic peptide consisting of residues 1–28 of A $\beta$  [72], or  $\tau$ -2 (Sigma). Briefly, the tissue was pretreated with formic acid (99%) (Merck) for 5 min at room temperature to enhance the immunostaining of tau protein and A $\beta$  [34] and rinsed in 5% normal sheep serum (Sigma) and 5% normal bovine serum (Gibco) in PBS. The sections were incubated for 48 h at room temperature in A $\beta$  (1:16000) rabbit or  $\tau$ -2 (1:8000) mouse antiserum. Sections were rinsed 3 times for 10 min each in PBS, followed by 5% normal sheep serum in PBS for 30 min. The tissue was then incubated for 90 min in biotin-SP-conjugated goat anti-rabbit or sheep anti-mouse immunoglobulin (Jackson) diluted 1:1000, and subsequently for 90 min in horse-radish peroxidase-conjugated streptavidin (Jackson) diluted 1:1000. All antibodies were diluted with PBS containing 5% normal sheep serum (Sigma). Each of the above steps was followed by rinsing in PBS. The antibody was visualized by a 5-min incubation with 3'3'-diaminobenzidine (Sigma) (50 mg/100 ml) as chromogen, nickel chloride (Reanal) (150 mg/100 ml) and 0.003% H<sub>2</sub>O<sub>2</sub>. If it was needed to amplify the end-product of immunohistochemistry, a modified [20] silver-gold intensification procedure was performed [13].

## RESULTS

### *Acetylcholinesterase alterations in the human olfactory bulb in Alzheimer's disease*

To understand the location of the neuropathological changes in the OB in AD, it is useful to view the structural localization of the layers (Fig. 1A) and the AChE patterns in these layers in the normal OB (Fig. 1B).

In the OB of AD brain samples, AChE has disappeared from the different layers, or remains diffusely restricted to small areas, without any well-defined neuronal structures (Fig. 1C). Staining was found in the diffuse SPs present in the internal plexiform layer (IPL), internal granule cell layer (IGCL) and in the white matter (WM) (Fig. 1C, D). The most severe damage was detected in the anterior olfactory nucleus (AON), from where most of the AChE-positive fibres had disappeared. In numerous NFTs and SPs, enzyme staining could be revealed (Fig. 1F; Table 3).

### *Neuropathological alterations in the human olfactory bulb in Alzheimer's disease*

With the silver impregnation technique, SPs could not be found in the control OBs (Fig. 2A). In the AD brain samples, amyloid staining was present in the olfactory nerve layer (ONL) (Fig. 2B) and in diffuse SPs present in a large number of glomeruli (Fig. 2B–F) and external plexiform layer (EPL) (Fig. 2F). In other layers, we found very few if any diffuse SPs. However, primary and diffuse SPs were numerous in the AON (Fig. 2G, I).



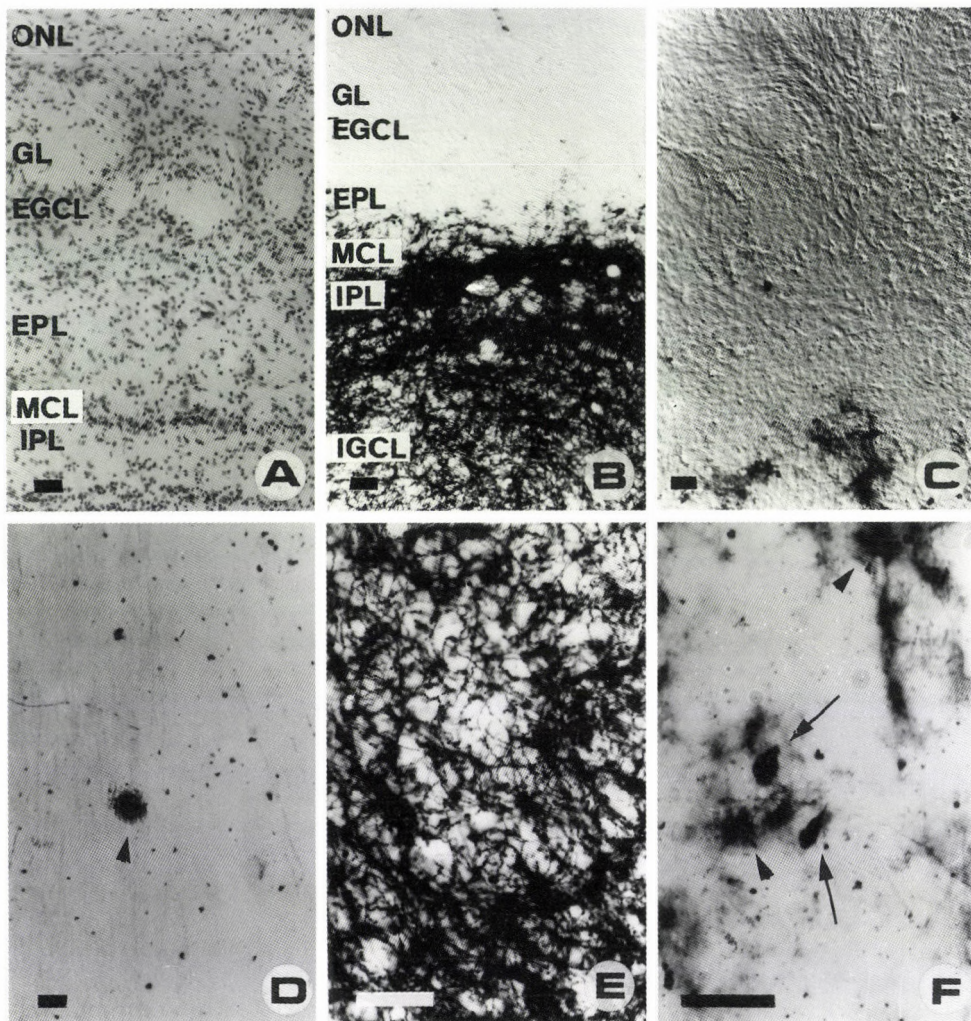


*Fig. 1.* Horizontal section of the control human (A) OB stained with cresyl violet, revealing the various layers: olfactory nerve layer (ONL), glomerular layer (GL), external granule cell layer (EGCL), external plexiform layer (EPL), mitral/tufted cell layer (MCL) and internal plexiform layer (IPL). Laminar distribution of AChE in the human OB (B). There were no AChE-positive axons in the ONL, the GL, the EGCL or the outer part of the EPL. In contrast, AChE-positive structures were present in the inner part of the EPL, the MCL, the IPL and the internal granule cell layer (IGCL). (For better visualization of the enzyme staining, Nomarski optics were applied.) In the OB of AD victims, most of the enzyme positivity has disappeared from the various layers and only some AChE staining in a patchy form can be seen in the IGCL (C). Various SPs showing AChE-positivity were found in the IPL, the IGCL and the white matter (WM) (arrowhead) (D). The most dramatic loss of cholinergic fibres was revealed in the AON of AD brain compared to the control samples (E). AChE-positive NFTs (arrows) and SPs (arrowheads) are present instead of stained cholinergic fibres (F). Scale bar = 100  $\mu$ m

*Table 3*  
Summary of pathological changes  
in the histochemical localization of AChE  
in the human OB

OB layers	Human OB AChE	
	Control	Pathology
ONL	–	–
GL	–	–
EGCL	–	–
EPL	+	–
MCL	+	–
IPL	++	Diffuse plaque
IGCL	+++	Diffuse plaque
WM	++	Diffuse plaque
OAN	++	NFTs + diffuse plaque

ONL: olfactory nerve layer, GL: glomerular layer, EGCL: external granular cell layer, EPL: external plexiform layer, MCL: mitral cell layer, IPL: internal plexiform layer, IGCL: internal granular cell layer, WM: white matter, OAN: anterior olfactory nucleus, NFT: neurofibrillary tangle  
+ : found, – : not found

Both in the control and in the AD samples, NFTs were scarcely to be found in the mitral cell layer (MCL). In contrast, a great number could be demonstrated within the AON in the AD samples (Fig. 2H, I). The neuropathologic alterations in the different layers are outlined in Table 4.

## DISCUSSION

### *Neuropathology of the human olfactory bulb in Alzheimer's disease*

#### Neuropathology of the cholinergic system

Investigation of the neuropathologic alterations in the cholinergic structures in the human OB revealed that in an advanced stage of AD the AChE positivity is weaker in the different layers, and is restricted to certain areas or disappears totally from the various layers. When and where the enzyme activity was present, the borders of AChE-stained areas were blurred or indistinct. The integrity of the cholinergic neuronal structures demonstrated that the density of AChE-positive axons was reduced, and the axons were beaded and dystrophic. Similarly as for the AON in the WM, AChE-positive diffuse SPs were detected. An estimate of the number of NFTs in the AON on the basis of the AChE histo-



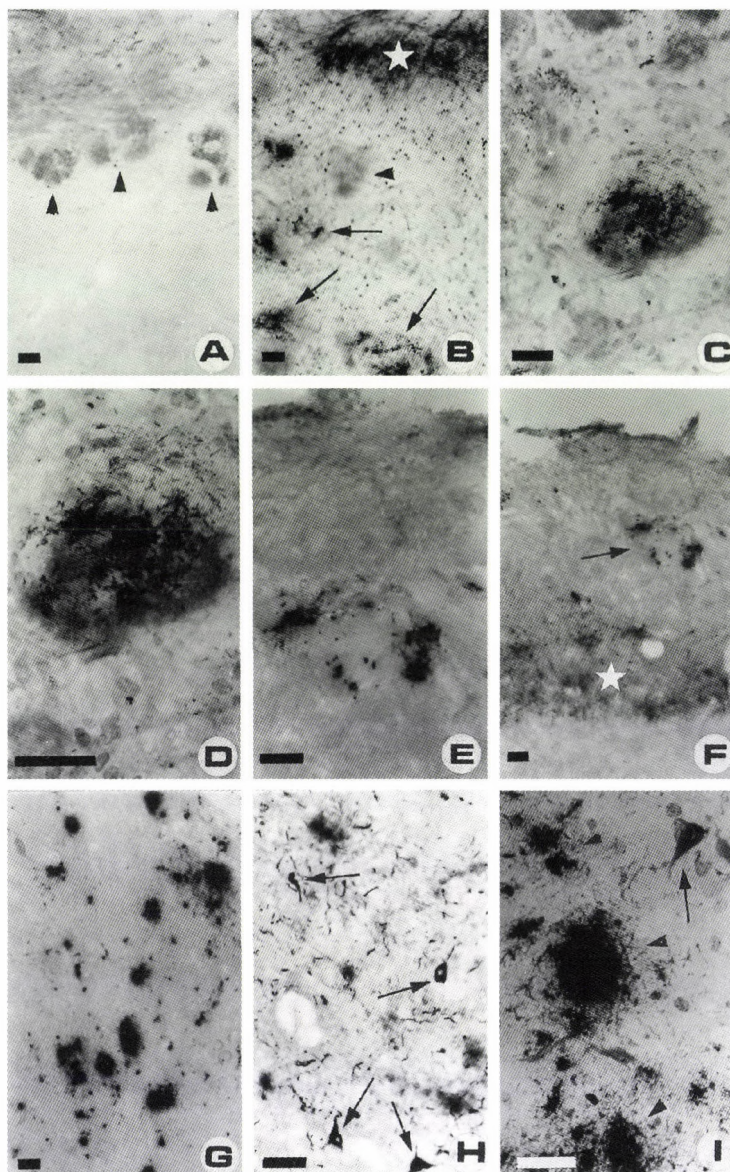


Fig. 2. Neuropathological changes of the human OBs in AD. In the control OB, A $\beta$ -positive structures cannot be observed either in the GL or in the other layers (A). In the AD samples, A $\beta$  staining is shown to be present in the ONL (white star) (B) and within a large number of glomeruli by either the silver impregnation technique (B–D) or immunostaining (E, F) (arrows), while it is absent from some others (arrowhead). At higher magnification, a characteristic diffuse A $\beta$  staining can be better seen within the glomeruli (D, E). Diffuse A $\beta$  staining was also found in the EPL when the immuno method was applied (white star) (F). In the advanced stage of AD, a number of SPs (arrowheads) (G, I) or NFTs (arrows) (H, I) or both (I) are present in the AON. Scale bar = 100  $\mu$ m

Table 4  
Summary of neuropathological changes  
in the various layers of the control human  
(non-AD) and AD OBs

OB layers	Human control		Human AD	
	SPs	NFTs	SPs	NFTs
ONL	–	–	*	–
GL	–	–	+	–
EGCL	–	–	+	–
EPL	–	–	++	–
MCL	–	–	–	Rare
IPL	–	–	–	–
IGCL	–	–	–	–
WM	–	–	+	–
AON	+	–	+++	+++

ONL: olfactory nerve layer, GL: glomerular layer, EGCL: external granular cell layer, EPL: external plexiform layer, MCL: mitral cell layer, IPL: internal plexiform layer, IGCL: internal granular cell layer, WM: white matter, AON: anterior olfactory nucleus, SP: senile plaque, NFT: neurofibrillary tangle  
+: relative occurrence of neuropathologic alterations, –: neuropathologic alterations not found \*: diffuse amyloid staining found

chemical technique indicated fewer positive neurons than with the silver impregnation staining. In the different layers, no NFTs were revealed, but in extremely rare cases NFTs were discovered in the MCL. In the OBs of non-AD patients, NFTs could not be detected with either AChE histochemistry or silver impregnation techniques.

Neurofibrillary tangles and amyloid beta protein deposits in human olfactory bulb

Our previous findings [31, 35–37, 75] were similar to those reported by other authors [2, 16, 17, 50, 65, 67] in that the most numerous primary and diffuse SPs were present in the AON, but they differed in that we could demonstrate Aβ deposits in the ONL, the EPL and the GL [31, 35–37, 75]. Further, the number of NFTs was highest in the AON, where there is a strong AChE activity in non-AD brain samples, which is severely reduced in AD. Additionally, we detected diffuse Aβ staining in the ONL, GL and EPL, inside a large number of glomeruli where no cholinergic axons are present [31, 35–37, 75]. In this respect, our findings support the suggestion [41, 48] that the presence of Aβ is not a conse-



quence of cholinergic hypoactivity. The diffuse A $\beta$  staining correlates rather with the localization of amyloid precursor-like protein [68] (APPLP2) which is present in the ONL.

### Cholinergic system and amyloid beta protein localization in human olfactory bulb

As concerns the close relationship between the A $\beta$  deposits and AChE-positive fibres in the same cortical laminae of the AD brain samples, some authors [7, 8, 49] have suggested that A $\beta$  deposits could degenerate cholinergic neurons and/or their axons. In contrast, others [41, 48] have demonstrated that the distribution of the cholinergic fibres and the deposition of amyloid SPs are independent.

## CONCLUSIONS

These results suggest that the deposition of amyloid SPs in some brain areas may not cause the degeneration of cholinergic neuronal elements. As regards the laminar distribution of cholinergic structures and neuropathologic alterations in AD OBs, our results strongly suggest that it is not only the cholinergic hypoactivity which is responsible for the production of A $\beta$ ; some other factors, e.g. free radicals [26, 30] or changes in calcium homeostasis [21, 33, 42, 54], may play a role. This suggestion is supported by the fact that, in the olfactory glomeruli, where a large number of A $\beta$  deposits could be demonstrated, no cholinergic axons are present. Our histochemical and neuropathological findings lend further support to the suggestion [35–37, 41, 48, 75] that there is not a close correlation between the A $\beta$  deposition and the cholinergic hypoactivity in some areas of AD brain samples.

## ACKNOWLEDGEMENTS

This work was supported by grants from the ETT (584/1996), OTKA (T022683).

## REFERENCES

1. Alzheimer, A. (1911) Über eigenartige Krankheitsfalle des späteren Alters. *Z. Gesamte. Neurol. Psychiatr.* 4, 356–385.
2. Averbach, P. (1983) Two new lesions in Alzheimer's disease. *Lancet* 2, 1203.
3. Balin, B. J., Broadwell, R. D., Salzman, M., El-Kalliny, M. (1986) Avenues for entry of peripherally administered protein to the central nervous system in mouse, rat, and squirrel monkey. *J. Comp. Neurol.* 251, 260–280.
4. Ball, M. J. (1977) Neuronal loss, neurofibrillary tangles and granulovacuolar degeneration in the hippocampus with aging and dementia: a quantitative study. *Acta Neuropathol.* 37, 111–118.
5. Ball, M. J. (1978) Topographic distribution of neurofibrillary tangles and granulovacuolar degeneration in hippocampal cortex of aging and demented patients. A quantitative study. *Acta Neuropathol.* 42, 73–80.

6. Bartus, R. T., Dean, R. L., Pontecorvo, M. J., Flicker, C. (1985) The cholinergic hypothesis: a historical overview, current perspective, and future directions. *Ann. Acad. Sci.* 444, 332–358.
7. Beach, T. G., McGeer, E. G. (1992) Senile plaques, amyloid beta-protein, and acetylcholinesterase fibres: laminar distributions in Alzheimer's disease striate cortex. *Acta Neuropathol.* 83, 292–299.
8. Beach, T. G., Honer, W. G., Hughes, L. H. (1997) Cholinergic fibre loss associated with diffuse plaques in the non-demented elderly: the preclinical stage of Alzheimer's disease? *Acta Neuropathol.* 93, 146–153.
9. Collerton, D. (1986) Cholinergic function and intellectual decline in Alzheimer's disease. *Neuroscience* 19, 1–28.
10. Crapper, D. R., Krishnan, S. S., Dalton, A. J. (1973) Brain aluminum distribution in Alzheimer's disease and experimental neurofibrillary degeneration. *Science* 180, 511–513.
11. Cruts, M., Backhovens, H., Wang, S. Y., Gassen, G. V., Theuns, J., De Jonghe, C. D., Wehnert, A., De Voecht, J., De Winter, G., Cras P. (1995) Molecular genetic analysis of familial early-onset Alzheimer's disease linked to chromosome 14q24.3. *Hum. Mol. Genet.* 12, 2363–2371.
12. Davies, P., Maloney, A. J. (1976) Selective loss of central cholinergic neurons in Alzheimer's disease. *Lancet* 2, 1403–1405.
13. Dobó, E., Dudás, B., Kalló, I., Liposits, Z. (1996) Novel immunohistochemical procedures for simultaneous detection of neuropeptides in human brain. *Neurobiology* 4, 139.
14. Duncan, H. J., Smith, D. V. (1995) Clinical disorders of olfaction. A review. In: Doty, R. L. (ed.) *Handbook of Olfaction and Gustation*. Marcel Dekker Inc., New York.
15. Esch, F. S., Keim, P. S., Beattie, E. C., Blacher, R. W., Culwell, A. R., Oltersdorf, T., McClure, D., Ward P. J. (1990) Cleavage of amyloid beta peptide during constitutive processing of its precursor. *Science* 248, 1122–1124.
16. Esiri, M. M., Wilcock, G. H. (1984) The olfactory bulbs in Alzheimer's disease. *J. Neurol. Neurosurg. Psychiatry* 47, 56–60.
17. Ferreyra-Moyano, H., Barragan, E. (1989) The olfactory system and Alzheimer's disease. *Int. J. Neurosci.* 49, 157–197.
18. Gallyas, F. (1971a) Silver staining of Alzheimer's neurofibrillary changes by means of physical development. *Acta Morphol. Acad. Sci. Hung.* 19, 1–8.
19. Gallyas, F. (1971b) A principle for silver staining of tissue elements by physical development. *Acta Morphol. Acad. Sci. Hung.* 19, 57–71.
20. Gallyas, F., Stankovics, J. (1987) Oxidation catalyzed by H<sup>+</sup> ions improves the silver intensification of 3,3'-diaminobenzidine staining by strongly suppressing tissue argyrophilia. *Histochemistry* 87, 615–618.
21. Gibson, G. E., Peterson, C. (1987) Calcium and the aging nervous system. *Neurobiol. Aging* 8, 329–343.
22. Greenamyre, J. T., Maragos, W. F., Albin, R. L., Penney, J. B., Young, A. B. (1988) Glutamate transmission and toxicity in Alzheimer's disease. *Prog. Neuropsychopharmacol. Biol. Psychiatry* 12, 421–430.
23. Gulya, K., Watson, M., Vickroy, T. W., Roeske, W. R., Perry, R., Perry, E., Duckles, S. P., Yamamura H. I. (1986) Examination of cholinergic and neuropeptide receptor alterations in senile dementia of the Alzheimer's type (SDAT). In: Fisher, A., Hanin, I., Lachman, C. (eds) *Alzheimer's and Parkinson's diseases. Advances in behavioral biology*. Plenum Press, New York.
24. Hardy, J. A., Higgins, G. A. (1992) Alzheimer's disease – The amyloid cascade hypothesis. *Science* 256, 184–185.
25. Hardy, J., Adolfsson, R., Alafuzoff, I., Bucht, G., Marcusson, J., Nyberg, P., Per Dahl, E., Wester, P., Winblad, B. (1985) Transmitter deficits in Alzheimer's disease. *Neurochem. Int.* 7, 545–563.
26. Hartman, D. (1993) Free radical theory of aging: A hypothesis on pathogenesis of senile dementia of the Alzheimer's type. *Age* 16, 23–30.
27. Herzog, A. G., Kemper, T. L. (1980) Amygdaloid changes in aging and dementia. *Arch. Neurol.* 37, 625–629.
28. Hyman, B. T., Trojanowski, J. Q. (1997) Consensus recommendations for the postmortem diagnosis of Alzheimer disease from the National Institute on Aging and the Reagan Institute Working Group



- on diagnostic criteria for the neuropathological assessment of Alzheimer disease. *J. Neuropathol. Exp. Neurol.* 56, 1095–1097.
29. Hyman, B. T., Van Hoesen, G. W., Damasio, A. R., Barnes, C. L. (1984) Alzheimer's disease: cell specific pathology isolates the hippocampal formation. *Science* 225, 1168–1170.
  30. Jesberger, J. A., Richardson, J. S. (1991) Oxygen free radicals and brain dysfunction. *Int. J. Neurosci.* 57, 1–17.
  31. Kása, P., Rakonczay, Z., Gulya, K. (1997) The cholinergic system in Alzheimer's disease. *Progr. Neurobiol.* 52, 511–532.
  32. Khachaturian, Z. S. (1985) Diagnosis of Alzheimer's disease. *Arch. Neurol.* 42, 1097–1105.
  33. Khachaturian, Z. S. (1989) The role of calcium regulation in brain aging: Re-examination of a hypothesis. *Aging J.* 17–34.
  34. Kitamoto, T., Ogomori, K., Tateishi, J., Prusiner, S. B. (1987) Formic acid pretreatment enhances immunostaining of cerebral and systemic amyloidosis. *Lab. Invest.* 57, 230–236.
  35. Kovács, I., Török, I., Zombori, J., Kása, P. (1996) Cholinergic structures and neuropathological changes in human olfactory bulb. *Clin. Neurosci.* 49, 23–24.
  36. Kovács, I., Török, I., Zombori, J., Kása, P. (1996) Neuropathologic changes in the olfactory bulb in Alzheimer's disease. *Neurobiology* 4, 123–126.
  37. Kovács, I., Török, I., Zombori, J., Kása, P. (1998) Cholinergic structures and neuropathological changes of the human olfactory bulb in Alzheimer's disease. *Brain Res.* (in press).
  38. Lang, W., Henke, H. (1983) Cholinergic receptor binding and autoradiography in brains of non-neurological and senile dementia of Alzheimer-type patients. *Brain Res.* 267, 271–280.
  39. Mann, D. M. A., Path, M. R. C., Esiri, M. M. (1988) The site of the earliest lesions of Alzheimer's disease. *New Engl. J. Med.* 318, 789–790.
  40. Mann, D. M. A., Tucker, C. M., Yates, P. O. (1988) Alzheimer's disease: an olfactory connection? *Mech. Ageing Dev.* 42, 1–15.
  41. Masliah, E., Terry, R., Buzsáki, G. (1989) Thalamic nuclei in Alzheimer's disease: evidence against the cholinergic hypothesis of plaque formation. *Brain. Res.* 493, 240–246.
  42. Mattson, M. P., Barger, S. W., Cheng, B., Lieberburg, I., Smith–Swintosky, V. L., Rydel, R. E. (1993)  $\beta$ -Amyloid precursor protein metabolites and loss of neuronal  $\text{Ca}^{2+}$  homeostasis in Alzheimer's disease. *Trends Neurosci.* 16, 409–414.
  43. Mattson, M. P., Guthrie, P. B., Kater, S. B. (1988) Intracellular messengers in the generation and degeneration of hippocampal neuroarchitecture. *J. Neurosci. Res.* 21, 447–464.
  44. McGeer, P. L., McGeer, E. G., Kawamata, T., Yamada, T., Akiyama, H. (1991) Reactions of the immune system in chronic degenerative neurological diseases. *Can. J. Neurol. Sci.* 18, Suppl. 3, 376–379.
  45. Mesulam, M. M. (1986) Alzheimer plaques and cortical cholinergic innervation. *Neuroscience* 17, 275–276.
  46. Mesulam, M.-M., Geula, C. (1992) Overlap between acetylcholinesterase-rich and choline acetyltransferase-positive (cholinergic) axons in human cerebral cortex. *Brain Res.* 577, 112–120.
  47. Miklóssy, J. (1993) Alzheimer's disease – a spirochetosis? *Neuroreport* 7, 841–848.
  48. Nakamura, S., Takenura, M., Suenaga, T., Akiyuchi, I., Kimura, J., Yasuhara, O., Kimura, T., Kitaguchi, N. (1992) Occurrence of acetylcholinesterase activity closely associated with amyloid  $\beta$ /A4 protein is not correlated with acetylcholinesterase-positive fibre density in amygdala of Alzheimer's disease. *Acta Neuropathol.* 84, 425–432.
  49. Nitta, A., Itoh, A., Hasegawa, T., Nabeshima, T. (1994)  $\beta$ -amyloid protein-induced Alzheimer's disease animal model. *Neurosci. Lett.* 170, 63–66.
  50. Ohm, T. G., Braak, H. (1987) Olfactory bulb changes in Alzheimer's disease. *Acta Neuropathol.* 73, 365–369.
  51. Parker, W. D. Jr. (1991) Cytochrome oxidase deficiency in Alzheimer's disease. *Ann. N.Y. Acad. Sci.* 640, 59–64.
  52. Pearson, R. C., Esiri, M. M., Hiorns, R. W., Wilcock, G. W., Powell, T. P. (1985) Anatomical correlates of the distribution of the pathological plaques in the neocortex in Alzheimer disease. *Proc. Nat. Acad. Sci. USA* 82, 4531–4534.

53. Perry, E. K., Gibson, P. H., Blessed, G., Perry, R. H., Tomlinson, B. E. (1977) Neurotransmitter enzyme abnormalities in senile dementia. *J. Neurol. Sci.* 34, 247–265.
54. Petersen, C. (1985) Changes in Calcium's role as a messenger during aging in neuronal and nonneuronal cells. *Ann. NY Acad. Sci.* 663, 279–293.
55. Reyes, P., Golden, G. T., Fagel, P. L., Fariello, R. G., Katz, L., Carner, E. (1987) The prepyriform cortex in dementia of the Alzheimer type. *Arch. Neurol.* 44, 644–645.
56. Rezek, D. L. (1987) Olfactory deficits as a neurologic sign in dementia of the Alzheimer type. *Arch. Neurol.* 44, 1030–1032.
57. Richter, J. A., Perry, E. K., Tomlinson, B. E. (1980) Decreased acetylcholine content in Alzheimer's disease. *Life Sci.* 26, 651–653.
58. Roberts, E. (1986) Alzheimer's disease may begin in the nose and may be caused by aluminosilicates. *Neurobiol. Aging* 7, 561–567.
59. Rylett, R. J., Ball, M. J., Calhoun, E. H. (1983) Evidence for high-affinity choline transport in synaptosomes prepared from hippocampus and neocortex of patients with Alzheimer's disease. *Brain Res.* 289, 169–175.
60. Shen, Z. X. (1994) Acetylcholinesterase provides deeper insights into Alzheimer's disease. *Med. Hypotheses* 43, 21–30.
61. Simpson, J., Yates, C. M. (1984) Olfactory tubercle choline acetyltransferase activity in Alzheimer-type dementia, Down's syndrome and Huntington's disease. *J. Neurol. Neurosurg. Psychiatry* 47, 1138–1140.
62. Sims, N. R., Bowen, D. M., Smith, C. C., Flack, R. H., Davison, A. N., Snowden, J. S., Neary, D. (1980) Glucose metabolism and acetylcholine synthesis in relation to neuronal activity in Alzheimer's disease. *Lancet* 1, 333–336.
63. Sternberger, N. H., Sternberger, L. A., Ulrich, J. (1985) Aberrant neurofilament phosphorylation in Alzheimer disease. *Proc. Natl. Acad. Sci. USA* 82, 4274–4276.
64. Strittmatter, W. J., Weisgraber, K. H., Huang, D. Y., Dong, L.-M., Salvesen, G. S., Pericak-Vance, M., Schmechel, D., Saunders, A. M., Goldgaber, D., Roses, A. D. (1993) Binding of human apolipoprotein E to synthetic amyloid  $\beta$  peptide: isoform-specific effects and implications for late-onset Alzheimer disease. *Proc. Natl. Acad. Sci. USA* 90, 8098–8102.
65. Struble, R. G., Clark, B. H. (1992) Olfactory bulb lesions in Alzheimer's disease. *Neurobiol. Aging* 13, 469–473.
66. Tago, H., Kimura, H., Maeda, T. (1986) Visualization of detailed acetylcholinesterase fibre and neuron staining in rat brain by a sensitive histochemical procedure. *J. Histochem. Cytochem.* 34, 1431–1438.
67. ter Laak, H. J., Renkawek, K., van Workum, F. P. A. (1994) The olfactory bulb in Alzheimer's disease: a morphologic study of neuron loss, tangles and senile plaques in relation to olfaction. *Alzheimer Dis. Assoc. Disord.* 8, 34–48.
68. Thinakaran, G., Kitt, C. A., Roskams, A. J., Slunt, H. H., Masliah, E., Von-Koch, C., Ginsberg, S. D., Ronnett, G. V., Reed, R. R., Price, D. L., Sisodia, S. S. (1995) Distribution of an APP homolog, APPLP2, in the mouse olfactory system: a potential role for APPLP2 in axogenesis. *J. Neurosci.* 15, 6314–6326.
69. Tomlinson, A. H., Esiri, M. M. (1983) Herpes simplex encephalitis: immuno-histological demonstration of spread of virus via olfactory pathways in mice. *J. Neurol. Sci.* 60, 473–484.
70. Whitehouse, P. J., Price, D. L., Struble, R. G., Clark, A. W., Coyle, J. T., DeLong, M. R. (1982) Alzheimer's disease and senile dementia: loss of neurons in the basal forebrain. *Science* 215, 1237–1239.
71. Wisniewski, H. M., Merz, P. A., Iqbal, K. (1984) Ultrastructure of paired helical filaments of Alzheimer's neurofibrillary tangle. *J. Neuropathol. Exp. Neurol.* 43, 643–656.
72. Yamaguchi, H., Hirai, S., Morimatsu, M., Shoji, M., Ihara, Y. (1988) A variety of cerebral amyloid deposits in the brains of the Alzheimer-type dementia demonstrated by  $\beta$  protein immunostaining. *Acta Neuropathol.* 76, 541–549.



73. Yamaguchi, H., Haga, C., Hirai, S., Nakazato, Y., Kosaka, K. (1990) Distinctive, rapid, and easy labeling of diffuse plaques in the Alzheimer brain by new methenamine silver stain. *Acta Neuropathol.* 79, 569–572.
74. Yates, C. M., Simpson, J., Gordon, A., Maloney, A. F., Allison, Y., Ritchie, I. M., Urquhart, A. (1983) Catecholamines and cholinergic enzymes in pre-senile and senile Alzheimer-type dementia and Down's syndrome. *Brain Res.* 280, 119–126.
75. Zombori, J., Kovács, I., Török, I., Kása, P. (1996) Structural localization of amyloid  $\beta$ -peptide in the olfactory bulb of Alzheimer's disease brain samples. *Clin. Neurosci.* 49, 46–47.

## EFFECTS OF BETA-AMYLOID ON CHOLINERGIC, CHOLINOCEPTIVE AND GABAergic NEURONS\*

Magdolna PÁKÁSKI<sup>1</sup>, Henrietta PAPP<sup>1</sup>, Mónika FORGON<sup>1</sup>, P. KÁSA JR.<sup>2</sup> and B. PENKE<sup>3</sup>

<sup>1</sup>Alzheimer's Disease Research Centre, <sup>2</sup>Department of Pharmaceutical Technology, <sup>3</sup>Department of Medical Chemistry, Albert Szent-Györgyi Medical University, Szeged, Hungary

(Received: 1998-06-12; accepted: 1998-06-26)

Alzheimer's disease is primarily characterized by neurofibrillary tangles, senile plaques and a cholinergic hypofunction. In this study, the morphological signs of toxicity of amyloid  $\beta$  (A $\beta$ ) 1–42 and short amyloid peptide fragments corresponding to amino acids 31–35 and 34–39 were investigated on cholinergic, cholinceptive and GABAergic neuronal populations of basal forebrain cultures.

The applied A $\beta$  fragments were toxic to cholinergic, cholinceptive and GABAergic neurons. In cholinergic and cholinceptive neurons, the toxic effect caused a redistribution of the acetylcholinesterase within the cells; the characteristic morphological changes in the GABAergic neurons involved the fragmentation and disappearance of the processes.

These results suggest that the vulnerability of neurons to A $\beta$  toxicity does not depend on their transmitter content, but the morphological manifestation of this vulnerability differs in the various neuronal populations. The results of experiments with short A $\beta$  fragments led to the conclusion that Leu<sup>34</sup> and Met<sup>35</sup> may be responsible for the toxicity of amyloid peptides.

**Keywords:** Alzheimer's disease – amyloid – neuronal culture – GABA immunocytochemistry – acetylcholinesterase – vesicular acetylcholine transporter

### INTRODUCTION

Alzheimer's disease (AD) is characterized by the extracellular deposition in the brain and its blood vessels of insoluble aggregates of the amyloid  $\beta$  (A $\beta$ ) peptide. AD can also be related to damage to the basal forebrain cholinergic system, and in particular the nucleus basalis of Meynert, which undergoes significant neuronal loss in AD [2, 4]. Although the GABAergic population is typically spared from severe neuronal loss in AD, the evidence does indicate the presence of neuritic abnormalities in these cells [25]. Previous studies have also demonstrated deficits of other neurotransmitters, including the GABA system, in patients with AD [15, 22].

\*Dedicated to Professor Péter Kása on the occasion of the 25th anniversary of his appointment as Head of the Central Research Laboratory and the Alzheimer's Disease Research Centre.

Send offprint requests to: Dr. Magdolna Pákáski, Alzheimer's Disease Research Centre, Albert Szent-Györgyi Medical University, H-6723 Szeged, Somogyi u. 4, Hungary. E-mail: pakaski@comser.szote.u.szeged.hu.



A $\beta$  has been shown to be toxic to neurons *in vitro* [3, 18, 26] and to rats and aged primates *in vivo* [10, 11]. Although the relationship between A $\beta$  toxicity and the cholinergic system was investigated *in vivo* [5, 6], we have little information about *in vitro* findings [17]. Another interesting question is how GABAergic neurons react to A $\beta$ . Earlier investigations provided controversial results concerning the resistance [19] and vulnerability [7, 8] of GABAergic neurons in response to A $\beta$  neurotoxicity.

The major protein component of the amyloid core of the senile plaques is the 40–42 amino acid residue A $\beta$ . Earlier reports concluded that A $\beta$ 25–35 causes morphological indications of neuronal degeneration similar to those of the full-length A $\beta$ 1–42. It has been suggested that this 11-amino acid internal sequence of amino acids is the biologically active fragment and may be responsible for the toxic effect of A $\beta$ 1–42 [26]. Further analysis of a series of peptides derived from the proposed active fragment of A $\beta$  revealed that A $\beta$ 29–35 is necessary for the neurotoxicity [20]. With regard to the cited data, the primary purpose of this study was to investigate the *in vitro* toxic effect of A $\beta$  on cholinergic or cholinceptive neurons in embryonic rat basal forebrain cultures; a second aim was to re-examine the morphological changes in the GABAergic neurons after A $\beta$  treatment. Cholinergic or cholinceptive neurons were identified by means of acetylcholinesterase (AChE) histochemistry and vesicular acetylcholine transporter (VACHT) immunohistochemistry. GABAergic neurons were demonstrated by GABA immunohistochemistry. These morphological methods were used to investigate the structural changes in the cholinergic, cholinceptive and GABAergic neurons after A $\beta$ 1–42 treatment. After initial characterization of the activity of full-length A $\beta$ 1–42, the toxicities of shorter fragments, such as A $\beta$ 31–35, A $\beta$ 34–39 and A $\beta$ 33–35, were compared. To prove the neuronal damage by biochemical means, measurements were made on the mitochondrial dehydrogenase activity (MTT) reduction and lactate dehydrogenase (LDH) release into the medium.

## MATERIALS AND METHODS

### *Tissue culture*

Since the basal forebrain is a region typically affected in AD, primary basal forebrain cultures were utilized in our experiments. Basal forebrain tissue from embryonic rat pups on days 16 or 17 (E16–17) was dissected and then digested for 10 min in 0.25% trypsin (Gibco) at 37 °C. Following mechanical dissociation of the tissue, the suspension was settled for 10 min at 1000  $\times$  g. The cell pellet was resuspended in Dulbecco's Modified Eagle Medium (DMEM) (Gibco) containing 10% fetal bovine serum (FBS) (Gibco), 100 U/ml penicillin and 100  $\mu$ g/ml streptomycin. Cells were plated onto coverslips coated with poly-L-lysine (Sigma) at a density of  $3.5\text{--}4 \times 10^4$  cells/cm<sup>2</sup> and were grown in a humidified incubator at 37 °C in 5% CO<sub>2</sub>.

### *Peptide solutions*

Human A $\beta$  was synthesized in the Chemical Department of our University by a solid-phase technique involving Boc chemistry, purified by HPLC, and subjected to electrospray mass spectral analysis [12]. A $\beta$ 1–42, A $\beta$ 31–35, A $\beta$ 34–39 or A $\beta$ 33–35 was solubilized in 35% acetonitrile plus 0.1% trifluoroacetic acid (ACN/TFA). Peptide solutions were diluted into the growth medium immediately after solubilization to yield a final concentration of 20  $\mu$ M for A $\beta$ s as described by Yankner et al. [26]. Peptides were added to cultures on 4 day *in vitro* (DIV 4) after plating. Control cultures were maintained in DMEM/10% FBS for 4 days, and then supplemented with vehicle alone. Morphological changes in the cells were monitored on days 1 (DIV 4+1), 3 (DIV 4+3) and 5 (DIV 4+5) after treatment.

### *AChE histochemistry*

To visualize the signs of A $\beta$  toxicity on cholinergic and cholinceptive neurons, the cultures were fixed in 4% paraformaldehyde for 20 min and then stained for AChE by the technique of Tago et al. [23]. Ethopropazine ( $10^{-4}$  M) was always used as non-specific cholinesterase inhibitor. After incubation with a reaction mixture containing acetylthiocholine iodide (1 mg/ml) as substrate, the reaction product was detected with 3,3'-diaminobenzidine tetrahydrochloride and NiCl<sub>2</sub>. During the microscopic examination, 300 AChE-positive neurons were counted both in the control and in the A $\beta$ 1–42-treated cultures and they were classified according to their size and the staining pattern.

### *VACHT immunohistochemistry*

For a more exact identification of cholinergic neurons, the cultures were immunostained for VACHT. The cells were fixed in 4% paraformaldehyde for 20 min and were incubated with 0.1% Triton X-100 and 5% normal rabbit serum (NGS) in Tris-buffered saline (TBS) for 2 h. The polyclonal antibody against VACHT (1:32 000, Chemicon, USA) was applied for 48 h. This was followed by incubation in rabbit-anti-goat IgG-biotin (1:200, Jackson ImmunoResearch Lab., USA) for 1 h, and then in streptavidin-horseradish peroxidase (1:500, Zymed, USA) for 1 h. The cultures were washed twice with 0.1 M TBS (pH 7.4) for 10 min between sera. The peroxidase reaction was developed by using 3,3'-diaminobenzidine tetrahydrochloride and NiCl<sub>2</sub>.

### *GABA immunohistochemistry*

To assess the neuronal damage caused to the GABAergic neurons by the A $\beta$ s, the cultures were immunostained for GABA by the peroxidase-antiperoxidase method. After fixation in 1% glutaraldehyde for 20 min, the cells were permeabilized and the non-specific staining was blocked by incubation with 0.2% Triton X-100 and 5% normal bovine serum



(NBS) in TBS for 4 h. The monoclonal antibody against GABA (1:3000; Immunotech, France) was applied overnight at 37 °C. Goat-anti-rabbit secondary antibody (1:30, Jackson ImmunoResearch Lab., USA) and rabbit peroxidase-antiperoxidase complex (1:200, Nordic Immun. Lab., Germany) were applied consecutively for 1 h at room temperature. Staining was revealed with a solution containing 3,3'-diaminobenzidine tetrahydrochloride,  $\text{NiCl}_2$  and  $\text{H}_2\text{O}_2$  in Tris-HCl. In immunocytochemical control experiments, immunostaining was blocked by deletion of the GABA antibody. The results of morphological observations were quantified by image analysis. A Leica Q500 MC colour image analyser (Germany) was employed to measure the numbers of GABAergic cells in the control and  $\text{A}\beta$ -treated cultures after different time intervals.

### *Biochemical investigations*

As one of the early indicators of toxicity of  $\text{A}\beta$ s [23], the MTT reduction was measured 2 and 6 h after  $\text{A}\beta$  treatment. 200  $\mu\text{l}$ /culture of 5 mg/ml MTT (3-[4,5-dimethylthiazol-2-yl]-2,5-diphenyltetrazolium bromide) stock was added and, after a 4 h incubation, 300  $\mu\text{l}$  of reaction solution containing 50% dimethylformamide and 20% SDS was added to solubilize the insoluble formazan precipitates produced by MTT reduction. The next day, the absorbance of the purple dye was read at 570 nm.

After a longer incubation with  $\text{A}\beta$ s (DIV4+3; DIV4+4 and DIV 4+5), the LDH activity in the culture medium was evaluated by measuring the rate of disappearance of NADH (after addition of pyruvate and NADH), monitored spectrophotometrically at 340 nm by the method of Wróblewski and LaDue [25].

## RESULTS

### *Demonstration of toxicity of $\text{A}\beta$ s on cholinergic and cholinceptive neurons*

In the control cultures, two types of neurons could be distinguished on the basis of their morphological features after AChE histochemistry. The majority of the AChE-positive neurons (66%–76%) were small and bipolar, but this basal forebrain culture contained a relatively large number of multipolar neurons with extensively arborized processes (24%–34%). The specific staining for AChE was localized on the perikarya and processes of neurons (Fig. 1A). After  $\text{A}\beta$ 1–42 treatment, the localization of the staining pattern was changed. It did not fill the whole perikarya and could be observed near the plasma membrane or sometimes near the somatodendritic region (Fig. 1B). Similarly, treatment of the cultures with shorter peptides ( $\text{A}\beta$ 31–35 or  $\text{A}\beta$ 34–39) also caused alterations in the enzyme localization within the cholinceptive and cholinergic neurons (Fig. 1C).  $\text{A}\beta$ 33–35 had no effect at all. Figure 2 demonstrates the quantitative distribution of the healthy and damaged AChE-positive neurons of different sizes in the control and  $\text{A}\beta$ 1–42-treated cultures. The numbers of both large, multipolar and small, bipolar neurons displaying diffuse

perikaryonal staining (healthy cells) were decreased after A $\beta$ 1–42 treatment. At the same time, the number of neurons with a staining pattern localized near the plasma membrane (damaged cells) was increased. The increase in the number of damaged cells was not essentially different in the small, bipolar (3-fold) and large, multipolar (4-fold) neurons.

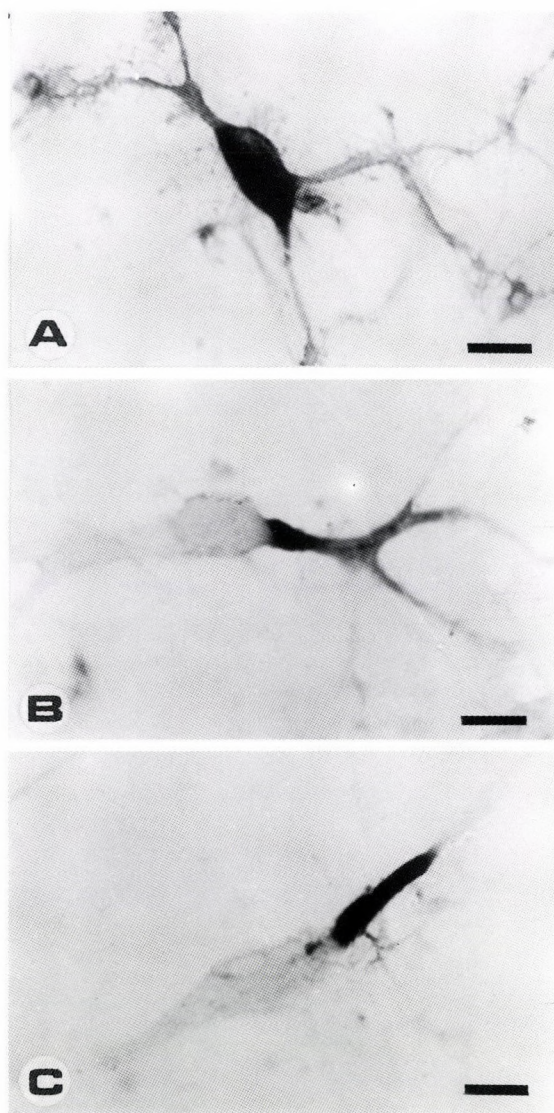


*Fig. 1.* Panels A–C: micrographs of basal forebrain cultures histochemically stained for AChE exposed for 1 day (DIV4+1) to the following treatments: A: solvent (control); B: 20  $\mu$ M A $\beta$ 1–42; and C: 20  $\mu$ M A $\beta$ 31–35. The neurons appear intact in the control culture; in contrast, the neurons are damaged after treatment (the specific staining is localized around the membrane). Scale bar = 10  $\mu$ m



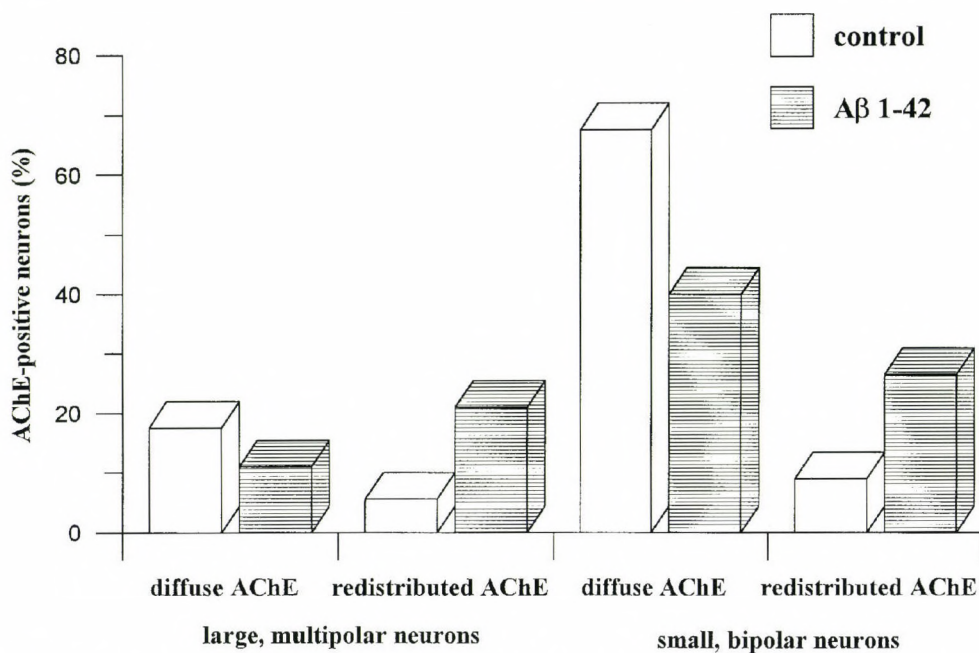


Fig. 2. Effect of Aβ1-2 on the localization of the AChE staining in the large, multipolar and small, bipolar AChE-positive neurons. The counted 300 cells of the cultures were taken as 100%

To confirm that the cultures really contained cholinergic neurons, the cells were immunostained for VACHT. Figure 3 illustrates the specific staining of cholinergic neurons. The immunostaining of VACHT was localized to the perikarya, where it appeared as vesicular distribution, and sometimes to the processes of neurons.

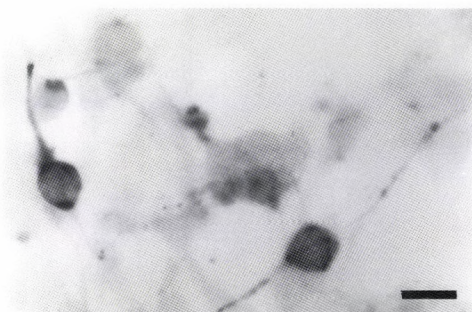


Fig. 3. Photomicrograph of basal forebrain cultures immunostained with VACHT antibody. Scale bar = 10 μm

*Demonstration of toxicity of A $\beta$ s on GABAergic neurons*

When the control and A $\beta$ -treated cultures were immunostained for GABA, there were again morphological differences between them. In the untreated cultures, the GABA-immunoreactive neurons were healthy and their long processes were intact (Fig. 4A). Initially (DIV4+1), tiny varicosities appeared on the processes of the GABA-positive neurons in the A $\beta$ 1–42 treated cultures (Fig. 4B). On longer incubation (DIV4+3), more fragmented neurites could be observed. By day 5 after A $\beta$ 1–42 treatment, the signs of degeneration had become more serious: the majority of the GABAergic cells had lost their processes and the number of this type of neurons had decreased. A $\beta$ 31–35 (Fig. 4C) and A $\beta$ 34–39 (Fig. 4D) had similar toxic effects on the GABAergic basal forebrain neurons. There were no changes in the morphology of GABA-immunoreactive neurons after A $\beta$ 33–35 treatment. Table 1 illustrates the effects of the A $\beta$ s on the numbers of GABAergic cells counted by image analysis. On day 1 after treatment, only A $\beta$ 1–42 caused a significant cell loss. By day 3 after treatment with A $\beta$ 1–42, A $\beta$ 31–35 or A $\beta$ 34–39, the number of GABA-immunoreactive cells had decreased to 50–60% of that in the

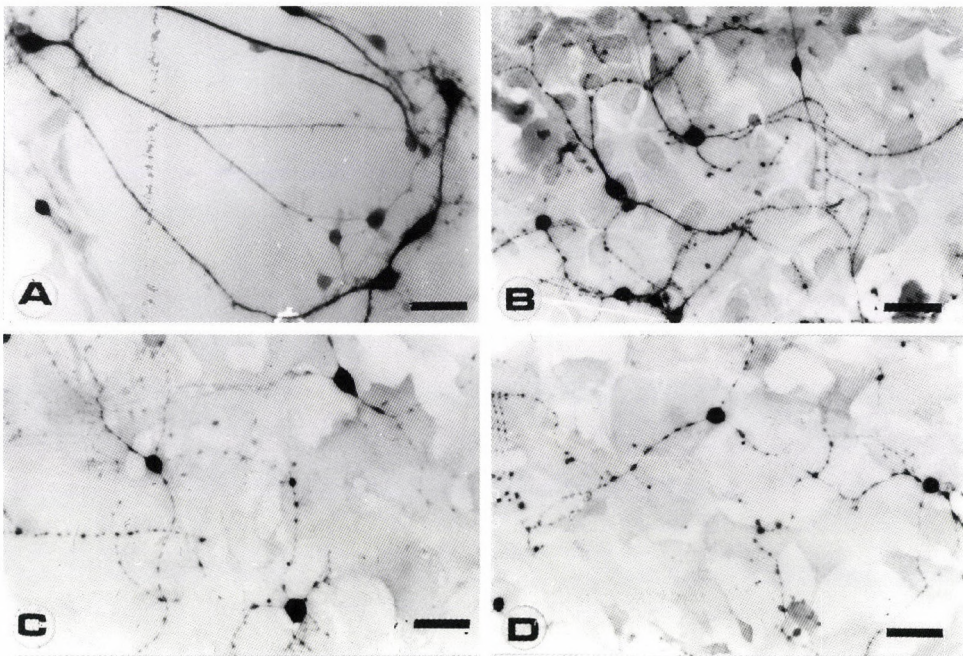


Fig. 4. Photomicrograph of basal forebrain cultures immunostained with GABA antibody exposed for 1 or 3 days (DIV4+1, DIV4+3) to the following treatments: A: solvent (control) (DIV4+1); B: 20  $\mu$ M A $\beta$ 1–42 (DIV4+1); C: 20 mM A $\beta$ 31–35 (DIV4+3) and D: 20 mM A $\beta$ 34–39 (DIV4+3); neurons have long, intact processes in the control culture; in contrast, the vast majority of the neurons are degenerated after treatment (fragmented neurites). Scale bar = 30  $\mu$ m



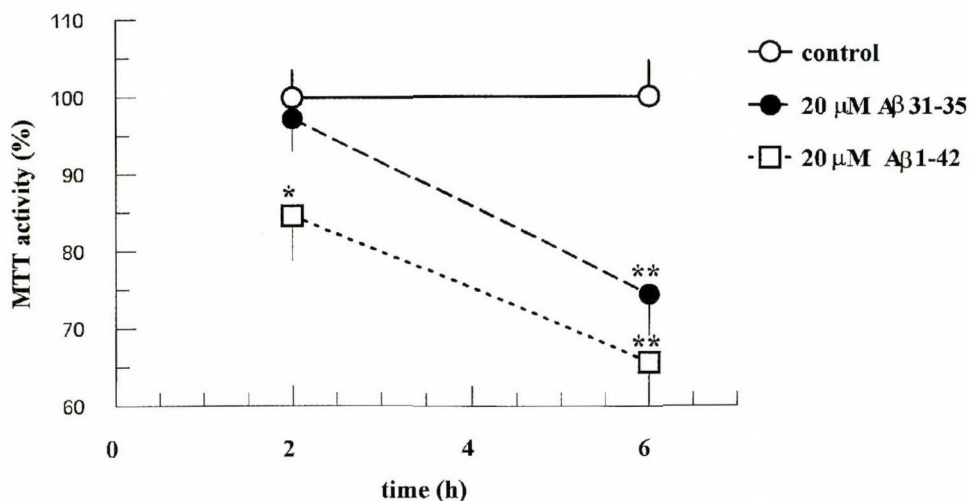


Fig. 5. Inhibition of MTT reduction caused by  $A\beta$ 1-42 and  $A\beta$ 31-35 in embryonic rat basal forebrain cultures. The values for untreated cultures (vehicle alone) were taken as 100%. Results on treated cultures are expressed as percentages of the control absorbance. Data are means  $\pm$  SD values of results on 5 separate sample. Significant toxicity is observed at 2 h after  $A\beta$ 1-42 treatment, and at 6 h after  $A\beta$ 1-42 or  $A\beta$ 31-35 treatment (\* $p$  < 0.001, \*\* $p$  < 0.002, paired Student's  $t$ -test)

control culture. Following a 5-day exposure to  $A\beta$ 1-42,  $A\beta$ 31-35 or  $A\beta$ 34-39, more serious damage to the GABAergic cells was observed. Treatment of the cultures with  $A\beta$ 33-35 did not induce a significant decrease in the number of GABA-positive cells.

### *Demonstration of toxicity of $A\beta$ s by biochemical means*

For further assessment of the toxicity of  $A\beta$ 1-42 and  $A\beta$ 31-35 on the basal forebrain neuronal culture, the MTT test was performed and LDH activity was measured. After a 2-h  $A\beta$  treatment, only  $A\beta$ 1-42 exhibited a diminished ability to reduce MTT. By 6 h after treatment,  $A\beta$ 31-35 also potentially inhibited the MTT reduction (Fig. 5).

The LDH activities of the media from the control and  $A\beta$ -treated cultures did not reveal any significant difference after a 3-day treatment period (DIV4+3). One and 2 days later (DIV4+4, DIV 4+5), both the full-length  $A\beta$ 1-42 and  $A\beta$ 31-35 caused significant elevations of LDH activities (Fig. 6).

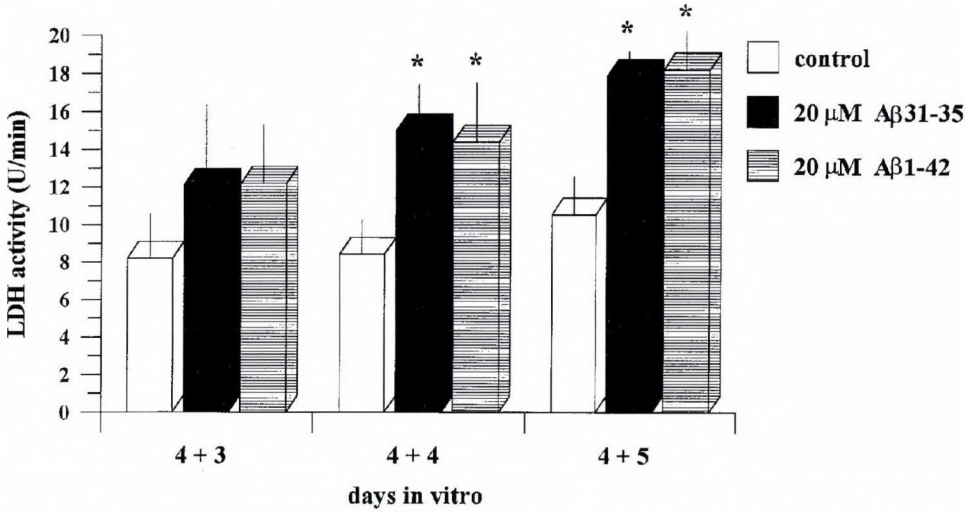


Fig. 6. Effects of Aβ1-42 and Aβ31-35 on LDH release from embryonic rat basal forebrain cultures. Data are means  $\pm$  SD values of results on 5 separate samples. Significant toxicity is observed on days 4 and 5 after Aβ1-42, Aβ31-35 and Aβ34-39 treatment (\* $p < 0.001$ , paired Student's  $t$ -test)

## DISCUSSION

The earliest data emphasized the relatively selective vulnerability of the cholinergic system of the basal forebrain in AD [2, 4]. A few years later, increasing evidence indicated damage to other transmitter systems, including the GABAergic neurons [15, 22, 25].

There were no *in vitro* or *in vivo* data relating to comparisons of the vulnerability of cholinergic and GABAergic neurons to Aβ toxicity. The present study revealed that Aβs are toxic to cholinergic, cholinceptive and GABAergic neurons in rat basal forebrain cultures.

Table 1  
Effects of different Aβs on numbers of GABAergic cells  
in embryonic rat basal forebrain cultures

	Aβ1-42	Aβ31-35	Aβ34-39	Aβ34-35
DIV4+1	74.5 $\pm$ 4.8*	97.4 $\pm$ 5.7	91.3 $\pm$ 9.7	109.7 $\pm$ 7.5
DIV4+3	52.0 $\pm$ 6.2*	61.0 $\pm$ 15*	53.0 $\pm$ 14*	89.7 $\pm$ 13.2
DIV4+5	15.9 $\pm$ 7.8*	19.9 $\pm$ 6.2*	25.6 $\pm$ 4.2*	83.1 $\pm$ 15.9

The values are expressed as % of control cultures. Data are means  $\pm$  SD values from 5 randomly selected fields ( $5 \times 0.3 \text{ mm}^2$ ) in each of 3 separate experiments. Significant toxicity is observed on day 1 after Aβ1-42 treatment, and on days 3 and 5 after Aβ1-42, Aβ31-35 and Aβ34-39 treatment (\* $p < 0.001$ , paired Student's  $t$ -test).



The histochemical results on the human cerebral cortex [14] indicate that the AChE-positive neurons that may be considered cholinergic exhibit extensive dendritic arborizations and the reaction of the secreted enzyme is also positive around the perikarya. Since our basal forebrain cultures contained a relatively large number of this latter type of AChE-positive neurons, the morphological changes in the cholinceptive and the cholinergic neurons in consequences of A $\beta$  toxicity had already been demonstrated [9]. This is the first *in vitro* study which provides information about the quantification of the signs of toxicity in cholinergic and cholinceptive neurons after treatment with full-length A $\beta$ . The change in localization of AChE within the cell can be regarded as an early sign of neurotoxicity [9], when the synthesis of the enzyme has almost totally stopped and it is translocated around the membrane.

The morphological signs of the toxic effects of A $\beta$ 1–42, A $\beta$ 31–35 and A $\beta$ 34–39 could also be detected on the GABAergic neurons, but they differed from those on the cholinergic and cholinceptive neurons. Our results disprove the data of Pike and Cotman [19], who found the GABAergic neurons to be resistant. We hypothesize that the controversial data may arise from differences in the solvent and in the concentrations of the peptides applied in the different experiments. Another difference lies in the age and origin of the cultures used by ourselves and by Pike and Cotman. Our previous results [15] demonstrated that the vulnerability of GABAergic neurons depends on their sizes: the most vulnerable GABA-immunoreactive neurons were the small ones (diameter 5–10  $\mu$ m), since only the number of these was decreased on 1 day after A $\beta$ 1–42 treatment. Monitoring the numbers of three different sizes of GABAergic neurons for 5 days after treatment revealed the relative resistance of the large cells to A $\beta$  treatment. We postulated that the differences in vulnerability within the GABAergic neurons may depend on other neurochemical differences. Since the GABAergic neurons are nearly always colocalized with one of several different calcium-binding proteins, our suggestion relates to the finding of Pike and Cotman [21], who reported the resistance of calretinin-immunoreactive neurons to A $\beta$  toxicity. On the basis of the results mentioned above, we proposed that the small GABAergic neurons do not contain one of the calcium-binding proteins, and they may therefore be vulnerable to A $\beta$ .

On the basis of the toxicity of both A $\beta$ 31–35 and A $\beta$ 34–39, we suggested that the amino acids Leu<sup>34</sup> and Met<sup>35</sup> may play a role in the neurodegenerative effect of  $\beta$ AP. This suggestion seems to confirm earlier results [11]. Manelli and Puttfarcken found that the amino acid substitution A $\beta$ 1–42(Nle<sup>35</sup>) decreased the toxicity towards rat hippocampal cells.

Abe and Kimura [1] demonstrated that A $\beta$  toxicity consists of two phases, which are distinguished on the basis of differences in duration and in Ca<sup>2+</sup> dependence. The early phase could be detected by the MTT assay, and the late phase by the LDH release assay. Our study, with these methods confirmed these findings. We found that the two phases of toxicity caused by A $\beta$ 31–35 can also be proved by these cytotoxic assays.

In summary, we have identified and characterized the morphological changes induced by A $\beta$  in cholinergic, cholinceptive and GABAergic neurons. The signs of toxicity display characteristic features for the given neuronal population. The results of experiments with short A $\beta$  fragments lead us to conclude that Leu<sup>34</sup> and Met<sup>35</sup> may also be important for the toxicity of amyloid peptides.

## ACKNOWLEDGEMENT

This work was supported by grants of OTKA T022683 and ETT 584/1996.

## REFERENCES

1. Abe, K., Kimura, H. (1996) Amyloid  $\beta$  toxicity of a  $\text{Ca}^{2+}$ -independent early phase and a  $\text{Ca}^{2+}$ -dependent late phase. *J. Neurochem.* 67, 2074–2078.
2. Bartus, R. T., Dean, R. L. III, Beer, B., Lippa, S. (1982) The cholinergic hypothesis of geriatric memory dysfunction. *Science* 217, 408–414.
3. Busciglio, J., Lorenzo, A., Yankner, B. A. (1992) Methodological variables in the assessment of beta amyloid neurotoxicity. *Neurobiol. Aging* 13, 609–612.
4. Coyle, J. T., Price, D. L., DeLong, M. R. (1983) Alzheimer's disease: a disorder of cortical cholinergic innervation. *Science* 219, 1184–1190.
5. Emre, M., Geula, C., Ransil, B. J., Mesulam, M.-M. (1992) The acute neurotoxicity and effects upon cholinergic axons of intracerebrally injected  $\beta$ -amyloid in the rat brain. *Neurobiol. Aging* 13, 553–559.
6. Harkány, T., Lengyel, Zs., Soós, K., Penke, B., Luiten, P. G. M., Gulya, K. (1995) Cholinotoxic effects of  $\beta$ -amyloid<sub>(1-42)</sub> peptide on cortical projections of the rat nucleus basalis magnocellularis. *Brain Res.* 695, 71–75.
7. Kása, P., Pákáski, M., Penke, B. (1992) Synthetic human beta amyloid has selective vulnerable effects on different types of neurons and glial cells in *in vitro* cultures derived from embryonic rat brain cortex. *Neurobiol. Aging* 13, Suppl. 1, S104.
8. Kása, P., Pákáski, M., Penke, B. (1993) Synthetic human beta amyloid has selective vulnerable effects on different types of neurons. In: Nicolini, M., Zatta, P. F., Corain, B. (eds) *Alzheimer's Disease and Related Disorders. Advances in the Biosciences* 12, Pergamon Press, Oxford, pp. 311–312.
9. Kása, P., Pákáski, M., Zarándi, M., Forgon, M., Papp, H., Rakonczay, Z. (1998) Alterations in the distribution of acetylcholinesterase within the cholinergic and cholinceptive neurons in *in vitro* tissue cultures in response to human amyloid  $\beta$  peptide and some of its fragments. *Neurobiol. Aging* 19, 549.
10. Kowall, N. W., Beal, M. F., Busciglio, J., Duffy, L. K., Yankner B. A. (1991) An *in vivo* model for neurodegenerative effects of  $\beta$  amyloid and protection by substance P. *Proc. Natl. Acad. Sci. USA* 88, 7247–7251.
11. Kowall, N. W., McKee, A. C., Yankner, B. A., Beal, M. F. (1992) In vivo neurotoxicity of beta amyloid [ $\beta$ (1-40)] and the [ $\beta$ (25-35)] fragment. *Neurobiol. Aging* 13, 537–542.
12. Laskay, G., Zarándi, M., Varga, J., Jost, K., Fónagy, A., Torday, C., Latzkovits, L., Penke, B. (1997) A putative tetrapeptide antagonist prevents  $\beta$ -amyloid-induced long-term elevation of  $[\text{Ca}^{2+}]_i$  in rat astrocytes. *Biochem. Biophys. Res. Commun.* 235, 479–481.
13. Manelli, A. M., Puttfarcken, P. S. (1995)  $\beta$ -Amyloid-induced toxicity in rat hippocampal cells: in vitro evidence for the involvement of free radicals. *Brain Res. Bull.* 38, 569–576.
14. Mesulam, M. M., Geula, C. (1992) Overlap between acetylcholinesterase-rich and choline acetyltransferase-positive (cholinergic) axons in human cerebral cortex. *Brain Res.* 577, 112–120.
15. Mountjoy, C. Q., Rossor, M. N., Iversen, L. L., Roth, M. (1984) Correlation of cortical cholinergic and GABA deficits with quantitative neuropathological findings in senile dementia. *Brain* 107, 507–518.
16. Pákáski, M., Farkas, Z., Kása, P. Jr., Forgon, M., Papp, H., Zarándi, M., Penke, B., Kása, P. (1998) Vulnerability of small GABAergic neurons to human  $\beta$ -amyloid pentapeptide. *Brain Res.* 796, 239–246.
17. Papp, H., Pákáski, M., Penke, B., Kása, P. (1996) Effects of  $\beta$ -amyloid and its fragments on cholinergic and cholinceptive neurons in vitro. *Clin. Neurosci.* 49, 49–50.
18. Pike, C. J., Walencewicz, A. J., Glabe, C. G., Cotman, C. W. (1991) In vitro aging of  $\beta$ -amyloid protein causes peptide aggregation and neurotoxicity. *Brain Res.* 563, 311–314.



19. Pike, C. J., Cotman, C. W. (1993) Cultured GABA-immunoreactive neurons are resistant to toxicity induced by  $\beta$ -amyloid. *Neuroscience* 56, 269–274.
20. Pike, C. J., Burdick, D., Walencewicz, A. J., Glabe, C. G., Cotman, C. W. (1993) Neurodegeneration induced by  $\beta$ -amyloid peptides in vitro: the role of peptide assembly state. *J. Neurosci.* 13, 1676–1687.
21. Pike, C. J., Cotman, C. W. (1995) Calretinin-immunoreactive neurons are resistant to  $\beta$ -amyloid toxicity in vitro. *Brain Res.* 671, 293–298.
22. Rossor, M. N., Garret, N. J., Johnson, A. L., Mountjoy, C. Q., Roth, M., Iversen, L. L. (1982) A post-mortem study of the cholinergic and GABA systems in senile dementia. *Brain* 105, 313–330.
22. Shearman, M. S., Ragan, C. I., Iversen, L. L. (1994) Inhibition of PC12 cell redox activity is a specific, early indicator of the mechanism of  $\beta$ -amyloid-mediated cell death. *Proc. Natl. Acad. Sci. USA* 91, 1470–1474.
23. Tago, H., Kimura, H., Maeda, T. (1986) Visualization of detailed acetylcholinesterase fiber and neuron staining in rat brain by a sensitive histochemical procedure. *J. Histochem. Cytochem.* 34, 1431–1438.
24. Walker, L. C., Kitt, C. A., Struble, R. G., Schmechel, D. E., Oertel, W. H., Cork, L. C., Price, D. L. (1985) Glutamic acid decarboxylase-like immunoreactive neurites in senile plaques. *Neurosci. Lett.* 59, 165–169.
25. Wróblewski, F., LaDue, J. S. (1955) Lactic dehydrogenase activity in blood. *Proc. Soc. Exp. Biol. Med.* 90, 210–213.
26. Yankner, B. A., Duffy, L. K., Kirschner, D. A. (1990) Neurotrophic and neurotoxic effects of amyloid  $\beta$  protein: reversal by tachykinin neuropeptides. *Science* 250, 279–282.

# CHOLINESTERASES IN ALZHEIMER'S DISEASE AND CHOLINESTERASE INHIBITORS IN ALZHEIMER THERAPY\*

Z. RAKONCZAY and I. KOVÁCS

Alzheimer's Disease Research Center, Albert Szent-Györgyi Medical University, Szeged, Hungary

(Received: 1998-06-12; accepted: 1998-06-24)

The central cholinergic neurons are known to be closely linked to intellectual functions such as memory and cognition. Alzheimer's disease (AD) is accompanied by a substantial loss of choline acetyltransferase (ChAT) and acetylcholinesterase (AChE) activities associated with cholinergic and cholinceptive neurons in several brain areas, especially in the cortex. Several reports suggest an altered form of AChE in AD. It may differ in its pH optimum and its responses to inhibitors, it may have lost its peripheral site and it has an anomalous molecular form as revealed by isoelectric focusing. All of these features point to the abnormality of the affected cholinergic neurons in AD.

The loss of cholinergic innervation in the brain of patients with AD has produced the "cholinergic hypothesis", which postulates that the memory dysfunction is a consequence of the cholinergic disturbances in the afflicted areas. This led to treatment attempts with cholinomimetics, including cholinesterase (ChE) inhibitors. AChE inhibitors function in AD by inhibiting AChE, which normally limits the amount of acetylcholine (ACh) in the brain. In consequence, those cells which are still alive and produce ACh may restore the cholinergic deficit at synaptic sites. The use of ChE inhibitors may therefore be the most appropriate palliative treatment in the early stages of the disease, before severe neuronal degeneration occurs. Some recent preliminary results suggest that long-term treatment with second- or third-generation ChE inhibitors may slow down the development of the disease. This paper provides an overview of the main therapeutic and diagnostic implications of ChEs in AD.

**Keywords:** Alzheimer's disease – acetylcholinesterase – acetylcholinesterase molecular forms – butyrylcholinesterase – cholinesterase inhibitors

## INTRODUCTION

Cholinesterases (ChEs) are enzymes found in many tissue types, including the nervous system. Mammalian brain ChEs can be differentiated by selective inhibitors alone or in combination with specific substrates into acetylcholinesterase (acetylcholine acetylhydro-

\*Dedicated to Professor Péter Kása on the occasion of the 25th anniversary of his appointment as Head of Central Research Laboratory and the Alzheimer's Disease Research Center.

Send offprint requests to: Dr. Zoltán Rakonczay, Alzheimer's Disease Research Center, Albert Szent-Györgyi Medical University, H-6720 Szeged, Somogyi u. 4, Hungary. E-mail: RZ@Comser.Szote.u-Szeged.Hu.



lase, EC 3.1.1.7, AChE) and butyrylcholinesterase (acylcholine acylhydrolase, EC 3.1.1.8, BuChE). Within the nervous system, AChE is the more abundant and its main function is the rapid hydrolysis of acetylcholine (ACh) at cholinceptive and cholinergic synapses, but why mammalian tissues, including the brain, contain BuChE is a question that has not been resolved.

ChEs also occur in high concentrations in non-cholinergic neurons, erythrocytes and embryonic tissues, and transiently concentrated in proliferating cells [31, 32]. It has therefore been proposed that, under certain developmental conditions, AChE and BuChE may function as peptidases and have the capacity to hydrolyze peptide bonds in naturally occurring neuropeptides, such as substance P and enkephalins [8, 9]. Recent results showed that the proteolytic activity of AChE may be associated with contamination of the preparations [7].

Considerable advances have been made in our understanding of the neurobiologic features of Alzheimer's disease (AD). Many other transmitter systems are affected by this disease, but the cholinergic system is the most consistently afflicted and the most studied [24], and it now forms one of the targets for therapeutic intervention [22, 29]. It has been confirmed that the cholinergic indices may be unique in their association with dementia severity [4].

Neurochemically, the cholinergic deficit relates to damage in the ascending cholinergic projections from the nucleus basalis of Meynert to the cerebral cortex [63]. Pathologically, AD is characterized by massive parenchymal deposits of totally insoluble amyloid protein, known as senile plaques (SPs). Another pathological hallmark is the neurofibrillary tangle (NFT), which is mainly composed of abnormally phosphorylated cytoskeletal protein tau and consists of paired helical filaments in the afflicted brain areas.

Our main goal here is to review the literature on ChEs in AD. Special attention has been paid to providing an insight into the histo-, immuno- and biochemical changes in ChE activities and their molecular forms in AD. A survey is also made of the AChE inhibitors *in vitro* and *in vivo* as tools for recent and future therapeutic approaches.

## MATERIALS AND METHODS

Membrane-associated AChE was extracted from normal human *post-mortem* brain. Briefly: Tissues were homogenized in 10 vol. of 12.5 mM phosphate buffer, pH 7.4, and centrifuged at 100,000 g for 1 h. The supernatant was discarded and the pellet was rehomogenized in the same buffer containing 0.5% Triton X-100. After centrifugation as above the supernatant was used as membrane-associated AChE [51]. BuChE was obtained from normal human serum. ChE activities were determined by spectrophotometric [13] or in the case of AChE molecular forms by radiometric [27] assays. AChE molecular forms were separated by density gradient ultracentrifugation [51]. In enzyme inhibition experiments, AChE or BuChE enzymes was preincubated with different concentrations of inhibitors for 30 min. and the reaction was started with the substrate acetylthiocholine or butyrylthiocholine. BW 284c51 ( $10^{-5}$  M) and ethopropazine ( $10^{-4}$  M) were used as specific AChE and BuChE inhibitors, respectively.

AChE histochemistry followed the method of Tago et al. [61]. Ethopropazine ( $10^{-4}$  M) was used to inactivate BuChE and BW281c51 ( $10^{-5}$  M) was added to control sections to demonstrate reaction specificity.

## RESULTS AND DISCUSSION

### *Histo- and immunochemical observations on cholinesterases in Alzheimer's disease*

In the normal human brain, the density of the cholinergic (AChE-positive) fibers is highest in the limbic and paralimbic cortical zones, intermediate in most sensory-motor and association zones, and lowest within the primary visual and visual association areas of the occipital lobe. In AD, an overall 55% loss of cortical cholinergic fibers has been detected [23]. However, a marked regional variation (18–85%) in the extent of this loss has been found in different cortical areas [20, 21, 23]. The temporal lobe, and particularly the temporal association areas, display a dramatic loss of cholinergic fibers (80–85%). By contrast, the anterior cingulate cortex, and the primary visual, primary somatosensory and primary motor cortices exhibit a relative preservation of cholinergic fibers (18–45%) [23].

Several reports have shown that AChE activity is associated with cortical and hippocampal SPs and NFTs in AD [17, 45, 59] (Fig. 1). The specificity of ChE histochemical reaction products found in the SP, the NFT and amyloid angiopathy was established by using ChE inhibitors [18, 35]. The reaction product associated with these lesions was completely inhibited by the specific AChE inhibitor 1,5-bis(allyldimethylammonium-phenyl)pentan-3-one dibromide, BW284c51 ( $10^{-4}$  M), but was not affected by the specific BuChE inhibitor tetraisopropyl pyrophosphoramidate, iso-OMPA ( $10^{-4}$  M), or ethopropazine ( $10^{-4}$  M). Conversely, the BuChE reaction product was reliably inhibited by iso-OMPA, but not by BW284c51. When sensitive histochemical techniques were applied for the visualization of ChEs, AChE activity was observed in a substantial population of SPs and NFTs throughout the cerebral cortex of AD patients [37, 38]. AChE-positive axons were severely depleted in the cerebral cortex of the AD brain. The location of the enzyme was demonstrated histochemically to be largely shifted to the SP or NFT. Histochemical observations have indicated that the AChE in normal neurons and ChEs associated with pathological lesions in AD differ in pH requirements for staining [37]. The AChE associated with normal neural elements was stained best at pH 8.0. At pH 6.8 to 7.0, enzyme activity was present in both mature and immature SPs, the amyloid core, the neuritic halo, and the extracellular tangles. On the other hand, the ChEs associated with normal neurons and axons differed from AD ChEs in their sensitivity to ChE inhibitors [18]. The formation of the AChE histochemical reaction products in normal neurons and axons was completely inhibited by  $10^{-7}$ – $10^{-6}$  M of the specific AChE inhibitor BW284c51. The AChE activity within the SPs and NFTs, however, required concentrations as high as  $10^{-5}$ – $10^{-4}$  M of BW284c51 for complete inhibition. The BuChE activity associated with the SPs and NFTs necessitated similarly high concentrations ( $10^{-5}$ – $10^{-4}$  M) of the BuChE inhibitor iso-OMPA for complete inhibition. The ChEs in AD samples



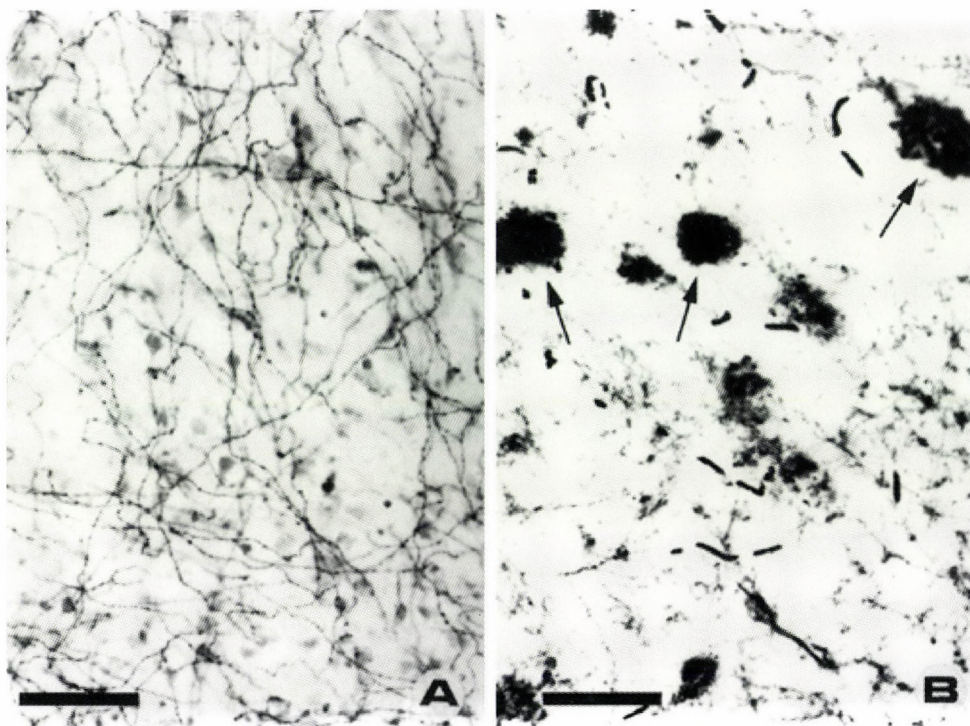


Fig. 1. AChE histochemistry of frontal cortex from control brain sample (A). Enzyme-positive axons display multiple varicosities. Scale bar = 100  $\mu$ m. Frontal cortex from a 72-year-old man with Alzheimer's disease (B). Note the presence of AChE-positive fibers and plaques (arrows). Scale bar = 100  $\mu$ m

therefore required 10–100 times higher concentrations of inhibitors for complete inhibition as compared with ChEs associated with normal neurons and axons. Indolamines such as serotonin and 5-hydroxytryptophan and the protease inhibitors bacitracin and carboxypeptidase inhibitor, at a concentration of  $5 \times 10^{-3}$  M, completely inhibited the histochemical reactivities of both AChE and BuChE in the pathological lesions of AD [64]. At the same concentration, these compounds had no effect on the AChE activity of normal neurons and fibers.

In many regions of the AD cerebral cortex, AChE- and BuChE-positive SPs and NFTs were intermingled throughout the depth of the cortex, suggesting that the AChE and BuChE activities might be colocalized within a single population of SPs and NFTs [10]. In some cortical areas, however, the superficial cortical layers contained predominantly AChE-positive NFTs, whereas the deep layers contained only BuChE-positive NFTs [10]. Histochemical observations indicate that BuChE accumulates in the plaques of  $\beta$ -amyloid ( $A\beta$ ) in AD, together with a form of AChE selectively expressed in the neuroglia. Many elderly individuals have extensive  $A\beta$  deposits in the brain without any evidence of dementia. The BuChE reactivity covers a greater portion of the SPs area in AD than in age-

matched control brains, suggesting that the accumulation of BuChE may be one of the factors that participates in the "ripening" and eventual pathogenicity of A $\beta$  deposits in AD [36]. Furthermore, in comparison to normal elderly individuals, AD brains displayed a significantly higher density of BuChE-positive glia and a lower density of AChE-positive glia in the entorhinal and inferotemporal cortices, but not in the primary somatosensory and visual cortices [65]. These observations may suggest that the glia are a likely source of the BuChE associated with the pathological lesions of AD.

In the entorhinal cortex of AD brains, immunohistochemistry with monoclonal antibodies [51] revealed AChE- and BuChE-like immunoreactivities in the SPs and NFTs, indicating that the histochemical ChE reactivity observed in the SP and NFT most probably originates from AChE and BuChE molecules [19].

The relationship between the cholinergic cortical innervation and the pathogenesis of these SPs is unknown. The character and the distribution of SPs in monkeys aged 4–31 years was analyzed with staining for AChE and also with Congo Red and silver stains [59]. It was found that both immature and mature SPs were rich in AChE. As the SPs matured, the amount of A $\beta$  increased, while the number of neurites and the activity of AChE decreased. End-stage amyloid-rich SPs lacked AChE [59]. These observations may indicate that changes in the cortical cholinergic innervation are important features in the pathogenesis and the evolution of neuritic SPs.

Heparan sulfate, heparinase lyase type I and to a lesser degree heparin and chondroitin sulfate are effective in solubilizing a large part of the ChE activity. Therefore, it has been proposed that AChE is anchored to and may be released from heparan sulfate glycosaminoglycans shown to be contained in the lesions [28]. It has also been suggested that the localization of ChEs is closely associated with the accumulation of the glycosaminoglycans in the SPs and NFTs [28].

A two-site immunoassay was performed for human brain AChE where autopsy samples of cortical regions A-9, A-10, A-17, A-21 and A-22 and subcortical regions (nucleus accumbens and hippocampus) from six non-neurological cases and five patients with AD were compared [25, 51]. A highly significant deficit of AChE protein was shown, averaging about 60%. Simultaneous immunoassays and measurements of enzyme activity, as determined spectrophotometrically, revealed a closely similar deficit in both cases. It was therefore concluded that in parallel with the enzyme activity decrease there is no immunoreactively impaired AChE in the AD brain. In other words, there is no accumulation of inactive AChE protein in the AD brain.

### *Cholinesterase activities and their molecular forms in the normal and the Alzheimer's disease central nervous system*

In the human brain, the total ChE level and the distributions of the molecular forms vary from region to region. Both AChE and BuChE are expressed as multiple molecular forms, including globular monomers ( $G_1$ ), dimers ( $G_2$ ) and tetramers ( $G_4$ ) of catalytic subunits, as well as asymmetric molecules with one ( $A_4$ ), two ( $A_8$ ) or three ( $A_{12}$ ) tetramers attached to a three-stranded collagen-like coiled structure. The molecular forms can be separated



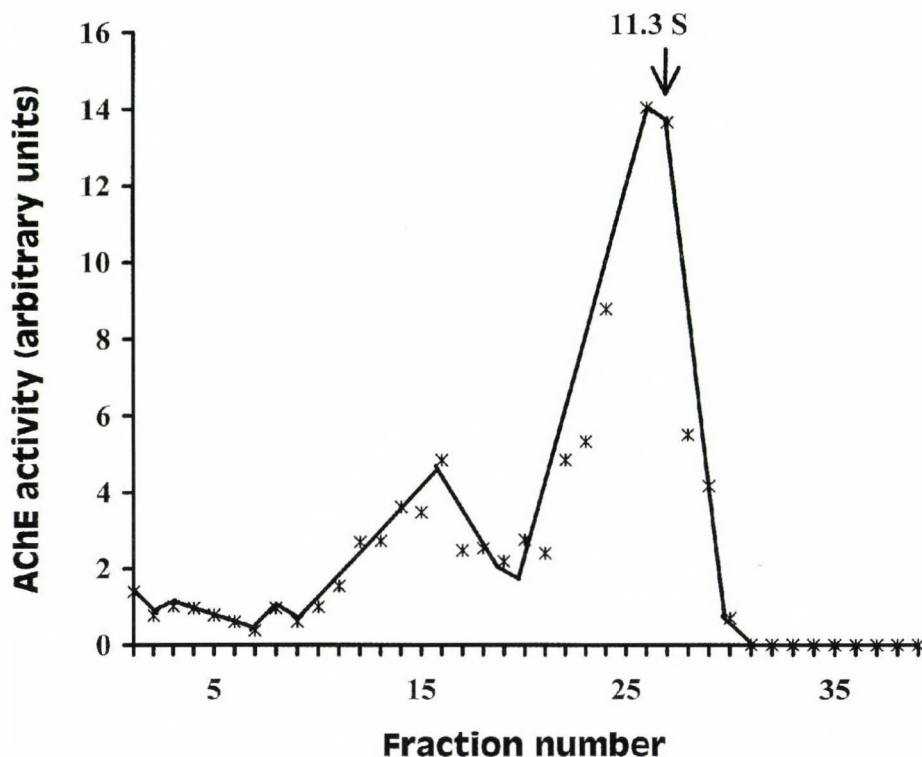


Fig. 2. Pattern of AChE molecular forms in human brain cortex. Tissues were homogenized in 10 vol. of 12.5 mM phosphate buffer, pH 7.4, and centrifuged at 100,000 g for 1 h. The supernatant was discarded and the pellet was rehomogenized in the same buffer containing 0.5% Triton X-100. After centrifugation as above, the supernatant was used as membrane-associated AChE. 0.4 ml supernatant was layered onto a 5-20% w/v sucrose gradient. The gradients were run in an SW 41 rotor for 18 h at 38,000 rpm (178,000 g) and fractions were collected from top to the bottom. Catalase (11.3 S) was used as an internal marker enzyme

by ultracentrifugation in sucrose density gradients and their sedimentation velocities can be determined. On the other hand, on the basis of the *in vitro* solubility characteristics, three main types of AChE can be distinguished: (1) high-salt-soluble, (2) low-salt-soluble and (3) detergent-soluble. The detergent-soluble forms are regarded as hydrophobic, membrane-associated enzymes, while the low- and high-salt-soluble enzyme forms are hydrophilic. The carbohydrate composition of the membrane-bound forms of AChE from the brain varies, as seen by interactions with lectins, suggesting an additional level of complexity of ChE polymorphism [34]. Although the significance of the different molecular forms is not clear, their tissue distribution is thought to reflect a specific physiological function and may change in pathological states [48, 50]. Within the central nervous system (CNS), the proposed physiological functions of the ChEs are probably mediated

through  $G_4$  AChE (10 S), though the  $G_1$  (4 S) is also present in small amounts in the human brain (Fig. 2).

Biochemically, the cholinergic deficit is reflected by a 10–60% loss of AChE in afflicted brain regions [11]. The selective loss of  $G_4$  (10S) AChE molecular forms in the parietal cortex (Brodmann area 40), together with a decrease in enzyme activity in autopsied material from patients with AD, was demonstrated about fifteen years ago [2]. The  $G_4$  form is of particular interest, since it is the most prevalent form in the brain [47]. Later, the above results were confirmed and extended to cover more brain areas [15, 55]. Taken together, all groups found decreases in the enzyme activity or in the ratio  $G_4/G_1$  in Brodmann areas 7, 8, 9, 10, 11, 21, 22 and 40 and the amygdala, but did not observe changes relative to age-matched controls in Brodmann areas 17 and 20, or in the hippocampus, nucleus caudatus, substantia nigra or cerebellum (Table 1). They proposed that there is a predominant loss of the  $G_4$  form of AChE in AD and that this loss is correlated with the degeneration of presynaptic elements which may be directly involved in the regulation of AChE transmission, sparing the cortical  $G_1$  form. The latter form is apparently associated with postsynaptic structures unaffected in this disease. In addition, the ratio  $G_4/G_1$  for BuChE was decreased by 20–40%, which was slightly less than the loss for AChE [1] (Table 1).

The changes in the distribution of the AChE molecular forms were studied in Brodmann area 21 of AD cases [67]. It was found that there were no changes in the distribution of the soluble  $G_1$  and  $G_4$  forms, but there was a significant (40%) decrease in the membrane-associated  $G_4$  AChE [54]. Moreover, 342% and 406% increases were noted in the asymmetric  $A_{12}$  and  $A_8$  AChE. These molecular forms are difficult to quantitate unless separated from the globular ones. The increases in the asymmetric forms were small in absolute terms, but large when expressed as percentages of the control. It has been suggested that the increase in asymmetric AChEs reflected an impairment of fast axonal transport on the axons of diseased cholinergic neurons projecting from the basal forebrain to the cerebral cortex [67]. Alternatively, this increase may be due to a sprouting phenomenon or neural plasticity to compensate degenerating cholinergic fibers in early AD. Interestingly, these asymmetric forms barely exist in the normal brain, and their elevated levels may be connected with the pathological lesions in AD.

Accumulation of AChE activities in AD brain fractions enriched with SPs and NFTs has been confirmed [39]. After digestion with collagenase and trypsin, only the  $G_4$  enzyme was found in the supernatant. From these results, it was concluded that the AChE in the SPs and NFTs might be of the asymmetric type, anchored to the SPs through a collagen tail.

Interestingly, a high abundance of  $G_1$  and a low ratio  $G_4/G_1$  were found for both AChE and BuChE in the human embryonic brain, resembling the pattern observed in AD [1]. On the other hand, both in the embryonic brain and in AD AChE shows no substrate inhibition, which is a constant feature of the enzyme in the adult human brain. It was therefore concluded that the degeneration of the cholinergic cortical afferentation in AD is reflected by a decrease in AChE  $G_4$ . This decrease is accompanied by the process of a neuritic sprouting response involved in SP formation, which is probably associated with the expression of a developmental form of the enzyme. On the other hand, substrate inhibition is



dependent on the integrity of the peripheral site, and it might therefore be possible that in AD point mutation(s) in AChE gene or *in situ* membrane disturbances are the actual cause of this phenomenon.

*Table 1*  
Ratios of molecular forms of cholinesterases  
in area dissected from postmortem brains of patients  
with Alzheimer's disease and controls

Area	AChE G <sub>4</sub> /G <sub>1</sub> ratio (% of control)	References
Broodman region		
A7	52.1	[1]
A9	49.5	[15]
A10	48.7	[15]
A11	45.5	[15]
A17	N.S.	[15]
A20	N.S.	[15]
A21	59.4	[15]
A22	32.8	[1]
A23	N.S.	[1]
A24	N.S.	[55]
A40	48.4	[15]
Amygdala		
Cortical nucleus	N.S.	[55]
Lateral basal nucleus	33.4	[55]
Medial basal nucl.	N.S.	[55]
Lateral nucl.	N.S.	[55]
Hippocampus	N.S.	[15]
Hippocampus area		
CA1	66.7	[55]
CA2/3	N.S.	[55]
CA4	69.7	[55]
Nucleus caudatus	N.S.	[1]
Nucleus basalis	54.9	[1]
Substantia nigra	N.S.	[55]
Cerebellum	N.S.	[15]
BuChE G <sub>4</sub> /G <sub>1</sub> ratio (% of control)		
Brodman region		
A7	68.7	[1]
A8	62.1	[1]
A20	75.4	[1]
Hippocampus	77.0	[1]
Nucleus caudatus	67.4	[1]
Nucleus basalis	59.7	[1]

Differences from controls are statistically significant unless indicated N.S. (= non significant).

ChAT and AChE were measured in the anterior and posterior gray matter of the lumbar spinal cord of AD patients and controls [66]. While the ChAT level was reduced, that of AChE was unaltered in the AD spinal cord. The decreased spinal cord ChAT level may be related to electrophysiological abnormalities that have been reported in the motor nerves of patients with AD. However, it should be noted that AD patients seldom present with motor symptoms.

*In vitro effects of clinically significant inhibitors on the cholinesterases and their molecular forms*

Table 3 shows the *in vitro* IC<sub>50</sub> values of 6 different inhibitors (Table 2) on human cholinesterases. They inhibit both AChE and BuChE to different degrees. Ambenonium has the highest specificity for AChE, followed by neostigmine. Physostigmine was equally well effective for both AChE and BuChE. Tacrine and heptyl-physostigmine inhibit BuChE more effectively than AChE.

Table 2  
Pharmacologically important cholinesterase inhibitors

Compound	Company	Clinical phase
Cognex (Tacrine)	Warner-Lambert	Registered
Aricept (Donepezil)	Eisai	Registered
Eptastigmine	Mediolanum	III
TAK-147	Takeda	III
ENA 713	Sandoz	III
Metrifonat	Bayer/Miles	III
Huperzin A	Chinese Acad. Sci.	III

Table 3  
Inhibition of human cholinesterases by representative drugs

Inhibitor	IC <sub>50</sub> (μM)		Selectivity BuChE/AChE
	AChE*	BuChE**	
Ambenonium	0.004	12.7	3175
Neostigmine	0.025	0.148	5.9
Physostigmine	0.018	0.018	1
Tacrine	0.45	0.063	0.14
Metrifonate	1.08	0.182	0.17
Heptyl-physostigmine	0.044	0.004	0.09

\*cortex, \*\*plasma



The effects of three clinically significant AChE inhibitors, physostigmine, a novel carbamate derivative of physostigmine (heptyl-physostigmine) and edrophonium, on the water-soluble AChE molecular forms in the caudate-putamen region were investigated [41]. Heptyl-physostigmine exhibited preferential inhibition for the  $G_1$  form. In contrast, edrophonium inhibited the  $G_4$  form more potently than the  $G_1$  form. Physostigmine inhibited the two forms with similar potency. These findings suggest a possible therapeutic application of a  $G_1$ -selective inhibitor in inhibiting the  $G_1$  form, which is relatively unchanged in the AD brain [41].

The influence of various AChE inhibitors ((+)(S)-N-ethyl-3-[(1-dimethylamino)ethyl]-N-methylphenylcarbamate hydrogentartrate (Sandoz, Basle, SDZ ENA 713, a novel centrally selective inhibitor), physostigmine, heptyl-physostigmine and 1,2,3,4-tetrahydro-9-aminoacridine, tacrine (THA) on the  $G_1$  and  $G_4$  forms of AChE isolated from *post-mortem* brain tissue from patients with AD was studied [14]. It was found that physostigmine and THA inhibited the  $G_1$  and  $G_4$  forms equally well, as expressed by the near unity value of the  $IC_{50}$  ratio  $G_4/G_1$ .

On the basis of the histochemical and biochemical investigations on AD brains, it has been suggested that ChEs have different properties as regards the interactions with substrates and inhibitors from those of the enzymes in the normal brain (see AChE histochemistry in AD). No difference in AChE activity between the control and AD groups was found in the hydrophilic, salt-soluble fraction [14]. However, the detergent-soluble membrane-bound enzyme activity was reduced by 70–80% in all brain regions (cortex, hippocampus and striatum) from AD cases [14]. Kinetic experiments revealed that the affinity of the enzyme for its substrate ( $K_m$ ) was similar in the control and the AD groups. As a consequence of the loss of enzyme, the apparent  $V_{max}$  values were decreased in the AD brains [4].

Highly potent, selective and low-cost bifunctional AChE inhibitors have been developed by utilizing computer modeling of ligand docking with target protein [42]. Eleven alkylene-linked bis-THA analogs were synthesized. These analogs were up to 10,000-fold more selective and 1,000-fold more potent than THA in inhibiting rat serum BuChE or rat brain AChE [42]. The computational studies strongly suggest that a low-affinity THA peripheral site exists in AChE. These compounds may be useful in the near future to replace THA; the therapeutic dose could thereby be lowered and the hepatotoxic side-effects prevented.

A novel AChE inhibitor, TAK-147 (3-[1-phenyl-4-piperidinyl]-1-(2,3,4,5-tetrahydro-1H-1-benzazepin-8-yl)-1-propanone fumarate, induced a potent and reversible inhibition of AChE activity in homogenates of the rat cerebral cortex ( $IC_{50} = 51.2$  nM). It was 3.0- and 2.4-fold more potent than THA and physostigmine, respectively [26]. In addition to AChE inhibition, TAK-147 also moderately activates the monoaminergic system [26].

Finally, it must be noted that almost all of the morphological and biochemical abnormalities seen in AD can also be seen (but to a much lower extent) in normal, non-demented, aged human brains. Moreover, in one-third of Parkinson's disease patients the cholinergic deficit is similar to that in AD [53]; the cholinergic deficit may therefore be one of the characteristic signs of dementia, but it does not seem to be specific for AD.

### *Therapeutic approaches to Alzheimer's disease with cholinesterase inhibitors*

Considerable advances have recently been made in our understanding of the neurobiologic features of AD. Many other transmitter systems are affected by this disease, but the cholinergic system is most consistently effected and most studied, and it now forms one of the targets for therapeutic intervention. Unfortunately, in clinical practice AD is a heterogeneous disorder; patient populations can be divided up into subgroups, e.g. familial versus sporadic disease, rapid versus slow progression, early versus late onset, or responders versus nonresponders to cholinergic therapy. Nevertheless, the best-developed approach to cholinergic therapy so far has been the use of cholinergic inhibitors and it is still the most promising (Table 2), since precursor loading with choline or phosphatidylcholine is ineffective. The concept behind the use of ChE inhibitors is the restoration of the cholinergic balance, at least for a while, through elevation of the ACh levels and augmentation of the function of the remaining ACh receptors. Drugs promoting the cholinergic function were therefore proposed for the treatment of AD. Particularly AChE and BuChE were used as molecular targets of pharmacological intervention.

There is generally some temporary improvement after anti-ChE treatment, but cholinergic side-effects due to peripheral ACh stimulation can sometimes be severe (abdominal cramps, nausea, diarrhea, vomiting, anorexia, weight loss, insomnia, myopathy, mental depression). Particularly in the cases involved in the earliest studies with the first generation of fairly specific AChE inhibitors such as physostigmine, the results were mixed but showed promise [12]. The disadvantages of using physostigmine include its very short duration of action (minutes) and the need for optimization for individual patients. Furthermore, the bioavailability of orally administered physostigmine is unpredictable and renders the handling of this drug difficult in the clinic. Nevertheless, the first positron emission tomography images of human brain AChE with [ $^{11}\text{C}$ ]physostigmine as tracer have recently been reported, showing the *in vivo* regional distribution of AChE. The cerebral distribution was typical of AChE activity: putamen-caudate > cerebellum > brainstem > thalamus > cerebral cortex [43]. It was suggested that this method allows a noninvasive *in vivo* determination of the cerebral AChE content, which is promising for study of the changes in AChE levels associated with neurodegenerative diseases such as AD. Moreover, it may provide an early diagnosis, and offers an assessment of the clinical efficacy of ChE inhibitor therapy.

The first long-acting anti-ChE drug, as a second generation of AChE inhibitors, to be approved by the Food and Drug Administration in the United States for use in AD therapy, is THA (Cognex), (Table 2). This drug penetrates the CNS and has a relatively low toxicity; it was first considered beneficial for AD patients [60]. However, THA has modest effects on 20–50% of the patients and has undesirable side-effects, including hepatotoxicity, which demands frequent monitoring of liver transaminases and autonomic symptoms. Furthermore, its bioavailability varies greatly from individual to individual. The experimental results reveal that THA exerts a wide variety of pharmacological actions in addition to its ability to block AChE: it also has regulatory effects on muscarinic and nicotinic receptors and on ACh synthesis, it inhibits GABA release, it stimulates dopamine,



histamine and 5-hydroxytryptamine release, it inhibits monoamine oxidase A and B, it has a marked ability to block potassium, sodium and calcium channels, and *in vitro* it can alter the secretion of amyloid precursor protein in cultured cell lines [16]. It is interesting to note that a subpopulation of AD patients, i.e. those lacking the ApoE4 allele, display a preferential improvement during THA treatment. In contrast, AD patients with at least one copy of the ApoE4 allele are insensitive to THA treatment [46]. However, there has recently been a report of a multicenter, double-blind, placebo-controlled trial of THA therapy, which included 663 patients suffering from mild to moderate AD. In this study, AD patients who were probably sensitive for THA therapy (>80 mg THA daily for 30 weeks) showed a delay in entering the nursing home [30].

The recently developed third generation of AChE inhibitors are donepezil (E2020, Aricept, 1-benzyl-4-[5,6-dimethoxy-1-indanon)-2-yl]methylpiperidine hydrochloride), heptyl-physostigmine, huperzine A and metrifonate (2,2,2-trichloro-1-hydroxyethylphosphonate, MTF), which have a longer duration and a lower toxicity. Donepezil-Aricept is the second drug approved by the FDA for treatment of the symptoms of mild to moderate AD. The results of multicenter, randomized, double-blind, placebo-controlled trials in the USA revealed that patients treated with donepezil showed dose-related improvements in the Alzheimer's Disease Assessment Scale, cognitive subscale and Mini Mental State Examination scores [52]. There was a statistically significant correlation between the plasma concentration of donepezil and the extent of AChE inhibition. In addition, donepezil had no clinically significant effect on vital signs, hematology or clinical biochemistry tests, was not associated with any hepatotoxicity and had fewer side-effects than observed with THA [52].

Heptyl-physostigmine (also known as eptastigmine) is a derivative of physostigmine (Table 2). Compared with physostigmine, heptylphysostigmine has less side-effects and a longer duration of action. A multicenter study was recently carried out according to a double-blind, randomized, placebo-controlled, unbalanced parallel-group design, with 83 subjects in the eptastigmine group and 20 in the placebo group [5]. This study showed that doses of 40–60 mg of eptastigmine per day are relatively safe and well tolerated, and that moderate AChE inhibition is associated with maximal cognitive efficacy.

(-)-Huperzine A is a very potent reversible blocker of AChE, with an average  $K_i$  value of 8 nM [33]. Racemic (+/-)-huperzine A was about twofold less potent than the more active (-) isomer in the inhibition of rat cortical AChE. It has also been suggested that it could be superior to physostigmine and THA for the treatment of AD and other cholinergic-related impairments [33]. Huperzine A can reduce glutamate-induced toxicity besides selectively inhibiting AChE [62]. Huperzine A could therefore be a potent neuroprotective agent not only where cholinergic neurons are impaired, but under conditions in which glutamatergic functions are compromised [62]. Accordingly, *in vivo* studies have indicated the potential of this drug to improve memory in humans [68].

A 3-month double-blind study has been completed to compare MTF with placebo in 50 patients with probable AD [3]. The MTF was dosed to achieve a 40–60% inhibition of red blood cell AChE activity. At completion of 3 months of treatment, the ADAS-cog subscale score in the MTF group differed from that in the placebo group by 2.6 points ( $p < 0.01$ ); there were also significant differences in the Global Improvement Scale

( $p < 0.02$ ) and Mini-Mental State Examination scores ( $p < 0.03$ ). Moreover, less than expected deterioration was found in AD patients who received MTF for up to 18 months [3]. It was concluded that MTF may slow the rate of decline in AD.

In clinical practice, AD is a heterogeneous disorder (see above). The evidence is clear that ChE inhibitors will not be a treatment that can be used on every patient with AD. The effects are modest, and the high incidence of side-effects and the intensive monitoring during treatment complicate the management. Given these considerations, it is possible to conclude that inhibitors are effective only in mild to moderate AD cases.

Finally, many new ChE inhibitors are now undergoing clinical trials (Table 2). The development of chemically novel AChE inhibitors that are relatively safe remains a therapeutic goal and hopefully some of them will come into clinical use in the very near future. However, although there is currently no way to stop progression, ChE inhibitors provide an effective temporary relief of symptoms in some patients. The final point is that there is a great need for better treatment, and especially treatment that has a more primary effect in preventing the development or possibly delaying the disease.

#### ACKNOWLEDGEMENT

Supported by grants OTKA T022683, T026470, ETT 652J96 and MKM 36 and an MKM Széchenyi Professorship.

#### REFERENCES

1. Arendt, T., Bruckner, M., Lange, M., Biegl, V. (1992) Changes in acetylcholinesterase and butyrylcholinesterase in Alzheimer's disease resemble embryonic development: a study of molecular forms. *Neurochem. Int.* 21, 381–396.
2. Atack, J. R., Perry, E. K., Bonham, J. R., Perry, R. H., Tomlinson, B. E., Blessed, G., Fairbairn, A. (1983) Molecular forms of acetylcholinesterase in senile dementia of Alzheimer's type: selective loss of the intermediate (10S) form. *Neurosci. Lett.* 40, 199–204.
3. Becker, R. E., Colliver, J. A., Markwell, S. J., Moriearty, P. L., Unni, L. K., Vicari, S. (1996) Double-blind, placebo-controlled study of metrifonate, an acetylcholinesterase inhibitor, for Alzheimer's disease. *Alzheimer Disease Assoc. Disorders* 10, 124–131.
4. Bierer, L. M., Haroutunian, V., Gabriel, S., Knott, J. P., Carlin, L. S., Purohit, D. P., Perl, D. P., Schmeidler, J., Kanof, P., Davis, K. L. (1995) Neurochemical correlates of dementia severity in Alzheimer's disease: Relative importance of the cholinergic deficits. *J. Neurochem.* 64, 749–760.
5. Canal, N., Imbimbo, B. P. (1996) Relationship between pharmacodynamic activity and cognitive effects of eptastigmine in patients with Alzheimer's disease. *Clin. Pharmacol. Ther.* 60, 218–228.
6. Carson, K., Geula, C., Mesulam, M.-M. (1991) Electron microscopic localization of cholinesterase activity in Alzheimer brain tissue. *Brain Res.* 540, 204–208.
7. Checkler, F., Vincent, J. P. (1989) Peptidatic activity associated with acetylcholinesterase are due to contaminating enzymes. *J. Neurochem.* 53, 924–928.
8. Chubb, I. W., Hodgson, A. J., White, G. H. (1980) Acetylcholinesterase hydrolyzes substance P. *Neuroscience* 5, 2065–2072.
9. Chubb, I. W., Ranieri, E., White, G. H., Hodgson, A. J. (1983) The enkephalins are amongst the peptides hydrolyzed by purified acetylcholinesterase. *Neuroscience* 10, 1369–1377.
10. Coleman, A. E., Geula, C., Price, B. H., Mesulam, M.-M. (1992) Differential laminar distribution of acetylcholinesterase and butyrylcholinesterase containing tangles in the cerebral cortex of Alzheimer's disease. *Brain Res.* 596, 340–344.



11. Davies, P., Maloney, A. J. F. (1976) Selective loss of central cholinergic neurons in Alzheimer's disease. *Lancet* 2, 1403.
12. Davis, K. L., Mohs, R. C., Tinklenberg, J. R., Davis, B. M., Pfefferbaum, A., Hollister, L. E., Koppell, B. S. (1978) Physostigmine: improvement of long-term memory process in normal humans. *Science* 201, 272–274.
13. Ellman, G. L., Courtney, D. K., Andres, V., Featherstone, R. M. (1961) A new and rapid colorimetric determination of acetylcholinesterase activity. *Biochem Pharmacol.* 7, 88–95.
14. Enz, A., Chappuis, A., Probst, A. (1992) Different influence of inhibitors on acetylcholinesterase molecular forms G1 and G4 isolated from Alzheimer's disease and control brains. In: Shafferman, A., Velan, B. (eds) *Multidisciplinary Approaches to Cholinesterase Functions*. Plenum Press, New York, pp. 243–249.
15. Fishman, E. B., Siek, G. C., MacCallum, R. D., Bird, E. D., Volicer, L., Marquis, J. K. (1986) Distribution of the molecular forms of acetylcholinesterase in human brain: alterations in dementia of Alzheimer type. *Ann. Neurol.* 19, 246–252.
16. Freeman, S., Dawson, R. M. (1991) Tacrine: A pharmacological review. *Progr. Neurobiol.* 36, 257–277.
17. Friede, R. L. (1965) Enzyme histochemical studies of senile plaques. *J. Neuropathol. Exp. Neurol.* 24, 447–491.
18. Geula, C., Mesulam, M.-M. (1989) Special properties of cholinesterases in the cerebral cortex of Alzheimer's disease. *Brain Res.* 498, 185–189.
19. Geula, C., Brimijoin, S., Mesulam, M.-M. (1992) Immunochemical detection of cholinesterases in Alzheimer's plaques and tangles. *Neurology* 41, 376.
20. Geula, C., Mash, D. C., Mesulam, M.-M. (1994) Loss of cortical cholinergic fibers in Alzheimer's disease: lack of a relationship with amyloid deposits and a strong relationship with tangle density. *Neurobiol. Aging* 15, S120.
21. Geula, C., Mesulam, M.-M. (1989) Cortical cholinergic fibers in aging and Alzheimers's disease: a morfometric study. *Neuroscience* 33, 469–481.
22. Geula, C., Mesulam, M.-M. (1995) Cholinesterases and pathology of Alzheimer disease. *Alzheimer Disease Assoc. Disorders* 9, Suppl. 2, 23–28.
23. Geula, C., Mesulam, M.-M. (1996) Systematic regional variations in the loss of cortical cholinergic fibers in Alzheimer's disease. *Cerebral Cortex* 6, 165–177.
24. Giacobini, E. (1997) From molecular structure to Alzheimer Therapy. *Jpn. J. Pharmacol.* 74, 25–241.
25. Hammond, P., Brimijoin, P. (1988) Acetylcholinesterase in Huntington's and Alzheimer diseases: Simultaneous enzyme assay and immunoassay of multiple brain regions. *J. Neurochem.* 50, 1111–1116.
26. Hirai, K., Kato, K., Nakayama, T., Hayako, H., Ishihara, Y., Goto, G., Miyamoto, M. (1997) Neurochemical effects of (3-[1-(phenyl)-4-piperidinyl]-1-(2,3,4,5-tetrahydro-1H-1-benzazepin-8-yl)-1-propanon fumarate (TAK-147), a novel acetylcholinesterase inhibitor, in rats. *J. Pharm. Exp. Ther.* 280, 1261–1269.
27. Johnson, C. D., Russel, R. L. (1975) A rapid, simple radiometric assay for cholinesterase, suitable for multiple determinations. *Anal Biochem.* 64, 229–238.
28. Kalaria, R. N., Kroon, S. N., Grahovac, I., Perry, G. (1992) Acetylcholinesterase and its association with heparan sulphate proteoglycans in cortical amyloid deposits of Alzheimer's disease. *Neuroscience* 511, 77–184.
29. Kása, P., Rakonczay, Z., Gulya, K. (1997) The cholinergic system in Alzheimer's disease. *Progr. Neurobiol.* 52, 511–535.
30. Knopman, D., Schneider, L., Davis, K., Talwalker, S., Smith, F., Hoover, T., Gracon, S. (1996) Long-term tacrine (Cognex) treatment: Effects on nursing home placement and mentality. *Neurology* 47, 166–177.
31. Layer, P. G. (1995) Novel function of cholinesterases in physiology, pathology and development. *Progr. Histochem. Cytochem.* 29, 1–92.

32. Layer, P. G. (1995) Nonclassical roles of cholinesterases in the embryonic brain and possible links to Alzheimer disease. *Alzheimer Disease Assoc. Disorders* 9, Suppl. 28, 29–36.
33. McKinney, M., Miller, J. H., Yamada, Tuckmantel, F. W., Kozikowski, A. P. (1991) Potencies and stereoselectivities of enantiomers of huperzine A for inhibition of rat cortical acetylcholinesterase. *Eur. J. Pharmacol.* 203, 303–305.
34. Meflah, K., Bernard, S., Massoulié, J. (1984) Interaction with lectins indicate differences in the carbohydrate composition of the membrane-enzymes acetylcholinesterase and 5'-nucleotidase in different cell types. *Biochimie* 66, 59–69.
35. Mesulam, M.-M., Carson, K., Price, B., Geula, C. (1992) Cholinesterases in the amyloid angiopathy of Alzheimer's disease. *Ann. Neurol.* 31, 565–569.
36. Mesulam, M.-M., Geula, C. (1994) Butyrylcholinesterase reactivity differentiates the amyloid plaques of aging from those of dementia. *Ann. Neurol.* 36, 722–727.
37. Mesulam, M.-M., Geula, C., C. Moran, M.A. (1987) Anatomy of cholinesterase inhibition in Alzheimer's disease: effect of physostigmine and tetrahydroaminoacridine on plaques and tangles. *Ann. Neurol.* 22, 683–691.
38. Mesulam, M.-M., Moran, M. A. (1987) Cholinesterases within neurofibrillary tangles related to age and Alzheimer's disease. *Ann. Neurol.* 22, 223–228.
39. Nakamura, S., Kawashima, S., Nakano, S., Tsuji, T., Araki, W. (1990) Subcellular distribution of acetylcholinesterase in Alzheimer's disease: abnormal localization and solubilization. *J. Neural Transm. Suppl.* 30, 13–23.
40. Navaratnam, D. S., Proddle, J. D., McDonald, B., Esiri, M. M., Robinson, J. R., Smith, A. D. (1991) Anomalous molecular form of acetylcholinesterase in cerebrospinal fluid in histologically diagnosed Alzheimer's disease. *Lancet* 337, 447–450.
41. Ogane, N., Giacobini, E., Struble, R. (1992) Differential inhibition of acetylcholinesterase molecular forms in normal and Alzheimer disease brain. *Brain Res.* 589, 307–312.
42. Pang, Z.-P., Quiram, P., Jelacic, T., Hong, F., Brimijoin, S. (1996) Highly potent, selective, and low cost bis-tetrahydroaminacrine inhibitors of acetylcholinesterase. *J. Biol. Chem.* 271, 23646–23649.
43. Pappata, S., Tavitian, B., Traykov, L., Jobert, A., Dalger, A., Mangin, J. F., Crouzel, C., Di Giambardino, L. (1996) In vivo imaging of human cerebral acetylcholinesterase. *J. Neurochem.* 67, 876–879.
44. Perry, E. K., Tomlinson, B. E., Blessed, G., Bergmann, K., Gibson, P. H., Perry, R. H. (1978) Correlation of cholinergic abnormalities with senile plaques and mental test scores in senile dementia. *Brit. Med. J.* 2, 1457–1459.
45. Perry, R. H., Blessed, G., Perry, E. K., Tomlinson, B. E. (1980) Histochemical observations on cholinesterase activities in the brains of elderly normal and demented (Alzheimer type) patients. *Age Aging* 9, 9–16.
46. Poirier, J., Delisle, M.-C., Quirion, R., Aubert, I., Forlow, M., Lahiri, D., Hiu, S., Bertrand, P., Nalbantoglu, J., Gilfix, B. G., Gauthier, S. (1995) Apolipoprotein E4 allele as a predictor of cholinergic deficits and treatment outcome in Alzheimer's disease. *Proc. Natl. Acad. Sci. USA.* 92, 12260–12264.
47. Rakonczay, Z. (1986) Mammalian brain acetylcholinesterase. In: Boulton, A. A., Baler, G. B., Yu, P. H. (eds), *Neuromethods. Neurotransmitter Enzymes*. Vol. 5, Humana Press, Inc. Clifton, New Jersey, pp. 319–360.
48. Rakonczay, Z. (1988) Cholinesterase and its molecular forms in pathological states. *Prog. Neurobiol.* 31, 311–330.
49. Rakonczay, Z., Vincendon, G., Zanetta, J.-P. (1981) Heterogeneity of rat brain acetylcholinesterase: A study by gel filtration and gradient centrifugation. *J. Neurochem.* 37, 662–669.
50. Rakonczay, Z., Brimijoin, S. (1988) Biochemistry and pathophysiology of the molecular forms of cholinesterases. *Subcell. Biochem.* 12, 335–378.
51. Rakonczay, Z., Brimijoin, S. (1988) Monoclonal antibodies to human brain acetylcholinesterase: Properties and applications. *Cell. Molec. Neurobiol.* 8, 85–93.



52. Rogers, S. L., Friedhoff, L. T. (1996) The Donepezil Study Group. The efficacy and safety of donepezil in patients with Alzheimer's disease: Results of a US multicentre, randomized, double-blind, placebo-controlled trial. *Dementia* 7, 293–303.
53. Ruberg, M., Rieger, F., Villageois, A., Bonnet, A. M., Agid, Y. (1986) Acetylcholinesterase and butyrylcholinesterase in frontal cortex and cerebrospinal fluid of demented and non-demented patients with Parkinson's disease. *Brain Res.* 362, 83–91.
54. Schegg, K. M., Harrington, L. S., Nielsen, S., Zweig, R. M., Peacock, J. H. (1992) Soluble and membrane-bound forms of brain acetylcholinesterase in Alzheimer's disease. *Neurobiol. Aging* 13, 697–704.
55. Siek, G. C., Katz, L. S., Fishman, E. B., Korosi, T. S., Marquis, J. T. (1990) Molecular forms of acetylcholinesterase in subcortical areas of normal and Alzheimer's disease brain. *Biol. Psychiatry* 27, 573–580.
56. Small, D. H., Michaelson, S., Sberna, G. (1996) Non-classical actions of cholinesterases: Role in cellular differentiation, tumorigenesis and Alzheimer's disease. *Neurochem. Int.* 28, 453–483.
57. Smith, A. D., Cuello, A. C. (1984) Alzheimer's disease and acetylcholinesterase-containing neurons. *Lancet* 331, 513.
58. Smith, A. D., Jobst, K. A., Navaratnam, D. S., Shen, Y. X., Priddle, J. D., McDonald, B., King, E., Esiri, M. M. (1991) Anomalous acetylcholinesterase in lumbar CSF of Alzheimer's disease. *Lancet* 338, 1538.
59. Struble, R. G., Cork, L. C., Whitehouse, P. L., Price, D. L. (1982) Cholinergic innervation in neuritic plaques. *Science* 216, 413–415.
60. Summers, W. K., Majovski, L. V., Marsh, G. M., Tachiki, K., Kling, A. (1986) Oral tetrahydroaminoacridine in long-term treatment of senile dementia, Alzheimer's type. *N. Engl. J. Med.* 315, 1241–1245.
61. Tago, H., Kimura, H., Meada, T. (1986) Visualization of detailed acetylcholinesterase fiber and neuron staining in rat brain by a sensitive histochemical procedure. *J. Histochem. Cytochem.* 34, 1431–1438.
62. Ved, H. S., Koenig, M. L., Dave, J. R., Doctor, B. P. (1997) Huperzin A, a potential therapeutic agent for dementia, reduces neuronal cell death caused by glutamate. *Neuroreport* 8, 963–968.
63. Whitehouse, P. L., Price, D. L., Clark, A. W., Coyle, J. T., DeLong, M. R. (1981) Alzheimer's disease: evidence for selective loss of cholinergic neurons in the nucleus basalis. *Ann. Neurol.* 10, 122–126.
64. Wright, C. I., Geula, C., Mesulam, M.-M. (1993) Protease inhibitors and indoleamines selectively inhibit cholinesterases in the histopathological structures of Alzheimer's disease. *Proc. natl. Acad. Sci. USA.* 90, 683–686.
65. Wright, C. I., Geula, C., Mesulam, M.-M. (1993) Neuroglial cholinesterases in the normal brain and in Alzheimer's disease: relationship to plaques, tangles and patterns of selective vulnerability. *Ann. Neurol.* 34, 373–384.
66. Yates, C. M., Simpson, J., Gordon, A., Christie, J. E. (1989) Cholinergic enzymes in spinal cord in Alzheimer-type dementia. *J. Neural Transm. P-D.* 1, 311–315.
67. Younkin, S. G., Goodridge, B., Katz, J., Lockett, G., Nafziger, D., Usiak, M. F., Younkin, L. H. (1986) Molecular forms of acetylcholinesterase in Alzheimer's disease. *Fed. Proc.* 45, 2982–2988.
68. Zhang, R.-W., Tang, X.-C., Han, Y.-Y., Sang, G.-W., Zhang, Y.-D., Ma, Z.-D., Zhang, C.-L., Yang, R.-M. (1991) Drug evaluation of huperzine-A in the treatment of senile memory disorders. *Acta Pharmacol. Sin.* 12, 250–252.

# AGED SYNTHETIC HUMAN AMYLOID $\beta$ -PEPTIDE 1-42 AND RELATED FRAGMENTS INDUCE DIRECT ACETYLCHOLINE RELEASE FROM RAT BASAL FOREBRAIN TISSUE SLICES\*

Mónika FORGON<sup>1</sup>, Z. FARKAS<sup>1</sup>, Magdolna PÁKÁSKI<sup>1</sup>, Márta ZARÁNDI<sup>2</sup> and B. PENKE<sup>2</sup>

<sup>1</sup>Alzheimer's Disease Research Centre and <sup>2</sup>Department of Medical Chemistry,  
Albert Szent-Györgyi Medical University, H-6720 Szeged, Hungary

(Received: 1998-06-12; accepted: 1998-06-26)

The direct effects of synthetic human amyloid  $\beta$ -peptide 1-42 (A $\beta$ 1-42), scrambled A $\beta$ 1-42 (MOD1 and MOD2), and related fragments (A $\beta$ 31-35, A $\beta$ 34-39, and A $\beta$ 17-21), either freshly dissolved (non-aged) or aged for 2, 4, 12 and 24 h, were studied on acetylcholine release from rat basal forebrain tissue slices. In *in vitro* tissue slices, A $\beta$ 1-42 aged for 2 h, and A $\beta$ 31-35 and A $\beta$ 34-39 aged for 24 h evoked acetylcholine release from the basal forebrain tissue slices in a Ca<sup>2+</sup>-dependent manner. Transmitter release was not observed on the use of freshly dissolved A $\beta$ 1-42 and scrambled A $\beta$ 1-42 (MOD1 and MOD2) and A $\beta$ 17-21 aged for 24 h. These data support the suggestion that it is the fibrillar (aggregated) form which is effective on the axon terminals and evokes direct acetylcholine release. It is proposed that one of the roles of A $\beta$  in the brain is the presynaptic modulation of acetylcholine release, in this way causing first an altered Ca<sup>2+</sup>-homeostasis, then cholinergic hypoactivity and finally the retrograde degeneration of cholinergic nerve cells.

**Keywords:** Amyloid  $\beta$ -peptide – aggregation – acetylcholine release – tissue slices – basal forebrain – Alzheimer's disease

## INTRODUCTION

Alzheimer's disease (AD) is a neurodegenerative disorder of the brain characterized by the presence of large numbers of degenerated nerve cells, neurofibrillary tangles and amyloid  $\beta$ -peptide (A $\beta$ )-containing senile plaques and a cholinergic hypofunction [for a review, see 12]. Morphological and neuropharmacological studies suggested that A $\beta$  contributes to the progression of AD and may be involved in the neuropathological degeneration of the cholinergic nerve cells. The exact mechanism of the cellular degeneration, however, is not yet understood. The results of neurotoxicologic studies revealed that the aggregated form of A $\beta$  may be the form that is toxic to different type of neurons [11, 26, 31]. Indeed, several authors have reported that freshly dissolved A $\beta$  has no effect, while the fibrillar and/or aggregated peptide may be toxic to cholinergic [10] and GABA-

\*Dedicated to Professor Péter Kása on the occasion of the 25th anniversary of his appointment as Head of the Central Research Laboratory and the Alzheimer's Disease Research Centre.

Send offprint requests to: Mónika Forgón, M.D., Alzheimer's Disease Research Centre, Albert Szent-Györgyi Medical University, H-6720 Szeged, Somogyi B. u. 4, Hungary.



ergic [21, 22] neurons. There is convincing evidence that the early degeneration of ascending cholinergic neurons contributes to AD dementia.

Preliminary *in vitro* neuropharmacological experiments demonstrated a prompt stimulatory effect of aged A $\beta$ 1-42 and related fragments (A $\beta$ 31-35 and A $\beta$ 34-39) on acetylcholine (ACh) release from rat brain tissue slices [10]. In contrast, freshly dissolved A $\beta$ 1-42 and A $\beta$ 1-40 and related peptides such as A $\beta$ 1-28 and A $\beta$ 25-35 inhibited the K<sup>+</sup>-evoked ACh release from slices of rat hippocampal and frontal cortex, but not the striatum [15, 16]. These controversial results led us to reinvestigate the effects of freshly dissolved (non-aged) and aged A $\beta$  peptides on ACh release from the rat basal forebrain, a region severely affected in AD. We examined the effects of freshly dissolved and aged A $\beta$  and some fragments and the effects of the presence and/or absence of Ca<sup>2+</sup> in the superfusion medium on the ACh release from basal forebrain tissue slices. The results demonstrate differences in the ACh release from tissue slices when freshly dissolved and aged A $\beta$  peptides are used. Moreover, the effects of these A $\beta$  peptides in enhancing A $\beta$ -evoked ACh release are Ca<sup>2+</sup>-dependent processes.

## MATERIALS AND METHODS

### *Materials*

Methyl-[<sup>3</sup>H]choline (choline chloride-methyl-<sup>3</sup>H; specific activity, 83 Ci/mmol) was purchased from Amersham International U.K.

Human A $\beta$  peptides, including A $\beta$ 1-42, A $\beta$ 31-35, A $\beta$ 34-39, MOD1, MOD2 and A $\beta$ 17-21, were synthesized in our Department of Medical Chemistry as described earlier [18]. The sequences of human A $\beta$ 1-42, the scrambled forms of A $\beta$ 1-42 and the related fragments used in our experiments were:

A $\beta$ 1-42:	DAEFRHDSGYEVHHQKLVFFAEDVGSNKGAIIGLMVGGGVIA
A $\beta$ 1-42 (MOD-1):	DAQSRHDSGAQSHHAKSASAAQDSGSNKGAIIGLMAGGSASA
A $\beta$ 1-42 (MOD-2):	DAQSRHDSGAQSHHAKSVFFAQDSGSASGAIIGLMAGGSASA
A $\beta$ 31-35:	IIGLM
A $\beta$ 34-39:	LMVGGV
A $\beta$ 17-21:	LVFFA

The purities of the peptides were checked by HPLC and their compositions were verified via their amino acid contents. NaCl, KCl, CaCl<sub>2</sub>, MgSO<sub>4</sub>, NaHCO<sub>3</sub>, NaH<sub>2</sub>PO<sub>4</sub>, D-glucose, acetonitrile, hemicholinium-3 (HC-3) and trifluoroacetic acid (TFA) were from Sigma (St. Louis, MO, USA). The scintillation cocktail Ultima Gold was from Packard (Groningen, NL).

### *Preparation of basal forebrain tissue slices and superfusion*

Adult male Sprague-Dawley rats (250–350 g) were used in the study. The animals were decapitated and the brains were immersed in ice-cold modified Krebs-Ringer buffer solution (KRS, in mM: NaCl 118, KCl 4.8,  $\text{CaCl}_2$  1.3,  $\text{MgSO}_4$  1.2,  $\text{NaHCO}_3$  25,  $\text{NaH}_2\text{PO}_4$  1.2 and D-glucose 10, adjusted to pH 7.4). A part of the basal forebrain was rapidly dissected out (Fig. 1), and 350- $\mu\text{m}$  thick slices were prepared with a McIlwain tissue chopper (Mickle Laboratory Engineering, Gomshall, Surrey, U.K.). The slices were washed and then incubated for 60 min at 37 °C in KRS containing 2  $\mu\text{Ci}/\text{ml}$  methyl- $[\text{}^3\text{H}]$ choline chloride (spec. act. 83 Ci/mmol) and 1.0 mM HC-3. No acetylcholinesterase inhibitor was added to the incubation medium; thus, the released  $[\text{}^3\text{H}]\text{ACh}$  converted to  $[\text{}^3\text{H}]\text{choline}$  is measured. The slices were then superfused for 70 min to remove any free tritium. Superfusion was maintained at a rate of 1.0 ml/min with KRS containing 1 mM HC-3, gassed continuously with 95%  $\text{O}_2/5\%$   $\text{CO}_2$ . Samples were collected every 3 min.

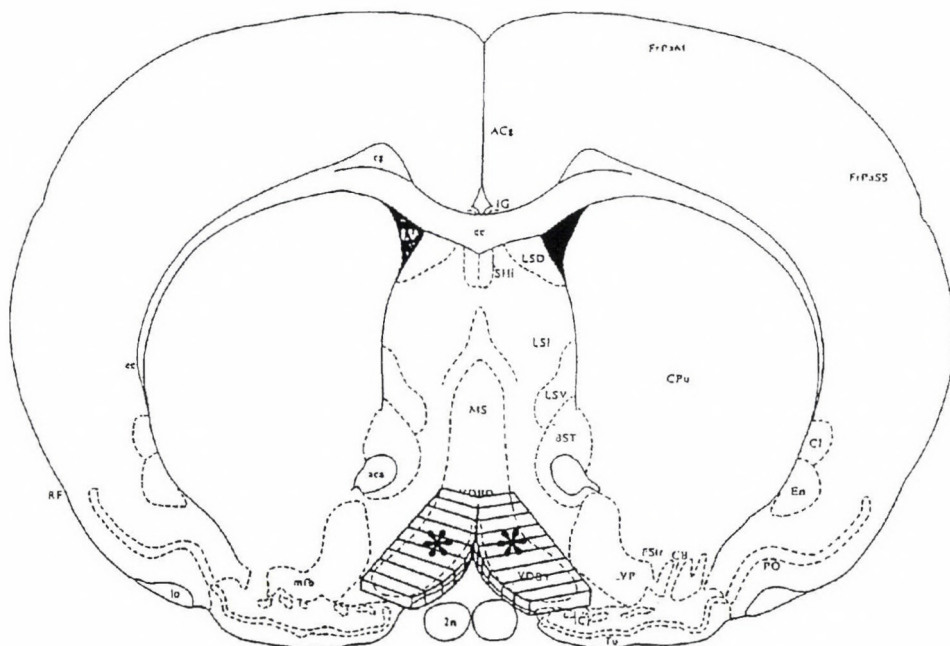


Fig. 1. Coronal section of rat brain, showing the basal forebrain region (caged area with asterisk) used in this study



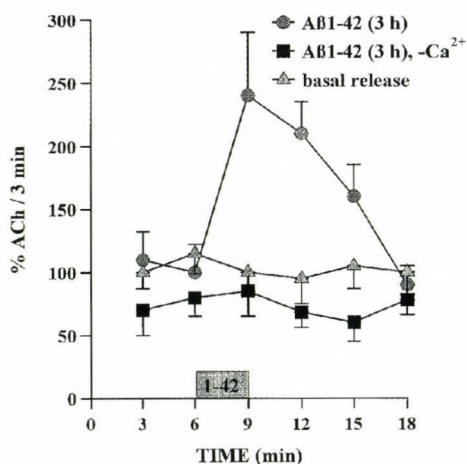


Fig. 2

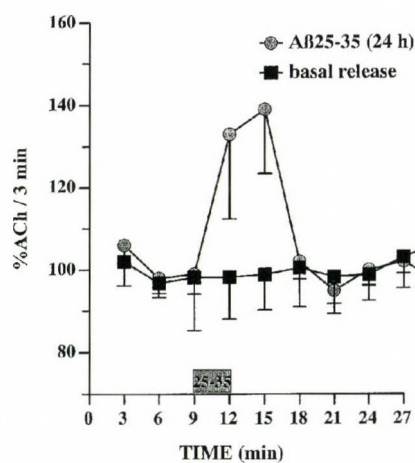


Fig. 3

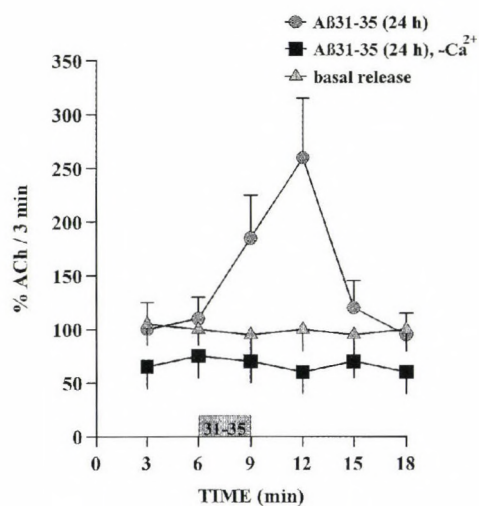


Fig. 4

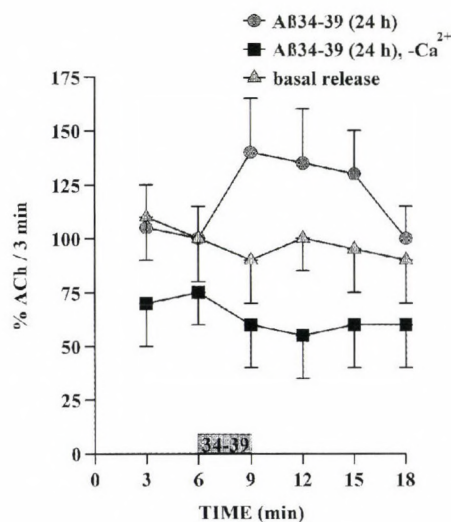


Fig. 5

Figs 2–5. Rates of ACh release induced with 20  $\mu$ M of A $\beta$ 1-42 aged for 3 h (Fig. 2), or A $\beta$ 25-35 (Fig. 3), A $\beta$ 31-35 (Fig. 4) and A $\beta$ 34-39 (Fig. 5) aged for 24 h. Note the effects of these peptides on the transmitter release and the effects of the omission of  $\text{Ca}^{2+}$  from the superfusion solution. No tritium release can be detected in the absence of  $\text{Ca}^{2+}$  from the superfusion solution

### Determination of tritium release

The tritium recovered following stimulation was analysed with a scintillation spectrometer. Tritium in the superfusate (3 ml) was detected, after addition of 6 ml of Ultima Gold LSC-cocktail, by liquid scintillation spectroscopy. After superfusion, the slices were homogenized in 0.5 ml KRS and transferred into scintillation vials containing 5 ml of Ultima Gold for determination of the radioactivity in the tissue slices. The recovery of radioactivity present in the superfusate and in the tissue slices was 95 to 98%.

### Preparation of $A\beta$ solution

$A\beta$ 1-42 was dissolved in acetonitrile and TFA solution at a concentration of 200  $\mu$ M (stock solution), and an aliquot was diluted tenfold with KRS and used as fresh solution. Other aliquots were aged for 2, 4, 12 or 24 h and used for further experiments.

## RESULTS

Figure 2 shows the rates of the  $A\beta$ 1-42-stimulated and the basal outflow of [ $^3$ H]choline from rat basal forebrain slices. Aged  $A\beta$ 1-42 (20  $\mu$ M) significantly increased the basal outflow of ACh in the presence of  $Ca^{2+}$ , but in the absence of  $Ca^{2+}$  the release of tritium fell below the basal ACh release. Similarly, 20  $\mu$ M  $A\beta$ 25-35 (Fig. 3), 20  $\mu$ M  $A\beta$ 31-35 (Fig. 4) and 20  $\mu$ M  $A\beta$  34-39 (Fig. 5) evoked transmitter release after aging for 12 or 24 h.

Figure 6 demonstrates that the shorter fragments of  $A\beta$  (31-35 and 34-39) also induced tritium release after aging for 24 h. No such effect was observed following the application of  $A\beta$ 17-21 or scrambled  $A\beta$ 1-42 (MOD1 and MOD2), even after aging for 24 h.

Figure 6 summarizes the results. It is demonstrated that the addition of freshly solubilized (non-aged)  $A\beta$ 1-42 and related fragments ( $A\beta$ 31-35 and  $A\beta$ 34-39) for 3 min to the medium superfusing basal forebrain tissue slices of rat preloaded with [ $^3$ H]choline caused

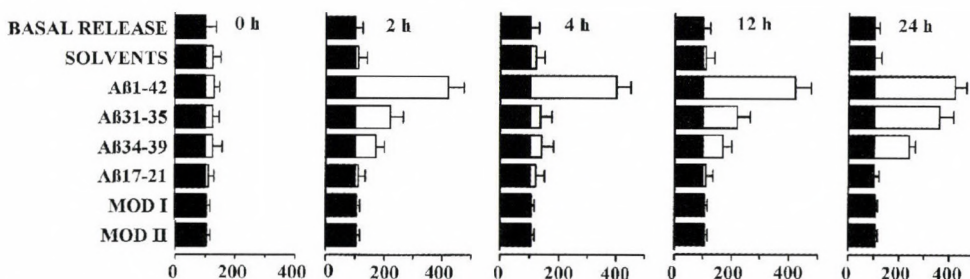


Fig. 6. The effects of aging of  $A\beta$ 1-42, MOD1 and MOD2, and the shorter peptide fragments on *in vitro* tritium release from the basal forebrain tissue slices of rat.  $A\beta$ 1-42 induces transmitter release within a period of 2 h, while similar effects of the other peptides can be demonstrated only after aging for 24 h



no significant tritium outflow over the basal values. Addition of A $\beta$ 1-42 aged for 2 h (in some experiments for 3 h), 4, 12 or 24 h to the superfusion solution significantly enhanced the tritium outflow, which subsequently (within 18 min after the onset of stimulation) returned to the basal values. No similar stimulation of tritium outflow was evoked by A $\beta$ 17-21 or the modified A $\beta$ 1-42 (MOD-1 and MOD-2).

## DISCUSSION

Our results clearly indicate that A $\beta$ 1-42 and related fragments (A $\beta$ 31-35 and A $\beta$ 34-39) can directly enhance the release of ACh *in vitro* from basal forebrain tissue slices [5, 11 and present results]. This effect is dependent on the presence of Ca<sup>2+</sup> in the superfusion solution. In contrast with our observations, others [1, 9, 15, 16] have reported that the release of ACh was decreased rather than increased by A $\beta$ 1-42, A $\beta$ 1-40, A $\beta$ 1-28 and A $\beta$ 25-35. Others observed various effects of A $\beta$ , such as an increase of neuronal membrane conductance [30], or of the choline conductance of PC12 cells [7], the induction of Ca<sup>2+</sup> currents in neuron-like human teratocarcinoma cells [28], an increase of Ca<sup>2+</sup> currents in rat cerebellar granule neurons [27], an enhanced leakage of choline out of cholinergic neurons [2], the opening of non-selective ion channels in rat cortical neurons [6], the decrease of ACh synthesis in a cell line derived from cholinergic neurons of the basal forebrain [25], a reduction of the GABA-induced Cl<sup>-</sup> current in *Aplysia* neurons [29], disruption of the Ca<sup>2+</sup> homeostasis by increasing the intraneuronal Ca<sup>2+</sup> concentration to induce an early and transient increase in the intracellular Ca<sup>2+</sup> level [2], and the induction of alterations in the intracellular Ca<sup>2+</sup> [17, 20, 32]. Although the various effects induced by A $\beta$  have been clearly demonstrated, there is as yet no agreement as to whether there is a specific receptor at the membrane surface for A $\beta$ , or whether the effect of the peptide is mediated through a non-specific physicochemical interaction with cell membranes [8], it opens channels for the entry of Ca<sup>2+</sup> [20], it forms channels for Ca<sup>2+</sup> [20] or it opens non-selective ion channels [6], resulting in neuronal degeneration. The first sign of this degeneration is the translocation of acetylcholinesterase from the endoplasmic reticulum to the membranes and to the dendrites of the cholinergic and/or cholinceptive neurons [13, 14].

The results in the *in vivo* [3] and *in vitro* [4, 23] effects of A $\beta$  clearly show that it has neurotoxic effects on cholinergic [10] and non-cholinergic neurons [22, 24]. However, the exact molecular mechanism of the degeneration of the different types of neurons and the resulting emergence of AD remains to be further elucidated, although it has been suggested that the peptide conformation [19] and aggregation may be responsible for the neurotoxicity.

## ACKNOWLEDGEMENTS

This work was supported by grants of OTKA T022683 and ETT 584/1996.

## REFERENCES

1. Abe, E., Casamenti, F., Giovannelli, L., Scali, C., Pepeu, G. (1994) Administration of amyloid  $\beta$ -peptides into the medial septum of rats decreases acetylcholine release from hippocampus in vivo. *Brain Res.* 636, 162–164.
2. Ehrenstein, G., Galdzicki, Z., Lange, G. D. (1997) The choline-leakage hypothesis for the loss of acetylcholine in Alzheimer's disease. *Biophys. J.* 73, 1276–1280.
3. Emre, M., Geula, C., Ransil, B. J., Mesulam, M. M. (1992) The acute neurotoxicity and effects upon cholinergic axons of intracerebrally injected  $\beta$ -amyloid in the rat brain. *Neurobiol. Aging* 13, 553–559.
4. Farkas, Z., Pákási, M., Penke, B., Kása, P. (1997) Acetylcholine release induced in vitro by beta-amyloid and its fragments. *Neurobiology* 5, 59–61.
5. Forgon, M., Farkas, Z., Gulya, K., Pákási, M., Penke, B., Kása, P. (1998) Amyloid  $\beta$ -peptide and its fragments induce acetylcholine release in *in vitro* basal forebrain tissue slices of rat brain, but do not affect the choline uptake. *Neurobiology* 6, 359–361.
6. Furukawa, K., Abe, Y., Akaïke, N. (1994) Amyloid  $\beta$  protein-induced irreversible current in rat cortical neurones. *Neuroreport* 5, 2016–2018.
7. Galdzicki, Z., Fukuyama, R., Wadhvani, K. C., Rapoport, S. I., Ehrenstein, G. (1994)  $\beta$ -amyloid increases choline conductance of PC12 cells: possible mechanism of toxicity in Alzheimer's disease. *Brain Res.* 646, 332–336.
8. Hertel, C., Terzi, E., Hauser, N., Jakob-Rotne, R., Seelig, J., Kemp, J. A. (1997) Inhibition of the electrostatic interaction between  $\beta$ -amyloid peptide and membranes prevents  $\beta$ -amyloid-induced toxicity. *Proc. Natl. Acad. Sci. USA* 94, 9412–9416.
9. Itoh, A., Nitta, A., Nadai, M., Nishimura, K., Hirose, M., Hasegawa, T., Nabeshima, T. (1996) Dysfunction of cholinergic and dopaminergic neuronal systems in beta-amyloid protein-infused rats. *J. Neurochem.* 66, 1113–1117.
10. Kása, P., Pákási, M., Penke, B. (1993) Synthetic human beta amyloid has selective vulnerable effects on different types of neurons. In: Nicolini, M., Zatta, P. F., Corain, B. (eds) *Alzheimer's Disease and Related Disorders. Advances in the Biosciences* 12, Pergamon Press, Oxford, pp. 311–312.
11. Kása, P., Farkas, Z., Pákási, M., Soós, K., Penke, B. (1996) Effects of  $\beta$ -amyloid peptides and their fragments on acetylcholine release in *in vitro* studies. *Ideggyógy. Szemle – Clin. Neurosci.* 49, 48–49.
12. Kása, P., Rakonczay, Z., Gulya, K. (1997) The cholinergic system in Alzheimer's disease. *Prog. Neurobiol.* 52, 511–535.
13. Kása, P., Pákási, M., Zarándi, M., Forgon, M., Papp, H., Rakonczay, Z. (1998) Alterations in the distribution of acetylcholinesterase within the cholinergic and cholinceptive neurons. *Neurobiol. Aging* 19, 549.
14. Kása, P., Penke, B., Pákási, M. (1998) Amyloid  $\beta$ -peptide treatment induces a redistribution of acetylcholinesterase within the enzyme-containing neurons in *in vitro* tissue cultures. *Neurobiology* 6, 369–371.
15. Kar, S., Seto, D., Gaudreau, P., Quirion, R. (1996)  $\beta$ -amyloid-related peptides inhibit potassium-evoked acetylcholine release from rat hippocampal slices. *J. Neurosci.* 16, 1034–1040.
16. Kar, S., Issa, A. M., Seto, D., Auld, D. S., Collier, B., Quirion, R. (1998) Amyloid  $\beta$ -peptide inhibits high-affinity choline uptake and acetylcholine release in rat hippocampal slices. *J. Neurochem.* 70, 2179–2187.
17. Koh, J., Yang, L. L., Cotman, C. W. (1990)  $\beta$ -amyloid protein increases the vulnerability of cultured cortical neurons to excitotoxic damage. *Brain Res.* 533, 315–320.
18. Laskay, G., Zarándi, M., Varga, J., Jost, K., Fónagy, A., Torday, C., Latzkovits, L., Penke, B. (1997) A putative tetrapeptide antagonist prevents  $\beta$ -amyloid induced long-term elevation of  $[Ca^{2+}]_i$  in rat astrocytes. *Biochem. Biophys. Res. Comm.* 235, 479–481.
19. Li, W. Y., Czilli, D. L., Simmons, L. K. (1995) Neuronal membrane conductance activated by amyloid  $\beta$  peptide: importance of peptide conformation. *Brain Res.* 682, 207–211.



20. Mattson, M. P., Cheng, B., Davis, D., Bryant, K., Lieberburg, I., Rydel, R. (1992)  $\beta$ -amyloid peptides destabilize calcium homeostasis and render human cortical neurons vulnerable to excitotoxicity. *J. Neurosci.* 12, 376–389.
21. Pákási, M., Farkas, Z., Soós, K., Penke, B., Kása, P. (1996) Role of Leu(34)-Met(35) in neurotoxicity caused by human  $\beta$ -amyloid (1-42) peptide in vitro. *Neurobiology* 4, 273–274.
22. Pákási, M., Farkas, Z., Kása, P. Jr., Forgón, M., Papp, H., Zarándi, M., Penke, B., Kása, P. Sr. (1998) Vulnerability of small GABAergic neurons to human  $\beta$ -amyloid pentapeptide. *Brain Res.* 796, 239–246.
23. Papp, H., Pákási, M., Penke, B., Kása, P. (1996) Effects of  $\beta$ -amyloid and its fragments on cholinergic and cholinceptive neurons in vitro. *Ideggyógy. Szemle – Clin. Neurosci.* 49, 49–50.
24. Papp, H., Pákási, M., Kása, P. Jr., Penke, B., Kása, P. Sr. (1998) Effects of human  $\beta$ -amyloid and its fragments on the subpopulation of GABAergic neurons. *Neurobiology* (in press).
25. Pedersen, W. A., Kloczewiak, M. A., Blusztajn, J. K. (1996) Amyloid  $\beta$ -protein reduces acetylcholine synthesis in a cell line derived from cholinergic neurons of the basal forebrain. *Proc. Natl. Acad. Sci. USA* 93, 8068–8071.
26. Pike, C. J., Walencewicz, A. J., Glabe, C. G., Cotman, C. W. (1991) In vitro aging of  $\beta$ -amyloid protein causes peptide aggregation and neurotoxicity. *Brain Res.* 563, 311–314.
27. Price, S. A., Held, B., Pearson, H. A. (1998) Amyloid  $\beta$  protein increases  $\text{Ca}^{2+}$  currents in rat cerebellar granule neurones. *Neuroreport* 9, 539–545.
28. Sanderson, K. L., Butler, L., Ingram, V. M. (1997) Aggregates of a  $\beta$ -amyloid peptide are required to induce calcium currents in neuron-like teratocarcinoma cells: relation to Alzheimer's disease. *Brain Res.* 744, 7–14.
29. Sawada, M., Ichinose, M. (1996) Amyloid  $\beta$  proteins reduce the GABA-induced  $\text{Cl}^-$  current in identified *Aplysia* neurons. *Neurosci. Lett.* 213, 213–215.
30. Simmons, M. A., Schneider, C. R. (1993) Amyloid  $\beta$  peptides act directly on single neurons. *Neurosci. Lett.* 150, 133–136.
31. Ueda, K., Fukui, Y., Kageyama, H. (1994) Amyloid  $\beta$  protein-induced neuronal cell death: neurotoxic properties of aggregated amyloid  $\beta$  protein. *Brain Res.* 639, 240–244.
32. Weiss, J. H., Pike, C. J., Cotman, C. W. (1994)  $\text{Ca}^{2+}$  channel blockers attenuate  $\beta$ -amyloid peptide toxicity to cortical neurons in culture. *J. Neurochem.* 62, 372–375.

## INVESTIGATION OF 2,6-DIMETHOXY-BENZOQUINONE IN EIGHT TREE SPECIES GROWN IN HUNGARY

Rita TÖMÖSKÖZI FARKAS<sup>1</sup>, M. HIDVÉGI<sup>2</sup> and R. LÁSZTITY<sup>3</sup>

<sup>1</sup>Birochem Ltd. and Central Food Research Institute, Budapest, Hungary

<sup>2</sup>Birochem Ltd. and Department of Biochemistry and Food Technology, Technical University of Budapest,  
Budapest, Hungary

<sup>3</sup>Department of Biochemistry and Food Technology, Technical University of Budapest, Budapest, Hungary

(Received: 1998-02-02; accepted: 1998-06-19)

Methoxy-substituted benzoquinone contents of eight wood samples collected from trees grown in Hungary were studied by a modified RP-HPLC method. Three samples (*Fraxinus excelsior*, *Fagus silvatica* and *Salix alba*) did not contain 2,6-dimethoxy-p-benzoquinone (2,6-DMBQ). Other samples (*Ailanthus altissima*, *Alnus glutinosa*, *Quercus robur*, *Populus balsamifera*, *Robinia pseudoacacia*) contained 0.02–0.3 mg/100 g of 2,6-DMBQ.

**Keywords:** 2,6-dimethoxy-benzoquinone – reversed-phased HPLC – trees

### INTRODUCTION

The important biological activity of some quinones is well known. Several quinones occur in the nature such as ubiquinones, plastoquinones, menaquinones, etc. They play an important role in the photosynthesis of some bacteria, in the respiratory chain of animal cells, in blood coagulation, etc. One of the most known quinones, vitamin K, influences the rate of blood coagulation. Quinone compounds may be formed *in vivo* from phenolic compounds e.g. dopaquinone is derivative of tyrosine. Several quinones are also used for therapeutic purposes. Adriamycin, daunorubicin, mitomycin c, etc. have cytostatic effects. Other benzo- and hydroquinones have antimicrobial effects [28, 40], and therefore are active components of Tetran-B, Metacyclin, Doxycyclin [37].

The biological activity of quinones is connected with their participation in redox-cycles in form of free reactive radicals. Their ability to produce aryl-nucleophil compounds, particularly by reaction with thiol and amino groups may explain the extreme activity of these compounds. In the skin or in other tissues and organs the nucleophiles are probably the functional groups of amino acids in protein, e.g. thiol group of cysteine or amino group of lysine. Quinones react with amines and amino acids *via* Michael addition, and they inhibit in some cases the activity of enzymes [6, 11, 37].

Send offprint requests to: Rita Tömösközi Farkas, Birochem Ltd. and Central Food Research Institute, Herman Ottó u. 15, H-1022 Budapest, Hungary



*Table 1*  
Occurrence of 2,6-DMBQ in different plants

Family	Genus (Literature)
Aceraceae	Acer [7]
Apocynaceae	Rauwolfia [11]
Asclepiadaceae	Marsdenia [11]
Asteraceae	Ambrosia, Gerberia [25, 41]
Betulaceae	Betula, etc. [22, 29]
Compositae	Baccharis, Verbesina, etc. [15, 16, 19]
Clusiaceae	Clusia [27]
Crotonoidae	Croton [2]
Dipterocarpaceae	Shorea [11]
Ebenaceae	Diospiros [3]
Ericaceae	Enkhiantus [11]
Fagaceae	Fagus, Quercus [8, 35]
Flacourtiaceae	Xylosma [4]
Gramineae	Sasa, Triticum etc. [28]
Guttiferae	Kielmeyera [5]
Hydrangeaceae	Hydrangea [12]
Iridaceae	Iris [1]
Lauraceae	Nectandra [11]
Leguminosae	Glycine, Phaseolus, etc. [14, 26, 32, 33]
Magnoliaceae	Liriodendron [11]
Melastomataceae	Tibouchia [11]
Meliaceae	Khaya, Cedrela, etc. [11]
Moraceae	Brosium [11]
Myristicaceae	Virola [11]
Proteaceae	Hakea [43]
Ranunculaceae	Adonis [20]
Rhizophoraceae	Kandelia [11]
Rubiaceae	Canthium [11]
Salicaceae	Populus [30, 31]
Sapotaceae	Thiegmella [11]
Simaroubaceae	Ailanthus, Simarouba, etc. [18, 23]
Thymelaeaceae	Peddia, Gyrinops etc. [34]
Ulmaceae	Ulmus [11]
Vochysiaceae	Vochysia [11]
Zingiberaceae	Afromomum [43]

In the recent decades researchers devoted more attention to immunostimulants and natural origin drugs. Szent-Györgyi had worked on compounds – 2,6-dimethoxy-*p*-benzoquinone (2,6-DMBQ) and 2-methoxy-*p*-benzoquinone (2MBQ) – which have been shown to have antimetastatic and bacteriostatic effect as well [10, 36, 37, 38, 39]. Occurrence of 2,6-DMBQ in different plants (Table 1) was reported by several authors. It was supposed that this compound was a product of degradation of lignin by different moulds [8, 9, 13, 21, 24]. The precursors of lignin, the sinapin and coniferyl alcohols, both contain methoxy groups in 2,6 resp. 2 positions.

The aims of this study were the following:

- adaptation and improvement of a HPLC method for determination of 2,6-DMBQ,
- collecting preliminary data about 2,6-DMBQ content of trees, grown in Hungary, as potential raw materials for natural preparations of this compound.

## MATERIALS AND METHODS

### 1. Materials

The samples (see Table 2) were collected in State Forest Farm in Fehérvársurgó in July 1992 and ground to fine powder in the Research Institute of Wood Industry in Budapest. All of the samples contained stem and cortex as well. Trees were 30–40 years olds from a heterogenous stand. Five tree samples were investigated all of species. We collected some trees which were described in literature (Fagaceae, Betulaceae, Salicaceae, Simaroubaceae) and some other species (Fabaceae, Oleaceae) which were grown in this area, but not published any data concerning 2,6-DMBQ.

Table 2  
2,6-DMBQ content of samples (ND – non detected)

Examined samples	2,6-DMBQ (mg/100 g sample)					
	water extr. (s)		ethanolic extr. (s)		chloroform. extr. (s)	
<i>Fagus silvatica</i> (Fagaceae)	ND	–	ND	–	ND	–
<i>Quercus robur</i> (Fagaceae)	ND	–	0.02	0.008	0.02	0.007
<i>Alnus glutinosa</i> (Betulaceae)	ND	–	ND	–	0.02	0.006
<i>Fraxinus excelsior</i> (Oleaceae)	ND	–	ND	–	ND	–
<i>Populus balsamifera</i> (Salicaceae)	0.08	0.013	ND	–	0.14	0.02
<i>Ailanthus altissima</i> (Simaroubaceae)	0.06	0.011	0.02	0.006	0.30	0.09
<i>Robinia pseudoacacia</i> (Fabaceae)	ND	–	0.02	0.008	0.16	0.04
<i>Salix alba</i> (Salicaceae)	ND	–	ND	–	ND	–



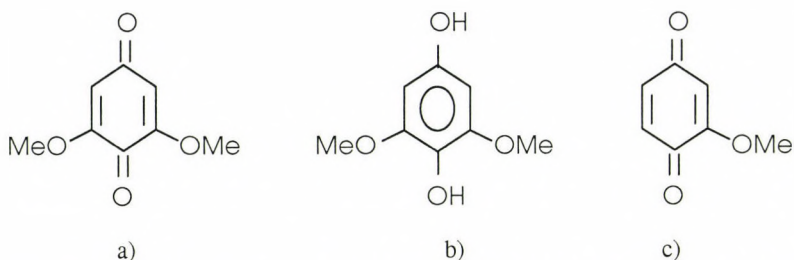


Fig. 1. Structure of a) 2,6-dimethoxy-*p*-benzoquinone (2,6-DMBQ), b) 2,6-dimethoxy-*p*-hydroquinone (2,6-DMHQ) and c) 2-methoxy-*p*-benzoquinone (2-MBQ)

The standards (2,6-DMBQ; 2,6-dimethoxy-*p*-hydroquinone, 2,6-DMHQ and 2-methoxy-*p*-benzoquinone, 2-MBQ; Fig. 1) were synthesised by Prof. Gábor Fodor (West Virginia University, Morgantown, USA) and donated to one of us (M.H.). The other chemicals, Na<sub>2</sub>HPO<sub>4</sub>, NaH<sub>2</sub>PO<sub>4</sub>, EDTA, NH<sub>2</sub>OH·HCl, methanol, ethanol, chloroform were produced by REANAL Fine Chemicals Co., Hungary. All reagents were used without additional cleaning.

## 2. Methods of extraction

Three procedures were used for extractions as follows:

- 50 g of sample was shaken in 600 cm<sup>3</sup> ethanol for 2 h. The extract was filtered and evaporated to dry in vacuum. The rest was dissolved in 5 cm<sup>3</sup> methanol.
- 50 g of sample was extracted with 400 cm<sup>3</sup> of chloroform for 2 h and treated as mentioned before.
- 50 g of sample was boiled in 500 cm<sup>3</sup> of distilled water for 2 h. The evaporated water was continuously replaced. The suspension was centrifuged, then the supernatant was extracted with chloroform (ratio 2:1) twice. The chloroform phase was evaporated to dry and dissolved in 5 cm<sup>3</sup> methanol [6].

## 3. RP-HPLC determination of quinones

The method of Huang et al. [17] was applied. A Beckmann 1114 M model pump, Labor MIM UV-detector, and Waters 740 integrator were used with a Chromsil C18, 10 micron column. The method was modified and adapted as described in "Results and Discussion".

## RESULTS AND DISCUSSION

### 1. Improvement of HPLC method

Although different chromatographic techniques are used for determination of benzoquinone derivatives, the most effective separation and determination may be achieved by reversed-phase high performance liquid chromatography (RP-HPLC). We started with use of method of Huang et al. [14] who reported about investigation of 12 derivatives of benzoquinone resp. hydroquinone using alkylsilica stationary phase and different solvent combinations as eluents. For prevention of oxidation of hydroquinones, EDTA (as complexing agent of ferri ions) and hydroxyl-ammonium phosphate were used. Our experiments showed that under conditions described Huang et al. [14] the oxidation of hydroquinones is not fully excluded. We succeeded to minimize the oxidation by stabilisation of pH at 6.05 using phosphate buffers. As eluent 10% methanol was used resulting in a good selectivity. The parameters of the improved method were the following:

- column: Chromsil C18, 10 microns
- flow rate: 2 ml/min.
- detection: at 290 nm
- eluent: phosphate ( $\text{Na}_2\text{HPO}_4$  – 2,5 mM +  $\text{NaH}_2\text{PO}_4$  – 2,5 mM) of pH = 6.05  
           $\text{Na}_2\text{EDTA}$  – 2,5 mM  
           $\text{NH}_2\text{OH}\cdot\text{HCl}$  – 5,0 mM  
          10% methanol.

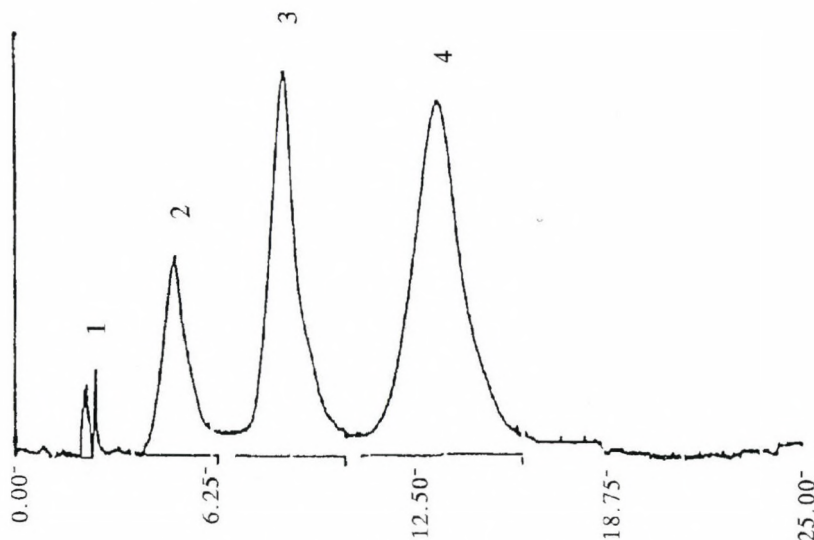


Fig. 2. Chromatogram of 2,6-DMBQ, 2,6-DMHQ and 2-MBQ



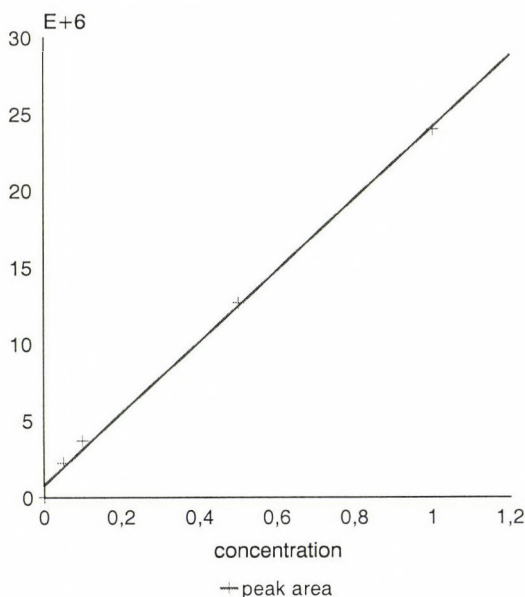


Fig. 3. Calibration curve of 2,6-DMBQ

## 2. Examination of wood samples

A typical chromatogram showing separation and determination of three benzoquinones (2-MBQ, 2,6-DMBQ, 2,6-DMHQ) is shown in Fig 2. Concentrations of standards were 0.1 mg/ml in each cases. A good selectivity was achieved. As it is seen, retention times of benzoquinones are higher than those of hydroquinones. The more functional methoxy groups the molecules contained the bigger is their respective retention time. Table 3 shows the data of retention times ( $t_R$ ) and capacity factors ( $k'$ ). In Fig. 3 the calibration curve serving for the determination of 2,6-DMBQ is shown. The quasi-linear curve has a correlation coefficient of 0.99.

Table 3  
Retention time ( $t_R$ ) and capacity  
factor of standards

Standard	$t_R$	$k'$
2,6-DMBQ	13.4	5.0
2,6-DMHQ	5.1	1.2
2-MBQ	8.5	2.7

## CONCLUSIONS

The 2,6-DMBQ content of wood samples (see Table 2) was determined by RP-HPLC method as described in the previous chapter. Three replications were made and the mean values are shown in Table 2. A characteristic chromatogram (for *Ailanthus altissima*) is shown in Fig. 4. As it is seen from the chromatogram the peak of 2,6-DMBQ is well separated, other compounds (contaminants) do not disturb the evaluation. The identification of 2,6-DMBQ was carried out by use of standard compound based on identity of retention time. In addition, the chromatogram of standard and the samples was prepared using DAD detector and the identity spectra was also controlled.

The concentration of 2,6-DMBQ in literature was between  $10^{-5}$ – $10^{-2}$  mg/g. The results showed that only five tree species (*Ailanthus altissima*, *Alnus glutinosa*, *Quercus robur*, *Populus balsamifera*, *Robinia pseudoacacia*) contain 2,6-DMBQ in a concentration range from 0.02 to 0.3 mg/100g. These results are correlated to the literature, but no data were found about family Fabaceae (*Robinia pseudoacacia*) concerning 2,6-DMBQ.

The highest quantities of quinones were extracted with chloroform. The best potential source of 2,6-DMBQ, among the trees studied, was *Ailanthus altissima*.

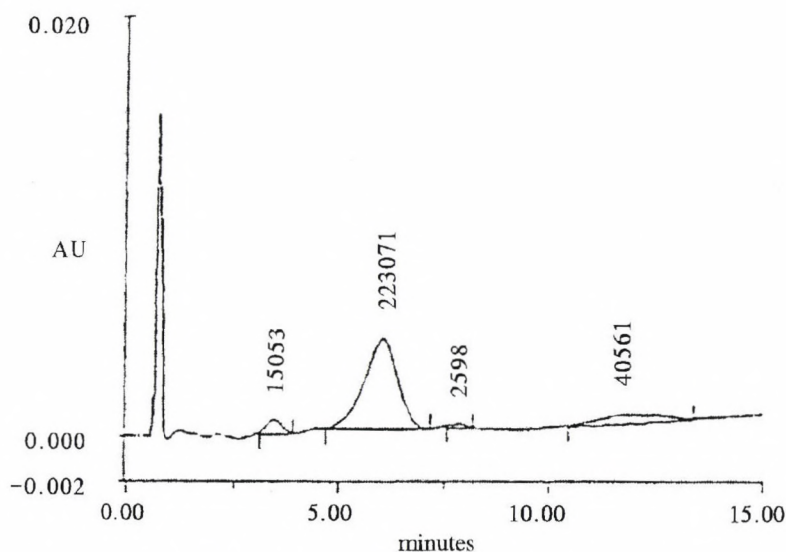


Fig. 4. Characteristic chromatogram of *Ailanthus altissima*



## ACKNOWLEDGEMENT

This work is supported by an OTKA grant (1998-2000), No. F 026196.

## REFERENCES

1. Agarwal, V. K., Tappa, R. K., Agarwal, S. G., Dhar, K. L. (1984) Phenolic constituents of *Iris mile-sii* Rhizomes. *Phytochemistry* 6, 1342-1343.
2. Bandara, B. M. R., Wimalasari, W. R. (1988) Diterpene alcohols from *Croton lacciferus*. *Phytochemistry* 27, 225-226.
3. Chen, C. C., Yu, H. J., Pan, T. M. (1994): Constituents of the heartwood of diospyros erinthia. *J. Chin. Chem. Soc.* 41, 195-198.
4. Cordell, A., Chang, P. T. O., Fong, H. H. S., Farnsworth, N. R. (1977) Xylosmacin, a new phenolic glucoside ester from *Xylosma velutina*. *Lloydia* 40, 340-343.
5. Correa deBarros, D., Fonseca eSilva, L. G., Gottlieb, O. R., Goncalves, S. J. (1970) Quinone and xanthone constituents of *Kielmeyera rupestris*. *Phytochemistry* 9, 447-451.
6. Farkas, R. (1993) *Investigation of Benzoquinone Derivates*. Dipl. Thesis, BME, Budapest.
7. Filipic, V. J., Underwood, J. C. (1963) Some aromatic compounds in sap composition of maple sap and sirup. *J. Food Sci.* 29, 464-468.
8. Freudenberg, K., Sidhu, G. S. (1961) Zur Kenntnis des Lignins der Buche und der Fichte. *Holzfor-schung* 2, 33-39.
9. Gupta, J. K., Jebsen, C., Kneifel, H. (1986) Sinapic acid degradation by the yeast *Rhodotorula glutinis*. *J. Gen. Microbiol.* 132, 2793-2799.
10. Halinska, A., Belej, T., O'Brien, P. J. (1996) Cytotoxic mechanisms of anti-tumour quinons in pa-rental and resistant lymphoblasts. *Br. J. Cancer*, Suppl. 74, 523-527.
11. Handa, S., Kinghorn, A. D., Cordell, G. A., Farnsworth, N. R. (1983) Plant anticancer agents. XXVI. *J. of Nat. Prod.* 46, 245-250.
12. Harasawa, A., Tagashira, A. (1994) Isolation of 2,6-dimethoxy-1,4-benzoquinone from *Hydrangea* and its deodorant activity against methyl mercaptan. *Biosci., Biotechnol. Biochem.* 58, 2073-2074.
13. Hartig, C., Merger, D., Fischer, K. (1990) Lignin-Biosynthese, Struktur, Biodegradation. *Zeitschrift Chem.* 30, 65-69.
14. Hausen, B. M., Schmalke, M. (1981) Quinonoid constituents as contact sensitizers in Australian Blackwood (*Acacia melanoxylon* RBR). *Brit. J. Ind. Med.* 38, 105-109.
15. Herz, W., Bruno, M. (1986) Heliangolides, kauranes and other constituents of *Helianthus hetero-phyllus*. *Phytochemistry* 25, 1913-1916.
16. Herz, W., Kumar, N. (1981) Aromatic and other constituents of four *Verbesina* species: Structure and stereochemistry of verbesindol. *Phytochemistry* 20, 247-250.
17. Huang, X., Bouvier, E. S. P., Stuart, J. D., Melander, W. R., Horváth, Cs. (1985) High-performance liquid chromatography of substituted p-benzoquinones and p-hydroquinones. *J. Chromatography* 330, 181-192.
18. Jain, M. K. (1963) Chemical examination of *Ailanthus excelsa* DC. *Indian J. Chem.* 2, 40.
19. Jarvis, B. B., Pena, B., Comezoglu, S. N., Rao, M. M. (1986) Non-trichotecenes from *Baccharia megapota*. *Phytochemistry* 25, 533-535.
20. Karrar, W. (1930) Über das Vorkommen von 2,6-Dimethoxy-chinon in *Adonis vernalis* L. *Helv. Chim. Acta* 13, 1424.
21. Kawai, S., Umezawa, T., Higuchi, T. (1988) Degradation mechanism of phenolic  $\beta$ -1 lignin sub-structure model compounds by laccase of *Coriolus versicolor*. *Arch. Biochem. Biophys.* 262, 99-100.
22. Kodaira, H., Ishikawa, M., Komoda, Y., Nakajima, T. (1981) Anti-platelet aggregation principles from the bark of *Fraxinus japonica* Blume. *Chem. Pharm. Bull.* 29, 2391-2393.
23. Kosuge, K., Mitsunaga, K., Koike, K., Ohmolo, T. (1994): Studies on the constituents of *Ailanthus integrifolia*. *Chem. Pharm. Bull.* 42, 1669-1671.

24. Leonowicz, A., Edgehill, R. I., Bollag, J. M. (1984) The effect of the transformation of syringic and vanillic acids by the laccases of *Rhizoctonia praticola* and *Trametes versicolor*. *Acta Microbiol.* 132, 89–96.
25. Lu, T., Parodi, F. J., Vargas, D., Quijano, L., Mertoetono, E. R., Hjortso, M. A., Fischer, N. H. (1993) Sesquiterpenes and thiarubines from *Ambrosia trifida* and its transformed roots. *Phytochemistry* 33, 113–116.
26. McPherson, D. D., Cordell, G. A., Soejarto, D. D., Pezzuto, J. M., Fong, H. H. S. (1983) Peltogenoids and homoisoflavonoids from *Caesalpinia pulcherrima*. *Phytochemistry* 22, 2835–2838.
27. Nagem, T. J., DaSilva, H. C., Mesquita, A. A. L., Silva, R. (1993): Constituents of *Clusia arboreocida*. *Fitoterapia* 64, 87.
28. Nishina, A., Haesgawa, K., Uchibori, T., Seino, H., Osawa, T. (1991) 2,6-dimethoxy-*p*-benzoquinone as an antibacterial substance in the bark of *Phyllostachys heterocyclo* var. *pubescens*, a species of thick-stemmed bamboo. *J. Agric. Food Chem.* 39, 266–269.
29. Nomura, M., Tokoroyama, T., Kubota, T. (1981) Biarylheptanoids and other constituents from wood of *Alnus japonica*. *Phytochemistry* 20, 1097–1104.
30. Pearl, I. A., Darling, S. F. (1968) Studies on the bark of the family *Salicaceae* – XIX. *Phytochemistry* 7, 1851–1853.
31. Pearl, I. A., Darling, S. F. (1968) Studies on the barks of the family *Salicaceae* – XVIII. *Tappi* 51, 537–539.
32. Schmalle, H. M. (1980) Acamelin, a new sensitizing furano-quinone from *Acacia melanoxylon*. *Tetr. Let.* 21, 149–152.
33. Schmalle, H. M., Jarchow, O. (1977) 2,6-Dimethoxy-1,4-benzoquinone, a new contact allergen in commercial woods. *Naturwissenschaften* 64, 534–535.
34. Schun, Y., Cordell, G. A. (1985) Studies on the *Thymelaeaceae* III. Constituents of *Gyrinops walla*. *J. Nat. Prod.* 48, 684–685.
35. Seikel, M. K., Hostettler, F. D., Niemann, G. J. (1971) Phenolics of *Quercus rubra* Wood. *Phytochemistry* 10, 2249–2251.
36. Sheh, I., Li, C. J. (1992): Citotoxicity studies some novel 2,6-dimethoxy-hydroquinone derivatives. *Anti-Cancer Drug Des.* 4, 315–327.
37. Szent-Györgyi, A. (1980) The living state and cancer. *Quant. Biol. Symp.* 7, 217–222.
38. Szent-Györgyi, A. (1982) Biological oxidation and cancer. *Quant. Biol. Symp.* 9, 27–30.
39. Szent-Györgyi, A. (1985) Metabolism and cancer. *Quant. Biol. Symp.* 12, 257–261.
40. Tahara, S., Matsukura, Y., Katsura, H., Mizutani, J. (1991): Naturally occurring antidotes against benzimidazole fungicides. *Z. Naturforschung, C: Biosci.* 48, 7575–7585.
41. Tak, H., Franczek, F. R., Fischer, N. H. (1995): A diterpene from *Garberia heterophylla*. *Phytochemistry*, 40, 185–189.
42. Varma, M., Varma, R. S., Parthasarathy, M. R. (1980) Minor Phenolic constituents of *Grevillea robusta* and *Hakea saligna*. *Naturforschung* 35, 344–345.
43. Vidari, G., Finzi, P. V., deBernardi, M. (1971) Flavonoids and quinones in stems of *Aframomum giganteum*. *Phytochemistry* 10, 3335–3339.





## DNA TECHNOLOGY AND ITS APPLICATION IN FORENSIC MEDICINE. A REVIEW

A. LÁSZIK<sup>1</sup>, A. FALUS<sup>2</sup>, L. KERESZTURY<sup>3</sup> and P. SÓTONYI<sup>1</sup>

<sup>1</sup>Department of Forensic Medicine, <sup>2</sup>Department of Genetics, Cell and Immunobiology,  
Semmelweis University Medical School, Budapest, Hungary

<sup>3</sup>Police Headquarters of Veszprém County, Veszprém, Hungary

(Received: 1998-02-18; accepted: 1998-06-09)

In the last years DNA technology became increasingly important in the forensic medicine. Conventional forensic serological analysis consists of the detection of genetic polymorphisms at the protein level, while DNA typing involves the study of individual variation directly at the level of nucleotide sequence. Today, DNA evidence is generally accepted by courts and greatly assists the resolution of criminal and civil investigations. This article reviews how molecular techniques used to detect genetic polymorphism in forensic science.

**Keywords:** DNA – genetic marker analysis – PCR – RFLP – forensic science

The concept of using polymorphic markers to solve forensic problems is far from being new since efforts were made to find matches by comparing similarities or dissimilarities to include or exclude a person as a perpetrator for a long while. The limited availability of useful marker systems was however a serious drawback for such works.

The ABO blood group system was the only one used on forensic samples for a long time. A significant breakthrough was achieved in the early 1970s when other protein and enzyme markers, which had been known to be polymorphic for a decade or more, were found to be useful for forensic evidence as well. The concept of applying genetically based polymorphic markers was largely extended to other systems to reach finally a considerable number of genetic marker systems. However, some of the more serious drawbacks like modest level of polymorphism and therefore low statistical evidentiary value, poor stability with rapid deterioration and occasional transformational artefacts leading to false exclusions reduced the value of these systems. Furthermore most of the markers are only present in blood and the investigation of body tissues was usually not possible [2].

The application of DNA typing is a natural extension of the forensic analysis of human biological evidence. Conventional forensic serological analysis consists of the detection of genetic polymorphisms at the protein level, while DNA typing involves the study of individual variation *directly* at the DNA sequence level.

Send offprint requests to: Prof. Dr. A. Falus, Department of Genetics, Cell and Immunobiology, Semmelweis University Medical School, P.O. B. 370, H-1445 Budapest, Hungary



Method of analysis:

- reliable, rapid, simple to perform
- detect unambiguous, qualitative differences between alleles
- consume little material

Nature of the marker:

- inherited independently of other markers being analyzed
- polymorphic with a high degree of heterozygosity
- population frequency data known

*Fig. 1. Criteria for useful forensic genetic markers*

The two major applications of DNA typing in forensic science are paternity testing and criminal investigations. DNA typing was first used for criminal investigation in 1985 in the United Kingdom and was first applied to case work in the United States by late 1986. The original "DNA fingerprinting" method, developed by Alec Jeffreys, examined many locations in the DNA of a genome at once. The result was a multi-banded pattern whose complexity suggested a fingerprint, and was probably unique to each individual [6].

Individuals can be distinguished by their genetic marker profile. The more markers compared, the more likely differences between individuals will be revealed. However, not all genetic markers are suitable for forensic applications, thus they must be carefully selected. The criteria by which genetic markers are evaluated for forensic use are outlined in Fig. 1.

The first technique that was adapted for forensic DNA analysis is called RFLP (Restriction Fragment Length Polymorphism). This kind of analysis determines variation in the length of a defined DNA fragment generated by digestion with endonuclease.

While most of the DNA sequences show modest variation between individuals, there are non-coding regions called minisatellites or Variable Number Tandem Repeats (VNTRs) that can exhibit an extraordinary level of length variation. This variation is based on regions of repeatedly arranged almost identical short (20–100 bp) DNA sequences which vary only in number of elements at a given locus [5, 6, 9].

RFLP still provides the highest degree of discrimination per locus. Unfortunately, this technique requires more and better quality DNA than some of the recently developed polymerase chain reaction (PCR) techniques. Since the forensic evidence is often old, degraded and of limited quantity, RFLP analysis is sometimes not possible. In RFLP analysis, all of the genomic DNA is processed, and the regions of interest are detected with labelled DNA probes.

Briefly, the process involves digestion of human genomic DNA with a restriction enzyme, separation of DNA fragments by electrophoresis, transfer of the fragments to a nylon membrane and incubation of the membrane with radioactive or alkaline phosphatase labelled probe (Fig. 2). The probe hybridizes to complementary sequences in the DNA fragments attached to the membrane, and the bound probe is visualized by autoradiography or alkaline phosphatase-catalyzed chemiluminescence (ECL).

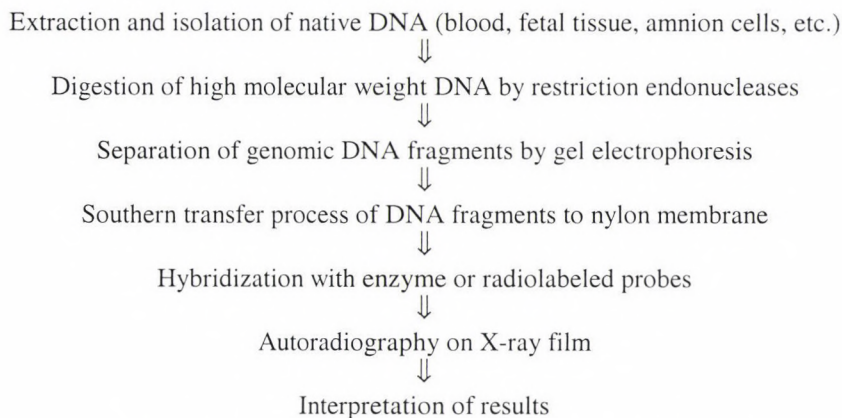


Fig. 2. Basic outlines of restriction fragment polymorphism (RFLP)

RFLP analysis is extremely suitable for the analysis of the drunken driver's blood samples, of difficult filiation cases involving relatives and missing persons. Additionally, prenatal paternity diagnosis is possible either with cultured amniotic fluid cells or chorionic tissue or abortion material, for instance after termination of pregnancy following rape [9]. The RFLP analysis, clearly shows the allele hereditary by Mendelian law [7].

The second type of technique is the polymerase chain reaction based DNA typing, which is a general technique for increasing the amount of a specific section of DNA in a sample. This means amplification of certain parts of DNA. It is generally designed so that only a small segment of the DNA of interest is copied, and this is accomplished with extremely high fidelity to the original (Fig. 3).

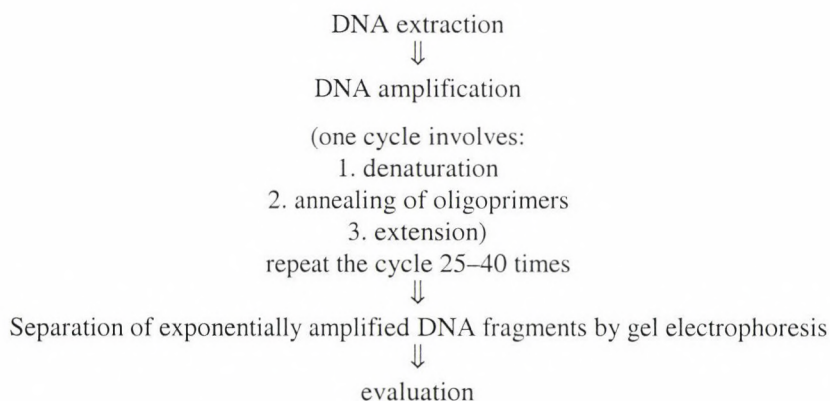


Fig. 3. Scheme of polymerase chain reaction



As a tool in forensic diagnostic, PCR based strategies have several advantages. First, PCR requires only trace quantities of DNA. Typically 10 ng of human DNA is optimal for the PCR, compared with 300–500 ng for RFLP typing. Consequently, it becomes realistic to type the DNA from minute samples, even a single hair root, sticked stamp or a cigarette butt containing epithelial cells [3]. Second, the PCR generates a large quantity of relatively pure product in a very short period of time, considerably less time than that required for typing by RFLP analysis. Third, degradation of the DNA sample is less of concern when using the PCR because PCR amplification targets a small segment of DNA [10, 11, 12].

The PCR technique is a highly sensitive method requiring special laboratory conditions, DNase free, sterile filtered, ultra pure water and ultra pure chemicals (Sigma, Fluka, Merck, etc.). In addition to standard techniques the DNA molecules can be obtained nowadays by the available up to date preparation kits (e.g. QIAamp Blood and Tissue Kit).

The first system, which became available for forensic analysis of PCR amplified DNA was HLA DQ A1 locus on chromosome 6. The type of variation present at this locus resides in the DNA sequence. Under appropriate conditions an amplified PCR product will hybridize to the immobilized probes only if they are exact sequence matches. Detection of the DQA1 alleles involves a colorimetric reaction. A streptavidin-horseradish peroxidase conjugate is then bound to the biotinylated PCR product. The peroxidase converts the chromogen (colorless substrate) into a blue precipitate. The final results are seen as series of blue dots on a paper-like strip. The strips are commercially available, and contain specific DNA sequences originating from the same locus in the genome as the DNA which has been amplified by PCR. When the probes are attached to the typing strip, the format is known as a reverse dot blot. Each probe is a specific sequence of DNA that defines an allele. These types of probes are known as sequence specific oligonucleotides (SSO). They are sometimes also referred to in the forensic science literature as allele specific probes (ASO). The chief advantages of this sequence polymorph system are the ability to investigate very small samples and the rapidity of analysis [4].

One of the more recent PCR systems to come on line in forensic science is called D1S80. D1S80 refers to the locus in the DNA that is being investigated. Like RFLP, the variation present at this locus is in the length of a defined DNA fragment as reflected by the number of tandem repeats (VNTR). However, because of its relatively smaller size, this fragment is amenable to amplification by PCR. In the forensic science literature, systems of this nature are called Amplified Fragment Length Polymorphisms (AmpFLPs). Each repeat unit in D1S80 is 16 bp long, except for the first repeat, which is 14 bp. The number of repeats varies from about 14 to 41, producing DNA fragments in the range of hundreds of base pairs, about an order of magnitude smaller than the fragments normally analyzed in RFLP typing. Thus D1S80 analysis combines the advantages inherent in any PCR system (specifically the ability to analyze samples of limited quantity and quality) with the greater variation generally seen in length-based systems. D1S80 loci are detected as discrete alleles and thus can be compared directly to a standard ruler made up of all possible alleles (allelic ladder) which is run on the same gel. The DNA is commonly detected by silver staining. Figure 4 shows the outcome of a rape case examination per-

formed in this system, lane 1 is the blood sample of the victim, lane 2 is the mixed vaginal swab, lane 3 is the blood sample of suspect 1 and lane 4 is the blood sample of suspect 2. "A" marks the allelic ladder. The first suspect's allele (lane 3) can be clearly identified in the mixed vaginal swab (lane 2).

Short Tandem Repeats (STRs) are similar to the D1S80 system described above, except that the repeat units are shorter. The loci chosen for forensic use generally have a tandem repeat unit of 3 or 4 bp and may be repeated from few to dozen of times. The size of the DNA fragments produced by amplification of STR loci tends to be in the range of hundreds of base pairs, rather than the thousands of base pairs found in RFLP fragments.



Fig. 4. The outcome of a rape case examination performed in D1S80 system. Lane 1 is the blood sample of the offended party, lane 2 is the mixed vaginal swab, lane 3 is the blood sample of suspect 1 and lane 4 is the blood sample of suspect 2. "A" marks the allelic ladder. The first suspect's allele can be clearly identified in the mixed vaginal swab



This makes STRs an ideal choice for degraded DNA [11, 12]. PCR amplification of several different loci is often performed simultaneously in the same tube, producing saving of time, materials, and most important, sample (multiplex PCR).

It is often useful to know if male and/or female components are present in a forensic sample. The amelogenin locus, which is coincidentally the gene for tooth pulp, shows a length variation between the sexes. One region of the female form of the gene contains a small deletion (6 bp) in non-essential DNA and produces a shorter product when amplified by PCR. When this region is analysed, a female with two X chromosomes will show one band. A male with both an X and Y chromosome will show two bands, one the same size as the female and one slightly larger.

PCR markers usually have fewer types per locus than the RFLP loci, but the frequencies of these types in the population are still lower than for conventional blood typing markers. When coupled with the fact that DNA tends to be far more stable than the conventional protein and enzyme markers, DNA typing is much more powerful than conventional typing of evidentiary material [4].

Another promising DNA-typing system utilizes *mitochondrial (mt) DNA* rather than nuclear DNA. The mitochondrial genome is 16569 bp and, of interest to forensic scientist, contains a noncoding hypervariable control region. In particular, there are two segments within this 1,100 bp control region, also called the D-loop, that tend to mutate with an extremely high frequency, at least 5 to 10 times of nuclear DNA. This high mutation rate makes the region attractive for use in individual identification. The variations exhibited in the two hypervariable regions are generally point mutations, although small deletions and insertions may also occur. Nuclear DNA is inherited in equal parts from both parents. Due to the technicalities of fertilization, genetic material from mitochondria is inherited only from the egg cell of the mother; thus mtDNA is said to exhibit *maternal inheritance*. Therefore the mtDNA type of an individual cannot be heterozygous, or exhibits two different types. A genetic element that lacks a homologous counterpart in the genome may be described as *hemizygous*; mtDNA is also sometimes referred to as *monoclonal*. This is a useful quality in tracking families and populations and also belies any possibility of new variations arising from chromosomal recombination. The complete nucleotide sequence of human mtDNA has been established for a reference individual [1].

Mitochondrial DNA is present in hundreds to thousands of copies per cell. Generally mt DNA typing involves PCR amplification followed by direct nucleotide sequencing of the allele. Because of its relatively small size in comparison to nuclear chromosomes and numerous multiple copies it is often the last typable DNA present in a small, old or badly treated sample. e.g. burnt or very decomposed corpses. If no results are obtained with any other systems, the mtDNA can be still typed [4].

PCR examinations performed in several systems can be successfully applied on the site of the crime, and for the identification of persons leaving a very low quantity of biological samples, even partly degraded DNA. New examination methods of molecular biology have opened up new ways for identification in forensic medicine. These methods can help us to answer questions, which cannot be answered by the conventional methods. At this time, DNA evidence is generally accepted by courts and greatly assists in the resolution of criminal and civil investigations.

## REFERENCES

1. Anderson, S., Bankier, A. T., Barrell, G. B. (1981) Sequence and organization of the human mitochondrial genome. *Nature*, 290, 457–465.
2. Bär, W. (1994) Past, present and future trends in forensic DNA technologies in Europe. *Acta Med. Leg.*, 20–25.
3. Higuchi, R., Beroldingen, von C. H., Sensabaugh, G. F., Erlich, H. A. (1988) DNA typing from single hairs. *Nature* 332, 543–546.
4. Inman, K., Rudin, N. (1997) *An Introduction to Forensic DNA Analysis*. CRC Press Inc., Boca Raton, New York, pp. 1–27.
5. Jeffreys, A. J., Wilson, V., Thein, S. L. (1985) Hypervariable “minisatellite” regions in human DNA. *Nature* 314, 67–73.
6. Jeffreys, A. J., Wilson, V., Thein, S. L. (1985) Individual specific fingerprints of human DNA. *Nature* 316, 76–79.
7. Lászik, A., Pöche, H., Mauer, V., Schneider, V. (1995) Apaságmegállapítás a DNS technológia (RFLP) alkalmazásának segítségével. *Orvosi Hetilap* 136, 2117–2119.
8. Lee, H. C., Ladd, C., Bourke, M. T., Pagliaro, E., Tirnady, F. (1994) DNA typing in forensic science. *Am. J. Forensic Med. Pathol.* 15, 269–282.
9. Nakamura, Y., Leppert, M., O’Connel, P., Wolff, R. (1987) Variable number of tandem repeat (VNTR) markers for human gene mapping. *Science* 235, 1616–1622.
10. Reynolds, R., Sensabaugh, G. (1991) Analysis of genetic markers in forensic DNA samples using the polymerase chain reaction. *Anal. Chem.* 63, 2–15.
11. Saiki, R. K., Scharf, S., Faloona, F. et al. (1985) Enzymatic amplification of  $\beta$ -globin genomic sequences and restriction site analysis for diagnosis of sickle cell anaemia. *Science* 230, 1350–1354.
12. Saiki, R. K., Gelfand, D. H., Stoffel, S. (1988) Primer directed enzymatic amplification of DNA with thermostable DNA polymerase. *Science* 239, 487–491.
13. Woller, J., Füredi, S., Pádár, Zs. (1997) Polimeráz láncreakción alapuló DNS-vizsgálatok a magyar igazságügyi gyakorlatban. *Orvosi Hetilap* 138, 3223–3228.
14. Wong, Z., Wilson, W., Jeffreys, A. J. et al. (1986) Cloning a selected fragment from a human DNA “Fingerprint”: isolation of an extremely polymorphic minisatellite. *Nucl. Acid. Res.* 14, 4605–4616.





## RAS-DEPENDENCE OF NERVE GROWTH FACTOR-INDUCED INHIBITION OF PROLIFERATION OF PC12 CELLS

Katalin KISS, B. BARTEK, Nóra NUSSEER and J. SZEBERÉNYI

Department of Biology, University Medical School of Pécs, Pécs, Hungary

(Received: 1998-04-04; accepted: 1998-06-15)

The PC12 rat pheochromocytoma cell line is the most frequently used model system to study neuronal differentiation: nerve growth factor (NGF) inhibits proliferation and causes easily scorable neurite formation in these cells. The central role of the monomeric guanine nucleotide binding Ras proteins in the pathway of NGF-induced differentiation is well documented. However, the possible involvement of Ras proteins in signal transduction processes mediating NGF-induced inhibition of proliferation has not been analyzed. To address this problem we studied PC12 subclones expressing a dominant inhibitory mutant Ras protein (Ha-Ras Asn17). Our results indicate that the cell cycle arrest characteristic of NGF-treated PC12 cells is mediated by a Ras-dependent signaling mechanism.

**Keywords:** PC12 cells – nerve growth factor – Ras proteins – Ha-Ras Asn17 mutant – proliferation

### INTRODUCTION

The PC12 cell line was established by the cloning of rat pheochromocytoma cells [6]. Under standard culturing conditions these cells have polygonal or spherical shape with a diameter of 10 to 20 micrometers. Resembling adrenal medullar chromaffin cells, they also have granules containing catecholamines. Upon treatment with nerve growth factor (NGF [8]) the cells stop proliferating, become quiescent in the G1 phase, extend several long, thin neurites, produce neurotransmitters and acquire other features characteristic of the phenotype of sympathetic neurons [6]. Since PC12 cells can differentiate into neuronal cells upon NGF treatment and survive in the absence of NGF, they are commonly used as a model system to study neuronal differentiation.

The signal transduction pathway mediating the differentiation response to NGF involves Ras proteins, members of the monomeric G-protein family (for a review see [13]). Ras proteins (Ha-Ras, Ki-Ras, N-Ras) can be found in all eukaryotic cells in association with the inner surface of cell membrane [1]. They alternate between GDP-bound, inactive, and GTP-bound, active forms. In their active state they relay signals from the NGF receptor to mitogen-activated protein kinase (MAPK) cascades. Stimulation of the MAPK-

Send offprint requests to: Prof. J. Szeberényi, Department of Biology, University Medical School of Pécs, Szigeti út 12, H-7643 Pécs, Hungary. E-mail: szeber@apacs.pote.hu.



pathway leads to the expression of a specific set of genes that, in turn, are believed to be responsible for the phenotypic changes accompanying neuronal differentiation (reviewed in [11, 13]).

The requirement for a functional Ras-pathway in NGF-induced neuritogenesis has been firmly established [7, 12]. Expression of a dominant negative mutant form of Ha-Ras [5] strongly inhibits NGF-induced stimulation of MAPKs [2, 15, 18], activation of early and secondary response genes, and neurite formation [9, 12]. PC12 subclones stably transfected with the mutant Ha-*ras* Asn17 gene (designated M17-subclones) are therefore useful tools to study the role of Ras in NGF-signaling.

Asynchronously cycling PC12 cells are pushed through a last cell cycle by NGF treatment, then arrested in G1 phase [10, 17] and start to grow neurites. The cessation of proliferation is accompanied by gradual alterations in the level and activity of key cell growth regulatory proteins [4, 16, 19]. Several members of the growth stimulatory cyclin-dependent protein kinase family (e.g. Cdc2, Cdk2, Cdk4, Cdk6) are down-regulated, while other proteins (e.g. cyclin D1, the Cdk inhibitor p21) are induced by NGF treatment. The link between the NGF receptor and the cell cycle machinery, however, has not been found yet. The aim of the experiments described in this paper was to analyze the role of Ras proteins in this signaling event. We found that while NGF-treated wild-type PC12 cells exited the cell cycle and started to grow neurites, the failure of M17-subclones to differentiate upon NGF treatment was accompanied by continuous growth of these cells. The antimitogenic effect of NGF in PC12 cells thus requires intact Ras function.

## MATERIALS AND METHODS

### *Cell culture*

Wild-type PC12 cells, as well as M17-subclones expressing Ha-Ras Asn17 at low (Z-M17-5) or high levels (M-M17-26) were used in these studies. The M17-subclones were previously described [12]. Cells were plated on 100-mm dishes and cultured in Dulbecco's modified Eagle medium (DMEM) supplemented with 5% horse and 2.5% fetal bovine serum (FBS).

### *Cell counting*

$10^4$  cells plated on 60-mm dishes were cultured in DMEM containing 5% horse serum and 2.5% FBS. (Preliminary experiments indicated that these serum concentrations properly supported the growth of all subclones used in these experiments.) NGF (20 ng/ml) was added to the cultures on the next day. Cell numbers were determined on duplicate plates on days 3, 6 and 9 after trypsinization, using a Burkner chamber.

*[<sup>3</sup>H]thymidine incorporation*

10<sup>5</sup> cells were plated on 100-mm dishes in DMEM containing 5% horse serum and 2.5% FBS. DNA synthesis was assayed by labeling with [<sup>3</sup>H]thymidine (1μCi/ml; 0.18 mM final concentration) for 3 h. The cells were washed twice with phosphate-buffered saline, and 2 ml of 0.2M NaOH containing calf thymus carrier DNA (40 μg/ml) was added to each plate. Samples were collected by filtration through Whatman GF/C glass fiber filters and washed with ice-cold 10% trichloroacetic acid and 95% ethanol. [<sup>3</sup>H]-incorporation into acid insoluble material was determined by scintillation counting. Cell numbers were counted on parallel plates and [<sup>3</sup>H]thymidine incorporations were expressed in cpm/10<sup>3</sup> cells (see Table 1).

Table 1  
The effect of NGF on [<sup>3</sup>H]thymidine incorporation in PC12 subclones

Cell lines →		PC12 cells		M-M17-26 cells	
Treatment ↓		<sup>3</sup> H-thymidine incorporation (cpm/10 <sup>3</sup> cells)	ratio (control/NGF- treated)	<sup>3</sup> H-thymidine incorporation (cpm/10 <sup>3</sup> cells)	ratio (control/NGF- treated)
day 1	control	620		933	
	NGF- treated	153	4.05	875	1.07
day 4	control	722		1208	
	NGF- treated	27	26.74	1364	0.89
day 7	control	850		733	
	NGF- treated	30	28.33	1000	0.73

For details of [<sup>3</sup>H]thymidine labeling see Materials and methods.

## RESULTS AND DISCUSSION

Previous characterization of several M17-subclones indicated that while intact Ras function is required for the NGF-induced differentiation of PC12 cells, the inhibition of endogenous Ras function does not affect the proliferative potential of these cells [12]. Therefore, M17-subclones provide suitable cell systems to study the role of Ras proteins in the antimitogenic signaling of NGF. In the present experiments, two M17-subclones (Z-M17-5 and M-M17-26) expressing low and high levels of Ha-Ras Asn17, respectively, were used. Both cell lines display inhibition of NGF-induced morphological differentiation, but early gene induction events appear to be unaffected in the low M17-expressor Z-M17-5 cell line. (For more detailed descriptions of these cell lines see [12, 14].) Comparison of the proliferative behaviour of these two cell lines toward NGF treatment might therefore give information on the role of early-response genes in the antimitogenic effect of NGF.



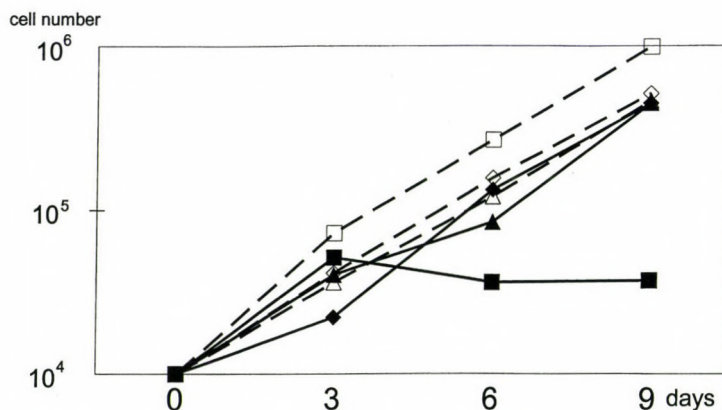


Fig. 1. Effect of NGF on proliferation of wild-type PC12 and M17-subclones.  $10^4$  PC12 ( $\square$ ,  $\dagger$ ), Z-M17-5 ( $\Delta$ ,  $\blacktriangle$ ), and M-M17-26 ( $\square$ ,  $\blacklozenge$ ) cells per plate were cultured in medium containing 5% horse serum and 2.5% FBS for 1 day and then treated with NGF (20 ng/ml, closed symbols); control cells (open symbols) were cultured in the medium only. Cell counts were taken at the indicated time points as described in Materials and methods

To clarify whether the antiproliferative effect of NGF is mediated by a Ras-dependent signal transduction pathway in PC12 cells, we examined the effect of NGF on the growth of wild-type PC12 cells and M17-subclones (Fig. 1). As expected, the number of control PC12 cells exponentially increased during the experiment, whereas upon NGF stimulation the cell number did not rise after the 3rd day of treatment. This is in agreement with earlier observations [10] that NGF promotes PC12 cells through one division cycle before the cessation of proliferation and the induction of differentiation. In contrast, the growth of Z-M17-5 and M-M17-26 subclones both with and without NGF treatment showed similar rates (Fig. 1). Since a number of Ras-independent effects of NGF (e.g. an increase in phosphoinositide turnover [14], stimulation of phosphatidylinositol-3 kinase activity [20]) are intact in these M17-subclones, the antiproliferative effect of NGF must be inhibited in these cells downstream of the receptor, presumably at the Ras proteins. We can thus conclude that the antimitogenic effect of NGF in PC12 cells requires intact Ras function: even partial inhibition of Ras-mediated signaling (as in Z-M17-5 cells) completely abolishes the cell cycle arrest caused by NGF.

In order to further confirm the involvement of the Ras-pathway in the antiproliferative effect of NGF we studied the incorporation of [ $^3$ H]thymidine into DNA in PC12 and M-M17-26 cells. [ $^3$ H]thymidine labeling of control and NGF-treated cultures was performed at different timepoints of the experiment and the ratios of [ $^3$ H]thymidine incorporations measured in untreated and NGF-treated cultures were calculated. Table 1 shows the results of a representative experiment. The high value of this index for PC12 cells even 1 day after the addition of NGF indicates that a subpopulation of cells is already arrested in G1 phase and is unable to progress into the S phase even before the overall growth rate of the culture is affected (see Fig. 1). The steep increase in the ratio of DNA synthesis in

untreated versus NGF-treated cells during the course of the experiment indicates a complete block of cell cycle progression caused by NGF. In sharp contrast, the index of [ $^3\text{H}$ ]thymidine incorporation did not change significantly in M-M17-26 cells indicating that even one week of NGF treatment was unable to block cell cycle progression in these cells.

Recent studies on PC12 cells revealed that NGF treatment has a profound effect on several regulatory components of the cell cycle machinery (see above in the Introduction). While these changes accompanying the G1 phase block are well documented, the link by which they are coupled to the activated NGF receptor remains to be determined. The binding of NGF to its receptor activates both Ras-dependent and -independent signaling events [14]. Activation of the Ras-dependent MAPK-pathway is absolutely required for the differentiation response [3]. Stimulation of Ras-independent mechanisms is by itself insufficient to mediate the neuritogenic effect of NGF, but synergizes with other pathways to stimulate neurite formation [14]. The results presented in this paper indicate that the antimitogenic effect of NGF requires intact Ras function. Inhibition of the antiproliferative effect of NGF in the low M17-expressor Z-M17-5 cells also indicates that the induction of several early-response genes (such as *c-fos*, *c-jun*, *zif268*, *pip92*, etc.) may not have a major role in the cell cycle arrest induced by NGF. Experiments to identify cell cycle regulatory proteins that may serve as downstream Ras targets in PC12 cells are underway in our laboratory.

#### ACKNOWLEDGEMENT

This study was supported by grants from the Hungarian National Research Foundation (OTKA T 012925 and T 026496), U.S.–Hungarian Joint Fund (93a-319) and the Hungarian Health Science Council (T-04 615/93).

#### REFERENCES

1. Barbacid, M. (1987) *Ras* genes. *Annu. Rev. Biochem.* 56, 779–827.
2. Boglári, G., Erhardt, P., Cooper, G. M., Szeberényi, J. (1998) Intact Ras function is required for sustained activation and nuclear translocation of extracellular signal-regulated kinases in nerve growth factor-stimulated PC12 cells. *Eur. J. Cell Biol.* 75, 54–58.
3. Cowley, S., Paterson, H., Kemp, P., Marshall, C. J. (1994) Activation of MAP kinase is necessary and sufficient for PC12 differentiation and for transformation of NIH3T3 cells. *Cell* 77, 841–852.
4. Dobashi, Y., Kudoh, T., Matsumine, A., Toyoshima, K., Akiyama, T. (1995) Constitutive overexpression of Cdk2 inhibits neuronal differentiation of rat pheochromocytoma PC12 cells. *J. Biol. Chem.* 270, 23031–23037.
5. Feig, L. A., Cooper, G. M. (1988) Inhibition of NIH 3T3 cell proliferation by a mutant ras protein with preferential affinity for GDP. *Mol. Cell. Biol.* 8, 3235–3243.
6. Greene, L. A., Tischler, A. S. (1976) Establishment of a noradrenergic clonal line of rat adrenal pheochromocytoma cells which respond to nerve growth factor. *Proc. Natl. Acad. Sci. USA* 73, 2424–2428.
7. Hagag, N., Halegoua, S., Viola, M. (1986) Inhibition of growth factor-induced differentiation of PC12 cells by microinjection of antibody to ras p21. *Nature* 319, 680–682.
8. Levi-Montalcini, R. (1987) The nerve growth factor: thirty-five years later. *EMBO J.* 6, 1145–1154.



9. Pap, M., Szeberényi, J. (1998) Differential Ras-dependence of gene induction by nerve growth factor and second messenger analogs in PC12 cells. *Neurochem. Res.* 23, 971–977.
10. Rudkin, B. B., Lazarovici, P., Levi, B.-Z., Abe, Y., Fujita, K., Guroff, G. (1989) Cell cycle-specific action of nerve growth factor in PC12 cells: differentiation without proliferation. *EMBO J.* 8, 3319–3325.
11. Szeberényi, J. (1996) Gene activation pathways of nerve growth factor signaling. A minireview. *Neurobiology* 4, 1–11.
12. Szeberényi, J., Cai, H., Cooper, G. M. (1990) Effect of a dominant inhibitory Ha-ras mutation on neuronal differentiation of PC12 cells. *Mol. Cell. Biol.* 10, 5324–5332.
13. Szeberényi, J., Erhardt, P. (1994) Cellular components of nerve growth factor signaling. *Biochim. Biophys. Acta* 1222, 187–202.
14. Szeberényi, J., Erhardt, P., Cai, H., Cooper, G. M. (1992) Role of Ras in signal transduction from the NGF receptor: Relationship to protein kinase C, calcium, and cyclic AMP. *Oncogene* 7, 2105–2113.
15. Thomas, S. M., De Marco, M., D'Arcangelo, G., Halegoua, S., Brugge, J. S. (1992) Ras is essential for nerve growth factor- and phorbol ester-induced tyrosine phosphorylation of MAP kinases. *Cell* 68, 1031–1040.
16. van Grunsven, L. A., Billou, N., Savatier, P., Thomas, A., Urdiales, J. L., Rudkin, B. B. (1996) Effect of nerve growth factor on the expression of cell cycle regulatory proteins in PC12 cells: dissection of the neurotrophic response from the anti-mitogenic response. *Oncogene* 12, 1347–1356.
17. van Grunsven, L. A., Thomas, A., Urdiales, J. L., Machenand, S., Choler, P., Durand, I., Rudkin, B. B. (1996) Nerve growth factor-induced accumulation of PC12 cells expressing cyclin D1: evidence for a G1 phase block. *Oncogene* 12, 855–862.
18. Wood, K. W., Sarnecki, C., Roberts, T. M., Blenis, J. (1992) Ras mediates nerve growth factor receptor modulation of three signal-transducing protein kinases: MAP kinase, Raf-1 and RSK. *Cell* 68, 1041–1050.
19. Yan, G. Z., Ziff, E. (1995) NGF regulates the PC12 cell cycle machinery through specific inhibition of the cdk kinases and induction of cyclin D1. *J. Neurosci.* 15, 6200–6212.
20. Yao, R., Cooper, G. M. (1995) Requirement for phosphatidylinositol-3 kinase in prevention of apoptosis by nerve growth factor. *Science* 267, 2003–2006.

# EVALUATION OF GENOTOXIC, MUTAGENIC AND ANTITUMOR PROPERTIES OF 2-AMINO-2-THIAZOLINE, L-THIOPROLINE AND 2-AMINO-2-THIAZOLINE $\epsilon$ -FORMYLAMINOCAPROATE

Vitalija ŠIMKEVIČIENĖ, J. STRAUKAS and Larisa CHAUSTOVA

Institute of Biochemistry, Vilnius, Lithuania

(Received: 1998-05-10; accepted: 1998-06-30)

In the present study the genotoxic, mutagenic and antitumor effects of 2-amino-2-thiazoline (R), L-thiopropine (N) and 2-amino-2-thiazoline  $\epsilon$ -formylaminocaproate (FAT) as well as their influence on bacterial growth and activity of the extracellular protease are discussed. On the basis of our study the following conclusions may be drawn: the investigated compounds, except N, had no strongly expressed genotoxic activity and none of them was found to be mutagenic. R and FAT were insignificantly toxic on bacterial growth, all compounds were ineffective against transplanted tumors and did not change the rate of the biosynthesis of *Bacillus subtilis* extracellular neutral protease.

**Keywords:** Genotoxicity – mutagenicity – antitumor activity – 2-amino-2-thiazoline – L-thiopropine – 2-amino-2-thiazoline  $\epsilon$ -formylaminocaproate

## INTRODUCTION

L-Thiazolidine-4-carboxylic acid (L-thiopropine, norgamem) and 2-amino-2-thiazoline hydrochloride (revercan) are capable of inducing reverse transformation in tumor cells [5, 10, 12]. L-Thiopropine possesses the ability to inhibit proliferation of chemically-transformed latent tumor cells [20]. Recently it has been reported that L-thiopropine slightly inhibited the growth of L 1210 mouse leukemia cells [9]. 2-Amino-2-thiazoline has been found to be of significant antitumor action in two autochthonous systems, that is, in mice with 1,2-dimethylhydrazine·HCl induced colon tumors and in the Friend virus system [21]. Although these agents were not active against any transplanted mice tumor, promising clinical effects were reported against advanced human cancer [2, 11].

It has been reported that thiopropine was a potent nitrite scavenger [29]. Thiopropine suppressed carcinogenesis induced by N-benzylmethylamine and nitrite in rats. Many human foodstuffs contain thiopropine, and this compound may act as an effective trapping agent of nitrite in the human body.

Send offprint requests to: Dr. Vitalija Šimkevičienė, Institute of Biochemistry, Mokslininkų 12, Vilnius 2006, Lithuania



We have recently reported that 2-amino-2-thiazoline  $\epsilon$ -formylaminocaproate (FAT) possessed a chemopreventive effect on cancer. FAT in experiments with mice reduced the lung tumor incidence up to 59% of that of control [25].

The rec assay as a bacterial genetic toxicology test is widely used for detection of potential chemical carcinogens [1, 16]. Evaluation of genotoxic and carcinogenic risk of the potential medicine ought to be taken into consideration. We report here the results of the study which was aimed at assessing the genotoxic and mutagenic properties of the above-mentioned agents by means of microbial short-term tests. Recent studies illustrate that the regulation of protease activity by both host and tumor tissue promises to become a new target for cancer therapy [19]. Therefore, in addition to genotoxicity and mutagenicity testing, a number of assays have been carried out with the aim of evaluating the influence of these compounds on the biosynthesis of the *Bacillus subtilis* extracellular neutral protease. Moreover, FAT in comparison with norgamen and revercan has been examined as antitumor agent in several rodent systems.

## MATERIALS AND METHODS

### *Agents*

2-Amino-2-thiazoline hydrochloride (revercan (R)) was prepared according to [8]. L-Thiazolidine-4-carboxylic acid (L-thioprolin) was synthesized according to Ratner and Clarke [23]. For the assay, sodium salt of L-thiazolidine-4-carboxylic acid (norgamem (N)) was used. 2-Amino-2-thiazoline  $\epsilon$ -formylaminocaproate (FAT) was synthesized according to the procedure described earlier [24].

### *Bacterial strains*

*Escherichia coli* K<sub>12</sub>C5013 as a wild (repair-proficient) strain, JC7902 (uvrA<sup>-</sup>, recA<sup>-</sup>), WP6 (polA1<sup>-</sup>), *Bacillus subtilis* BD170 (rec<sup>+</sup>), BD190 (rec<sup>-</sup>), *Salmonella typhimurium* TA100 strains were used in this study. All strains were kindly provided by the Institute of High Molecular Compounds, Moscow, Russia.

### *Growth medium*

Nutrient broth (NB, Difco) with 0.5% NaCl added and LB (Difco) were used for bacterial cells growth. A solid medium contained 2% agar (Difco, USA). Cultures for tests were grown overnight at 37 °C on a rotary shaker [17].

### *Toxicity and genotoxicity assays*

Inhibition of bacterial growth was evaluated after the suitable period of the bacteria suspension incubation with and without the studied agent. The number of cells was determined by measuring optical density (OD<sub>590</sub>) and compared with the cells number in control wild strain suspension. Optical density was measured on photoelectrocolorimeter KFK-2-UKhL 4.2 (Russia), green filter. All experiments were performed in triplicate.

The micro-suspension method, as a bacterial genetic toxicology test, using *Escherichia coli* repair deficient strains, has been used with some modifications [16]. In our study overnight growing bacteria were concentrated at 5000 rpm for 5 min and resuspended in potassium phosphate buffer (0.1 M Na<sub>2</sub>HPO<sub>4</sub> × 7H<sub>2</sub>O, 0.1 M NaH<sub>2</sub>HPO<sub>4</sub> × H<sub>2</sub>O, pH 7.5) to 10<sup>8</sup> cells/ml, studied compounds were added and incubation was continued at 37 °C with shaking. Inhibition of bacterial growth was evaluated after 6 h, the samples were taken for measuring of optical density. Each tester strain was exposed to two concentrations of each compounds. All experiments were performed in triplicate for each strain.

### *Mutagenic assay*

Mutagenic properties were determined according to the procedure [14, 18]. *Salmonella* tester strain was TA100. 0.02 M nitrosomethylurea (NMU) standard mutagen was used as positive control in the same experiments.

### *The extracellular neutral protease activity assay*

The extracellular neutral protease activity was determined by spectrophotometric method by Anson with some modifications according to [3, 13] at pH 7.2 in 0.02 M phosphate buffer with *p*-sulphodiasobenzene N,N-dicarbamidoethylcaseine ("Fermentas", Vilnius) as substrate. To 0.5 ml of 0.8% substrate 0.1 ml of supernatant was added. After incubation of 10 min at 30 °C 0.5 M trichloroacetate acid was added. Solution was centrifugated and supernatante was estimated on spectrophotometer Perkin Elmer 550 (Germany) under OD<sub>400</sub>. Activities are expressed in international units (IU) according to the certain calculation.

The studied compounds were dissolved in physiological solution (0.9% NaCl).

### *Animals*

Mice 42(C<sub>57</sub>B1/6\* DBA/2) F<sup>1</sup>, 30 CC<sub>57</sub> Br, 30 C<sub>57</sub> B1/6, 129 BALB/C and 30 Wistar rats were used in our study. The animals were kept at the laboratory conditions for at least 5 days prior to the test. Before the test animals were randomised and assigned to the treatment groups. Mice body mass was 22–24 g. Animals were obtained from the Latvian State Pharmaceutical Company "GRINDEX", Riga. Throughout the study mice were



cared for in accordance with European Convention and the Guide for the Care and Use of Laboratory Animals [6, 22, 26, 28]. The response of each animal to the killing procedure was recorded by the same person [7].

### *Toxicity testing in vivo*

The survival of mice (4-6 weeks old), treated intraperitoneally with graduated dose levels of each compound was observed for 14 days. The LD<sub>50</sub> value was determined by the method of Lithfield and Wilcoxon [15].

### *Antitumor activity*

Antitumor activity was determined by using the following tumor models: *murine ascite tumor* Nk/Ly (Nk/Ly), *Ehrlich ascite carcinoma* (EAC), *hemocitoblastoses La* (La), *lymphoidic leukaemia L 1210* (L1210), *Sarcoma 180* (S 180), *planacellular cancer of fore-stomach* (PCF) and *Walker-256 carcinoma* (W-256) [27]. Tumor models were kindly supplied by the Cancer Research Centre (Moscow, Russia). Nk/Ly, EAC, L 1210 and La tumor cells were inoculated intraperitoneally, S 180, W-256 were inoculated subcutaneously at the axillary regions of animals and PCF-intramuscularly. Treatment of tumor-bearing animals with test compounds was generally initiated on the 2–3 days following solid tumor implant or 24 h after ascite tumor inoculation and continued for a period of 5 days. The solutions of test compounds (in various doses) were injected intraperitoneally to each animal mg/kg basis individually, according to the body weight. For the evaluation of antitumor activity against subcutaneously and intramuscularly inoculated tumors (S 180, W-256 and PCF) the tumor weight was measured and expressed as per cent inhibition of tumor growth.

The criteria for effectiveness against solid and ascites tumors were the tumor growth inhibition (TGI %) and ascites growth inhibition (AGI %) values of 50 and more. The antitumor activity against intraperitoneally inoculated tumors was evaluated by calculating the percentage of increase in life (ILS %). The criteria of effectiveness were the ILS (%) values of 25 and more.

The statistical significance was determined by  $t$  = Student's test ( $P < 0.05$ ).

## RESULTS AND DISCUSSION

The toxic effect is presented as the inhibition effect of the compounds on the cells viability of the wild strain. Results presented in Table 1 show, that the viability of the *Escherichia coli* wild strain cells is decreased after the 1 h incubation with N (1mM) to 10%, with R and FAT – to 35% at the same concentration. Our study has shown that R and FAT were more toxic than N. In order to evaluate the genotoxic activity of the studied compounds we carried out our experiments with *Escherichia coli* strains with repair defi-

cient system. Genotoxicity was defined as the ability of the compounds to preferentially kill DNA repair-defective strains. The rec assay detected N as evident genotoxic agent. All studied compounds inhibited the bacterial growth of JC7902 strain. The analysis of our data demonstrated that R and FAT did not show strongly expressed genotoxic activity at 1 mM on WP6 strain. The level of toxicity and genotoxic activity in both repair-proficient and -deficient strains at the 0.1 mM of all compounds, except N, was the same. The rec assay was dependent on the relative inability of a postreplication repair-defective (*recA*<sup>-</sup>) bacterial strain to repair DNA damage caused by physical or chemical agents, therefore, the strains with defects in both excision repair (*uvrA*<sup>-</sup>) and postreplication repair (*recA*<sup>-</sup>) were extremely sensitive to small amounts of DNA damage [4, 16]. As it was expected, in all cases among the repair-deficient strains, JC7902 was by far the most sensitive strain in revealing the direct genotoxicity of the 3 compounds.

Present results provide evidence that of 3 compounds evaluated, only N exhibited evident genotoxic activity in a DNA-repair test relative to other compounds. FAT synthesized by us did not show significant genotoxic activity on WP6 strain under two concentration of the tested compounds. This indicates that FAT is not able to induce significant DNA damages, which are irreversible in repair-deficient bacteria.

Our study in vitro demonstrates that 2-amino-2-thiazoline hydrochloride (R) as well as the salt of 2-amino-2-thiazoline  $\epsilon$ -formylaminocaproic acid (FAT) from the standpoint of toxic and genotoxic properties are almost alike.

Other experiments were carried out in order to determine the mutagenic properties of the compounds. Mutagenic activity was observed by the number of the his<sup>+</sup> revertants. Results presented in Table 2 provide evidence that all compounds are devoid of mutagenic activity in the Ames reversion test. Compounds studied, except R, do not possess antimutagenic properties with respect to nitrosomethylurea (Table 2). On the basis of our results the conclusion is that no significant difference exists between the mutagenic activities of R and N as well as that of the salt of 2-amino-2-thiazoline  $\epsilon$ -formylaminocaproic acid (FAT).

The extracellular protease activity was determined with *Bacillus subtilis* rec<sup>+</sup> and rec<sup>-</sup> strains. Agents studied did not change the rate of the culture growth during 6 h incubation.

Table 1  
Evaluation of genotoxicity using *Escherichia coli* strains

Compounds	mM	<i>Escherichia coli</i> strains cell viability, %. 6 h		
		K <sub>12</sub> C5013	JC7902	WP6
R	1	67	50	67
	0.1	90	100	83
N	1	90	30	45
	0.1	92	50	100
FAT	1	65	36	87
	0.1	100	69	100



Table 2  
Mutagenic activity of the revercan (R), norgamem (N)  
and their analogous (FAT)  
on the *Salmonella thyphimurium* TA100

Tested compounds	No. of the his <sup>+</sup> revertants on the plate	+NMU 0.002 M
R	110	1200
N	160	1000
FAT	74	880
Control	77	720

Values presented are the means of 3 replicates.  $P < 0.05$ .  
All compounds were used in 1 mM.

The data presented in Table 3 have shown that the secretion of the protease into the incubation medium was observed in normal range and with the strains with damages in the reparation system (rec<sup>-</sup>). Then *Bacillus subtilis* cells were grown to the stationary growth phase on milk agar medium. Only R stimulated protease extraction into the medium up to 30% (data not shown). Present results confirm and correlate with the low toxicity of investigated compounds.

### *Toxicity and antitumor activity in vivo*

The toxic doses and MTD (maximal tolerated doses) of compounds are listed in Table 4. All compounds were moderately toxic (3rd class of toxicity). The toxicity data of N on mice resembled data obtained by other authors [20]. Neither compound did cause a solid tumor inhibition effect. Treatment of Nk/Ly R failed to increase the life span, in spite of the marked inhibitory effect of ascites growth (50%). We suggest that the cause of the

Table 3  
Effect of tested compounds on the proteolytic activity  
of *Bacillus subtilis* BD 170 rec<sup>+</sup> and BD 190 rec<sup>-</sup> strains

Concentration, mM	R		N		FAT	
	rec <sup>+</sup>	rec <sup>-</sup>	rec <sup>+</sup>	rec <sup>-</sup>	rec <sup>+</sup>	rec <sup>-</sup>
1	32	30	34	34	41	36
0.5	30	36	28	–	40	34
0.2	36	26	34	32	38	34
0.1	38	36	36	36	40	32
control	36	32	36	32	36	32

Protealytic activity is presented in IU, (–) – untested.

Table 4  
Toxicity and antitumor activity of tested compounds

Test compounds	Dosage, mg/kg LD50	MTD	Optimal therapeutic dose, mg/kg × days	Model	Inhibition, %	P <
R	200 (190–210)	150	20 x 5	Nk/Ly	50.0 <sup>a)</sup>	0.05
			20 x 5	EAC	28.8 <sup>a)</sup>	0.05
			25 x 5	La	40.3 <sup>b)</sup>	0.5
			25 x 5	L 1210	7.7 <sup>b)</sup>	0.01
			20 x 5	S 180	–16.0 <sup>c)</sup>	0.5
N	160 (155–165)	100	20 x 5	Nk/Ly	30.0 <sup>a)</sup>	0.01
			20 x 5	EAC	14.0 <sup>b)</sup>	0.5
			25 x 5	La	5.3 <sup>b)</sup>	0.5
			25 x 5	L 1210	7.7 <sup>b)</sup>	0.01
			20 x 5	S 180	–43.0 <sup>c)</sup>	0.5
FAT	350 (340–370)	200	40 x 5	Nk/Ly	0 <sup>a)</sup>	0.05
			40 x 5	EAC	0 <sup>b)</sup>	0.5
			–	La	–	–
			35 x 5	L 1210	0 <sup>b)</sup>	0.01
			40 x 5	W-256	9.1 <sup>c)</sup>	0.5
			20 x 5	PCF	–45.2 <sup>c)</sup>	0.01

a) – ascite growth inhibition

b) – increase of life span per cent

c) – tumor growth inhibition

death of the mice was a common latent toxicity. R was insignificantly effective in increasing life span of La leukemia-bearing mice. N and FAT were ineffective, too. Our experimental system has confirmed that N and R, as noncytotoxic anticancer agents, were not active in experimental tumor systems of mice, including L 1210. Although they have shown clinical efficacy in treating epidermoid carcinoma of head and neck with pulmonary metastases [2]. R and N as well as FAT was not active inhibitor of transplanted tumors.

## CONCLUSIONS

All the studied compounds are devoid of mutagenic activity and, except N, are not strongly genotoxic, hence it follows that they do not induce irreversible damages to DNA structure. Thus, the following conclusion may be drawn: revercan and 2-amino-2-thiazoline  $\epsilon$ -formylaminocaproate, as potential medicine, presumably seem to be of no danger. Attention ought to be paid to the possible hazard of norgamem. The data obtained by us can promote the elucidation of chemical and biochemical basis of the mechanism of action of the studied compounds as the inductors of the reversal transformation of tumor cells.



## ACKNOWLEDGEMENT

The authors are grateful to D. Šaduikytė for the help in preparing this paper.

## REFERENCES

1. Benvenuti, S., Severi, F., Sacchetti, A., Melegari, M., Vampa, G. (1997) Synthesis, antimicrobial and genotoxic properties of some benzoimidazole derivatives. *Il Farmaco* 52, 231–235.
2. Brugarolas, A., Gosálvez, M. (1980) Treatment of cancer by an inducer of reverse transformation. *Lancet* 1, 68–70.
3. Colowick, S. P., Kaplan, N. O. (1970) *Methods in Enzymology*. New York–London, pp. 651.
4. De Flora, S., De Renzi, G. P., Camoirano, A., Astengo, M., Basso, C., Zancacchi, P., Bennicelli, C. (1985) Genotoxicity assay of oil dispersants in bacteria (mutation, differential lethality, SOS DNA-repair) and yeast (mitotic crossing-over). *Mutation Res.* 158, 19–30.
5. Diaz-Gil, J. J., Gosálvez, M. (1981) Reverse transformation of HeLa cells by 2-amino-2-thiazoline HCl, an analogues of thioproline. *Proc. AACR and ASCO* 22, 52.
6. European Convention for the Protection of Vertebrate Animals for Experimental and Other Scientific Purposes, Strasbourg. Council Directive (86/609/EEC), 1986.
7. Flekneil, P. A. (1966) *Laboratory Animals Anesthesia*. Academic. Press, 2nd ed.
8. Gabriel, S. (1889) Zur Kenntniss des Bromäthylamins. *Ber.* 22, 1139–1154.
9. Garofalo, A., Balconi, G., Botta, M., Corelli, F., D'Incalci, M., Fabrizi, G., Fiorini, I., Lambia, D., Nacci, V. (1993) Thioanalogues of anti-tumor antibiotics. 2. Synthesis and preliminary in vitro cytotoxicity evaluation of tricyclic [1,4] benzothiazepine derivatives. *Eur. J. Med. Chem.* 28, 213–220.
10. Gosálvez, M. (1979) The plasma membrane as a target in anticancer chemotherapy. *Proc. AACR and ASCO* 20, 17.
11. Gosálvez, M. (1980) Norgamem and revercan. The first two inducers of reverse transformation (transrecers) in anticancer therapy. *Proc. AACR and ASCO*. 21, 132.
12. Gosálvez, M., Vivero, C., Alvarez, J. (1979) Restoration of contact inhibition in tumour cells in tissue culture by treatment with thiazolidine-4-carboxylic acid. *Biochem. Soc. Trans.* 7, 191–192.
13. Kaverzneva, E. D. (1971) *Applied Biochemistry and Microbiology*. Moscow, 2nd ed., p. 225.
14. Killbey, B. J., Legator, M., Nichols, W., Ramel, C. (1984) *Handbook of Mutagenicity. Test Procedures*. Amsterdam–New York–Oxford, pp. 1–13.
15. Litchfield, J. T., Wilcoxon, F. (1949) A simplified method of evaluating dose-effects experiments. *J. Pharmacol. Exp. Ther.* 96, 99–113.
16. Mamber, S. W., Bryson, V., Katz S. E. (1983) The *Escherichia coli* WP2/WP100 rec assay for detection of potential chemical carcinogens. *Mutation Res.* 119, 135–144.
17. Maniatis, T., Fritsch, E. F., Sambrook, J. (1982) *Molecular Cloning: A Laboratory Manual*. Cold Spring Harbor, N.Y.
18. Maron, D. M., Ames, B. N. (1983) Revised methods for the *Salmonella* mutagenicity test. *Mutation Res.* 113, 173–215.
19. Opdenakker, G., Paemen, L., Norga, K., Masure, S. (1997) Proteinase inhibition in invasive cancer therapy: four control levels of matrix degradation. *Int. J. Cancer.* 70, 628–630.
20. Parks, R. C., Jones, T., Banks, A. R., Hessek, E. (1982) Thioproline: an inhibitor of chemical carcinogenesis. *Neoplasma* 29, 535–537.
21. Pine, M. J., Mirand, E. A., Ambrus, J. L., Bock, F. G. (1983) Antitumor studies of 2-amino-2-thiazoline and other tumor-modifying agents. *J. Med.* 14, 433–449.
22. Pizzocheri, F., Zaninelli, B. (1990) Safety test for the notification of new chemicals: EEC directive 79/831. Ivrea, Italy.
23. Ratner, S., Clarke H. T. (1937) The action of formaldehyde upon cysteine. *J. Am. Chem. Soc.* 59, 200–206.

24. Straukas, J., Dirvianskyte, N., Jankauskas, R., Yavorovskaja, V. E., Yevstropov, A. N., Kiseliova, V. N. (1996) Synthesis and antiviral activity of N- and O-substituted amino acids. *Khim.-Farm. Zh.* 30, 18–21 (in Russian).
25. Šimkevičienė, V., Straukas, J. (1997) The experimental study in chemoprevention of cancer with 2-amino-2-thiazoline  $\epsilon$ -formylaminocaproate. 1st Int. Congr. of Asia Pacific Ass. of Med. Toxicology and the 5th Iranian Congr. of Toxicology and Poisoning. Teheran, Iran, p. 176.
26. Sandoe, P., Crips, R., Holtung, N. (1966) *Animal Ethics. Report*. Univ. Copenhagen, pp. 1–20.
27. Sofiina, Z., Syrkin, A., Goldin, A., Kline, A. (1980) *Experimental Evaluation of Anti-tumor Drugs in the USSR and in the USA*. Meditsina, Moskva (in Russian).
28. Department of Health and Human Services. Guide for the Care and Use of Laboratory Animals. Bethesda, 1985.
29. Wakabayashi, K., Nagao, M., Sugimura, T. (1992) Heterocyclic amines, lipophilic ascorbic acid, and thioproline: ubiquitous carcinogens and practical anticarcinogenic substances. In: Wattenberger, L. W. (ed.) *Cancer Chemoprevention*. CRC: Boca Raton, Fla. pp. 311–325.





## GROWTH HORMONE INHIBITS THE INTERLEUKIN-6 INDUCED *junB* PROTOONCOGENE AND FIBRINOGEN EXPRESSION IN HEPG2 HUMAN HEPATOMA CELLS

P. IGAZ, Beáta DÉRFALVI, Sára TÓTH and A. FALUS

Department of Genetics, Cell- and Immunobiology, Semmelweis University Medical School,  
Budapest, Hungary

(Received: 1998-06-16; accepted: 1998-07-18)

Growth hormone (GH) and interleukin-6 (IL-6) play important regulatory roles in multiple endocrinological and immunological functions. In this study we examined whether GH can modulate the actions of IL-6. In HepG2 human hepatoma cells we studied the effects of different GH concentrations on the expression of the *junB* mRNA as an *early* and on the biosynthesis of fibrinogen protein as a *late* model of IL-6-related hepatic response. Both GH and IL-6 alone induced the expression of *junB* and fibrinogen but GH significantly inhibited the actions of higher (10 and 20 ng/ml) IL-6 concentrations in a dose dependent manner. These findings further underline the importance of interplay between the effectiveness of IL-6 and GH in various physiological processes.

**Keywords:** Growth hormone – interleukin-6 – *junB* mRNA – fibrinogen

### INTRODUCTION

Growth hormone (GH) is a peptide hormone produced mainly by the anterior lobe of the hypophysis. Its activities include the regulation of the growth of skeletal and soft tissues and metabolic actions. Recent observations call the attention to the immunomodulating potential of GH. GH has been shown to stimulate the proliferation of T-cells, the generation of cytotoxic T-cells and also the proliferation and immunoglobulin synthesis of B-cells [1, 13]. Apart from being synthesised in the hypophysis, lymphocytes were shown to produce GH. Lymphocytes not only synthesise GH but have specific “cytokine-like” receptors for it [1, 12].

Interleukin-6 (IL-6) is a cytokine with pleiotropic effects regulating haematopoiesis, hepatic acute-phase protein production, B-cell development [2].

Both the GH and IL-6 receptors belong to the receptor family called GH/PRL/cytokine receptor family [7, 11, 14] with some common structural elements. Both the GH and IL-6 receptors were found to associate with JAK family kinases and activate STAT proteins as

Send offprint requests to: Prof. Dr. András Falus PhD, Dsc, Department of Genetics, Cell- and Immunobiology, Semmelweis University Medical School, 1445 Budapest, Nagyvárad tér 4, Hungary. P.O. Box: 370, email: faland@net.sote.hu



transcription factors [9, 15, 16] that findings allude to the possibility of common signal-transduction pathways utilized by the two receptors.

We examined the expression of the *junB* mRNA and the secretion of fibrinogen protein in response to IL-6 stimulation in the presence or absence of different concentrations of GH on the HepG2 human hepatoma cell line. IL-6 is known to induce both the expression of the *junB* mRNA and fibrinogen protein in hepatic cells [2].

## MATERIALS AND METHODS

### *Cell culture and treatments*

HepG2 cells were cultured in six-well plates in 10% FCS (Gibco) containing RPMI1640 medium. Each well contained  $3 \times 10^6$  cells.

Cultures were treated for 0.5, 2, 6 and 24 h with IL-6 (Gibco) or GH (Pharmacia and Upjohn) or with the combination of the two. Concentrations of IL-6 and GH used were 2, 5, 10, 20 ng/ml and 10, 100 and 1000 ng/ml, respectively. All possible combinations were tested.

Cells were harvested for RNA preparation by the end of all treatment periods, in addition, supernatants were collected for the ELISA assay measuring fibrinogen production in the case of 24 h treatments.

### *Isolation of RNA*

Total cellular RNA was prepared from cultures using the guanidium-thiocyanate method [6]. Concentration of RNA was measured on 260 nm with a Spectronics Genesys 2 spectrophotometer. To judge the purity of RNA preparation and the accuracy of RNA concentration measurements we also ran the RNA-s on 1% agarose gels containing 10% formaldehyde on 40 V for 2 h.

The identical intensities of the 28S rRNA bands were considered as indicators of the equal amounts of RNA included in the RT-PCR reaction.

### *Quantitative (competitive) RT-PCR for *junB* mRNA*

RT-PCR for *junB* mRNA was performed as described. Briefly: RT was made using a Perkin-Elmer RT-PCR kit in a volume of 20  $\mu$ l. The mixture contained 2  $\mu$ l 10 $\times$  RT buffer, 5 mM MgCl<sub>2</sub>, 0.5  $\mu$ M oligo-dT, 4  $\times$  1 mM dNTP-s, 25 U MuLV reverse transcriptase, 10 U RN-ase inhibitor, 1  $\mu$ g RNA.

PCR was performed in 50  $\mu$ l volume containing 5  $\mu$ l 10 $\times$  PCR buffer (Promega), 1.5 mM MgCl<sub>2</sub> (Promega), 4  $\times$  0.2 mM dNTP-s (Promega), 50 pmol *junB* primer (sense + antisense), 1 U Taq Polymerase (Promega), 2  $\mu$ l cDNA. The RT-PCR reaction was carried out on a Pharmacia Gene Aaq Controller. The primers (synthesised by Pharmacia) used in the PCR reaction are specific primers for *junB* as described [10]. The sequences of

the primers are: sense: CCAGTCCTTCCACCTCGACGTTTACAAG, antisense: GACTAAGTGCGTGTTTCTTTTCCACAGTAC

Competitive PCR for junB was performed as described by us [8]. Briefly: we amplified the cDNA-s in the presence of a plasmid containing competitor sequence generated by mismatch-cloning. This competitor plasmid is amplified by the same primers as the junB product to be determined but due to its different molecular weight it can be separated from it by an electrophoresis. Using serial dilutions of the competitor the amount of junB mRNA can be determined. By this method we could determine the effects of treatments relative to the untreated control (x-fold).

PCR products were run on 2% agarose gels in 1× TBE buffer on 100 V for 1 h.

### *ELISA assay for fibrinogen*

The protein production of fibrinogen by HepG2 cells was determined from supernatants of cultures treated for 24 h. Fibrinogen was determined by a sandwich ELISA assay as described [5]. Rabbit anti-human fibrinogen and peroxidase conjugated antibodies were purchased from Dakopatts.

### *Statistical analysis*

Results of both the competitive junB RT-PCR and the fibrinogen ELISA assays were analyzed statistically by Student's *t*-probe.

## RESULTS

### *junB mRNA expression*

Both IL-6 and GH dose dependently induced the expression of junB. The effect of IL-6, however, was more prominent. (10 ng/ml IL-6 induced junB expression in 30 min. treatments 10.33-fold, while 1000 ng/ml GH induced it 8.41-fold (Fig. 1).)

In 0.5 h treatments GH moderately enhanced the junB inducing effect of 2 ng/ml IL-6. The enhancing effect was significant only in the highest concentration of GH applied (1000 ng/ml). In the cases of higher (5, 10 and 20 ng/ml) IL-6 concentrations GH dose dependently inhibited the action of IL-6 in the 0.5 h treatment periods. In the 2 and 6 h treatment periods GH did not significantly influence the action of 2 ng/ml IL-6. The induction of junB expression by higher IL-6 concentrations, however, was dose dependently inhibited by GH. In 24 h treatments we could not detect a modulating effect of GH (data not shown).



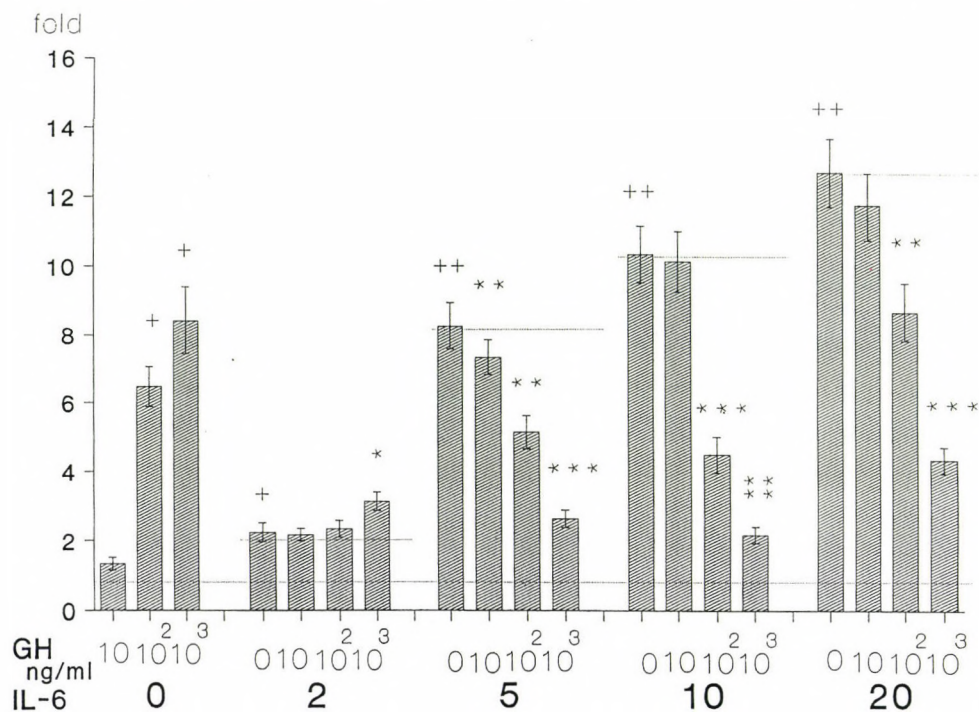


Fig. 1. Results of the competitive junB RT-PCR assay ( $n = 3$ ) in 30 minute treatment periods. Data are expressed relative to the control (x-fold). Treatments with GH or IL-6 alone were compared to the untreated control (+ =  $p < 0.01$ , ++ =  $p < 0.005$ ). Combined IL-6 + GH treatments were compared to the corresponding IL-6 treatments (\* =  $p < 0.05$ , \*\* =  $p < 0.02$ , \*\*\* =  $p < 0.01$ , \*\*\*\* =  $p < 0.005$ )

### Biosynthesis of fibrinogen

In the case of fibrinogen production (Table 1) the tendency of results is similar to that of junB expression. Both GH and IL-6 stimulated the production of fibrinogen on their own, IL-6 again was the more effective (10 ng/ml IL-6 produced a 2.51-fold increase in fibrinogen production, while 1000 ng/ml GH only a 1.92-fold). GH produced a moderate, non-significant, dose-dependent increase in the fibrinogen production elicited by 2 ng/ml IL-6, but significantly decreased that of 10 and 20 ng/ml in a dose dependent way. No tendencies could be observed when 5 ng/ml IL-6 was applied.

### DISCUSSION

Hormones (e.g. GH) are found to have paracrine, cytokine-like effects, and cytokines (e.g. IL-6) to have endocrine, hormone-like actions [4]. Both the receptors of IL-6 and GH and their signal-transduction pathways have similar elements [3, 11].

*Table 1*  
The effect of growth hormone and interleukin-6  
on fibrinogen production by HEPG2 human hepatoma cells

Treatments	mean $\pm$ SD	p
Control	1.00 $\pm$ 0.09	
<i>10 ng/ml GH</i>	<i>1.02 <math>\pm</math> 0.11</i>	<i>NS</i>
<i>100 ng/ml GH</i>	<i>1.84 <math>\pm</math> 0.17</i>	<i>p &lt; 0.01</i>
<i>1000 ng/ml GH</i>	<i>1.92 <math>\pm</math> 0.24</i>	<i>p &lt; 0.02</i>
<i>2 ng/ml IL-6</i>	<i>1.22 <math>\pm</math> 0.13</i>	<i>NS</i>
2 ng/ml IL-6 + 10 ng/ml GH	1.25 $\pm$ 0.15	NS
2 ng/ml IL-6 + 100 ng/ml GH	1.43 $\pm$ 0.22	NS
2 ng/ml IL-6 + 1000 ng/ml GH	1.41 $\pm$ 0.28	NS
<i>5 ng/ml IL-6</i>	<i>1.62 <math>\pm</math> 0.24</i>	<i>p &lt; 0.05</i>
5 ng/ml IL-6 + 10 ng/ml GH	1.36 $\pm$ 0.17	NS
5 ng/ml IL-6 + 100 ng/ml GH	1.42 $\pm$ 0.19	NS
5 ng/ml IL-6 + 1000 ng/ml GH	1.38 $\pm$ 0.16	NS
<i>10 ng/ml IL-6</i>	<i>2.51 <math>\pm</math> 0.43</i>	<i>p &lt; 0.02</i>
10 ng/ml IL-6 + 10 ng/ml GH	1.69 $\pm$ 0.11	p < 0.05
10 ng/ml IL-6 + 100 ng/ml GH	1.15 $\pm$ 0.04	p < 0.02
10 ng/ml IL-6 + 1000 ng/ml GH	0.93 $\pm$ 0.11	p < 0.02
<i>20 ng/ml IL-6</i>	<i>2.83 <math>\pm</math> 0.55</i>	<i>p &lt; 0.02</i>
20 ng/ml IL-6 + 10 ng/ml GH	1.85 $\pm$ 0.19	NS
20 ng/ml IL-6 + 100 ng/ml GH	1.40 $\pm$ 0.23	p < 0.05
20 ng/ml IL-6 + 1000 ng/ml GH	0.99 $\pm$ 0.06	p < 0.02

HepG2 cells were treated for 24 h. Results are expressed relative to the control (x-fold). NS = non significant. Treatments with GH or IL-6 alone (in italics) were compared to the untreated control, combined IL-6 + GH treatments were compared to the corresponding IL-6 treatments (n=3).

We therefore surmised the possibility of GH influencing the actions of IL-6. We studied the effects of GH treatments on responses elicited by IL-6 in the HepG2 human hepatoma cell line. We examined two responses: the expression of the junB mRNA that is an early response and the production of the fibrinogen protein as a late one.

We obtained similar results with the two systems. GH seemed to induce both the expression of junB mRNA and the fibrinogen protein in a dose dependent manner. IL-6, however, was found to be more potent in inducing these responses.

No effects of GH were observed on the junB expression elicited by IL-6 in 24 h treatment periods. Since junB is an early gene [17], it may be possible, that the stimuli that lead to its activation cease by this longer period. One may speculate that among physiological conditions when GH and IL-6 occur together during acute phase response to sur-



gery, in follicular fluid [4, 15] or during therapeutical application of GH in children with broad spectrum of pediatric diseases related with short stature or growth failure this type of interplay may modulate the local effects of interleukin-6.

The interaction between these two mediators might occur at receptor level a more "downstream", during signal transduction. Since both the GH and IL-6 receptors were shown to activate JAK kinases and STAT family proteins [9, 15, 16], there may be both cooperative and competitive interplay between these mediators when GH and IL-6 are simultaneously present.

#### ACKNOWLEDGEMENT

This work was supported by grants OTKA 021175/1995 and MKM 90/1997.

#### REFERENCES

1. Auernhammer, C. J., Strasburger, C. J. (1995) Effects of growth hormone and insulin-like growth factor I on the immune system. *Eur. J. Endocrinol.* 133, 63–65.
2. Baumann, H., Marinkovic-Pajovic, S., Won, K. A. (1992). The action of interleukin-6 and leukaemia inhibitory factor on liver cells. In: *Polyfunctional Cytokines: IL-6 and LIF*. Wiley, Chichester (Ciba Foundation Symposium 167), pp. 100–124.
3. Bazan, J. F. (1990) Haemopoietic receptors and helical cytokines. *Immunol. Today* 11, 350–354.
4. Besedovsky, H. O., del Rey, A. (1996) Immune-neuro-endocrine interactions: facts and hypotheses. *Endocrine Rev.* 17, 64–102.
5. Biró, J., Bosze, Sz., Hudecz, F., Nagy, Z., Rajnavölgyi, É., Schmidt, B., Rákász, É., Falus, A. (1995) The effect of WSEWS pentapeptide and WSEWS-specific monoclonal antibodies on constitutive and IL-6 induced acute-phase protein production by a human hepatoma cell line, HepG2. *Immunol. Lett.* 46, 183–187.
6. Chomczynski, P., Sacchi, N. (1987) Single-step method of RNA isolation by acid guanidinium thiocyanate-phenol-chloroform extraction. *Anal. Biochem.* 162, 156–159.
7. Hirano, T., Matsuda, T., Nakajima, K. (1994) Signal transduction through gp130 that is shared among the receptors for the interleukin-6 related cytokine subfamily. *Stem. Cells* 12, 262–277.
8. Igaz, P., Fejér, G., Szalai, Cs., Tóth, S., Falus, A. (1998) Development of competitive mRNA PCR for the quantification of interleukin-6 responsive junB oncogene expression. *Biotechniques* 24, 854–860.
9. Ihle, J. N., Kerr, I. M. (1995) Jaks and Stats in signaling by the cytokine receptor superfamily. *TIG* 11, 69–74.
10. Irving, J., Feng, J., Wistrom, C. (1992) An altered repertoire of fos/jun (AP-1) at the onset of replicative senescence. *Exp. Cell Res.* 202, 161–166.
11. Kelly, P. A., Goujon, L., Sotiropoulos, A. (1994) The GH receptor and signal transduction. *Hormone Res.* 42, 133–139.
12. Kiess, V., Butenandt, O. (1985) Specific growth hormone receptors on human peripheral mononuclear cells: reexpression, identification and characterization. *J. Clin. Endocrinol. Metab.* 60, 740–746.
13. Murphy, W. J., Rui, H., Longo, D. L. (1995) Effects of growth hormone and prolactin on immune development and function. *Life Sci.* 57, 1–14.
14. Postel-Vinay, M. C., Finidori, J. (1995) Growth hormone receptor: structure and signal transduction. *Eur. J. Endocrinol.* 133, 654–659.
15. Schindler, C., Darnell, J. (1995) Transcriptional responses to polypeptide ligands: The JAK-STAT pathway. *Ann. Rev. Biochem.* 64, 621–651.
16. Vanderkuur, J. A., Wang, X., Zhang, L. (1994) Domains of the growth hormone receptor required for association and activation of JAK2 tyrosine kinase. *J. Biol. Chem.* 34, 21709–21717.
17. Vogt, P. K., Bos, T. J. Jr. (1990) Oncogene and transcription factor. *Adv. Cancer Res.* 55, 1–35.

## HOMOPLASTIC A12,753G MITOCHONDRIAL DNA MUTATION IN A HUNGARIAN FAMILY

Andrea KIS<sup>a</sup>, A. MATOLCSY<sup>b</sup>, L. VÉCSEI<sup>c</sup>, G. KOSZTOLÁNYI<sup>c</sup>, K. MÉHESE<sup>a,d</sup>  
and B. MELEGH<sup>a,d,e</sup>

<sup>a</sup>MTA-POTE Clinical Genetics Research Group of the Hungarian Academy of Sciences,  
Department of <sup>b</sup>Pathology, <sup>d</sup>Pediatrics and <sup>c</sup>Medical Genetics, University Medical School of Pécs, Pécs;  
Department of <sup>e</sup>Neurology, Szent-Györgyi Albert University Medical School of Szeged, Szeged, Hungary

(Received: 1998-05-25; accepted: 1998-07-23)

A 42-year-old male patient with clinical symptoms resembling multiple sclerosis but showing slight unusual myopathic features was referred to our clinic. Analysis of mtDNA isolated from the patient's skeletal muscle revealed two homoplasmic *Pvu* II restriction sites instead of the usual single one. At the same time, digestion of the DNA with *Bam*H I and with *Sac* I resulted in the normal one and two restriction fragments, respectively. For search of the mutation as the possible background of the patient's disease, serial PCR amplifications were carried out, and the new *Pvu* II site was tentatively located within the 12,352 and 12,914 bp. This region of the patient's mtDNA was sequenced and an A to G transition at the 12,753 bp position was found. According to the sequence analysis, this mutation was responsible for generation of the new *Pvu* II restriction site. The mutation caused a modification of the CAA triplet at the 12,751 position to CAG. Since both triplets encode glutamine in the mtDNA, the mutation could not have been responsible for the patient's disease. The same mutation was identified in the healthy brothers of the patient. Our investigation seems to have recognized a variant of the mtDNA in a Hungarian family which has not been revealed so far in any European haplogroup.

**Keywords:** Mitochondrial DNA – polymorphism – population genetics

### INTRODUCTION

The human mitochondrial DNA (mtDNA) is a closed circular molecule which was first completely sequenced by Anderson et al. [1]. The sequence evolution rate of human mtDNA is more than ten times higher than that of the nuclear genes [7, 17], resulting in the natural occurrence of several variants of mtDNA in normal individuals. Haplotype and phylogenetic analyses of the human mtDNA became a useful approach for clarification of several issues concerning the origin of humans, including time-course and colonization patterns in various regions of the world, and the genetic relationships of the existing human populations [11, 13–15].

On the other hand, a continuously growing number of diseases is associated with mtDNA defects. These include, among others, the multisystem disorders of encephalomyopathy, cardiomyopathy: it seems, that tissues with high oxidative capacity, like the

Send offprint requests to: Béla Melegh, M.D., Ph.D., Associate Professor of University Medical School of Pécs, H-7623 Pécs, József A. 7, Hungary, email: meleghb@apacs.pote.hu



nervous system and the muscle tissues are the most vulnerable to such kind of defects [8, 9, 10, 17, 18].

Here we report on a case of male patient who had neuromuscular symptoms. During the molecular biology investigations a new type of mtDNA variant was established. Although the mutation could not have been responsible for the patient's disease, since the same alteration was later detected in the patient's healthy family members as well, it represents a new natural mtDNA mutation variant, which has not been detected so far in Europe.

## MATERIALS AND METHODS

A 42-year-old male patient developed clinical symptoms resembling multiple sclerosis seven years prior to the examinations reported here. As an unusual feature in multiple sclerosis, he had skeletal muscle involvement evidenced by increasing fatigue, intolerance of normal muscle work, which had not been problem before the beginning of his disease. He became clumsy, later retinal degeneration appeared with retrobulbar neuritis. Among others, the possibility of mitochondrial disease had been arisen, and the DNA extracted from the muscle of the patient was sent for analysis of a possible mtDNA deletion.

The total DNA from the muscle and peripheral blood was phenol extracted using standard procedures [12]. For search of mtDNA deletion the method based on Southern blotting was used as previously described [8]; the probe was human mtDNA extracted from placenta, labeled with [32]P dATP using a random prime labeling kit (Megaprime, Amersham International). For digestion of the total DNA *Pvu* II, *Sac* I and *Bam* H I restriction enzymes were used.

For search of the location of the extra *Pvu* II site several amplifications with different primers were applied. Finally, the primers harboring between 12,352-12,368 np (5'ACTATAACCACCCTAAC3') and 12914-12898 np (5'GAGTGTAGGATAAATCA3') were used. Amplifications were performed in 50  $\mu$ l total volume, the mixture contained 100 ng of total DNA, 2.5 mM  $MgCl_2$ , 10 mM Tris HCl buffer, pH 9.0, 50 mM KCl, 200  $\mu$ M of each of four dNTPs, 20 pmol of each primer and 2 U of *Taq* DNA polymerase. The thermal conditions were as follows: the first cycle of 5 min at 95 °C denaturation, 50 °C annealing for 2 min, and elongation at 72 °C for 3 min was followed by 30 cycles of 95 °C 1 min, 50 °C 2 min, 72 °C 3 min. The final extension was: 95 °C 1 min, 50 °C 2 min, and 72 °C 10 min, and the PCR product was agarose gel electrophoresed and visualized by ethidium bromide staining [12]. The amplification product was also used to detect the presence of the new *Pvu* II site, and was used for sequencing of the mtDNA, as well.

The PCR products were cloned into pCR<sup>TM</sup> II vector using the TA cloning system (Invitrogen, San Diego, CA), following the manufacturer's instructions. The DNA sequencing was performed from a small-scale plasmid preparation using the Sequenase version 2.0 (USB, Cleveland, OH) system according to the instructions and the usual procedures [12].

## RESULTS

In the DNA extracted from the skeletal muscle of the patient two homoplasic *Pvu* II sites (5'CAG↓CTG3') were detected with Southern blotting (Fig. 1) instead of the normal single one located at the 2,650 bp position at the reference sequence [1]. At the same time, digestion of the DNA with *Bam* H I and *Sac* I resulted in generation of homoplasic 16.6 Kb single, and 9.6 plus 6.9 Kb double restriction sites, respectively, as it occurs normally on the Cambridge sequence [1]. There was no evidence for significant mtDNA deletion in the patient.

During the sequence analysis of the mtDNA actually the H chain was sequenced (Fig. 2). In the amplified mtDNA region spanning between 12,352 and 12,914 bp the whole sequence was identical to the reference sequence except for one base difference: at 12,753 bp an a T → C substitution was found in the patient's mtDNA (Fig. 2), which corresponded to a A → G substitution in the coding L chain. Thus, the substitution changed the original CAA triplet at 12,751 bp to CAG in the L chain of the mtDNA.

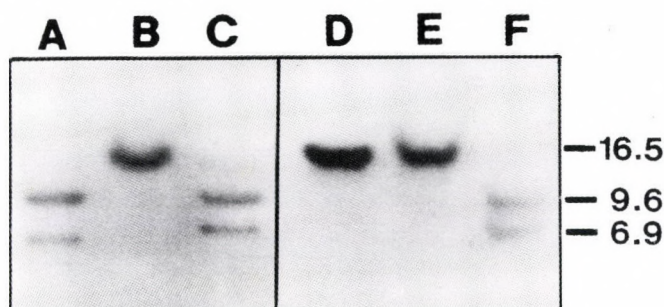


Fig. 1. Analysis of the patient's DNA (left panel) with restriction enzymes. For the Southern blot the following enzymes were used: *Pvu* II (lanes A and D), *Bam* H I (lanes B and E), and *Sac* I (lanes C and F). In the mtDNA of the patient two homoplasic *Pvu* II sites were detected (lane A), instead of the normal one (the control patient is on the right panel; *Pvu* II digestion in the lane C). Digestion with *Bam* H I and with *Sac* I resulted in the normal one and the normal two digestion products, respectively, both in the patient and in the healthy control (right panel)

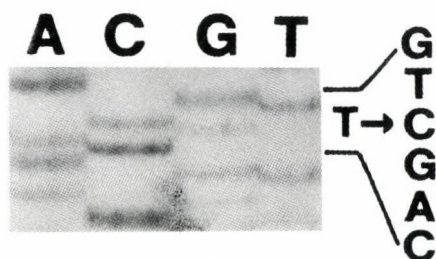


Fig. 2. Sequence of the H chain of the mtDNA of the patient. A T → C substitution was found at the position of 12,753 bp



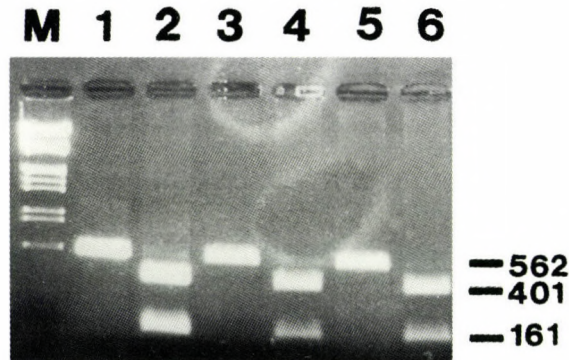


Fig. 3. Restriction analysis of the amplified segment of mtDNA spanning between 12,352 and 12,914 np from the patient (lanes 1 and 2), and from the patient's brothers (lanes 3–4 and 5–6). The amplification of the DNAs resulted in a single 562 np amplification product in each cases (lanes 1, 3 and 5); the digestion of the amplified DNA with *Pvu* II lead to the generation of two digestion products (401 and 161 bp) in each cases (lanes 2, 4 and 6)

Using the total DNA extracted from peripheral blood of the patient and from his two clinically healthy brothers, the mtDNA was amplified using the same primers as detailed above. The amplified 562 bp segment was totally digestible with *Pvu* II, the digestion resulted in two pieces of product (401 and 161 bp, as it could be calculated) in both cases indicating, that the mutation was inherited in the patient's family (Fig. 3). The death of the patient's mother several years before the examinations disabled us to analyze her DNA.

## DISCUSSION

Several types of mutation of the mtDNA have been described to cause neuromuscular diseases, including deletions and point mutations of the mitochondrial genom [5, 9, 10, 17, 18]. Since our patient exhibited unusual clinical features, we analyzed his DNA bearing in mind a possible mutation which could have been related to his disease. Finally, a homoplasmic A → G substitution was found at the 12,753 np position, which changed the CAA triplet to CAG at the 12,751 np.

In the mtDNA both CAA and CAG triplets encodes glutamine. Regarding the nuclear genome, a minimum of 32 tRNAs are required to read the genetic code according the wobble principle [3, 4], by contrast, in the mitochondria the codon-anticodon pairing is more simplified and only 22 tRNAs are available to read the information deriving from the mtDNA [1, 2]; one mitochondrial tRNA can recognize the entire four-member codon family rather than the two tRNA per codon family in the nuclear genetic code. Since again, both CAA and CAG triplets encodes glutamine, and there is no evidence for different binding characteristics for the two tRNAs in the mitochondrial translation, which could act on the protein synthesis, the mutation detected in the patient seems not to be responsible for his disease. This is strengthened by the fact, that the brothers of the patient had no clinical evidence for neuromuscular disease at the time of the examination.

Since mtDNA is maternally transmitted and therefore does not undergo recombination, and it has a high sequence evolution rate, the mutations radiated along the maternal lineages and accumulated in the different human populations can be used as haplogroup markers [11, 13–15]. Since in the most extensive studies [11, 13–15] the region of mtDNA affected in our family has not been examined, therefore its natural occurrence in the European populations cannot be predicted. Moreover, no firmly established case of this mutation can be found in the literature; only in one single Non-Ainu Japanese individual the authors [6] concluded the existence of this variant based on the digestion pattern, but it was not established by sequencing. Probably further studies can reveal if this mutation-variant in combination with others can be regarded and used as a sub-population haplogroup marker.

#### ACKNOWLEDGEMENTS

The authors are indebted to Antonio Torroni for his help in the sequence search within his own data in the Emory Database. This work was supported in part from grants of the Hungarian National Science Foundation, OTKA T 019301, T 023588; the Ministry of Welfare ETT 377/1996, 365/1996, and of the Ministry of Education MKM 739/1996, FKFP 1261/1997.

#### REFERENCES

1. Anderson, S., Bankier, A. T., Barrell, B. G., de Bruijn, M. H. L., Coulson, A. R., Drouin, J., Eperon, I. C., Nierlich, D. P., Roe, B. A., Sanger, F., Schreier, P. H., Smith, A. J. H., Staden, R., Young, I. G. (1981) Sequence and organisation of human mitochondrial genome. *Nature* 290, 457–465.
2. Barelli, B. G., Anderson, S., Bankier, A. T., de Bruijn, M. H., Chen, E., Coulson, A. R., Drouin, J., Eperon, I. C., Nierlich, D. P., Roe, B. A., Sanger, F., Schreier, P. H., Smith, A. J., Staden, R., Young, I. G. (1980) Different pattern of codon recognition by mammalian mitochondrial tRNAs. *Proc. Natl. Acad. Sci. USA* 77, 3164–3174.
3. Crick, F. H. (1966) The genetic code-Yesterday, today, and tomorrow. *Cold Spring Harb. Symp. Quant. Biol.* 31, 1–31.
4. Crick, F. H. (1966) The genetic code. *Sci. Amer.* 215, 55–61.
5. Editorial (1998) Mitochondrial encephalomyopathies: gene mutation. *Neuromusc. Disord.* (updated in each issue).
6. Harihara, S., Hirai, M., Omoto, K. (1986) Mitochondrial DNA polymorphism in Japanese living in Hokkaido. *Jpn. J. Human Genet.* 31, 73–83.
7. Miyata, T., Hayashida, H., Kikuno, R., Hasegawa, M., Kobayashi, M., Koike, K. (1982) Molecular clock of silent substitution: at least six-fold preponderance of silent changes in mitochondrial genes over those in nuclear genes. *J. Mol. Evol.* 19, 28–35.
8. Melegh, B., Bock, I., Gáti, I., Méhes, K. (1996) Multiple mitochondrial DNA deletions and persistent hyperthermia in a patient with Brachmann–De Lange phenotype. *Am. J. Med. Genet.* 65, 82–88.
9. Molnar, M., Zanssen, S., Buse, G., Schröder, J. M. (1996) A large-scale deletion of mitochondrial DNA in a case with a pure mitochondrial myopathy and neuropathy. *Acta Neuropathol.* 91, 654–658.
10. Nishino, I., Komatsu, M., Kodama, S., Horai, S., Nonaka, I., Goto, Y. (1996) The 3260 mutation in mitochondrial DNA can cause mitochondrial myopathy, encephalopathy, lactic-acidosis, and stroke-like episodes (MELAS). *Muscle Nerve* 19, 1603–1604.



11. Passarino, G., Semino, O., Bernini, F. L., Santachiara-Benerecetti, S. A. (1996) Pre-caucasoid and caucasoid genetic features of the Indian population, revealed by mtDNA polymorphisms. *Am. J. Hum. Genet.* 59, 927–934.
12. Sambrook, J., Fritsch, E. F., Maniatis, T. (1989) Molecular cloning. In: *A Laboratory Manual*, 2nd. edition. Cold Spring Harbor Laboratory Press, Cold Spring Harbor, New York.
13. Torroni, A., Schurr, T., Yang, C.-C., Szathmary, E. J. E., Williams, R. C., Schandfield, M. S., Troup, G. A., Knowler, W. C., Lawrence, D. N., Weiss, K. M., Wallace, D. C. (1992) Native American mitochondrial DNA analysis indicates that the Amerind and the Nadene populations were founded by two independent migrations. *Genetics* 130, 153–162.
14. Torroni, A., Schurr, T. G., Cabell, M. F., Brown, M. D., Neel, J. V., Larsen, M., Smith, D. G., Vullo, C. M., Wallace, D. C. (1993) Asian affinities and continental radiation of the four founding Native American mitochondrial DNAs. *Am. J. Hum. Genet.* 53, 563–590.
15. Torroni, A., Neel, J. V., Barrantes, R., Schurr, T. G., Wallace, D. C. (1994 c) A mitochondrial DNA “clock” for the Amerinds and its implication for timing their entry into North America. *Proc. Natl. Acad. Sci. USA* 91, 1158–1162.
16. Wallace, C. D. (1992) Diseases of the mitochondrial DNA. *Ann. Rev. Biochem.* 61, 1175–1212.
17. Wallace, D. C., Ye, J. H., Neckelmann, S. N., Singh, G., Webster, K. A., Greenberg, B. D. (1987) Sequence analysis of cDNAs for the human and bovine ATP synthase beta subunit: mitochondrial DNA genes sustain seventeen times more mutations. *Curr. Genet.* 12, 81–90.
18. Zeviani, M., Servidei, S., Gellera, C., Bertini, E., DiMauro, S., DiDonato, S. (1989) An autosomal dominant disorder with multiple deletions of mitochondrial DNA starting at the D-loop region. *Nature* 339, 309–311.

## COLORMAPPING: A NON-MATHEMATICAL PROCEDURE FOR GENETIC MAPPING

G. B. KISS, A. KERESZT, P. KISS and Gabriella ENDRE

Institute of Genetics, Biological Research Center of the Hungarian Academy of Sciences, Szeged, Hungary

(Received: 1998-06-23; accepted: 1998-09-14)

We describe a new procedure, called colormapping, a non-mathematical method for genetic mapping. Numerical scores representing the genotypes of the markers are converted to colors and these are used to display the genotypes of the markers for each individual in a segregating population. Color genotypes are arranged in a matrix where each row corresponds to a marker – ordered according to their position in the appropriate Linkage Group – and each column represents an individual in the mapping population. The picture is called colormap by which the genotypes of the chromosomal segments can be shown for each individual in the segregating population. A colormap can be used for whole genome analysis which is profitable in genetic and breeding experiments and is suitable for genetic mapping, too. The location of a new marker is found by recognizing similarities between the color pattern of the individuals for the new marker and the ordered markers in the colormap. Colormapping can also be used to find linkages which cannot be determined unambiguously by conventional mapping programs. Moreover, colormaps are extremely powerful for troubleshooting by indicating inaccurate genotypes caused by errors of different origin. Colormap(ping) is generally applicable to genetic mapping/analysis of any organisms.

*Keywords:* Genetic linkage map – colormapping – *Medicago sativa*

### INTRODUCTION

The efficient analysis of complex genomes like those of the plants started with the work of Gregor Mendel who discovered the basic principles of the inheritance of traits [9]. By the work of T. H. Morgan and A. H. Sturtevant, traits determined by genes could be assigned to Linkage Groups (LGs), and within one LG the order of the genes could be established, thereby genetic maps could be constructed [11]. Until 1980, different morphological mutants, distinguishable forms of enzymes (allozymes/isozymes), and other traits like resistance against pathogens were used as genetic markers for the construction of genetic maps of different plants (e.g. pea, maize, rice, etc.). Genetic mapping based on the above types of markers was time consuming and limited concerning the number of markers. Since the introduction of molecular markers for mapping [2], the construction of ge-

Send offprint requests to: Dr. G. B. Kiss, Institute of Genetics, Biological Research Center of the Hungarian Academy of Sciences, H-6701 Szeged, Hungary. P.O. Box 521. E-mail: kgb@everx.szbk.u-szeged.hu



netic maps of many organisms including plant species has been extremely accelerated and become relatively simple. It was demonstrated for the first time in 1980 [2] that DNA sequence differences between two crossable individuals can be detected by Southern hybridization [10], and used as codominant genetic markers for mapping. This new technique, called Restriction Fragment Length Polymorphism (RFLP), became a powerful tool to construct genetic map of different organisms. Since 1990 several PCR-based techniques (Random Amplified Polymorphic DNA (RAPD) [14]; Arbitrary Primed PCR (AP-PCR) [13]; DNA Amplification Fingerprinting (DAF) [4]; Amplified Fragment Length Polymorphism (AFLP) [12]) have been rapidly developed in order to increase the number of DNA markers on the maps. PCR-based techniques have several advantages over RFLP such as speed, handling more samples, and avoidance of isotopes. On the other hand, they also have drawbacks like dominant inheritance in many cases and some degree of ambiguity compared to RFLP.

The construction of the genetic maps is based on the calculation of the recombination frequencies (RF) from the genotype scores for the marker pairs of a segregation population. By this, the large number of genotypic data, which were equal to the number of individuals in the segregation populations were abstracted into single RF values between two markers. RF values were then converted to genetic distances, which were then used to draw the genetic map. Accordingly, markers were shown next to a vertical bar according to their order and proportionally to their calculated genetic distance. The vertical bars constituting all the linkage groups of an organism represented the genetic map. This presentation of the marker orders did not reflect the genotype of the markers and the individuals in the mapping population, that is the raw data used for the calculations were not shown. Raw data are genotypes which were usually designated by characters (numbers or letters) and stored as tabulated data. Raw data in this form were impracticable and could not be easily handled since the mass of the numbers or letters in the matrix was confusing for the eyes. However, replacing the characters by graphical or color symbols made the raw data manageable. Graphical and color representation of the genotypes could be used for whole genome [15] or pedigree analysis [3].

During our mapping work we realized that the use of color representation of the genotypes can be further improved and this type of visualization could be applied as a powerful tool for genetic mapping. In this communication we describe the so-called colormapping which is a non-mathematical procedure for genetic mapping. Colormapping is an interactive, computer based but manually performed operation by which the position of a new marker can be easily determined. Genotypes of the markers for each individual in the mapping population were converted to and represented by colors, and computer spreadsheet program was used to display the color genotypes as a genetic colormap. The genotypes of a new marker were displayed by a color patterned row which in turn could be inserted between two marker rows of the colormap according to their best match compared to the flanking color pattern. This mapping procedure is fast, facile, reliable, avoids mathematical calculations and allows powerful troubleshooting by highlighting genotypes which do not match the surrounding genomic region.

## MATERIALS AND METHODS

### *The origin of the data used in this study*

In order to construct a colormap the determination of the genotypes of the markers for the individuals in a segregation population is needed. The genotypes which were used to deduce the colormap from numerical characters are taken from the *mouse.raw* data file of the program MAPMAKER/EXP 3.0 [7, 8] which contains the genotypes for 15 loci of chromosome 10 for the 46 individual mouse progeny in a segregating population. The name, location and distances of these markers can be found on page 45 of the MAPMAKER/EXP 3.0 manual. Software and manual of MAPMAKER/EXP 3.0 can be obtained from Dr. Eric Lander (Whitehead Institute, 9 Cambridge Center, Cambridge, MA 01242, USA, Fax: 617 258 6505; Internet: mapmaker@genome.wi.mit.edu). The above-mentioned 15 markers are used for Figs 1–3. The genotype data for the markers of the LGs 2, 6 and 7 of diploid *Medicago sativa* shown in Figs 4 and 5 are the results of the mapping work on alfalfa in our laboratory [Káló et al., submitted].

### *Conversion of the numerical genotypes to color symbols*

The numerical genotypes throughout the paper are as follows: 1 and 3 maternal and paternal homozygous, respectively; 2 heterozygous; 4 paternal dominant; 5 maternal dominant genotypes; 0 missing data. These genotypes are converted to colors by EXCEL program using short Macro programs utilizing the "Format\Cells...\Patterns\Cell shading\color" functions. These Macro programs convert the white shading of the cells containing the numerical characters to colors as follows: Character 0, 1, 2, 3, 4 and 5 are converted to gray, yellow, green, purple, metal-blue, and light green, respectively.

### *Procedure of colormapping using EXCEL program*

Colormapping is carried out by the computer program EXCEL which is available for both IBM compatible and Macintosh/Apple computers. Data are interchangeable between the computer systems through ASCII text file format. Genotypes are converted to colors (see above) which results in a color pattern (see Results). Care has to be taken to introduce the genotype scores of a new marker in the same order as the order of the individual plants in the colormap to be used. Mapping manipulation starts by opening a window with two horizontal parts, one is steady, this contains the color pattern of the new marker in one row (usually at the bottom of the screen), the other is rolled and contains as many rows of the markers from the colormap as possible or convenient. The markers in the later window are scrolled from the first marker until the last one by using the mouse on the scrolling arrowhead on the right side of the window. The human eyes recognize easily when the color pattern of the new marker and that of the markers in the colormap are similar. When best fit is achieved, scrolling is stopped and the new marker is inserted into the



colormap by the "Cut" and the "Insert cut cells" functions of the "Edit" menu. This operation takes less than one minute after having the combined color genotype data of the new marker introduced into the spreadsheet. Program EXCEL v. 5.0 for IBM compatible computers allows to handle 256 columns and 16384 rows that is there is room for more than 4,000,000 genotype data. The best way to handle the data is to have a master file ("frame colormap") containing only limited number of core markers (preferentially codominant ones), as well as individual files for each LG with all markers mapped. Conveniently "rough" mapping is done first in the "frame colormap". Once a new marker has been mapped then it is transferred to the file containing the appropriate LG where "fine" mapping can be performed. It is of choice whether the newly mapped marker becomes the member of the core markers.

## RESULTS

### *Generation of color pattern from raw data, and the colormap*

Genetic mapping has been based till now on mathematical analysis of the incidence rate of the genotypes for the loci segregated in the individuals of a mapping population. Irrespective of the type of the segregation population (whether it is inbred line, F2 intercross or backcross) genotypes are scored similarly. The individual genotype for a locus can be homozygous for the maternal allele, homozygous for the paternal allele or heterozygous. This kind of genotype allocation can only be used when the evaluation is codominant. In the case of dominant inheritance, however, heterozygous configuration is indistinguishable from the dominant homozygous. Traditionally in diploid organisms the following symbols were introduced taking  $a_1$  and  $a_2$  as the maternal and paternal alleles, respectively:  $a_1a_1$ , maternal homozygous;  $a_2a_2$ , paternal homozygous;  $a_1a_2$ , heterozygous;  $a_1-$ , maternal dominant ( $a_1$  is dominant over  $a_2$ , therefore either  $a_1a_1$ , or  $a_1a_2$ );  $a_2-$ , paternal dominant ( $a_2$  is dominant over  $a_1$ , therefore either  $a_2a_2$ , or  $a_1a_2$ ). These scoring symbols obey the traditional designation highlighting the genotype of both chromosomes of the homologue pair. The application of computer programs for the calculation of genetic linkages for several markers, as well as the ambiguity which may arise from the genetic configuration of two markers with heterozygous genotypes ( $a_1a_2/b_1b_2$  is indistinguishable from  $a_2a_1/b_1b_2$ ) single character symbols representing combined genotypes or scores have been introduced (see for example MAPMAKER/EXP 3.0). These symbols (numeric or alphabetic) can be defined for example as follows: 1 = maternal homozygous ( $a_1a_1$ ); 3 = paternal homozygous ( $a_2a_2$ ); 2 = heterozygous ( $a_1a_2$  or  $a_2a_1$ ); 4 = paternal dominant ( $a_2-$ ); 5 = maternal dominant ( $a_1-$ ).

For the estimation of the recombination frequencies between marker pairs mathematical calculations are generally applied (most frequently the maximum likelihood method is used [1]. For these calculations (which are computerized nowadays), the genotypes of the loci of the individuals in a segregation population have to be fed into the computer one after another. Genotypes are scored as numerical or alphabetical characters (see above) and stored favorably in a spreadsheet file (in our case program EXCEL is used). The cre-

ated file contains the genotypes of the markers for the individuals in a mapping population as shown in Fig. 1. The markers highlighted in the first column of Fig. 1A are not in the order of their chromosome location since their linkage relationships have not been determined yet. To establish the gene order computer program MAPMAKER/EXP 3.0 is used. Running MAPMAKER/EXP 3.0 with data shown in Fig. 1A, the following gene order is obtained: T031 - M153 - M024 - M139 - A114 - M067 - D030 - L062 - M003 - A037 - M007 - M172 - T032 - A063 - M175 (compare this order with the genetic map of chromosome 10 of mouse on page 45 in MAPMAKER/EXP 3.0 manual). In Fig. 1 the 15 markers are displayed random (Fig. 1A) or in ordered (Fig. 1B) sequence, respectively. Looking at the black and white characters it is very hard to observe the changes in the pattern of the numerical data (i.e. recombination), since human eye is not sensitive enough to distinguish black characters on a white background. To make pattern perception more obvious by visual sensation numerical characters are simply replaced by well selected colors, since "Colour is what eye sees best" [5]. Conversion of the genotypes to colors is described in the Materials and Methods, and shown in Fig. 2. The changes in the color pattern after determining the linkage order is striking (compare Fig. 2A with Fig. 2B). In Fig. 2B the long vertical stretches of colors represent homozygous maternal and paternal (yellow and purple, respectively), or heterozygous (green) chromosomal regions. Color transitions reflect recombination events therefore the genotypes of genomic regions and their changes along the chromosomes for each individual can be comprehensively analyzed. The resulting display in Fig. 2B is the so-called colormap. The colored bars next to each other in the colormap are representing the combined genotypes of the 15 ordered markers of the homologue chromosome pair of LG 10 for 46 mouse individuals in an F2 segregating population.

### *Properties of the colormaps*

The colormap shown in Fig. 2B presents the marker order of LG 10 and the combined genotypes of the appropriate individuals for the given genetic markers. This primary colormap, however, does not reflect the proper genetic distances between the markers. Markers and their pertaining genotypes can be arranged according to the genetic distances between the marker pairs as shown in Fig. 3A. Genetic distances have to be calculated from the recombination frequencies using the Haldane or Kosambi map functions. Missing genotypes of the chromosomal regions located between the mapped markers are represented by gray color (refer to Figs 2 and 3A). One can see that the ordered genetic markers determine fixed positions on the chromosome to serve as reference points (i.e. core markers) for subsequent mapping.

A highly saturated genetic map possesses thousands of markers, yet these reference points are far from each other in terms of physical distance. Core markers are flanked by hundreds of genes with undetermined genotypes (see gray zones in Fig. 3A), that is fixed points represent only a very tiny portion of the whole genome. To handle the LGs as continuous genotype segments instead of interrupted ones, the genotypes of the flanking regions can be predicted [15]. The prediction can be carried out easily on the colormap to



## A

	1	2	3	4	5	6	7	8	9	10	11	12	13	14	15	16	17	18	19	20	21	22	23	24	25	26	27	28	29	30	31	32	33	34	35	36	37	38	39	40	41	42	43	44	45	46			
L062	3	2	3	2	1	3	2	2	2	1	2	2	2	2	2	1	2	3	2	2	2	2	2	2	2	2	2	1	2	1	2	2	1	2	2	2	2	2	2	1	2	3	0	1	3	2	1		
D030	2	3	3	2	1	2	2	1	2	1	2	2	1	1	2	1	1	3	1	2	2	2	2	2	3	2	1	2	1	2	3	1	2	2	2	2	2	2	2	1	1	3	3	1	3	2	1		
M175	3	1	2	2	2	3	1	3	1	3	2	2	2	2	1	1	2	3	2	2	1	2	2	3	2	1	2	1	1	2	2	0	1	2	3	1	2	3	1	3	2	2	2	3	1	2			
M067	2	3	3	2	1	2	2	1	2	1	2	2	1	1	2	1	1	3	1	2	2	2	2	2	2	2	2	1	2	1	2	3	1	2	2	2	2	2	1	2	1	3	3	1	3	2	1		
M003	3	2	3	2	2	3	2	2	2	1	2	3	2	2	2	1	2	3	2	2	2	2	2	2	2	2	2	1	2	1	2	2	1	2	2	2	2	2	2	1	2	3	2	1	3	2	1		
M024	5	3	5	3	5	5	5	5	5	5	5	5	5	5	5	5	5	5	5	5	5	5	5	5	5	5	5	5	5	5	5	5	5	5	5	5	5	5	5	5	5	5	3	5	3	5			
M172	3	2	3	2	2	3	1	3	2	1	2	3	2	2	2	1	2	3	2	2	2	2	2	2	2	2	1	1	2	1	2	2	1	2	2	3	2	2	2	1	3	2	2	2	3	1	2		
T031	2	2	2	3	1	2	2	1	2	1	0	2	1	1	2	2	2	2	2	2	2	3	2	2	2	0	2	1	2	1	2	2	2	1	2	2	2	2	1	3	2	2	1	0	2	1	2	2	3
T032	3	1	3	2	2	3	1	3	2	2	2	3	2	2	2	0	2	3	2	2	2	2	2	2	2	2	1	2	2	1	2	2	1	2	2	3	2	2	2	1	3	2	2	2	3	1	2		
M139	2	3	2	3	1	2	2	1	2	1	2	2	1	1	2	1	2	3	2	2	2	2	2	2	2	2	2	1	2	1	2	3	1	2	2	2	2	2	1	2	1	3	3	1	3	2	3		
M007	3	2	3	2	2	3	2	3	2	1	2	3	2	2	2	1	2	3	2	2	2	2	2	2	2	2	2	1	1	2	1	2	2	1	2	2	3	2	2	2	1	3	3	2	2	3	1	2	
M153	2	2	2	3	1	2	2	1	2	1	2	2	1	1	2	2	2	3	2	2	2	2	3	2	2	2	2	2	1	2	1	2	2	1	2	2	2	1	3	2	2	1	3	2	1	2	2	3	
A037	3	2	3	2	2	3	2	3	2	1	2	3	2	2	2	1	2	3	2	2	2	2	2	2	2	2	2	1	1	2	1	2	2	1	2	2	3	2	2	2	1	3	3	2	1	3	2	2	
A114	2	3	3	3	1	2	2	1	2	1	2	2	1	1	2	1	2	3	2	2	2	2	2	2	2	2	2	1	2	1	2	3	1	2	2	2	2	2	2	1	2	1	3	3	1	3	2	3	
A063	3	1	3	2	2	3	1	3	2	2	2	3	2	2	1	1	2	3	2	2	1	2	2	2	2	2	2	1	2	1	1	2	2	1	2	2	3	1	2	2	1	3	2	2	2	3	1	2	

## B

	1	2	3	4	5	6	7	8	9	10	11	12	13	14	15	16	17	18	19	20	21	22	23	24	25	26	27	28	29	30	31	32	33	34	35	36	37	38	39	40	41	42	43	44	45	46			
T031	2	2	2	3	1	2	2	1	2	1	0	2	1	1	2	2	2	2	2	2	2	3	2	2	0	2	1	2	1	2	2	1	2	2	2	1	3	2	2	1	0	2	1	2	2	3			
M153	2	2	2	3	1	2	2	1	2	1	2	2	1	1	2	2	2	3	2	2	2	3	2	2	2	2	1	2	1	2	2	2	2	1	3	2	2	1	3	2	1	2	2	3					
M024	5	3	5	3	5	5	5	5	5	5	5	5	5	5	5	5	5	3	5	5	5	5	5	5	5	5	5	5	5	5	5	5	5	5	5	5	5	5	5	5	3	5	3	5	3				
M139	2	3	2	3	1	2	2	1	2	1	2	2	1	1	2	1	2	3	2	2	2	2	2	2	2	2	1	2	1	2	3	1	2	2	2	2	2	1	2	1	3	3	1	3	2	3			
A114	2	3	3	3	1	2	2	1	2	1	2	2	1	1	2	1	2	3	2	2	2	2	2	2	2	2	1	2	1	2	3	1	2	2	2	2	2	2	1	2	1	3	3	1	3	2	3		
M067	2	3	3	2	1	2	2	1	2	1	2	2	1	1	2	1	1	3	1	2	2	2	2	2	2	2	1	2	1	2	3	1	2	2	2	2	2	2	1	2	1	3	3	1	3	2	1		
D030	2	3	3	2	1	2	2	1	2	1	2	2	1	1	2	1	1	3	1	2	2	2	2	2	3	2	1	2	1	2	3	1	2	2	2	2	2	2	2	1	1	3	3	1	3	2	1		
L062	3	2	3	2	1	3	2	2	2	1	2	2	2	2	1	2	3	2	2	2	2	2	2	2	2	2	1	2	1	2	2	2	1	2	2	2	2	2	2	1	2	3	0	1	3	2	1		
M003	3	2	3	2	2	3	2	2	2	1	2	3	2	2	2	1	2	3	2	2	2	2	2	2	2	2	2	1	2	1	2	2	2	1	2	2	2	2	2	2	2	1	2	3	2	1	3	2	1
A037	3	2	3	2	2	3	2	3	2	1	2	3	2	2	2	1	2	3	2	2	2	2	2	2	2	2	1	1	2	1	2	2	1	2	2	3	2	2	2	1	3	3	2	1	3	2	2		
M007	3	2	3	2	2	3	2	3	2	1	2	3	2	2	2	1	2	3	2	2	2	2	2	2	2	2	2	1	1	2	1	2	2	1	2	2	3	2	2	2	1	3	3	2	2	3	1	2	
M172	3	2	3	2	2	3	1	3	2	1	2	3	2	2	2	1	2	3	2	2	2	2	2	2	2	2	2	1	1	2	1	2	2	1	2	2	3	2	2	2	1	3	2	2	2	3	1	2	
T032	3	1	3	2	2	3	1	3	2	2	2	3	2	2	2	0	2	3	2	2	2	2	2	2	2	2	1	2	2	1	2	2	1	2	2	3	2	2	2	1	3	2	2	2	3	1	2		
A063	3	1	3	2	2	3	1	3	2	2	2	3	2	2	1	1	2	3	2	2	1	2	2	2	2	2	2	1	2	1	2	2	1	2	2	3	1	2	2	1	3	2	2	2	3	1	2		
M175	3	1	2	2	2	3	1	3	1	3	1	3	2	2	2	1	1	2	3	2	2	1	2	2	3	2	1	2	1	1	2	2	0	1	2	3	1	2	3	1	3	2	2	2	3	1	2		

Fig. 1. Genotypes of the markers of the mouse chromosome 10 taken from the *mouse.raw* data file of program MAPMAKER/EXP 3.0 [7, 8]. For simplicity, markers belonging to chromosome 10 were only extracted (see page 45 of the MAPMAKER/EXP 3.0 manual; and see Materials and Methods). The matrix displays the genotypes of 15 loci (first column) of the 46 individuals of the mouse progeny (first row) in the segregating population. Numerical values are: 1 and 3, maternal and paternal homozygous, respectively; 2, heterozygous, 5, maternal dominant genotypes. To handle and edit the raw data program EXCEL for Macintosh or IBM compatible computers was used. Panel A and B show non-ordered and ordered marker sequences, respectively

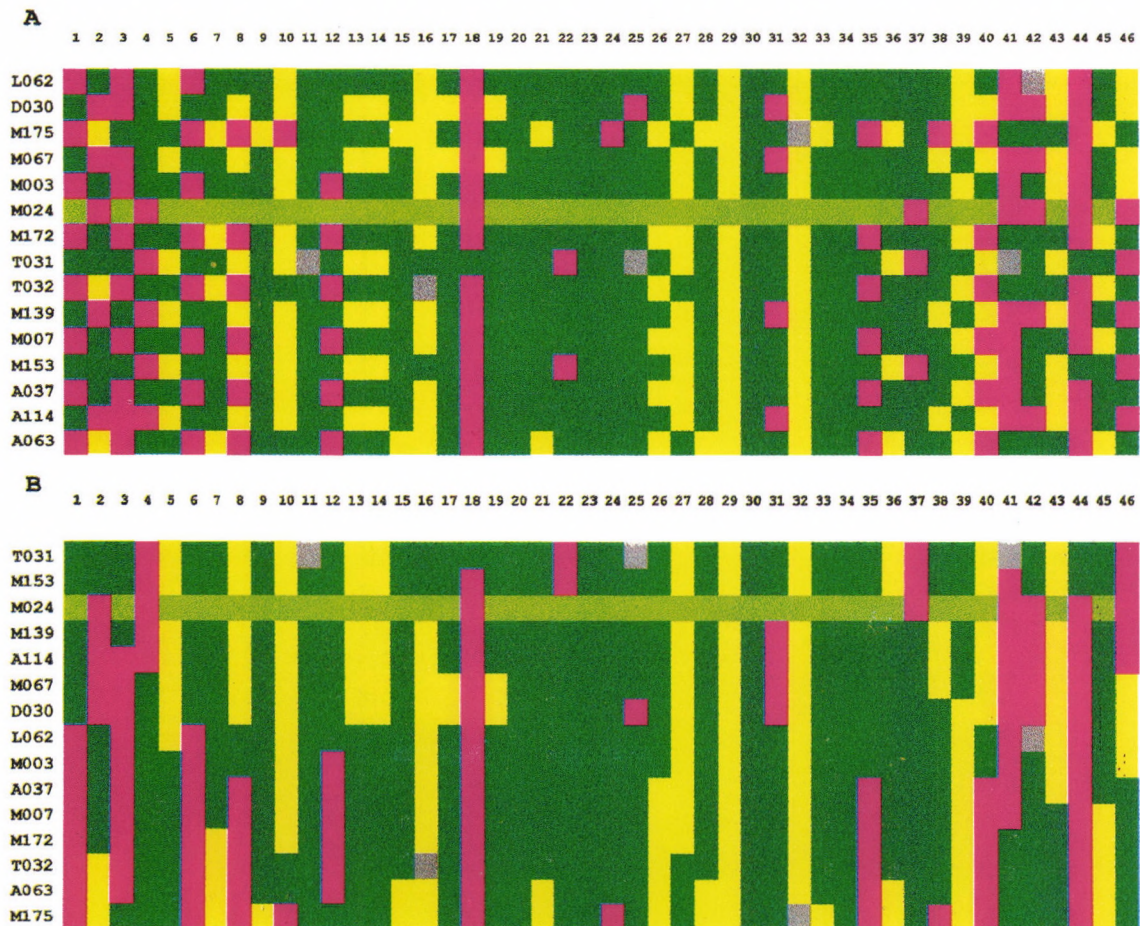


Fig. 2. Genotypes of the mouse markers on chromosome 10 displayed in Fig. 1 are represented here by colors. Maternal (number 1), paternal (number 3) homozygous genotypes are replaced by yellow and purple colors, respectively. Heterozygous (number 2) and maternal dominant (number 5) genotypes are highlighted by green and pale green colors, respectively. Missing data are gray. The numerical characters were replaced by the appropriate color background by the Format "background pattern" function of the *EXCEL* program for either Macintosh or IBM compatible personal computer. Adjusting the column height and row width the desired picture size can be achieved. Panel A and B show disordered and ordered marker sequences, respectively



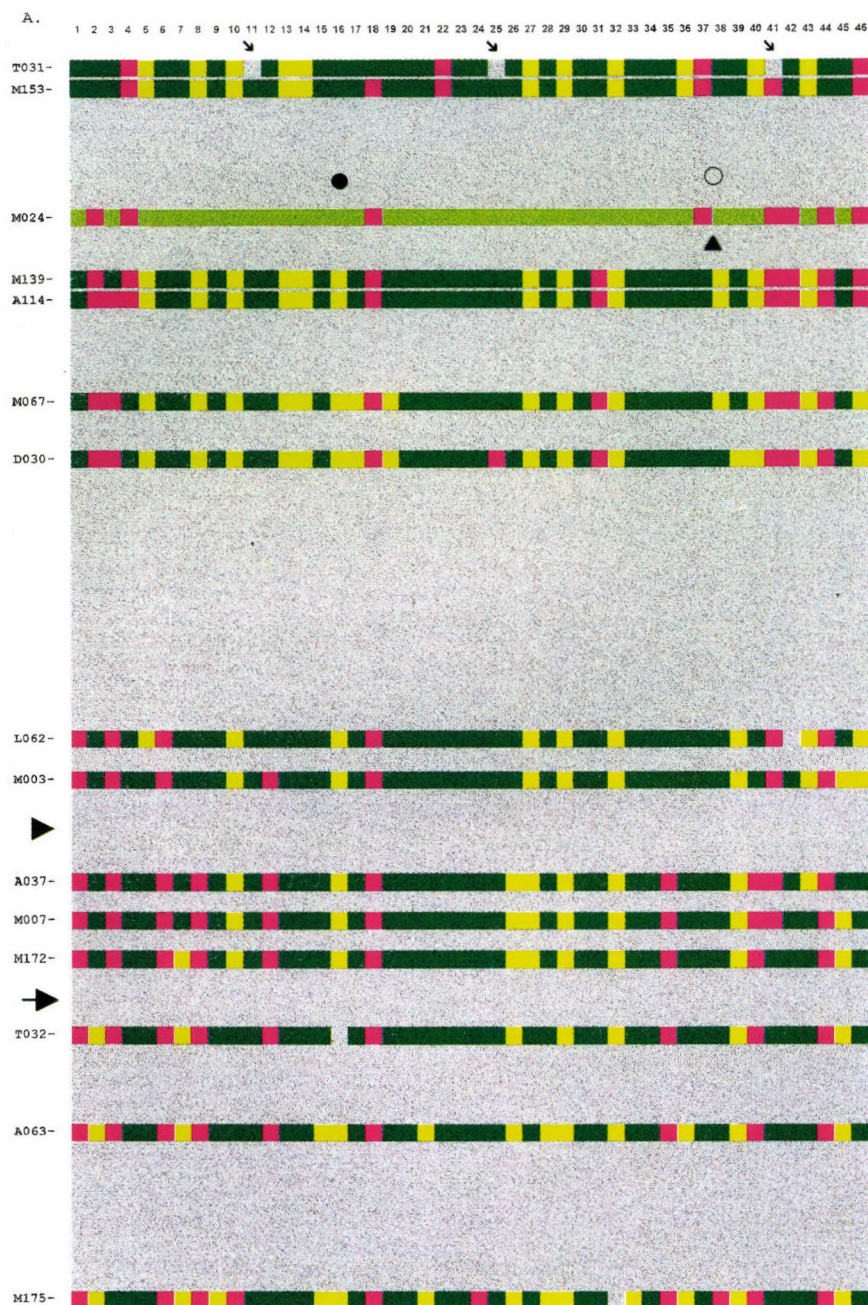
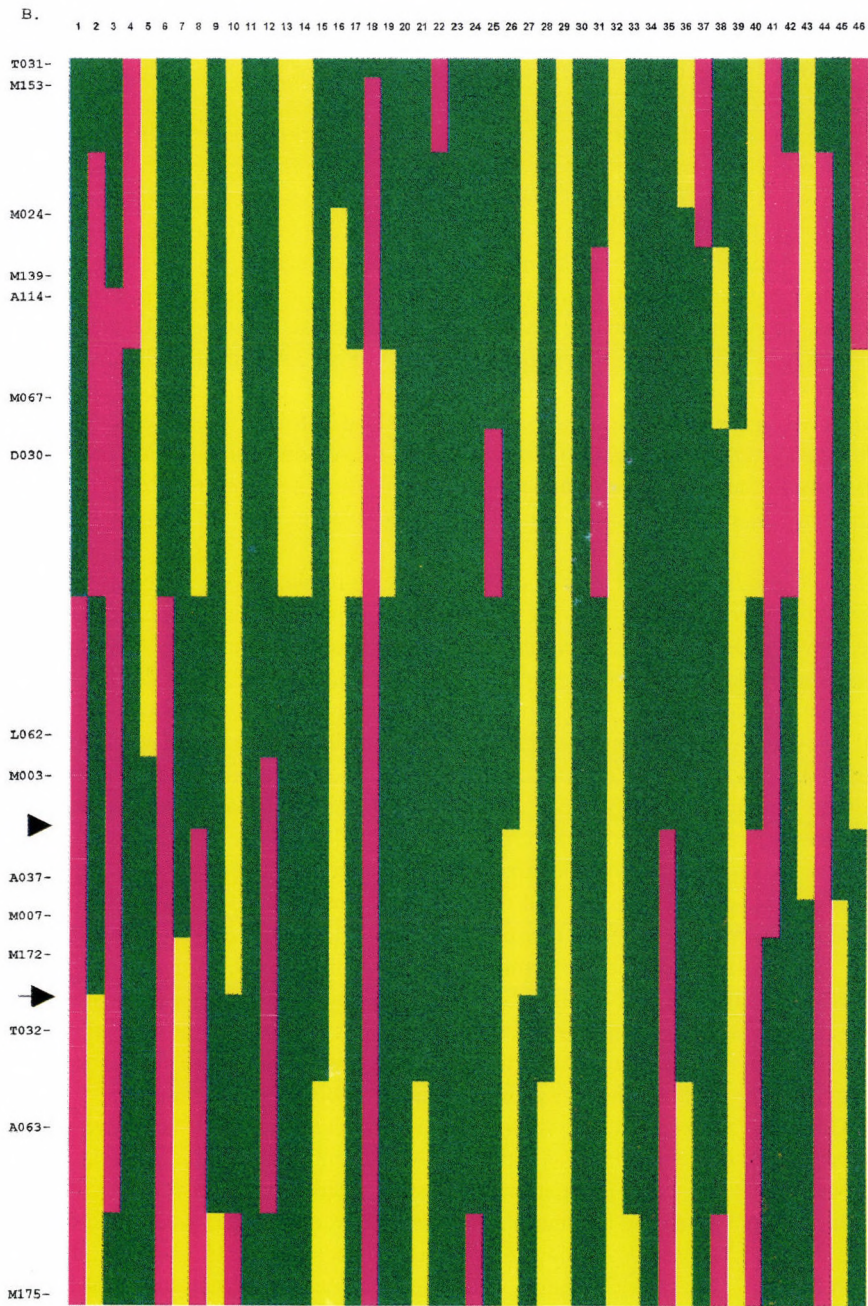


Fig. 3. The ordered marker sequence of chromosome 10 of mouse displayed in Fig. 2B after introducing the relative distances between markers. Panels A and B show non-predicted and predicted color genotypes, respectively. Horizontal arrowheads show predictable and predicted paternal genotype in panel A and B, respectively, between markers M003 and A037 for the mouse individual number 1. Horizontal





arrows show predictable and predicted recombination site in panel A and B, respectively, between markers M172 and T032 for the mouse individual number 2. Slanting arrowheads in panel A show predictable genotypes for the last marker T031 for mouse individuals number 11, 25 and 41



get a continuous color pattern and thereby a continuous genotype strip (compare Fig. 3A with Fig. 3B). The predictions are according to the follows:

(1) If the combined genotypes of the two flanking markers were the same the following assumption was made: the genotypes of the intermediate genes (chromosomal segment) were inferred from that of the flanking markers because no recombination event was supposed (the principle of maximum parsimony). It means that if the flanking markers displayed maternal, paternal homozygous, or heterozygous genotypes than the genotypes of the intermediate genes are most likely maternal or paternal homozygous, or heterozygous, respectively (see for example the horizontal arrowhead between markers M003 and A037 for mouse individual number 1 in Figs 3A and 3B). However, it is important to keep in mind that even, but not odd number of recombinations could have occurred between the markers, consequently an "island" of a different genotypic segment (abbreviated as island afterwards) could interrupt the region. These hidden islands can be revealed by further fine genetic mapping in the region. The shorter the distance between the reference markers, the more probable that no even number of recombinations took place, that is no island is present.

(2) If the combined genotypes of the two flanking markers were different it is supposed that only one recombination took place (the principle of maximum parsimony) somewhere between the markers. Recombination is supposed to take place halfway between the flanking markers, therefore sequences located in one or the other side of the assumed recombination site "inherit" the genotype of the closer marker (see for example the horizontal arrow between markers M172 and T032 for mouse individual number 2 in Figs 3A and 3B). Three or more odd number of recombinations would result in island(s). The shorter the genetic distance between the markers, the more probable that no three or more odd number of recombinations occurred. Determination of the genotypes of additional markers in the region makes the localization of the recombination spots(s) more accurate.

(3) If the last genotype at the end of the LG was missing no recombination was supposed, consequently the same genotype was predicted that the closest proximal flanking marker had (see for example the slanting arrows at marker T031 for mouse individuals number 11, 25, and 41, in Fig. 3A). Similarly, the genotype of the chromosomal region located distal from the last marker to the telomer was inferred from the genotype of the last marker. It is not excluded that further mapping reveals recombination. The closer the end marker to the telomer, the less probable the recombination event was.

(4) Dominant markers located between two codominant markers can provide more reliable prediction of genotypes and recombination events. For example marker M024 in mouse individual number 37 is paternal recessive (combined genotype is 3, that is purple). This fact positions the recombination event between markers M024 and M139 (see triangle in Fig. 3A) instead of being in the middle of markers M153 and M139 (see open circle in Fig. 3A). On the other hand, if the genotype was maternal dominant (combined genotype is 5, that is pale green) as in the case of marker M024 in mouse individual 16, no additional information is obtained since this genotype is heterozygous (recombination is between M024 and M139) or maternal homozygous (recombination is between M024

and M153), therefore the predicted recombination should be placed in halfway between markers M153 and M139 (see closed circle in Fig. 3A).

It is advised that determined and predicted genotypes should be distinguished. For that purpose numerical characters can be used in the data sheet where scores are stored. However, when computer calculation is to be carried out, these characters have to be converted either to zero (missing data), or to numbers 1, 2, 3, 4, 5. Zero replacement gives the so-called non-predicted raw data, while predicted data will yield predicted values for the calculation of linkage.

### *Colormapping as a novel procedure for genetic mapping of new markers*

Colormaps displayed on a monitor by the help of the *EXCEL* program can be used efficiently for genetic mapping. The principal role of colormapping is to find the best match between the color pattern of the new marker to be mapped and that of the colormap (see Fig. 4). Program *EXCEL* makes it possible to divide the opened window on the monitor in two horizontal parts at the same time. This feature of the program is used to find the correct map position of the new marker. The first window contains as many marker rows of an LG as possible including all or several individuals (columns) in the mapping population. This can be achieved by adjusting the column height and row width to the desired value. Below this, another narrow window is opened containing the color genotypes of the individuals for the new marker to be mapped (the order of the individuals must be the same in both windows). Mapping is done by visual comparison of the color pattern of the markers in the upper and lower windows. To find the position of the new marker, the rows of the upper window are rolled upwards to show the color pattern of the upcoming markers until the best match of the patterns is found. If the end of the LG was reached without unambiguous matching, the next LG is started to be screened, and so on. During this procedure visual evaluation is needed to catch the region of the map to which the new marker shows the highest degree of color pattern match – thereby the less recombination event. When this region is found the new marker is inserted between those two markers where the new marker fits the best. The procedure of colormapping is illustrated in Fig. 4. An RFLP marker CAD5B is mapped between RFLP markers U189A and L295 on LG 2 of alfalfa. By inserting the new marker CAD5B (that is the row of a color pattern) into this region of the colormap the minimal number of color transition (recombination) is generated. This mapping procedure takes usually less time than running any of the computer programs which calculate recombination frequencies and map distances using mathematical formulas. On the other hand, colormapping produces the same order of loci as mathematical approaches without determining the genetic distance.



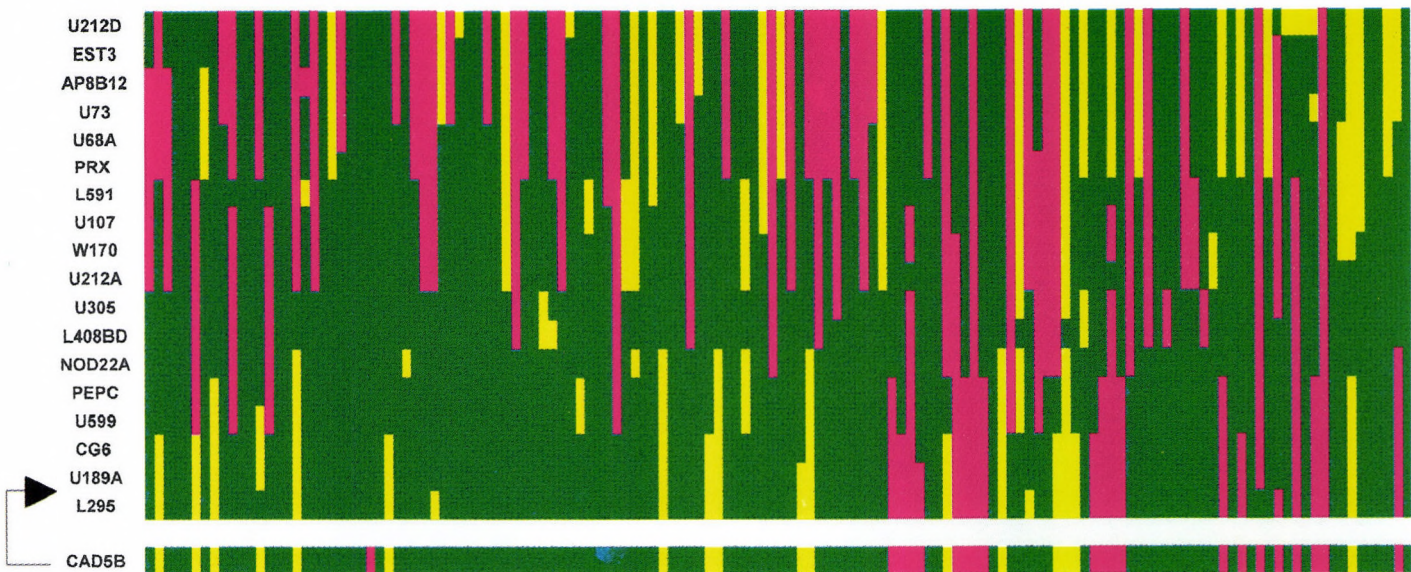


Fig. 4. Mapping a new marker CAD5B to LG 2 of the genetic map of alfalfa. The color genotypes of CAD5B are shown at the bottom of the Fig. 4. According to the color pattern similarities CAD5B was mapped in LG2 and can be placed between U189A and L295. The minimum number of color transitions (recombinations) were generated by inserting the new marker between U189A and L295. This manipulation was carried out by the “Cut” and “Insert cut cells” functions of the computer program *EXCEL* as described in the “Materials and Methods” and the “Results” sections in more detail

### *Colormapping in distorted regions*

During our mapping work on alfalfa some markers showed distorted segregation ratios, i.e. individuals with heterozygous genotype for these markers were in excess. An RFLP marker U286 showed extreme distorted segregation (8 homozygous genotypes out of 137 individuals, see Fig. 5). According to the computer program MAPMAKER/EXP 3.0 this marker gave recombination frequencies of less than 0.1 with two other markers OAD16A and U62, respectively, which belonged to two different LGs (LG 6 and 7, respectively). When LG 6 and 7, as well as the above markers were analyzed in the form of colormap it could be demonstrated unambiguously that markers OAD16A and U286 are unlinked (zero "homozygous link" out of 7 and 8 homozygous genotypes, respectively), while U62 and U286 are linked (6 "homozygous link" out of 8 and 7 homozygous genotypes, respectively). The analysis of these color patterns shed light also to the linkage relation between the two halves of LG 6 and 7, respectively. Marker OAD16A connects the two halves of LG 6, while U286 is the "bridge" between the two parts of LG 7 as shown in Fig. 5.

### *Troubleshooting with colormap*

One of the most advantageous properties of the colormaps is their powerful troubleshooting capacity. Troubleshooting is usually done on the raw data introduced as numerical genotypes into a matrix. On the one hand, the genotypes should be checked again on the autoradiograms or on the photos, on the other hand, the genotypes have to be verified by proofreading the characters one by one. These procedures are time consuming, laborious, and still doubtful. Whereas, a newly introduced marker into the colormap according to the position of its best fit immediately gives a spectacular color view of the new marker and its neighborhood. One can obviously perceive whether the color of the new marker matches unambiguously their flanking regions (markers) for each individual or not. The following situations may occur:

(1) the genotypes of the flanking markers are the same, and the new marker matches this pattern; no discrepancy that is no recombination occurred.

(2) the genotypes of the flanking markers are the same but the genotype of the new marker differs from both in one or more individuals; in this case either recombination events occurred on both sides of the new marker (see for example the genotype of the U286 for individuals 70 and 103 on LG 7 in Fig. 5.), therefore islands were generated, or errors were made.

(3) the genotypes of the flanking markers are different and the genotype of the new marker coincides with one of the flanking genotypes. In this case, the recombination event has occurred between the new marker and the marker with the diverse genotype (see for example the genotypes of U286 for individuals 22, 23, 24, etc. on LG 7 in Fig. 5).

(4) the genotypes of the flanking markers are different and the genotype of the new marker does not coincide with any of the flanking genotypes. In this case, recombination events have occurred on both sides of the new marker or miss-genotyping.



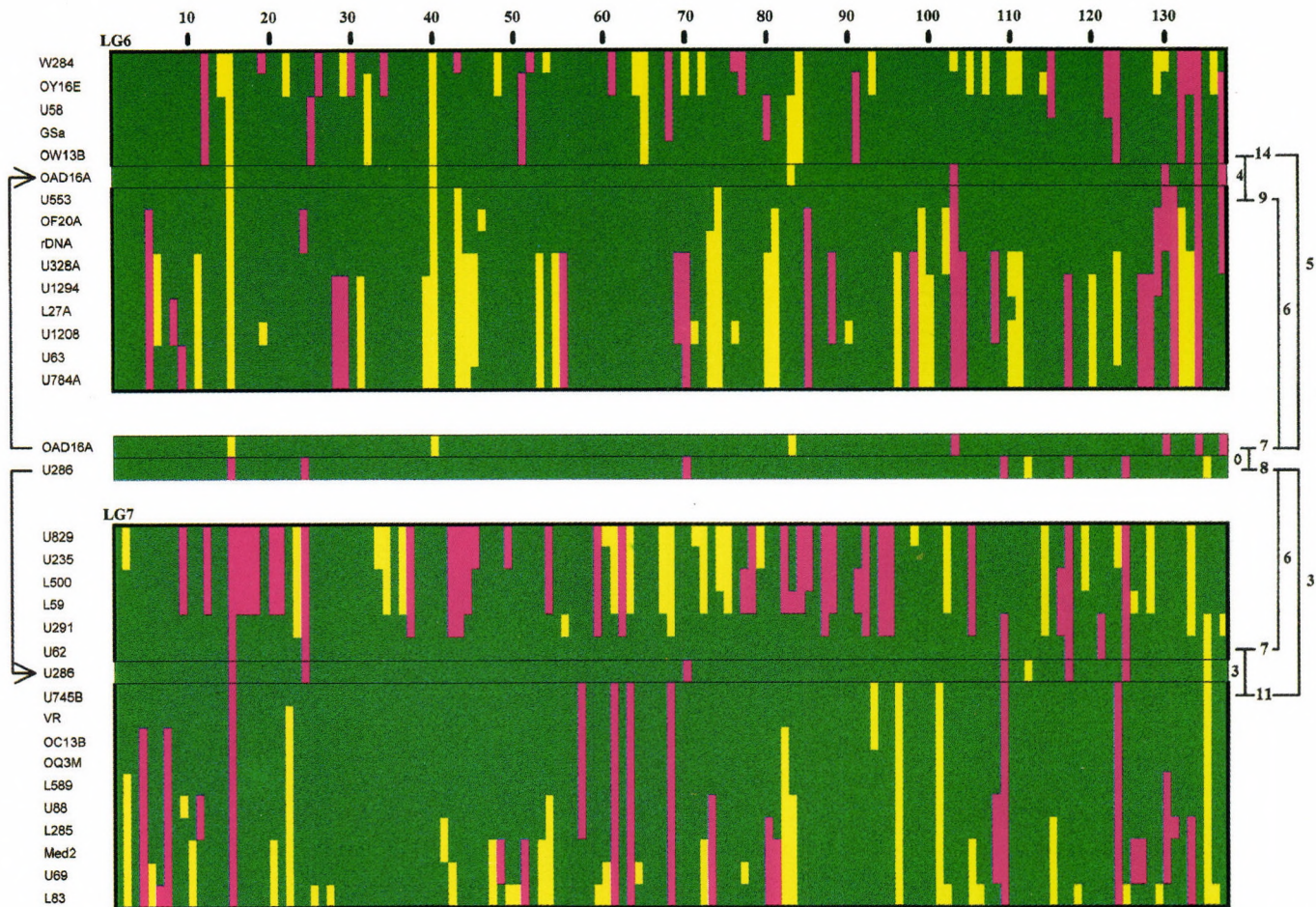


Fig. 5. Colormapping of markers with ambiguous location. The markers are placed according to their order but the distances are out of scale. The values on the top of the Fig. show the serial numbers of the plants in the population. On the right side of the colormap the values represent the total numbers of individuals with homozygous genotype of the appropriate markers as well as the numbers of individuals with homozygous links to the flanking markers.

The explanation of this Fig. is described in the "Results" section of the paper



The presence of an island can be confirmed by mapping new marker(s) with the same genotype next to the marker by which the island was generated in the appropriate individual, or thrown out if repeated experiments disproved the genotype. For example, in the case of the marker U286 for the plant individual number 70 on LG 7 in Fig. 5, the homozygous paternal genotypic island (purple color) was confirmed by a new dominant marker OAH11A (data not shown). In the case of an island one should keep in mind that it may be the result of miss-genotyping caused by personal mistakes or technical errors. The color display of the genotypes (that is the colormap) is extremely powerful to highlight ambiguities, consequently facilitates troubleshooting. In the case of discrepancy the genotypes of only those marker/individual combinations have to be rechecked or re-determined which produced conflicting results. This kind of troubleshooting helped us tremendously during our mapping work to pick up discrepancies and to correct genotypes, consequently experimental mistakes could be eliminated or reduced to a large extent.

## DISCUSSION

In this paper we described the concept of colormap and its use for colormapping which is a non-mathematical method for genetic mapping. Combined color genotypes of ordered markers are used to display the genetic composition throughout the entire genome of each individuals in a segregation population. This display is the colormap which can be used for colormapping that is to find the location of new markers on the map quickly and with high fidelity. Colormapping can also be used to find genuine linkage between regions with distorted segregation ratios which are ambiguously sorted out by conventional computer programs. Moreover, colormaps are extremely powerful for troubleshooting to pick up incorrect genotypes caused by errors of different origin.

As compared to the concept of graphical genotype [15], colormaps have a major advantage: the alleles appeared in a locus of the homologue chromosome pair are integrated into a combined genotype and this is displayed as color. Maternal and paternal homozygous, heterozygous, or maternal and paternal dominant configurations are displayed by different colors. The resulting color picture, that is the genotypes of the ordered markers of the individuals in a segregation population is the colormap. Colored genotypic pattern of any genomic segment can be analyzed more easily as compared to either graphical or numerical patterns. Recently the representation of the genotypes by color was introduced for using in marker-based pedigree analysis [3] but no colors were used before to represent combined genotypes which facilitate the genetic mapping.

Colormaps are extremely useful in plant genetics and breeding when whole genome analysis is required. The selection of individuals with a desired genotype among the progeny is simple and straightforward even if more than one locus is looked at, e.g. in the case of multiple loci selection. Colormaps display the genetic composition of the individuals in a segregation population giving a concise and comprehensive color image where the entire genome is highlighted. Taking the color genotype of an individual plant, transition from one color to another mirrors recombination event. Similarly to the graphical genotype, cis or trans heterozygous configuration of the alleles cannot be revealed by



colormaps, consequently cis or trans heterozygous configuration of the alleles has to be determined, if necessary, by progeny analysis.

Colormaps can be used for genetic mapping. This new approach is called colormap-ping since the location of the new markers is found by the best match of the color pattern of the new marker compared to the already existing colormap. Strikingly, colormapping is efficient, and even faster than mathematical calculations to find the position of the new markers. This is achieved by the fact that the perception of color patterns by the human eyes is extremely sensitive [5]. Colormapping is carried out by the help of a computer spreadsheet program called *EXCEL* which is available for both Macintosh and IBM computers, in addition *EXCEL* is compatible with other spreadsheet programs e.g. *LOTUS 1-2-3*. The new marker to be mapped is shown as a color patterned row in a part of the window separated from the other one displaying the already established colormap, which is followed by finding the best match between the patterns of the new marker and the appropriate region of the colormap as described in Results. After inserting the new marker into its adequate position it is becoming a new component of the map. Since colormapping does not determine the genetic distances, a colormap displays the order of the markers disproportionately. Genetic distances have to be calculated by other methods and the appropriate distances can be incorporated afterwards into the colormap as shown in Fig. 3B. It has to be emphasized, that the construction of colormaps can be started from scratch. Similar color patterns of markers can be separated one by one, and by continuing this sorting out LGs can be established as was performed with scrambled markers for the eight LGs of alfalfa (data not shown).

Colormaps can be used to find linkage relationship between markers and partial linkage groups if mathematical approaches give ambiguous results as was demonstrated for LGs 6 and 7 in this study. If the segregation ratio of given markers are extremely distorted as in the case of some chromosomal regions in the outcrossing diploid alfalfa mapping population [6], calculating the recombination frequencies may result in false values (heterozygous marker pairs are not neutral but enhance linkage). Displaying the appropriate color patterns visual sensation can perceive the more important homozygous links or color transitions, by which linkage or non-linkage can be strengthened or rejected.

An extremely important advantage of colormaps to our experience is the immediate realization of surprising results or experimental mistakes. The appearance of a different color that is an "island" in a genetically uniform region may indicate double recombination events or mistakes in the determination of the genotype or typing. Repeating the determination of the genotype for the appropriate locus can confirm or reject the genotype of the island. This is of great help when genotyping is carried out by RAPD [14] or other PCR-based techniques with non-specific primers, since PCR amplifications may result in false patterns for different reasons. RFLP patterns [2] can also produce incorrect genotypes if sampling mistakes, slot shift or mixing up individual plants occurred. In these cases colormaps highlights strikingly the irregular pattern. Improper genotyping can also occur if wrong allele allocation was made. This can happen when the parents of the F<sub>2</sub> population were heterozygous for the appropriate locus and the origin of the alleles can not be determined unambiguously. In this case, colormap highlights discrepancies by showing opposite color pattern, and the appropriate genotype can be corrected.

Troubleshooting is extremely important in genetic mapping. Some experimental mistakes cannot be detected by computer when recombination frequencies are calculated using mathematical algorithms. Most of the above errors would be resulted in an outcome called "unlinked" and some mistakes would give longer genetic distances. Analyzing the color pattern of colormaps genotype errors can be corrected after which more reliable values can be calculated.

Colormap(ping) is not restricted only to plant genomes, it is applicable for any Genome Projects like human, *Drosophila*, *Caenorhabditis*, yeast and others, which could benefit from it by displaying the combined color genotypes making possible genome analysis, comparison, troubleshooting and mapping.

#### ACKNOWLEDGEMENTS

The authors thank Mrs. P. Somkúti, Mrs. L. Tóth, Mrs. K. Katona, Ms. Z. Liptay and Mr. S. Jenei for their skillful technical assistance. This work was supported partly by grants OTKA (Hungarian Scientific Research Fund) T025467, OTKA T016935, AKP 96-360/62, OMFB (National Committee for Technical Development, Hungary), Dr. János Bátyai Holczer Foundation, Volkswagen Stiftung grant no. I/72 244, INCO COPERNICUS/BIOTECH grant no. PL962170 and by the C.N.R.S. – Hungarian Academy of Sciences collaborative program.

#### REFERENCES

1. Allard, R. W. (1956) Formulas and tables to facilitate the calculation of recombination values in heredity. *Hilgardia* 24, 235–278.
2. Botstein, D., White, R. L., Skolnick, M., Davis, R. W. (1980) Construction of a genetic linkage map in man using restriction fragment length polymorphisms. *Am. J. Hum. Genet.* 32, 314–331.
3. Boutin, S. R., Young, N. D., Lorenzen, L. L., Shoemaker, R. C. (1995) Marker-based pedigrees and graphical genotypes generated by supergene software. *Crop Sci.* 35, 1703–1707.
4. Caetano-Annollés, G., Bassam, B. J., Gresshoff, P. (1993) Enhanced detection of polymorphic DNA by multiple arbitrary amplicon profiling of endonuclease-digested DNA: identification of markers tightly linked to the supernodulation locus in soybean. *Mol. Gen. Genet.* 241, 57–64.
5. Chaparro, A., Stomeyer III, C. F., Huand, E. P., Kronauer, R. E., Eskew, R. T. Jr. (1993) Color is what the eye sees best. *Nature* (London) 361, 348–362.
6. Kiss, G. B., Csanádi, G., Kálmán, K., Kaló, P., Ökrész, L. (1993) Construction of a basic genetic map for alfalfa using RFLP, RAPD, isozyme and morphological markers. *Mol. Gen. Genet.* 238, 129–137.
7. Lander, E. S., Green, P., Abrahamson, J., Barlow, A., Daly, M. J. (1987) MAPMAKER: An interactive computer package for constructing primary genetic linkage maps of experimental and natural populations. *Genomics* 1, 174–81.
8. Lincoln, S., Daly, M., Lander, E. (1992) *Constructing genetic maps with MAPMAKER/EXP 3.0*. Whitehead Institute Technical Report, 3rd edition.
9. Mendel, G. (1866) Versuche über Pflanzen-Hybriden. *Verhandlungen des naturforschenden Vereines in Brünn* 4, 3–47.
10. Southern, E. M. (1975) Detection of specific sequences among DNA fragments separated by gel electrophoresis. *J. Mol. Biol.* 98, 503–517.
11. Sturtevant, A. H. (1913) The linear arrangement of six sex-linked factors in *Drosophila*, as shown by their mode of association. *J. Exp. Zool.* 14, 203–204.
12. Vos, P., Hogers, R., Bleeker, M., Reijans, M., van de Lee, T., Hornes, M., Frijters, A., Pot, J., Peleman, J., Kuiper, M., Zabeau, M. (1995) AFLP: a new technique for DNA fingerprinting. *Nucl. Acids Res.* 23, 4407–4417.



13. Welsh, J., McClelland, M. (1990) Fingerprinting genomes using PCR with arbitrary primers. *Nucleic Acids Res.* 18, 7213–7218.
14. Williams, J. G. K., Kubelik, A. R., Livak, K. J., Rafalski, J. A., Tingey, S. (1990) DNA polymorphism amplified by arbitrary primers are useful as genetic markers. *Nucleic Acids Res.* 18, 6531–6535.
15. Young, N. D., Tanksley, S. D. (1989) Restriction fragment length polymorphism maps and the concept of graphical genotypes. *Theor. Appl. Genet.* 77, 95–101.

# EFFECTS OF ADMINISTRATION OF CYPROTERONE ACETATE ON SEMINAL VESICLE AND TESTICULAR ACTIVITY, AND SERUM TESTOSTERONE AND ESTRADIOL-17- $\beta$ LEVELS IN THE CATFISH *CLARIAS BATRACHUS*

M. S. SINGH and K. P. JOY

Department of Zoology, Banaras Hindu University, Varanasi, India

(Received: 1998-04-04; accepted: 1998-08-11)

Cyproterone acetate (CA) was administered in the catfish *Clarias batrachus* (BW 60-65 g) in a dose of 1 mg/fish daily for 21 days in the prespawning (June) phase of the reproductive cycle. The treatment caused a marked decrease in the size and weight of both testis and seminal vesicle (SV). Spermatogenesis was retarded, inhibiting the transformation of spermatids into spermatozoa. The SV was greatly regressed; the lobules were small with empty lumina or collapsed and fibrosed together with the interstitium in many areas. The CA treatment decreased significantly the concentrations of total proteins, fructose, hexosamines and sialic acid in both the SV and testis, and serum levels of testosterone and estradiol-17 $\beta$ . The results indicate that the regressive changes in the SV and testis were a sequel to decreased androgen level and blockade of androgen actions by interrupting, most likely, the androgen receptor mechanisms.

**Keywords:** Seminal vesicle – testis – catfish – total protein – fructose – hexosamine – sialic acid-estradiol 17 $\beta$  – cyproterone acetate

## INTRODUCTION

Cyproterone acetate (CA; 1,2 $\alpha$ -methylene 6-chloro-pregn-4,6-diene-17 $\alpha$ -ol-3,20-diene-17 $\alpha$ -acetate) is a commonly used antiandrogen to study androgen control of male reproductive physiology of animals and man. CA influences a number of androgen-dependent functions, notably spermatogenesis, sex accessory gland activity, sexual differentiation, behaviour, etc. [11, 18–25]. It also elicits antigonadotropic properties due to progestational properties [20]. In nonmammals, only limited studies are available demonstrating CA effects on spermatogenesis and secondary male sexual characteristics [2, 6, 7, 27, 28]. In teleosts, CA administration is only partially effective to block secondary sexual characters [31] or has failed to inhibit the masculinizing effect of testosterone propionate or 11-ketotestosterone [27]. Murhpy [16] reported that CA failed to prevent gonad maturation but decreased the gonadotropic cell size and plasma androgen (11-ketotestosterone) level in Atlantic salmon parr. Seminal vesicle is an accessory reproductive gland

Send offprint requests to: Prof. K. P. Joy, Department of Zoology, Banaras Hindu University, Varanasi-221005, India; e-mail: kpjoy@banaras.ernet.in.



characteristic of the male reproductive system of some teleosts, like catfishes, blennies and gobies [13, 17, 40]. Apart from exocrine secretion and sperm storage, it is steroidogenic and synthesizes a number of androgens [29, 30, 33, 34]. Additionally, it is an important conjugation site of androgens which have pheromonal function [39]. It shows seasonal activity in correlation with the testis [17]. In an extensive study in *Clarias batrachus*, Rai [26] has reported seasonal changes in chemical constituents, such as total proteins, fructose, hexosamines and sialic acid of both testis and SV and stimulatory effects of testosterone administration on these parameters. In the catfish *Heteropneustes fossilis*, Sundararaj and Nayyar [38] reported based on histology that castration led to hyperactivity of the SV and administration of CA in castrates prevented this hyperactivity.

The objective of the present study was to evaluate CA effects on SV and testicular functions, and serum levels of testosterone and estradiol-17 $\beta$  (E<sub>2</sub>) in the catfish *C. batrachus*.

## MATERIALS AND METHODS

### 1. Collection and maintenance

Catfish (60-65 g) were collected in the prespawning phase (May-June) of the reproductive cycle. Males were separated and maintained under normal photoperiod and temperature (L:D cycle 13.3:10.7, and ambient temperature  $32 \pm 7$  °C in May) and acclimatized for 15 days. During acclimation, fish were treated with benzanthine penicillin (1.00.000/litre) for 1 h daily for 3 days to prevent skin infection. They were fed goat liver during the period of acclimation and experiment.

### 2. Experimental design

One hundred and eighty acclimatized fish were divided into three groups of 60 each. The first group served as initial control. The fish in this group were sacrificed before the start of the experiment. They were weighed and blood was collected by caudal puncture for serum collection and sera were stored at -20 °C for radioimmunoassay (RIA) of E<sub>2</sub> and testosterone. They were then sacrificed by decapitation. SV and testis were removed quickly and weighed. The tissues were fixed in Bouin's fluid for histology or stored at -20 °C for biochemical estimations. The second group was injected with olive oil which serves as vehicle control. The third group was injected with cyproterone acetate (CA, a generous gift of Schering AG, Germany) intraperitoneally daily for 21 days, in a dose of 1.0 mg/fish/day. CA was dissolved in olive oil. After termination of the experiment, the fish were weighed and blood was withdrawn for serum collection. They were sacrificed by decapitation. The testis and SV were removed and stored at -20 °C for biochemical estimations or fixed in Bouin's fluid for histology.

### 3. Study parameters

#### a) SV – Somatic Index (SVSI)

The weight of the SV was expressed in 100 g BW.

#### b) Gonadosomatic Index (GSI)

The weight of the testis was expressed in 100 g BW.

#### c) Histology

The tissues were processed for paraffin embedding and 7  $\mu$ m paraffin sections were taken in transverse plane and stained with Ehrlich's hematoxylin-eosin.

#### d) Radioimmunoassay of serum testosterone and estradiol 17 $\beta$ (E<sub>2</sub>)

E<sub>2</sub> and testosterone RIAs were carried out according to the standard procedure of Abraham [1]. [2,4,6,7,<sup>3</sup>H(N)] E<sub>2</sub> (sp. act. 87.0 Ci/mMol) and [1,2,6,7,<sup>3</sup>H(N)]-testosterone (sp. act. 92.1 Ci/mMol) were purchased from NEN, Boston, MA, USA and were used for the assays. E<sub>2</sub> antibody was a generous gift of Professor G. D. Niswender, Colorado State University, Fort Collins, Co., USA and testosterone antibody was a generous gift of the Indian Council of Medical Research, New Delhi, through the courtesy of Dr. C. Das, AIIMS, New Delhi.

The sensitivity of both assays was 10 pg/ml. E<sub>2</sub> antiserum cross-reacted with estrone (4%) and estriol (0.5%). The testosterone antiserum cross-reacted with 5 $\alpha$ -dihydrotestosterone (3%),  $\Delta^4$ -androstenedione (4.3%), 5 $\alpha$ -androstanediol (1.9%), progesterone (1.1%), androstane-3 $\alpha$ -diol (1.5%), cortisol (0.096%), androstane-3 $\beta$ -diol (2.5%), estradiol-17 $\beta$  (0.061%) and dehydroisoandrosterone sulphate (0.72%). The intra- and interassay coefficients of variation (n = 5, mean  $\pm$  SD) for E<sub>2</sub> were 2.28% (SD  $\pm$  0.011) and 5.3% (SD  $\pm$  0.025), respectively and those for testosterone were 1.43% (SD  $\pm$  0.014) and 2.40% (SD  $\pm$  0.023), respectively.

#### e) Estimation of total proteins, fructose, hexosamines and sialic acid

The concentrations of total proteins, fructose, hexosamines and sialic acid in the SV and testis were measured by standard procedures according to the methods of Lowry et al. [14], Mann [15], Elson and Morgan [5] as modified by Davidson [3] and Warren [41], respectively.

### 4. Statistical analysis

Data were expressed as means  $\pm$  SEM (standard error of means). Student's *t*-test was used to show significance between CA and control group data.



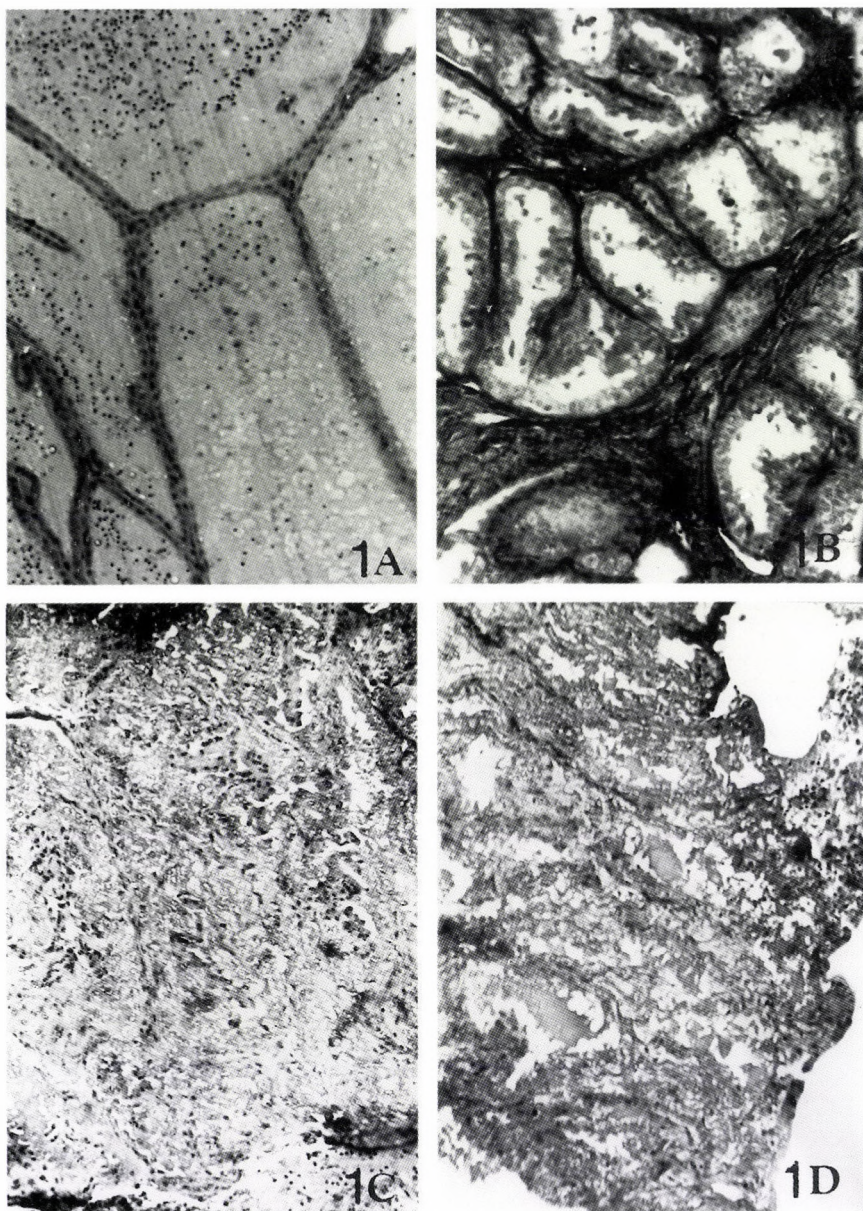
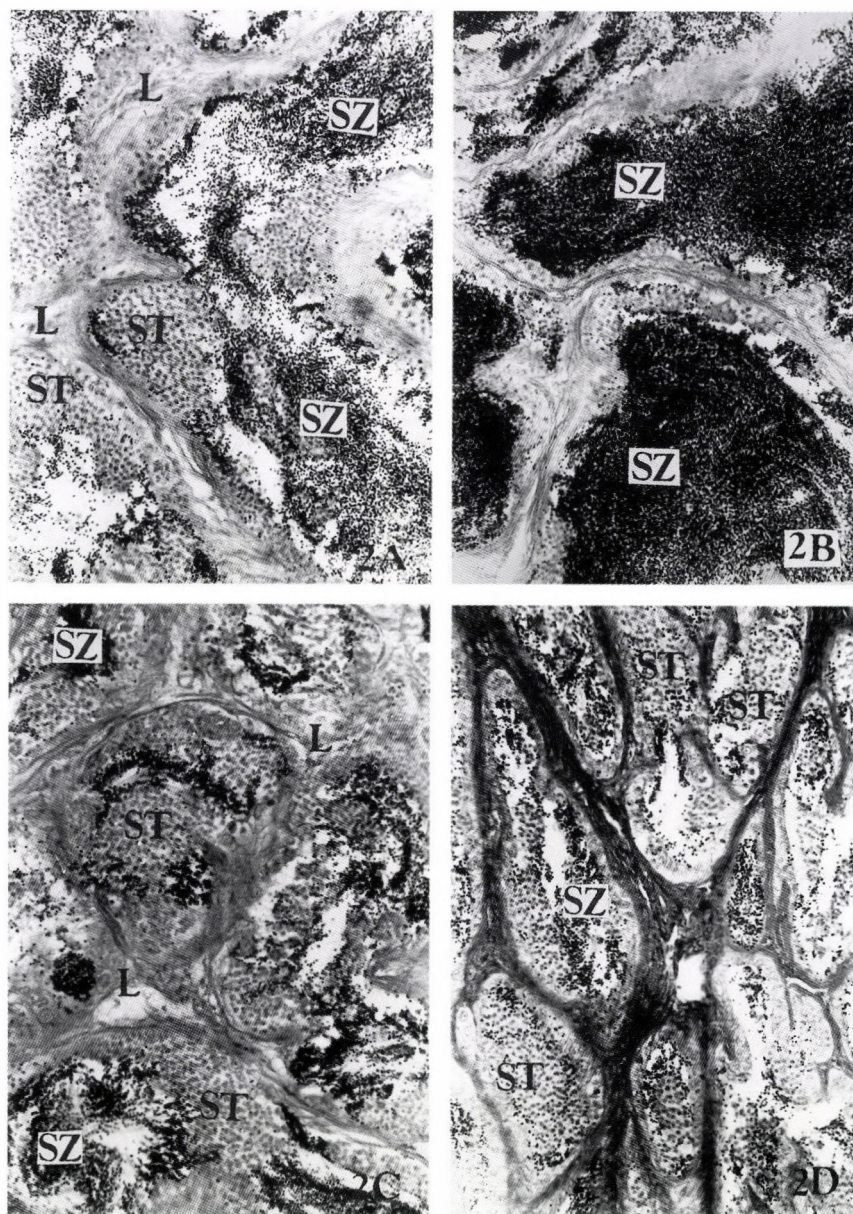


Fig. 1A–D. Effect of administration of cyproterone acetate (CA) on histology of the seminal vesicle of *Clarias batrachus* in prespawning phase. Ehrlich's hematoxylin-eosin,  $\times 240$

Fig. 1A. A TS of the SV of a vehicle control fish. The SV lobules are large and distended with flat epithelia and secretion-filled lumina. Spermatozoa are seen embedded in the secretion. Figs 1B–D. TS of the SV of a CA-treated fish. Extensive regressive changes are seen in the SV. The lobules are empty and the interstitium thick (B), or are extensively fibrosed (C), or are collapsed and in the process of fibrosis (D)





Figs 2A–D. Effect of administration of cyproterone acetate (CA) on the histology of the testis in *C. batrachus*. Ehrlich's hematoxylin-eosin. L – Leydig cells; ST – spermatids; SZ – spermatozoa,  $\times 240$

Fig. 2A. A TS of the testis of an initial control fish. The seminiferous tubules contained a moderate population of spermatozoa. Fig. 2B. A TS of the testis of an olive oil-treated control fish. The seminiferous tubules are enlarged and contained large masses of spermatozoa. Figs 2C, D. A TS of the testis after CA treatment. The seminiferous tubules are small in size and contained less number of spermatozoa (C) and the interstitium is thick (D)



## RESULTS

## 1. Effect of CA on SV histology

The SV lobules in the vehicle control group were large and distended with flat epithelium and secretory material-filled lumen. Spermatozoa can be seen embedded in the secretion (Fig. 1A). The administration of CA produced extensive regressive changes in the SV. Lobules in some regions of the SV were reduced in size and their lumina were mostly empty containing only lumps of secretory material. The epithelium was tall and columnar, but did not show any secretory activity (Fig. 1B). The interstitium was thick and fibrosed. In other regions, the lobules were collapsed (Fig. 1C) and lost their histoarchitecture with extensive fibrotic changes (Fig. 1D).

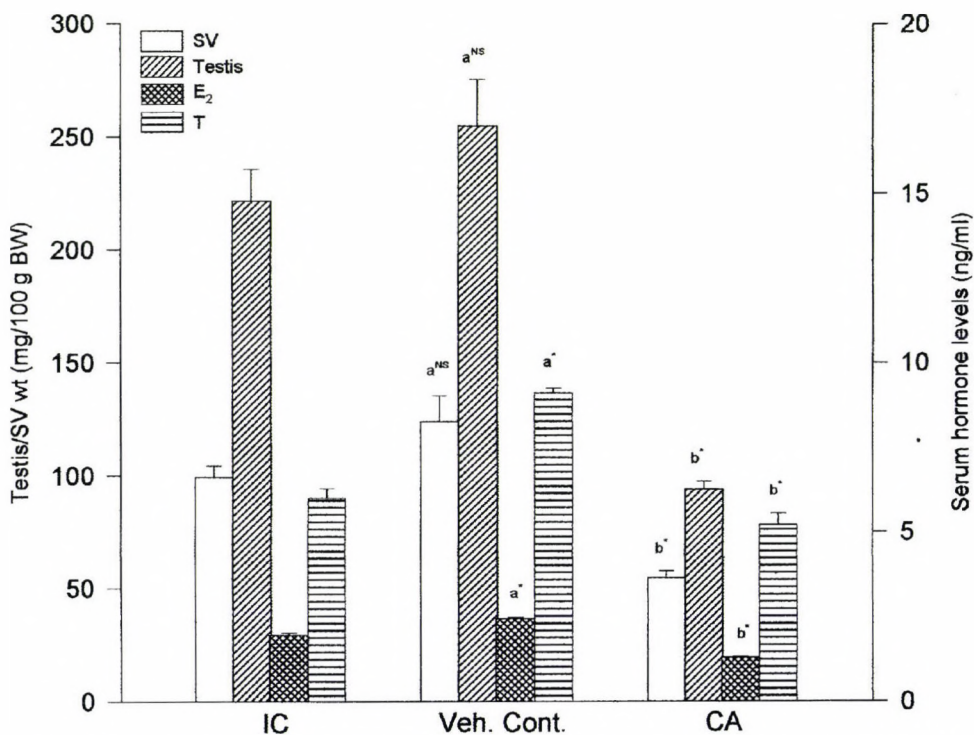


Fig. 3. Effect of administration of cyproterone acetate (CA) on the weights of testis (GSI) and seminal vesicle (SVSI), and serum levels of estradiol-17 $\beta$  (E<sub>2</sub>), testosterone (T) in *Clarias batrachus* (mean  $\pm$  SEM; n = 5). **a** – comparison between the initial control (IC) and vehicle control groups, \*p < 0.001; **b** – comparison between the vehicle control and CA-treated groups, \*p < 0.001; NS – not significant (Student's *t*-test)

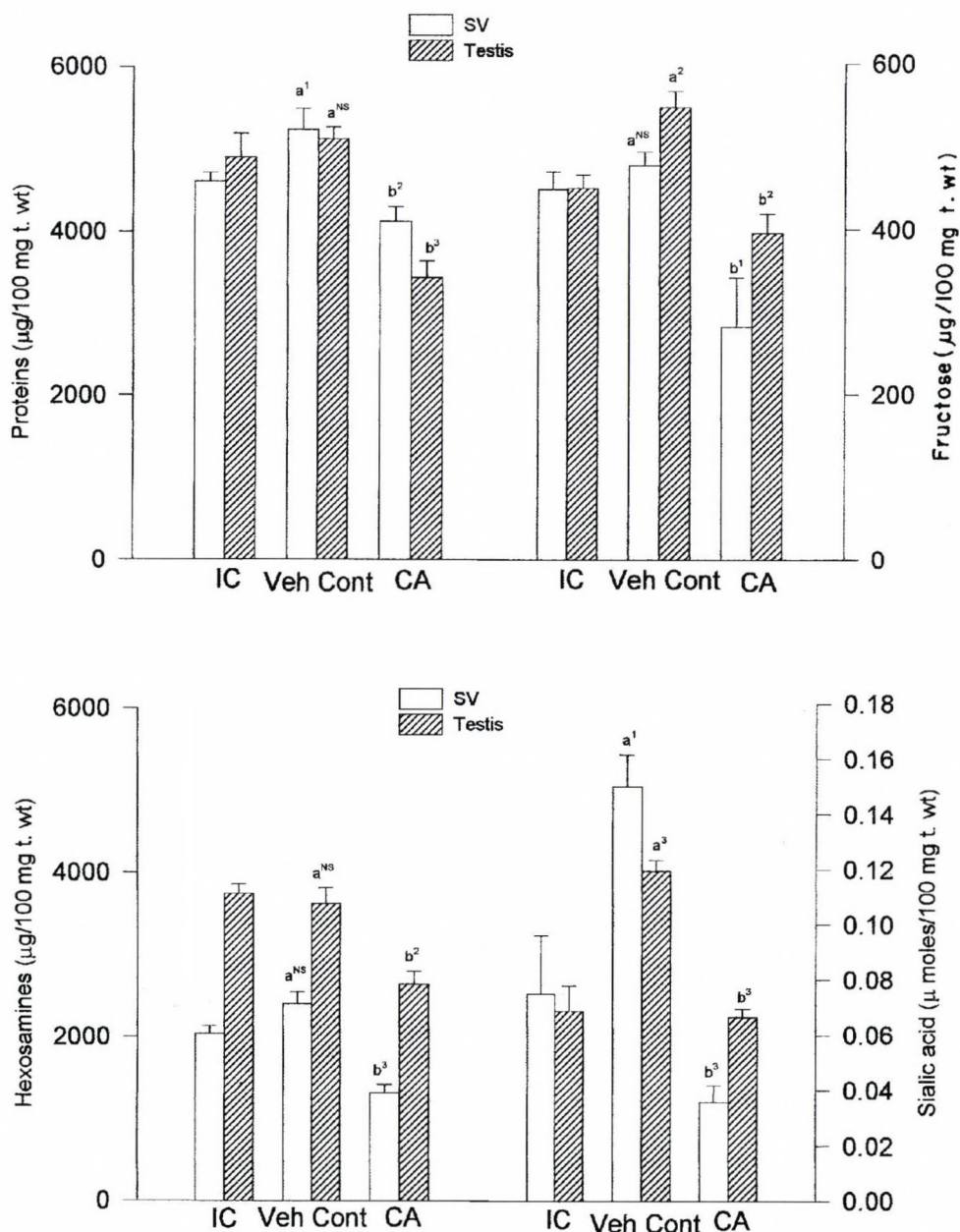


Fig. 4. Effect of administration of cyproterone acetate (CA) on total proteins, fructose, hexosamines and sialic acid levels in *Clarias batrachus* (means  $\pm$  SEM;  $n = 5$ ). **a** – initial control vs. vehicle control group, 1 –  $p < 0.05$ , 2 –  $p < 0.01$ ; 3 –  $p < 0.001$ ; **b** – vehicle control vs. CA group, 1 –  $p < 0.05$ , 2 –  $p < 0.01$ , 3 –  $p < 0.001$  (Student's *t*-test)



## 2. Effect of CA on spermatogenesis

In the testis of initial control fish, the seminiferous tubules contained moderate population of spermatozoa (Fig. 2A). In the olive oil-treated control, the tubules were enlarged and the lumina were filled with large masses of spermatozoa (Fig. 2B). The CA treatment reduced markedly the tubular size and retarded the pace of spermatogenesis. The tubules contained a less number of spermatozoa and a large number of spermatids (Figs 2C, D) compared to control fish. The interstitium and the germinal layer were thick in some areas (Fig. 2D).

## 3. Effect of CA on SVSI, GSI and serum levels of hormones

The administration of CA decreased significantly ( $p < 0.001$ ) the SVSI, GSI and the levels of testosterone and  $E_2$  compared to that of the vehicle control group (Fig. 3).

## 4. Effect of CA on total proteins, fructose, hexosamines and sialic acid concentrations in the SV and testis

The administration of CA decreased significantly the concentrations of proteins (SV,  $p < 0.01$ ; testis,  $p < 0.001$ ), fructose (SV,  $p < 0.05$ ; testis,  $p < 0.01$ ), hexosamines (SV,  $p < 0.001$ ; testis,  $p < 0.01$ ), and sialic acid ( $p < 0.001$ ) when compared with those of the vehicle control group (Fig. 4).

## DISCUSSION

The accessory sex glands are target organs for androgens and, therefore, for antiandrogens as well [23]. By this criterion, the SV of the catfish which is an androgen-dependent gland responded to the antiandrogen treatment along the expected line. The data showed that CA treatment inhibited significantly the normal activity of the male reproductive system. In the SV, the histological changes varied from reduction of the lobules with empty lumina to their total collapse and fibrosis. Apparently, such variations might be due to different stages of the secretory activity within the lobules. Sundararaj and Nayyar [38] have reported a decrease in the weight of the SV (SVSI) following CA treatment in castrated *Heteropneustes fossilis*. The present investigation has provided for the first time quantitative chemical analysis data of some SV components. The CA treatment inhibited significantly the concentrations of total proteins, fructose, sialic acid and hexosamines. The concentrations of these biochemical correlates have been shown to increase with the progress of gonadal recrudescence and stimulated by exogenous testosterone treatment [26]. Investigations in mammals have shown that CA inhibits the levels of proteins and sialic acid in epididymis, fructose in Cowper's glands and dorsal prostate [25], and the contents of DNA, RNA, and zinc in the prostate [21]. Similar inhibitory effects were also

reported after flutamide (a nonsteroidal 'pure' antiandrogen) treatment in rats [4] and musk shrew [36].

The CA treatment has also inhibited testicular activity as evident from the decreased GSI and impaired spermatogenesis. The tubules contained mainly spermatids. In the Atlantic salmon parr, CA treatment did not arrest spermatogenesis although a decrease in plasma androgen (11-ketotestosterone) level was reported [16]. On the other hand, Rouse et al. [31] have reported inhibition of the development of both spermatids and spermatozoa in CA-treated sticklebacks. In rainbow trout, Billard [2] has shown that there was no testicular growth when the antiandrogen treatment was started before the initiation of spermatogenesis and a limited effect was observed when treated after the beginning of spermatogenesis. In all mammals, including man, CA inhibits spermatogenesis but the degree of inhibition varies with doses and species [21, 24]. According to these authors, medium doses inhibited spermatozoal maturation, high doses impaired meiosis and extremely high doses resulted in depopulation of the tubules; only spermatogonia and spermatocytes persisted. According to Schenck and Neumann [32] and Neumann and Schenck [24], the inhibition of spermatogenesis is a secondary effect due to the inhibition of Sertoli cell function. These authors have reported a parallel decrease of the testis weight and androgen binding protein reduction in the CA-treated rat. The inhibition of total proteins, fructose, hexosamines and sialic acid in the testis of the CA-treated catfish suggests a direct action of the antiandrogen on testosterone-mediated secretory activity of the Sertoli (cyst) cells.

The regressive changes in the SV and retardation of spermatogenesis in the CA-treated catfish may be ascribed to the antiandrogen competitively inhibiting the binding of androgens to the cytosol receptor in the target organs and the resulting inhibition of the cytosol-androgen receptor translocation into the nucleus and androgen-dependent transcriptional and translocational activities, as reported in mammals [10, 20, 22]. The androgen receptor dynamics in relation to CA treatment has to be investigated in the catfish.

In the CA-treated fish, serum levels of testosterone and  $E_2$  were significantly decreased. The decreased level of testosterone might have further augmented the antiandrogenic action of the compound at peripheral targets. Schreck [35] has reported decreased plasma testosterone level and uptake of  $H^3$ -testosterone by the testis of CA-treated rainbow trout (*Salmo gairdneri*). Murphy [16] reported a decrease in plasma 11-ketotestosterone level in CA-treated Atlantic salmon parr. Likewise, in human volunteers and laboratory animals, a decrease in testosterone level was reported following CA treatment which was attributed to decreased LH levels [12, 21]. A direct action of CA on Leydig cells is very likely and may be responsible for the low serum level of testosterone in the CA-treated intact fish. CA has been shown to inhibit  $\Delta 5$ - $3\beta$ -hydroxysteroid dehydrogenase activity in the ovaries and livers of female tadpoles [9]. Haider [8] reported that CA influences the differentiation of rat peritubular Leydig cells and hydroxysteroid dehydrogenases to varying degrees. In Indian wall lizard, CA treatment inhibited  $\Delta 5$ - $3\beta$ -hydroxysteroid dehydrogenase and glucose-6-phosphate dehydrogenase activities and caused the accumulation of sudanophilic lipid material in Leydig cells [7]. The decreased  $E_2$  level suggests the decreased rate of aromatization of testosterone which is the precursor of  $E_2$ . A decrease in  $E_2$  level was also reported in CA-treated human volunteers [12]. Srivastava



et al. [37] have reported that CA displaces  $E_2$  selectively from sex hormone-binding globulin in female monkey plasma.

In conclusion, the regressive changes in the SV and testis are caused by decreased secretion and activity of androgen by CA.

#### ACKNOWLEDGEMENTS

This work was supported by a research grant to KPJ from the Indian Council of Agricultural Research, New Delhi. The authors are grateful to Schering AG, Germany for a generous gift of cyproterone acetate and to Prof. G. D. Niswender, Department of Physiology, University of Colorado, Co, USA for  $E_2$  antiserum and the Indian Council of Medical Research, New Delhi and Dr. C. Das, AIMS, New Delhi for testosterone antiserum.

#### REFERENCES

1. Abraham, G. E. (1974) Radioimmunoassay of steroids in biological materials. *A. Endocrinol.* 183 (Suppl. 75), 1–42.
2. Billard, R. (1982) Attempts to inhibit testicular growth in rainbow trout with antiandrogens (cyproterone, cyproterone acetate, oxymetholone) and busulfan given during the period of spermatogenesis. *Gen. Comp. Endocrinol.* 48, 33–48.
3. Davidson, E. A. (1966) Analysis of sugars found in mucopolysaccharides. In: E. F. Neufeld, V. Ginsburg (eds) *Methods in Enzymology*, Vol. VIII. Academic Press, New York, pp. 52–60.
4. Dhar, J. D., Setty, B. S. (1976) Studies on the physiology and biochemistry of mammalian epididymis: Effect of flutamide, a nonsteroidal antiandrogen, on the epididymis of the rat. *Fertil. Steril.* 5, 566–576.
5. Elson, L. A., Morgan, W. J. T. (1933) A colorimetric method for the determination of glucosamine and galactosamine. *Biochem. J.* 27, 1824–1828.
6. Gaitoude, S. G., Gouder, B. Y. (1983) Effect of cyproterone acetate on the testis and male accessory reproductive organs in the lizard, *Calotes versicolor*. *Monit. Zool. Ital.* 17, 217–230.
7. Haider, S., Rai, U. (1986) Effects of cyproterone acetate and flutamide on the testis and epididymis of the Indian wall lizard, *Hemidactylus flaviviridis* (Ruppel). *Gen. Comp. Endocrinol.* 64, 321–329.
8. Haider, S. G., Urban, A., Hilscher, B., Hilscher, W., Passia, D. (1983) Cyproterone acetate induced changes in the behavior of hydroxysteroid dehydrogenases in rat Leydig cells during perinatal development. *Andrologia* 15, 498–506.
9. Hsu, C. Y., Hsu, L. H., Liang, H. M. (1979) The effect of cyproterone acetate on the activity of  $\Delta^5$ -3 $\beta$ -hydroxysteroid dehydrogenase in tadpole sex transformation. *Gen. Comp. Endocrinol.* 39, 404–410.
10. Jänne, O. A., Bardin, C. W. (1984) Androgen and antiandrogen receptor binding. *Ann. Rev. Physiol.* 46, 107–118.
11. Jost, A. (1971–72) Use of androgen antagonists and antiandrogens in studies on sex differentiation. *Hormones and Antagonists: Gynec. Invest.* 2, 180–201.
12. Knuth, U. A., Hano, R., Niesch-Lag, E. (1984) Effect of flutamide or cyproterone acetate on pituitary and testicular hormones in normal men. *J. Clin. Endocrinol. Metab.* 59, 963–969.
13. Lahnsteiner, F., Richtarski, U., Patzner, R. A. (1990) Functions of the testicular gland in two blennioid fishes, *Salarias (= Blennius) pavo* and *Lipophrys (= Blennius) dalmatinus* (Blenniidae, Teleostei) as revealed by electron microscopy and enzyme histochemistry. *J. Fish Biol.* 37, 85–97.
14. Lowry, O. H., Rosenbrough, N. J., Farr, A. L., Randall, R. J. (1951) Protein measurement with folin-phenol reagent. *J. Biol. Chem.* 193, 265–275.
15. Mann, T. (1964) *The biochemistry of semen and of the male reproductive tract*. Methuen, London.

16. Murphy, T. M. (1980) The effect of methallibure and cyproterone acetate on the gonadotrophic cells, plasma androgen levels and testes of precocious 1 + male Atlantic salmon parr *Salmo salar* (L.). *J. Fish Biol.* 17, 673–680.
17. Nayyar, S. K., Sundararaj, B. I. (1970) Seasonal reproductive activity in the testes and seminal vesicles of the catfish, *Heteropneustes fossilis* (Bloch). *J. Morphol.* 130, 207–226.
18. Neumann, F. (1971–72) Use of cyproterone acetate in animal and clinical trials. *Hormones and antagonists: Gynec. Invest.* 2, 150–179.
19. Neumann F., Elger, W. (1984) Sexual differentiation: studies with antiandrogens. In: M. Serio et al. (eds) *Sexual Differentiation: Basic and Clinical Aspects*. Raven Press, New York, pp. 191–208.
20. Neumann, F., Gräf, K.-J., Hasan, S. H., Schenck, B., Steinbeck, H. (1977) Central action of antiandrogens. In: L. Martini, M. Motta (eds) *Androgens and Antiandrogens*. Raven Press, New York, pp. 163–177.
21. Neumann F, Habenicht, U. F., Schacher, A. (1984) Androgens and target cell response: different in vivo effects of cyproterone acetate, flutamide and cyproterone. In: K. W. McKerns, A. Aakvaag, V. Hansson (eds) *Regulation of Target Cell Responsiveness*. Vol. 2. Plenum Press, New York, pp. 489–527.
22. Neumann, F., Jacobi, G. H. (1982) Antiandrogens in tumour therapy. *Clinics in Oncol.* 1, 41–64.
23. Neumann, F., Richter, K. D., Schenck, B., Tunn, U., Senge, TH. (1980) Action of antiandrogens on accessory sexual glands. In: F. H. Schroder, H. J. de Voogt (eds) *Steroid Receptors, Metabolism and Prostatic Cancer*. Amsterdam, Excerpta Medica, pp. 22–40.
24. Neumann, F., Schenck, B. (1980) Anti-androgens: Basic concepts and clinical trials. In: G. R. Cunningham, W.-B. Schill, E. S. E. Hafez (eds) *Regulation of Male Fertility*. The Hague, Martinus Nijhoff, pp. 93–104.
25. Prasad, M. R. N., Rajalakshmi, M., Reddy, P. R. K. (1971–72) Action of cyproterone acetate on male reproductive functions. *Hormones and Antagonists: Gynec. Invest.* 2, 202–212.
26. Rai, M. S. (1996) *Reproductive Endocrinology of Catfish: Aspects of Structure and Physiology of Seminal Vesicle in Clarias batrachus* (L.). Ph. D. Thesis Banaras Hindu University, Varanasi, India.
27. Rastogi, R. K., Chieffi, G. (1975) The effects of antiandrogens and antiestrogens in nonmammalian vertebrates. *Gen. Comp. Endocrinol.* 26, 79–91.
28. Rastogi, R. K., Chieffi, G., Iela, L. (1971–72) Effects of antiestrogen and antiandrogen in Amphibia. *Hormones and Antagonists: Gynec. Invest.* 2, 271–275.
29. Resink, J. W., Schoonen, W. G. E. J., Van den Hurk, R., Viveen, W. J. A. R., Lambert, J. G. D. (1987) Seasonal changes in steroid metabolism in the male reproductive organ-system of the African catfish, *Clarias gariepinus*. *Aquaculture* 63, 59–76.
30. Resink, J. W., Van den Hurk, Voorthuis, P. K., Terlouw, M., De Leeuw, R., Viveen, W. J. A. R. (1987) Quantitative enzyme histochemistry of steroid and glucuronide synthesis in testes and seminal vesicles, and its correlation to plasma gonadotropin level in *Clarias gariepinus*. *Aquaculture* 63, 97–114.
31. Rouse, E. F., Coppenger, C. J., Barnes, P. R. (1977) The effect of an androgen inhibitor on behaviour and testicular morphology in the stickleback *Gasterosteus aculeatus*. *Horm. Behav.* 9, 8–18.
32. Schenck, B., Neumann, F. (1978) Influence of anti-androgens on Sertoli cell function and intra-testicular androgen transport. *Int. J. Androl.* 1, 459.
33. Schoonen, W. G. E. J., Lambert, J. G. D. (1986) Steroid metabolism in the seminal vesicles of the African catfish, *Clarias gariepinus* (Burchell), during the spawning season, under natural conditions, and kept in ponds. *Gen. Comp. Endocrinol.* 61, 355–367.
34. Schoonen, W. G. E. J., Lambert, J. G. D. (1987) Gas chromatographic mass spectrometric analysis of steroids and steroid glucuronides in the seminal vesicle fluid of the African catfish, *Clarias gariepinus*. *Gen. Comp. Endocrinol.* 68, 375–386.
35. Schreck, C. B. (1973) Uptake of <sup>3</sup>H-testosterone and influence of an antiandrogen in tissues of rainbow trout (*Salmo gairdneri*). *Gen. Comp. Endocrinol.* 21, 60–68.
36. Singh, S. K. (1984) Effect of flutamide on the testis and accessory sex glands of the musk shrew, *Suncus murinus* L. *Exp. Clin. Endocrinol.* 84, 20–26.



37. Srivastava, A. K., Dey, S. B., Roy, S. K. (1983) Interaction of cyproterone acetate with sex hormone binding globulin of monkey plasma. *Exp. Clin. Endocrinol.* 82, 232–234.
38. Sundararaj, B. I., Nayyar, S. K. (1969) Effects of estrogen, SU-9055, and cyproterone acetate on the hypersecretory activity in the seminal vesicles of the castrate catfish, *Heteropneustes fossilis* (Bloch). *J. Exp. Zool.* 172, 399–408.
39. Van den Hurk, R., Resink, J. W. (1992) Male reproductive system as sex pheromone producer in teleost fish. *J. Exp. Zool.* 261, 204–213.
40. Van den Hurk, R., Resink, J. W., Peute, J. (1987) The seminal vesicle of the African catfish, *Clarias gariepinus*. A histological, histochemical, enzyme-histochemical, ultrastructural and physiological study. *Cell Tiss. Res.* 247, 573–582.
41. Warren, L. (1959) The thiobarbituric acid assay of sialic acids. *J. Biol. Chem.* 234, 1971–1975.

# BODY PERCEPTION AND CONSCIOUSNESS. CONTRIBUTIONS OF INTEROCEPTION RESEARCH<sup>1</sup>

R. HÖLZL, A. MÖLTNER and C. NEIDIG

Laboratory of Clinical Psychophysiology, Otto-Selz-Institute of Psychology and Education Science, University of Mannheim, Mannheim, Germany and Faculty of Natural Sciences, Department of Comparative Physiology, Eötvös Loránd University, Budapest, Hungary

(Received: 1998-07-08; accepted: 1998-07-21)

Wer will was *Lebendig's* erkennen und beschreiben,  
Sucht erst den *Geist* heraus zu treiben,  
Dann hat er die *Teile* in seiner Hand,  
Fehlt leider nur das *geistige Band*.<sup>2</sup>

J. W. VON GOETHE [1]

## INTRODUCTION

In looking back at the last three decades of interoception research in the Department of Comparative Physiology at Eötvös Loránd University Budapest from the standpoint of an external cooperating group it seems appropriate to consider its impact on recent and future developments in the field and related areas of psychobiology. We will do this by concentrating on a series of experiments inspired by our cooperation with G. Ádám's group since 1985 [2–5]. Their results have important bearings on a current issue in the consciousness debate.

Dedicated to György Ádám on the occasion of his 75th birthday.

Send offprint requests to: Prof. Dr. R. Hözl, Laboratory of Clinical Psychophysiology, Otto-Selz-Institute of Psychology and Education Science, University of Mannheim, Postfach 103462, D-68131 Mannheim, Germany

<sup>1</sup>This report is based on an invited paper read by the first author before the Hungarian Academy of Sciences at the 30th Anniversary Symposium of the Department of Comparative Physiology, Eötvös Loránd University, and the Human Psychophysiology Group of the Hungarian Academy of Sciences, Budapest, 18th December 1997.

<sup>2</sup>English translation (R. H.): "Who would know and describe a living thing / Tries first to drive its spirit out, / Then with the pieces in his hand, / He lacks their spiritual bond" [1].



### *Visceroception and somatosensation*

The issue in question is on the role of body perception in general and perception of visceral events in particular in the constitution of a conscious self through the construction of the so-called "*body self*". This term has become fashionable again since Damasio's best-selling book on "*Descartes' Error*" [6] and refers to the embodied "*Me*" as the integrative centre around which *perceptions* and *orientation in space, feelings* and *thoughts, plans* and *volitional acts* are organized by the brain.

Damasio's model of "*somatic markers*" particularly emphasizes the contribution of *visceral feedback* in affect and action control, that is, from our *inner organs*, the heart and the guts, in addition to tactile signals from the skin and proprioceptive signals from muscles, joints and the labyrinth.

The model implies a crucial role of central body representation in the constitution of a conscious self, but *its dynamics*, the ways in which somatosensory and viscerosensitive afferent flows become integrated into the experience of the embodied self, remained obscure. In this respect, we seem to know not much more than the early researchers on the "body schema" like Horowitz, Schilder, Penfield or Luria, to name a few [7–11].

### *The role of awareness*

In particular, we do not know at which level of *awareness* the information from somatic and visceral afferents is processed and combined to exert their alleged control on affect, intention, and action. This seems strange as there is a *long tradition of research* on somatosensation on the one side and on viscerosensitive on the other, the latter being connected much with the Department of Comparative Physiology.

But it is as if we had only the pieces in our hands and would be lacking in the "*geistige Band*", the conceptual bond, to which Johann Wolfgang referred in the motto above. The situation might change considerably when those two traditions could be combined.

Beginning with Ádám's classic on "*Interoception and Behavior*" 30 years ago [12], psychophysiological knowledge has accumulated showing that interoceptive information may control behavior requiring highest brain levels such as discriminative learning without necessarily reaching awareness by the subject.

But little is known about the *differences in processing* with – as compared to without – awareness. Not much is known either about these differences in somatosensation, and almost nothing is known about *mutual influences between the two sensory channels* at different levels of awareness over and above the older physiological and clinical work on referred pain etc. since Head and others [13–14].

Knowledge on such *somato-visceral interactions* at the perceptual level would be basic, however, to a better understanding of those integrative mechanisms at the highest level of the body schema, the *body image*, to which Damasio was referring to.

### *Somatovisceral interactions*

Before my colleagues and I started out on this question only a single psychophysiological study had appeared in 1990 dealing with somatovisceral interactions in visceral perception of humans, and, as you might have guessed, it stemmed from Ádám's group [15]. It investigated the *masking* (No. 1 in Fig. 1) of a visceral distension stimulus by an abdominal stimulus in a special preparation with colostomy patients by way of a so-called signal detection approach. But it did not directly address the relation between *awareness* and somatovisceral masking (Nos 3 and 5).

The question of *awareness-specific effects in interoception* was what we have been primarily interested in since we started out on interoception about 10 years ago with a series of studies on the *psychophysics* of intestinal mechanoreception, on the *discriminability* between internal and external, abdominal stimuli, and on their *interactions* below and above conscious sensation.

In the following I will shortly describe two experiments of this series, one taking up Ádám's lead on somatovisceral masking, the other on its counterpart, summation, about which no study had been done so far.

#### INTERACTIONS BETWEEN SOMATOSENSORY AND VISCERAL SIGNALS IN BODY PERCEPTION

##### 1. Mutual Masking

**Task:** Stimulus detection & Identification

##### 2. Summation

**Task:** Stimulus detection only

##### 3. Role of Awareness

**Differentiating Role:** Differences of masking (summation) effects with as compared to without Conscious Sensation

##### 4. Mode-specific Interaction Effects

##### 5. Mode-specific Awareness Effects

Fig. 1. Somatovisceral Interactions – Level of interaction and role of awareness in masking and summation



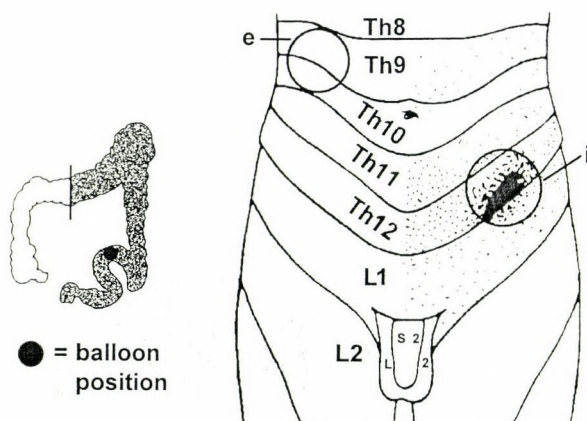


Fig. 2. Stimulation sites in somatovisceral interactions studies

## SOMATOVISCERAL MASKING

Figure 2 illustrates the stimulation sites which we used for the somatovisceral interaction studies: The visceral stimulus was applied by a balloon probe in the sigmoid colon, the external abdominal stimuli by a ring-shaped stimulator as in Ádám's study at two abdominal sites (Fig. 2, marks i and e), one within, the other outside the abdominal reference zone from which visceral and somatic afferents converge at the spinal level according to neurophysiological studies [16].

The psychophysical method differed from Ádám's in two important respects:

(1) A continuous tracking method called *multiple staircase* was used to assess interoceptive and somatosensory thresholds concurrently within the same subject. This controls for instationarities of perceptual thresholds over prolonged periods of testing and for interindividual variance. The method is a somewhat sophisticated version of the famous *Békésy-method* of continuous auditory threshold estimation in which the intensity of the stimulus is tracked up or down depending on subject's discrimination response, except that a multiple of thresholds is tracked in parallel.

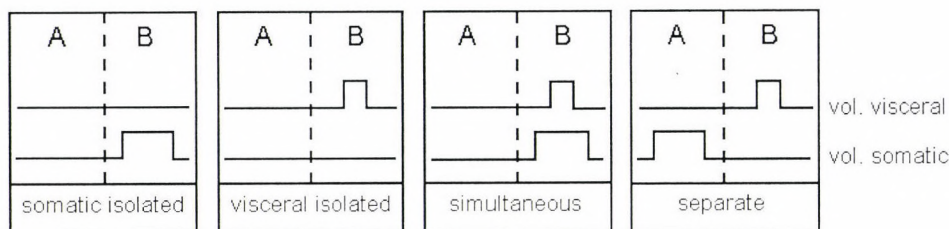


Fig. 3. Trial structure of concurrent somatovisceral masking procedure

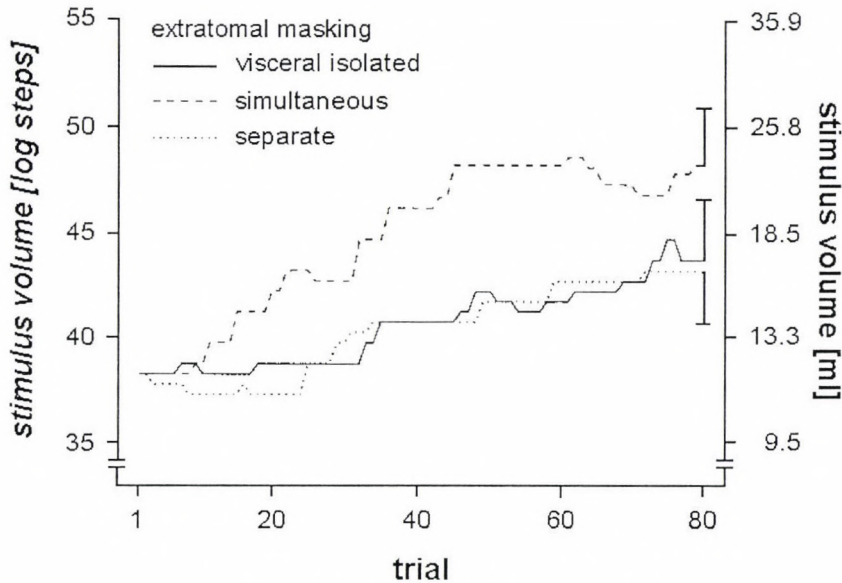


Fig. 4. Mean tracking curves in masking experiment

(2) A forced-choice paradigm with two observation intervals A and B (Fig. 3) was applied in which the subject is forced to decide in which interval the stimulus had occurred even when he has not felt anything.

In addition, a subjective rating of the intensity felt, ranging from “not felt” to “strongly felt”, was requested at the end of the trial. This allowed concurrent testing of discrimination with or without conscious sensation – and the sensation itself which all were to be compared.

In the case of somatovisceral masking illustrated in Fig. 3, four kinds of stimuli or stimulus combinations are presented and their corresponding discrimination thresholds were continuously assessed by the multiple staircase:

- Visceral distension “isolated” (first frame in Fig. 3),
- abdominal pressure “isolated” (second frame in Fig. 3),
- visceral and abdominal stimulus *overlapping* (third frame in Fig. 3), and
- visceral and abdominal stimulus *combined*, but in *separate* observation intervals as control (last frame in Fig. 3).

The subject is asked in which of the observation intervals the visceral and the abdominal stimulus occurred. The intensity is adjusted in the next trial depending on hit or miss of the subject for the particular stimulus.

As one can see from the group trackings in Fig. 4, combining visceral and somatic stimulus resulted in *distinct elevation of visceral thresholds* shown by the upper curve in the case of overlapping combination, but not in the separate combination which gave the



same thresholds as when the visceral stimulus was presented alone. This demonstrates *somatosensory masking of the visceral stimulus*.

There are two interesting aspects in the results of this study which differ from other masking experiments in exteroception:

*Firstly*, the masking relation is asymmetric, that is, the abdominal stimulus is not masked by the visceral stimulus.

*Secondly*, the masking effect on the visceral stimulus is not greater when the abdominal stimulus is presented within the spinal reference zone as compared to outside. This shows that the effect is not produced by somatovisceral convergence neurons at the spinal level but supraspinally, presumably in the somatosensory cortex, S(II).

*Thirdly, and most important*, there are *specific differences* in visceral and somatosensory discrimination performance when the subject had also had a conscious sensation as to compared when he had not.

This is shown in Fig. 5 which may look a bit complicated at first, although its message is rather simple, that is, there is a qualitative difference between visceroreception and somatosensation under different awareness conditions:

– Hit rates in trials in which the subject had a conscious sensation were higher than those in trials where no sensation occurred – as one would expect.

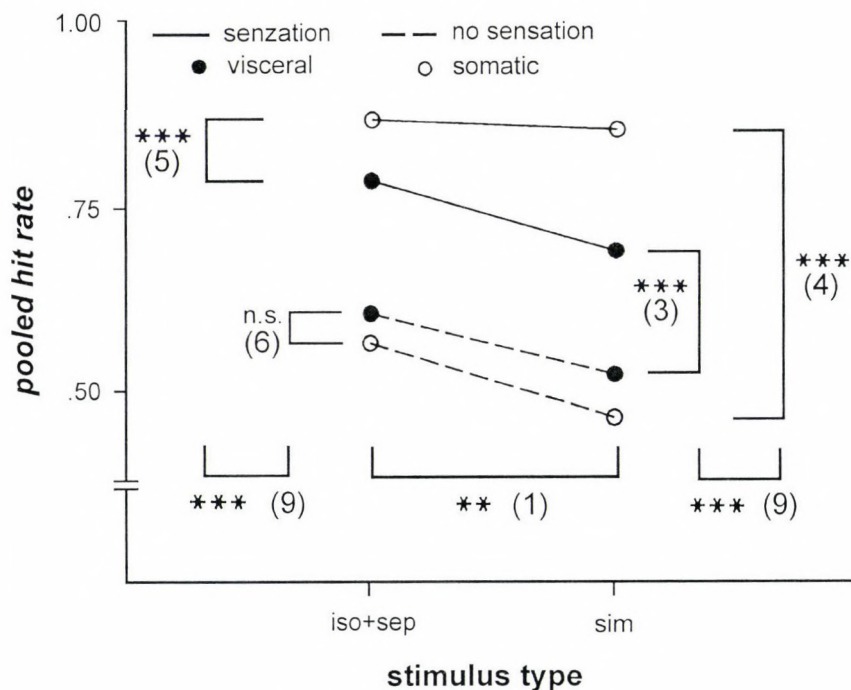


Fig. 5. Awareness and discrimination

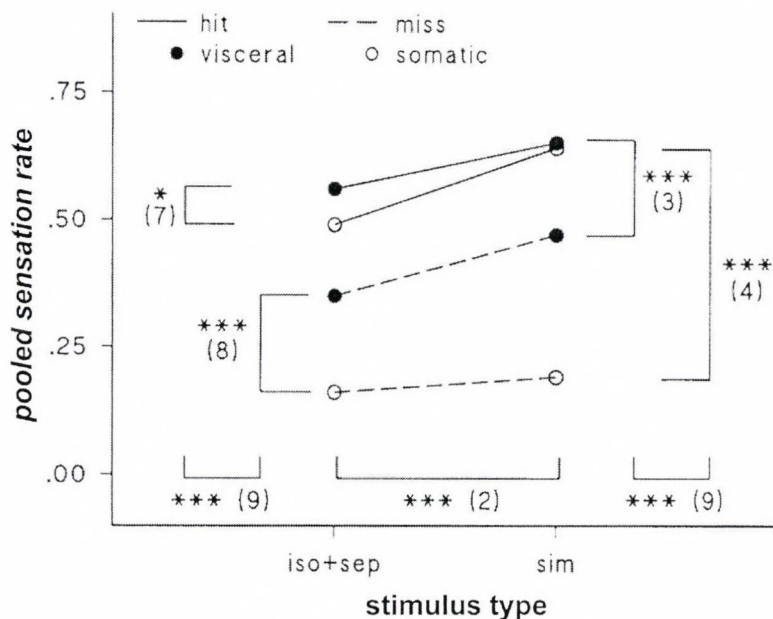


Fig. 6. Sensation and discrimination

– But, in addition, the difference between hit rates under the two awareness conditions is much greater for the abdominal, that is, the somatic stimulus as compared to the difference for the visceral stimulus.

As it seems, the visceral discrimination is *less strongly coupled to conscious sensation* than is the tactile discrimination on the abdomen!

– And finally, the difference is accentuated by the effective masking of the visceral stimulus by the somatosensory abdominal stimulus: Hit rates of the visceral discrimination are higher in the presence of a conscious sensation when presented separately, but do not drop to chance level under masking ( $= 0.50$ ). In contrast, they do for discriminations without sensation. Again, this is different from somatosensation.

Analogous specifics appear when sensation rate is considered as a function of hits or misses of the forced choice discrimination which is illustrated in Fig. 6.

The details would lead too far here. It will be sufficient for the present purpose to note that there are not only characteristic somatic-visceral differences in masking as such but also in the masking effect on the relation between forced stimulus detection and conscious sensation of the stimulus.



## SOMATOVISCERAL SUMMATION

Because lack of space we will not describe the second experiment on somatovisceral summation in any detail but would like to add just this much:

In the summation task the subject is not to identify the sensory mode or channel (visceral or somatic) as in the masking condition but he has only to detect any stimulus at all. In this case, internal and external signals may be combined to increase detection rate when presented in combination.

This is in fact the case and thresholds drop while hit rates go up. The interesting thing is, that in this condition *no decoupling of sensation and discrimination* takes place and *visceral and somatic discrimination do not differ* in this respect.

### CONTRIBUTIONS OF INTEROCEPTION RESEARCH

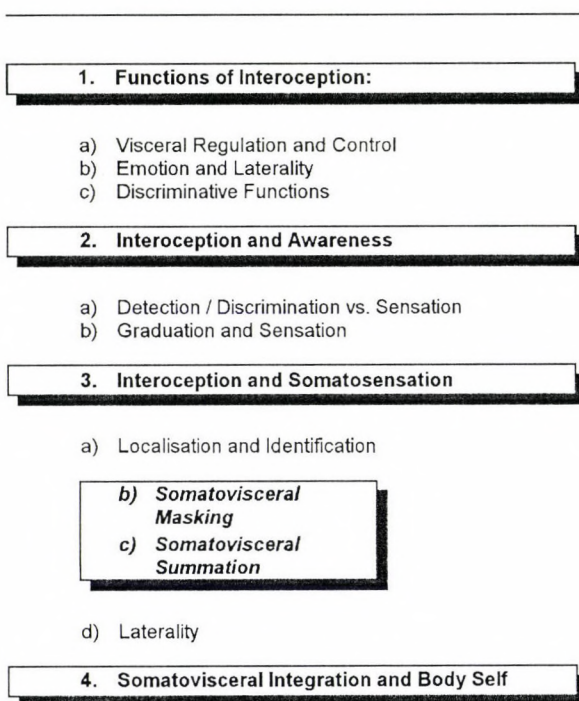


Fig. 7. Contributions of interoception research

## CONCLUSION

As one can (or should) see from the examples, *mode-specific effects of awareness* may be found when taking a closer look at visceroreception and somatosensation and their relations.

And, in addition, this may *vary with the kind of information* the subject has to extract from the dual sensory inflow from the body to solve a given task, for instance, *discriminating between sensory modes* or *using both* in conjunction.

*This is the kind of perceptual dynamics* that we would like to know if we were *to build a model* of how and at what cognitive level visceral signals become integrated with somatosensory inflow – and if talk of “body self” and “somatic markers” is to become *more than a façon de parler*.

It is our conviction that such a model would have to make systematic use of old and new contributions of interoception research to the problem of central body representation as summarized in Fig. 7.

And it is our hope that this might finally provide us with the “*geistige Band*” we have referred to in the beginning – although we, too, presented only *pieces in our hands*.

## ACKNOWLEDGEMENTS

The research in the Laboratory of Clinical Psychophysiology at the University of Mannheim and the collaboration with Dr. Ádám's group in Budapest was generously supported by the Deutsche Forschungsgemeinschaft, DFG, by continuing grants to the first author since 1985 (Ho 904/3 through 8). Without this support neither the particular experiments nor the inspiring cooperation with the Human Psychophysiology Group of the Hungarian Academy of Sciences would have been possible. The DFG also supported several research visits of our group in Budapest and a visit of Dr. Ádám in Mannheim jointly with the Hungarian Academy of Sciences.

## REFERENCES

1. Goethe J. W. v. (1790/1808) *Faust. Ein Tragödie*. 1. Teil cited after: 1963, “Hamburger Ausgabe”, comm. by Trunz, E. (p. 63, vv 1936–1939). Hamburg, Chr. Wegener Verlag.
2. Ádám, G. (1998) *Visceral perception: Understanding Internal Cognition*. Plenum, New York–London–Washington–Moscow.
3. Fent, J., Balázs, L. Buzás, G. Erasmus, L.-P., Hölzl, R., Kovács, Á., Weisz, J., Ádám, G. (1998) Colonic sensitivity in irritable bowel syndrome and normal subjects according to their hemispheric preference and cognitive style. *Internat. J. Psychophysiol.* 30, in press.
4. Hölzl, R., Erasmus, L.-P., Möltner, A. (1996) Detection, discrimination and sensation of visceral stimuli. *Biol. Psych.* 42, 199–214.
5. Hölzl, R., Möltner, A., Neidig, C. W., Erasmus, L.-P. (1998) *Somato-visceral interactions in visceral perception: abdominal masking of colonic stimuli*. Integrative physiological and behavioral science, in press.
6. Damasio, A. R. (1994). *Descartes' error*. Grosset/Putnam, New York.
7. Horowitz, E. L. (1935) Spatial localization of the self. *J. Soc. Psychol.* 6, 379–387. (Cited after [8].)
8. Hilgard, E. R. (1949) Human motives and the concept of the self. *Am. Psychol.* 4, 374–382.
9. Schilder, P. (1975) *Das Körperschema*. Suhrkamp, Frankfurt/M: (Orig.: Berlin, 1923.)
10. Penfield, W., Boldrey, E. (1937) Somatoic motor and sensory representation in the cerebral cortex of man as studied by electrical stimulation. *Brain* 60, 389–443.



11. Luria, A. R. (1972) *The Man with a Shattered World*. Basic Books, New York. (Orig.: Moscow, 1968.)
12. Ádám, G. (1967) *Interoception and Behaviour. An Experimental Study*. Akadémiai Kiadó, Budapest.
13. Head, H. (1893) On disturbances of sensation with especial reference to the pain of visceral disease. *Brain* 16, 1–133.
14. MacKenzie, J. (1893) Some points bearing on the association of sensory disorders and visceral disease. *Brain* 16, 321–353.
15. Ádám, G., Balázs, L., Vidos, T., Keszler, P. (1990) Detection of colon distension in colonostomy patients. *Psychophysiology* 27, 451–456.
16. Cervero, F. (1994) Sensory innervation of the viscera: peripheral basis of visceral pain. *Physiol. Rev.* 74, 95–138.

PRINTED IN HUNGARY

Akadémiai Nyomda, Martonvásár





## DIRECTIONS TO CONTRIBUTORS

ACTA BIOLOGICA HUNGARICA publishes original works in the field of experimental biology.

Manuscripts should be addressed to Dr. JÁNOS SALÁNKI, Editor, *Acta Biologica Hungarica*, H-8237 Tihany, Hungary.

Only original papers will be published and a copy of the Publishing Agreement will be sent to the authors of papers accepted for publication. Manuscripts will be processed only after receiving the signed copy of the agreement.

The manuscripts should not exceed 16 typed pages in general. The manuscripts should be typed double-spaced, on one side of the paper. In order to assure rapid publication, contributors are requested to submit two copies of the manuscript including an abstract (max. 200 words), tables and figures. An electronic version of the manuscript (including the figures) should also be submitted on a 3.5" diskette, using Word for Windows 7.0, 6.0 or 2.0 wordprocessor package in Microsoft Windows '95 or Windows 3.1 system. Each table should be typed on a separate sheet, numbered and provided with a title. All figures, either photographs or drawings or graphs, should be numbered consecutively. Figure legends should be typed in sequence on a separate sheet. Color plates (micrographs and drawings) will be charged to the authors (in 1998 US\$ 280 per page).

Papers should be headed with the title of the paper, the names of the authors (male authors use initials, female authors use one given name in full), department, institute and town where the work was performed. A running title, not to exceed 50 letter spaces, should be included on a separate sheet and immediately following the summary 5 keywords must be supplied.

The *full paper* should be divided into the following parts in the order indicated:

1. *Abstracts*
2. *Introduction*
3. *Materials and Methods*
4. *Results*
5. *Discussion*
6. *References.* Papers – the essential ones only – cited in the manuscript should be listed on a separate

sheet in alphabetical order according to the first author's surname. The references should be numbered so that each may be referred to in the text by its number only.

Examples:

1. Boas, N. F. (1953) Method for determination of hexosamine in tissue. *J. biol. Chem.* 204, 553–563.
2. De Duve, C. (1959) Lysosomes, a new group of cytoplasmic particles. In: Hayashi T. (ed.) *Subcellular Particles*. Ronald Press, New York, pp. 1–72.
3. Umbreit, W. E., Burris, R. H., Stauffer, I. F. (1957) *Manometric Techniques*. Burgess Publishing Co., Minneapolis.

*Short communication.* Manuscripts, in English, should not exceed 1000 words (4 types pages) including references. The text of manuscripts containing tables and/or figures must be correspondingly shorter. Accepted short communications will be published within six months after submission of manuscripts. In order to speed up publication, no proof will be sent to authors.

Authors will be furnished, free of charge, with 25 reprints. Additional reprints may be obtained at cost.





307218

# **Acta Biologica Hungarica**

78

VOLUME 49, NUMBERS 2-4, 1998

EDITOR

**J. SALÁNKI**

EDITORIAL BOARD

V. CSÁNYI, D. DUDITS, K. ELEKES, L. FERENCZY, A. FALUS, E. FISCHER,  
B. FLERKÓ, K. GULYA, F. HAJÓS, J. HÁMORI, L. HESZKY, P. KÁSA,  
J. KOVÁCS, J. NEMCSÓK, P. PÉCZELY, M. SIPICZKY, **G. SZABÓ**,  
J. SZEBERÉNYI, GY. SZÉKELY, A. TIGYI



**Akadémiai Kiadó, Budapest**

ACTA BIOL. HUNG. ABAHAU 49 (2-4) 165-477 (1998) HU ISSN 0236-5383



# ACTA BIOLOGICA HUNGARICA

A QUARTERLY OF THE HUNGARIAN  
ACADEMY OF SCIENCES

---

*Acta Biologica Hungarica* publishes original papers on experimental biology.

*Acta Biologica Hungarica* is published in yearly volumes of four issues by

AKADÉMIAI KIADÓ  
H-1117 Budapest, Prielle K. u. 4, Hungary  
<http://www.akkrt.hu>

Manuscripts and editorial correspondence should be addressed to

*Acta Biologica Hungarica*  
H-8237 Tihany, Hungary  
  
Phone: (36-87) 448-244  
Fax: (36-87) 448-006  
E-mail: [salanki@tres.blki.hu](mailto:salanki@tres.blki.hu)

Orders should be addressed to

AKADÉMIAI KIADÓ  
H-1519 Budapest, P.O. Box 245, Hungary  
Fax: (36-1) 464-8221  
E-mail: [kiss.s@akkrt.hu](mailto:kiss.s@akkrt.hu)

Subscription price for Volume 49 (1998) in 4 issues US\$ 136.00, including normal postage, airmail delivery US\$ 20.00.

"This periodical is included in the document delivery program THE GENUINE ARTICLE of the Institute of Scientific Information, Philadelphia. The articles published in the periodical are available through *The Genuine Article* at the Institute for Scientific Information, 3501 Market Street, Philadelphia PA 19104."

---

*Acta Biologica Hungarica* is abstracted/indexed in Biological Abstracts, Chemical Abstracts, Current Contents-Agriculture, Biology and Environmental Sciences, database (EMBASE), Index Medicus, International Abstracts of Biological Sciences

---

## CONTENTS

Preface. M. SZILÁGYI, E. TYIHÁK .....	165
An evolutionary role of formaldehyde. M. P. KALAPÓS .....	167
Related $^{15}\text{N}$ - and $^{14}\text{N}$ -methyltransferases methylate the large and small subunits of Rubisco. Z. YING, R. M. MULLIGAN, N. JANNEY, M. ROYER, R. L. HOUTZ .....	173
Methylation and gene mutation in eukaryotic DNA. C.-Q. LIU, J.-F. HUANG, YING WANG, W.-B. LIU .....	185
Role of formaldehyde in direct formation of glycine and serine in bean leaves. Á. NOSTICZIUS .....	193
Effect of methionine enrichment on the biological activities of food proteins. GYÖNGYI HAJÓS, SZ. FARKAS, EMÓKE SZERDAHELYI, MARIANNE POLGÁR .....	201
L-carnitine as essential methylated compound in animal metabolism. An overview. M. SZILÁGYI .....	209
Addition of $\text{CH}_2\text{O}$ to arginine – a theoretical study by <i>ab initio</i> method. CORNELIA KOZMUTZA, E. M. EVLETH, L. UDVARDI, J. PIPEK .....	219
Formaldehyde cycle and the natural formaldehyde generators and capturers. E. TYIHÁK, L. ALBERT, ZS. I. NÉMETH, GY. KÁTAY, ZS. KIRÁLY-VÉGHÉLY, B. SZENDE .....	225
Formaldehyde in the plant kingdom. G. BLUNDEN, B. G. CARPENTER, MARICELLA ADRIAN- ROMERO, M.-H. YANG, E. TYIHÁK .....	239
Plant tissue culture as a model for study of diversity in formaldehyde binding. I. LÁSZLÓ, ÉVA SZÓKE, ZS. NÉMETH, L. ALBERT .....	247
Determination of endogenous formaldehyde in plants (fruits) bound to L-arginine and its relation to the folate cycle, photosynthesis and apoptosis. L. TRÉZL, L. HULLÁN, T. SZARVAS, A. CSIBA, B. SZENDE .....	253
The hydrazine derivative aminoguanidine inhibits the reaction of tetrahydrofolic acid with hydroxymethylarginine biomolecule. L. HULLÁN, L. TRÉZL, T. SZARVAS, A. CSIBA .....	265
Induction of resistance of wheat plants to pathogens by pretreatment with N-methylated sub- stances. KLÁRA MANNINGER, MÁRIA CSÖSZ, E. TYIHÁK .....	275
Identification and measurement of resveratrol and formaldehyde in parts of white and blue grape berries. ZSUZSA KIRÁLY-VÉGHÉLY, E. TYIHÁK, L. ALBERT, ZS. I. NÉMETH, GY. KÁTAY .....	281
Relationship between dimedone concentration and formaldehyde captured in plant tissues. ÉVA SÁRDI, E. TYIHÁK .....	291
The use of HPLC for the detection and quantification of formaldehyde in the Pteridophyta. MARICELA ADRIAN-ROMERO, G. BLUNDEN, B. G. CARPENTER, SHEILA LUCAS, E. TYIHÁK .....	303



Drought stress, peroxidase activity and formaldehyde metabolism in bean plants. ÉVA STEFANOVITS-BÁNYAI, ÉVA SÁRDI, SUSAN LAKATOS, M. ZAYAN, I. VELICH .....	309
The increase of formaldehyde level in some rare pathological cases of teeth determined with the use of quantitative TLC. T. KATARZYNA RÓŻYŁO, R. SIEMBIDA, ANNA SZYSZKOWSKA, ANNA JAMBROŻEK-MANKO .....	317
Formaldehyde generators and capturers as influencing factors of mitotic and apoptotic processes. B. SZENDE, E. TYIHÁK, L. TRÉZL, ÉVA SZŐKE, I. LÁSZLÓ, GY. KÁTAY, ZS. KIRÁLY-VÉGHÉLY .....	323
Reduction of apoptosis of <i>in vitro</i> cultured lymphocytes of HIV-positive persons by N <sup>G</sup> -hydroxy-methylated-L-arginine and l'-methyl-ascorbigen. J. BOCSI, K. NAGY, E. TYIHÁK, L. TRÉZL, B. SZENDE .....	331
Formaldehyde generation by N-demethylation. H. KALÁSZ, MÁRIA BÁTHORI, E. TYIHÁK .....	339
Formaldehyde-induced modification of hemoglobin <i>in vitro</i> . R. FARBISZEWSKI, ELŻBIETA SKRZYDLEWSKA, AGNIESZKA ROSZKOWSKA .....	345
Change of biotransformation steps of formaldehyde cycle in water-melon plants after infection with <i>Fusarium oxysporum</i> . ÉVA SÁRDI, E. TYIHÁK .....	353
The effect of heat shock on the formaldehyde cycle in germinating acorns of European turkey oak. L. ALBERT, ZS. I. NÉMETH, SZ. VARGA .....	363
Changes in formaldehyde contents of germinating acorns of <i>Quercus cerris</i> L. under low temperature stress conditions. ZS. I. NÉMETH, L. ALBERT, SZ. VARGA .....	369
Alteration of endogenous formaldehyde level following mercury accumulation in different pig tissues. T. RÉTFALVI, ZS. I. NÉMETH, I. SARUDI, L. ALBERT .....	375
Investigation of some methylated compounds and peroxidase activity during plant ontogenesis in snap bean. ÉVA SÁRDI, ÉVA STEFANOVITS-BÁNYAI .....	381
Formaldehyde as a proof and response to various kind of stress in some <i>Basidiomycetes</i> . ANNA JAROSZ-WILKOŁAZKA, MONIKA FINK-BOOTS, ELŻBIETA MALARCZYK, A. LEONOWICZ .....	393
Relationships between demethylase activity, formaldehyde and oxygen during incubation of <i>Rhodococcus erythropolis</i> with veratrate. MARZANNA PAŹDZIOCH-CZOCHRA, ELŻBIETA MALARCZYK .....	405
Comparative quantitative chromatographic determination of formaldehyde in different groups of physiological and pathological hard tissues of teeth. T. KATARZYNA RÓŻYŁO, R. SIEMBIDA .....	413
Are the reductions in nematode attack on plants treated with seaweed extracts the result of stimulation of the formaldehyde cycle? T. JENKINS, G. BLUNDEN, YUE WU, S. D. HANKINS, B. O. GABRIELSEN .....	421
Effect of l'-methylascorbigen on the resistance potential of plants to pathogens. GY. KÁTAY, E. TYIHÁK .....	429
Analogies and differences in the excited reactions of formaldehyde and D-glucose. L. TRÉZL, L. HULLÁN, T. SZARVAS, A. CSIBA, J. PIPEK .....	437
Microbial urea-formaldehyde degradation involves a new enzyme, methylenediurease. T. JAHNS, ROSWITHA SCHEPP, C. SIERSDORFER, H. KALTWASSER .....	449
Differential detection of N-heterocyclic compounds and their N-methylated derivatives by immunoanalysis. HONG M. LE, GYÖNGYVÉR HEGEDŰS, A. SZÉKÁCS .....	455
Urea-formaldehyde resins and free formaldehyde content. VIKTÓRIA VARGHA .....	463

## PREFACE

It is a pleasure for us to present the proceedings of the 4th International Conference (July 1-4, 1998, Budapest, Hungary) on the "Role of Formaldehyde in Biological Systems – Methylation and Demethylation Processes". The aim of this Conference was to provide a suitable environment for mutual understanding and discussion between scientists coming from various new fields of formaldehyde research.

Formaldehyde is "a two-face molecule". On the one hand, formaldehyde is a widely spread common, environmental pollutant. It has also been reported to be – under certain conditions – mutagenic and carcinogenic. On the other hand, formaldehyde is also a normal and indispensable component of different biological systems similar to hydrogen peroxide. These two small molecules are constantly produced intra- and extracellularly, and so there is a real possibility for their interaction in which excited, killing molecules can be liberated.

A number of rapid formaldehyde pathways in different tissues exist through labile hydroxymethyl groups linked to various acceptor molecules. It follows from these facts that all biological systems possess a formaldehyde-yielding potential which can originate from enzymatically controlled methylation and demethylation processes as well as from other uncontrolled biological oxidation processes, alike. More detailed knowledge of these fundamental biotransformation steps and their abnormalities will facilitate elucidation of certain perplexing phenomena.

It is our hope that these proceedings will give an up-to-date and representative view of the research being conducted in a wide range of fields, all of which is contributing to the understanding of functions of formaldehyde in biological systems.

On behalf of the Hungarian Biochemical Society Section for Environmental Biochemistry and the scientific and organizing committees of the Conference we would like to express our appreciation to Dr. Károly Elekes, editor of the *Acta Biologica Hungarica*, for his help throughout the preparations of the proceedings. Finally, the organizers of the Conference would like to gratefully acknowledge the financial support of different agencies and corporations.

MIHÁLY SZILÁGYI  
(Herceghalom)

ERNŐ TYIHÁK  
(Budapest)





## AN EVOLUTIONARY ROLE OF FORMALDEHYDE\*

M. P. KALAPOS

Theoretical Biology Research Group, Budapest, Hungary

(Received: 1998-10-28; accepted: 1998-11-25)

The evolution can be divided into three stages: chemical, prebiological and biological evolution. Most of the problems emerge when the development of cellular organization, the so-called prebiological evolution, is investigated. Here the possible evolutionary roles for formaldehyde as well as for the methylglyoxalase pathway are proposed. The theory, on the one hand, ascertains a pathway serving as an anaplerotic route for the reductive citric acid cycle of surface metabolists and using formaldehyde as raw molecule. On the other hand, an explanation for the glyoxalase enigma is offered hoping that in this way a long lasting mystery of almost nine decades biochemical research can be solved.

*Keywords:* Formaldehyde – methylglyoxal – glyoxalase – surface metabolism

### INTRODUCTION

There is an ubiquitous enzyme system, the so-called glyoxalase system, which is found in almost all the species and tissues investigated until now [11]. The glyoxalase system comprises two enzymes, glyoxalase I (E.C. 4.44.1.5., lactoylglutathione lyase) and glyoxalase II (E.C. 3.1.2.6., hydroxyacyl glutathione hydrolase), and consumes a catalytic amount of reduced glutathione [11]. The catalytic function of this enzyme system is to convert  $\alpha$ -oxoaldehydes into their corresponding  $\alpha$ -hydroxycarboxylic acid counterparts in two consecutive steps via the intermediate S-D-lactoylglutathione [11]. However, the problem is that the biological function of this enzyme system in biochemical machinery is still unknown. This biochemical puzzle has adhered several out of the brilliant biochemists of our century, without any need for fullness I mention here the names of Hopkins, Neuberg, Lohmann, Racker and Szent-Györgyi. Despite the endeavours the problem has as yet remained open. The most influential theories in this regard have been as follows: (i) participa-

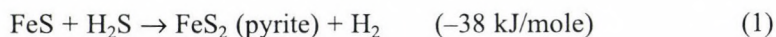
\* Presented at the 4th International Conference on the Role of Formaldehyde in Biological Systems, July 1-4, 1998, Budapest, Hungary.

Send offprint requests to: M. P. Kalapos, Theoretical Biology Research Group, H-1029 Budapest, Dámvad utca 18, Hungary.



tion in glycolysis, (ii) regulation of cell division (promine and retine) and (iii) detoxication of methylglyoxal. Nevertheless, either of those have proved to be able to give an acceptable answer to the long lasting problem emerged concerning the function of this pathway. The glycolysis operates through another pathway, through the three carbon-phosphates [9]. The role of glyoxalases in cell division regulation needs further experimental supports and the promine/retine theory that describes this regulation suffers from intramural contradictions [5, 7]. And the role of glyoxalase pathway in detoxication eventhough exactly describes a function for the glyoxalases, it does not give the reason of why it is of ubiquitous nature [1]. So here is the first starting point to our suggestion, namely, there is an enzyme system with widespread distribution and presence in all living organisms but without any obvious recognized function in the extant cells. That is we face with an enigma.

The second branch of the problems is related to the biochemical evolution. As far as it is known, Oparin was the first in the 1920s, who presented a trial on the emergence of cellular life [4]. The so-called primeval soup theory was thought at that time as to be an answer to how the organization of matter into living might have started [4]. I do not want to go into details in this regard since the literature on Oparin's theory is unaccountable. However, here it has to be stressed that one of the most crucial problems of the primeval soup theory is that the primeval ocean as a solution of organic compounds should have been very diluted retaining the probability of bumping of different molecules very low. To overcome this obstacle, in the 1980s Wachtershauser presented his surface metabolism concept by throwing out the primeval soup theory into the sink. The most important statements of surface metabolism theory are shown as follows: (i) flat refusal of the prebiological soup theory (Oparin's theory), (ii) organic compounds are enched to a charged surface, (iii) a chemoautotrophic system operates in which the source of energy for carbon fixation is the pyrite formation as depicted in the Equation (1)



(pH 7, T = 25 °C, 1 M H<sub>2</sub>S)

(iv) the reductive citric acid cycle is a nonenzymic archaic precursor cycle, (v) the constituents of the cycle coexist in an equilibrium with their thioanalogues and finally (vi) the anaplerotic route operates through one of the listed pathways: acetyl-coA pathway, glycine synthetase pathway or the oxalate route [8, 12].

From biochemical point of view it is obvious that small, simple molecules had been needed as prerequisites to any function for the ignition of the cycle. That is the anaplerotic route for the cycle is very critical. In this regard there are concerns. It has also to be noticed that there are several other critical remarks concerning the theory [2, 6]. But the discussion of those is out of the scope of the talk.

The third starting point is the well-known formose cycle. And with this cycle we have arrived at formaldehyde. Formaldehyde is one of the most abundant organic compounds in the intrastellar space and comets. It can also be produced in labora-

tories under so-called prebiotic conditions [10]. And it is a simple and reactive compound. Furthermore, through formose reaction it leads to the generation of a wide variety of carbohydrates, therefore, it is an ideal chemical to participate in the early stage of evolution.

## THE THEORY

**The theory** is that the early methylglyoxalase pathway functioning without any participation of enzymes was the link between the formose cycle and the reductive citric acid cycle of surface metabolists, thus providing a bridge between these cycles and a fuel for the archaic reductive citric acid cycle.

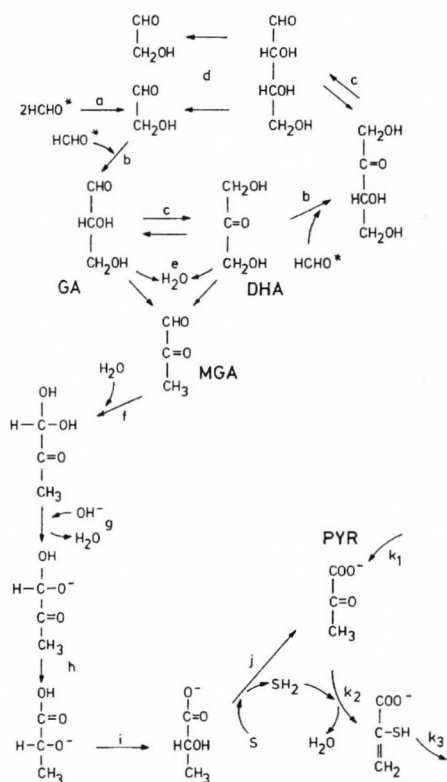


*Fig. 1.* Reactions that lead to pyruvate formation from formaldehyde a., self-condensation, b., aldol-condensation, c., carbonyl shift isomerization, d., aldol-retroaldol reaction, e., dehydration, f., hydration, g–i., suggested disproportionation of methylglyoxal to lactate in which reaction h. is slow while reaction i. is fast [3], j., oxidation linked to  $\text{H}_2\text{S}$  formation,  $k_{1-3}$ , reactions in the archaic reductive citric acid cycle as defined in the literature [12]. Asterisks indicate the molecules of formaldehyde that should be prebiotically synthesized in the surroundings. Abbreviations in the figure:  $\text{PYR}$  = pyruvate,  $\text{MGA}$  = methylglyoxal,  $\text{GA}$  = glyceraldehyde,  $\text{DHA}$  = dihydroxyacetone



The formose reaction is well known (Fig. 1). After the condensation of two molecules of formaldehyde glycolaldehyde is generated which enhances its own synthesis from formaldehyde. By using up two additional molecules of formaldehyde two molecules of glycolaldehyde are produced after one turn of the cycle.

Turn to methylglyoxal generation and its further conversion to lactate. If we look at the conversion of methylglyoxal into lactate it is immediately clear that the reaction itself is an intramolecular Cannizzaro reaction.

Follow the steps of the pathway (Fig. 1).

The first reaction is to lead to the formation of methylglyoxal from either glyceraldehyde or dihydroxyacetone. This dehydration reaction is an acid-base catalyzed reaction. So as an offshoot of the formose cycle methylglyoxal is generated.

In the second step the hydration of methylglyoxal takes place which is followed by an attack by a hydroxy group resulting in a giving down of one molecule of water.

The subsequent steps are not fully corroborated, but it seems that through the steps h and i (Fig. 1) lactate is resulted from the reaction pathway and hydride ion is transferred from one carbon to another one. Also a crucial point is the conversion of lactate into pyruvate. It should be mentioned that based on thermodynamical calculations, just like in the extant metabolism, lactate production is favoured over the production of pyruvate which means that the flow of matter is possible only in that case when there is a continuous consumption of pyruvate. This happens when the citric acid cycle works. That is the most simple regulation is seen here. The produced  $\text{SH}_2$  is used up in the cycle as a sulfur supply for the exchange of oxygen to sulfur [6].

To sum up, in my view the ubiquitous nature of glyoxalase pathway predicts an important role for this pathway in the evolution. This role according to my suggestion would have been to operate as an anaplerotic route for the reductive citric acid cycle of surface metabolists.

I have only taken you into my workshop without giving final answer to the questions and maybe in this way I have left you with more doubts than facts. But you should remember, it is a long way to arrive at the end of a scientific problem. And even the longest way starts with the first few steps. Perhaps this rule applies to glyoxalase research, too.

#### ACKNOWLEDGEMENT

This research was supported by the grant from the National Scientific Research Fund (OTKA), Budapest, Hungary (T 022914).

#### REFERENCES

1. Aronsson, A. C., Mannervik, B. (1977) Characterization of glyoxalase I purified from pig erythrocytes by affinity chromatography. *Biochem. J.* 165, 503–509.
2. De Duve, C., Miller, S. L. (1991) Two dimensional life? *Proc. Natl. Acad. Sci. USA* 88, 10014–10017.

3. Fedoronko, M., Königstein, J. (1971) Kinetik und Mechanismus der Disproportionierung von Methylglyoxal zu Milchsäure. *Collection Czechoslov. Chem. Commun.* 36, 3424–3430.
4. Haldane, J. B. S. (1967) The origin of life. In: Bernal, J. D. (ed.) *The Origin of Life*, William Clowes and Sons, Ltd., London and Beccles, pp. 242–249.
5. Kalapos, M. P. (1994) Methylglyoxal toxicity in mammals. *Toxicol. Lett.* 73, 3–24.
6. Kalapos, M. P. (1997) Possible evolutionary role of methylglyoxalase pathway: Anaplerotic route for reductive citric acid cycle of surface metabolists. *J. Theor. Biol.* 188, 201–206.
7. Kalapos, M. P. (1998) On the promine/retine theory of cell division. *Biochim. Biophys. Acta* 1426, 1–16.
8. Maden, B. E. H. (1995) No soup for starters? Autotrophy and origins of life. *Trends Biol. Sci.* 20, 337–341.
9. Meyerhof, O. (1948) New investigations of enzymatic glycolysis and phosphorylation. *Experientia* 4, 169–176.
10. Miller, S. L. (1987) Which organic compounds could have occurred on the prebiotic Earth? *Cold Spring Harbor Symp. Quant. Biol.* 52, 17–26.
11. Vander Jagt, D. L. (1989) The glyoxalase system. In: Dolphin, D., Poulson, R., Avramovic, O. (eds) *Glutathione: Chemical, Biochemical and Medical Aspects. Part A*. John Wiley and Sons, Inc. New York, pp. 597–641.
12. Wachtershauser, G. (1990) Evolution of the first metabolic cycles. *Proc. Natl. Acad. Sci. USA* 87, 200–204.





## RELATED $\alpha$ N- AND $\epsilon$ N-METHYLTRANSFERASES METHYLATE THE LARGE AND SMALL SUBUNITS OF RUBISCO\*

Z. YING<sup>a,1</sup>, R. M. MULLIGAN<sup>b</sup>, N. JANNEY<sup>a,2</sup>, M. ROYER<sup>a</sup> and R. L. HOUTZ<sup>a,3</sup>

<sup>a</sup>Plant Physiology/Biochemistry/Molecular Biology Program, Department of Horticulture & Landscape Architecture, University of Kentucky, Lexington, USA

<sup>b</sup>Department of Developmental and Cell Biology, University of California, Irvine, USA

(Received: 1998-10-28; accepted: 1998-11-25)

Ribulose-1,5-bisphosphate carboxylase/oxygenase (Rubisco) is methylated at the  $\alpha$  amino position of the N-terminal methionyl residue of the processed and assembled form of the small subunit (SS), and is also methylated in some species at the  $\epsilon$ -amino group of lysine-14 in the large subunit (LS). The gene (*rbcMT-S*) and cDNAs for the SS  $\alpha$ N-methyltransferase (SSMT) from spinach (*Spinach oleracea*) have been cloned, sequenced, and expressed. The gene is closely related to a previously characterized LS methyltransferase (Rubisco LSMT) cDNA from pea (Rubisco LSMT) and a Rubisco LSMT gene from tobacco. Sequence analysis of the cDNA and transcript mapping experiments demonstrate that the *rbcMT-S* pre-mRNAs experience alternative 3' splice site selection, such that mRNAs for a long form with a four amino acid insertion and a short form are expressed at approximately equal abundance. The coding sequence of spinach SSMT includes a putative targeting presequence with sequence identity at a plastid processing site. A N-terminal truncated form of spinach SSMT was expressed and purified from *E. coli* cells. Both long and short forms of the cDNAs were shown to catalyze methylation of the  $\alpha$  amine of the N-terminal methionine of the SS of Rubisco.

**Keywords:** Rubisco – protein methylation – trimethyllysine – N-methylmethionine – N-methyltransferases

### INTRODUCTION

Ribulose-1,5-bisphosphate carboxylase/oxygenase (Rubisco) experiences several types of post-translational modifications during the expression, import and assembly of the protein. The large subunit (LS) is encoded by a plastid gene, and the mature form of the spinach LS is processed by removal of the N-terminal Met-1 and Ser-2

\* Presented at the 4th International Conference on the Role of Formaldehyde in Biological Systems, July 1-4, 1998. Budapest, Hungary.

<sup>1</sup>Current address: Tropical Research and Education Center, University of Florida/IFAS, 18905 SW 280th St., Homestead, FL 33031.

<sup>2</sup>Current address: GenApps Inc., A169 ASTeCC Building, University of Kentucky, Lexington, KY 40506.

Send offprint requests to: Dr. Robert L. Houtz, Dept of Horticulture & Landscape Architecture, N318 Agriculture Science North, University of Kentucky, Lexington KY 40546-0091 USA; rhoutz@ca.uky.edu (email).



residues and acetylation of Pro-3 [7, 15]. In addition, the LS from many species contains a trimethyllysyl residue at Lys-14 [5, 6, 7]. The small subunit of Rubisco (SS) is also post-translationally modified. The polypeptide is post-translationally imported into chloroplasts and processed by a stromal processing peptidase which removes the targeting presequence. The resultant N-terminal methionine residue of the processed SS is subjected to  $^{\alpha}$ N-methylation [4] prior to assembly with the LS into the holoenzyme.

The methylation of Lys-14 in the LS is catalyzed by S-adenosyl-L-methionine (AdoMet):Rubisco LS (lysine)  $^{\epsilon}$ N-methyltransferase (Rubisco LSMT, Protein Methylase III, EC 2.1.1.127) [10]. Rubisco LSMT genes, cDNAs and polypeptides have been characterized from pea and tobacco [10, 24]. Lys-14 methylation has been detected in many plant species (pea, tobacco, tomato, soybean, cucumber, petunia, pepper, and cowpea), but in some species (spinach, wheat, and corn) the methylation does not occur [5, 7].

The observation that LS polypeptides from some species are methylated at Lys-14, while methylation is not detectable in other species such as spinach is a curious observation. Several proteins contain trimethyllysyl residues such as cytochrome c, calmodulin, and histones, and the protein-specific  $^{\epsilon}$ N-methyltransferases for these proteins have been described; however, there has not been an explanation for the existence of identical proteins in a nonmethylated state.

In this study we report a homologue of Rubisco LSMT from spinach that encodes an enzyme that methylates the SS of Rubisco (Rubisco SSMT). This is the first reported eukaryotic  $^{\alpha}$ N-methyltransferase. In addition, recombinant tobacco Rubisco LSMT expressed in *E. coli*, and both recombinant and purified pea Rubisco SSMT, also catalyzed the methylation of the  $\alpha$  amino group of the processed form of the SS. Thus, the  $^{\alpha}$ N- and  $^{\epsilon}$ N-methyltransferases which methylate the LS and SS of Rubisco are related and in some cases identical enzymes.

## MATERIALS AND METHODS

Spinach (*Spinacea oleracea* L. cv. Melody) plants were cultured in ProMix<sup>TM</sup> soil media in a greenhouse at approximately 20 °C with a natural light photoperiod during the winter season (Lexington, Kentucky).

Two *rbcMT-S* cDNAs were obtained by RT-PCR and RACE. For RT-PCR, 5  $\mu$ g of total RNA isolated from spinach leaves using Trizol (GIBCO/BRL) was reverse-transcribed with an oligo d(T)<sub>17</sub> primer. The resulting first-strand cDNA product was amplified by PCR with *Taq* polymerase (GIBCO/BRL) using degenerate oligonucleotide primers (Fig. 1) corresponding to conserved peptide sequences between pea [10] and tobacco [24] Rubisco LSMTs. The PCR product was cloned into Bluescript II KS(+) vector (Stratagene) for sequencing.

For 5' RACE, reverse-transcription was the same as described above and was followed by poly d(C)-tailing as described in [23]. The PCR products were digested with *SacI* and *XbaI*, gel-purified and cloned into Bluescript II KS(+) vector for

sequencing. Two different clones were identified: S-40' has a 12-bp auxiliary exon (auxon) and S-38' lacks the auxon.

For 3' RACE, 5 µg of total RNA from spinach leaves was reverse-transcribed with an adapter-primer (AP-1, 5' GGC CAC GCG TCG ACT AGT ACT (T)<sub>16</sub>). Amplification was performed by PCR as described above with oligonucleotide AP-1 and a spinach specific primer (SF-9). The PCR product was cloned into pCR-Scrip Direct SK(+) vector (Stratagene) for sequencing.

Both strands of each clone were sequenced by the dideoxy chain termination method [18] using Sequenase (US Biochemical) and <sup>35</sup>S-dATP (NEN) with M13 reverse and S-40 primers.

Both full-length S-38 and S-40 cDNAs (GenBank accession #'s AF071544 and AF071545, respectively) were obtained by ligation of clones S2' and S25' to S-38' and S-40', accordingly, based on restriction sites within the overlapped regions. N-terminally truncated forms of S-38 and S-40 were obtained by PCR with primers designed to remove the first 43 amino acids and replace Cys-44 with Met. Both full length and N-terminally truncated forms of S-38 and S-40 were cloned into pET-23d for expression in pLysS cells.

The *rbcsMT-S* gene (GenBank accession #AF071543) was cloned by PCR. Spinach nuclear DNA was isolated using Floraclean (Bio101, Inc.), and 100 ng amplified by PCR with *Taq* polymerase (GIBCO/BRL). The PCR product was cloned into pCR-Script SK(+) for sequencing.

For DNA gel blot analysis, spinach nuclear DNA was digested with *Eco*RI or *Sca*I, electrophoresed on a 0.7% agarose gel and transferred onto nylon membranes (MSI) [17]. The DNA blot was hybridized with the cDNA probe I (*Sf*/I fragment, 1056-bp) labeled with digoxigenin-UTP according to the procedure provided by the manufacturer (Boehringer Mannheim).

Clone pS40XR0.4 was transcribed with T3 RNA polymerase in the presence of <sup>32</sup>P-rATP (800 Ci/mMol) to produce a radiolabeled antisense transcript (Fig. 3A). The radioactive probe (~100,000 cpm) was precipitated with 5 µg of tRNA and 0, 2.5, 10, or 20 µg of total RNA isolated from mature spinach leaves. After hybridization the RNA duplexes were digested by addition of 200 units of RNase T1 (Boehringer Mannheim) and 250 ng RNase A (Sigma). The protected RNA fragments were dissolved, denatured, and electrophoresed on 6% polyacrylamide gels with 8 M urea. Gels were dried and analyzed by autoradiography.

Individual clones (S-40 and S-38, both full-length and N-terminally truncated in pET-23d expression vector) were cultured in pLysS host cells. After induction with 0.5 mM IPTG, cells were collected by centrifugation, washed twice with deionized water, resuspended in 100 ml of buffer A (50 mM TRIS-K<sup>+</sup>, pH 8.2, 5 mM MgCl<sub>2</sub>, 1 mM EDTA, 1 mM PMSF, and 10 µg/ml leupeptin) and frozen at -80 °C. The activity of Rubisco LSMT was determined in the thawed cell lysates as described previously [22]. Rubisco SSMT activity was determined by incubation of pLysS cell lysates, or purified S-38 and S-40, with lysates from spinach chloroplasts isolated according to [14]. Reactions contained 5 ml to 10 ml of [<sup>3</sup>H-methyl]AdoMet (70–80 Ci/mmol), 10 µg to 20 µg of chloroplast lysate protein, and either 10 µg of protein



from pLysS cell lysates or 1 µg of purified S-38 or S-40 protein. Reactions were terminated by addition of SDS-PAGE sample preparation buffer, electrophoresed on 15% acrylamide gels, and after transfer to a PVDF membrane, radioactivity visualized using a <sup>3</sup>H phosphor-imager screen (Molecular Dynamics Model 425, Sunnyvale, CA).

## RESULTS

LSMT-specific primers were designed to highly conserved sequences of pea and tobacco Rubisco LSMT and were used to amplify a 786-bp fragment from first-strand cDNAs. The remaining 5' and 3' end sequences of the spinach cDNA were obtained by 5' and 3' RACE to complete the coding sequence [3].

Amplification of 5' coding sequences resulted in the identification of two 5' RACE products (836-bp and 848-bp fragments). The 848 bp product (designated as S-40') had a 12-bp insertion relative to the 836 bp fragment (designated as S-38'). The 5' RACE products (S-38', S-40') and the initial PCR product amplified with LSMT specific primers (S-25') had complete sequence identity in the regions that overlapped, except for the 12-bp insertion in S-40' (Fig. 1).

Amplification of 3' coding sequence was performed by RACE using an adapter-primer (AP-1) for first-strand cDNA synthesis and also as a reverse primer, and SF-9 as the *rbcMT-S*-specific primer for PCR amplification, and a single 761-bp PCR product was obtained. Sequence analysis confirmed the identity of the 3' RACE product as encoding the predicted 3' portion of the *rbcMT-S* protein including the 3' untranslated region. Two cDNA sequences (S-40 and S-38) were assembled from these overlapping clones.

Both *rbcMT-S* cDNAs encode polypeptides of 495-aa (S-40) and 491-aa (S-38) with predicted molecular masses of 55.5 kD and 55.0 kD, respectively, similar to the masses of pea (55.0 kD) and tobacco (56.0 kD) Rubisco LSMT (Fig. 1). In addition, the deduced amino acid sequence includes five imperfect copies of a leucine-rich repeat (LRR), similar to pea and tobacco LSMT (Fig. 1) [11]. The deduced amino acid sequence from the *rbcMT-S* cDNAs shows 60% and 62% identity with the amino acid sequences of pea and tobacco Rubisco LSMT, respectively.

A 3.1 kb genomic clone that included the entire coding region of the *rbcMT-S* gene was obtained and sequenced (see GenBank accession #AF071543). Comparison of the genomic DNA with the cDNA sequences allowed the precise location of the six exons and five introns. The 12-bp insertion in the *rbcMT-S* S-40 cDNA corresponds to the 3' 12 nt of intron III (Fig. 2). Examination of the DNA sequence of this intron and flanking regions suggested that either of two 3' splice sites (separated by the 12-bp sequence) could be utilized during splicing of the *rbcMT-S* transcripts. Thus, as illustrated in Fig. 2, when the intron III sequence is completely removed, a S-38 mRNA encoding a 55.0 kD polypeptide is produced. However, if splicing occurs at the alternative site, a S-40 mRNA that retains a 12-nt portion of the 3' end of intron

Spinach40	MATLFTLIPS-SMSTFLNPFKTTQHSKLHFATPSPTFNPLSIRCFRPPETDTPPEIQKFWG	62
Spinach38	MATLFTLIPS-SMSTFLNPFKTTQHSKLHFATPSPTFNPLSIRCFRPPETDTPPEIQKFWG	62
Pea	MATIFSGG---SVSPFLFHTNKGTSFTPKAPILHLKRSFSAKSVASVGTPELSLPAVQTFWK	60
Tobacco	MASVFSVHPLPSSSFLCLKTKSRTHKHQTFYTYQKILINSLOLQTELDPKIPQVQTFWK	63
Spinach40	LSDKGIISPKCPVKPGIVPEGLGLVAQKDISRNEVLEVPQKFWINPDVAAEISGVCNGLK	125
Spinach38	LSDKGIISPKCPVKPGIVPEGLGLVAQKDISRNEVLEVPQKFWINPDVAAEISGVCNGLK	125
Pea	LQEEGVITAKTPVKASVVTPEGLGLVAKDISRNDVLOVPKRLWINPDVAAEISGRVCELK	123
Tobacco	LCKEGVTTKTPVKPGIVPEGLGLVAKRDIAGKETVLOVPKRLWINPDVAAEISGVNCSGLK	126
Spinach40	PWVSVALFLMRKKLGNSSSWKPYIDILPDSTMTIYWESEELSELQGSQLLNTLIGVKELVA	188
Spinach40	PWVSVALFLMRKKLGNSSSWKPYIDILPDSTMTIYWESEELSELQGSQLLNTLIGVKELVA	188
Pea	PWLSVILFLIRER-SREDSVMKHFGILPQRTOSTIYWESEELQELQGSQLLKTTVSKEYVK	185
Tobacco	PWISVALFLLREK-WRDDSKWKYIMDVLPKSTOSTIYWESEELSEIGTQLLSTMTSVKDYQ	188
Spinach40	NEFAKLEEVLPVHKQLFPFDVTQDDFWAFGMLRSRAFTCLEGQSLVLIPLADLVVQQAHS	251
Spinach38	NEFAKLEEVLPVHKQLFPFDVTQDDFWAFGMLRSRAFTCLEGQSLVLIPLADLVVQQAHS	247
Pea	NECLKLQSIILPNKRLPDPVTLQDDFWAFGILRSRAFSRLRNENLVVPMADL----INHS	244
Tobacco	NEFQKVEEVILANKQLFPFPITLQDDFWAFGILRSRAFSRLRNQNLTVPFADL----TNHN	247
Spinach40	PDITAPKYAMEIRG-AGLFSRELVSRLNPTPVKAGDOVLIOYDLMKSNALALDYGLTESRS	313
Spinach38	PDITAPKYAMEIRG-AGLFSRELVSRLNPTPVKAGDOVLIOYDLMKSNALALDYGLTESRS	209
Pea	AGVTTEHAYEVKGAAGLFSMDYLFSLKSPSVKAGEQVYIOYDLMKSNALALDYGIEPME	307
Tobacco	ARVTTEHAYEVKGAAGLFSMDLFLSLRSLKLAGDQLFIQYDLMKSNADMALDYGIEPSS	310
Spinach40	ERNAYTLTLEIPESDSFYGDKLDIAESNGMESAYFDIVLEQPLPAMHLPYLRLVALGGEDVF	376
Spinach38	ERNAYTLTLEIPESDSFYGDKLDIAESNGMESAYFDIVLEQPLPAMHLPYLRLVALGGEDVF	372
Pea	NRHAYTLTLEISESDPFDDKLDVAESNGFAQTAYFDIFYMTLPPGLLPYLRLVALGGTDAF	370
Tobacco	ARDAFTLTLEISESDEFYGDKLDIAETNGIGETAYFDIKIGQSLPPTMIPYLRLVALGGTDAF	373
Spinach40	LLLESIFRNSINGHLDLPISPANEEELICQVIRDACTSALSGYSTTIAEDEKLLAEGDIDPRLEI	439
Spinach38	LLLESIFRNSINGHLDLPISPANEEELICQVIRDACTSALSGYSTTIAEDEKLLAEGDIDPRLEI	435
Tobacco	LLLESIFRNSVNGHLGLPVSRAMEELICKVVRDACKSALSGYHTTIEDEKLMEEGWLSTRLOI	436
Pea	LLLESIFRDTINGHLVSRDNEELCKAVREACKSALAGYHTTIEQDEL-KEGNLDSRLAI	432
Spinach40	AITIRLGEKRVLQDIDEEFKEREMELGGYEYQERRKDLGLAGEQGEKLPWIGEV	495
Spinach38	AITIRLGEKRVLQDIDEEFKEREMELGGYEYQERRKDLGLAGEQGEKLPWIGEV	491
Pea	AVGIRGEKRVLQDIDGIEQKELDLQLEYEQERRKDLGLAGEQGEKLPWIGEV	489
Tobacco	AVGIRLGEKRVLQDIDDFRERELDELEYEQERRKDLGLAGEQGEKLPWIEPK	491

Fig. 1. Comparison of the deduced amino acid sequences of S-38 and S-40, with tobacco and pea Rubisco LSMTs. Identical residues are indicated by vertical lines and similar residues by dots. Gaps introduced to maximize alignment are indicated by dashes. Leucine-rich repeat-like motifs are underlined. The four amino acid sequence, WVQQ, deduced from the 12-nt auxon is shown in bold italic letters. The conserved peptide sequences, from which the primers are derived to clone the *rbcMT-S*, are indicated by arrows

III is generated, and subsequently a 4-amino acid longer polypeptide of 55.5 kD is produced.

Since DNA gel blot analysis revealed that the *rbcMT-S* is a single copy gene (data not shown) RNase protection studies were performed to analyze the relative expression of the S-38 and S-40 mRNAs in spinach leaves. The results revealed that S-40 and S-38 mRNAs were present in approximately equal abundance (Fig. 3). Control reactions that omitted spinach leaf RNA (lane 2) or substituted a heterologous RNA (maize mitochondrial, lane 6) failed to protect any RNA fragments. Thus, two tran-



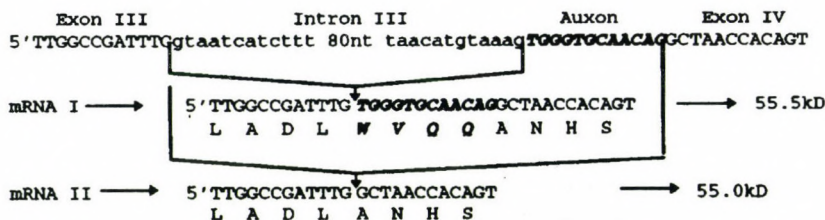


Fig. 2. Alternative splicing of intron III of *rbcMT-S* mRNA. The top portion shows the sequence of intron III and flanking regions. Shown below are the two types of mRNAs (S-40 and S-38) produced by alternative splicing. When the second 3' splice site is utilized, the 12-nt auxon is retained to produce S-40 mRNA (center), which encodes a 55.5 kD polypeptide. If the first 3' splice site is utilized, the auxon is absent and S-38 mRNA is produced (bottom), which encodes a 55.0 kD polypeptide

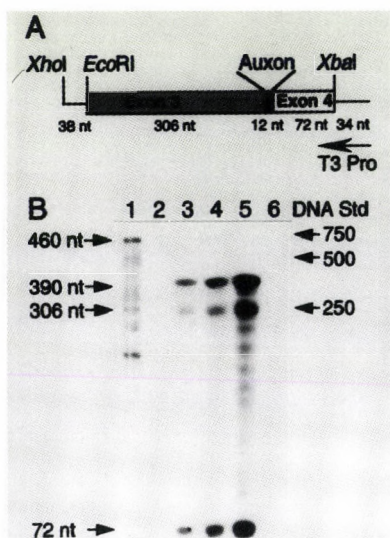


Fig. 3. Two forms of *rbcMT-S* mRNAs are produced as a result of alternative splice site selection. (A) pS40XR0.4 was produced by cloning the 390 nucleotide EcoRI/XbaI fragment of the S-40 cDNA into pBluescript SK+. The clone spans exon III, the auxon, and exon IV. A 460 nucleotide antisense probe was produced by transcription from the T3 promoter to the XhoI site. The long form of the mRNA protects a 390 nucleotide fragment of the probe, and the short form of the mRNA protects a 306 and a 72 nucleotide fragment. (B) RNase protection was performed to demonstrate the relative abundance of the long and short forms of *rbcMT-S*. The 460 nucleotide antisense probe (lane 1) was annealed to 0, 2.5, 10, or 20 µg of total RNA from mature spinach leaves (lanes 2, 3, 4, and 5) and digested with RNase A and RNase T1. The 390 nucleotide fragment is protected by the long form of *rbcMT-S* and the 306 and 72 nucleotide fragments are protected by the short form of *rbcMT-S*. The intensities of the 390 and 306 nucleotide fragments are similar, indicating that the long and short forms are approximately equivalent in abundance. Omission of spinach RNA (lane 2) or the substitution of a heterologous RNA (maize mitochondrial RNA, lane 6) resulted in complete sensitivity of the probe to RNase. The migration of a radio-labeled DNA size ladder (250 bp ladder, Gibco/BRL) is shown on the right margin

scripts of a single *rbcMT-S* gene are expressed in spinach leaves that differ by a 12 bp insertion as a result of 3' alternative splice site selection.

Examination of the N-terminal sequence of S-38 and S-40 identified a putative chloroplast processing site from Ser-41 to Cys-44 (Ser-Ile-ArgCys), with exact identity to the chloroplast processing site for spinach nitrate reductase [1]. The putative chloroplast targeting presequence was removed, and expression of N-terminally truncated forms of spinach S-38 and S-40 resulted in the synthesis of large amounts of protein in inclusion bodies. This form was easily collected and purified, and could be denatured in 6 M urea and refolded to a soluble form after exhaustive dialysis. Polyclonal antibodies were prepared against purified N-terminally truncated S-38 and used to detect translation products from S-38 and S-40 transcripts. A single immunoreactive polypeptide was detected in spinach chloroplast lysates, at a similar molecular mass to the N-terminally truncated form of S-38 (~50.6 kD, Fig. 4).

The presence of chloroplast-localized translation products for S-38 and S-40 with homology to both pea and tobacco Rubisco LSMT suggested that these proteins may have a different, but related type of methyltransferase activity. A recent report of a-methylation of the N-terminus of the processed form of the SS of Rubisco [4] lead us to examine the possibility that the S-38 and S-40 cDNAs coded for an  $\alpha$ N-methyltransferase for the SS of spinach Rubisco. Cell lysates from bacterial expression of N-terminally truncated S-38 and S-40 constructs were assayed for methyltransferase

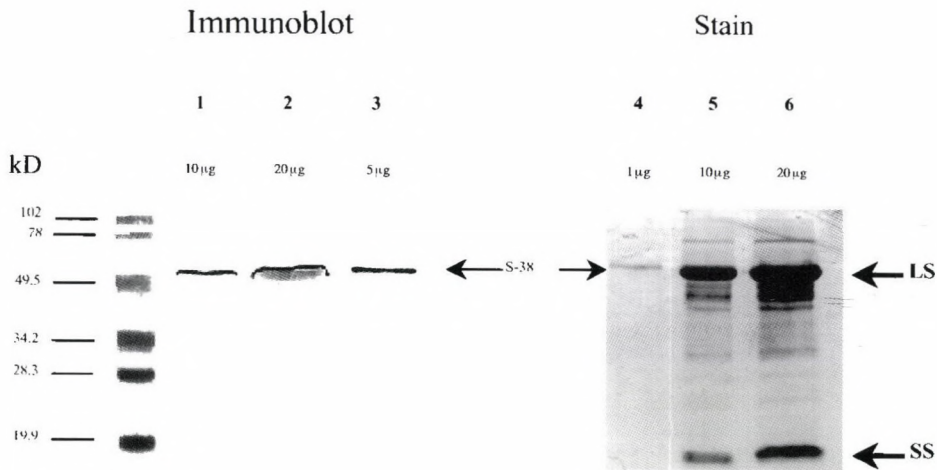
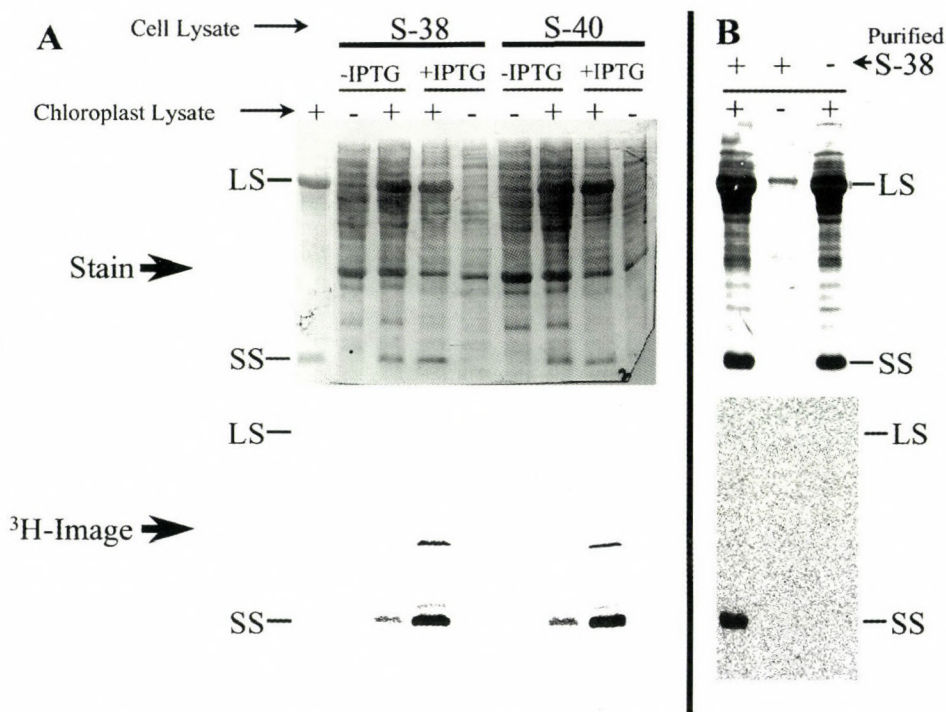


Fig. 4. Immunodetection of translation products from *rbcMT-S* in spinach chloroplasts. Isolated intact chloroplasts from spinach leaves were lysed and the stromal fraction loaded on SDS-PAGE (15% acrylamide) gels. After electrophoresis, proteins were electrophoretically transferred to PVDF membranes and either stained for several minutes with Coomassie Brilliant Blue R-250 (Stain), or developed with antibodies prepared against purified S-38 protein (Immunoblot). Lanes 1, 2, 5, and 6 are chloroplast lysates with total protein loads as indicated above the lanes. Lanes 3 and 4 are purified S-38 protein at the indicated levels. LS and SS identify the large and small subunits of spinach Rubisco, respectively





**Fig. 5.** S-38 and S-40 expression-dependent incorporation of  $^3\text{H}$ -radiolabel from [ $^3\text{H}$ -methyl]AdoMet into the small subunit of Rubisco in spinach chloroplast lysates. (A) Lysates (~15 mg total protein) from induced (+IPTG) and non-induced (-IPTG) pLysS cells harboring S-38 or S-40 cDNAs cloned into pET21d expression vector were incubated in the presence and absence of spinach chloroplast lysates (~12  $\mu\text{g}$  total protein) and [ $^3\text{H}$ -methyl]AdoMet (1.8 mM, 70–80 Ci/mmol). After incubation at 30 °C for 30 min, samples were electrophoresed on 15% SDS-PAGE gels, and electrophoretically transferred to PVDF membranes. The PVDF membranes were briefly stained with Coomassie Brilliant Blue R-250, then destained with 100% methanol, washed with  $\text{dH}_2\text{O}$ , and imaged for radioactivity. LS and SS refer to the locations of the large and small subunits of Rubisco, respectively. (B) Purified S-38 (~2  $\mu\text{g}$ ) was incubated in the presence and absence of spinach chloroplast lysates (~18  $\mu\text{g}$  total protein) and [ $^3\text{H}$ -methyl]AdoMet (1.8 mM, 70–80 Ci/mmol) for 30 min at 30 °C. After electrophoresis and transfer, the PVDF membrane was stained and imaged as described above.

activity with spinach chloroplast lysates as a proteinaceous substrate. Tritium radiolabel incorporation from [ $^3\text{H}$ -methyl]AdoMet into spinach chloroplast polypeptides was assessed by SDS-PAGE, electrophoretic transfer to PVDF membranes, and phosphor image analysis. Incorporation of radiolabel was detected into a region corresponding to the SS of Rubisco (Fig. 5A), which was dependent on the addition of chloroplast lysates and induced by IPTG. Both S-38 and S-40 were capable of catalyzing methylation of the SS (Fig. 5A). Highly purified S-38 obtained from inclusion bodies and refolded as a soluble protein was shown to exclusively catalyze

transfer of radiolabel into the region corresponding to the SS of Rubisco (Fig. 5B). Similar results were obtained with purified S-40. These results suggest that a small pool of free SSs exists in the stromal fraction from spinach chloroplasts as has been previously demonstrated in chloroplasts from *Chlamydomonas* [19] and peas [8].

Unequivocal demonstration that purified recombinant S-38 catalyzed SS methylation at the N-terminal Met of processed SS was documented by Edman degradation of the SS with simultaneous determination of radioactivity. During the first cycle of Edman degradative sequencing, 92% of the radiolabel incorporated into the small subunit region of the PVDF blot was released (Fig. 6). The amino acid residue in this cycle did not correspond to any of the standard amino acids, but migrated as an

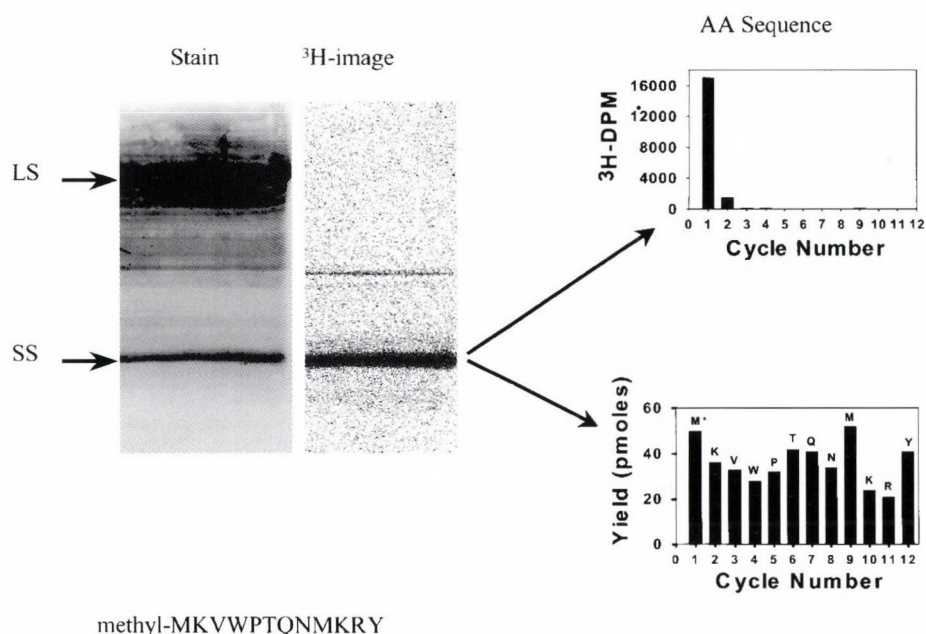


Fig. 6. Radiosequencing of the spinach Rubisco SS. A spinach chloroplast lysate containing 100  $\mu$ g of total protein was incubated with purified S-38 protein (10  $\mu$ g) and [ $^3$ H-methyl]AdoMet (1.8 mM, 70–80 Ci/mmol) for 30 min at 30  $^{\circ}$ C. The sample was electrophoresed on a 15% SDS-PAGE gel, and proteins electrophoretically transferred to a PVDF membrane. The PVDF membrane was briefly stained with Coomassie Brilliant Blue R-250, then imaged for radioactivity, and the protein band at the position of the SS of Rubisco subjected to Edman degradative sequencing. During each cycle of sequencing a portion of the PTH-derivatized amino acid pool was diverted prior to separation by HPLC for determination of radioactivity. Amino acid residues identified are indicated, all other residues were <5 pmoles. LS and SS refer to the locations of the large and small subunits of Rubisco, respectively. The sequence obtained, identified at the bottom of the figure, is identical with the sequence reported for the SS of spinach Rubisco beginning with the second lysyl residue [13]. The first residue released during sequencing, identified as a modified Met residue (indicated by an asterix in the sequence bar graph) migrates slightly behind N'-diphenylurea (DPU), and is consistent with the sequence and recently reported mass spectroscopy identification of methyl-N-methionine as the N-terminal residue of the SS of spinach Rubisco [4]



unknown with a retention time just slightly greater than DPU, similar to that reported for methylated Met in other work [4]. The next 11 amino acid residues corresponded exactly to the known N-terminal residues of the SS of spinach Rubisco [13]. Given that a thorough chemical and physical structural analysis of the N-terminal residue of the SS of spinach Rubisco has already identified this residue as N-methylmethionine, the results presented here demonstrate that the two gene products from the *rbcMT-S* gene code for enzymes capable of methylating the N-terminal Met residue of the processed form of the small subunit of Rubisco. We propose that these enzymes be referred to as Rubisco small subunit  $\alpha$ N-methyltransferase or Rubisco SSMT.

## DISCUSSION

A spinach gene responsible for  $\alpha$ -methylation of the N-terminal methionine residue of the processed form of the SS of Rubisco has been cloned, expressed, and assayed. The spinach enzyme specifically methylates the SS of Rubisco, but shows a high degree of homology to a previously characterized tobacco gene and pea cDNA. The *rbcMT-S* gene is present as a single copy in the spinach genome, and two splice forms of the mRNA are detected by PCR and by RNase protection.

A single immunoreactive polypeptide localized in the chloroplast was detected with polyclonal antibodies to S-38. The small mass difference between the protein forms of S-38 and S-40 precludes determination of whether or not both of these proteins are present *in vivo*. Both S-38 and S-40 have identical SS methyltransferase activity.

Methylation of the SS of spinach Rubisco was initially characterized as stoichiometric and specific for the SS only at low concentrations of AdoMet [2], and methylation of the N-terminal Met of the SS was recently confirmed by protein sequence analysis [4]. Methylation of the SS of Rubisco is apparently widespread since N-methyl-Met was detected as the N-terminal residue in the SS of Rubisco from pea, corn, and barley [4]. We have also detected N-methyl-Met as the N-terminal residue in the SS of tobacco Rubisco (data not shown). In addition, an enzymatic assay demonstrated that chloroplast lysates catalyzed methylation of bacterially expressed SS using AdoMet as a methyl donor [4]. The expression of a spinach gene with homology to known protein  $\epsilon$ N-methyltransferases (Rubisco LSMT from pea and tobacco) was initially anomalous, given that Lys-14 in the LS of spinach Rubisco is not methylated. Additionally, the gene and coding sequences reported for pea and tobacco Rubisco LSMT do not contain substantial homology with any reported nucleotide or amino acid sequences, including those of other protein, DNA, and small metabolite methyltransferases. Thus, methylation of Rubisco SS in spinach is catalyzed by a homologue of a bifunctional methyltransferase in pea that methylates both LS and SS. The functional significance of this post-translational modification is obscure however, and has only been speculated to be involved in processes as diverse as protection against proteolytic degradation [9, 16, 20], proper cellular localization

of proteins, and/or assembly of macromolecular structures [21]. Protection against proteolytic degradation is a possible function since the stroma of pea chloroplasts contains at least three aminopeptidases, one of which has specificity for Met residues [12].

The identification of a homologue of pea and tobacco LSMT in spinach was initially confounding because the enzyme had no obvious function. Structural analyses of the methylation status of Lys-14 in the LS of spinach Rubisco have unequivocally established this residue as unmodified [5, 15], and spinach Rubisco is an excellent *in vitro* substrate for pea Rubisco LSMT [6, 22]. Additional studies in our laboratory have demonstrated that the absence of methylation at Lys-14 in the LS of spinach Rubisco is consistent throughout the development of spinach plants, and is not influenced by several environmental stresses (unpublished data). Our original interest was in defining the molecular basis for this dichotomy and to determine in spinach whether or not genes exist which are related to the already identified protein  $\epsilon$ N-methyltransferase, responsible for formation of trimethyllysyl residues in the LS of Rubisco. The unique nature and interrelatedness of these amino acid and nucleotide sequences suggests that the protein  $\alpha$ N- and  $\epsilon$ N-methyltransferase described here may represent a new family of protein methyltransferases.

#### REFERENCES

1. Back, E., Burkhart, W., Moyer, M., Privalle, L., Rothstein, S. (1988) Isolation of cDNA clones coding for spinach nitrite reductase: Complete sequence and nitrate induction. *Mol. Gen. Genet.* 212, 20–26.
2. Black, M. T., Meyer, D., Widger, W. R., Cramer, W. A. (1987) Light-regulated methylation of chloroplast proteins. *J. Biol. Chem.* 262, 9803–9807.
3. Frohman, M. A. (1990) RACE: rapid amplification of cDNA ends. In: Innis, M. A., Gelfand, D. H., Sninsky, J. J., White, T. J. (eds) *PCR Protocols: A Guide to Methods and Applications*, Academic Press, San Diego, pp. 28–38.
4. Grimm, R., Grimm, M., Eckerskorn, C., Pohlmeier, K., Rohl, T., Soll, J. (1997) Postimport methylation of the small subunit of ribulose-1,5-bisphosphate carboxylase in chloroplasts. *FEBS Letters* 408, 350–354.
5. Houtz, R. L., Poneleit, L., Jones, S. M., Royer, M., Stults, J. T. (1992) Post-translational modifications in the amino-terminal region of the large subunit of ribulose-1,5-bisphosphate carboxylase/oxygenase from several plant species. *Plant Physiol.* 98, 1170–1174.
6. Houtz, R. L., Royer, M., Salvucci, M. E. (1991) Partial purification and characterization of ribulose-1,5-bisphosphate carboxylase/oxygenase large subunit  $\epsilon$ N-methyltransferase. *Plant Physiol.* 97, 913–920.
7. Houtz, R. L., Stults, J. T., Mulligan, R. M., Tolbert, N. E. (1989) Post-translational modifications in the large subunit of ribulose bisphosphate carboxylase/oxygenase. *Proc. Natl. Acad. Sci. USA* 86, 1855–1859.
8. Hubbs, A., Roy, H. (1992) Synthesis and assembly of large subunits into ribulose bisphosphate carboxylase/oxygenase in chloroplast extracts. *Plant Physiol.* 100, 272–283.
9. Keeling, P. J., Doolittle, W. F. (1996) Methionine aminopeptidase-1: The MAP of the mitochondrion? *Trends Biochem. Sci.* 21, 285–286.
10. Klein, R. R., Houtz, R. L. (1995) Cloning and developmental expression of pea ribulose-1,5-bisphosphate carboxylase/oxygenase large subunit N-methyltransferase. *Plant Mol. Biol.* 27, 249–261.



11. Kobe, B., Deisenhofer, J. (1994) The leucine-rich repeat: A versatile binding motif. *Trends Biochem. Sci.* 19, 415–421.
12. Liu, Z.-Q., Jagendorf, A. T. (1986) Neutral peptidases in the stroma of pea chloroplasts. *Plant Physiol.* 81, 603–608.
13. Martin, W., Mustafa, A.-Z., Henze, K., Schnarrenberger, C. (1996) Higher-plant chloroplast and cytosolic fructose-1,6-bisphosphatase isoenzyme: Origins via duplication rather than prokaryote-eukaryote divergence. *Plant Mol. Biol.* 32, 485–491.
14. Mills, W. R., Joy, K. W. (1980) A rapid method for isolation of purified, physiologically active chloroplasts, used to study the intracellular distribution of amino acids in pea leaves. *Planta* 148, 75–83.
15. Mulligan, R. M., Houtz, R. L., Tolbert, N. E. (1988) Reaction-intermediate analogue binding by ribulose biphosphate carboxylase/oxygenase causes specific changes in proteolytic sensitivity: The amino-terminal residue of the large subunit is acetylated proline. *Proc. Natl. Acad. Sci. USA* 85, 1513–1517.
16. Pettigrew, G. W., Smith, G. M. (1977) Novel N-terminal protein blocking groups identified as dimethylproline. *Nature* 265, 661–662.
17. Sambrook, J., Fritsch, E. F., Maniatis, T. (1989) *Molecular Cloning: A Laboratory Manual*, 2nd Ed. Cold Spring Harbor Lab. Cold Spring Harbor, NY.
18. Sanger, F., Nicklen, S., Coulsin, A. R. (1977) DNA sequencing with chain-terminating inhibitors. *Proc. Natl. Acad. Sci. USA* 74, 5463–5467.
19. Schmidt, G. W., Miskind, M. L. (1983) Rapid degradation of unassembled ribulose 1,5-bisphosphate carboxylase small subunits in chloroplasts. *Proc. Natl. Acad. Sci. USA* 80, 2632–2636.
20. Stock, A., Stock, J. (1988) Methylation, demethylation and deamidation of glutamate residues in membrane chemoreceptor proteins. In: Zappia, V., Galletti, P., Porta, R. (eds) *Advances in Post-Translational Modifications of Proteins and Aging*, Plenum Press, New York, pp. 201–212.
21. Strom, M. S., Lory, S. (1993) Structure-function and biogenesis of the type-IV pili. *Annu. Rev. Microbiol.* 47, 565–596.
22. Wang, P., Royer, M., Houtz, R. L. (1995) Affinity purification of ribulose-1,5-bisphosphate carboxylase/oxygenase large subunit N-methyltransferase. *Prot. Expr. Pur.* 6, 528–536.
23. Ying, Z., King, M. L. (1996) Isolation and characterization of *xnov*, a *Xenopus laevis* ortholog of the chicken *nov* gene. *Gene* 171, 243–248.
24. Ying, Z., Janney, N., Houtz, R. L. (1996) Organization and characterization of the ribulose-1,5-bisphosphate carboxylase/oxygenase large subunit <sup>ε</sup>N-methyltransferase gene in tobacco. *Plant Mol. Biol.* 32, 663–671.

## METHYLATION AND GENE MUTATION IN EUKARYOTIC DNA\*

C.-Q. LIU,<sup>1</sup> J.-F. HUANG,<sup>1</sup> YING WANG<sup>1</sup> and W.-B. LIU<sup>2</sup>

<sup>1</sup> Laboratory of Cellular and Molecular Evolution, Kunming Institute of Zoology,  
Chinese Academy of Sciences, Kunming, Yunnan, P. R. China

<sup>2</sup> Modern Biological Center, Yunnan University, Kunming, Yunnan, P. R. China

(Received: 1998-10-28; accepted 1998-11-25)

5-methylcytosine ( $m^5C$ ) as a rare base exists in eukaryotic genomes, which is a normal constitution in many eukaryotic DNA and the existence of  $m^5C$  is a feature of eukaryotic DNA. Under regular physiological conditions, cytosine of eukaryotic DNA is usually methylated. Up to the present, many people consider that the  $m^5C$  may be mutation hotspots by the deamination leading to gene mutation. Our study indicated that the spontaneous mutation caused by the transition of G-C  $\rightarrow$  A-T, in eukaryotic DNA, may result from the tautomer changing of base pairs and may also be caused by other factor actions, however it could not be caused by the deamination of  $m^5C$ .

**Keywords:** DNA methylation – 5-methylcytosine – deamination – gene mutation – molecular electrostatic potential

### INTRODUCTION

Methylation of cytosine which is widespread in DNA of eukaryotes may play an important role in some biological processes, such as DNA replication, transcription, recombination, gene expression, cell differentiation, maintenance of chromosomal structure, establishment of preferred sites for mutation, and directing genetic trigger during cell development [4, 6-8, 18, 19]. Despite the wealth of information accumulated on DNA methylation and biological function, the biological significance of methylated bases in DNA is still far from being understood. Of these problems, the relation between hydrolytic deamination and gene mutation of  $m^5C$  in eukaryotic DNA is puzzling scientists for a long time and still unclear at present.

In theory, the deamination of cytosine and 5-methylcytosine ( $m^5C$ ) may lead to the production of uracil and thymine (T) respectively (Fig. 1). It is believed that uracil is an abnormal base in DNA and can be enzymatically removed *in vivo*, how-

\*Presented at the 4th International Conference on the Role of Formaldehyde in Biological Systems, July 1-4, 1998, Budapest, Hungary.

Send offprint requests to: Dr. J.-F. Huang, Junnan 650223, P. R. China, E-mail: tbrg@public.km.yn.cn



ever, on the other hand, uracil may also serve as a rare base existing in DNA. Thymine is a normal constituent of DNA, which is not recognized by the uracil repair system [1, 5, 18, 19]. Thereupon, the deamination from m<sup>5</sup>C to thymine, after the next round of replication of DNA, will make G·C mutated to A·T. This will change one sequence to another, for example, from sequence CCAGG → Cm<sup>5</sup>CAGG → CTAGG. If the UAG triplet took place this mutation, it would cause a nonsense mutation [20].

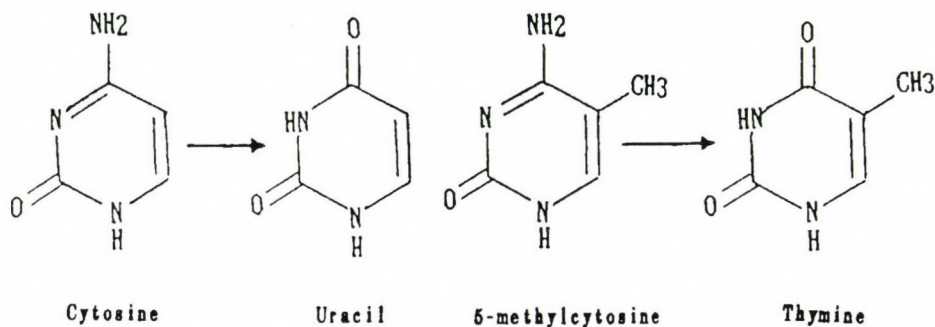


Fig. 1. The deamination reactions

Coulondre et al. [5] have reported some experimental evidence which demonstrated m<sup>5</sup>C causing directly base substitution hotspots. For example, the m<sup>5</sup>C in bacterial DNA is known to be associated with high mutability for the G·C → A·T transition. They suggested that methylated sites may be mutation "hot spots" in *E. coli*. A major hot spot in the *Iac* repressor gene is the sequence CC(A/T)GG, in wild-type *E. coli*, which is always methylated [18]. For this gene, m<sup>5</sup>C are preferred sites for spontaneous mutations [5, 9]. The deamination of m<sup>5</sup>C will lead to a heritable change in DNA by the transition from G·C → A·T and could influence differentiation [18]. Since m<sup>5</sup>C in bacteria are known to be associated with high mutability for G·C → A·T transition, and the dinucleotide CpG is deficient in the genomes of higher eukaryotes [3], the dinucleotide CpG deficiency in some eukaryotes was thought of being due to the increased mutability of m<sup>5</sup>C by deamination to thymidine, after cytosine methylated into m<sup>5</sup>C [3]. Some data of m<sup>5</sup>C deamination *in vivo* have been found in some prokaryotes [5]. However, mutagenic deamination of m<sup>5</sup>C, in high eukaryotes, is still short of convincing evidences, and the investigations of Barker et al. [2] may serve as a reference in this aspect. Similarly, m<sup>5</sup>C deamination *in vitro* has been observed, after the treatment with alkali, high temperature (at neutral PH), or sodium bisulfate [21], when the m<sup>5</sup>C will be deaminated. But, any explanation about the relation between m<sup>5</sup>C and mutation "hot spots" in eukaryotic genomes must reckon

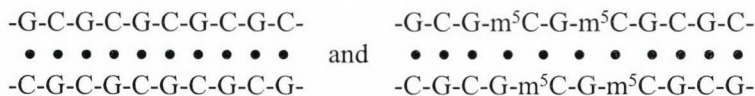
on with the fact that  $m^5C$  is absent in the genomes of *Drosophila* and other arthropods [4, 10, 17], and other factors which will result in the possibility of  $G \cdot C \rightarrow A \cdot T$  transition.

Although many studies suggested that spontaneous deamination of  $m^5C$  in DNA takes easily place, and gives rise to  $G \cdot C \rightarrow A \cdot T$  transition, thereby leads to a heritable change [1–7, 10, 16–21], some data are controversial. For example, Razin and Friedman [19] considered that the methylated bases in DNA could serve either as “hot spots” for mutations or in contrast, play a role in protecting DNA from mutations. In addition, *in vivo* experiments strongly suggest that enzyme-catalyzed deaminations of cytosine do not play a major role in making methylation sites in *E. coli* hot spots for mutations [23].

The biological significance of DNA methylation is still far from being understood, and the results from experiments are somewhat ambiguous, therefore we have studied whether DNA methylation can cause the transition from  $G \cdot C \rightarrow A \cdot T$ , and then result in gene mutation.

## MATERIALS AND METHODS

Both double helix segments of unmethylated and methylated B-DNA, as follows, have been employed during computation.



Electronic wave functions of bases, phosphodiester and deoxyribose that are involved in computing molecular electrostatic potentials (MEP) of methylated and unmethylated B-DNA segments are calculated by *ab initio* SCF method. All calculations of energy functions are based on our previous methods [15].

## RESULTS

The computed results show that the minimum values and distribution of MEP between unmethylated and methylated B-DNA are different. The minimum values of MEP in unmethylated B-DNA are  $-452.22 \sim -406.90$  kcal/mol, but the values in methylated B-DNA are  $-498.45 \sim -445.45$  kcal/mol (Fig. 2). In 4-hydroxyl-5-methylcytosine as the intermediate during the deamination from  $m^5C$  to T, the bond order of C4-N7 (0.862) is larger than that of C4-O (0.605) (Fig. 3).



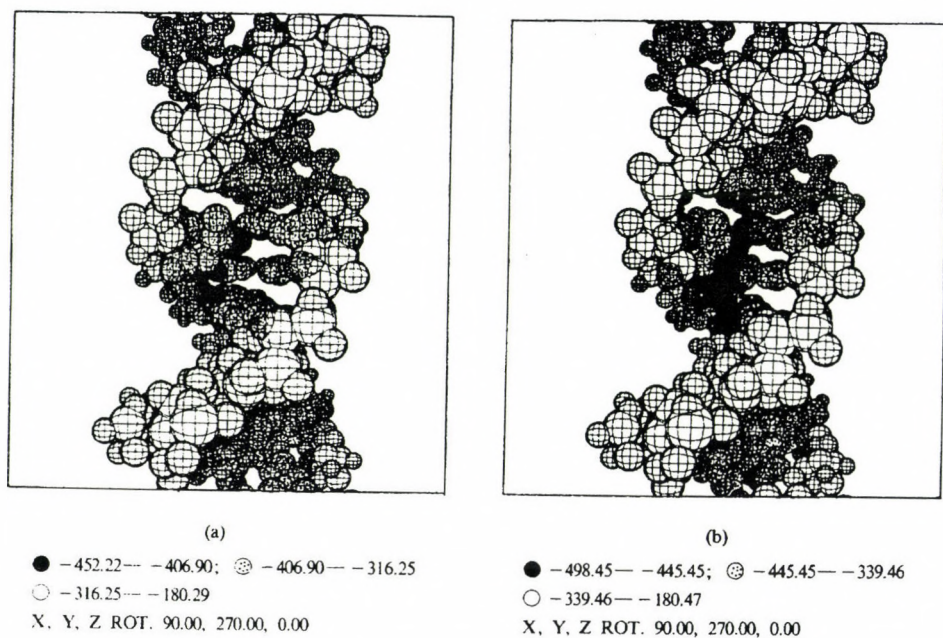


Fig. 2. Molecular electrostatic potential in the segment of B-DNA double helix. (a) The unmethylated B-DNA double helix; (b) the methylated B-DNA double helix

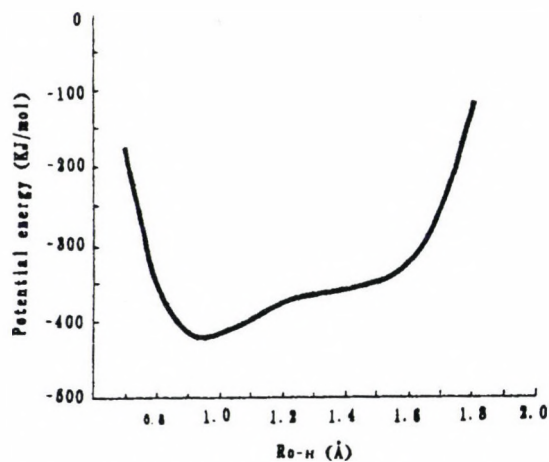


Fig. 3. The potential energy curve of proton transfer in O-HN...N intramolecular hydrogen bond system of 4-hydroxyl-5-methylcytosine

## DISCUSSION

Our previous studies have suggested that both cytosine and  $m^5C$  hold similar reacting activity, so they can pair with guanine [11–15], which has been proved by experiments. The reactivity is not apparently influenced by the introduction of the methyl group to C5 position in the single, base pair and nucleotide. In the cases of nucleotide and a segment of B-DNA double helix, this is due to the methylation giving rise to a more obvious change in MEP, thus the change of MEP may alter the affinity with some specific proteins and can affect greatly the combination of protein with DNA and the interaction with other molecules. Because MEP can reflect the electrostatic character of the whole molecule, and show the effect of whole structure on reactive sites and activity, the results suggest that the effect of a methyl group on MEP of unmethylated DNA is localized and MEP minimum values are distributed along the relative positions of the major groove. In methylated DNA, the distribution of MEP minimum values is relatively focused in the regions between the 4<sup>th</sup> and 7<sup>th</sup> base pairs. The most conspicuous feature is that the methylated helix has the strongest MEP (Fig. 2). Since methylation can cause MEP changing in localized regions, it could change the affinity of DNA with a specific protein. Therefore, it could affect the interaction between DNA and regulatory proteins, which protect DNA from being degraded or inhibit DNA transcription, etc.

In the process of  $m^5C$  hydrolytic deamination, the reacting intermediate, 4-hydroxyl-5-methylcytosine (Fig. 4) will deaminate the methyl group into T, so this intermediate must undergo a changeable process of intramolecular hydrogen bonding (we take the relationship among the three atoms of O, H10 and N7 for a linear intramolecular hydrogen bond, *i.e.* O–H...N in Fig. 4). How can this process be realized? It depends mainly on the probability of proton transfer. The potential energy curve of proton transfer in O–H...N intramolecular hydrogen bond system of 4-hydroxyl-5-methylcytosine shows that the potential well in the right is not striking and the potential well in the left is deeper than that in the right. Thus suggest that the probability of proton transfer from oxygen atom to nitrogen atom is a low, which is adverse to the deamination. In addition, the comparison of bond order of C4–N7 and

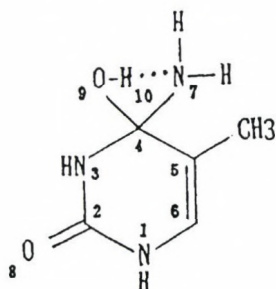
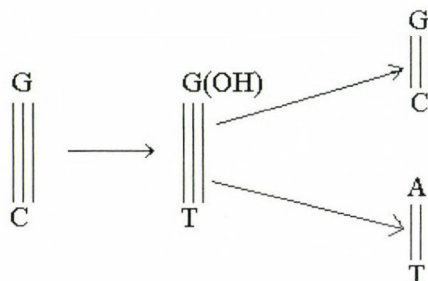


Fig. 4. The reaction intermediate-O–HN...N intramolecular hydrogen bond of 4-hydroxyl-5-methylcytosine



C4-O suggest that C4-O bond is easily broken and is also adverse to the deamination in energy.

In theory, one base can have several existing types, and the positions of its combination with H atoms are different in these types. Because each of them can form the hydrogen bonds at several positions, the nucleotides can be paired with each other by many pairing ways. In common condition of G pairing with C, if a H atom of G were transferred to make  $G_{(OH)}$ , and  $G_{(OH)}$  could pair with T, in next pairing, G (if it had renewed to common keto-type) would pair with C, and T would pair with A. Thus the sequence of bases would take place the change, as follows:



According to the change, when a base G appeared as an enol-tautomer, it would result in the spontaneous mutation. Lowdin [16] suggested that the proton tunnel in pairing bases may lead to the formation of the tautomers, and therefore, it may be a reason of mutation in the replication process. In addition, our previous calculation suggested that both  $G_{(OH)} \cdot T$  and  $G \cdot T_{(OH)}$  pairs are more stable even than G-C pair (where  $G_{(OH)}$  is enol-tautomer of guanine and  $T_{(OH)}$  is enol-tautomer of thymine) [22]. Therefore, we infer that the spontaneous mutation caused by the transition of  $G \cdot C \rightarrow A \cdot T$ , in eukaryotic DNA, may be a result caused by the tautomer changing base pairs and may also be caused by other actions, whereas it could not be caused by the deamination of  $m^5C$ .

#### REFERENCES

1. Adams, R. L. P., Burdon, R. H. (1985) *Molecular Biology of DNA Methylation*. Springer-Verlag, New York.
2. Barker, D., Schafer, M., White, R. (1984) Restriction sites containing CpG show a higher frequency of polymorphism in human DNA. *Cell* 36, 131–138.
3. Bird, A. P. (1980) DNA methylation and frequency of CpG in animal DNA. *Nucleic Acids Res.* 8, 1499–1504.
4. Cooper, D. N. (1983) Eukaryotic DNA methylation. *Hum. Genet.*, 64, 315–333.
5. Coulondre, C., Miller, J. H., Farabaugh, P. J., Gilbert, W. (1978) Molecular basis of base substitution hotspots in *Escherichia coli*. *Nature* 274, 775–780.
6. Eden, S., Ceder, H. (1994) Role of DNA methylation in the regulation of transcription. *Cur. Opin. Genet. Develop.* 4, 255–259.
7. Ehrlich, M., Wang, R. Y.-H. (1981) 5-Methylcytosine in eukaryotic DNA. *Science* 212, 1350–1357.

8. Holliday, R. (1987) The inheritance of epigenetic defects. *Science* 238, 163–170.
9. Holliday, R., Grigg, G. W. (1993) DNA methylation and mutation. *Mutat. Res.* 285, 61–67.
10. Levine, M., Garen, A., Lepesant, J.-A., Lepesant-Kejzlarova, J. (1981) Constancy of somatic DNA organization in developmentally regulated regions of the *Drosophila* genome. *Proc. Natl. Acad. Sci. USA*, 78, 2417–2421.
11. Liu, C.-Q., Wang, Y., Zhou, M.-P., Tang, C.-K. (1984) Study on the DNA methylation I. Quantum biology investigation of methylation of cytosine. *J. Mol. Sci.* 4, 501–506.
12. Liu, C.-Q., Cao, H., Wang, Y., Huang, J.-F. (1986) The effect of 5-methylcytosine on the interaction between stacked base and amino acid-codon. *J. Mol. Sci.* 6, 301–306.
13. Liu, C.-Q., Wen, Y.-K., Cao, H., Chen, H. (1989) *An Introduction to Quantum Biology*. Science Press, Beijing.
14. Liu, C.-Q. (1990) *Quantum Biology and Its Application*. Higher Education Press, Beijing.
15. Liu, C.-Q., Wang, Y., Huang, J.-F., Zhang, H. (1991) A quantum biological approach to the relations of DNA methylation with gene transcription and mutation. *J. Theor. Biol.* 148, 145–155.
16. Lowdin, P. O. (1964) Some aspects on DNA replication; incorporation errors and proton transfer. In: Pullman, B. (ed.) *Electronic Aspects of Biochemistry*. Academic Press, New York and London.
17. Rae, P. M. M., Steele, R. E. (1979) Absence of cytosine methylation at C-C-G-G and -G-G-C-C sites in the rDNA coding regions and intervening sequences of *Drosophila* and the rDNA of other higher insects. *Nucleic Acids Res.* 6, 2987–2995.
18. Razin, A., Urieli, S., Pollack, Y., Gruenbaum, Y., Glaser, G. (1980) Studies on the biological role of DNA methylation: IV. Mode of methylation of DNA in *E. coli* cells. *Nucleic Acids Res.* 8, 1783–1792.
19. Razin, A., Friedman, J. (1981) DNA methylation and its possible biological roles. *Prog. Nucleic Acids Res. Mol. Biol.* 25, 33–52.
20. Razin, A. (1984) DNA methylation patterns: formation and biological functions. In: Razin, A. (ed.) *DNA Methylation, Biochemistry and Biological Significance*. Springer-Verlag, New York.
21. Wang, R. Y.-H., Gehrke, C. W., Ehrlich, M. (1980) Comparison of bisulfite modification of 5-methyldeoxycytidine and deoxycytidine residues. *Nucleic Acids Res.* 8, 4777–4790.
22. Wang, Y., Liu, C.-Q., Huang, J.-F. (1990) Quantum biological researches in the influences of base tautomers upon base pairing. *Acta Biochim. Biophys. Sinica* 22, 263–270.
23. Wyszynski, M., Gabbara, S., Bhagwat, A. S. (1994) Cytosine deaminations catalyzed by DNA cytosine methyltransferases are unlikely to be the major cause of mutational hot spots at sites of cytosine methylation in *Escherichia coli*. *Proc. Natl. Acad. Sci. USA*, 91, 1574–1578.





## ROLE OF FORMALDEHYDE IN DIRECT FORMATION OF GLYCINE AND SERINE IN BEAN LEAVES\*

Á. NOSTICZIUS

Department of Chemistry, Faculty of Agricultural Sciences, Pannon University,  
Mosonmagyaróvár, Hungary

(Received: 1998-10-28; accepted: 1998-11-25)

In our early study [2] labelled formaldehyde, glyoxylate, glycine and serine were formed from  $^{14}\text{CO}_2$  during 1 min incubation. Continuing the detailed work by unlabelled  $\text{HCO}_3^-$  with short (1 min) incubation time in numerous experiments, there were significant changes in the amount of formaldehyde, glyoxylate, glycine and serine. The main product was glycine. In illuminated leaves after  $\text{HCO}_3^-$  intake, the formaldehyde content increased. However, in dark in the presence of 5 mM  $\text{HCO}_3^-$  the formaldehyde content decreased and the amount of glyoxylate, glycine and serine increased in green leaves.

The transamination is improbable as the amount of glutamate and aspartate did not decrease during the glycine and serine formation. The change in the amount of the measured free amino acids and glyoxylate was hindered by (aminoxy)acetic acid (AOA) and amethopterin. AOA, which is an inhibitor of pyridoxal phosphate has no effect on formaldehyde alteration. In the presence of amethopterin which inhibits the activity of tetrahydrofolate the formaldehyde amount increased in dark kept  $\text{CO}_2$  containing green leaves instead of decreasing. This shows that tetrahydrofolate has a role in glyoxylate formation from formaldehyde and  $\text{CO}_2$ .

A direct formation of glycine and serine can be supposed in definite circumstances during photosynthesis, in which pyridoxal phosphate has an important role.

**Keywords:** Formaldehyde – glyoxylate – photosynthesis – direct formation of glycine

### INTRODUCTION

The presence of formaldehyde in green leaves has been proved for years. In our early study [2] labelled formaldehyde, glyoxylate, glycine and serine were formed from  $^{14}\text{CO}_2$  during one and two minutes incubation. The quantity of all measured compounds increased in growing light intensity about 10–50% except glycine, the growing light intensity caused eleven times increase in glycine content. It seems that formaldehyde, glyoxylate, glycine and serine form photosynthetically, and the main

\* Presented at the 4th International Conference on the Role of Formaldehyde in Biological Systems, July 1–4, 1998, Budapest, Hungary.

Send offprint requests to: Prof. Á. Nosticzius, Chemical Department of Pannon University, H-9200 Mosonmagyaróvár, Lucsony u. 15. Hungary.



product is glycine. It is unlikely that all  $\text{CO}_2$  which are in leaves take part in this process.

Vermaas and Govindjee [4] and Stemler [3] have given a good summary about the  $\text{CO}_2$  (or  $\text{HCO}_3^-$ ) which is bound to the chloroplast inner membrane. This  $\text{CO}_2$  is necessary for light reactions. Studying the pH which is necessary for binding it was experienced that at pH 6.8 the binding is the largest. Studies were made by  $^{14}\text{CO}_2$  and radiation was measured. Thylakoid bound  $\text{CO}_2$  was written by the authors which was released when light reactions were taken place. It is possible that formaldehyde was present because  $\text{CO}_2$  was reduced by light reactions, but only the radiation of  $^{14}\text{C}$  were measured. This  $^{14}\text{C}$  can be present both in  $\text{CO}_2$  or in formaldehyde.

Glycine and serine as early products were present in the study of Benson and Calvin [1], the aim was – at that time – to explain the formation of carbohydrates. At present it seems that glycine and serine originate from formaldehyde.

For the detailed examination of formaldehyde, glyoxylate, glycine and serine formation unlabelled  $\text{HCO}_3^-$  was used with short (1 min) incubation time.

## MATERIALS AND METHODS

Plants were grown in a plant raising chamber. Temperature was raised gradually from 20 °C to 28 °C during 8 hours and reduced gradually to 20 °C during 8 hours. Meanwhile the light intensity was 80 W/m<sup>2</sup>. During the third 8 hours the plants were kept in dark at 20 °C.

Neutralised aqueous 0.1% dimedone solution was suctioned into green leaves. This solution was made with 5 mM  $\text{NaHCO}_3$  or without, with enzyme inhibitors or without. Vacuum infiltration was followed by 1 min incubation in dark or in other case in light (10 W/m<sup>2</sup> fluorescent day light). After this, leaves were taken into boiling 1% trichloroacetic acid solution. The leaves were powdered after drying by 50 °C flowing air. From well-known amount (0.3–0.4 g) of leaf powder the formaldehyde-dimedone was extracted by ethanol. From an other well-known part of the sample the glyoxylate and free amino acids were extracted by distilled water. All the two extracts were evaporated by vacuum and the solid residues were dissolved in 1 ml solvent. Formaldehyde-dimedone dissolved in ethanol, glyoxylate and free amino acids in 0.1% aqueous dimedone solution. For quantitative transformation of glyoxylate to glyoxylate-dimedone 48 hours are necessary. The separation of free amino acids is possible from this solution immediately but the glyoxylate determination only after 48 hours because only the glyoxylate-dimedone (the dimedone and its derivatives) is fluorescent after the chemical reaction.

For separation of different substances TLC method was used (Merck silica gel 60 plate). The following eluents were used:

for formaldehyde-dimedone: petroleum ether and ethanol in 100 : 7 ratio and for glyoxylate-dimedone: toluene, ethyl acetate, formic acid in 60 : 30 : 15 ratio, for glycine, glutamic acid and aspartic acid: acetone, distilled water, urea in 70 : 30 : 0.5 proportion and for serine: acetone, distilled water in 70 : 30 ratio.

For the quantitative determination of separated spots fluorimetry was used after chemical reaction. For formaldehyde-dimedone determination the plate was sprayed with 0.1% 2,4-dichloroquinone-4-chloroimide (in ethanol) and then with a mixture, which contained 14% (m/m) sucrose, 6.5% (m/m)  $\text{Na}_2\text{CO}_3$ , 1 M NaOH in 6 : 2 : 0.5 proportion. The best fluorescence is accessible if the plates stay about 10–15 min in below 0 °C, and then are dried with hair-drier. For glyoxylate determination the plate was sprayed with 0.1% 2,4-dichloroquinone-4-chloroimide and then with a mixture containing 28.6% (m/m) sucrose, 13% (m/m)  $\text{Na}_2\text{CO}_3$  and 2 M NaOH in 2 : 1 : 1 ratio. The fluorescence will be the best if the plate stay about 5 °C at night after spraying. For glycine, glutamic and aspartic acid determination the plate was sprayed with a mixture of 10 ml 0.05% o-phthalaldehyde in acetone and 2 ml concentrated acetic acid. After spraying it was necessary to heat the plate for 25–30 min at 110 °C because the serine has a disturbing effect which can be eliminated by heating. For serine determination the plate must be sprayed with a freshly mixed composition of acetylacetone solution and saturated (about 0.02 M)  $\text{KIO}_4$  as well as buffer solution in proportion 2 : 1 : 1. The acetylacetone solution contained 2 ml acetylacetone in 20 ml n-propanol and 80 ml distilled water. The buffer solution contained 50 ml 15% (m/m) ammonium acetate and 10 ml ammonia solution (25%). After spraying the plate must be heated about 10 min in 100–110 °C.

After reaction the formaldehyde-dimedone and glyoxylate-dimedone, glycine, glutamic acid and aspartic acid as well as serine have a yellow fluorescence under 365 nm light. The fluorescence was measured for quantitative determination in all cases.

## RESULTS

The question was whether it is possible to demonstrate the formation of formaldehyde, glyoxylate, glycine and serine from unlabelled  $\text{HCO}_3^-$  during short incubation time?

The formaldehyde content of green leaves has been measured for many years. The formaldehyde content sometimes increased, sometimes decreased during incubation with  $\text{HCO}_3^-$ . Table 1 shows that in leaves picked in light the formaldehyde content increased when 5 mM  $\text{NaHCO}_3$  was present and the formaldehyde content decreased in the presence of 5 mM  $\text{NaHCO}_3$  when the leaves were kept in dark at least 10 min after plucking. It appears that formaldehyde forms from  $\text{HCO}_3^-$  in light and  $\text{HCO}_3^-$  ( $\text{CO}_2$ ) reacts with formaldehyde in dark in green plant leaves.

During the light reactions of photosynthesis pH difference takes place between the two sides of chloroplast inner membrane. On the other hand  $\text{CO}_2$  ( $\text{HCO}_3^-$ ) was bound to each photosystem II complex as showed Vermaas and Govindjee [4] and Stemler [3]. The amount of  $^{14}\text{CO}_2$  bound to chloroplast depends on pH, the maximum was at pH 6.8 [3]. The pH must have strong influence on photosynthetic transformation of  $\text{CO}_2$ . Table 2 shows the effect of pH on the formation of formaldehyde and glyoxylate. The scale was 0.5 pH in this study. Maximum formaldehyde and gly-



Table 1

The effect of  $\text{HCO}_3^-$  on the amount of formaldehyde in dark kept and light kept green leaves  
Values are means of 7 experiments in  $10^{-5}$  g/g dry weight

	Leaves picked under	
	light	dark
1. Untreated	0.1430	0.0783
2. 5 mM $\text{NaHCO}_3$	0.1851	0.0628
1-2		0.0155
2-1	0.04212	
LSD <sub>5%</sub>	0.0271	0.0108
LSD <sub>1%</sub>	0.0366	

Table 2

The effect of pH on the amount of formaldehyde and glyoxylate  
Values are means of 8 horse bean experiments in  $10^{-5}$  g/g dry weight

A			B		
pH	formaldehyde	glyoxylate	pH	formaldehyde	glyoxylate
5.5	(0.4721)	(1.3492)	5.5	(0.6397)	(1.3185)
6.0	0.4798	1.0623	6.0	0.5539	1.2697
6.5	0.5577	1.6704	6.5	0.6966	1.9925
7.0	0.7248	3.0379	7.0	0.8395	3.0051
7.5	0.4214	1.1551	7.5	0.4685	1.1008
8.0	(0.5567)	(1.0762)	8.0	(0.6403)	(0.9582)
LSD <sub>5%</sub>	0.2196	1.8082	LSD <sub>5%</sub>	0.2459	1.8521
7.0-6.0	0.245	1.9756	7.0-6.0	0.2856	1.7354
7.0-7.5	0.3034	1.8828	7.0-7.5	0.3710	1.9043

Treatment:

A = after vacuum infiltration by 0.1 M phosphate (4 cases) or 0.1 M Tris-HCl buffer (4 cases) 15 min in dark

B = after vacuum infiltration by phosphate or Tris-HCl buffer 10 min dark and 5 min in light

Date in parenthesis are not involved in calculation of LSD.

oxylate amount can be measured at  $\text{pH} = 7$ . It is almost the same with the case of chloroplast bound  $\text{CO}_2$ , where the maximum was 6.8 pH. It is imaginable that formaldehyde forms from the  $\text{CO}_2$  which is bound to photosystem II complex.

Table 3

The effect of enzyme inhibitors on the amount of formaldehyde, glyoxylate and glycine in bean leaves, during 1 min incubation

Values are means of 7 experiments in  $10^{-5}$  g/g dry weight

		Formaldehyde	Glyoxylate	Glycine
1. Untreated	D	0.1187	0.7245	9.67
2. Untreated	L	0.1075	0.7456	9.19
3. 5 mM $\text{HCO}_3^-$	D	0.0668	1.0535	15.93
4. 5 mM $\text{HCO}_3^-$	L	0.0920	0.6763	15.84
5. 1 mM AOA	D	0.1028	0.9169	11.58
6. 1 mM AOA	L	0.0945	0.8583	12.50
7. 5 mM $\text{HCO}_3^-$	D	0.0630	0.9248	11.58
8. +1 mM AOA	L	0.0797	1.1407	9.17
9. 1 mM amethopterin	D	0.0881	1.1855	11.41
10. 1 mM amethopterin	L	0.1005	1.4352	12.72
11. 5 mM $\text{HCO}_3^-$	D	0.1240	1.0037	11.34
12. + amethopterin	L	0.1087	1.2028	11.28
LSD <sub>10%</sub>				4.58
LSD <sub>5%</sub>		0.0281	0.65	5.45
LSD <sub>1%</sub>		0.0481		

D = 1 min incubation in dark

L = 1 min incubation in  $10 \text{ W/m}^2$  light

In the case of Tables 3 and 4 it is better to pay attention to the dark incubated samples, because light may cause new processes. In Table 3 the effect of (aminooxy)acetic acid (AOA) and amethopterin on formaldehyde, glyoxylate and glycine formation can be seen. AOA is an inhibitor of pyridoxal phosphate. Amethopterin is an inhibitor of tetrahydrofolate which should transfer the active  $\text{C}_1$ -units. In the samples without enzyme inhibitor  $\text{HCO}_3^-$  causes decrease in formaldehyde content, significant difference at formaldehyde is in 1% probability level. At AOA the difference lessens, the significant difference is only 5% probability level. At amethopterin formaldehyde content increases in the presence of  $\text{HCO}_3^-$ , instead of decreasing, while the glyoxylate amount do not increase. It seems that tetrahydrofolate is necessary to form glyoxylate from formaldehyde and  $\text{CO}_2$ . Both inhibitors prevent the formation of glyoxylate and glycine from  $\text{HCO}_3^-$ .

Table 4 shows the effect of (aminooxy)acetic acid and  $\text{HCO}_3^-$  on the amount of glyoxylate, glycine, serine, glutamic- and aspartic acid. The effect of  $\text{HCO}_3^-$  can be seen in the difference of samples 3 and 1. It seems that glycine is the main product which forms from  $\text{HCO}_3^-$ . The significant difference is in 1% probability level at (3–1) and is in 5% probability level at (3–7). The glyoxylate difference at (3–1) is



5% probability level and the serine difference at (3–1) is significant only 10% probability level.

Glycine is the single product which absolute amount with  $\text{HCO}_3^-$  and without inhibitor is significantly more than its amount with  $\text{HCO}_3^-$  and with enzyme inhibitor. In Table 3 in the sample 3 (with  $\text{HCO}_3^-$ , without inhibitor) the glycine amount is more than in the sample 7 (with  $\text{HCO}_3^-$  and with AOA). The significant difference between sample 3 and sample 11 is in 10% probability level.

In Table 4 the glycine amount in sample 3 (with  $\text{HCO}_3^-$  and without AOA) is more, than the glycine amount of sample 7 (with  $\text{HCO}_3^-$  and with AOA), this difference is significant at 5% probability level. Their difference (3–7) is significant neither glyoxylate, nor serine.

The amount of glutamic acid and aspartic acid did not decrease during glycine and serine formation. The amount of glutamic and aspartic acid is a bit more (but not significantly) in sample 3 than in sample 1. The transamination from these two amino acids is improbable.

Table 4

The effect of  $\text{HCO}_3^-$  and (aminooxy)acetic acid in green bean leaves on the amount of glyoxylate, glycine, serine, glutamic and aspartic acid during 1 min incubation  
Values are means of 13 experiments in  $10^{-5}$  g/g dry weight

		Glyoxylate	Glycine	Serine	Glutamic acid	Aspartic acid
1. Untreated	D	0.9251	10.35	8.66	26.75	8.38
2. Untreated	L	1.0681	10.88	8.52	29.34	8.96
3. 5 mM $\text{HCO}_3^-$	D	1.5209	15.28	10.92	30.73	10.25
4. 5 mM $\text{HCO}_3^-$	L	1.440	15.03	10.74	30.95	10.05
5. 1 mM AOA	D	1.4947	12.45	10.64	31.97	10.25
6. 1 mM AOA	L	1.2669	11.81	9.23	29.76	8.94
7. 1 mM AOA +	D	1.4734	11.09	9.56	27.83	8.51
8. 5 mM $\text{HCO}_3^-$	L	1.5348	9.80	9.11	25.86	8.75
LSD <sub>10%</sub>		0.4245		2.19	5.31	2.25
LSD <sub>5%</sub>		0.5088	3.72			
LSD <sub>1%</sub>			4.92			

D = 1 min incubation in dark

L = 1 min incubation in 10 W/m<sup>2</sup> light

## DISCUSSION

It is possible that formaldehyde forms from  $\text{CO}_2$  which is bound to chloroplast membrane. It is not the same with  $\text{CO}_2$  which takes place in dark reaction and reacts with ribulose-1,5-biphosphate or phosphoenol pyruvate. After illumination the formed formaldehyde removes from membrane.

It is supposed that formaldehyde reacts with  $\text{CO}_2$  ( $\text{HCO}_3^-$ ) and glyoxylate can be formed.

Formation of glycine from glyoxylate is imaginable, but without transamination, because along this pathway the amount of glutamic acid and aspartic acid (pools of amino group) do not decrease. However, pyridoxal phosphate is necessary for this pathway because AOA prevents the formation of glycine and serine.

The role of formaldehyde in the direct formation of a few amino acids (e.g. glycine) is also imaginable. It is not necessary to suppose glycine or serine formation from earlier formed 3-phosphoglyceric acid. The transformation between glycine and serine with the participation of tetrahydrofolate is well known, it is attributed to photorespiration. However, in the excess of  $\text{HCO}_3^-$ , and in dark incubation the participation of that latter process is improbable.

## REFERENCES

1. Benson, A. A., Calvin, M. (1950) Carbon dioxide fixation by green plants. *Ann. Rev. Plant Physiol.* 1, 25–42.
2. Nosticzius, Á., Szarvas, T., Molnár, Z. (1992) *Photosynthesis and formaldehyde formation*. In: Proc. 3<sup>rd</sup> Intern. Conf. on Role of formaldehyde in biological systems. Hungarian Biochemical Society. Budapest, pp. 151–156.
3. Stemler, A. (1982) Bicarbonate and Photosystem II. In: Govindjee P. (ed.) *Photosynthesis* Vol. 2. Academic Press, New York, pp. 513–539.
4. Verma, F. J., Govindjee P. (1982) Bicarbonate or carbon dioxide as a requirement for efficient electron transport on the acceptor side of photosystem II. In: Govindjee (ed.) *Photosynthesis* Vol. 2. Academic Press, New York, pp. 541–558.



MAGYAR  
TUDOMÁNYOS AKADÉMIA  
KÖNYVTÁRA

## EFFECT OF METHIONINE ENRICHMENT ON THE BIOLOGICAL ACTIVITIES OF FOOD PROTEINS\*

GYÖNGYI HAJÓS,<sup>1</sup> SZ. FARKAS,<sup>1</sup> EMŐKE SZERDAHELYI<sup>1</sup> and MARIANNE POLGÁR<sup>2</sup>

<sup>1</sup>Central Food Research Institute, Budapest, Hungary

<sup>2</sup>Madarász Children's Hospital, Budapest, Hungary

(Received: 1998-10-28; accepted: 1998-11-25)

A special enzymatic technique, the enzymatic peptide modification (EPM) reactions have been worked out in our laboratory, by which proteins can be modified with respect to their biological activities. Enzymatic modification methods provide several advantages in producing proteins of desired nutritional properties. Proteolytic modification, particularly when combined with methionine enrichment, significantly altered the biological activities and leads to increased nutritional value.

**Keywords:** Methionine enrichment – biological activity – enzymatic peptide modification – antinutritive character

### INTRODUCTION

During enzymatic modification under appropriate reaction conditions, L-amino acids (generally in ester form) are partially covalently incorporated into the peptide chains of a protein hydrolysate [1]. Thus, these enzymatic modification reactions with amino acid enrichment would be expected to be more important from health aspects than other modification processes without covalent amino acid enrichment.

Because of their antitoxin and antioxidant effects, SH-containing amino acids are able to act as reducing agents, scavengers and inducers of cellular detoxification [2-4]. With respect to biological utilisation and safety it is important to note that only nutritious sulfur amino acids should be applied for food uses. However, sulfur amino acids, first of all methionine, are the limiting essential amino acid in most plant proteins. In order to improve the nutritional quality of foods free L-methionine fortification is not the best method because of the toxic or antinutritional effect of high levels of free methionine in the diet [3, 9].

\* Presented at the 4th International Conference on the Role of Formaldehyde in Biological Systems, July 1-4, 1998, Budapest, Hungary.

Send offprint requests to: Dr. Gyöngyi Hajós, Central Food Research Institute, H-1022 Budapest, Herman O. u. 15, Hungary.



Summarizing the above, proteolytic modification of proteins by covalent sulfur amino acid enrichment could be a suitable method for producing protein-based reducing agents, scavengers and inducers of cellular detoxification, that is for improvement in the safety of foods.

The enzymatic modification of proteins is one of the best ways to reduce their antigenic/allergenic character. While cleaving of the polypeptide chain during enzymatic modification, the antigenic architecture of the protein molecule collapses. While sequential epitopes might survive the steps of enzymatic hydrolysis, epitopes are rapidly altered depending on the actual conformation of the protein.

Legume seeds contain a number of antinutrients, mainly lectin and trypsin inhibitors. The efficiency of the nutritional utilization of diets containing soybean is well below that expected on the basis of chemical composition [7]. In order to reduce the extent of this constraint, at present, all soy products go through expensive heat-treatment or other processing procedures which can lead to losses of essential amino acids and to the production of toxic by-products. In addition, most plant proteins are inherently deficient in one or more amino acids. Methionine is the limiting essential amino acid of soybeans [8].

The goal of our study was to apply enzymatic modification as a tool for alteration of safety and quality of food proteins. In the course of these studies we have elaborated a method for covalent amino acid enrichment of proteolytic hydrolysates of soy proteins. Methionine was chosen as the amino acid to be enriched because of its nutritional importance: Met is (i) one of the limiting essential amino acids especially in the case of plant proteins, (ii) an important methylating agent, (iii) an amino acid with a strong hydrophobic character, (iv) a component having a role in the safety of foods as S-containing amino acid.

## MATERIALS AND METHODS

Soybean (*Glycine max*) albumin and soybean agglutinin (SBA) were purified from soybeans [8].

### *Enzymatic hydrolysis*

Soy proteins were hydrolysed in a solution at a concentration of 2% (w/v) with pepsin at pH 2.0 (substrate: enzyme, 100 : 1, w/w). Incubation was carried out at 37 °C for 2 h. The reaction mixture was stirred during hydrolysis and after that freeze dried.

### *Enzymatic peptide modification*

The peptic hydrolysate of soybean albumin fraction was used to produce EPM-products in the presence of  $\alpha$ -chymotrypsin (at pH 6.0) or pepsin (at pH 4.0) in a solution of 20% w/v. For methionine enrichment methionine ethyl ester in different

proportions (L-methionine at a ratio of 0.15 : 1, 0.34 : 1, 0.48 : 1, 0.63 : 1, 0.92 : 1 to protein) was added to the reaction mixture. The reaction mixture was incubated (substrate: enzyme, 100 : 1, w/w) for 16 hours at 37 °C without stirring, dialysed against distilled water at 5 °C for 24 hours to remove the excess of free methionine and methionine ethyl ester and freeze dried.

### *Amino acid content*

Aliquots of the samples were hydrolyzed with 6 M HCl in a tube flushed with N<sub>2</sub> at 105 °C for 24 h and the amino acids were subjected to thin layer ion-exchange chromatography. Methionine spots were evaluated by a Biotec Fischer video densitometer (identified and compared to the control methionine).

### *SDS-PAGE electrophoresis*

Samples were separated in a vertical polyacryl amide slab gel (15% acryl amide) with a stacking gel (6% acryl amide). Samples were incubated at 100 °C for 2 min. After electrophoresis the gels were stained with 0.5% Coomassie Blue R (Sigma).

### *Immunoblotting technique*

After running SDS-PAGE the proteins were blotted electrophoretically onto nitrocellulose membranes using a semidry blot apparatus (at 2.5 mA/cm<sup>2</sup>). The blots were reacted with anti-soy bean agglutinin antibodies, followed by peroxidase-antiperoxidase reaction, and finally the colours were developed with 4-chloronaphthol-H<sub>2</sub>O<sub>2</sub> reagent as described earlier [5, 6].

## RESULTS AND DISCUSSIONS

In our laboratory enzymatically modified and methionine-enriched soybean albumin was produced without heat treatment and antinutritive properties of the products were measured. During the process of the enzymatic modification of soy albumin, the antinutrients of soybean have been partially eliminated.

The proteinase-induced covalent incorporation of methionine shows an optimum curve in the function of the quantity of methionine ethyl ester added to the reaction mixture (Fig. 1). The covalent methionine-enrichment was maximal at the value of 0.34 g methionine/1 g in this enzyme-catalyzed process. This optimal methionine-enrichment was used for our further EPM reactions. Behind this point, interestingly



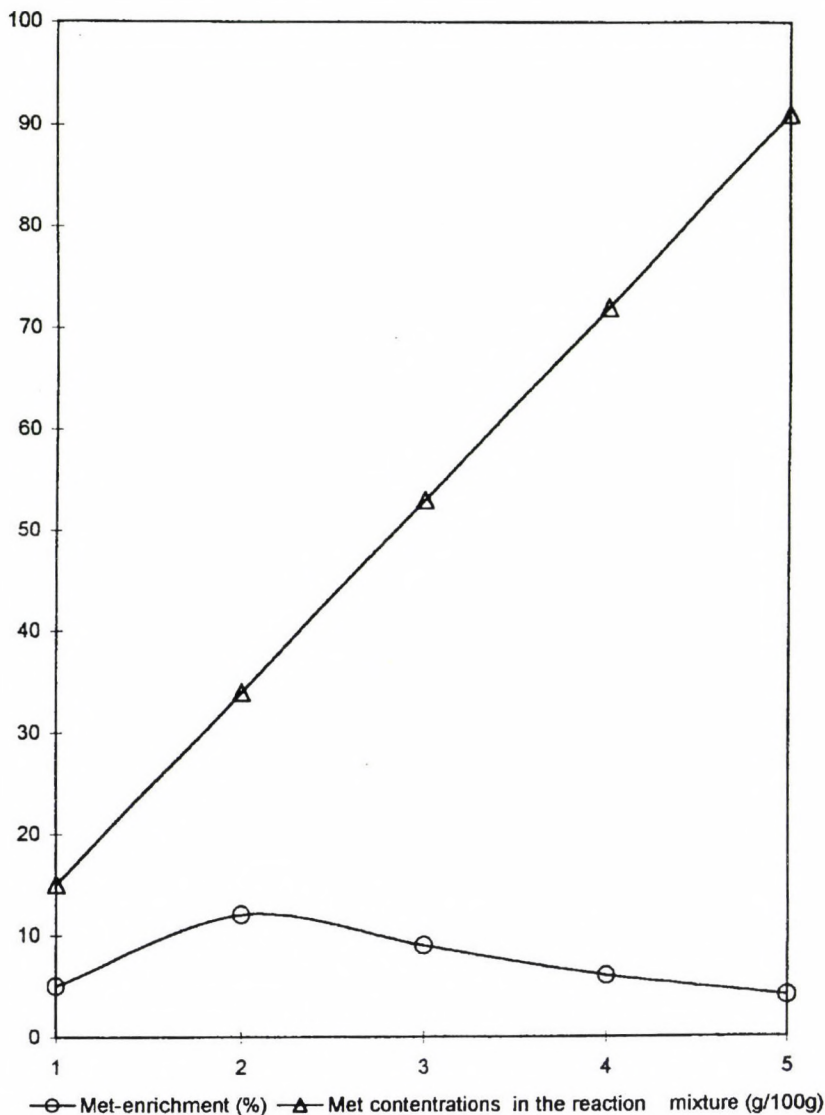


Fig. 1. Optimum curve of the quantity of methionine enrichment and quantities of methionine ethyl ester added to the reaction mixture

enough, the higher amount of methionine (in form of ethyl ester) was added to the reaction mixture, the lower amount of covalently bound methionine was found in the product. A possible interpretation of this result is that the changes in the ratio

between methionine ethyl ester and peptides of the protein hydrolysate influences the degree of the amino acid incorporation and thereby the primary structure of the products, and alters the mode of the transpeptidation and the efficacy of the amino acid enrichment.

The content and immunological activity of soybean agglutinin in soy albumin and modified soy albumin samples was investigated. After an SDS-PAGE separation of the proteins in soy albumin samples, the proteins were electrophoretically transferred to a membrane and detected immunologically using antibody to soybean agglutinin and visualizing the soybean agglutinin antibody complex by rabbit IgG antibody.

Evaluation of the SDS-PAGE patterns after Coomassie Blue staining and immunoblotting (Fig. 2) of the samples of soybean albumin, peptic hydrolysates of soybean albumin, different peptic EPM products with and without methionine enrichment produced from the peptic hydrolysate of soybean albumin,  $\alpha$ -chymotryptic EPM product with methionine enrichment produced from peptic hydrolysate of soybean albumin showed, that the number and intensity of zones corresponding to soybean agglutinin was reduced during the peptic hydrolysis and further reduced after both the peptic and  $\alpha$ -chymotryptic EPM methods. The videoden-

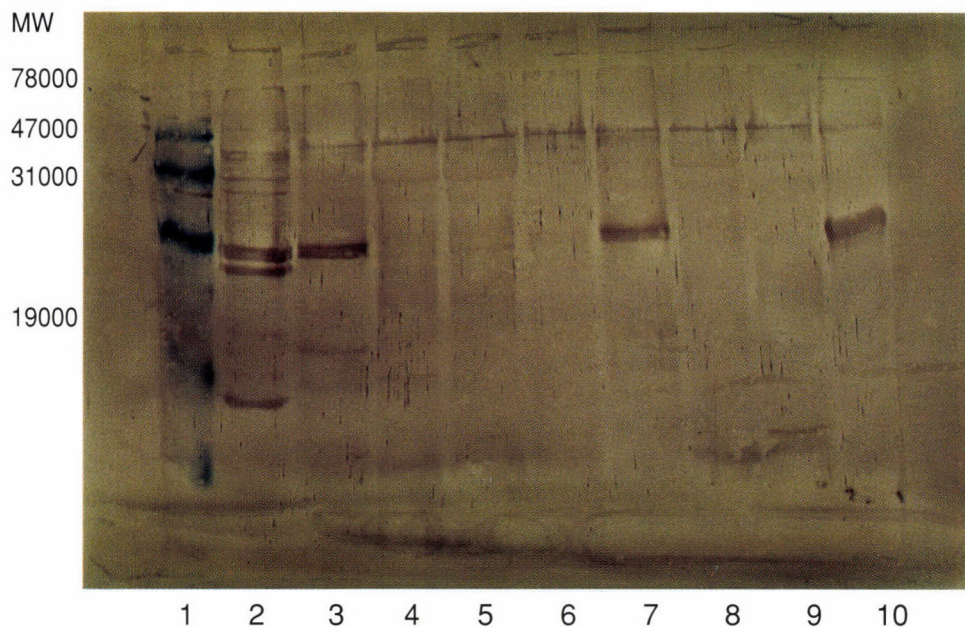


Fig. 2. Immunoblotting of the samples of soybean albumin and modified products of soybean albumin. The lanes contained the following materials: 1. LMW control (prestained), 2. Soy albumin, 3 and 7. Peptic hydrolysate of soy albumin, 4., 8. and 9. Peptic EPM-product (without Met-enrichment) produced from the peptic hydrolysate of soy albumin, 5. Peptic EPM-product with methionine enrichment produced from the peptic hydrolysate of soy albumin, 6.  $\alpha$ -chymotryptic EPM-product with Met-enrichment produced from the peptic hydrolysate of soy albumin, 10. Soybean agglutinin



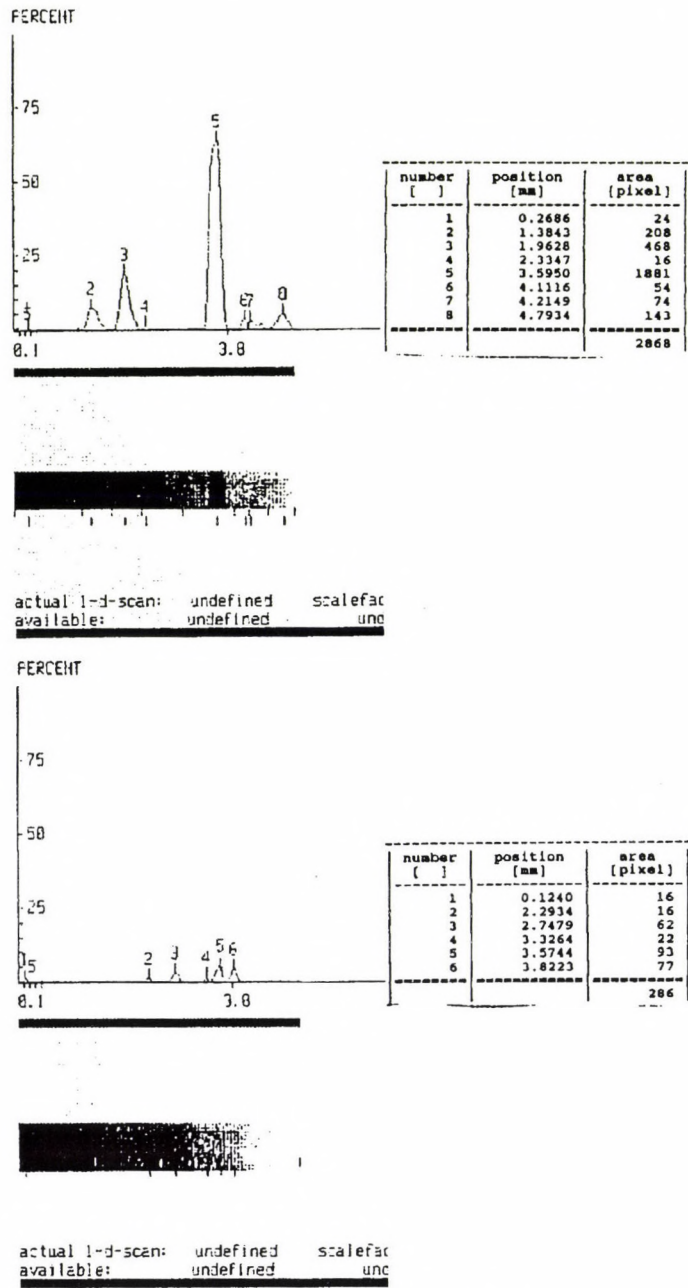


Fig. 3. The video-densitometric evaluation of the peptic hydrolysate and the peptic EPM (produced with methionine enrichment) samples, see Fig. 2

sitometric evaluation shows the significant difference in the immunoreactivity of the peptic hydrolysate to compare to the peptic EPM (produced with methionine enrichment) product (Fig. 3) against anti-soybean agglutinin.

The untreated soy albumin showed considerable soybean agglutinin activity and the lectin content (soybean agglutinin) of soy albumin was slightly reduced during the peptic hydrolysis. However, neither the sample of peptic-EPM-soy albumin nor  $\alpha$ -chymotryptic-EPM-soy albumin indicated any significant activity against anti-soybean agglutinin rabbit IgG antibody.

In conclusion, the enzymatic modification methods (EPM) by transpeptidation and methionine enrichments are suitable to improve the nutritional values of soy proteins partly by modifying the structure of the soybean lectin, partly by compensating for their methionine deficiency by covalently bound methionine enrichment. The combination of the incorporation of a strong hydrophobic amino acid, methionine into the terminals of the protein chains and of modification by proteolysis and resynthesis of peptide bonds in the soy proteins can lead to modification in protein conformation resulting in decreased antinutritive activity and increased biological value.

It is expected that due to enzymatic modification reactions leading to amino acid enrichment, the resulting proteins should be more valuable for healthy nutrition than other products in which the modification occurred without covalent enrichment with methionine.

#### ACKNOWLEDGEMENTS

The skillful assistance of Ms. Éva Kiss, Ms. Betty Zárai and Ms. Katalin Sólyom is gratefully acknowledged. This work was supported by the Hungarian Scientific Research Fund (OTKA, No. T 022836).

#### REFERENCES

1. Aso, K., Tanimoto, S., Yamashita, M., Arai, S., Fujimaki, M. (1979) Chemical properties of enzymatically modified proteins produced from soy protein by covalent attachment of methionine. *Agric. Biol. Chem.* 49, 1649.
2. Csomós, G., Fehér, J. (1992) *Free Radicals and the Liver*. Springer-Verlag, Berlin.
3. Friedman, M. (1994) Improvements in the safety of foods by SH-containing amino acids and peptides. A review. *J. Agric. Food Chem.* 42, 3–11.
4. Hajós, Gy., Gelencsér, É., Blázovics, A., Fehér, J. (unpublished)
5. Hajós, Gy., Gelencsér, É., Grant, G., Bardocz, S., Sakhri, M., Duguid, T. J., Newman, A. M., Pusztai, A. (1996) Effect of proteolytic modification and methionine enrichment on the nutritional value of soya albumins for rats. *J. Nutritional Biochemistry* 7, 481–487.
6. Hajós, Gy., Gelencsér, É., Pusztai, Á., Grant, G., Sakhri, M., Bardocz, S. (1995) Biological effects and survival of trypsin inhibitors and the agglutinin from soybean in the small intestine of the rat. *J. Agric. Food Chem.* 43, 165–170.
7. Pellett, P., Young, V. R. (1980) *Nutritional Evaluation of Food Protein*. United Nation University.
8. Pusztai, A. (1991) *Plant Lectins, Chemistry and Pharmacology of Natural Products*. Cambridge University Press, Cambridge.
9. Siemensma, A. D., Weijer, W. J., Bak, H. J. (1993) The importance of lengths in hypoallergenic infant formulae. *Trends in Food Science & Technology* 4, 16.





## L-CARNITINE AS ESSENTIAL METHYLATED COMPOUND IN ANIMAL METABOLISM. AN OVERVIEW\*

M. SZILÁGYI

Research Institute for Animal Breeding and Nutrition, Herceghalom, Hungary

(Received: 1998-10-28; accepted: 1998-11-25)

Certain kinds of N-methylated compounds proved to be essential for animals. L-Carnitine is a small-molecular-weight quaternary amine which occurs naturally in micro-organisms, plants and animals. Generally, plants contain little carnitine compared to animals where especially high levels may be found in heart and skeletal muscle.

The main function of L-carnitine is the translocation of long-chain fatty acids from the extramitochondrial space to the mitochondrial space. It also facilitates the removal from mitochondria of short-chain and medium-chain fatty acids that accumulate as a result of normal and abnormal metabolism. This pathway provides a means to regenerate the intramitochondrial free coenzyme A under conditions where short-chain acyl-CoA esters are produced at a rate faster than they can be utilized.

L-Carnitine is synthesized by most animals but its supplementation can be beneficial under certain condition including insufficient carnitine synthetic enzyme activity, metabolic abnormalities, dietary deficiencies or malnutrition.

Several studies on pigs, fish, foal, quail and broiler chickens demonstrate a growth improvement by feeding extra dietary L-carnitine. It has been also found that L-carnitine supplementation resulted in lowered muscle and liver lipid contents.

Formaldehyde is involved in metabolism, methylation–demethylation processes of these compounds.

*Keywords:* L-Carnitine – animal metabolism – performance – carcass quality – formaldehyde

### INTRODUCTION

Methylated compounds, especially naturally occurring quaternary ammonium compounds constitute a class of metabolites, including such well-known representatives as choline, betaines and carnitine. They are of widespread, probably ubiquitous phylogenetic occurrence. They have evolved as a versatile strategy for adaptation of organisms to fluctuating or stressing environmental conditions.

\* Presented at the 4th International Conference on the Role of Formaldehyde in Biological Systems, July 1–4, 1998, Budapest, Hungary.

Send offprint requests to: Dr. M. Szilágyi, Research Institute for Animal Breeding and Nutrition, H-2053 Herceghalom, P.O. Box 2, Hungary.



During the phylogenesis each of them has been selected to assist in metabolism and/or to interact with specific receptors. Some of them serve to oppose exogenic stress.

L-Carnitine is a small-molecular-weight quaternary amine [ $\beta$ -OH-( $\gamma$ -N-trimethyl-amino)-butyrate] which occurs almost ubiquitously in the biosphere and is probably phylogenetically very ancient, dating back to the evolution of mitochondria. Generally, plants contain little carnitine compared to animals where especially high levels may be found in heart and skeletal muscle [7].

The concentration of carnitine in different species and tissues varies over a wide range and its levels are influenced by age and nutritional status of the animal [1, 10, 20, 34, 44]. The highest concentrations reported have been found in horseshoe crab muscle [13] and rat epididymal fluid [8].

Highest concentrations of carnitine were found in maternal tissues including liver, placenta, kidney, myocardium, and choroid plexus of mice. High retention of tissue carnitine in excess of blood levels suggests the existence of concentrative uptake mechanism. Labelled carnitine was not detectable in either maternal or fetal brain. This suggests that the brain barrier systems limit the access of L-carnitine to the brain. In fetus, the level of carnitine was less than that seen in the maternal tissues, however, the tissue distribution was similar. The fetal tissue carnitine concentration increased with time. These findings suggest that relief of encephalopathy due to toxic organic anions in metabolic disorders following L-carnitine supplementation appears to be peripheral metabolic effects rather than direct access to the central nervous system. However, the physiological role for the concentrative uptake of L-carnitine by the choroid plexus remains to be determined. Transport of carnitine into fetal tissues via placenta further suggests the possibility of prenatal therapy in pregnancies at risk for certain inherited metabolic disorders [21].

In mammalian tissues and body fluids, L-carnitine is present in free and esterified forms. Under conditions of undisturbed intermediary metabolism, the great majority of the carnitine ester in serum and urine are represented by acetylcarnitine. Acetylcarnitine represents about 20–30% of carnitine in serum and about 50% of carnitine in urine. Free carnitine, however, is quantified by about 80% of serum carnitine under normal conditions, with a normal acylcarnitine to free carnitine ratio (AC/FC) of 0.25 [50].

In general, carnitine is low in foods and feeds of plant origin and high in animal ones.

Considering the differing amounts of carnitine and acylcarnitines present in various cells and cell organelles, it is clear that a regulated energy demanding path for uptake and efflux of these metabolites must exist [2].

## BIOSYNTHESIS

Although carnitine is widely distributed in nature, elucidation of the precursors and the pathway for carnitine biosynthesis remained an enigma for many years. Early studies demonstrated that the methyl groups of methionine are incorporated into car-

nitine, but the precursors for the carbon and nitrogen moiety remained unknown, even though it was known that gamma-butyrobetaine could be converted to carnitine. With the discovery that lysine served as a precursor of carnitine in *Neurospora crassa*, documentation of the conversion of protein-bound trimethyllysine to carnitine quickly appeared.

In mammals, lysine is a precursor of carnitine via protein-bound trimethyllysine, in contrast to yeast, where free lysine is methylated via S-adenosylmethionine. Thus, the biosynthesis of carnitine requires two essential amino acids, lysine and methionine, in the presence of ferrous ions and a number of vitamins: ascorbate, niacin and pyridoxine, which are required as cofactors for the enzymes involved in the metabolic pathway of L-carnitine [12, 22, 31, 37].

## FUNCTIONS

A role for carnitine in metabolism was established by Fraenkel and colleagues, when they demonstrated that carnitine is an essential growth factor for larvae of the mealworm, *Tenebrio monitor*. Almost 50 years after its discovery, parallel investigations by Bremer and colleagues and Fritz and colleagues established a role for carnitine in beta-oxidation of long-chain fatty acids [4]. Several roles for carnitine in mammalian metabolism have been proposed, both direct and indirect, most of which involve conjugation of acyl residues to the beta-hydroxyl group with subsequent translocation from one cellular compartment to another [4, 7]. This process affects both availability of activated acyl residues and availability of CoASH.

The main function of L-carnitine is the translocation of long-chain fatty acids from the extramitochondrial space, where they are activated, to the mitochondrial space, where they are oxidized. It also facilitates the removal from mitochondria of short-chain and medium-chain fatty acids that accumulate as a result of normal and abnormal metabolism. This pathway provides a means to regenerate the intramitochondrial free coenzyme A under conditions where short-chain acyl-CoA esters are produced at a rate faster than they can be utilized. These two important functions have been reviewed by several investigators [6, 31, 32].

Carnitine also has a role in detoxification of some of the organic acids, which are produced in excessive amounts in certain organic acidurias [4].

## L-CARNITINE AND ITS METABOLISM IN SKELETAL MUSCLE

Muscles of sheep, cattle and goats contain quite large amounts of carnitine, most of which is present in the free form, under normal conditions.

The total carnitine content of a particular muscle (e.g. *M. biceps femoris*) can vary with the season. This variation is probably related to the different pasture conditions. Pastures are poorer quality in Australian summer conditions and muscle carnitine content is significantly greater than in winter. In this respect the carnitine content of



blood of lactating ewes on a low nutritional plane was found to be significantly greater than those on a high nutritional plane [43].

The total carnitine content of the same muscle varies with age and is considerably less in younger animals. The total carnitine content of *M. biceps femoris* of lambs dramatically rises immediately after birth. Only a very small rise in liver carnitine is seen at the same time. A 2–3-fold increase in muscle carnitine was observed in rats during the first week after birth [5].

This it would appear that the rapid rise in muscle carnitine is not due to biosynthesis in the liver. However, biosynthesis of carnitine in the muscle tissue of the lamb is a possibility. Hydroxylation of gamma-butyrobetaine to carnitine by skeletal muscle from adult sheep has been also demonstrated. Moreover, a significant increase in the carnitine content of muscle tissue occurs in adult diabetic sheep, suggesting possible biosynthesis in this tissue as no significant uptake of carnitine from the blood by skeletal muscle was observed in the severe diabetic state [43].

The most likely source of this muscle carnitine in the lamb is carnitine derived from the mother's milk. Ewes' milk is relatively rich in carnitine and a young lamb could receive 30–40 g of carnitine via the milk during a 10-week lactation [43]. It has been shown that in suckling rats uptake of carnitine from the mother's milk gives rise to an increased carnitine content of liver and heart tissue [35].

The rapid rise of muscle carnitine in the young lamb following birth and its possible derivation from the mother's milk could mean that the new-born lamb is at risk in cold stress situations, for short-term cold stress in goats has been shown to significantly decrease carnitine secretion in the milk [43].

The carnitine content of a particular muscle may vary between breeds in one species (e.g. sheep), although this could be related to differing nutritional conditions. However, more importantly, the carnitine content of muscle appears to be inversely related to the CoA content, those muscles with a very low CoA content containing relatively high levels of carnitine. These observations may suggest that carnitine transport into muscle tissues, or biosynthesis is regulated by the CoA content or vice versa.

The varying carnitine content of muscles with age and in particular the inverse relationship to CoA content raise questions as to the main function of carnitine in muscle tissues. Obviously carnitine is essential for the oxidation of long-chain fatty acids as these form a significant proportion of the metabolizable fuel in ruminant muscle.

However, it is surprising that long-chain acylcarnitine (acid-insoluble fraction) constitutes only a very small fraction of the total carnitine in the muscle of sheep, even in the diabetic state. The high concentration of carnitine present in ruminant muscles could be necessary for the oxidation of acetate. Acetate is a major calorific fuel in ruminants which is mainly oxidized in extra hepatic tissues. However, as acetate readily penetrates the inner mitochondrial membrane, and in muscle tissues of the sheep the acetate thiokinase is located mainly in the mitochondria, in the matrix, the high content of carnitine in ruminant muscles is not necessary for acetate oxidation.

It would seem that a major role of carnitine in muscle tissues, particularly in stress conditions, is in an acetyl buffer system, removing acetyl groups from inside the muscle mitochondria and thereby relieving "acetyl pressure" on the very small amounts of CoA present in muscle, 95% of which is localized in the mitochondria.

A further significant role of carnitine in muscle tissues, particularly in times of metabolic stress, may be in the metabolism of branched-chain amino acids. Skeletal muscle is the main site for the oxidation of branched-chain amino acids in the rat and the capacity to degrade these acids is increased 3–5-fold in fasting and diabetes.

Significant quantities of isobutyryl-carnitine have been found in skeletal muscle of sheep. Isobutyryl-carnitine is derived from the oxidation of valine. There was a slight net uptake of valine by muscles of the hind limb of the sheep, as judged by tarsal venous versus femoral arterial concentrations, in the diabetic state.

## L-CARNITINE EFFECTS ON BLOOD CONSTITUENTS

It has been reported that supplemental carnitine (0.3% of the diet) caused reductions in the concentration of triglycerides and total cholesterol in liver and serum of rats fed on a high-fat diet [42]. They also demonstrated that addition of carnitine to a high-cholesterol diet resulted in decreased levels of cholesterol and lipids in serum, but cholesterol remained higher than in controls. L-Carnitine has also been shown to lower serum triglycerides, phospholipids and free fatty acids in infants and rats [11, 31]. Research with foals has shown that animals fed L-carnitine (10 g per animal per day for 78 days) had lower levels of serum triglycerides and higher concentrations of urea in serum than those of the control group [14]. L-Carnitine has also been reported to decrease plasma total cholesterol concentrations in cholesterol-fed rabbits [41].

Studies on fish have demonstrated that supplemental dietary L-carnitine (between 100 and 250 mg/kg wet fish weight per day) reduced plasma lipids, primarily triglycerides, of sea bass fed on high-fat diets [38]. However, sea bass fed a standard diet, low in fat, without supplemented carnitine had plasma lipid concentrations similar or lower than sea bass fed high-fat diets plus carnitine.

In poultry, Leibetseder [22] observed no effect of supplemental dietary L-carnitine on serum levels of triglycerides or cholesterol of pullets during the early stages of egg production cycle.

## L-CARNITINE EFFECTS ON GROWTH PERFORMANCE

L-Carnitine is synthesized by most animals but its supplementation can be beneficial under certain condition including insufficient carnitine synthetic enzyme activity, metabolic abnormalities, dietary deficiencies or malnutrition [6, 12, 33].

Several studies on pigs, fish, foal, quail and broiler chickens demonstrate a growth improvement by feeding extra dietary L-carnitine. Santulli and D'Amelio [38] demonstrated that supplemental carnitine increased growth of sea bass



(*Dicentrarchus labrax* L.) fry. They also found that carnitine supplementation resulted in lowered muscle and liver lipid contents. Weeden et al. [49] reported that feeding a diet containing 1000 mg carnitine per kg reduced carcass fat and improved feed to gain ratio of weanling pigs. Lettner et al. [23] indicated that feeding diets supplemented with L-carnitine up to 60 mg/kg significantly affected the fatty acid composition of abdominal fat (a marked increase in percent of C18 : 2 fatty acid was noted) and tended to improve fattening performance of broiler chickens. Torreele et al. [45] reported improvements in growth rate and feed conversion and a reduction in body fat of African catfish (*Clarias gariepius*) fed diets supplemented with L-carnitine. Schuhmacher et al. [40] concluded that carnitine seemed effective in improving body weight gain and feed conversion in groups of animals (fish, piglets and quail) fed diets marginally deficient in lysine and methionine plus cystine, respectively. Hausenblasz et al. [14] reported that body weight gain and degree of protein conversion (efficiency of protein utilization) achieved by foals that received (10 g per animal per day) supplemental dietary L-carnitine for 78 days were significantly greater than those of the control group.

In contrast, Cartwright [9] reported that performance of broilers, in terms of body weight, feed consumption, carcass fat and abdominal fat content, was not affected by feeding diet supplemented with 0.5% (5000 mg/kg) L-carnitine of the diet from 5 to 7 wk of age. Likewise, Barker and Sell [3] observed no effect of added dietary L-carnitine, at levels of 0, 50 or 100 mg/kg diet, on performance or carcass composition of broiler chickens and young turkeys fed low- or high-fat diets. Leibetseder [22] investigated the effectiveness of carnitine and its precursors (lysine and methionine) to reduce formation of the abdominal fat in broilers fed diets supplemented with 0 or 5% fat. He found that performance (body weight gain and feed conversion) and abdominal fat content of broilers were not influenced by dietary carnitine (L- or DL-form) at a level of 200 mg/kg diet. He also reported that carnitine concentrations in liver, kidney, heart and certain skeletal muscles significantly increased in response to dietary supplementation of L-carnitine. Other investigators dealing with pigs and fish failed to observe favourable growth responses to supplemental dietary L-carnitine [15, 17, 36]. One can expect that the metabolic impact of dietary supplements to vary with species, age and physiological status of the animal, namely growth, maturity, pregnancy or lactation [31].

## L-CARNITINE EFFECTS ON PERFORMANCE OF BROILER CHICKENS

L-carnitine addition resulted in significant increases ( $P < 0.05$ ) in body weight gains of broilers in the growing period. Abdominal fat contents of 46-day-old broilers were significantly decreased, both as absolute weights ( $P < 0.05$ ) and as percentages of body weight ( $P < 0.01$ ), by added L-carnitine in the growing period [29].

Feeding L-carnitine-supplemented diets of different dietary protein levels to broilers a significant interaction between added L-carnitine and dietary protein level was

noted on body weight gain and feed conversion of broilers from 18 to 32 days of age [26]. Amount and percentage of abdominal fat and ether extract contents of breast meat of 53-day-old broilers were significantly reduced in response to L-carnitine supplementation.

Responses to supplemental dietary L-carnitine of broilers fed diets with different levels of metabolizable energy were investigated [30] from 18 to 53 days of age. Added L-carnitine increased body weight gain and improved feed conversion during the first two weeks of study. Feed conversion was also improved during the fourth week of experiment. Weights of breast yield and thigh meat yield were significantly increased whereas quantity and percentage of abdominal fat were reduced by added L-carnitine. A significant interaction was noted between supplemental dietary L-carnitine and dietary energy level on body weight gain and feed conversion during the second wk of study.

### L-CARNITINE EFFECTS ON LAYING PERFORMANCE

Leibetseder [22] investigated whether the supplementation of a commercial layers' ration with either 500 mg L-carnitine or 500 mg nicotinic acid or both per kg reduces the cholesterol concentration in the egg yolk. He found that dietary treatments had no effect on feed intake, egg production, body weight or concentrations of yolk or serum cholesterol. In another trial in the same report, Leibetseder [22] found that egg hatchability increased from 83% to 87% and from 82.4% to 85.3% when broiler breeders were fed on diets supplemented with L-carnitine at levels of 50 and 100 mg/kg diet, respectively.

Performance, certain parameters of egg quality and composition of egg of pullets fed L-carnitine supplemented diets from 18 to 29 wk of age were investigated [28]. Albumen quality was improved by added L-carnitine. Yolk index was improved after 7 wk of supplementation. Concurrently, absolute and relative weights of egg yolk were decreased while percentage of egg white increased in response to added L-carnitine. After 11 wk of feeding L-carnitine, eggs produced by the treated group contained smaller yolks than those of control. All other criteria were not affected by L-carnitine. It was concluded that L-carnitine had positive effects on interior egg quality during the early stages of egg production.

The effects of L-carnitine supplementation of a practical layer diet on the performance of laying hens and some parameters of egg quality were studied, for 8 weeks, using 65-week-old hens [27]. Albumen quality was improved, while yolk index and yolk color score were not affected by dietary L-carnitine. The percentage of egg white increased and that of egg yolk decreased in response to dietary supplementation of L-carnitine. Dietary L-carnitine did not influence laying performance (egg production rate, mean egg weight, daily feed intake, daily egg mass and feed conversion) or external egg quality measured by egg weight, egg shape index or by egg shell quality, either measured directly as shell breaking strength or indirectly as shell weight, shell thickness or shell weight per unit surface area. Based on the



results reported herein, L-carnitine had a beneficial effect on albumen quality and could modify the components of the edible part of the egg during the late laying period.

## PUTATIVE MECHANISMS OF ACTION OF L-CARNITINE

It is known that S-adenyl-L-methionine (SAM) serves as a methyl donor in all transmethylation reactions [18, 24], including the fully N<sup>ε</sup>-methylation of L-lysine in polypeptide bound [25]. In mammals, the free N<sup>ε</sup>-trimethyl-L-lysine is the precursor of L-carnitine. According to recent investigations, formation of formaldehyde (HCHO) from S-methyl group of SAM is linked to the enzymatic transmethylation of different substances [16, 47, 48]. This observation brings into question the existence of a methyl cation or methyl radical in the enzymatic transmethylation reaction, clearly relating to the formation of HCHO from the methyl moiety of SAM.

It is better known that during the demethylation process, HCHO and a demethylated compound can be formed [19]. As a result of heat shock, the level of three potential HCHO generators (trigonelline, choline and trimethyl lysine) moderately decreased [46].

The measurable HCHO level is dramatically elevated in parts of water melon (*Citrullus vulgaris* L.) immediately after a nonlethal infection with *Fusarium oxysporum*. At the same time the level of some quaternary ammonium compounds, as potential HCHO generators, are considerably decreased [39].

It is obvious from these results that HCHO measurable can originate from methylation and demethylation processes, not as a side product, but as a basic and indispensable substance required for different biological systems. These statements may be valid for L-carnitine as fully N-methylated compound. In this case the formation of methyl groups takes place originally in the case of L-lysine bound in polypeptide chain. However, there is a possibility for the formation of HCHO from the N-methyl groups of L-carnitine by means of demethylases or special peroxidases.

Another possibility of HCHO formation from N-methyl groups of L-carnitine may be similar to demethylation of choline through the formation of methylamine [52]. Methylamine is an endogenous substrate for SSAO and HCHO, H<sub>2</sub>O<sub>2</sub> and NH<sub>3</sub> can be formed which are all potentially cytotoxic [51].

## REFERENCES

1. Alhomida, A. S., Duhaime, A. S., Al-Jafari, A. A., Junaid, M. A. (1995) Determination of L-carnitine, acylcarnitine and total carnitine levels in plasma and tissues of camel (*Camelus dromedarius*). *Comp. Biochem. Physiol.* 111B, 441–445.
2. Anthoni, U., Christophersen, C., Hougaard, L., Nielsen, H. (1991) Quaternary ammonium compounds in the biosphere. – An example of a versatile adaptive strategy. *Comp. Biochem. Physiol.* 99B, 1–18.
3. Barker, D. L., Sell, J. L. (1994) Dietary carnitine did not influence performance and carcass composition of broiler chickens and young turkeys fed low- or high-fat diets. *Poultry Sci.* 73, 281–287.

4. Bieber, L. L. (1988) Carnitine. *Ann. Rev. Biochem.* 57, 261–283.
5. Borum, P. R. (1986) Carnitine function. In: Borum, P. R. (ed.), *Clinical Aspects of Human Carnitine Deficiency*. Pergamon Press, New York, pp. 25–36.
6. Borum, P. R. (1987) Role of carnitine in lipid metabolism. In: Bracco, U., Horisberger, M. (eds) *Lipids in Modern Nutrition*, Nestlé Nutrition, Vevey/Raven Press, New York, pp. 51–58.
7. Bremer, J. (1983) Carnitine. *Ann. Rev. Nutr.* 63, 1420–1480.
8. Brooks, R. G., Hamilton, D. W., Mallek, A. H. (1974) Carnitine and glycerophosphorylcholine in the reproductive tract of the male rat. *J. Reprod. Fertil.* 36, 141–160.
9. Cartwright, A. L. (1986) Effect of carnitine and dietary energy concentration on body weight and body lipid of growing broilers. *Poultry Sci.* 65 (Suppl. 1), Abstr. 21.
10. Curto, M., Piccinini, M., Mioletti, S., Mostert, M., Bruno, R., Ricciardi, M. P., Rinaudo, M. T. (1994) Levels of carnitine and glycogen in rabbit tissues during development. *Int. J. Biochem.* 26, 163–169.
11. Dayanandan, A., Kumar, P., Kalaiselvi, T., Panneerselvam, C. (1994) Effect of L-carnitine on blood lipid composition in atherosclerotic rats. *J. Clin. Biochem. Nutr.* 17, 81–87.
12. Feller, A. G., Rudman, D. (1988) Role of carnitine in human nutrition. *J. Nutr.* 118, 541–547.
13. Frenkel, R. A., McGarry, J. D. (1980) In: *Carnitine Biosynthesis and Functions* (eds) Frenkel, R. A., McGarry, J. D., Academic Press, New York.
14. Hausenblasz, J., Ács, M., Petri, Á., Mézes, M. (1996) Effect of L-carnitine on some metabolic parameters of foals. *Állat. Takar.* 45, 397–403.
15. Hoffman, L. A., Ivers, D. J., Ellersieck, M. R., Veum, T. L. (1993) The effect of L-carnitine and soybean oil on performance and nitrogen and energy utilization by neonatal and young pigs. *J. Anim. Sci.* 71, 132–138.
16. Huszti, S., Tyihák, E. (1986) Formation of formaldehyde from S-adenyl-L-(methyl-<sup>3</sup>H) methionine during enzymatic transmethylation of histamine. *FEBS Letters* 209, 362–366.
17. Ji, H., Bradley, T. M., Tremblay, G. C. (1996) Atlantic salmon (*Salmo salar*) fed L-carnitine exhibit altered intermediary metabolism and reduced tissue lipid, but no change in growth rate. *J. Nutr.* 126, 1937–1950.
18. Katoh, Y. (1990) Changes in the contents of S-adenosyl-methionine and 1-methyl-histidine in Hiproly barley callus after auxin withdrawal. *Agric. Biol. Chem.* 54, 3117–3122.
19. Kedderis, G. L., Hollenberg, P. F. (1983) Peroxidase-catalysed N-demethylation reactions. *J. Biol. Chem.* 259, 663–668.
20. Khan, L., Bamji, M. S. (1979) Tissue carnitine deficiency due to dietary lysine deficiency: Triglyceride accumulation and concomitant impairment in fatty acid oxidation. *J. Nutr.* 109, 24–31.
21. Kim, C. S., Roe, C. R. (1992) Maternal and fetal tissue distribution of L-carnitine in pregnant mice: low accumulation in the brain. *Fundam. Appl. Toxicol.* 19, 222–227.
22. Leibetseder, J. (1995) Studies of L-carnitine effects in poultry. *Arch. Anim. Nutr.* 48, 97–108.
23. Lettner, V. F., Zollitsch, W., Halbmayer, E. (1992) Use of L-carnitine in the broiler ration. *Bodenkultur* 43, 161–167.
24. Paik, W. K., Kim, S. (1980) *Protein Methylation*. Wiley, New York.
25. Paik, W. K., Kim, S. (1990) *Protein Methylation*. CRC Press, Boca Raton.
26. Rabie, M. H., Szilágyi, M., Gippert, T. (1997a) Effects of dietary L-carnitine supplementation and protein level on performance and degree of meatiness and fatness of broilers. *Acta Biol. Hung.* 48, 221–239.
27. Rabie, M. H., Szilágyi, M., Gippert, T. (1997b) Effects of dietary L-carnitine on the performance and egg quality of laying hens from 65–73 weeks of age. *Brit. J. Nutr.* 78, 615–623.
28. Rabie, M. H., Szilágyi, M., Gippert, T. (1997c) Influence of supplemental dietary L-carnitine on performance and egg quality of pullets during the early laying period. *Állattenyésztés és Takarmányozás* 46, 457–468.
29. Rabie, M. H., Szilágyi, M., Gippert, T., Votisky, E., Gerendai, D. (1997d) Influence of dietary L-carnitine on performance and carcass quality of broiler chickens. *Acta Biol. Hung.* 48, 241–252.
30. Rabie, M. H., Szilágyi, M. (1998) Effects of L-carnitine supplementation to diets differing in energy levels on performance, abdominal fat content, and yield and composition of edible meat of broilers. *Brit. J. Nutr.* 80, 391–400.



31. Rebouche, C. J. (1992) Carnitine function and requirements during the life cycle. *FASEB J.* 6, 3379–3386.
32. Rebouche, C. J., Paulson, D. J. (1986) Carnitine metabolism and function in humans. *Ann. Rev. Nutr.* 6, 41–66.
33. Rebouche, C. J., Bosch, E. P., Chenard, C. A., Schabold, K. J., Nelson, S. E. (1989) Utilization of dietary precursors for carnitine synthesis in human adults. *J. Nutr.* 119, 1907–1913.
34. Rinaudo, M. T., Curto, M., Bruno, R., Piccinini, M., Marino, C. (1991) Acid soluble, short chain esterified and free carnitine in the liver, heart, muscle and brain of pre- and post-hatched chicks. *Int. J. Biochem.* 23, 59–65.
35. Robles-Valdes, C., McGarry, J. D., Foster, D. W. (1976) Maternal-fetal carnitine relationships and neonatal ketosis in the rat. *J. Biol. Chem.* 251, 6007–6012.
36. Rodehutsord, M. (1995) Effects of supplemental dietary L-carnitine on growth and body composition of rainbow trout (*Oncorhynchus mykiss*) fed high fat diets. *J. Anim. Physiol. Anim. Nutr.* 73, 276–279.
37. Sándor, A., Kispál, Gy., Kerner, J., Alkonyi, I. (1983) Combined effect of ascorbic acid deficiency and underfeeding on hepatic carnitine level in guinea-pigs. *Experientia* 39, 512–513.
38. Santulli, A., D'Amelio, V. (1986) Effects of supplemental dietary carnitine on growth and lipid metabolism of hatchery-reared sea bass (*Dicentrarchus labrax* L.). *Aquaculture* 59, 177–186.
39. Sárdi, É., Tyihák, E. (1992) Effect of *Fusarium* infection on the formaldehyde cycle in parts of watermelon (*Citrullus vulgaris* L.) plants. In: Tyihák, E. (ed.) *Role of Formaldehyde in Biological Systems* Hungarian Biochemical Society, Budapest, pp. 145–150.
40. Schuhmacher, A., Eissner, C., Gropp, J. M. (1993) Carnitine in fish, piglets and quail. In: Flachowsky, G., Schubert, R. (eds) *Vitamine und weitere Zusatzstoffe bei Mensch und Tier* 4th Symposium, Jena, pp. 407–412.
41. Seccombe, D. W., James, L., Hahn, P., Jones, E. (1987) L-carnitine treatment in the hyperlipidemic rabbit. *Metabolism* 36, 1192–1196.
42. Shimura, S., Hasegawa, T. (1993) Changes of lipid concentrations in liver and serum by administration of carnitine added diets in rats. *J. Vet. Med. Sci.* 55, 845–847.
43. Snoswell, A. M., Henderson, G. D. (1980) Carnitine and metabolism in ruminant animals. In: Frenkel, R. A., McGarry, J. D. (eds) *Carnitine Biosynthesis, Metabolism, and Functions*. Academic Press, New York, pp. 191–205.
44. Szilágyi, M., Lindberg, P., Sankari, S. (1992) Serum L-carnitine concentration in domestic animals. In: Ubaldi, A. (ed.) *Proc. 5th Congr. Int. Soc. Animal Clinical Biochem.*, pp. 389–391.
45. Torreele, E., Sluiszen, A.-van der, Verreth, J. (1993) The effect of dietary L-carnitine on the growth performance in fingerlings of the African catfish (*Clarias gariepinus*) in relation to dietary lipid. *Br. J. Nutr.* 69, 289–299.
46. Tyihák, E., Király, Z., Gullner, G., Szarvas, T. (1989) Temperature-dependent formaldehyde metabolism in bean plants. The heat shock response. *Plant Sci.* 59, 133–139.
47. Tyihák, E., Rozsnyai, S., Sárdi, É., Gullner, G., Trézl, L., Gáborjányi, R. (1994) Possibility of formation of excited formaldehyde and singlet oxygen in biotic and abiotic stress situations. *Acta Biol. Hung.* 45, 3–10.
48. Tyihák, E., Trézl, L., Szende, B. (1998) Formaldehyde cycle, and the phases of stress syndrome. In: Csermely, P. (ed.) *Stress of Life: from Molecules to Man*. Ann. New York Acad. Sciences, 851, 259–270.
49. Weeden, T. L., Nelssen, J. L., Hansen, J. A., Fitzner, G. E., Goodband, R. D. (1991) The effect of L-carnitine on starter pig performance and carcass composition. *J. Anim. Sci.* 69 (Suppl.), Abstr. 105.
50. Winter, S. C., Zorn, E. M., Vance, W. H. (1990) Carnitine deficiency. *Lancet* 1, 981–982.
51. Yu, P. H. (1997): Deamination of methylamine and angiopathy; toxicity of formaldehyde, oxidative stress and relevance to protein glycoxidation in diabetes. *J. Neural. Transm. (Suppl.)* 52, 207–222.
52. Zeisel, S. H., Wishnok, J. S., Blusztajn, J. K. (1983) Formation of methylamines from ingested choline and lecithin. *J. Pharmacol. Exp. Ther.* 225, 320–324.

## ADDITION OF CH<sub>2</sub>O TO ARGININE – A THEORETICAL STUDY BY *AB INITIO* METHOD\*

CORNELIA KOZMUTZA,<sup>1</sup> E. M. EVLETH,<sup>2</sup> L. UDVARDI<sup>1</sup> and J. PIPEK<sup>1</sup>

<sup>1</sup>Physics Institute, Technical University of Budapest, Budapest, Hungary

<sup>2</sup>Laboratoire de Chimie Theorique, Universite P. et M. Curie, Paris, France

(Received: 1998-10-28; accepted: 1998-11-25)

Arginine is an acid possessing a guanidine side group which is protonated at all biological pHs, R–NH–C(=NH<sub>2</sub><sup>+</sup>)–NH<sub>2</sub>. We have performed computations on the neutral species by the *ab initio* method using MINI and 6-31G(d) basis sets. Geometry optimization at the HF SCF level has also been carried out using the 6-31G(d) basis set. We investigated the addition of formaldehyde to both the NH<sub>2</sub>– and H–N=C– sites of the guanidine side group. The calculated exothermicities of the reactions with formaldehyde were found different for the above structures. We are planning to determine the energy barriers for these reactions in the near future.

**Keywords:** Arginine – formaldehyde – *ab initio* method

### INTRODUCTION

The role of formaldehyde in biological systems and processes is expected to be very important by scientists for a long time [2, 8, 10 and references therein]. The theoretical study of the reaction of CH<sub>2</sub>O is, therefore, of interest.

Arginine is an unusual acid possessing an unusual guanidine side group which is protonated at all biological pHs. Except in a kinetic sense, one does not find the neutral form present. Free arginine, not incorporated in a protein, has three pKs (1.8, 9.0 and 13.2, respectively). Our theoretical study aimed to investigate the interaction of the arginine with formaldehyde.

\* Presented at the 4th International Conference on the Role of Formaldehyde in Biological Systems, July 1–4, 1998, Budapest, Hungary.

Send offprint requests to: Dr. Cornelia Kozmutza, Institute of Physics, Department of Theoretical Physics, Technical University of Budapest, Budafoki u. 8, H-1521 Budapest, Hungary.



## MATERIALS AND METHODS

We started with the computations on the neutral species using several basis sets. Accurate evaluations of the pKs is not yet possible. Our calculations were performed using well-known basis sets at the HF SCF level. A complete geometry optimization using the 6-31G(d) basis set was also carried out by one of the authors (E.M.E.).

The main goal is to investigate the addition of formaldehyde to both the  $\text{NH}_2$ - and  $\text{H}-\text{N}=\text{C}$ - sites of the guanidine group. These structures showed no indication of interaction of the added  $\text{HO}-\text{CH}_2$ - group with other parts of the arginine. Because of the large size of the arginine group certain considerations had to be taken into account, namely:

- (a) we used relatively small basis sets,
- (b) we performed the calculations at the HF SCF level (i.e. the correlation energy contributions have not been calculated).

We did perform calculations, on the other hand, for eliminating the basis set superposition error (BSSE): the energy quantities were corrected by using the well-known counter-poise (CP) method [1] in each case.

In spite of the above restrictions, we expect, that our results obtained for the reactions studied are relevant, as

- (a) the basis sets used are known to give acceptable results for systems and reactions of similar type (see [4–5]),
- (b) the interaction energy calculated at the HF SCF level is expected to cover a dominant part of the total one for interactions of the type studied (see [3 and 6]).

## RESULTS

Our preliminary calculations were performed for the  $\text{CH}_2\text{O}+\text{NH}_3$  system (see several earlier studies on this adduct in ref. 4. and references therein). Some results are collected in Table 1. Two important conclusions can be drawn when looking at the interaction energies calculated at various C–N separations. First, the results obtained by the MINI basis set follow the same trend viz. the C–N separation as the values calculated by the larger, 6-31G(d) basis set. Second, it can be seen in Table 1, that when the 6-31G(d) basis set was used in the calculation, the SCF level covers the dominant part of the interaction energy (the contribution of the correlation energy obtained at the MP2 level, e.g., does not exceed the 10% calculated at the optimized geometry using the 6-31G(d) basis set).

The first calculations for the  $\text{CH}_2\text{O}$  + arginine structures (for both Adducts) were performed using the MINI basis set. It was not expected that numerically relevant results will be obtained for the interaction energies. The differences, however, calculated for Adduct I (i.e. arginine +  $\text{CH}_2\text{O}$  to the  $\text{NH}_2$ -C- site) and for Adduct II (i.e. arginine +  $\text{CH}_2\text{O}$  to the  $\text{H}-\text{N}=\text{C}$ - site) should be demonstrated. The values obtained affirmed the expectation: the difference between the energies which correspond to Adduct I and Adduct II suggests a slightly larger exothermicity for Adduct II.

*Table 1*  
Interaction energy quantities for the CH<sub>2</sub>O + NH<sub>3</sub> system with and without CP correction  
(values are in atomic units)

	C-N separation	Level of method	Without CP	Including CP
Basis set: MINI	4.0 bohr	SCF	+0.0246	+0.0322
		MP2	-0.0074	-0.0015
	5.0 bohr	SCF	+0.0014	+0.0041
		MP2	-0.0023	-0.0007
	6.0 bohr	SCF	-0.0012	-0.0005
		MP2	-0.0005	-0.0002
Basis set: 6-31G(d)	4.0 bohr	SCF	+0.0278	+0.0292
		MP2	-0.0009	+0.0268
	5.0 bohr	SCF	+0.0037	+0.0038
		MP2	-0.0012	+0.0025
	6.0 bohr	SCF	-0.0043	-0.0010
		MP2	-0.0035	-0.0015
	Optimized	SCF	-0.0058	-0.0043
		MP2	-0.0042	-0.0041

The calculations for Adduct I and Adduct II were performed by using basis set 6-31G(d) at the geometry optimized structures and the following results were obtained. The values obtained unambiguously suggest that the exothermicity for Adduct II is about 30% larger than for Adduct I. The binding of the CH<sub>2</sub>O to arginine (for both structures) is furthermore about three times larger than that found for the CH<sub>2</sub>O+NH<sub>3</sub> system (for the basis sets used).

The coordinates for the arginine are listed in Table 2. The structure of the arginine is given in Fig. 1, while Fig. 2 demonstrates Adduct I and Fig. 3 shows Adduct II, respectively.



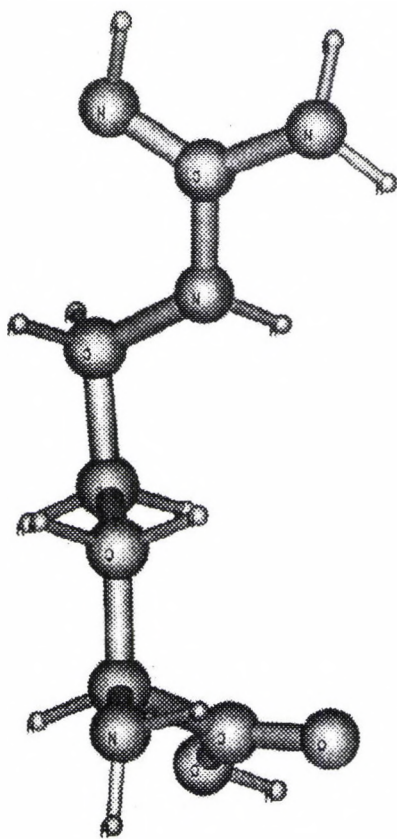


*Fig. 1.* The structure of the arginine

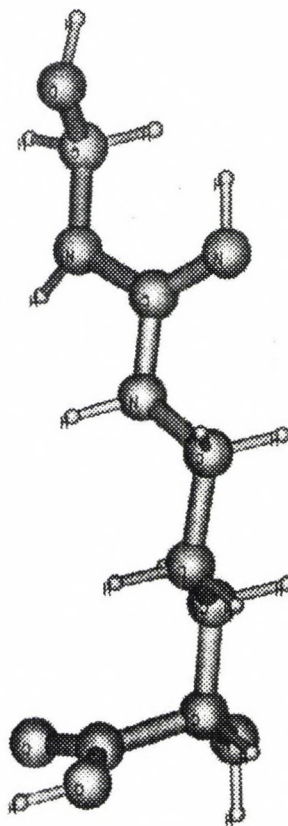


*Fig. 2.* The structure of Adduct I  
(addition of CH<sub>2</sub>O to the NH<sub>2</sub>- site of arginine)

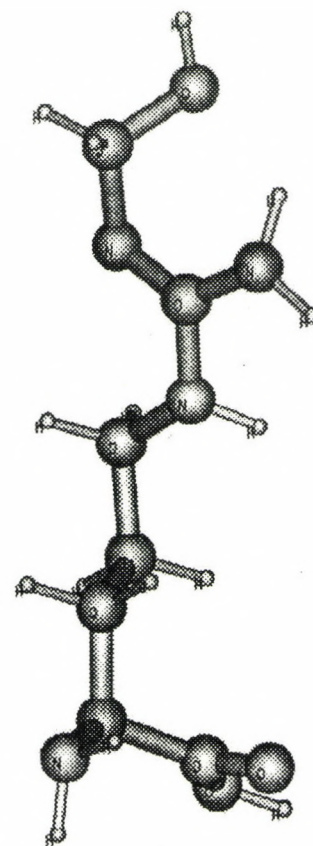


*Fig. 3.* The structure of Adduct II (addition of  
CH<sub>2</sub>O to the H-N=C- site of arginine)

Table 2  
Geometrical structure of the arginine molecule

Center number	Atomic number	Coordinates (Angstroms)		
		X	Y	Z
1	7	-3.826517	1.501596	0.441325
2	6	-3.373384	0.242009	0.087688
3	7	-2.033968	0.213075	-0.230733
4	6	-1.431934	-1.032226	-0.672701
5	6	0.085739	-0.895035	-0.767440
6	6	0.752838	-0.635871	0.585733
7	6	2.289042	-0.606452	0.559259
8	6	2.773832	0.511746	-0.353348
9	7	2.780865	-0.452978	1.913649
10	8	2.842079	1.656608	-0.035971
11	8	3.111247	0.092038	-1.569055
12	1	3.382043	0.848164	-2.081874
13	7	-4.062129	-0.816789	0.105475
14	1	-3.238975	2.282536	0.253668
15	1	-4.793513	1.677928	0.287120
16	1	-4.984617	-0.650165	0.461870
17	1	-1.705350	1.020074	-0.715995
18	1	-1.835066	-1.343698	-1.633322
19	1	-1.700889	-1.797076	0.040708
20	1	0.330985	-0.104537	-1.474741
21	1	0.478614	-1.811799	-1.199406
22	1	0.473110	-1.414848	1.286032
23	1	0.397168	0.300438	1.003032
24	1	2.658403	-1.544732	0.164167
25	1	3.779523	-0.528931	1.945302
26	1	2.547397	0.458114	2.260504

## DISCUSSION

The results obtained should be viewed with caution for some reasons. First, a solvent effect could modify the results. Second, not too large basis sets were used. Third, the methods used are not of too high level. Concerning these points of view, however, it should be added, that

(a) the consideration of the correlated level does not seem to exert significant effect on the calculated interaction energy in systems of the same type (see Table 1 and [4]),



(b) similar results to ours were obtained by other authors [7] for the C–N separation in the  $\text{CH}_2\text{O}+\text{NH}_3$  system, e.g., and

(c) several experimental results affirm [9] that the addition of the  $\text{CH}_2\text{O}$  to the arginine is stronger than that found for the  $\text{CH}_2\text{O} + \text{NH}_3$  system. Our results also suggest that the addition of the  $\text{CH}_2\text{O}$  to the arginine leads to larger binding than that obtained for the  $\text{CH}_2\text{O} + \text{NH}_3$  system (where the binding energy does not exceed the 3.5 kcal/mol when calculated by 6-31G(d) basis set).

#### ACKNOWLEDGEMENT

Thanks are due to Professor Kapuy for many valuable discussions. The calculations partly were performed by the support of grants of OTKA (No. T019741 and T024136).

#### REFERENCES

1. Boys, S. F., Bernardi, B. (1970) The calculation of small molecular interactions by the differences of separate total energies. *J. Mol. Phys.* 19, 553–566.
2. Evleth, E. M. (1998) Lecture given at the 4th International Conference on the Role of Formaldehyde in Biological Systems, Budapest.
3. Kozmutza, C., Ozoroczy, Zs., Kapuy, E. (1990) The structure of the  $\text{CH}_2\text{O}-\text{NH}_3$  system. *J. Mol. Structure (Theochem)* 207, 259–268.
4. Kozmutza, C., Evleth, E. M., Kapuy, E. (1991) Interaction energy of formaldehyde with ammonia. *J. Mol. Structure (Theochem)* 233, 139–145.
5. Kozmutza, C., Kapuy, E., Evleth, E. M., Pipek, J., Trézl, L. (1996) Application of the localized representation for studying interaction energies. *Int. J. Quant. Chem.* 57, 775–780.
6. Kozmutza, C., Tfirst, E. (1998) A study of weakly interacting systems in localized representation, including the many-body effect. *Advances in Quantum Chemistry* 31, 231–250.
7. Ospina, E., Villareces, J. L. (1993) Theoretical calculation of the reaction-mechanism between ammonia and formaldehyde. *J. Mol. Structure (Theochem)* 106, 201–209.
8. Scheiner, S., Lipscomb, W. N., Kleier, D. A. (1976) Molecular orbital studies of enzyme activity 2. *J. Am. Chem. Soc.* 98, 4770–4777.
9. Trézl, L. (1998) Personal communication.
10. Tyihák, E., Trézl, L., Rusznák, I. (1980) Spontaneous N-methylation of L-lysine by formaldehyde. *Pharmazie* 35, 19–20.

## FORMALDEHYDE CYCLE AND THE NATURAL FORMALDEHYDE GENERATORS AND CAPTURERS\*

E. TYIHÁK,<sup>1</sup> L. ALBERT,<sup>2</sup> ZS. I. NÉMETH,<sup>2</sup> GY. KÁTAY,<sup>1</sup>  
ZS. KIRÁLY-VÉGHÉLY<sup>3</sup> and B. SZENDE<sup>4</sup>

<sup>1</sup>Plant Protection Institute, Hungarian Academy of Sciences, Budapest, Hungary

<sup>2</sup>Institute for Chemistry, University of Sopron, Sopron, Hungary

<sup>3</sup>Research Institute for Viticulture and Enology of Agricultural Ministry,  
Experimental Wine Cellar, Budapest, Hungary

<sup>4</sup>Institute of Pathology and Experimental Cancer Research, Semmelweis University of Medicine,  
Budapest, Hungary

(Received: 1998-10-28; accepted: 1998-11-25)

S-adenosyl-L-methionine serves as a methyl donor in virtually all of the vast number of enzymatic transmethylation reactions including DNA methylation. On the basis of our former experiences we questioned the formation of a methyl cation or methyl radical in the enzymatic transmethylation reactions. The formation of formaldehyde from the methyl moiety of S-adenosyl-L-methionine has been demonstrated. It became increasingly evident that there is a formaldehyde cycle in biological systems in which the formation of the methyl group of L-methionine takes place through formaldehyde and the formation of formaldehyde from S-adenosyl-L-methionine is linked to different enzymatic transmethylation reactions. It is also known that during demethylation processes both formaldehyde and demethylated compound can be formed. The abnormalities of the originally controlled formaldehyde cycle and the uncontrolled enzymatic production of formaldehyde from endogenous and/or exogenous substrates may be potential risk factors in pathogenesis of different disorders. The formaldehyde generator and capturer molecules may potentially normalise these abnormal processes.

*Trans*-resveratrol (trans-3,5,4'-trihydroxystilbene), which is as phytoalexin, occurs naturally in grapes and a variety of medicinal plants. According to our present observations it is a natural concentration-dependent formaldehyde capture molecule. It would seem that elimination of the uncontrolled formaldehyde with resveratrol may exert a double effect in biological systems. The elimination of formaldehyde with resveratrol (first step) may cause a cardioprotective effect and the reaction products between resveratrol and formaldehyde (second step) may act as a chemopreventive factor against cancer.

**Keywords:** Betaines – cardioprotective effect – chemoprevention – formaldehyde – formaldehyde cycle – resveratrol

### INTRODUCTION

Formaldehyde (HCHO) is a common environmental pollutant found in tobacco smoke, many occupational settings, certain forms of home insulations and consumer products and as a component of exhaust from diesel and gasoline combustion [4, 46]. It has also been reported that formaldehyde could be both genotoxic and carcinogenic

\* Presented at the 4th International Conference on the Role of Formaldehyde in Biological Systems, July 1–4, 1998, Budapest, Hungary.

Send offprint requests to: Dr. E. Tyihák, Plant Protection Institute, Hungarian Academy of Sciences, P.O. Box 102, H-1525 Budapest, Hungary.



[13, 14, 23, 31]. HCHO is also formed within the cell by oxidative demethylation (via demethylases and special peroxidases) of a variety of endogenous and/or exogenous N-, O- and S-methyl compounds [7, 10, 19, 20], and by uncontrolled enzymatic production of HCHO from endogenous and/or exogenous substrates may be a potential risk factor in pathogenesis of different clinical disorders [48]. Methylamine and aminoacetone are endogenous substrates for semicarbazide-sensitive amine oxidase (SSAO) [5]. The deaminated products are the HCHO and methylglyoxal, as well as  $\text{H}_2\text{O}_2$  and ammonia, which are all potentially cytotoxic. Excessive SSAO-mediated deamination may directly initiate endothelial injury and plaque formation, increase oxidative stress, which can potentiate oxidative glycation and/or LDL oxidation. HCHO is capable of exacerbating advanced glycation, and thus increase the complexity of protein cross-linking [48, 49].

HCHO and  $\text{H}_2\text{O}_2$ , which can be constantly formed intra- and extracellularly in all cells [15, 22, 45], can interact endogenously, and the very reactive singlet oxygen and excited HCHO [37] are the reaction products [42, 45]. These reactive molecules may be determining factors of disease resistance, however, at the same time they may be potential risk factors.

We have demonstrated that radiolabelled formaldemethone is formed from the radiolabelled methyl group of S-adenosyl-L-methionine (SAM) in the course of enzymatic conversion of histamine to N<sup>ε</sup>-methylhistamine in the presence of dime-done, suggesting that the formation of HCHO is probably linked to the enzymatic transmethylation of histamine [16]. This observation brings into question the existence of a methyl cation or methyl radical in the enzymatic transmethylation reaction [16, 39, 45], and relating this phenomenon to the formation of HCHO from the methyl moiety of SAM.

It is well known that HCHO is a cytotoxic compound. Endogenously formed HCHO, however, is supposedly detoxified at the cellular level via the tetrahydrofolate pathways and oxidised to format and  $\text{CO}_2$  [22]. It would seem that low and non-toxic equilibrium concentrations of HCHO might be maintained in the cell.

All these considerations open a new horizon in understanding earlier controversial results, as well as providing the impetus for studying the HCHO cycle [39, 41, 45] as a fundamental biological pathway system.

### *Theoretical aspects of the formaldehyde cycle*

#### **On the metabolism of SAM**

S-adenosyl-L-methionine (SAM) is formed in a cytosolic enzymatic reaction from L-methionine and ATP. SAM serves as a methyl donor in virtually all of the vast number of enzymatic transmethylation reactions, including DNA methylation [1, 6, 24, 28, 29]. The reaction of SAM with a nucleophilic acceptor molecule results in the formation of S-adenosyl-L-homocysteine (SAH) and the methylated acceptor (Fig. 1).

SAH is further metabolised to cystathionine and homocysteine. SAM can undergo decarboxylation to yield decarboxylated SAM, from which the propylamino moiety forms polyamines and leaves methylthioadenosine. Methylthioadenosine can be reconverted to L-methionine and, with subsequent additional conversion, to ethylene, format,  $\text{CO}_2$  and ammonia [24, 39].

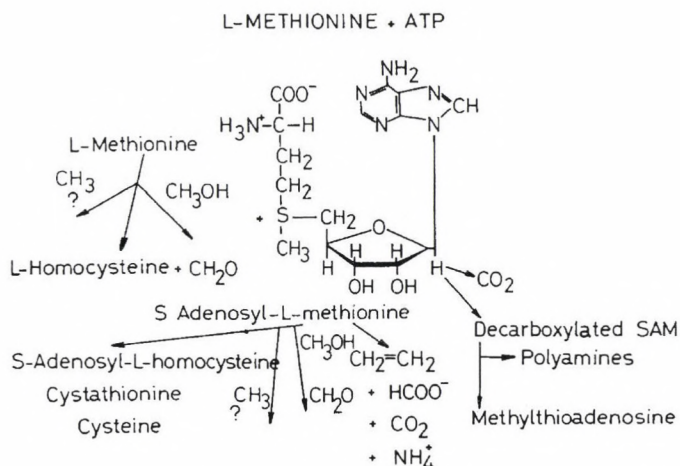


Fig. 1. Metabolism pathways of SAM

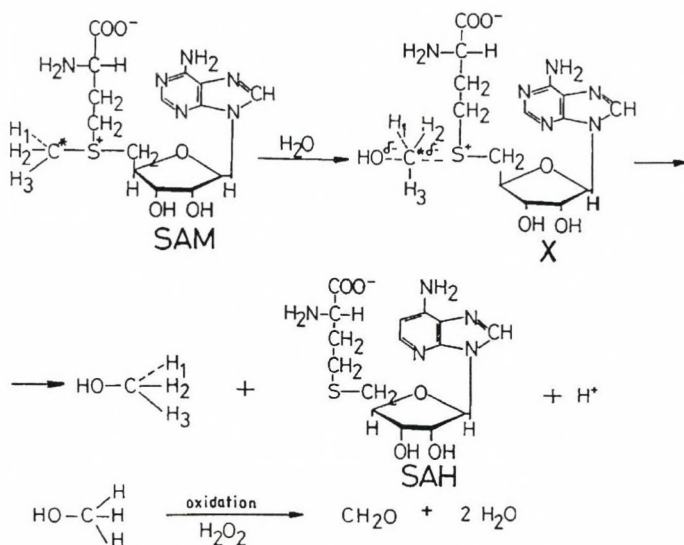


Fig. 2. Demethylation process of SAM



Figures 1 queries the existence of a  $\text{CH}_3$ -group in the enzymatic transmethylation reaction, clearly relating to formation of HCHO from the methyl moiety of SAM.

Figures 2 illustrates the demethylation process of SAM as a sulfonium ion. SAM is unique among known biological sulfonium compounds in possessing three different substituents attached to the sulphur atom; a condition which results in the formation of an optically active centre [6, 24].

As can be seen in Fig. 2, the first biotransformation pathway for SAM containing the S-methyl moiety is the subsequent cleavage of the S-C bond. Hydroxyl ion, as a strongly electronegative group – under appropriate conditions – forces cleavage of the chiral  $\text{CH}_3$  group in the form of methanol, while the remaining bonds of the carbon atom (responding to the effect of the hydroxyl ion electron couple) shift to inversion of configuration [39].

In this demethylation process, X is an intermediate product and the methanol is further metabolised to HCHO.

It should be pointed out that there are earlier reports regarding the formation of methanol from SAM (summarised in reference [28]) however, the authors offered no [28]; explanation for the formation of methanol.

### On the mechanism of enzymatic methylation

It has recently been shown that radiolabelled formaldemethone is formed from the radiolabelled methyl group of SAM in the course of enzymatic conversion of histamine to N-methylhistamine in the presence of dimedone [16]. This observation was the first to reveal that the formation of HCHO from SAM was linked to an enzymatic transmethylation.

From the proposed scheme shown in Fig. 3, it can be seen that the guanidine group of the L-arginine plays a key function in the mechanism of enzyme activity; namely, that transmethylase enzyme protein participates in the process of methylation.

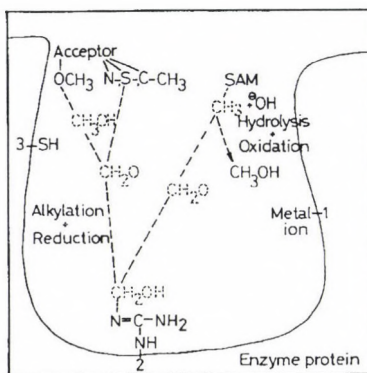


Fig. 3. Schematic drawing of enzymatic methylation in accordance with the more recent observations

In recent years, arginine-specific reagents such as 1,2-cyclohexanedione and phenylglyoxal have been used to demonstrate the existence of essential arginine residues in a number of different enzymes [16].

## New aspects of the synthesis of L-methionine

Synthesis of L-methionine occurs in a number of reactions. It is known that the primary pathway for the breakdown of SAH in eukaryotic cells is via SAH hydrolase to yield adenosine and L-homocysteine (Fig. 1) [6, 50]. In the presence of 5-methyltetrahydrofolate ( $N^5CH_3THF$ ), the L-homocysteine formed is methylated to regenerate L-methionine; hence, the carbon skeleton of L-methionine is recycled several times before being eliminated via cystathione (Fig. 1).

Enzymatic formation of HCHO from  $N^5CH_3THF$  was demonstrated by formation of a tetrahydroisoquinoline ring [24] and in xenobiotic transformation [22]. It has been established that  $N^5CH_3THF$  is not a methyl donor for biogenic amines.

Formation of HCHO from  $N^5CH_3THF$  appears not to be a side reaction of these biotransformations, but rather a process which is very similar to the reaction of SAM with histamine [16]. It is hypothesised that HCHO plays a role in the formation of L-methionine, too.

## On the putative HCHO cycle

Experimental evidence and the aforementioned biochemical arguments suggest that in biological systems a rapid, primary HCHO cycle [39, 41, 45] exists (Fig. 4), in which formation of L-methionine from L-homocysteine and the HCHO-yielding function of SAM are essential components of such fundamental biological pathway system.

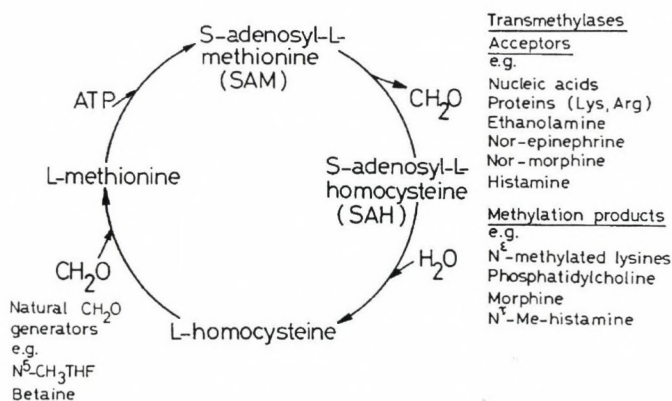


Fig. 4. Biotransformation steps of the putative HCHO cycle



A number of rapid HCHO pathways in different tissues exists through hydroxymethyl groups linked to various acceptor molecules [8, 9, 35, 36, 41, 45].

More detailed knowledge of the biotransformation steps of this putative HCHO cycle will facilitate elucidation of certain perplexing phenomena (e.g. random methylation, mechanisms of mutagenesis, carcinogenesis, resistance, etc.).

## MATERIALS AND METHODS

### *Chemicals*

All chemicals were obtained from Merck Chemical Co. (Darmstadt, Germany) and Sigma Co. (St. Louis, USA) as well as from Reanal Chemical Co. (Budapest, Hungary) and were of analytical purity grade. Formaldemethone was prepared by adding HCHO solution (20 mL of 48% solution) to a solution of dimedone (5 g) in hot ethanol (30 mL) and water (5 mL). The white precipitate was filtered and recrystallized from aqueous methanol (product melting point – 191°C) [32].

### *Microbial, plant and animal material*

The fresh plant and animal tissues and the spores of fungi were frozen in liquid nitrogen, powdered and aliquots (0.25 g) were treated with 0.7 mL methanolic dimedone solution. This suspension was centrifuged at 1000×g for 10 min at 4 °C. The clear supernatant was used for analysis by overpressured layer chromatography (OPLC) [27] or it was diluted with methanol in the ratio 1 : 11 for analysis by high performance liquid chromatography (HPLC), or with methanol in the ratio 1 : 400 for matrix assisted laser desorption/ionisation mass spectrometry (MALDI MS) [2].

### *Reaction mixtures between resveratrol and HCHO*

Aliquot parts of diluted formalin and resveratrol in methanol were mixed at room temperature. The interactions between HCHO and resveratrol were carried out at constant and increasing concentrations of both resveratrol and HCHO.

### *Characteristics of automatic personal OPLC instrument*

This separation instrument is capable of providing high external pressure (max. 5.0 MPa) and has four main parts: holding unit, hydraulic unit, layer cassette and an attached drain valve. The cassette envelops the sealed chromatoplate. On the inside part of the PTFE cover of the cassette which directly contacts the sorben layer there are two directing channels (troughs). One trough at the beginning of the sorbent layer

generates the formation of the straight front line and the other one at the end of the sorbent layer serves to collect the eluent in the case of unexpected overflow.

The computer controlled liquid delivery system has two pump heads, one for the eluent delivery and the other for the hydraulic liquid. All parameters for simple or repeated developments can be given and stored in the software [27].

Chromatograms were evaluated instrumentally using a Shimadzu CS-930 (Kyoto, Japan) dual wavelength TLC scanner [27].

### *Analysis of HCHO as dimedone adduct and as well as resveratrol by TLC and automatic personal OPLC instrument*

Aliquot amounts of plant and animal tissue or spore extracts were applied to the chromatoplates by means of TLC Applicator AS30 (DESAGA Co., Heidelberg, Germany) in nitrogen atmosphere for the measurement of formaldemethone in the dimedone adduct and separately for betaines. In order to limit air access after application of the samples, the application sites were covered totally with a glass plate because the laboratory air contains always a small quantity of HCHO.

The chromatogram was developed immediately after application. Chloroform-dichlormethane (10 : 30, V/V) as mobile phase was used for determining the formaldemethone. For the separation of betaines an eluent mixture containing i-propanol-methanol-0.1M Na-acetate (20 : 3 : 30, V/V) was used [43]. Calibration curves were made in each case.

For the separation of reaction products from the interaction between resveratrol and HCHO conventional TLC technique was used: sorbent layer, silica gel 60 F<sub>254</sub>; eluent, chloroform-methanol mixtures; spots or bands were evaluated visually by UV illumination (254 and 366 nm) and instrumentally by using a Shimadzu CS-930 densitometer (305 nm for resveratrol and oligomers, 295 nm for hydroxy-, hydroxymethyl derivatives).

### *Quantification of formaldemethone and resveratrol derivatives by HPLC*

The HPLC equipment consisted of a Gynkotek (Germering, Germany) model M480 pump fitted with a Rheodyne (California, USA) model 8125 injector with a 20 µL sample loop, connected to column (130×4.6 mm i.d.) filled with Chromspher C18 (5 µm; of particle size) (Chrompack, Bergen op Zoom, Netherlands). The UV detector employed was a Tosoh (Kyoto, Japan) model TSK 6040 UV instrument measuring at  $\lambda = 260$  nm, and the output was passed through an Elektroflex GM (Szeged, Hungary) model EF 2012 ADDA converter and processed using a personal computer. The mobile phase was methanol: 0.01 n hydrochloric acid (77 : 23, V/V; pH 2.60) at a flow rate of 1 mL/min [2].



In the case of resveratrol derivatives the mobile phase was methanol-water (70 : 30, V/V) at flow-rate of 1.0 mL/min and the detection was carried out at 270 nm.

### *Identification of formaldemethone, betaines and resveratrol derivatives by MALDI MS*

An aliquot (0.5  $\mu$ L) of the diluted supernatant mentioned above or reaction product of resveratrol and HCHO was mixed with 0.5  $\mu$ L  $\alpha$ -cyano-4-hydroxycinnamic acid (ACH) matrix [(10 mg ACH/mL in acetonitrile: water (7 : 3, V/V)] directly on a disposable sample slide. The droplet was allowed to dry naturally prior to MALDI MS analysis. The sample preparation for the authentic formaldemethone and others was the same as before but using a standard solution ( $2 \times 10^{-5}$  M) instead of diluted supernatant [2]. The mass spectrometer used in this work was a Finnigan LASERMAT 2000 (Finnigan MAT Ltd., Hennel Hempstead, UK).

## RESULTS AND DISCUSSION

### *HCHO and its potential generators in the biosphere*

Figure 5 illustrates the level of HCHO and its potential endogenous generators in the leaves of a tree species, *Gymnocladus dioicus* (L.) C. Koch depending on the season. It can be seen that the amount of HCHO was very high in spring and autumn leaves and, at the same time, the amount of fully N-methylated compounds, as marker molecules, was very high only in the spring. In this latter case the HCHO originated from methylation processes while in autumn the level of fully N-methylated substances decreased continuously by demethylation process. Such a relationship is practically valid for all tree species [45].

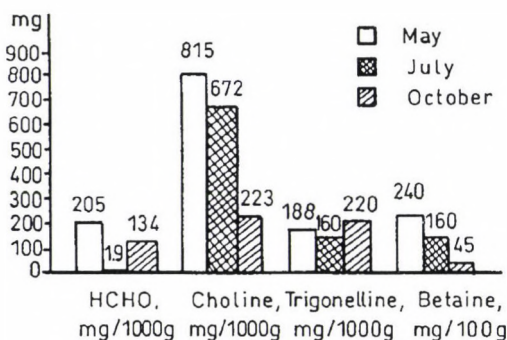


Fig. 5. Change HCHO and its generators in *Gymnocladus dioicus* (L.) C. Koch depending on the season. Details of the experiment are given under Materials and Methods

Figure 6 shows the amount of HCHO as its dimedone adduct in different animal tissues. The measurable quantity of bound HCHO by dimedone from fresh animal tissues depends on the concentration of the dimedone in solution. The level of HCHO produced increases with increased dimedone concentration until a maximum is reached [30].

Under acidic conditions the hydroxymethyl groups are in equilibrium with, for example, iminium, oxonium and thionium ions which, in the presence of dimedone, lead to the formation of formaldemethone [44]. It has to point out that dimedone was always in excess in the reaction mixture. It would seem that HCHO is bound in cells to acceptor molecules (e.g. L-arginine) with different binding force [8, 9, 15, 16, 35].

In Fig. 7 it can be seen that similar relationships are valid for all compared biological systems, that is, HCHO is a normal component of all cells similar to occurrence of  $H_2O_2$ . It was shown in earlier studies that HCHO can be originated from methylation [41] and demethylation [7] as well as from other biological oxidation processes [23, 25, 34, 48]. It is obvious that HCHO is practically under controlled regulation in the formaldehyde cycle [39], however, the uncontrolled enzymatic production of HCHO from endogenous and/or exogenous substrates may exert a risk in pathogenesis of different disorders [47, 48]. Although analysable HCHO may be derived from a number of sources the level of this aldehyde is characteristic for a

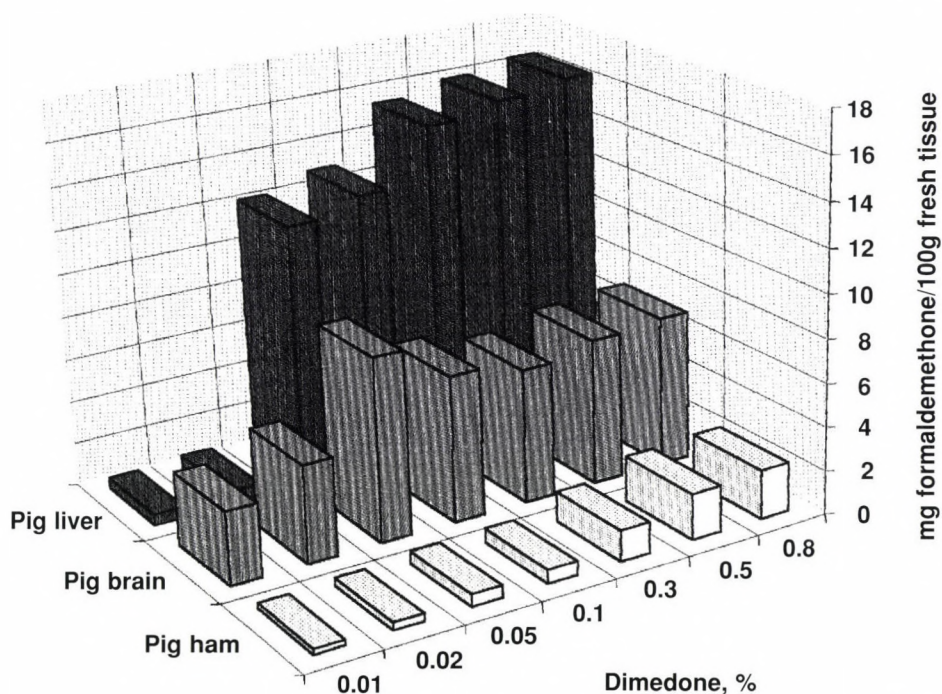


Fig. 6. Effect of dimedone concentration on the amount of HCHO captured from different animal tissues. Details of the experiment are given under Materials and Methods



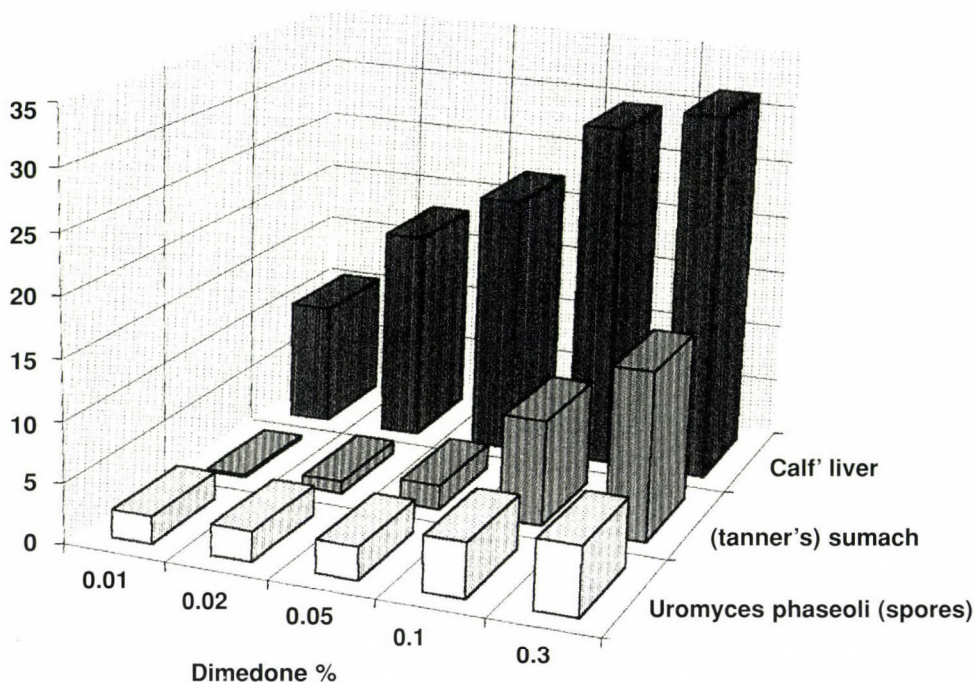


Fig. 7. Change of the amount of HCHO in three totally different biological samples. Details of the experiment are given under Materials and Methods

given system [3]. It is also important to stress that HCHO is not a side product but a basic and indispensable substance required for various biological processes.

Finally, it has to note that under physiological conditions HCHO can be activated by  $H_2O_2$  and, as a result, singlet oxygen and excited HCHO can be simultaneously formed [37, 45]. The invasive (stress situation) or non-invasive (stress-free condition) formation of these excited molecules play a role in disease resistance killing the pathogens [42] however at that time, they also could be potential risk factors.

### *Possible mobilisation of the endogenous HCHO*

We do not know exactly the functions of the endogenous bound HCHO. Are its metabolic [endogenous] pathways influenced by e.g. food constituents? In this paper we report in our preliminary experimental results using a common dietetic substance, resveratrol. Resveratrol, a phytoalexin [17], is well known as a common constituent of the human diet, and it has a considerable cardioprotective [11, 12, 21, 38], as well as a cancer chemopreventive [18, 26] effect.

The *trans*-resveratrol, as a stilbene derivative has a characteristic double bond and the phenolic hydroxyl groups generate electron withdrawal effect, thus this mol-

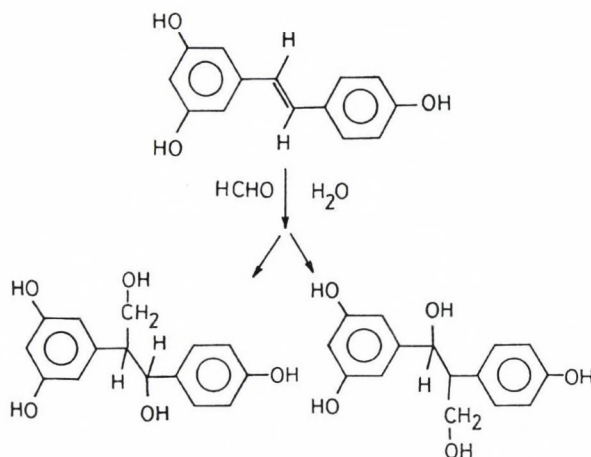


Fig. 8. Supposed mechanism of reaction between resveratrol and HCHO

ecule could be an endogenous HCHO capturer molecule. Figure 8 shows the putative mechanism of reaction between resveratrol and HCHO. It can be seen that there is a possibility for the formation of two isomers of the reaction product.

Using a TLC separation method we isolated a special substance from the reaction mixture of resveratrol and diluted formaline solution which has a characteristic  $m/z$  value of 276.41. This corresponds to 7-hydroxymethyl-, 8-hydroxy-resveratrol and 7-hydroxy-, 8-hydroxymethyl-resveratrol, respectively (these are trivial names of the two isomers). Figure 9 illustrates the separation of two isomers of the hydroxy-, hydroxymethyl-resveratrol by means of a HPLC technique.

As a result of this reaction resveratrol by elimination of HCHO of different origin from coronaria and other vessels may reduce the development of e.g. atherosclerotic plaques. Furthermore, the hydroxy-, hydroxymethyl-resveratrol isomers formed in

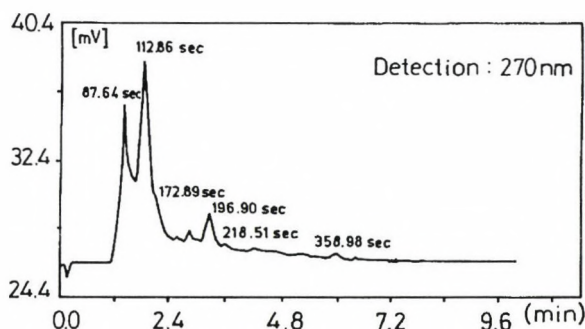


Fig. 9. Separation of hydroxy-, hydroxymethyl-resveratrol isomers by HPLC. Conditions Materials and Methods



this elimination reaction may exert a killing activity to cancer cells and pathogens, similar to other hydroxymethylated substances [36] in other words, this new molecule and similar reaction products may be responsible for the cancer chemopreventive activity of the dietetic resveratrol at three major stages of carcinogenesis as initiation, promotion and progression [18]. The apoptotic effect of resveratrol was also demonstrated [33].

One can conclude from these preliminary results that resveratrol can mobilise a special part of the chemically labile bound HCHO forming thereby several resveratrol derivatives with tumor cell killing activity.

The double effect of resveratrol with the mobilisation of the endogenous HCHO opens new horizons on influencing two important disease groups with a common dietetic substance. Furthermore, these results give an impetus for searching similar endogenous HCHO capturer molecules.

#### REFERENCES

1. Adams, R. L. P., Burdon, R. H. (1985) *Molecular Biology of DNA methylation*. Springer-Verlag, New York, Berlin, Heidelberg, Tokyo.
2. Albert, L., Németh, Zs., Barna, T., Varga, Sz., Tyihák, E. (1998) Measurement of endogenous formaldehyde in the early development stages of European Turkey oak (*Quercus cerris* L.). *Phytochem. Anal.* 9, 227–231.
3. Blunden, G., Carpenter, B. G., Adrian-Romero, Maricella, Yang, M.-H., Tyihák, E. (1998) Formaldehyde in plant kingdom. *Acta Biol. Hung.* 49, 239–246.
4. Bolt, H. M. (1987) Experimental toxicology of formaldehyde. *J. Can. Res. Clin.* 13, 305–309.
5. Boor, P. J., Trent, M. B., Lyes, G. A., Tao, M., Ansari, G. A. S. (1992) Methylamine metabolism to formaldehyde by vascular semicarbaside-sensitive amine oxidase. *Toxicology* 73, 251–258.
6. Borek, E., Salvatore, F., Zappia, V. (eds) (1977) *The Biochemistry of Adenosyl-methionine*. Columbia University Press, New York.
7. Chelvarajan, R. L., Fannin, F. F., Bush, L. P. (1993) Study of nicotine demethylation in *Nicotiana glauca*. *J. Agric. Food Chem.* 41, 858–862.
8. Csiba, Á., Trézl, L., Tyihák, E., Graber, H., Vári, É., Téglás, G., Rusznák, I. (1982) Assumed role of L-arginine in mobilization of endogenous formaldehyde. *Acta Physiol. Acad. Sci. Hung.* 59, 35–41.
9. Csiba, Á., Trézl, L., Tyihák, E., Szarvas, T., Rusznák, I. (1986) N<sup>G</sup>-Hydroxymethyl-L-arginines: new serum and urine components. Their isolation and characterization by ion-exchange TLC. In: Tyihák, E. (ed.) *Proc. Int. Symp. TLC with Special Emphasis on OPLC*. Szeged, Hungary, 1984, Labor MIM, Budapest.
10. Fannin, F. F., Bush, L. P. (1992) Nicotine demethylation in *Nicotiana*. *Med. Sci. Res.* 20, 867–868.
11. Frankel, E. N., Waterhouse, A. L., Kinsella, J. E. (1993) Inhibition of human LDL oxidation by resveratrol. *The Lancet* 341, 1103–1104.
12. Fuhrman, B., Lavy, A., Aviram, M. (1995) Consumption of red wine with meals reduces the susceptibility of human plasma and low-density lipoprotein to lipid peroxidation. *Am. J. Clin. Nutr.* 61, 49–54.
13. Grafström, R. C., Fornace, A., Jr., Harris, C. C. (1984) Repair of DNA damage caused by formaldehyde in human cells. *Cancer Res.* 44, 4323–4332.
14. Grafström, R. C., Curren, R. D., Yang, L. L., Harris, C. C. (1985) Genotoxicity of formaldehyde in cultured human fibroblasts. *Science* 228, 89–91.
15. Heck, H. d'A., Casanova, M., Starm, T. B. (1990) Formaldehyde toxicity – new understanding. *Crit. Rev. Toxicol.* 20, 397–426.

16. Huszti, S., Tyihák, E. (1986) Formation of formaldehyde from S-adenosyl-L-(methyl-<sup>3</sup>H)methionine during enzymic transmethylation of histamine. *FEBS Letters* 209, 362–366.
17. Ingham, J. L. (1976) 3,5,4'-Trihydroxystilbene as a phytoalexin from groundnuts (*Arachis hypogaea*). *Phytochemistry* 15, 1791–1793.
18. Jang, M. J., Cai, L., Udeani, G. O., Slowing, K. V., Thomas, C. F., Beecher, C. W. W. H. S. S., Farnsworth, N. R., Kinghorn, A. D., Mehta, R. J., Moon, R. C., Pezzuto, J. M. (1997) Cancer chemopreventive activity of resveratrol, a natural product derived from grapes. *Science* 275, 218–220.
19. Kapoor, M., Lewis, J. (1987) Heat shock induces peroxidase activity in *Neurospora crassa* and confers tolerance toward oxidative stress. *Biochem. Biophys. Res. Commun.* 147, 904–910.
20. Kedderis, G. L., Hollenberg, P. F. (1983) Peroxidase-catalysed N-demethylation reactions. *J. Biol. Chem.* 259, 663–668.
21. Kerry, N. L., Abbey, M. (1997) Red wine and fractionated compounds prepared from red wine inhibit low density lipoprotein oxidation in vitro. *Atherosclerosis* 135, 93–102.
22. Kucharczyk, N., Yang, Y. T., Wang, K. K., Sofia, R. D. (1984) The formaldehyde-donating activity of N<sup>5</sup>, N<sup>10</sup>-methylene-tetrahydrofolic acid in xenobiotic biotransformation. *Xenobiotica* 14, 667–676.
23. Kuykendall, J. R., Trela, B. A., Bogdanffy, M. S. (1995) DNA-protein crosslink formation in rat nasal epithelial cells by hexamethylphosphoramide and its correlation with formaldehyde production. *Mut. Res.* 343, 209–218.
24. Manchester, J. L., Chemaly, S. L. (1983) S-adenosyl-methionine and ammonium compounds in biochemistry. *South Afr. J. Sci.* 79, 442–444.
25. Meller, E., Rosengarten, H., Friedhoff, A. J., Stebbins, R. D., Silber, R. (1975) 5-Methyl-tetrahydrofolic acid is not a methyl donor for biogenic amines: enzymatic formation of formaldehyde. *Science* 187, 171–173.
26. Mgboneyebi, O. P., Russo, I. H. (1998) Antiproliferative effect of synthetic resveratrol on human breast epithelial cells. *Intern. J. Oncol.* 12, 865–869.
27. Mincsovičs, E., Ferenczi-Fodor, K., Tyihák, E. (1996) Overpressured layer chromatography In: J. Sherma, B. Fried (eds), *Handbook of Thin-Layer Chromatography*. Marcel Dekker, New York, NY, pp. 171–203.
28. Paik, W. K., Kim, S. (1980) *Protein Methylation*. Wiley, New York.
29. Paik, W. K., Kim, S. (eds) (1990) *Protein Methylation*. CRC Press, Boca Raton.
30. Sárdi, É., Tyihák, E. (1998) Relationship between dimedone concentration and formaldehyde captured in plant tissues. *Acta Biol. Hung.* 49, 291–301.
31. Sawinski, E., Sawinski, C. R. (1978) *Aldehydes-Photometric Analysis*, Vol. 5, Formaldehyde Precursors, Academic Press, New York.
32. Spencer, D., Henshall, T. (1955) The kinetics and mechanisms of the reaction of formaldehyde with dimedone (Part I). *J. Am. Chem. Soc.* 77, 1943–1948.
33. Szende, B., Tyihák, E., Trézl, L., Szőke, É., László, I., Kátay, Gy., Király-Véghely, Zs. (1998) Formaldehyde generators and capturers as influencing factors of mitotic and apoptotic processes. *Acta Biol. Hung.* 49, 323–329.
34. Thorndike, J., Beck, W. S. (1977) Production of formaldehyde from N<sup>5</sup>-methyltetrahydrofolate by normal and leukemia leukocytes. *Cancer Res.* 37, 1125–1132.
35. Trézl, L., Csiba, Á., Rusznák, I., Tyihák, E., Szarvas, T. (1981) L-Arginine as an endogenous formaldehyde carrier in human blood and urine. In: Proc. 21st Hung. Annu. Meet. Biochem. Veszprém, Hungary, Hung. Biochem. Soc. Rosdy, B. (ed.), Budapest, 1981. *Chem. Abstr.* 96, 159 825b, 1982.
36. Trézl, L., Szende, B., Csiba, Á., Rusznák, I., Lapis, K. (1986) In vitro and in vivo inhibition of tumor cell proliferation by N<sup>G</sup>-hydroxymethyl-L-arginines as a natural cell component. Abstr. In: 14th Int. Cancer Congr. Akadémiai Kiadó, Budapest.
37. Trézl, L., Pipek, J. (1988). Formation of excited formaldehyde in model reactions simulating real biological systems. *J. Mol. Struct. (Theochem)* 170, 213–223.
38. Turrens, J. F., Lariccia, J., Nair, G. M. (1997) Resveratrol has no effect on lipoprotein profile and does not prevent peroxidation of serum lipids in normal rats. *Free Rad. Res.* 27, 557–562.



39. Tyihák, E. (1987) Is there a formaldehyde cycle in biological systems? In: Tyihák, E., Gullner, G. (eds), *Proc. 2nd Int. Conf. on the Role of Formaldehyde in Biological Systems*, SOTE Press, Budapest, pp. 155–181.
40. Tyihák, E., Szende, B., Trézl, L. (1990) Biological effects of methylated amino acids. In: Paik, W. K., Kim, S. (eds), *Protein Methylation*. CRC Press, Inc., Boca Raton, pp. 363–388.
41. Tyihák, E., Rozsnyay, S., Sárdi, É., Szőke, É. (1992) Formaldehyde cycle and the cell proliferation: plant tissue as a model. In: Tyihák, E. (ed.), *Proc. 3rd Int. Conf. Role of Formaldehyde in Biological Systems – Methylation and Demethylation Processes*, pp. 139–144. Hungarian Biochemical Society, Budapest.
42. Tyihák, E., Rozsnyay, S., Sárdi, É., Gullner, G., Trézl, L., Gáborjányi, R. (1994) Possibility of formation of excited formaldehyde and singlet oxygen in biotic and abiotic stress situations. *Acta Biol. Hung.* 45, 3–10.
43. Tyihák, E., Szőke, É. (1996) Measurement of formaldehyde and some fully N-methylated substances in tissue cultures of *Datura innoxia*. *Plant Growth Regulation* 20, 317–320.
44. Tyihák, E., Blunden, G., Yang, M. H., Crabb, T. A., Sárdi, É. (1996) Formaldehyde, as its dimedone adduct, from *Ascophyllum nodosum*. *J. Appl. Phycol.* 8, 211–215.
45. Tyihák, E., Trézl, L., Szende, B. (1998) Formaldehyde cycle and the phases of stress syndrome. *Ann. N. Y. Acad. Sci.* 851, 259–270.
46. Walker, J. K. (1964) *Formaldehyde*. Kieger, R. E. Publ. Co., Huntington, New York.
47. Yu, P. H., Zuo, D. M. (1995) Formaldehyde produced endogenously via deamination of methylamine; a potential risk factor for initiation of endothelial injury. *Atherosclerosis* 120, 189–197.
48. Yu, P. H. (1997) Deamination of methylamine and angiopathy; toxicity of formaldehyde, oxidative stress and relevance to protein glycooxidation in diabetes. *J. Neural. Transm. (Suppl.)* 52, 207–222.
49. Yu, P. H. (1998) Increase of formation of methylamine and formaldehyde in vivo after administration of nicotine and potential cytotoxicity. *Neurochem. Res.* 23, 1205–1210.
50. Zappia, V., Rydek-Cwick, C. R., Schlenk, F. (1969) The specificity of S-adenosylmethionine derivatives in methyl transfer reactions. *J. Biol. Chem.* 244, 4499–4509.

## FORMALDEHYDE IN THE PLANT KINGDOM\*

G. BLUNDEN,<sup>1</sup> B. G. CARPENTER,<sup>1</sup> MARICELLA ADRIAN-ROMERO,<sup>1,2</sup>  
M-H. YANG<sup>1</sup> and E. TYIHÁK<sup>3</sup>

<sup>1</sup>School of Pharmacy and Biomedical Sciences, University of Portsmouth, Portsmouth, U.K.

<sup>2</sup>Faculty of Pharmacy, University of Los Andes, Mérida, Venezuela

<sup>3</sup>Plant Protection Institute, Hungarian Academy of Sciences, Budapest, Hungary

(Received: 1998-10-28; accepted: 1998-11-25)

Formaldehyde, at its dimedone adduct, formaldemethone, has been detected by thin-layer and high-performance liquid chromatography in extracts of all species tested of marine algae, macrofungi, lichens, bryophytes, pteridophytes, gymnosperms and angiosperms. The yields of formaldehyde recorded in this study varied from 30 µg/g to 4060 µg/g, fresh weight.

**Keywords:** Formaldehyde – formaldemethone – plant kingdom – HPLC analysis – disease resistance

### INTRODUCTION

Betaines and other quaternary ammonium compounds have been shown to confer plants with an increased resistance to pathogen attack. For example, trigonelline has been reported as a potential resistance inducer in plants against obligate biotrophic fungi [4]. Application of  $\gamma$ -aminobutyric acid betaine,  $\delta$ -aminovaleric acid betaine and glycinebetaine to tomato plants resulted in significantly reduced numbers of second stage juveniles of the root-knot nematodes, *Meloidogyne javanica* and *M. incognita*, invading the roots. Significantly reduced egg recovery from the established females was also recorded [11, 12].

A formaldehyde cycle has been proposed for biological systems [7]. All methyl groups are potential precursors and thus betaines are potential sources of formaldehyde, the formation of which has been linked to the induction of disease resistance in plants [5]. If the formaldehyde cycle is a feature of plants, then there should be analyzable amounts of this compound in plant tissues. However, its identification has been restricted to a few angiosperms, for example, Gersbeck et al. [2] and Sardi and

\* Presented at the 4th International Conference on the Role of Formaldehyde in Biological Systems, July 1–4, 1998, Budapest, Hungary.

Send offprint requests to: Professor Dr. G. Blunden, School of Pharmacy and Biomedical Sciences, White Swan Road, Portsmouth, Hampshire, PO1 2DT, U.K.



Tyihák [6] and marine algae [9, 13]. With the latter, formaldehyde was detected, after transformation to formaldemethone, in all species studied.

In this present study, angiosperms, gymnosperms, pteridophytes, bryophytes, macrofungi, lichens and marine algae have been investigated to determine whether they contain detectable amounts of formaldehyde.

## MATERIALS AND METHODS

The plant species studied and their places and dates of collection are given in Table 1. The plant material was carefully sorted to reduce contamination with extraneous material, and observed epibionts were removed by scraping with a knife. As soon as possible after collection, the plant material was stored at  $-20^{\circ}\text{C}$  until required for processing.

### *Isolation and characterization of formaldemethone*

Fresh *Ulva lactuca* (500 g), *Amanita muscaria* (100 g), *Xanthoria parietina* (30 g), *Phyllitis scolopendrium* (100 g), *Thuidium tamariscinum* (100 g), *Taxus baccata* (100 g) and *Hedera helix* (100 g) were separately frozen, powdered in liquid nitrogen and mixed with either 1 L (*U. lactuca*) or 500 mL (remaining species) of 0.2% dimedone solution in methanol. After standing for 24 h, each suspension was filtered and the filtrate concentrated under reduced pressure to remove the methanol. The aqueous residues were extracted with  $2 \times 50$  mL chloroform. The chloroform layers were combined, concentrated to small volume under reduced pressure and subjected to preparative thin-layer chromatography (preparative TLC) using 500  $\mu\text{m}$  layers of silica gel (Merck grade 7749, TLC grade with fluorescent indicator) and chloroform as the development solvent. Examination under UV light at 254 nm revealed a distinct blue band, which was eluted from the silica with chloroform and characterised from proton nuclear magnetic resonance ( $^1\text{H}$  NMR) spectroscopic and electron impact (EI) mass spectrometric data.  $^1\text{H}$  NMR spectra were obtained in deuterated chloroform using a Jeol GSX 270 FT-NMR spectrometer. The EI mass spectra were recorded using a Jeol DX 303 spectrometer coupled to DA 5000 data system.

### *Detection and quantification of formaldemethone by thin-layer and high-performance liquid chromatography*

Frozen plant material of each species (500 mg) was powdered in liquid nitrogen and mixed with 2 mL 0.2% dimedone solution in methanol. As a control, a further sample (500 mg) was treated in the same way, but with 2 mL methanol. After standing for 24 h, the suspensions were centrifuged at 1500 g for 10 min and the clear supernatants separated for examination first by TLC and secondly by high performance

liquid chromatography (HPLC). TLC was performed on 250  $\mu\text{m}$  layers of silica gel (Merck grade 7749, TLC grade with fluorescent indicator) with chloroform as the development solvent. Formaldemethone was detected under UV light as a blue spot.

The content of formaldemethone in every sample was determined using the HPLC method of Adrian-Romero et al. [1], which employed a Hypersil C<sub>18</sub> column and methanol-water (60 : 40) as the mobile phase. Formaldemethone and unreacted dimedone were detected using a UV detector set at 258 nm. Quantification was based on peak height using, as reference, a standard injection of ethyl paraben.

## RESULTS AND DISCUSSION

Samples of one marine alga (*Ulva lactuca*), one fungus (*Amanita muscaria*), one lichen (*Xanthoria parietina*), one pteridophyte (*Phyllitis scolopendrium*), one bryophyte (*Thuidium tamariscinum*), one gymnosperm (*Taxus baccata*) and one angiosperm (*Hedera helix*), when frozen and powdered in liquid nitrogen and mixed with a solution of dimedone in methanol, produced a compound which, when isolated, had identical TLC, HPLC, <sup>1</sup>H NMR spectroscopic and EI mass spectrometric characteristics to formaldemethone [9].

Samples of angiosperms gymnosperms, pteridophytes, bryophytes, lichens, macrofungi and marine algae (five of each) were tested for the presence of formaldehyde, after conversion to formaldemethone, using TLC and HPLC. The compound was detected in the extracts of all species analysed, but was absent from the methanol extracts of these plants. The quantity of formaldemethone present in the extracts of each plant was estimated using an HPLC procedure (Table 1).

Considerable differences between species were recorded for their formaldehyde contents. In this study the highest yield was that from the angiosperm *Cordyline australis* (4060  $\mu\text{g/g}$ ) and the lowest from the gymnosperm *Ephedra equisetina* (30  $\mu\text{g/g}$ ). The results quoted were obtained from single samples. However, we have shown that leaf samples collected at the same time from different parts of the same plant produced widely differing results (*Hedera helix*, collected in March 1998: 1470, 1240, 920, 940, 920, 1240, 1220, 890  $\mu\text{g/g}$ ; *Buddleja davidii*, collected in March 1998: 1140, 1170, 2050, 2280, 2000, 2130, 2210  $\mu\text{g/g}$ ).

Tyihák [7] and Tyihák et al. [8] have proposed that the methyl group of L-methionine is formed via formaldehyde and that this compound, derived from SAM, is linked to different enzymic transmethylation reactions [3, 7, 8]. Formaldehyde pathways in different tissues exist through hydroxymethyl groups linked to various acceptor molecules [10]. It follows from this that formaldehyde should be present in biological systems in detectable amounts. The results obtained demonstrate that this is probably true for all plants.



*Table 1*  
Formaldehyde (as Formaldemethone) concentrations in species of angiosperms, gymnosperms, pteridophytes, bryophytes, lichens, macrofungi and marine algae

Species	Place of collection	Date of collection	Formaldehyde ( $\mu\text{g/g}$ fresh tissue)
ANGIOSPERMAE			
DICOTYLEDONES			
<i>Hedera helix</i>	Havant, Hampshire	January 1998	310
<i>Beta vulgaris</i> ssp. <i>maritima</i>	Langstone, Harbour, Hampshire	January 1998	230
<i>Rumex sanguineus</i>	Havant, Hampshire	January 1998	160
MONOCOTYLEDONES			
<i>Arum maculatum</i>	Havant, Hampshire	January 1998	1290
<i>Cordyline australis</i>	Havant, Hampshire	April 1998	4060
GYMNOSPERMAE			
GINKGOALES			
<i>Ginkgo biloba</i>	Szeged, Hungary	November 1997	610
CONIFERAE			
<i>Abies pinsapo</i>	Cambridge Botanic Garden	November 1997	50
<i>Sequoiadendron giganteum</i>	Cambridge Botanic Garden	November 1997	510

Species	Place of collection	Date of collection	Formaldehyde (µg/g fresh tissue)
TAXALES			
<i>Taxus baccata</i>	Havant, Hampshire	January 1998	260
GNETALES			
<i>Ephedra equisetina</i>	Cambridge Botanic Garden	November 1997	30
PTERIDOPHYTA			
<i>Dryopteris felix-mas</i>	Cambridge Botanic Garden	November 1997	50
<i>Phyllitis scolopendrium</i>	Uppark, W. Sussex	December 1997	310
<i>Azolla filiculoides</i> *	Romsey, Hampshire	January 1998	11
<i>Doodia maxima</i>	Cambridge Botanic Garden	November 1997	80
<i>Polypodium vulgare</i>	Plympton, Devon	January 1998	<10
BRYOPHYTA			
Musci			
<i>Thuidium tamariscinum</i>	Firestone Copse, near Havenstreet, Isle of Wight	January 1998	130
<i>Eurhynchium praelongum</i>	Havant, Hampshire	February 1998	130
<i>Homalothecium sericeum</i>	Bovey Tracey, Devon	February 1998	760
<i>Fontinalis antipyretica</i>	Widecombe-in-the-Moor, Devon	February 1998	690



(Cont. Table 1)

Species	Place of collection	Date of collection	Formaldehyde ( $\mu\text{g/g}$ fresh tissue)
HEPATICAE			
<i>Lunularia cruciata</i>	Havant, Hampshire	September 1998	80
MACROFUNGI			
Basidiomycota			
<i>Agaricus silvicola</i>	Warblington, Hampshire	November 1997	590
<i>Amanita muscaria</i>	Waterlooville Golf Club, Hampshire	November 1997	170
<i>Lycoperdon perlatum</i>	Stansted Woods, Hampshire	November 1997	1090
<i>Coriolus versicolor</i>	Kingley Vale, W. Sussex	January 1998	1290
ASCOMYCOTA			
<i>Daldinia concentrica</i>	Kingley Vale, W. Sussex	January 1998	570
LINCHES			
<i>Hypogymnia physodes</i>	Kingley Vale, W. Sussex	December 1997	460
<i>Xanthoria parietina</i>	Havant, Hampshire	December 1997	380
<i>Evernia prunastri</i>	Pondwell, Isle of Wight	January 1998	270
<i>Ramalina siliquosa</i>	Wembury, Devon	January 1998	310
<i>Lichina pygmaea</i>	Kimmeridge, Dorset	February 1998	1830

Species	Place of collection	Date of collection	Formaldehyde (µg/g fresh tissue)
MARINE ALGAE			
Chlorophyta			
<i>Ulva lactuca</i>	Langstone Harbour, Hampshire	November 1997	1300
PHAEOPHYTA			
<i>Pilayella littoralis</i>	Kimmeridge, Dorset	March 1997	720+
<i>Fucus spiralis</i>	Southsea, Hampshire	April 1997	1220
RHODOPHYTA			
<i>Chondrus crispus</i>	Kimmeridge, Dorset	July 1995	440+
<i>Porphyra leucosticta</i>	Kimmeridge, Dorset	March 1997	1350+

All locations are in the United Kingdom, unless otherwise stated.

\*Co-occurs with the cyanobacterium *Anabaena*.

+ From Tyihak et al. [9]





## REFERENCES

1. Adrian-Romero, M., Blunden, G., Carpenter, B. G., Lucas, S., Tyihák, E. (1998) The use of HPLC for the detection and quantification of formaldehyde in the Pteridophyta. *Acta Biol. Hung.* 49, 303–308.
2. Gersbeck, N., Schönbeck, F., Tyihák, E. (1989) Measurements of formaldehyde and its main generators in *Erysiphe graminis* infected barley plants by planar chromatographic techniques. *J. Planar Chromatogr.* 2, 86–89.
3. Huszti, Z., Tyihák, E. (1988) Formation of formaldehyde from S-adenosyl-L(methyl-<sup>3</sup>H) methionine during enzymatic transmethylation of histamine. *FEBS Letters* 290, 362–366.
4. Kraska, T., Schönbeck, F. (1992) Resistance induction in plants by trigonelline and possible mechanisms. In: Tyihák, E. (ed.) *Proceedings of the 3rd International Conference on Role of Formaldehyde in Biological Systems. Methylation and Demethylation Processes*. Hungarian Biochemical Society, Budapest, pp. 163–168.
5. Manninger, K., Csösz, M., Tyihák, E. (1992) Biochemical immunisation of wheat plants to biotrophic fungi by endogenous, fully N-methylated compounds. In: Tyihák, E. (ed.) *Proceedings of the 3rd International Conference on Role of Formaldehyde in Biological Systems. Methylation and Demethylation Processes*. Hungarian Biochemical Society, Budapest, pp. 157–162.
6. Sardi, E., Tyihák, E. (1992) Effect of *Fusarium* infection on the formaldehyde cycle in parts of water melon (*Citrullus vulgaris* plants). In: Tyihák, E. (ed.) *Proceedings of the 3rd International Conference on Role of Formaldehyde in Biological Systems. Methylation and Demethylation Processes*. Hungarian Biochemical Society, Budapest, pp. 145–150.
7. Tyihák, E. (1987) Is there a formaldehyde cycle in biological systems? In: Tyihák, E. and Gullner, G. (eds) *Proceedings of the 2nd International Conference on the Role of Formaldehyde in Biological Systems*. SOTE Press, Budapest, pp. 155–181.
8. Tyihák, E., Gullner, G., Trézl, L. (1993) Formaldehyde cycle and possibility of formation of singlet oxygen in plant tissue. In: Mózaik, G., Emerit, I., Féher, J., Matkovics, B. and Vincze, Á. (eds) *Proceedings of the International Symposium on Oxygen Free Radicals and Scavengers in the Natural Sciences*. Akadémiai Kiadó, Budapest, pp. 21–28.
9. Tyihák, E., Blunden, G., Yang, M-H., Crabb, T. A., Sárdi, E. (1996) Formaldehyde, as its dimedone adduct, from *Ascophyllum nodosum*. *J. appl. Phycol.* 8, 211–215.
10. Tyihák, E., Rozsnyay, S., Sárdi, E., Gullner, G., Trézl, L., Gáborjányi, R. (1994) Possibility of formation of excited formaldehyde and singlet oxygen in biotic and abiotic stress situations. *Acta Biol. Hung.* 45, 3–10.
11. Wu, Y., Jenkins, T., Blunden, G., Whapham, C., Hankins, S. D. (1997) The role of betaines in alkaline extracts of *Ascophyllum nodosum* in the reduction of *Meloidogyne javanica* and *M. incognita* infestations of tomato plants. *Fundam. appl. Nematol.* 20, 99–102.
12. Wu, Y., Jenkins, T., Blunden, G., von Mende, N., Hankins, S. D. (1998) Suppression of fecundity of the root-knot nematode, *Meloidogyne javanica*, in monoxenic cultures of *Arabidopsis thaliana* treated with an alkaline extract of *Ascophyllum nodosum*. *J. Appl. Phycol.* 10, 91–94.
13. Yang, M-h., Blunden, G., Tyihák, E. (1998) Formaldehyde from marine algae. *Biochem. System. Ecol.* 26, 117–123.

## PLANT TISSUE CULTURE AS A MODEL FOR STUDY OF DIVERSITY IN FORMALDEHYDE BINDING\*

I. LÁSZLÓ,<sup>1</sup> ÉVA SZŐKE,<sup>1</sup> ZS. NÉMETH<sup>2</sup> and L. ALBERT<sup>2</sup>

<sup>1</sup>Institute of Pharmacognosy, Semmelweis University of Medicine, Budapest, Hungary

<sup>2</sup>Institute for Chemistry, University of Sopron, Sopron, Hungary

(Received: 1998-10-28; accepted: 1998-11-25)

The effect of endogenous formaldehyde (HCHO) deprivation with dimedone – as abiotic stress – was investigated on the methylation-demethylation reactions in *Datura innoxia* Mill. callus cultures. The matrix assisted laser desorption/ionization mass spectrometric (MALDI MS) investigation of the culture extracts revealed characteristic differences between the tissues cultivated in light and dark. MALDI MS data show the presence of a precursor molecule and its mono- and tri-hydroxymethyl derivative, only in the cultures maintained in light. The relative amount of the different derivatives changed considerably, as a consequence of dimedone application in the culture medium and during the extraction.

**Keywords:** *Datura innoxia* Mill. – formaldehyde – hydroxymethyl group – matrix assisted laser desorption/ionization mass spectrometry – methylation-demethylation

### INTRODUCTION

The role of HCHO in methylation and demethylation reactions has been studied in several experiments. HCHO can be captured and measured as formaldemethone, which is the dimedone adduct form of this aldehyde [9]. The formation of radiolabelled HCHO during the enzymic conversion of histamine to N<sup>ε</sup>-methyl-histamine is proved [4]. The methylation reactions, including DNA methylation [8] may be an important regulating factor in the mitotic and apoptotic events of cells [11]. During different demethylation processes HCHO and demethylated compound can be formed [2, 3, 5]. Accumulation of endogenous HCHO and reduced level of fully-N-methylated molecules (e.g. trimethyl-L-lysine, choline) could be measured for the effect of biotic and abiotic stress conditions [1, 10, 12].

In *D. innoxia* Mill. callus cultures a high level of HCHO could be measured in young tissues, as a result of methylation reactions [13]. However, in old cultures the

\* Presented at the 4th International Conference on the Role of Formaldehyde in Biological Systems, July 1–4, 1998, Budapest, Hungary.

Send offprint requests to: I. László, Institute of Pharmacognosy, Semmelweis University of Medicine, H-1085 Budapest, Üllői út 26, Hungary. E-mail: laszim@drog.sote.hu.



measurable HCHO amount elevated again which was an aftermath of increased demethylation processes. At the same time the concentration of some fully-N-methylated compounds decreased [13].

In our previous experiment we studied the effect of HCHO deprivation with dimedone – as a special abiotic stress – on the growth of *D. innoxia* Mill. callus cultures [6]. Dimedone in culture medium influenced characteristically the growth of tissues. The results showed that the HCHO concentration of the cultures cultivated in light were significantly higher in dimedone-free and in dimedone-stressed cultures as well [6]. These differences between the cultures cultivated in dark and in the light led us to investigate the molecular basis of this phenomenon, and to find special HCHO precursors in the cultures.

The main purpose of this work is to demonstrate the effect of HCHO deprivation with dimedone on the methylation-demethylation reactions in *D. innoxia* Mill. callus cultures.

## MATERIAL AND METHODS

### *Callus tissues*

The test material was secondary callus tissue isolated from shoots of *D. innoxia* Mill. organized culture. The callus tissues were grown in light (2500 Lux, 12 hours per day) and in dark at 25 °C on AMS solid medium (0.7% agar) containing 30 g l<sup>-1</sup> of sucrose (Reanal), 5.0 mg l<sup>-1</sup> of Ca-pantothenate (Reanal), 4.43 g l<sup>-1</sup> of Murashige and Skoog basal medium [7] (Sigma), 1.0 mg l<sup>-1</sup> of kinetin (Fluka) and 1.0 mg l<sup>-1</sup> of 2,4-D (BDH Chemicals).

In comparison with the control, the applied dimedone concentration was 1000 ppm. The dimedone solution was made up in distilled water at room temperature and added into the culture medium.

Milled freeze dried tissues (0.05 g) were extracted with methanol (96%, 1.2 ml), or with dimedone solution in methanol (0.01%, 1.2 ml). The extracts were centrifuged (6500 min<sup>-1</sup>, 8 min). The supernatant was used for MALDI MS analysis.

### *MALDI MS analysis*

The MALDI mass spectrometer used in this work was a Finnigan LASERMAT 2000 (Finnigan MAT Ltd., Hemel Hempstead, UK). The matrix material was  $\alpha$ -cyano-4-hydroxycinnamic acid (ACH) (Sigma). The sample (0.5  $\mu$ l) was diluted with methanol in ratio 1 : 100, than it was mixed with 0.5  $\mu$ l  $\alpha$ -cyano-4-hydroxy cinnamic acid (ACH) matrix (2 mg/ml in 60% methanol] 40% water) directly on the disposable sample slide. The droplet was allowed to dry naturally to the analysis.

## RESULTS AND DISCUSSION

During the MALDI MS investigations the peak of the matrix material was used for the comparative determination of the amount of different components. The matrix signal can be observed at 384 mass number, which is the peak of the protonated sandwich molecule of the used ACH matrix (Figs 1, 2). The study of MALDI MS spectral data revealed the presence of a molecule in the cultures maintained in light which seems to be a potential HCHO generator. Figures 1A and 1B show the MALDI MS spectra of the extract of control (dimedone-free) *D. innoxia* Mill. callus tissues, cultivated in light. The peak of the protonated precursor molecule can be observed at 142 mass number. At 172 mass number there is the signal of the mono-hydroxymethyl derivative, while the signal at 232 correspond to the tri-hydroxymethyl derivative of the precursor. The tri-hydroxymethyl molecule was the main component after the extraction with methanol. However, after the administration of dimedone-methanol solution the relative amount of the mono-hydroxymethyl derivative increased considerably coupled with decrease of relative amount of the tri-hydroxymethyl molecule. This observation shows that these changes are the result of dimedone application, and of the collection of hydroxymethyl groups. The di-substituted derivative was not detectable.

Figures 2A and 2B show the MALDI MS results of dimedone-stressed (1000 ppm dimedone in culture medium) callus cultures. The relative amount of the tri-hydroxymethyl compound was originally lower, as a result of dimedone application in the culture medium. However, the use of dimedone during extraction decreased its amount again.

Table 1 illustrates the results in summarised form. The amount of the tri-hydroxymethyl molecule decreased and the quantity of the mono-hydroxymethyl derivative

Table 1

Change of relative peak intensity of the hydroxymethyl substituted molecule in *Datura innoxia* Mill. callus cultures (maintained in the light, extracted with methanol 96%, or 0.01% solution of dimedone in methanol)

Mass number	141 (+1)	171 (+1)	201 (+1)	232 (+0)
Assumed structure	X	X-CH <sub>2</sub> OH	X-(CH <sub>2</sub> OH) <sub>2</sub>	X <sup>+</sup> -(CH <sub>2</sub> OH) <sub>3</sub>
relative peak intensity				
Control (Dimedone-free) culture + Methanol	Low	Low	—	High
Control (Dimedone-free) culture + Dimedone solution	Low	High	—	Low
1000 ppm Dimedone in culture medium + Methanol	Low	Medium	—	High
1000 ppm Dimedone in culture medium + Dimedone solution	Low	High	—	Low



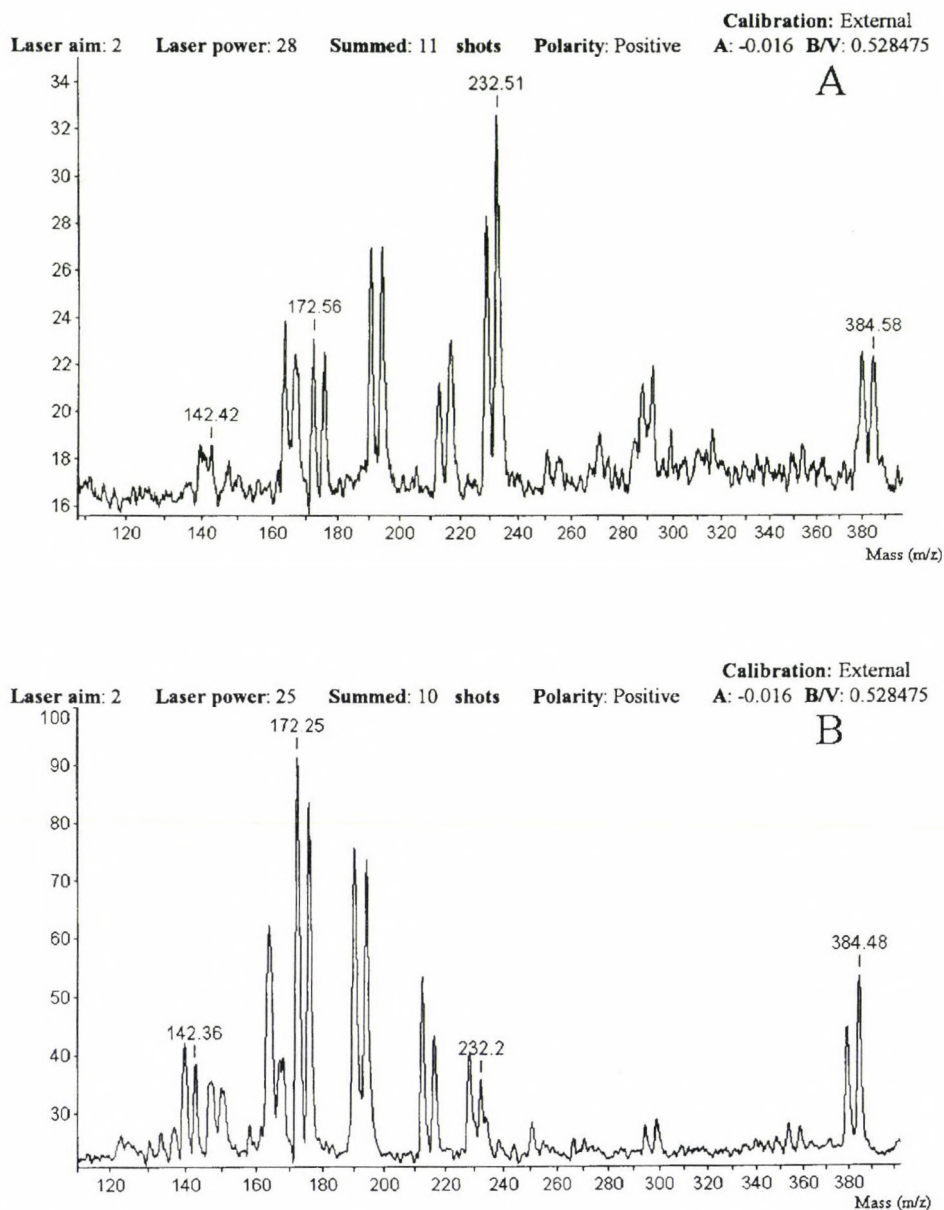


Fig. 1. MALDI MS spectra of *Datura innoxia* Mill. callus tissue (cultivated in light on dimedone-free solid medium). A: extraction with methanol, and B: extraction with 0.01% dimedone solution

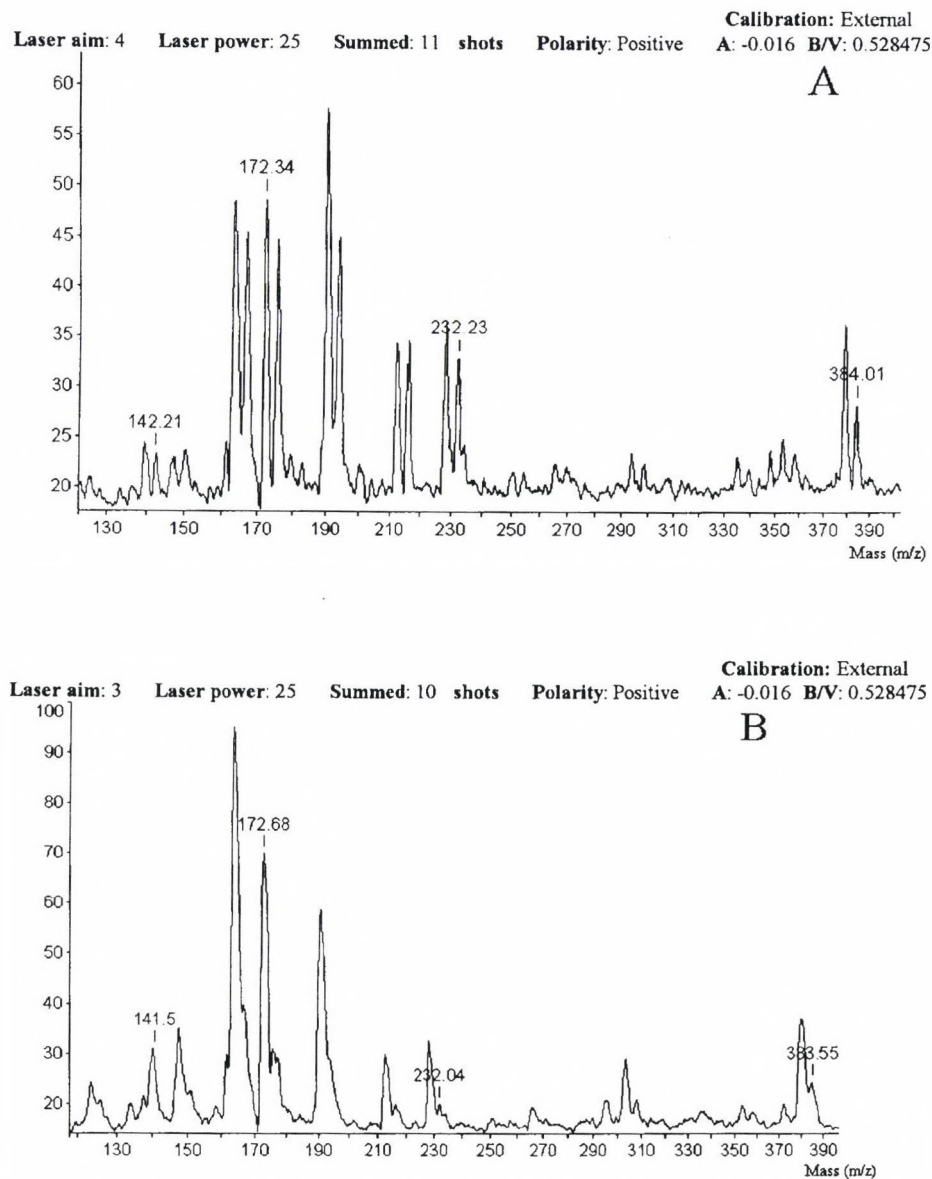


Fig. 2. MALDI MS spectra of *Datura innoxia* Mill. callus tissue (cultivated in light on 1000 ppm dimedone containing solid medium). A: extraction with methanol, and B: extraction with 0.01% dimedone solution



increased in both cases – in dimedone-free, and dimedone-stressed cultures as well – after extraction with dimedone solution. These results were supported by the previously performed quantitative OPLC analysis [6].

It seems that there is a special molecule in *D. innoxia* Mill. callus tissues cultivated in light which is a potential HCHO generator, and these hydroxymethyl groups correspond to the measured, increased concentration of HCHO. These results also sign that there are differences in the methylation-demethylation processes in *D. innoxia* Mill. cultures in dark and in the light.

The identification of this tropine-like molecule is in progress. The HPLC and MALDI MS investigation of the callus tissues confirmed that these cultures did not contain tropane alkaloids in measurable quantities. We plan to make further investigations in determination of alkaloid and HCHO content of genetically modified, tropane alkaloid containing hairy-root cultures in order to study the relationship between the methylation-demethylation reactions and alkaloid biosynthesis.

#### REFERENCES

1. Burgyán, J., Szarvas, T., Tyihák, E. (1982) Increased formaldehyde production from L-methionine-(S-<sup>14</sup>CH<sub>3</sub>) by crude enzyme of TMV-infected tobacco leaves. *Acta Phytopathol. Acad. Sci. Hung.* 17, 11–15.
2. Chelvarajan, R. L., Fannin, F. F., Bush, L. P. (1993) Study of nicotine demethylation in *Nicotiana glauca*. *J. Agric. Food Chem.* 41, 858–862.
3. Fannin, F. F., Bush, L. P. (1992) Nicotine demethylation in *Nicotiana glauca*. *Med. Sci. Res.* 20, 867–868.
4. Huszti, T., Tyihák, E. (1986) Formation of formaldehyde from S-adenosyl-L-[methyl-<sup>3</sup>H]methionine during enzymic transmethylation of histamine. *FEBS Letters*, 209, No. 2, 362–366.
5. Kedderis, G. L., Hollenberg, P. F. (1983) Peroxydase-catalysed N-demethylation reactions. *J. Biol. Chem.* 259, 663–668.
6. László, I., Szőke, É., Tyihák, E. (1998) Relationship between abiotic stress and formaldehyde concentration in tissue culture of *Datura innoxia* Mill. *Plant Growth Regul.* 25, 195–199.
7. Murashige, T., Skoog, F. (1962) A revised medium for rapid growth and bio-assays with tobacco tissue culture. *Physiol. Plant* 15, 473–497.
8. Paik, W. K., Kim, S. (1990) *Protein methylation*, CRC Press, Boca Raton.
9. Sárdi, É., Tyihák, E. (1994) Simple determination of formaldehyde in dimedone adduct form in biological samples by high performance liquid chromatography. *Biomed. Chromatogr.* 8, 313–314.
10. Szarvas, T., János, E., Gáborjányi, R., Tyihák, E. (1982) Increased formaldehyde formation, an early event of TMV infection in hypersensitive host. *Acta Phytopathol. Acad. Sci. Hung.* 17, 7–10.
11. Szende, B., Tyihák, E., Szókán, Gy., Kátay, Gy. (1995) Possible role of formaldehyde in the apoptotic and mitotic effect of 1-methyl-ascorbigen. *Pathol. Oncol. Res.* 1, 38–42.
12. Tyihák, E., Király, Z., Gullner, G., Szarvas, T. (1989) Temperature-dependent formaldehyde metabolism in bean plants. The heat shock response. *Plant Sci.* 59, 133–189.
13. Tyihák, E., Szőke, É. (1996) Measurement of formaldehyde and some fully N-methylated substances in tissue cultures of *Datura innoxia*. *Plant Growth Regul.* 20, 317–320.

# DETERMINATION OF ENDOGENOUS FORMALDEHYDE IN PLANTS (FRUITS) BOUND TO L-ARGININE AND ITS RELATION TO THE FOLATE CYCLE, PHOTOSYNTHESIS AND APOPTOSIS\*

L. TRÉZL,<sup>1</sup> L. HULLÁN,<sup>2</sup> T. SZARVAS,<sup>3</sup> A. CSIBA<sup>4</sup> and B. SZENDE<sup>5</sup>

<sup>1</sup>Technical University of Budapest, Department of Organic Chemical Technology, Budapest, Hungary

<sup>2</sup>National Institute of Oncology, Department of Biochemistry, Budapest, Hungary

<sup>3</sup>Institute of Isotopes, Co., Ltd., Department of Clinical Chemistry, Budapest, Hungary

<sup>4</sup>Veterinary and Food Control Station, Budapest, Hungary

<sup>5</sup>Institute of Pathology and Experimental Cancer Research, Semmelweis University, School of Medicine, Budapest, Hungary

(Received: 1998-10-28; accepted: 1998-11-25)

A very powerful nucleophilic reagent, hydralazine(1-hydrazino-phthalazine) proved to be suitable for determination of the endogenous formaldehyde level in biological samples. It was found that in different plants (vegetables, fruits, especially in red beet, cauliflower, kohlrabi, grapes) is a large amount of releasable endogenous formaldehyde (0.5–1.0 mM) bound to L-arginine mainly in the form of N<sup>G</sup>-tri-hydroxymethyl-L-arginine (TriHMA).

N<sup>G</sup>-hydroxymethyl-L-arginines (HMA) were proved to transfer their hydroxymethyl groups to tetrahydrofolic acid producing N<sup>5</sup>,N<sup>10</sup>-methylene-tetrahydrofolate, the coenzyme of thymidylate synthase. HMA was found to inhibit the cell proliferation of HT-29 cell culture (human colon adenocarcinoma ATCC HT-B 38) causing apoptosis. Photosynthetic experiments produced confirmatory evidences that <sup>14</sup>CH<sub>2</sub>O could be formed in photosynthesis already after 10 seconds of <sup>14</sup>CO<sub>2</sub> fixation in the seedlings of *Zea mays* L. (single cross) and the <sup>14</sup>CH<sub>2</sub>O was immediately trapped by L-arginine mainly as TriHMA.

**Keywords:** Endogenous formaldehyde – plants – L-arginine – apoptosis – photosynthesis – folate cycle

## INTRODUCTION

In the last years many data have been accumulated that there is an endogenous formaldehyde (CH<sub>2</sub>O) level in human and animal organisms and in different plants (mainly in fruits) [5, 8, 10, 13]. The questions are arisen, how the endogenous CH<sub>2</sub>O could be formed and what is its role in biological systems.

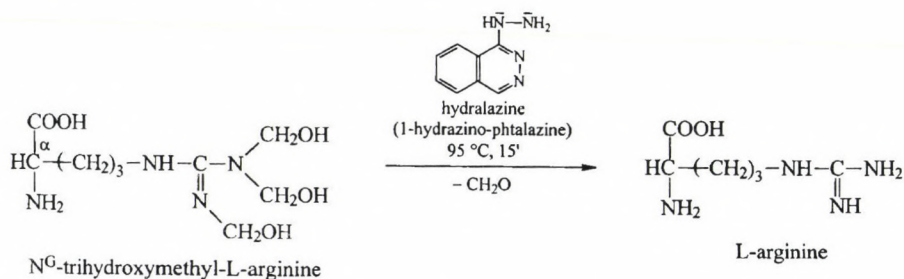
Our research team belonging to several research institutes in Hungary has been dealing with the role of CH<sub>2</sub>O in biological systems for more than two decades. Our

\* Presented at the 4th International Conference on the Role of Formaldehyde in Biological Systems, July 1–4, 1998, Budapest, Hungary.

Send offprint requests to: Dr. L. Trézl, Department of Organic Chemical Technology, Technical University of Budapest, H-1111 Budapest, Műgyetem rkp. 5, Hungary.



team discovered new chemical reactions of  $\text{CH}_2\text{O}$  with amino acids, primary amines, nucleic acids, ascorbic acid, etc. The reactions are novel in organic chemistry as well [7, 8, 11, 12]. We reinvestigated and reevaluated the so-called "Sørensen formol titration" which could take place between amino acids and  $\text{CH}_2\text{O}$  and can be found in textbooks and university handbooks since 1908 up to now. The investigations were carried out with L-lysine and L-arginine. L-Lysine could spontaneously be methylated and formylated by  $\text{CH}_2\text{O}$  on the  $\epsilon$ -amino group, while L-arginine could only be hydroxymethylated by  $\text{CH}_2\text{O}$  on the guanidino group. The hydroxymethylated arginine derivatives could be isolated from reaction mixture [1, 6, 10]. The  $\text{N}^\epsilon$ -methylated-L-lysine derivatives are biologically active compounds, they increase the cell proliferation.  $\text{N}^G$ -hydroxymethylated arginine derivatives (HMA) have been shown to have antiproliferative properties and are nontoxic compounds [9]. The guanidino group of L-arginine can bind one, two, or three molecules of  $\text{CH}_2\text{O}$  and in the reaction mono-, di-, and trihydroxymethylated arginine derivatives could be formed. The hydroxymethylated derivatives of L-arginine are relatively stable compounds. Consequently, L-arginine is suitable to carry the endogenous  $\text{CH}_2\text{O}$  in form of hydroxymethyl group in biological systems. The hydroxymethyl groups are attached to guanidino group by reversible bonds. A very powerful nucleophilic reagent, hydralazine (1-hydrazino-phthalazine) proved to be suitable to eliminate the bound  $\text{CH}_2\text{O}$  from arginine because hydralazine (a hydrazine derivative) is much more nucleophilic compound than the guanidino group of arginine. The statement was proved by model experiments. The removed  $\text{CH}_2\text{O}$  formed with hydralazine *s*-triazolo-(3,4- $\alpha$ )-phthalazine (Tri-P) under mild acidic condition and the reaction products were separated by reversed-phase HPLC [5].



HMA showed apoptotic effect, *in vitro*, on human colon tumor cells (human colon adenocarcinoma ATCC HT-B 38). Based on theoretical considerations HMA was supposed to react with tetrahydrofolate (THF). The reaction between HMA and THF could be proved by thymidylate synthase, as the product of HMA and THF reaction was  $\text{N}^5, \text{N}^{10}$ -methylene-THF, the coenzyme of thymidylate synthase. Photosynthetic experiments produced confirmatory evidences that  $^{14}\text{CH}_2\text{O}$  could be formed in photosynthesis already after 10 seconds of  $^{14}\text{CO}_2$  fixation in the seedlings of *Zea mays* L. (single cross) and the  $^{14}\text{CH}_2\text{O}$  was immediately trapped by L-arginine mainly as TriHMA.

## MATERIALS AND METHODS

### *Reversed phase HPLC*

Reagent grade hydralazine hydrochloride (HP-HCl) was purchased from Sigma, reagent grade  $\text{CH}_2\text{O}$  35% p.a. from Reanal (Budapest, Hungary) and acetonitrile for the mobile phase was of HPLC grade from Carlo Erba (Milan, Italy). All other chemicals used were of analytical grade and from Sigma.

### *Standard solution*

A standard solution of  $\text{CH}_2\text{O}$  was prepared by diluting reagent grade  $\text{CH}_2\text{O}$  in distilled water. For the recovery study, plant samples were spiked with various amounts of  $\text{CH}_2\text{O}$  in the range of 0.025–2  $\text{mg L}^{-1}$ .

Detection of Tri-P in plant extracts was performed as follows: Aliquots of extracts were injected through a 20  $\mu\text{l}$  loop (Rheodyne, USA) onto HPLC columns (250 mm  $\times$  4 mm ID) in tandem. The HPLC column were packed with reversed-phase Nucleosil – C18, 10  $\mu\text{m}$  (Macherey-Nagel, Düren, Germany) maintained at room temperature. The mobile phase was 30% acetonitrile in 0.05 M  $\text{KH}_2\text{PO}_4$  (pH : 4.5) delivered by Waters model 501 HPLC pump, at a flow rate of 1  $\text{ml min}^{-1}$ . Detection was carried out using a Waters 470 spectrofluorometric detector at 237 nm (excitation) and 370 nm (emission). The sensitivity/attenuation of the detector was 100 $\times$ 1. Retention time of the  $\text{CH}_2\text{O}$  adduct product (Tri-P) was 9.15 min.

### *Thymidylate synthase enzyme assay*

Charcoal, 2'-deoxyuridine 5'-monophosphate (dUMP) and dl-L-tetrahydrofolic acid were Sigma products. 5- $^3\text{H}$ -dUMP was purchased from The Radiochemical Centre (Amersham UK).

Thymidylate synthase activity was estimated, essentially as described by Roberts [3]. Reaction mixture (0.15 ml) contained 4.5 nmol 5- $^3\text{H}$ -dUMP (22 kBq), 20 nmol tetrahydrofolate, 20 nmol  $\text{CH}_2\text{O}$ , 1.5  $\mu\text{mol}$  2-mercapto-ethanol, 7.5  $\mu\text{mol}$  NaF, 7.5  $\mu\text{mol}$  Tris-HCl buffer (pH 7.5) and 0.11 ml of cytosol prepared from P388 ascites tumor cells. Tumor transplantation, the check of tumor growth and cytosol preparation were carried out as written before [2]. Reaction was started by adding the cytosol and after incubation (0–30 min) at 37 °C was terminated by addition of 0.5 ml of 3.35% TCA and 0.5 ml of charcoal suspension (55 mg/ml). The samples were centrifuged at 1000  $\times$  g for 15 min. Radioactivity of supernatant was counted in LSC. Nonadsorbable and total radioactivity were determined in appropriate controls. Reaction velocity was linear with time under the conditions employed. The enzyme activities varied by less than 5% in the control.



### *Methods of cell proliferation*

HT-29 cell culture (human colon adenocarcinoma ATCC HTB28) was used. The cell number at plating was  $7 \times 10^4/\text{ml}$ . The culture medium was RPMI(Sigma) + 10% bovine serum (Serva). The cells were cultured in 24-hole Greiner plates (Kremsmünster, Austria) in humidified  $\text{CO}_2$  incubator at 37 °C.

### *Treatment of HT-29 cell culture*

$\text{NG}$ -hydroxymethyl-L-arginine (HMA) was dissolved in RPMI medium and added to the cultures 24 hours after plating. No serum was used (the serum-supplemented medium was discarded before treatment). The dose of HMA was 1, 10, and 100  $\mu\text{g}/\text{ml}$ . Three parallels were used in each doses and control in each point of sampling (24, 48, and 72 hours after treatment). Samples were taken 24, 48 and 72 hours after treatment. Cell count was determined using Buerker's chamber.

### *Investigation of apoptosis*

HT-cells were cultured on cover slips in 6-hole Grainer plates ( $10^5$  cells/ml), using the same culture and treatment methods as described above. At 24, 48 and 72 hours after treatment the cover slips were put into methanol for 5 minutes and stained with hematoxylin and eosin as well as Tunel reaction (Apop-Tag Kit, Oncor, USA) was performed.

### *Photosynthetic $^{14}\text{CO}_2$ fixation*

$\text{Ba}^{14}\text{CO}_3$  (specific radioactivity : 2.03 Gbq/mmol,) was the product of Amersham. The seedlings of *Zea mays* L. (single cross) were cultivated for 12 days for  $^{14}\text{CO}_2$ . It was carried out in the assimilation apparatus previously described [4]. The leaves were exposed to  $^{14}\text{CO}_2$  (40 MBq) for 10 s and 30 s.

In addition, certain experiments involved pretreatment with arginine and dime-done. Maize leaves were enclosed in a glass chamber and illuminated with their cut bases standing to a depth of 5 mm in a 0.57 mM/200  $\mu\text{l}$  aqueous solution of arginine and 0.014 mM/300  $\mu\text{l}$  of dime-done. Experiments were carried out also with maize leaves pretreated in aqueous solution of  $\text{CH}_2\text{O}$  formaldehyde- $^{14}\text{C}$  (380 kBq/200  $\mu\text{l}$  and hydroxymethylated- $^{14}\text{C}$ -arginine (210 kBq/200  $\mu\text{l}$ )).

### *Analysis of $^{14}\text{C}$ -labelled arginine derivatives in plant*

Liquid nitrogen frozen samples were ground and the powder was extracted with 25.0 ml of 50% ethanol and in the case of pretreatment with aqueous solution of dimedone with 25.0 ml of chloroform, respectively. After concentrating of the ethanolic extracts to 2 ml the amino acids thus obtained were separated by ion exchange chromatography on a column of cationic resin and eluted with 10% of  $\text{NH}_4\text{OH}$  then the solution was concentrated and chromatographed on IONEX-25 SA Na cation exchange thin-layer. Distribution of the radioactivity was determined with Berthold scanner. Arginine derivatives (hydroxymethylated- $^{14}\text{C}$ -arginines) were identified with standard hydroxymethylated- $^{14}\text{C}$ -arginine prepare (Fig. 3).

### *Preparation of hydroxymethylated- $^{14}\text{C}$ -L-arginine derivative*

1 mmol of L-arginine was dissolved in 5 ml distilled water and was reacted with 5 mmol of  $^{14}\text{CH}_2\text{O}$  (specific radioactivity : 0.5 mCi/mmol) for 4 hours at 70 °C in a glass apparatus with reflux condenser. The reaction product was precipitated with 50 ml of acetone and was put into a refrigerator and kept there for 5 hours. After sometimes acetone was decanted and the crystalline product was scuffed again with 50 ml of anhydrous acetone. The crystals were filtered, washed with acetone and dried under vacuum. Their specific radioactivity was determined in LSC (Berthold BF 5000, liquid scintillation cocktail : CLINISOSOL<sup>®</sup>, Institute of Isotopes, Budapest, Hungary). Specific radioactivity : 0.4–0.5 mCi/mmol. The chromatographic separation of hydroxymethyl- $^{14}\text{C}$ -L-arginine derivatives were carried out on IONEX-25 SA-Na cation exchange thin-layer and the distribution of radioactivity was determined with Berthold Chromatogram Scanner.

The integrated area of peaks: 1.  $\text{N}^{\text{G}}$ -trihydroxymethyl- $^{14}\text{C}$ -L-arginine (Tri HMA) 67,936 dpm, (43.49%). 2.  $\text{N}^{\text{G}}$ -dihydroxymethyl- $^{14}\text{C}$ -L-arginine (Di HMA) 41 680 dpm (26.62%). 3.  $\text{N}^{\text{G}}$ -monohydroxymethyl- $^{14}\text{C}$ -L-arginine (Mo HMA) 29 618 dpm (18.92%) (see Fig. 3). Preparation of mixture of  $\text{N}^{\text{G}}$ -mono,-di,- and trihydroxymethyl-L-arginine derivatives (HMA), the chromatographic separation,  $^1\text{H}$ ,  $^{13}\text{C}$  (solid phase) NMR investigations, stability studies, Mp determination and C,H,N analysis were discribed elsewhere [1, 6, 9, 10].

## RESULTS AND DISCUSSION

The endogenous  $\text{CH}_2\text{O}$  levels determined by the hydralazine method in various plants (medicinal plants), vegetables and fruits are given in Table 1. In some fruits (banana, grape) the endogenous  $\text{CH}_2\text{O}$  level is very high (>0.5 mmol/kg), however, this level is extremely high (~1 mmol/ kg, or higher than 1 mmol/kg) in some other vegetables (cauliflower, kohlrabi, red beet).



*Table 1*  
Endogenous (releasable) formaldehyde content of different biological samples

The name of biological samples	Formaldehyde content mmol/kg
<i>Vegetables</i>	
carrot (root)	0.22
onion	0.36
potato seed (raw)	0.65
red beet d < 5 cm	0.62
red beet d > 10 cm	0.74
cabbage white	0.73
cabbage red	0.87
cauliflower	0.87
kohlrabi tuber (ripened)	1.03
young kohlrabi tuber	0.21
young kohlrabi leaf	0.85
<i>Budlets</i>	
cherry	0.82
poplar (populus)	0.78
<i>Fruits (ripened)</i>	
water melon (inside)	0.22
water melon (rind)	0.30
apricot	0.32
plum	0.37
apple (winter type)	0.42
tomato	0.44
banana	0.54
sour-cherry	0.60
grape (white, ripened)	0.74
grape young leaf	0.71
wine (white)	0.66
<i>Medicinal plants</i>	
althea root	0.24
mistletoe ( <i>Viscum album</i> )	0.22
common comfrey	0.39

It means that we "eat" every day considerable amount of endogenous CH<sub>2</sub>O with fruits and vegetables.

Biochemical investigations were extended to thymidylate synthase (EC 2.1.1.45). The enzyme catalyzes the reductive methylation of dUMP to thymidine 5',-monophosphate using N<sup>5</sup>,N<sup>10</sup>-methylene-tetrahydrofolate coenzyme. To prove our idea that HMA may react with THF 1.2 μmol HMA was incubated with 1.2 μmol THF at 37 °C, for 1 hour in the presence of 7.5 μmol Tris-HCl buffer pH = 7.5. As a control the same amount of CH<sub>2</sub>O and THF were incubated in the same condition as HMA and THF. The CH<sub>2</sub>O and THF reaction is used for the production of the extremely

labile coenzyme [3]. The reaction mixture of HMA + THF, or HCHO + THF produced considerable amount of labelled product during the thymidylate synthase reaction and the radioactivity values were proportional to the reaction time (Fig. 1). As the Roberts method is highly specific for thymidylate synthase, the results proved that HMA reacted with THF producing  $N^5,N^{10}$ -methylene-tetrahydrofolate coenzyme. Therefore, the experiment proved that THF received a  $C_1$ -fragment from HMA. Vegetables and fruits can thus serve as a  $CH_2O$  generator for us, because endogenous  $CH_2O$  is bound to L-arginine and the  $N^G$ -hydroxymethylated arginine derivatives can carry this  $CH_2O$  to the folate cycle increasing the  $C_1$  pool in the form of  $N^5,N^{10}$ -methylene-tetrahydrofolate.

The main question is that how could endogenous  $CH_2O$  be formed and bound to L-arginine in plants? The photosynthesis was supposed to be responsible for the formation of  $CH_2O$  and for its reaction with L-arginine, because early investigation of Szarvas et al. in 1983 have shown that  $^{14}CH_2O$  was formed from  $^{14}CO_2$  in photosynthesis and the formed  $^{14}CH_2O$  was captured by dimedone [4]. We supposed that L-arginine (which is present in large amount in leaves) is suitable to trap the  $CH_2O$  in leaves. The photosynthetic experiments (see Fig. 2, 10 sec with  $^{14}CO_2$ ) produced

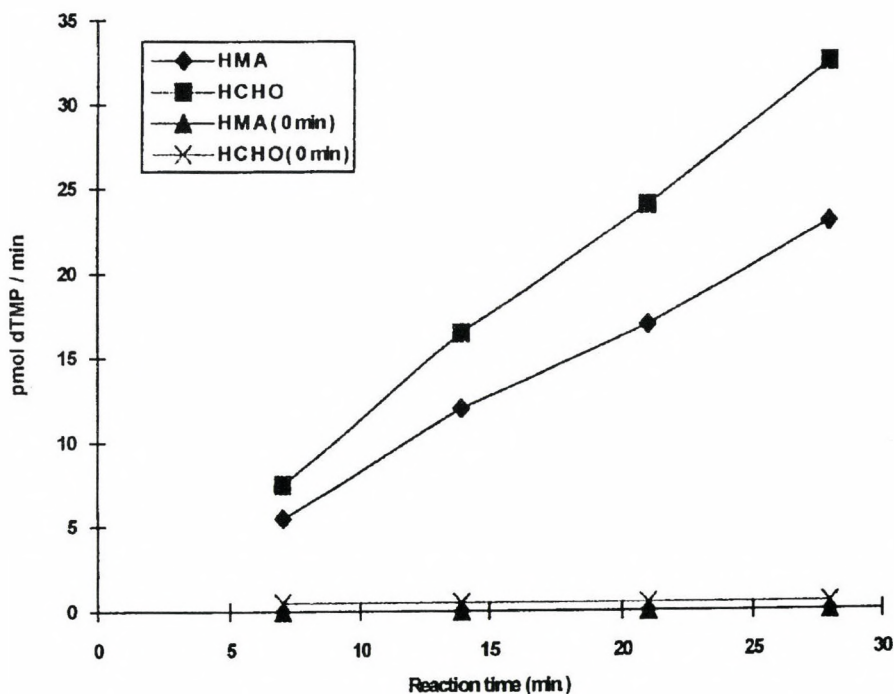


Fig. 1. Reaction of HMA and THF tested by thymidylate synthase assay. 1.2  $\mu$ mol HMA and 1.2  $\mu$ mol THF as well as 1.2  $\mu$ mol HCHO and 1.2  $\mu$ mol THF were incubated in 7.5  $\mu$ mol Tris-HCL buffer (pH = 7.5) for 1 hour and 37 °C



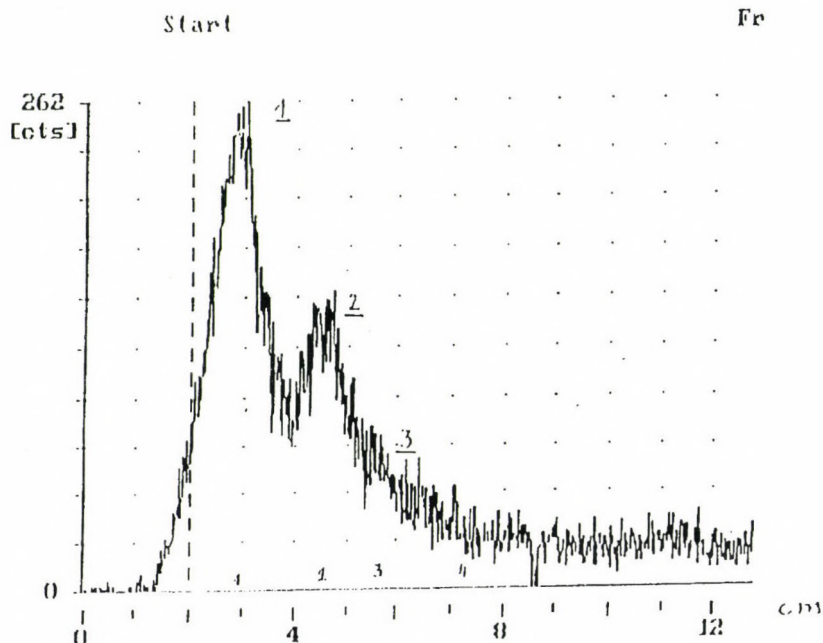


Fig. 2. Radioactivity distribution of  $N^G$ -hydroxymethyl- $^{14}C$ -L-arginines formed in photosynthesis in the seedlings of *Zea mays* already after 10 s of  $^{14}CO_2$  fixation on IONEX 25 SA Na cation exchanging thin layer sheet (Macherey-Nagel). (1 TriHMA, 2 DiHMA, 3 MoHMA)

confirmatory evidence that endogenous  $^{14}CH_2O$  could be formed in maize leaves during  $^{14}CO_2$  fixation almost in short-time experiments (10 sec) and the  $^{14}CH_2O$  is bound to L-arginine mainly as  $N^G$ -trihydroxymethyl- $^{14}C$ -L-arginine (TriHMA) beside DiHMA and MoHMA) (Fig. 2).

Comparing the radioactivity distributions of Fig. 2 and Fig. 3 it can be seen that the distributions are very similar in the model synthetic reaction (Fig. 3) and in leaves (Fig. 2). The only difference is that the hydroxymethyl-arginine derivatives could be formed in a very short-time in leaves, suggesting enzyme(s) catalysis. The results could be explained by the possibility that the  $CH_2O$  may be one of the product of photosynthesis beside or in the Calvin cycle. Calvin excluded the formation of  $CH_2O$  in photosynthesis because of its toxicity. However,  $CH_2O$  could immediately be bound by L-arginine producing the group of biomolecules,  $N^G$ -hydroxymethyl-arginines, which have no toxicity.

Finally, we emphasize the unique properties of  $N^G$ -hydroxymethylated arginines synthesized not only in our laboratory but in leaves, too. They inhibit tumorous cell proliferation [9] and cause apoptosis. Light microscopic study of the fixed and stained HT 29 cell cultures (human colon adenocarcinoma ATCC HTB 38) showed that the decline in cell number after high doses of HMA was due to apoptotic cell death of the cultured HT 29 tumor cells. Considerable amount of decrease in cell

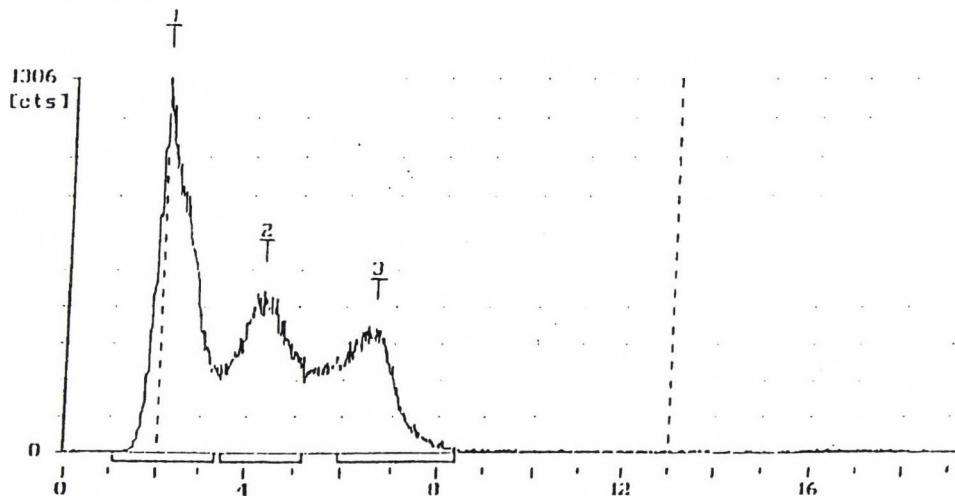


Fig. 3. Radioactivity distribution of  $N^G$ -hydroxymethyl- $^{14}C$ -L-arginines prepared from the reaction mixture of L-arginine and  $^{14}CH_2O$  (specific radioactivity : 0.5 mCi/mmol) (for 4 hours at 70 °C) on IONEX 25 SA Na cation exchanging thin-layer sheet (Macherey-Nagel) (1 TriHMA, 2 DiHMA, 3 MoHMA)

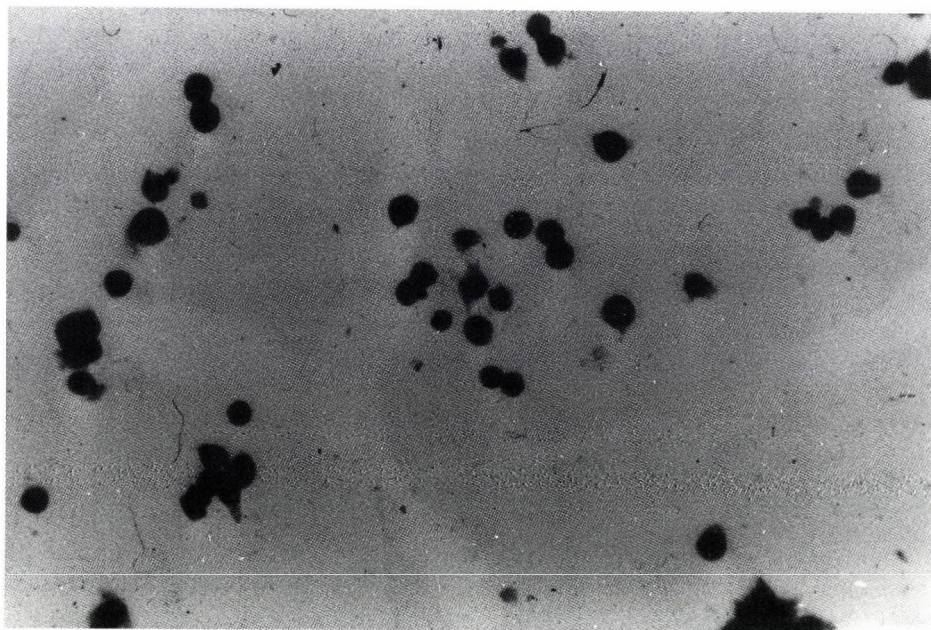


Fig. 4. Apoptotic cell death of HT 29 cells (human colon adenocarcinoma ATCC HTB-38) treated with 100 µg/ml HMA for 48 hours



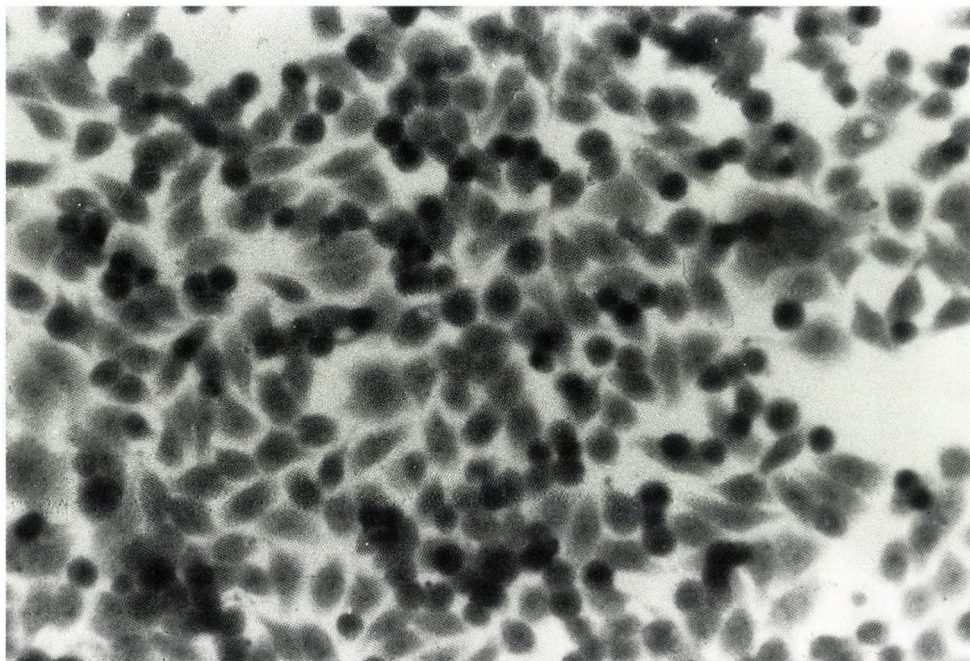


Fig. 5. HT 29 cells (human colon adenocarcinoma ATCC HTB-38) were cultured as described in method for 48 hours (control, untreated cells)

number, shrinkage of cells and condensation of chromatin were observed after 48 hours treatment of HMA (100  $\mu\text{g/ml}$ ) (Fig. 4) compared to the untreated control of HT 29 cells (Fig. 5).

#### REFERENCES

1. Csiba, A., Trézsl, L., Tyihák, E., Graber, H., Vári, É., Téglás, G., Rusznák, I. (1982) Assumed role of L-arginine in mobilisation of endogenous formaldehyde. *Acta Physiol. Acad. Sci. Hung.* 59, 35–45.
2. Hullán, L., Szikla, K., Tusnady, G., Holczinger, L. (1988) Thymidylate synthase and thymidine kinase activities and methotrexate cytotoxicity during growth of L 1210 an Ehrlich ascites tumor. *Cancer Biochem. Biophys.* 10, 131–139.
3. Roberts, D. (1966) An isotopic assay for thymidylate synthetase. *Biochemistry* 5, 3546–3551.
4. Szarvas, T., Pozsár, B. I., Simon, L. P. (1983) Detection of endogenous free formaldehyde in plants and its relationship with photosynthesis. *Acta Agron. Acad. Sci. Hung.* 32, 313–330.
5. Trézsl, L., Csiba, A., Juhász, S., Szentgyörgyi, M., Lombai, G., Hullán, L. (1997) Endogenous formaldehyde level of foods and its biological significance. *Z. Lebensm. Unters. Forsch. A.* 205, 300–304.

6. Trézl, L., Rusznák, I., Náray-Szabó, G., Szarvas, T., Csiba, A., Ludányi, Á. (1988) Essential differences in spontaneous reaction of L-lysine and L-arginine with formaldehyde and its quantum chemical interpretation. *Period. Politech.* 32, 251–260.
7. Trézl, L., Rusznák, I., Tyihák, E., Szarvas, T. (1982) L-aszkorbinsavval gátolt spontán N-metilezési és N-formilezési reakciók L-lizin és formaldehid között és ennek biokémiai vonatkozásai. *Biológia* 30, 55–71.
8. Trézl, L., Rusznák, I., Tyihák, E., Szarvas, T., Szende, B. (1983) Spontaneous N<sup>ε</sup>-methylation and N<sup>ε</sup>-formylation reactions between L-lysine and formaldehyde inhibited by L-ascorbic acid. *Biochem. J.* 214, 289–292.
9. Trézl, L., Szende, B., Csiba, A., Rusznák, I., Lapis, K. (1986) *In vivo and in vitro inhibition of tumor cell proliferation by N<sup>G</sup>-hydroxymethyl-L-arginines as a natural cell component.* Abstr. No. 3594, 14<sup>th</sup> Int. Cancer Congr. Budapest.
10. Trézl, L., Tyihák, E., Lotlikar, P. D. (1990) Nonenzymatic Protein Methylation and its biological significance in Paik, W. K., Kim, S. (eds) *Protein Methylation*. CRP Press, Boca Raton, Florida.
11. Tyihák, E., Trézl, L., Kolonits, P. (1985) The isolation of N<sup>ε</sup>-formyl-lysine from the reaction between formaldehyde and L-lysine and its identification by OPLC and NMR spectroscopy. *J. Pharm. Biomed. Anal.* 3, 343–349.
12. Tyihák, E., Trézl, L., Rusznák, I. (1980) Spontaneous N<sup>ε</sup>-methylation of L-lysine by formaldehyde. *Pharmazie* 35, 18–20.
13. Tyihák, E., Trézl, L., Szende, B. (1998) Formaldehyde cycle and phases of stress syndrome. *Annals of N.Y. Acad. Sci.* 851, 259–270.





# THE HYDRAZINE DERIVATIVE AMINOGUANIDINE INHIBITS THE REACTION OF TETRAHYDROFOLIC ACID WITH HYDROXYMETHYLARGININE BIOMOLECULE\*

L. HULLÁN,<sup>1</sup> L. TRÉZL,<sup>2</sup> T. SZARVAS<sup>3</sup> and A. CSIBA<sup>4</sup>

<sup>1</sup>National Institute of Oncology, Budapest

<sup>2</sup>Technical University of Budapest

<sup>3</sup>Institute of Isotopes, Budapest

<sup>4</sup>Veterinary and Food Control Station, Budapest, Hungary

(Received: 1998-10-28; accepted: 1998-11-25)

Aminoguanidine (AG), a hydrazine derivative is known to inhibit the formation of Advanced Glycosylation Endproducts (AGE) and AG has been proposed as an agent in prophylaxis of diabetic complications. However, treatment with hydrazine produced liver and lung tumors by formation of N<sup>7</sup>- and O<sup>6</sup>-methylguanine in the DNA of rodents. The hydrazine derivative, isonicotinic acid hydrazide induced pulmonary tumors in mice. N<sup>G</sup>-hydroxymethyl-arginine (HMA) was synthesized by our research group and it showed anticancer effect against experimental tumors. HMA was found earlier in human blood and urine, and recently in many plants (in fruits and vegetables). We could demonstrate a reaction (pH = 7.5, 37 °C, 1<sup>h</sup>) between HMA and tetrahydrofolate (THF) producing N<sup>5</sup>,N<sup>10</sup>-methylene-tetrahydrofolate (CH<sub>2</sub>-THF), the coenzyme of thymidylate synthase (TS). In model experiments AG proved to react with formaldehyde (HCHO) and to eliminate the C<sub>1</sub>-fragment of HMA, but not that of CH<sub>2</sub>-THF. In the presence of AG burst chemiluminescence and a higher speed of the formylation and methylation reactions were found in the AG, HCHO, hydrogen peroxide (H<sub>2</sub>O<sub>2</sub>) and L-lysine system than without AG.

**Conclusions:** HMA as a biomolecule is one of the compounds which are responsible for the endogenous HCHO level. The biochemical function of HMA may be the direct supply of C<sub>1</sub>-fragment for the folate cycle. AG can disturb the above function of HMA. The reaction between AG and HCHO seems to be dangerous for biological systems because of the possible presence of L-lysine and H<sub>2</sub>O<sub>2</sub>. The burst chemiluminescence indicates excited molecules with extreme high energy producing uncontrolled formylation and methylation reactions. Considering the results of the experiments with AG its use as a medicament seems to be questionable.

**Keywords:** Aminoguanidine – hydroxymethylarginine – folate cycle – endogenous formaldehyde – thymidylate synthase

## INTRODUCTION

In spite of the fact that free formaldehyde (HCHO) is toxic and carcinogenic it can always be found using different nucleophilic reagents in various biological materials. The literature distinguishes exogenous and endogenous HCHO. The exogenous

\* Presented at the 4th International Conference on the Role of Formaldehyde in Biological Systems, July 1-4, 1998, Budapest, Hungary.

Send offprint requests to: Dr. L. Hullán, National Institute of Oncology, H-1122 Budapest, Ráth György u. 7/9, Hungary.



HCHO attacks the various organisms in free form originating from the environment, while the endogenous HCHO is supposed to be liberated from nontoxic biomolecules of the cells. Till now it was questionable what is the biochemical role of endogenous HCHO in living organisms.

N<sup>G</sup>-hydroxymethylarginine (HMA) was synthesized from HCHO and L-arginine. The imino and amino nitrogen of guanidino group carry one, two, or three hydroxymethyl group [17]. HMA was shown to inhibit the growth of some experimental tumors [15]. HMA was found in human blood and urine [4] and recently, in plants (fruits and vegetables) in about ten times higher concentration than in human samples [12]. HMA showed apoptotic effect *in vitro* on human colon tumor cells [11] and there are evidences that the biosynthesis of HMA may occur during photosynthesis [13]. Based on quantumchemical data HMA carries the hydroxymethyl group in a relatively labile form and HMA was supposed to belong to the biomolecules responsible for the endogenous HCHO level of cells.

Hydrazine has been shown to react with endogenous HCHO forming formaldehyde hydrazone. It methylates DNA guanine at the N<sup>7</sup>- and O<sup>6</sup>-positions and produces liver and lung tumors [9]. Chronic exposure to hydrazine leads to hypomethylation of total target organ DNA and that the hypomethylation is dose related to the development of liver cancer [5]. The hydrazine derivative, isonicotinic acid hydrazide (the most important antituberculous agent) induced pulmonary tumors in mice [1, 7].

Aminoguanidine (AG) inhibits the Maillard reaction, the formation of AGEs among others on hemoglobin of patients with diabetes, too. The results initiated clinical studies on AG as an agent of potential benefit in prophylaxis of diabetic complications [2]. Recently, AG turned to be very well-known (more than 400 papers were dealing with it in the last two years), because AG inhibits the inducible NO synthase [3].

In our experiments, reactions of HMA were investigated. Based on theoretical considerations HMA was supposed to react both with tetrahydrofolate (THF) and AG. The reaction between HMA and THF could be proved by thymidylate synthase (TS), as the product of HMA and THF reaction was N<sup>5</sup>,N<sup>10</sup>-methylene-THF (CH<sub>2</sub>-THF), the coenzyme of thymidylate synthase. The TS assay was suitable for the investigation of the reaction between AG and HMA, too. The amount of coenzyme formed in the reaction of HMA and THF decreased, due to the previous reaction of AG with the hydroxymethyl group of HMA. Consequently, TS activities decreased also in the Roberts assay of TS modified appropriately to the experiments. Investigations of chemiluminescence emission and the products of reactions either with hydrogen peroxide (H<sub>2</sub>O<sub>2</sub>), or H<sub>2</sub>O<sub>2</sub> and L-lysine (LYS) proved that AG initiated excited HCHO with extreme high energy and increased the speed of uncontrolled methylation and formylation reactions.

## MATERIALS AND METHODS

### *Chemicals*

AG bicarbonate salt, dl-L-tetrahydrofolic acid, 2'-deoxyuridine 5'-monophosphate (dUMP) and charcoal were Sigma products. (5-<sup>3</sup>H)dUMP was purchased from The Radiochemical Centre (Amersham UK). <sup>14</sup>C-HCHO was manufactured in Institutes of Isotopes.

### *Enzyme assay*

TS activity was estimated, essentially as described by Roberts [10] with some modifications. Reaction mixture (0.15 ml) contained 4.5 nmol (5-<sup>3</sup>H)dUMP (22 kBq), 20 nmol tetrahydrofolate, 20 nmol HCHO, 1.5  $\mu$ mol 2-mercapto-ethanol, 7.5  $\mu$ mol NaF, 7.5  $\mu$ mol Tris-HCl buffer, pH = 7.5 and 0.11 ml of cytosol prepared from P388 ascites tumor cells. Tumor transplantation, the check of tumor growth and cytosol preparation were carried out as written before [6].

Reaction started by adding the cytosol and after incubation (0–30 min) at 37 °C was terminated by addition of 0.5 ml of 3.35% trichloroacetic acid and 0.5 ml of charcoal suspension (55 mg/ml). The samples were centrifuged at  $1.000 \times g$  for 15 min. Radioactivity of supernatant was counted in a liquid scintillation spectrometer. Nonadsorbable and total radioactivity were determined in appropriate controls.

Reaction velocity was linear with time under the conditions employed. The enzyme activities varied by less than 5% in the control.

### *Chemiluminescence (CL) emission measurements*

CL emission measurements were carried out in Packard TriCarb LSC using coincidence operating mode on <sup>3</sup>H channel.

### *Investigations with labelled compounds*

Reaction products were analysed by TLC (Kieselgel HF<sub>254</sub>) as a function of reaction time. 0 min sample was put on the TLC layer as quick as possible after having completed the reaction mixture. Running solution was n-buthanol-acetic acid-water = 8 : 1 : 1.



## RESULTS AND DISCUSSION

The reaction between HCHO and THF producing CH<sub>2</sub>-THF was published more than forty years ago [8]. CH<sub>2</sub>-THF participates as a coenzyme in the reductive methylation of deoxyuridine-5'-monophosphate to thymidylate by TS in the *de novo* nucleotide biosynthesis. The extreme labile coenzyme can be produced by the reaction of HCHO and THF for the TS assay [10]. The spontaneous reaction of HCHO and THF (as a control) and the TS assay were used in our experiments in which we wanted to know whether HMA reacts with THF. The reaction between HMA and THF was supposed to be probable because of theoretical considerations.

1.2  $\mu$ mol HMA and 1.2  $\mu$ mol THF in 7.5  $\mu$ mol Tris-HCl buffer (pH = 7.5) were kept for 1 hour and 37 °C as well as 1.2  $\mu$ mol HCHO and 1.2  $\mu$ mol THF were kept in the same way. Both reaction mixtures were tested in the conventional TS assay of Roberts [10] but modified as necessary.

The reaction mixture of HMA plus THF, or HCHO plus THF produced considerable amount of labelled product during the TS reaction and the radioactivity value was proportional to the reaction time (Fig. 1). There was no radioactivity in the samples if TCA was given prior to the cytosol (0 minute reactions). Consequently, the results were similar if either HMA, or HCHO was preincubated with THF. As the Roberts method is highly specific for TS, the results proved that HMA reacted with THF producing CH<sub>2</sub>-THF. Therefore, THF received a C<sub>1</sub>-fragment from HMA. The source of the C<sub>1</sub>-fragment must be the hydroxymethyl group of the arginine derivative, because arginine did not produce the coenzyme with THF (data is not given in detail).

HMA was found in human blood and urine [4], in plants (fruits and vegetables) as well [12], but in about ten times higher concentration than in human samples. Consequently, HMA is a biomolecule belonging to the molecules responsible for the endogenous HCHO level. CH<sub>2</sub>-THF, a very important biomolecule, is produced by the reaction of HMA and THF biomolecules. It occurs without any enzyme, however, under physiological conditions. There are evidences that HMA may be synthesized during photosynthesis [13]. HMA may provide a direct supply of C<sub>1</sub>-fragment for folate cycle from the flora to the fauna. The biochemical role of endogenous formaldehyde or at least of HMA may be a functional reserve for C<sub>1</sub>-fragment of folate cycle intracellularly.

Hydrazine has been shown to react with endogenous HCHO of various cell fractions prepared from rat liver [9]. The hydrazine derivative AG was investigated in model experiments to know whether AG has similar chemical characteristics as hydrazine. The model reactions were evaluated using the TS assay.

1.2  $\mu$ mol HCHO and various amounts of AG (0, 2.4, 4.8, or 12  $\mu$ mol) were kept in 7.5  $\mu$ mol Tris-HCl buffer (pH 7.5) for 1 hour at 37 °C. After 1 hour 1.2  $\mu$ mol THF was given to each reaction mixtures and they were kept for 1 hour at 37 °C again. Then the reaction mixtures were tested in the TS assay (Fig. 2). AG decreased the TS activities. The AG concentrations and the TS activities were in indirect proportion.

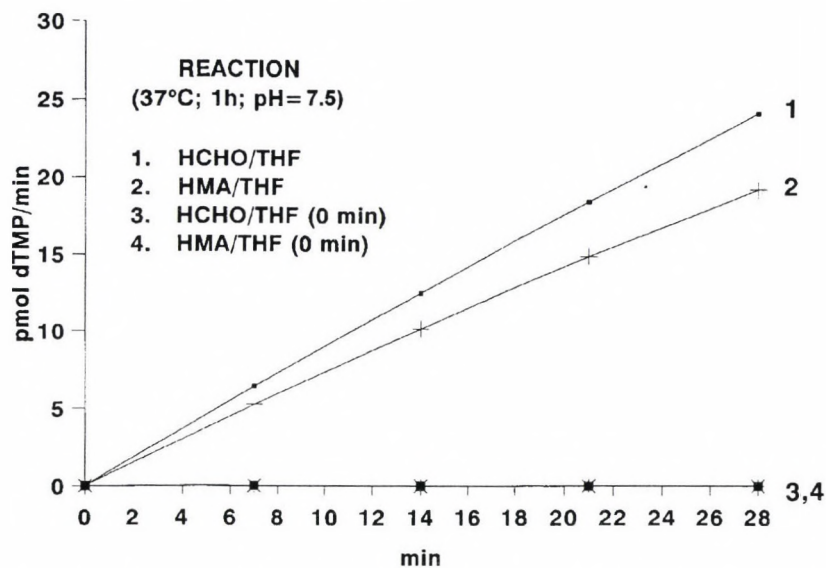


Fig. 1. Reaction of HMA and THF. 1.2  $\mu\text{mol}$  HMA and 1.2  $\mu\text{mol}$  THF as well as 1.2  $\mu\text{mol}$  HCHO and 1.2  $\mu\text{mol}$  THF were kept in 7.5  $\mu\text{mol}$  Tris-HCl buffer (pH 7.5) for 1 hour and 37 °C. Both reaction mixtures were tested by the TS assay

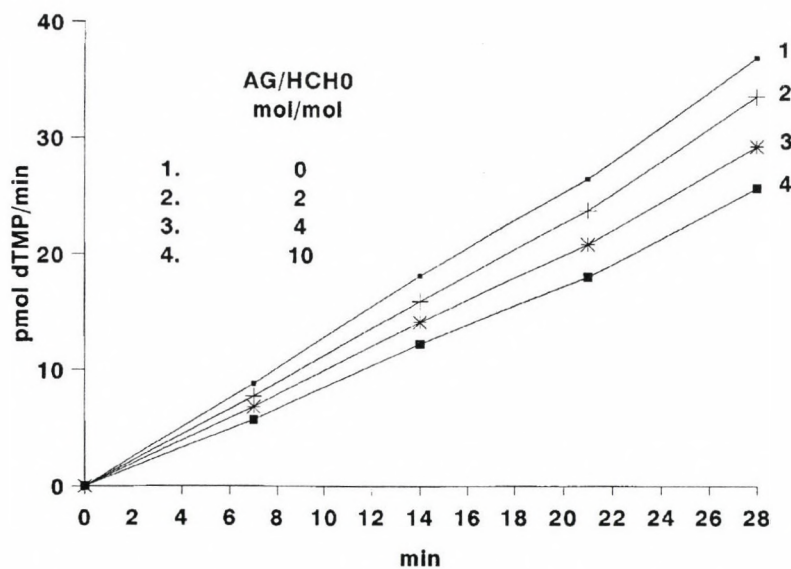


Fig. 2. Reaction of AG and HCHO. 1.2  $\mu\text{mol}$  HCHO were kept in the presence of various concentrations of AG in 7.5  $\mu\text{mol}$  Tris-HCl buffer (pH 7.5) for 1 hour at 37 °C. Then 1.2  $\mu\text{mol}$  THF was added to each reaction mixture and they were kept for 1 hour at 37 °C prior to the TS test



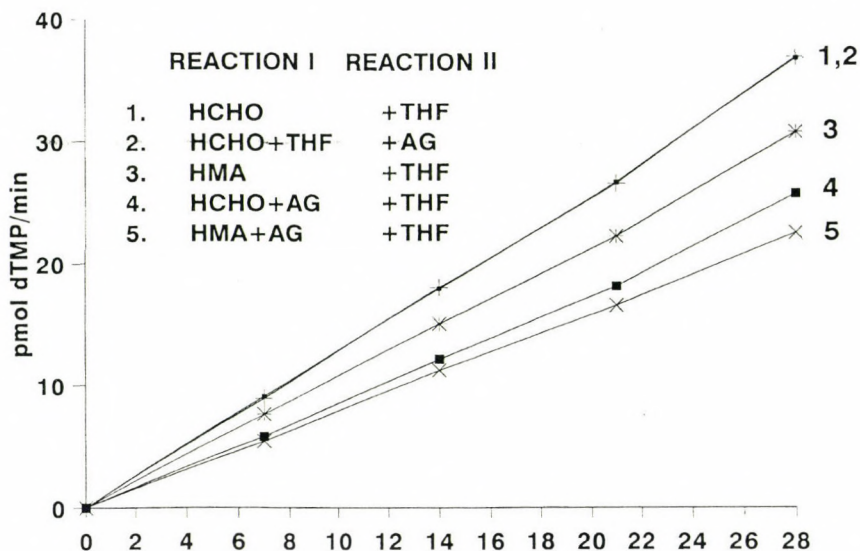


Fig. 3. Reaction between AG + HMA and AG + HCHO. 1.2  $\mu$ mol HCHO, 1.2  $\mu$ mol HMA, 1.2  $\mu$ mol THF and 12  $\mu$ mol AG were used in the various reaction mixtures. Two incubation periods, 1 hour each, followed at 37 °C and pH 7.5 in each case

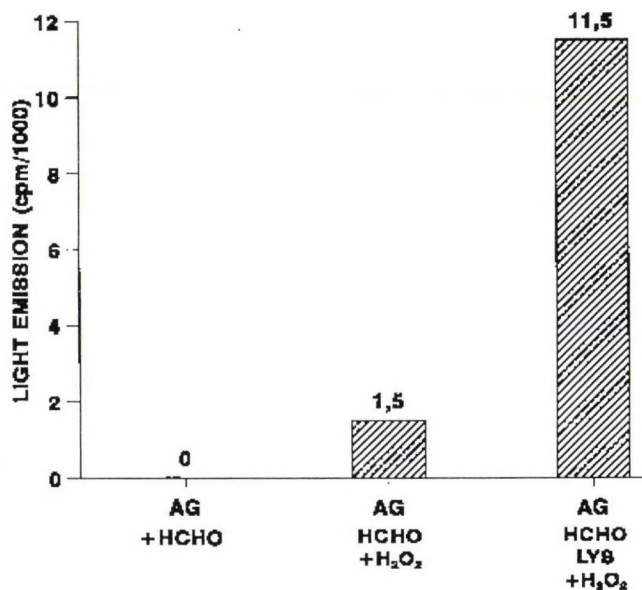


Fig. 4. Burst chemiluminescence emission in the reaction mixtures of equimolar (1 mmol) AG + HCHO + H<sub>2</sub>O<sub>2</sub> and AG + HCHO + LYS + H<sub>2</sub>O<sub>2</sub>

In the next experiment various reaction mixtures were incubated and compared to each other by the TS assay at the same time in the same experimental system (Fig. 3). Two incubation periods, 1 hour each, followed at 37 °C and pH 7.5 in each case. In the two controls, 1.2  $\mu$ mol HCHO, as well as 1.2  $\mu$ mol HMA were kept alone and then together with 1.2  $\mu$ mol THF for 1 hour each. 1.2  $\mu$ mol HCHO as well as 1.2  $\mu$ mol HMA were kept first with 12  $\mu$ mol AG, then with 1.2  $\mu$ mol THF. Both reaction mixtures produced significantly lower TS activities than the appropriate controls did. When HCHO (1.2  $\mu$ mol) was incubated first with THF (1.2  $\mu$ mol), AG (12  $\mu$ mol) did not decrease the enzyme activities even if the first incubation time was very short.

The experiments proved that AG, similar to hydrazine, must be very nucleophilic. AG reacted not only with the free HCHO but it removed the hydroxymethyl group of HMA and did not give further to THF. Therefore, AG showed the characteristic reaction of hydrazine decreasing the endogenous HCHO level represented by the HMA biomolecule in our experiments. It is important to emphasize that AG did not remove the C<sub>1</sub>-fragment of CH<sub>2</sub>-THF coenzyme. Consequently, AG may disturb the folate cycle only indirectly decreasing the amount of C<sub>1</sub>-fragment source carried by HMA and probably other biomolecules, too.

It is known that various aldehydes can be activated by H<sub>2</sub>O<sub>2</sub> especially in the presence of the  $\epsilon$ -amino group of L-lysine (LYS) [14]. Both LYS and endogenous H<sub>2</sub>O<sub>2</sub> may occur intracellularly. To investigate in model reaction the effect of *in vivo* circumstances on the reaction of AG and HCHO chemiluminescence emission was determined in various reaction mixtures containing the above-mentioned compounds (Fig. 4). All investigated compounds were in equimolar concentration (1 mmol in 5 ml total volume) containing 7.5  $\mu$ mol Sørensen buffer (pH 7.5). The chemiluminescence emission was measured 20 sec after mixing the reagents. There was no light emission value in the reaction of AG and HCHO, while considerable high light emission was found in the reaction of AG, HCHO and H<sub>2</sub>O<sub>2</sub>. Chemiluminescence emission was especially high when both H<sub>2</sub>O<sub>2</sub> and L-lysine were together with AG and HCHO.

The AG, HCHO, LYS and H<sub>2</sub>O<sub>2</sub> system was investigated by radiochromatography because considerable amount of N<sup>ε</sup>-formyl-L-lysine and N<sup>ε</sup>-methyl-L-lysine has been found due to the excited HCHO in the reaction mixture of HCHO, LYS and H<sub>2</sub>O<sub>2</sub> [16]. 1 mmol AG, 1 mmol LYS, 2 mmol <sup>14</sup>C-HCHO (18.5 MBq/mmol) and 2 mmol H<sub>2</sub>O<sub>2</sub> were reacted in 500  $\mu$ l Sørensen buffer (Fig. 5). AG has an enforcing effect on the formylation and methylation of lysine. The speed of formylation reaction is much higher and the amount of methylated lysine is also higher than those in the HCHO, LYS and H<sub>2</sub>O<sub>2</sub> system were. The results of chemiluminescence measurements and product analysis proved unambiguously that the excited HCHO in the presence of AG is extremely reactive. The random, uncontrolled formylation and methylation of lysine suggest similar reactions for other biomolecules, too. The results make questionable the planned use of AG as a medicament and they should be considered concerning the theoretical experiments in which AG is involved.



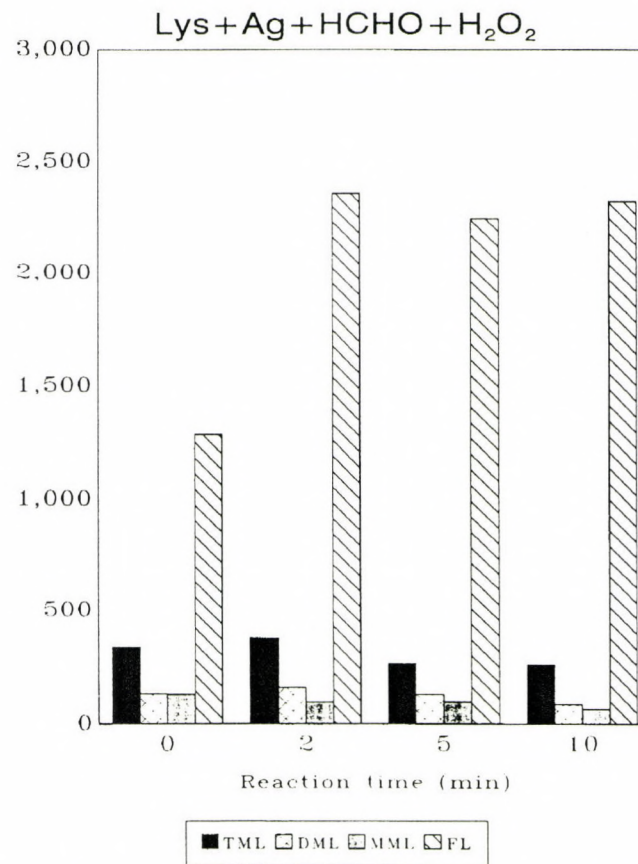
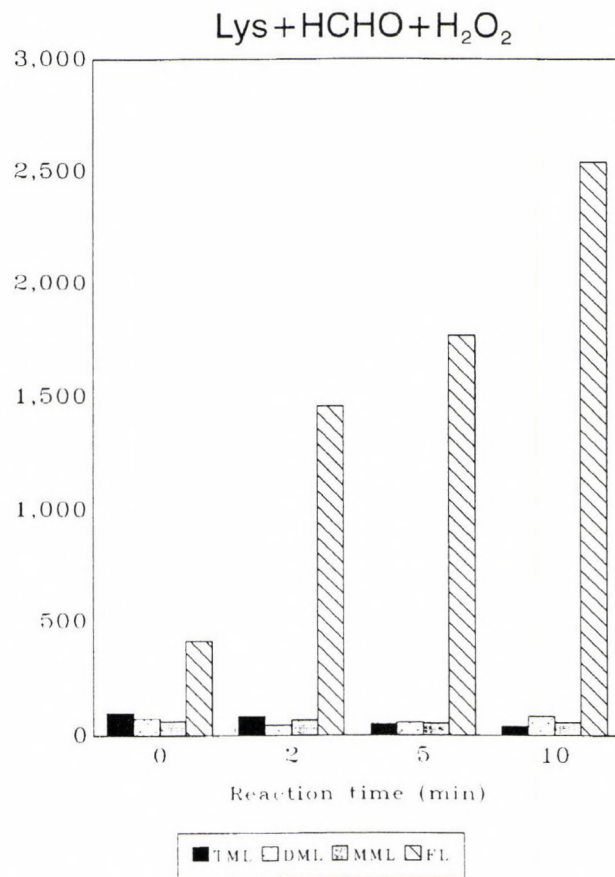


Fig. 5. Products in the reaction mixtures of LYS + HCHO + H<sub>2</sub>O<sub>2</sub> and LYS + AG + HCHO + H<sub>2</sub>O<sub>2</sub>. (TML, DML and MML = tri-, di- and monomethyl-lysine, FL = formyl-lysine)

## REFERENCES

1. Bianciffiori, C., Ribacchi, R. (1962) Pulmonary tumours in mice induced by oral isoniazid and its metabolites. *Nature* 194, 488–489.
2. Cerami, A. (1994) The role of the Maillard reaction in vivo. In: Labuza, T. P., Reieccius, G. A., Monnier, V., O'Brien, J., Baynes, J. (eds) *Maillard Reactions in Chemistry, Food, and Health*. The Royal Society of Chemistry.
3. Corbett, J. A., Tilton, R. G., Chang, K. et al. (1992) Aminoguanidine, a novel inhibitor of nitric oxide formation, prevents diabetic vascular dysfunction. *Diabetes* 41, 552–556.
4. Csiba, A., Trézl, L., Rusznák, I. (1986) N<sup>G</sup>-Hydroxymethyl-L-arginines: Newly discovered serum and urine components-isolation and characterization on the basis of cation-exchange thin-layer chromatography. *Biochem. Med. and Metab. Biol.* 35, 271–274.
5. FitzGerald, B. E., Shank, R. (1996) Methylation status of DNA cytosine during the course of induction of liver cancer in hamsters by hydrazine sulfate. *Carcinogenesis* 17, 2703–2709.
6. Hullán, L., Szikla, K., Tusnády, G., Holczinger, L. (1988) Thymidylate synthetase and thymidine kinase activities and methotrexate cytotoxicity during growth of L1210 and Ehrlich ascites tumor. *Cancer Biochem. Biophys.* 10, 131–139.
7. Juhász, J., Baló, J., Kendrey, G. (1957) Über die geschwulsterzeugende Wirkung des Isonicotinsäurehydrazid (INH). *Zeitschrift für Krebsforschung* 62, 188–196.
8. Kisliuk, R. L. (1957) Studies on the mechanism of formaldehyde incorporation into serine. *J. biol. Chem.* 227, 805–814.
9. Lambert, C. E., Shank, R. C. (1988) Role of formaldehyde hydrazone and catalase in hydrazine-induced methylation of DNA guanine. *Carcinogenesis* 9, 65–70.
10. Roberts, D. (1966) An isotopic assay for thymidylate synthetase. *Biochemistry* 5, 3546–3548.
11. Szende, B., Tyihák, E., Trézl, L., Szőke, É., László, I., Kátay, Gy., Király-Véghely, Zs. (1998) Formaldehyde generators and capturers as influencing factors of mitotic and apoptotic processes. In: *4th Int. Conf. on Role of formaldehyde in biological systems. Methylation and demethylation processes*. (Budapest) p. 18.
12. Trézl, L., Csiba, A., Juhász, S., Szentgyörgyi, M., Lombai, G., Hullán, L. (1997) Endogenous formaldehyde level of foods and its biological significance. *Z. Lebensm. Unters. Forsch. A.* 205, 300–304.
13. Trézl, L., Hullán, L., Szarvas, T., Csiba, A., Szende, B. (1998) Determination of endogenous formaldehyde in plants (fruits) bound to-L-arginine and its relation to the folate cycle, photosynthesis and apoptosis. In: *4th Int. Conf. on Role of formaldehyde in biological systems. Methylation and demethylation processes*. (Budapest) p. 24.
14. Trézl, L., Ludányi, Á., Rusznák, I., Horváth, V., Szarvas, T., Vasvári, G., Tyihák, E. (1989) Lizin bázikus végcsoportjainak gyorsító hatása hidrogén-peroxid és formaldehid közötti reakciókban. *Magyar Kémiai Folyóirat* 95, 131–139.
15. Trézl, L., Szende, B., Csiba, A., Rusznák, I., Lapis, K. (1986) In vivo and in vitro inhibition of tumor cell proliferation by N-hydroxymethyl-arginines as a natural cell component. In: *14th Int. Cancer Congress*, Budapest, No. 3594.
16. Trézl, L., Török, G., Vasvári, G., Pipek, J., Hullán, L. (1992) Formation of burst chemiluminescence, excited aldehydes, and singlet oxygen in model reactions and from carcinogenic compounds in rat liver S9 fractions. *Periodica Polytechnica Ser. Chem. Eng.* 36, 239–247.
17. Trézl, L., Tyihák, E., Lotlikar, P. D. (1990) Nonenzymatic protein methylation and its biological significance. In: Paik, W. K., Kim, S. (eds) *Protein Methylation*, CRC Press, Boca Raton Fla, pp. 407–433.





# INDUCTION OF RESISTANCE OF WHEAT PLANTS TO PATHOGENS BY PRETREATMENT WITH N-METHYLATED SUBSTANCES\*

KLÁRA MANNINGER,<sup>1</sup> MÁRIA CSÖSZ<sup>2</sup> and E. TYIHÁK<sup>1</sup>

<sup>1</sup>Plant Protection Institute, Hungarian Academy of Sciences, Budapest, Hungary

<sup>2</sup>Cereal Research Non Profit Company Szeged, Hungary

(Received: 1998-10-28; accepted: 1998-11-25)

It has been established that the application of N-methylated compounds as N, N-dimethyl-L-tyrosine and glycine-betaine can induce resistance to biotrophic fungi (*Erysiphe graminis*, *Puccinia recondita*) in wheat (Yubileynaya) at two different pretreatment concentrations. This dose-dependent “double immune response” of plants is the basic phenomenon of the biochemical immunization. These N-methylated compounds are potential formaldehyde generators and the formaldehyde formed can take part in the induction of resistance of wheat plants. It seems that the dose-dependent “double immune response” of plants is in correlation with the biotransformation steps of formaldehyde cycle as a fundamental biochemical pathway.

**Keywords:** Biochemical immunization – biotrophic fungi – double immune response – induction of resistance – N-methylated substances

## INTRODUCTION

Systemic acquired resistance (SAR) is a widely distributed plant defence system that confers a broad spectrum of disease resistance [11]. The onset of SAR correlates with the expression of SAR genes in the infected as well as uninfected (systemic) tissues.

Biochemical plant pathology is now beginning to provide the insights into mechanisms of host-pathogen interaction which should allow disease control chemicals to be designed on a rational basis. These should include not only chemicals with a direct action against the pathogen, but also those, which may act indirectly by simulating host defence mechanisms [2, 11].

The responses of plants to pathogen attack include synthesis of various small molecules (e.g. toxic phytoalexins). There is also evidence for production of active oxygen species that aid in cell wall strengthening and in attacking the pathogen. The ini-

\* Presented at the 4th International Conference on the Role of Formaldehyde in Biological Systems, July 1–4, 1998, Budapest, Hungary.

Send offprint requests to: Dr. Klára Manninger, Plant Protection Institute, Hungarian Academy of Sciences, H-1525 Budapest, P.O. Box 102, H-1525 Hungary.



tial infection by a necrotizing pathogen results in a plant with increased systemic disease resistance to broad spectrum of pathogens [7, 8, 12].

According to recent investigations all biological systems possess a formaldehyde (HCHO)-yielding potential which may originate from methylation and demethylation processes, alike [1, 3, 6]. Recently, it has been shown that the formation of HCHO from S-methyl group of S-adenosyl-L-methionine (SAM) is linked to an enzymatic transmethylation [6]. The level of HCHO and some fully N-methylated substances (e.g. N-trimethyl-L-lysine, TML) as marker molecules is higher in all cases in the top (youngest) leaves than in elder ones. The high level of HCHO and at the same time accumulation of N-methylated substances during early development stages and in rapidly dividing cells are originated from the transmethylation reactions [18].

It is well known that during demethylation process HCHO and demethylated compound can be formed as it has been previously demonstrated [1, 4]. The measurable HCHO level is dramatically elevated in virus or other microbial infected tissues (biotic stress) and in the case of heat shock or salt stress as well as for the application of different exogenous substances (abiotic stress). At the same time the level of different methylated compounds as potential HCHO generators are considerably decreased [16, 18].

The accumulation of HCHO in spring is originating mainly from the enzymatic transmethylation reactions, while in autumn the high level of HCHO is in correlation with the demethylation processes [17].

There is a HCHO cycle in biological systems, that is, the formation of L-methionine from L-homocysteine takes place through HCHO and the HCHO-yielding from S-methyl group of SAM during the transmethylation reaction is essential step in this fundamental biochemical pathway [17, 18].

According to earlier investigations the pretreatment of plants with endogenous N-methylated compounds as choline, glycine betaine etc. increases the resistance potential of plants to pathogens. More exactly, the application of N-methylated compounds can induce resistance to biotrophic fungi in host plants. The time dependence of induction (at least 2 days) may be due to metabolic changes of these N-methylated substances in host plants being the prerequisite for the enhanced resistance [9, 15, 17]. The dosage dependent double immune response of plants to pathogens is based on an indirect effect and can manifest through the rearrangement of the methyl groups in frame of HCHO cycle [15, 17].

The aim of the present paper is to demonstrate the applicability of endogenous N-methylated substances as potential HCHO-donating inducers on induction of disease resistance in wheat plants against biotrophic fungi.

## MATERIALS AND METHODS

### *Plants and pathogens*

Wheat (*Triticum aestivum* cv. Yubileynaya) plants were cultivated in commercial compost in a greenhouse.

*Erysiphe graminis* and *Puccinia recondita* were maintained on wheat plants in greenhouse.

### Induction of resistance

An aqueous solution of DL-carnitine HCL (Sigma-Aldrich Kft., Budapest, Hungary) and N, N-dimethyl-L-tyrosine (DMT) with concentrations from  $10^{-3}$  to  $10^{-12}$  mol/l was used. The solutions were sprayed onto the leaves ( $4-5 \mu\text{l cm}^{-2} \cdot \text{leaf}$ ). Plants treated with water were used as controls.

### Inoculations

Plants were inoculated with a spore suspension of the pathogen 6 days after treatment with inducer-solution and then incubated at  $18-20^\circ\text{C}$  for 24 hours at high relative humidity. Pustule densities were assessed 10 days after inoculation and disease severity was expressed as pustules/cm<sup>2</sup>.

### Evaluation of the data

The mathematical evaluation of data was carried out by polynomial regression analysis.

## RESULTS AND DISCUSSION

Figure 1 and Fig. 2 illustrate the biochemical immunization of wheat plants to *Erysiphe graminis* and *Puccinia recondita* using different concentration of N, N-dimethyl-L-tyrosine and glycine betaine, respectively as inducers. It can be seen that there is a double immune response of plants. In this case the resistance phase of the stress syndrome is divisible to two ranges.

All the types of resistance so also induced resistance ultimately depend on a resistance potential which is obviously the most important means of disease control [13]. It seems that disease resistance is not a static but an elastic feature of plants. However, the chemical nature of the substances which are responsible for the resistance is poorly understood. It is evident that in induced resistance the mechanism of interaction between the pathogen and chemical agent is to be indirect, involving a characteristic change in host plant metabolism.

We demonstrated that the application of N-methylated compounds as glycine-betaine can induce resistance to biotrophic fungi (*Erysiphe graminis*, *Puccinia recondita*) in wheat plants (e.g. Yubileynaya) at two characteristic pre treatment concentrations.



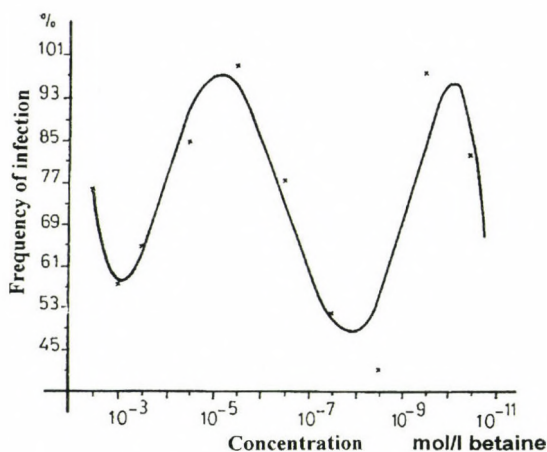


Fig. 1. Effect of glycine betaine on the infection frequency of *Puccinia recondita* on wheat. Polynomial regression analysis:  $Y = 273.6 - 369.4 + 219.7 X - 54.8X + 6.0X - 0.2X$ .  $r = 0.8707$ .  $F = 12.40^*$

This dose-dependent “double immune response” of plants is the basic phenomenon of the biochemical immunization.

These N-methylated compounds used are the endogenous constituents of wheat plants and their concentration level in the tissues is variety-dependent. These N-methylated compounds are potential formaldehyde (HCHO) generators and the HCHO formed can take part in the induction of resistance of wheat plants. It seems that the dose-dependent double immune response of plants is in correlation with the

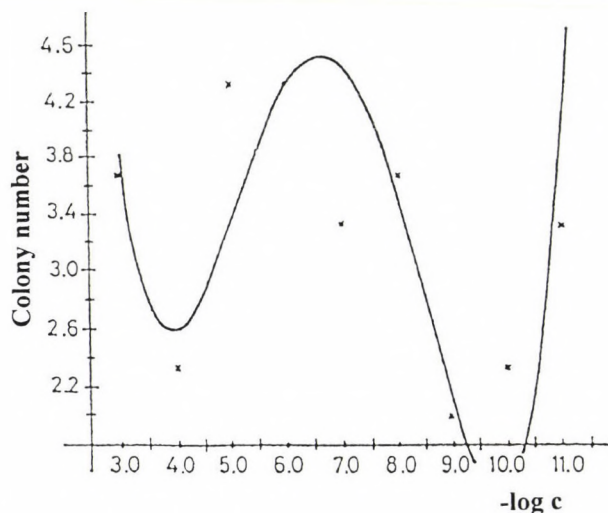


Fig. 2. Relationship between colony number and  $\log c$  (DMT) (wheat cv. Yubileynaya, *Erysiphe graminis*).  $R = 0.96$   $F = 39.34^{***}$

biotransformations steps of formaldehyde cycle as a fundamental biochemical pathway.

According to earlier observation  $\text{H}_2\text{O}_2$  as a small molecule is also present in different plant tissues [1, 3, 4]. It should be pointed out that the level of the HCHO and  $\text{H}_2\text{O}_2$  as normal endogenous components depends on plant age, leaf position [3, 16]. It follows from these facts that there is a real possibility of formation of excited HCHO ( $\text{H}^*\text{CHO}$ ) and singlet oxygen ( $^1\text{O}_2$ ) in the reaction between HCHO and  $\text{H}_2\text{O}_2$  [14, 16]. Because  $\text{H}_2\text{O}_2$  may participate directly in the oxidative demethylation of the given N-methylated compound so these two small molecules can meet immediately during the demethylation process. This consecutive demethylation process may be a fundamental step of the biochemical immunization of plants.

It has to be emphasized that  $^1\text{O}_2$  and  $\text{H}^*\text{CHO}$  have extremely high reactivity [14] and possibly attack not only the cellular components as nucleic acids and proteins but also microbial systems within plant tissues. It is obvious that the manifestation of their activity depends on the level of quenching systems in plant tissues [16].

#### REFERENCES

1. Chelvarajan, J. L., Fannin, F. F., Bush, L. P. (1993) Study of nicotine demethylation in *Nicotiana glauca*. *J. Agric. Food Chem.* 41, 858–862.
2. Görlach, J., Volrath, S., Knauf-Beiter, G., Hengy, G., Beckhove, U., Kogel, K.-H., Oostendorp, M., Staub, T., Ward, E., Kessmann, H., Ryals, J. (1996) Benzothiadiazole, a novel class of inducers of systemic acquired resistance, activates gene expression and disease resistance in wheat. *The Plant Cell* 8, 629–643.
3. Gullner, G., Tyihák, E. (1987) Hydrogen peroxide dependent N-demethylase activity in the leaves of normal and heat-shocked bean plants. *Plant Sci.* 52, 21–27.
4. Hao, D.-Y., Yeoman, M. M. (1996) Nicotine N-demethylase in cell-free preparations from tobacco cell cultures. *Phytochem.* 42, 325–329.
5. Hoffland, E., Hakulinen, J., van Pelt J. A. (1966) Comparison of systemic resistance induced by avirulent and non pathogenic *Pseudomonas* species. *Phytopathology* 56, 757–762.
6. Huszti, S., Tyihák, E. (1986) Formation of formaldehyde from S-adenosyl-L-(methyl- $^3\text{H}$ ) methionine during enzymic transmethylation of histamine. *FEBS Letters* 209, 362–366.
7. Kuc, J. (1982) Induced immunity to plant disease. *BioScience* 32, 854–860.
8. Kuc, J. (1987) Translocated signals for plant immunization. *Ann. N. Y. Acad. Sci.* 494, 221–223.
9. Manninger, K., Csősz, M., Tyihák, E. (1992) Biochemical immunization of wheat plants to biotrophic fungi by endogenous fully N-methylated compounds. In: *Proc. 3rd Intern. Conf. Role of Formaldehyde in Biological Systems-Methylation and Demethylation Processes*. 18–22 May, 1992, Sopron, Hungary, Hung. Biochem. Soc. Budapest. Tyihák, E. (ed.), pp. 157–162.
10. Mettraux, J.-P., Signer, H., Ryals, J., Ward, E., Wyss-Benz, M., Gaudin, J., Raschdorf, K., Schmid, E., Blum, W., Inverardi, B. (1990) Increase in salicylic acid at the onset of systemic acquired resistance in cucumber. *Science* 250, 1004–1006.
11. Morris, S. W., Vernooij, B., Titatam, S., Starrett, M., Thomas, S., Wiltse, C. C., Frederiksen, R. A., Bhandhufalck, A., Hulbert, S., Uknes, S. (1998) Induced resistance responses in maize. *Molec. Plant-Microbe Interact.* 11, 643–658.
12. Ryals, J., Uknes, S., Ward, E. (1994) Systemic acquired resistance. *Plant Physiol.* 104, 1109–1112.
13. Schönbeck, F., Steiner, Ulrike, Kraska, T. (1993) Induzierte Resistenz: Kriterien, Mechanismen, Anwendung und Bewertung. *J. Plant Dis. Protect.* 100, 541–557.



14. Trézl, L., Pipek, J. (1988) Formation of excited formaldehyde in model reactions simulatin real biological systems. *J. Mol. Struct. (Theochem)* 170, 213–223.
15. Tyihák, E., Steiner, Ulrike, Schönbeck, F. (1989) Induction of disease resistance by N-trimethyl-L-lysine in bean plants against *Uromyces phaseoli*. *J. Phytopath.* 125, 253–256.
16. Tyihák, E., Rozsnyay, Zs., Sárdi, E., Gullner, G., Trézl, L., Gáborjányi, R. (1994) Possibility of formation of excited formaldehyde and singlet oxygen in biotic and abiotic stress situations. *Acta Biol. Hung.* 45, 3–10.
17. Tyihák, E., Manninger, K., Csősz, M. (1995) Formaldehyde cycle “double immune response” and biochemical immunization of plants. In: M. Manka (ed.) *Environmental Biotic Factors in Integrated Plant Disease Control*. The Polish Phytopath. Soc., Poznan, pp. 571–574.
18. Tyihák, E., Trézl, L., Szende, B. (1998) Formaldehyde cycle and the phases of stress syndrome. *Ann. N.Y. Acad. Sci.* 851, 443–453.
19. Uknes, S., Mauch-Mani, B., Mozer, M., Potter, S., Williams, S., Dincher, S., Chandler, D., Slusarenko, A., Ward, E., Ryals, J. (1992) Acquired resistance in *Arabidopsis*. *Plant Cell* 4, 645–656.

## IDENTIFICATION AND MEASUREMENT OF RESVERATROL AND FORMALDEHYDE IN PARTS OF WHITE AND BLUE GRAPE BERRIES\*

ZSUZSA KIRÁLY-VÉGHÉLY,<sup>1</sup> E. TYIHÁK,<sup>2</sup> L. ALBERT,<sup>3</sup> ZS. I. NÉMETH<sup>3</sup> and GY. KÁTAY<sup>2</sup>

<sup>1</sup>Research Institute for Viticulture and Enology of Agricultural Ministry,  
Experimental Wine Cellar, Budapest

<sup>2</sup>Plant Protection Institute, Hungarian Academy of Sciences, Budapest

<sup>3</sup>Institute for Chemistry, University of Sopron, Sopron, Hungary

(Received: 1998-10-28; accepted: 1998-11-25)

The phytoalexin resveratrol (3,5,4'-trihydroxy-trans-stilbene) and formaldehyde (as its dimer adduct, formaldehydethone) have been identified and measured in the extracts of parts of white and blue grapes as well as in white and red wines by overpressured layer chromatography (OPLC), high performance liquid chromatography (HPLC) and from matrix assisted laser desorption/ionization mass spectrometric data. It has been established that the level of resveratrol was very high in skin and in some cases in the stem. Blue grape varieties and red wines always contained a considerably higher amount of resveratrol than white grapes and wines. The measurable level of formaldehyde as well as the resveratrol content was always parallelly high in the same parts of the berries, however, the formaldehyde level was higher in white grapes than in blue ones. The simultaneous occurrence of resveratrol and formaldehyde gives a possibility for interaction between these two special molecules, consequently, hydroxymethyl derivatives of resveratrol can be formed. These resveratrol derivatives may be responsible for special biological activities of resveratrol in grapes and dietetically (cardioprotective effect and chemopreventive effect against cancer) in the human organism.

**Keywords:** Formaldehyde – OPLC – HPLC – MALDI MS – resveratrol – *Vitis vinifera* L.

### INTRODUCTION

Several plants, including grapevine, synthesize the stilbene type resveratrol as a phytoalexin and other stilbenes [5, 10, 15]. Stilbene biosynthesis specifically requires the presence of stilbene synthase [18], using one molecule of 4-coumaroyl-CoA and 3 molecules of malonyl-CoA as substrates [17] both of which are commonly present in plants. Stilbene synthase genes derived from peanut [23] or grapevine [24] have already been transferred to other plant species such as tobacco [7], oilseed rape [22], and rice [20]. A slight increase in resistance to the pathogen *Botrytis cinerea* was reported for transgenic tobacco plants possessing genes coding for grapevine stilbene

\* Presented at the 4th International Conference on the Role of Formaldehyde in Biological Systems, July 1–4, 1998, Budapest, Hungary.

Send offprint requests to: Dr. Zs. Király-Véghely, Research Institute for Viticulture and Enology of Agricultural Ministry, Experimental Wine Cellar, H-1105 Budapest, Maláta u. 4, Hungary.



synthase [8]. Accumulation of resveratrol was detectable after fungal inoculation, resulting in a considerable increase in the resistance of transgenic tomato to the hemibiotrophic pathogen *Phytophthora infestans* [22, 23]. A dramatic accumulation of resveratrol but no significant increase in resistance occurred after inoculation of transgenic tomato plants with the perthotrophic pathogen *Botrytis cinerea*, and the necrotrophic pathogen *Alternaria solani* [24].

It follows from these results that the phytoalexin resveratrol as a product of stilbene-synthase has a function in plant responses to pathogens, however, the mechanism of action is practically unknown and in some cases the increase in disease resistance is controversial [24].

The roots of some plants (e.g. *Polygonum* species) which contain resveratrol have been used to treat diseases such as hyperlipaemia and arteriosclerosis, allergic diseases and inflammatory disease [14]. Furthermore, Kimura et al. [14] reported that stilbenes showed antileukaemic activity, due to their effect on arachidonate metabolism in leukocytes.

It is especially interesting that the phytoalexin resveratrol is produced in grapevines [5], consequently it has also been discovered in wine [15]. Several epidemiological studies have indicated that while excessive alcohol intake may result in tissue injury, there is universal relationship between moderate red wine consumption and low incidence of coronary heart disease [6]. Chemical analyses of wine and in particular red wine, have demonstrated the presence of resveratrol in its two isomers *trans* and *cis* [15], because the *trans*-isomer can be transformed easily into the *cis*-isomer (e.g. by UV rays) [15]. However, there was a slight difference between the biological activity of these two isomers (e.g. antiaggregating effect or antiplatelet activity) [2,16]. More recently, the antimutagenic activity of *trans*-resveratrol was demonstrated by the umu test and Ames test [27]. These results suggest that the presence of hydroxyl groups is important for antimutagenic activity.

The potential practical importance of resveratrol may be increased by the finding that resveratrol inhibits the development of preneoplastic lesions in carcinogen-treated mouse mammary glands in culture and retards tumorigenesis in a mouse skin cancer model [26] resveratrol, as a phytoalexin, was also shown to have cancer chemopreventive activity in assays representing three major stages of carcinogenesis such as initiation, promotion and progression [12].

According to recent investigations, a detectable amount of formaldehyde (HCHO) was found in biological systems that originates from methylation [9] and demethylation [13] as well as from uncontrolled enzymatic processes [28]. It has become increasingly evident that there is a HCHO cycle in biological systems [25] in which formation of the methyl group of L-methionine that takes place through HCHO from S-adenosyl-L-methionine (SAM) is linked to different enzymatic transmethylation reactions [9]. It is known that during the demethylation process, HCHO and a demethylation compound can be formed [4]. Although, analysable HCHO may be derived from a number of sources, the measurable level of HCHO is characteristic for a given system.

This paper describes the identification and measurement of resveratrol and HCHO as two potential interactive endogenous substances in parts of grape berries of white and blue grapevine varieties.

## MATERIALS AND METHODS

### *Chemicals*

All chemicals were obtained from Merck Chemical Co. (Darmstadt, Germany) and Sigma Co. (St. Louis, USA) as well as Reanal Chemical Co. (Budapest, Hungary). Formaldemethone was prepared by a known preparative method [19].

### *Plant material*

The fresh tissue parts from white and blue berries were frozen in liquid nitrogen, powdered and aliquot (e.g. 0.25) was used for analysis by layer liquid chromatographic techniques and for matrix assisted laser desorption/ionization mass spectrometry (MALDI MS) [1].

### *Analysis of HCHO as dimedone adduct and resveratrol by TLC and automatic personal OPLC instrument*

An aliquot of powdered grape tissue (0.25 g) was treated with 0.7 mL of 0.20% dimedone solution. This suspension was centrifuged at 1000 g for 10 min. at 4 °C. The clear supernatant was used for overpressured layer chromatographic (OPLC) separation of formaldemethone [26]. Aliquot amounts of the samples were applied to the chromatoplates by means of TLC Applicator AS 30 (Desaga Co., Heidelberg, Germany) in nitrogen atmosphere. In order to limit air access after application of the samples the application sites were covered totally with a glass plate because the laboratory air contains always a small quantity of HCHO. The chromatogram was developed immediately after application. Chloroform-dichloromethane (10 : 30, V/V) as mobile phase was used for determining the formaldemethone [26].

For the separation of resveratrol conventional TLC and automatic overpressured layer chromatographic (OPLC) technique were used: sorbent layer, silica gel 60F<sub>254</sub>; eluent, chloroform-methanol mixtures; spots or bands were evaluated visually by UV elimination (254 and 366 nm) and instrumentally by using a Shimadzu CS-930 densitometer (305 nm).



### *Identification of resveratrol by MALDI MS*

An aliquot (0.5  $\mu$ L) of the extract solution was mixed with 0.5  $\mu$ L  $\alpha$ -cyano-4-hydroxycinnamic acid (ACH) matrix (10 mg/mL ACH in acetonitrile : water (7 : 3, V/V)) directly on a disposable sample slide. The droplet was allowed to dry naturally prior to MALDI MS analysis. The sample preparation for the authentic substances was the same as before but using a standard solution ( $2 \times 10^{-5}$  M) instead of diluted supernatant. The mass spectrometer used in this work was a Finnigan LASERMAT 2000 (Finnigan MAT Ltd., Hennel Hempstead, UK) [1].

## RESULTS AND DISCUSSION

### *Resveratrol investigations*

The MALDI-MS spectrum of authentic resveratrol is shown in Fig. 1, while Fig. 2 demonstrates the identification of resveratrol ( $m/z$  value of 227) in an extract of skin of blue berries (Soproni Kékfrankos variety).

Figure 3 illustrates the distribution of resveratrol content in different parts of berries of several blue grape varieties. It can be seen that the level of resveratrol is especially high in the skin and in some cases in the stem.

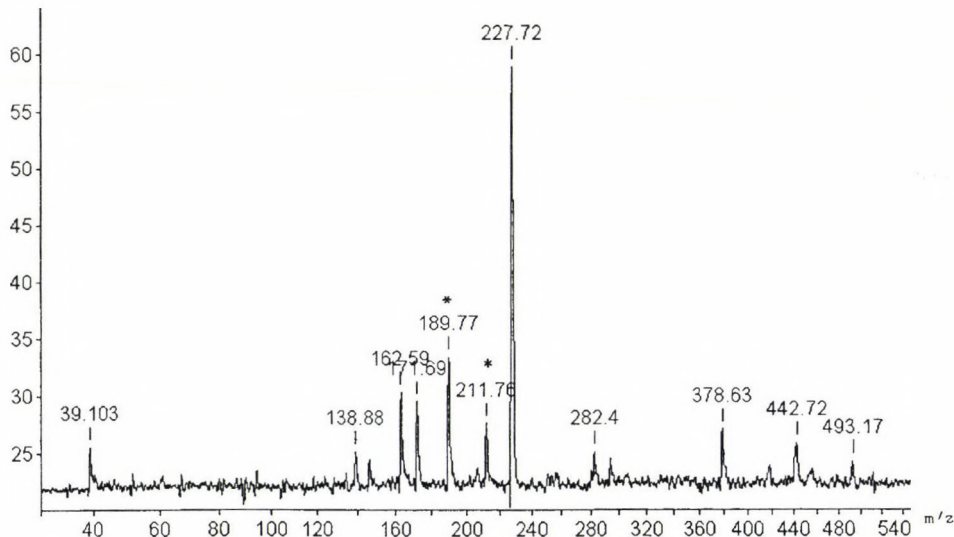


Fig. 1. MALDI MS spectrum of resveratrol. Peaks marked with \* are signals produced by the sample matrix. For sample preparation protocol and MS conditions see the Materials and Methods

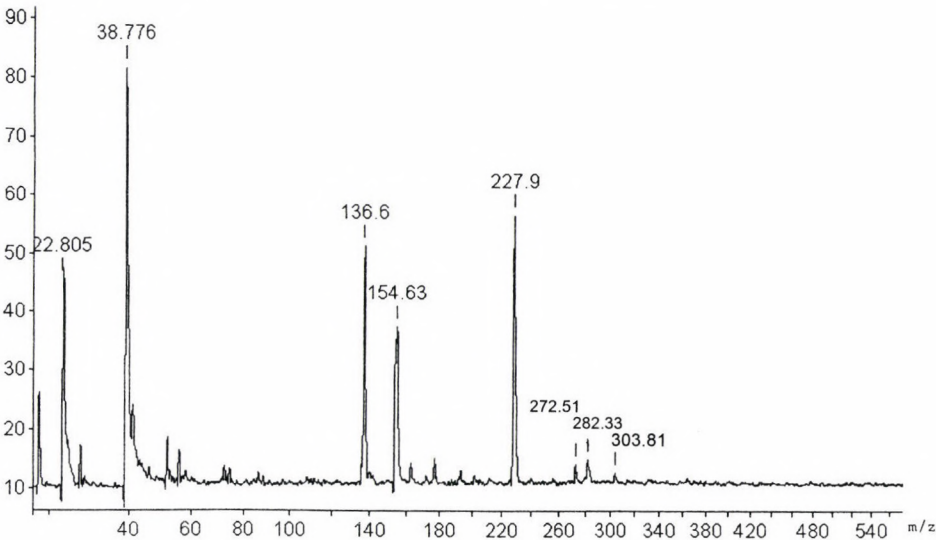


Fig. 2. MALDI MS spectrum of an extract of skin of Soproni Kékfrankos variety. Conditions as at Fig. 1

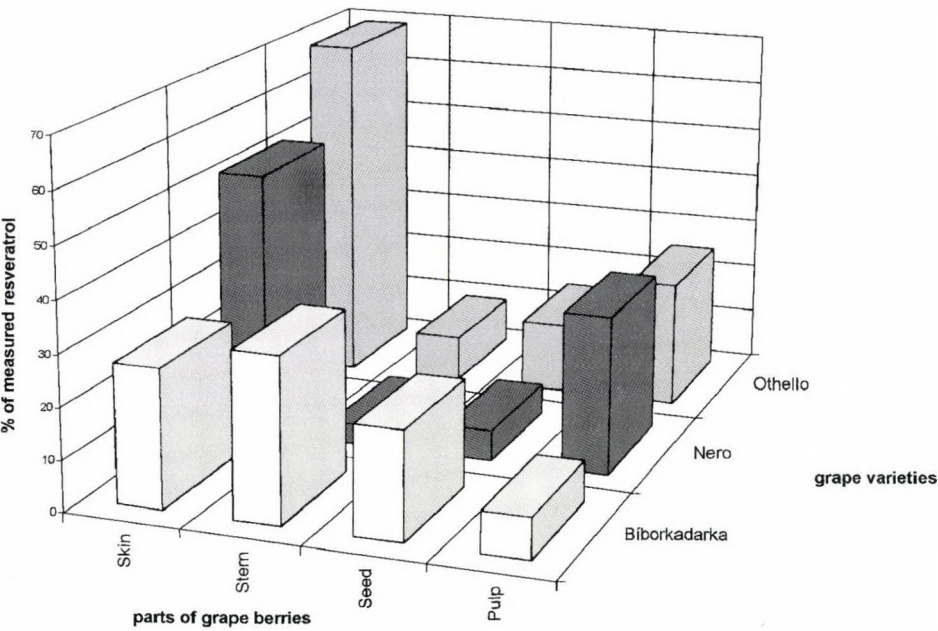


Fig. 3. Distribution of resveratrol in parts of white and blue grape berries (in %). Conditions in Materials and Methods



Table I summarizes the results of our comparative investigations for white and red wines. It can be seen that the level of resveratrol is generally higher in red wines than in white ones. These results are in agreement with some earlier data [5, 15].

*Table I*  
Content of resveratrol in some Hungarian wines

Wines	Resveratrol, mg/l
<i>White wines</i>	
Szamorodni	0.05
Furmint	0.06
Tokaji Aszú	0.09
Hárslevelű	0.07
Chardonnay	0.04
<i>Red wines</i>	
Burgundi	1.14
Kékfrankos	1.38
Cabernet sauvignon	3.07
Kadarka	1.63
Merlot	3.19
Oporto	3.70
Egri bikavér	4.40

Harvesting time: 28.08.1998.

### *HCHO investigations*

It is known that in the reaction between HCHO and dimedone, as a HCHO capture molecule, an adduct (formaldemethone) is formed in an irreversible process.

Figure 4 summarizes the levels of formaldehyde measured in parts of white and blue berries. It can be seen that the levels of formaldehyde showed characteristic values, however, the measurable HCHO content was higher in skin and stem than in other parts of the berries. These results demonstrate clearly that there is a simultaneous accumulation of these two substances in different parts of berries of grapes. It has been established that the level of HCHO is higher in the parts of white grapes.

### *A putative interaction between resveratrol and HCHO*

These preliminary results perhaps will help to understand the special activity of resveratrol as a stilbene derivative. Trans-resveratrol is a normal component of parts of grapes and it may participate in defence mechanisms of plant tissues [7, 8, 24].

It was supposed that the special structure (double bond) of resveratrol is suitable for an interaction with HCHO which – according to present investigations – normal-

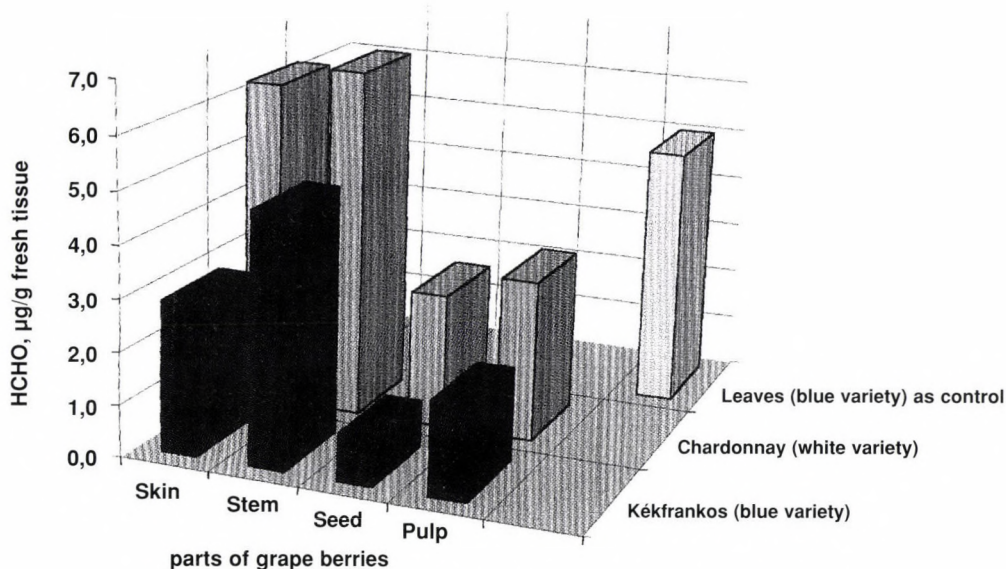


Fig. 4. Level of HCHO measurable in parts of white and blue grape berries.  
Conditions in Materials and Methods

ly occurs in a chemically labile bound form in grapevine plant. This idea is supported by the fact that the main accumulation sites of both substances (resveratrol and HCHO) are always in the same parts of the berries. There is a possibility for a continuous formation of resveratrol derivatives (mainly hydroxymethyl derivatives) in different tissues and one can suppose that these special derivatives of resveratrol could be responsible for the disease resistance response of grapevine plants. The isolation and identification of such natural resveratrol derivatives are in progress. This idea is supported further by preliminary chemical investigations in which we were able to illustrate an interaction between resveratrol and HCHO. From the reaction mixture two isomers were as 7-hydroxymethyl-, 8-hydroxy-resveratrol and 7-hydroxy-, 8-hydroxymethyl-resveratrol isolated and identified by means of HPLC and MALDI MS data [26].

Indirect evidences suggest that the presence of resveratrol in white and red wine may explain the reduced risk of coronary heart disease associated with moderate wine consumption [6]. This effect has been attributed to the inhibition of platelet aggregation and coagulation, in addition to the antioxidant and antiinflammatory activity of resveratrol [2, 6, 16]. Furthermore, recent reports show that resveratrol is a potent cancer chemopreventive agent [3] in assays representing three major stages of carcinogenesis [12], however, the precise mechanism of the cardioprotective effect as well as the antitumor activity is not well understood. One can suppose that the reaction of resveratrol with endogenous HCHO molecules may also influence chemoprevention of cancer [21, 26].



## REFERENCES

1. Albert, L., Németh, Zs., Barna, T., Varga, Sz., Tyihák, E. (1998) Measurement of endogenous formaldehyde in the early development of European Turkey oak (*Quercus cerris* L.). *Phytochem. Anal.* 9, 227–231.
2. Bertelli, A. A. E., Giovannini, L., DeCaterina, R., Bernini, W., Migloari, M., Fregoni, M., Bavaresco, L., Bertelli, A. (1996) Antiplatelet activity of cis-resveratrol. *Drugs Exptl. Clin. Res.* XXII, 61–63.
3. Clement, M.-V., Hirpara, J., Chawdhury, Pervaiz, S. (1998) Chemopreventive agent resveratrol, a natural product derived from grapes, triggers CD95 signaling-dependent apoptosis in human tumor cells. *Blood* 92, 996–1002.
4. Chelvarajan, R. L., Fannin, F. F., Bush, L. P. (1993) Study of nicotine demethylation in *Nicotiana glauca*. *J. Agric. Food Chem.* 41, 858–862.
5. Creasy, L. L., Coffee, M. (1988) Phytoalexin production potential of grape berries. *J. Amer. Soc. Hort. Sci.* 113, 230–234.
6. Fuhrman, B., Lavy, A., Aviram, M. (1995) Consumption of red wine with meals reduces the susceptibility of human plasma and low-density lipoprotein to lipid peroxidation. *Am. J. Clin. Nutr.* 61, 49–54.
7. Hain, R., Bieseler, B., Kindl, H., Schröder, G., Stöcher, R. (1990) Expression of a stilbene synthase gene in *Nicotiana tabacum* results in synthesis of the phytoalexin resveratrol. *Plant Mol. Biol.* 15, 325–335.
8. Hain, R., Reif, H. J., Krause, E., Langebastels, R., Kindl, H., Vornam, B., Wiese, W., Schmecker, E., Schreier, P. H., Stöcker, R., Stenzel, K. (1993) Disease resistance results in foreign phytoalexin expression in a novel plant. *Nature* 361, 153–156.
9. Huszti, S., Tyihak, E. (1986) Formation of formaldehyde from S-adenosyl-L-(methyl-<sup>3</sup>H)methionine during enzymic transmethylation of histamine. *FEBS Letters* 209, 362–366.
10. Ingham, J. L. (1976) 3,5,4'-Trihydroxy-stilbenes a phytoalexin from groundnuts (*Arachis hypogaea*). *Phytochemistry* 15, 1791–1793.
11. Ingham, J. L. (1978) Isoflavonoid and stilbene phytoalexins of the genus *Trifolium*. *Biochem. Syst. Ecol.* 6, 217–223.
12. Jang, M., Cai, L., Udeani, G. O., Slowing, K. V., Thomas, C. F., Beecher, C. W. W., Fong, H. S., Farnsworth, N. R., Kinghorn, A. D., Mehta, R. G., Moon, R. C., Pezzuto, J. M. (1997) Cancer chemopreventive activity of resveratrol, a natural product derived from grapes. *Science* 275, 218–220.
13. Kedderis, G. L., Hollenberg, P. F. (1983) Peroxidase-catalysed N-demethylation reactions. *J. Biol. Chem.* 259, 663–668.
14. Kimura, Y., Okuda, Y., Namba, T., Negishi, T., Hayatsu, H. (1985) Effects of stilbenes on arachidonate metabolism in leukocytes. *Biochim. Biophys. Acta* 834, 275–278.
15. Lamuela Raventos, R. M., Romero-Perez, A. I., Waterhouse, A. I., de la Torre-Boronat, M. C. (1995) Direct HPLC analysis of cis- and trans-resveratrol and piccid isomers in Spanish red *Vitis vinifera* wines. *J. Agric. Food Chem.* 43, 281–283.
16. Orsini, F., Pelizzoni, F., Verotta, L., Aburjai, T. (1997) Isolation, synthesis and antiplatelet aggregation activity of resveratrol 3-O- $\beta$ -D-glucopyranoside and related compounds. *J. Nat. Prod.* 60, 1082–1087.
17. Rupprich, N., Kindl, H. (1978) Stilbene synthases and stilbene carboxylate synthases I. Enzymatic synthesis of 3,5,4'-trihydroxystilbene from p-coumaroyl CoA and malonyl CoA. *Hoppe-Seyler's Z. Physiol. Chem.* 359, 165–172.
18. Schröder, J., Lanz, T., Schröder, G. (1989) Genes for the biosynthesis of stilbene-type phytoalexins. In: Lamb, C., Beachy, R. (eds) *Plant Gene Transfer*. A. R. Liss Inc., New York.
19. Spencer, D., Henshall, T. (1955) The kinetics and mechanisms of the reaction of formaldehyde with dimedone (Part I). *J. Am. Chem. Soc.* 77, 1943–1948.
20. Stark-Lorenzen, P., Nelke, B., Hänssler, G., Mühlbach, H. P., Thomzik, J. E. (1997) Transfer of a grapevine stilbene synthase gene to rice (*Oryza sativa* L.). *Plant Cell Reports* 16, 668–673.

21. Szende, B., Tyihák, E., Trézsl, L., Kátay, Gy., Király-Véghely, Zs. (1998) Formaldehyde generators and capturers as influencing factors of mitotic and apoptotic processes. *Acta Biol. Hung.* 49, 323–329.
22. Thomzik, J. E. (1995) Agrobacterium-mediated transformation of stem disks from oilseed rape (*Brassica napus* L.). In: Davey, M., Gastland, K. (eds) *Methods in Molecular Biology*. Vol. 44. Agrobacterium protocols. Clifton, Humana Press, New Jersey.
23. Thomzik, J. E. (1996) Gene transfer in plants. *PflSchutz Nachrichten Bayer* (special issue) 49, 5–23.
24. Thomzik, J. E., Stenzel, K., Stöcker, R., Schreier, P. H., Hain, R., Stahl, D. J. (1997) Synthesis of a grapevine phytoalexin in transgenic tomatoes (*Lycopersicon esculentum* Mill) conditions resistance against *Phytophthora infestans*. *Physiol. Molec. Plant Pathol.* 51, 265–278.
25. Tyihák, E., Trezl, L., Szende, B. (1998) Formaldehyde cycle and the phases of stress syndrome. *Ann. N.Y. Acad. Sci.* 851, 259–270.
26. Tyihák, E., Albert, L., Németh, Zs., Kátay, Gy., Király-Véghely, Zs., Szende, B. (1998) Formaldehyde cycle and natural formaldehyde generators and capturers. *Acta Biol. Hung.* 49, 225–238.
27. Uenobe, F., Nakamura, S-i, Miyazawa, M. (1997) Antimutagenic effect of resveratrol against Trp-P-1. *Mut. Res.* 373, 197–200.
28. Yu, P. H. (1997) Deamination of methylamine and angiopathy; toxicity of formaldehyde, oxidative stress and relevance to protein glycooxidation in diabetes. *J. Neural. Transm. (Suppl.)* 52, 207–222.





## RELATIONSHIP BETWEEN DIMEDONE CONCENTRATION AND FORMALDEHYDE CAPTURED IN PLANT TISSUES\*

ÉVA SÁRDI<sup>1</sup> and E. TYIHÁK<sup>2</sup>

<sup>1</sup> Department of Genetics and Plant Breeding, University of Horticulture and Food Industry,  
Budapest, Hungary

<sup>2</sup> Plant Protection Institute, Hungarian Academy of Sciences, Budapest, Hungary

(Received: 1998-10-28; accepted: 1998-11-25)

In different parts of water-melon plants (*Citrullus vulgaris* L.) formaldehyde (HCHO), in dimedone adduct form (formaldemethone), and fully N-methylated substances were identified and determined by OPLC as well as HPLC, capillary GC and GC-MS methods using authentic substances. The HCHO captured originates from dynamic methylation and demethylation processes in which this simplest aliphatic aldehyde is bound in the form of highly reactive hydroxymethyl groups. Dimedone will react with the small quantity of HCHO in equilibrium with the hydroxymethyl groups and it follows from this that the rate of HCHO captured as the dimedone adduct will increase parallel to the increasing concentration of dimedone applied, as a methanolic solution, until a plateau is reached. The level of HCHO was very high in the roots of water-melon seedlings.

**Keywords:** *Citrullus vulgaris* L. – formaldehyde – dimedone – methylation – demethylation

### INTRODUCTION

According to recent investigations, all biological systems possess a HCHO-yielding potential which can originate from methylation and demethylation processes, alike [6, 8, 9, 18]. Recently, it has been shown that radiolabelled formaldemethone is formed from the S-CH<sub>3</sub>-<sup>3</sup>H of S-adenosyl-L-methionine (SAM) in the course of the enzymic conversion of histamine to N<sup>ε</sup>-methylhistamine in the presence of dimedone as a HCHO capture molecule; this suggests that the formation of HCHO is probably linked to the enzymic transmethylation of histamine [6]. HCHO, from S-CH<sub>3</sub>-<sup>3</sup>H of SAM might be coupled with an NH<sub>2</sub> group of an amino acid (e.g. arginine) of the active site of the histamine-N-methyltransferase (HNMT), forming a hydroxymethyl-protein and then this hydroxymethyl-protein might yield its labile hydroxymethyl (-CH<sub>2</sub>OH) group to the acceptor molecule. A complete loss of enzyme activity by modifying arginine residues of HNMT seems to confirm this assumption [6]. It also

\* Presented at the 4th International Conference on the Role of Formaldehyde in Biological Systems, July 1-4, 1998, Budapest, Hungary.

Send offprint requests to: Dr. Éva Sárdi, Department of Genetics and Plant Breeding, University of Horticulture and Food Industry, Budapest, H-1502 P.O. Box 53, Hungary.



follows from these results that the high level of HCHO and, at the same time, accumulation of N-methylated substances during early development stages and in rapidly dividing cells originate from the intensive transmethylation reactions [18].

It is better known that during the demethylation process HCHO and the demethylated compound can be formed [2, 8, 9]. As a result of disease stress, the amount of HCHO considerably increased in virus-infected tobacco leaves and it was supposed that this was the result of enhanced enzymic demethylation processes (biotic stress) [11, 14]. With L-methionine and SAM as substrates the demethylase activity was significantly high [1]. A strong correlation exists between the external temperature and the amount of measurable HCHO in Pinto bean leaf tissues [15]. As a result of heat stress (HS), the level of 3 potential HCHO generators (trigonelline, choline and TML) moderately decreased. The higher activity of demethylases at elevated temperatures, including HS is the cause of higher amounts of HCHO (abiotic stress) [4].

It is more and more evident that there is a HCHO cycle in biological systems [16, 17], that is, formation of the methyl group of L-methionine takes place through HCHO and the formation of HCHO from SAM is linked to different enzymatic transmethylation reactions [6, 16, 17]. There exists a number of quick HCHO pathways through the hydroxymethyl groups in different tissues [17]. It follows from these new results that there is an analyzable amount of HCHO in different biological systems and that HCHO is not a side product, but a basic and indispensable substance of the biological processes.

This paper describes the isolation, identification and measurement of HCHO in parts of water-melon as a test plant with special emphasis on the earliest phases of ontogenesis as well as on the effect of dimedone concentration applied on the measurable amount of HCHO.

## MATERIALS AND METHODS

### *Plant material*

Water-melon plants (*Citrullus vulgaris* L. cv. Szigetcsépi 51 F<sub>1</sub> hybrid) were cultivated in commercial compost in a greenhouse. The seeds were collected from field experiments (1993) according to the practice of the Department of Genetics and Plant Breeding.

### *Chemicals*

All the chemicals were of analytical grade and were purchased from REANAL Co. (Budapest, Hungary) and Merck Co. (Darmstadt, Germany).

### *Synthesis of formaldemethone (1,3,1'3'-tetraketo-5,5,5',5'-tetramethyl-4,4'-dicyclomethane)*

Formaldemethone was prepared by adding formaldehyde solution (10 cm<sup>3</sup> of 38% solution) to a solution of dimedone (2.5 g) in hot ethanol (15 cm<sup>3</sup>) and water (2.5 cm<sup>3</sup>). The white precipitate formed was removed by filtration and recrystallized from aqueous ethanol, m.p. 191 °C [13].

### *Chemical preparation of plant samples*

The seeds and the fresh parts of plants were frozen with liquid nitrogen, powdered and treated with dimedone solution (from 0.71 mM to 142.86 mM methanolic dimedone solution) (e.g. 0.25 g plant powder/0.7 cm<sup>3</sup> of dimedone solution) for 30 min. This suspension was centrifuged at 1500 g for 10 minutes at 4 °C. The clear supernatant was promptly used for overpressured layer chromatographic (OPLC) [19] and (after dilution) for high performance liquid chromatographic (HPLC) separations [12] (A long storage of the reaction mixture with or without tissues may result in decrease of the formaldemethone value).

### *Preparation of seedling roots with dimedone in different solvents*

The fresh root tissue of seedlings was frozen with liquid nitrogen, powdered and treated with dimedone (1.43 mM and 3.57 mM) in different solvents (acetonitrile, acetone, ethanol and methanol) (e.g. 0.25 g powder/0.7 cm<sup>3</sup> dimedone solution) for 30 min. These suspensions were centrifuged at 1500 g for 10 min at 4 °C. The clear supernatants were promptly used for OPLC separations [14].

### *Reaction of HCHO solutions with methanolic dimedone solutions of different concentration*

The 50 and 500 µmol formaldehyde solutions were treated with dimedone solution (from 0.71 mM to 142.86 mM methanolic dimedone solution) and analysed by OPLC [19].

### *OPLC system for the consecutive separation of formaldemethone and dimedone*

Off-line OPLC separations were carried out with a Chrompres 25 OPLC chromatograph (Factory of Laboratory Instruments Co., Ltd., Budapest, Hungary). Samples were applied with a Hamilton syringe (Bonaduz, Switzerland). Separation of formaldemethone was carried out with a chloroform-methylene chloride eluent mixture (35 : 65, V/V) on silica gel 60 F<sub>254</sub> chromatoplates with impregnated edges [3]. For the separation of residual dimedone, acetone was used. The densitograms were recorded with a Shimadzu CS 930 scanner (Shimadzu Co., Kyoto, Japan) at  $\lambda = 260$  nm for formaldemethone after the 1st separation step.



### *Isolation of formaldemethone from the root tissue extract of water-melon seedlings*

The fresh root tissue of water-melon seedlings was frozen with liquid nitrogen, powdered and treated with dimedone solution (1.0 g plant powder in 2.0 cm<sup>3</sup> of dimedone solution (21 mM) in methanol). After centrifugation, an aliquot of the supernatant was applied as a broad band (15 cm) to a silica gel 60 F<sub>254</sub> chromatoplate (Merck Co., Germany) with impregnated edges by means of a Linomat III automatic sample applicator (Camag Co., Muttensz, Switzerland).

A Chrompres 25 OPLC system, operated at an overpressure of 25 bar, was used for the off-line separation applying chloroform-methylene chloride (30 : 90, V/V) as eluent to a migration distance of 19 cm. The formaldemethone band with an R<sub>f</sub> of ca. 0.3, corresponding to authentic formaldemethone was scraped from the sorbent layer into a glass tube and the powder extracted with acetone. After centrifugation the supernatant was used, after partial evaporation, for GC-MS studies (from the 0.25 mg/cm<sup>3</sup> acetone solution) and then, as an identified sample, was used for OPLC and HPLC investigations alongside authentic formaldemethone.

The UV-spectrum of formaldemethone was recorded by a Shimadzu CS 930 scanner directly from the sorbent layer after OPLC separation.

### *HPLC separation of formaldemethone*

A Liquochrom Mode 2010 liquid chromatograph equipped with an UV 308 detector (Factory of Laboratory Instruments Co., Ltd., Budapest, Hungary), OH-814 recorder (RADELKIS Co., Budapest, Hungary), Digint-180 Integrator (Servintern Co., Budapest, Hungary) and a 20 µl loop was used. The formaldemethone was eluted with methanol at a flow-rate of 0.7 cm<sup>3</sup>/min and UV detection (260 nm) using a BST Si-100-S C-18 column (250 mm × 4 mm I.D., 10 µm) (Bioseparation Technical Co., Budapest, Hungary) [12].

### *Capillary column gas chromatography-mass spectrometry of dimedone and formaldemethone*

GC analyses were performed using a Shimadzu GC-4A gas chromatograph (Shimadzu Co., Kyoto, Japan) fitted with a fused silica capillary column (Rtx-5) (30 cm × 0.25 mm I.D.) coated with a 0.25 µm film thickness of the immobilized 5% phenyl-, 95% dimethyl-polisiloxane stationary phase and a flame ionization detector (FID). The conditions used were as follows: carrier gas, nitrogen at a flow-rate of 13.5 cm<sup>3</sup>/sec and N<sub>2</sub>/H<sub>2</sub> (1 : 1 V/V) was used as the gas for the FID, which was set to 250 °C; inlet pressure of make-up gas, 1.3 bar; pressure of air, 1.5 bar; injector temperature, 220 °C (isothermal); splitting ratio, 1 : 20. The retention time of authentic dimedone and formaldemethone were as follows: between 1.0 and 2.0 min and 5.8

and 6.0 min, respectively. For GC-MS a model Shimadzu GC-MS-QP 2000 fitted with the same column as above was used. The chromatographic conditions were as follows: carrier gas, helium at a flow-rate of 25 cm<sup>3</sup>/s. The mass spectrometric conditions were as follows: electron energy, 70 eV; temperature 250 °C; ion multiplier potential, 1.4 kV [7].

## RESULTS

### *Identification of HCHO, in dimedone adduct form, from different parts of water-melon plants*

Figure 1 illustrates the UV-spectrum of the authentic and isolated formaldemethone which were recorded directly from the sorbent layer after OPLC separation.

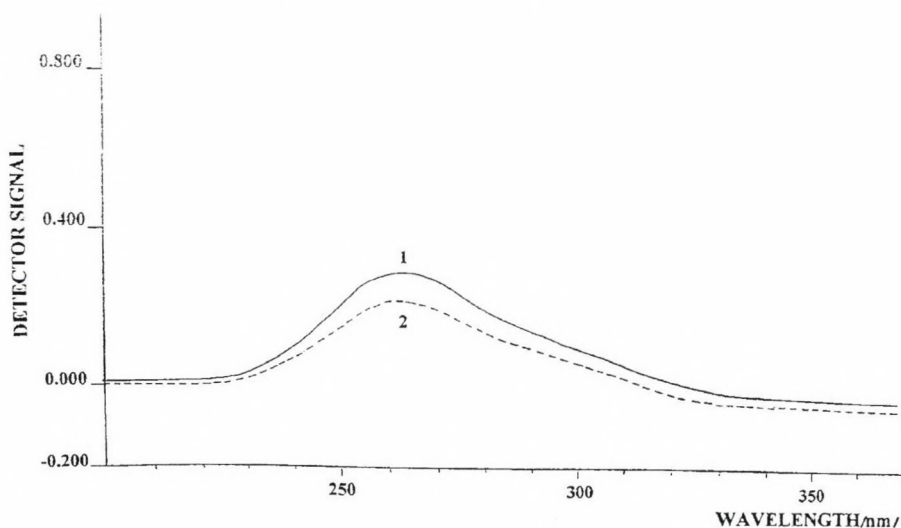


Fig. 1. The UV-spectrum of authentic (1) and isolated (2) formaldemethone

The capillary GC system was used suitable for the identification of HCHO, as its dimedone adduct, isolated from the roots of water-melon seedlings. The retention time was 5.9 min for both the authentic and isolated formaldemethone.

Mass spectrometric data (Table 1) confirm that the compound isolated was formaldemethone.

Figure 2 illustrates representative HPLC chromatograms of extracts made with methanolic dimedone solution of three parts of *Citrullus vulgaris* L. cv. Szigetcsépi 51 F<sub>1</sub> hybrid. It can be seen clearly that the level of dimedone decreased in correla-



tion with the quantity of formaldehyde formed. This simple, sensitive HPLC method was successfully used for the measurement of HCHO, in dimedone adduct form, from the different parts of water-melon plants.

Table 1

Mass numbers and relative intensities of authentic formaldehyde and formaldehyde isolated from root of water-melon seedlings

m/z	Relative intensity, %	m/z	Relative intensity, %
authentic		isolated	
292 (M+)	70	292 (M+)	88
191	18	191	18
165	90	165	92
124	32	124	35
97	30	97	38
83	70	83	88
69	49	69	54
55	77	55	88
41	64	41	90

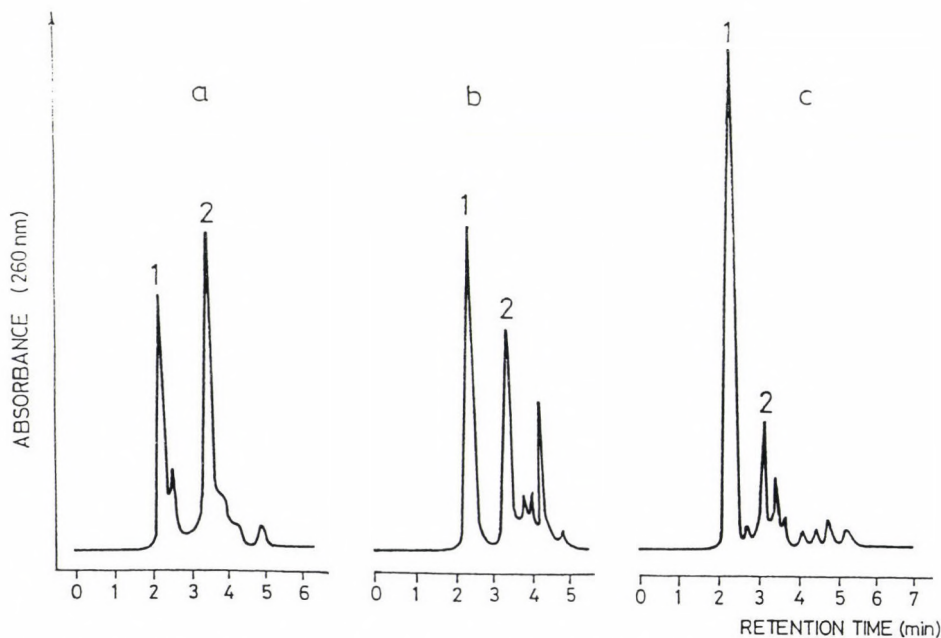


Fig. 2. Level of formaldehyde in extracts of different parts of water-melon plants (a: root of seedling, b: seed leaf, c: seed). Representative HPLC chromatograms, 1: dimedone, 2: formaldehyde

### Effect of dimedone concentration on the amount of HCHO bound

Figure 3 illustrates clearly that the amount of HCHO bound by dimedone from the fresh parts of water-melon plants depends considerably on the concentration applied of this capture molecule.

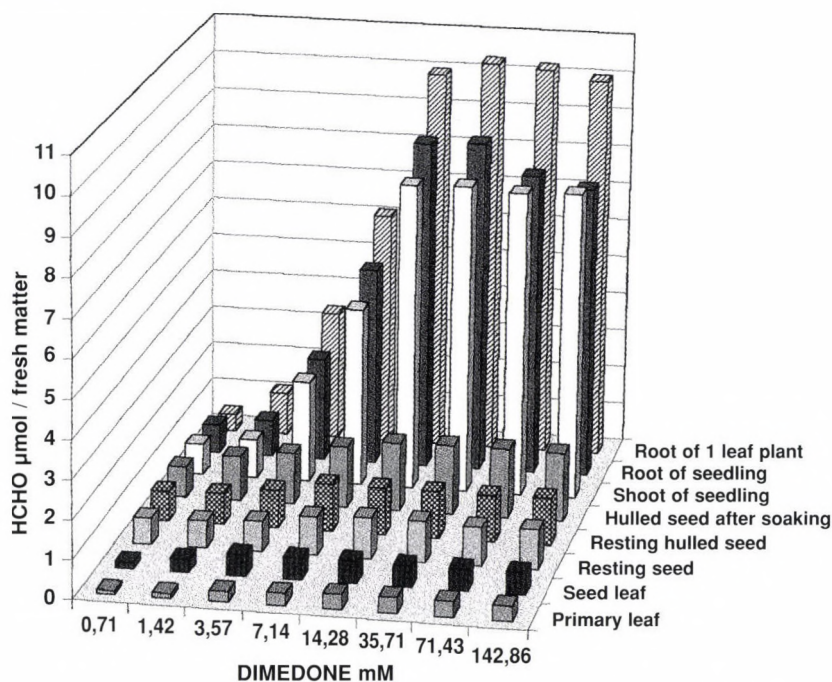


Fig. 3. Effect of dimedone concentration on the amount of HCHO bound

Table 2 illustrates these results converted to  $\mu\text{mol/g}$  dry matter. It can be seen from Figure 3 and Table 2 that in all cases the level of HCHO was increased with increasing concentration of dimedone. This observation is especially true in the case of roots of young plants where we could detect a surprisingly high level of HCHO using different dimedone concentrations. The results also show that at higher dimedone concentrations (over 0.5%) the measurable amount of HCHO is not significantly higher and a saturation level is reached.

For controlling and understanding this special reaction mechanism, firstly we reacted diluted formalin solutions with methanolic dimedone solutions of different concentration; more exactly those originally used for the capture of HCHO from plant tissues. There was practically no difference between the measured formaldemethone values; that is, the amount of HCHO captured with dimedone did not increase with the increase in concentration.



*Table 2*  
Effect of dimedone concentration on the amount of HCHO dissociated

Dimedone mM	0.71	1.42	3.57	7.14	14.28	35.71	71.43	142.86
	HCHO $\mu\text{mol/g}$ dry matter							
Resting seed	$0.66 \pm 0.02$	$0.80 \pm 0.04$	$0.81 \pm 0.04$	$1.01 \pm 0.04$	$1.06 \pm 0.03$	$1.12 \pm 0.04$	$1.07 \pm 0.04$	$1.10 \pm 0.03$
Resting hulled seed	$0.78 \pm 0.03$	$0.83 \pm 0.03$	$1.06 \pm 0.04$	$1.31 \pm 0.05$	$1.30 \pm 0.06$	$1.31 \pm 0.05$	$1.30 \pm 0.06$	$1.31 \pm 0.04$
Hulled seed after soaking 24 h	$1.31 \pm 0.04$	$1.43 \pm 0.05$	$2.37 \pm 0.05$	$2.82 \pm 0.07$	$3.14 \pm 0.07$	$3.19 \pm 0.06$	$3.19 \pm 0.07$	$3.18 \pm 0.06$
Shoot of seedling	$9.97 \pm 0.22$	$12.47 \pm 0.20$	$32.62 \pm 0.66$	$57.50 \pm 0.97$	$98.97 \pm 1.25$	$99.43 \pm 1.18$	$98.19 \pm 1.15$	$98.87 \pm 1.19$
Root of seedling	$14.60 \pm 0.31$	$18.80 \pm 0.35$	$53.44 \pm 0.95$	$103.26 \pm 1.85$	$172.02 \pm 2.01$	$173.44 \pm 2.00$	$171.10 \pm 2.11$	$170.10 \pm 2.15$
Primary leaf of 1 leaf plant	$2.22 \pm 0.06$	$2.64 \pm 0.07$	$10.55 \pm 0.20$	$24.69 \pm 0.51$	$37.76 \pm 0.68$	$37.54 \pm 0.69$	$37.61 \pm 0.60$	$37.57 \pm 0.68$
Seed leaf of 1 leaf plant	$1.07 \pm 0.05$	$1.47 \pm 0.07$	$3.76 \pm 0.07$	$7.40 \pm 0.15$	$11.97 \pm 0.21$	$19.91 \pm 0.34$	$19.89 \pm 0.04$	$19.57 \pm 0.05$
Root of 1 leaf plant	$6.20 \pm 0.19$	$7.70 \pm 0.18$	$40.24 \pm 0.70$	$81.83 \pm 1.35$	$140.33 \pm 2.17$	$142.52 \pm 3.15$	$142.02 \pm 2.21$	$140.00 \pm 2.25$

Table 3  
Relationship between the dimedone concentration in methanol and the "pseudo pH"

Dimedone %	"Pseudo pH"
0.01	4.95
0.02	4.70
0.05	4.50
0.07	4.40
0.10	4.20
0.20	3.80
0.50	3.60
0.70	3.60
1.00	1.60
MeOH	6.40

When ethanol, acetonitrile and acetone were used to prepare dimedone solutions, the amount of HCHO detected, as formaldemethone, was very similar in all cases. However, methanolic dimedone solution gave a reaction mixture which was more advantageous for quantitative chromatographic evaluation (e.g. in the case of dimedone solution in acetone, condition favoured the formation of other unknown dimedone derivatives as well).

Finally it is supposed that by increasing dimedone concentration in methanol the amount of active hydrogen atoms will increase in the methanolic solution and there is a possibility for measuring "pseudo pH" values. Table 3 supports our original theory: "the pseudo pH" decreases parallel with the increase in dimedone concentration. These hydrogen ions can dissociate the HCHO from the labile hydroxymethyl groups.

## DISCUSSION

The occurrence of HCHO, captured as its dimedone adduct, was demonstrated in different parts of water-melon plants by means of different chromatographic and spectroscopic techniques.

It is known that HCHO can be bound in the form of labile reactive groups to endogenous molecules (e.g. guanidine groups of proteins, glutathione) [6, 10]. The basis of the formaldemethone formation is that the small quantity of HCHO in equilibrium with the hydroxymethyl groups will react with dimedone to form formaldemethone. This will disturb the equilibrium and more HCHO will be formed, which, in turn, will react with dimedone.

It also follows from our experiments that water-melon tissues possess a HCHO-yielding potential which can originate from methylation and demethylation process-



es. It is obvious that the ratio between HCHO from methylation and demethylation processes depends on the age of the plant part in normal environmental conditions. A biotic and/or abiotic stress situation(s) provides favourable conditions for the formation of HCHO. Our results support the earlier observations [18] that the accumulation of HCHO in hydroxymethyl groups of different binding force is especially intensive in the early development stages and in rapidly dividing cells. However, we first demonstrated that a large amount of HCHO can be isolated from the roots of plants where the main transmethylation and other reactions take place.

These studies firstly provide a detailed analysis of the occurrence of HCHO in different parts of a plant. The relatively high level of HCHO in the seed samples can originate from a continuous formation of HCHO from the effects of peroxidases and other demethylases on the methylated substances. This HCHO (mainly in excited form) can participate in the prevention of attack of seed tissues by pathogens [17]. However, the finding that the HCHO yield from plant parts is dependent on the dione concentration used opens a new horizon for studying the fundamental functions of this aliphatic aldehyde in different biological-biochemical processes. It also follows from these results that in future we should use the same dione concentration in comparative studies. In future these new facts about HCHO have to be taken into account in other biological systems, as well [5, 10].

#### ACKNOWLEDGEMENTS

We wish to thank Prof. Dr. J. Balla (Technical University of Budapest) for capillary GC and GC-MS measurements and Dr. A. Végh for the densitometric evaluation of OPLC chromatograms.

#### REFERENCES

1. Burgyán, J., Szarvas, T., Tyihák, E. (1982) Increased formaldehyde production from L-methionine- $(S-^{14}CH_3)$  by crude enzyme of TMV infected tobacco leaves. *Acta Phytopathol. Acad. Sci. Hung.* 17, 11–15.
2. Fannin, F. F., Bush, L. P. (1992) Nicotine demethylation in *Nicotiana*. *Med. Sci. Res.* 20, 867–868.
3. Gersbeck, N., Schönbeck, F., Tyihák, E. (1989) Measurement of formaldehyde and its main generators in *Erysiphe graminis* infected barley plants by planar chromatographic techniques. *J. Planar Chromatogr.* 2, 86–89.
4. Gullner, G., Tyihák, E. (1987) Hydrogen peroxide dependent N-demethylase activity in the leaves of normal and heat-shocked bean plants. *Plant Sci.* 52, 21–27.
5. Heck, H. d'A., Casanova, M., Starm, T. B. (1990) Formaldehyde toxicity – new understanding. *Crit. Rev. Toxicol.* 20, 397–426.
6. Huszti, Z., Tyihák, E. (1986) Formation of formaldehyde from S-adenosyl-L-(methyl-3H) methionine during enzymatic transmethylation of histamine. *FEBS Letters* 209, 362–366.
7. János, É., Balla, J., Tyihák, E., Gáborjányi, R. (1980) Gas-liquid chromatographic analysis of dione derivatives of formaldehyde and other aliphatic aldehydes on capillary column. *J. Chromatogr.* 191, 239–244.
8. Kawata, S., Sugiyama, T., Iami, J., Minami, Y., Tarui, S., Okamoto, M., Yamano, T. (1983) Hepatic microsomal cytochrome P-450 dependent N-demethylation of methylguanidine. *Biochem. Pharmacol.* 32, 3723–3728.

9. Kucharczyk, N., Yang, J. T., Wong, K. K., Sofia, R. D. (1984) The formaldehyde-donating activity of N<sup>5</sup>, N<sup>10</sup>-methylene tetrahydrofolic acid in xenobiotic biotransformation. *Xenobiotica* 14, 667–676.
10. Paik, W. K., Kim, S. (1980) *Protein Methylation*. Wiley and Sons, New York, pp. 132–136.
11. Sárdi, É., Tyihák, E. (1992) Effect of *Fusarium* infection on the formaldehyde cycle in parts of water-melon (*Citrullus vulgaris* L.) plants. In: E. Tyihák (ed.) *Proc. of 3rd Intern. Conf. on Role of Formaldehyde in Biological Systems*. Sopron, Hungary 1992. Hung. Biochem. Soc., Budapest, pp. 145–150.
12. Sárdi, É., Tyihák, E. (1994) Simple determination of formaldehyde in dimedone adduct form in biological samples by high performance liquid chromatography. *Biomed Chromatogr.* 8, 313–314.
13. Spencer, D., Henshall, T. (1955) The kinetics and mechanisms of the reaction of formaldehyde with dimedone. (Part I.) *J. Am. Chem. Soc.* 77, 1943–1948.
14. Tyihák, E., Balla, J., Gáborjányi, R., Balázs, E. (1978) Increased free formaldehyde level in crude extract of virus infected hypersensitive tobaccos. *Acta Phytopath. Acad. Sci. Hung.* 13, 29–31.
15. Tyihák, E. (1987) Is there a formaldehyde cycle in biological systems? In: E. Tyihák, G. Gullner (eds) *Proc. of 2nd Intern. Conf. on the Role of Formaldehyde in Biological Systems*, Keszthely, Hungary, SOTE Press. Budapest, 137–144.
16. Tyihák, E., Király, Z., Gullner, G., Szarvas, T. (1989) Temperature-dependent formaldehyde metabolism in bean plants. The heat shock response. *Plant Sci.* 59, 133–139.
17. Tyihák, E., Gullner, G., Trézsl, L. (1993) Formaldehyde cycle and possibility of formation of singlet oxygen in plant tissues. In: Gy. Mózsik et al. (eds) *Proc. Intern. Symp. on Oxygen free radicals and scavengers in the natural sciences*. Akadémiai Kiadó, Budapest, pp. 21–28.
18. Tyihák, E., Rozsnyay, Zs., Sárdi, É., Szőke, É. (1992) Formaldehyde cycle and the cell proliferation: plant tissue as a model. In: Tyihák, E. (ed.) *Proc. of 3rd Intern. Conf. on Role of Formaldehyde in Biological Systems*. Sopron, Hung. Biochem. Soc., Budapest, pp. 139–144.
19. Tyihák, E. (1987) Overpressured layer chromatographic methods in the study of the formaldehyde cycle in biological systems. *Trends Anal. Chem.* 6, 90–94.





## THE USE OF HPLC FOR THE DETECTION AND QUANTIFICATION OF FORMALDEHYDE IN THE PTERIDOPHYTA\*

MARICELA ADRIAN-ROMERO,<sup>1,2</sup> G. BLUNDEN,<sup>1</sup> B. G. CARPENTER,<sup>1</sup>  
SHEILA LUCAS<sup>1</sup> and E. TYIHÁK<sup>3</sup>

<sup>1</sup>School of Pharmacy and Biomedical Sciences, University of Portsmouth, Portsmouth, U.K.

<sup>2</sup>Faculty of Pharmacy, University of Los Andes, Mérida, Venezuela

<sup>3</sup>Plant Protection Institute, Hungarian Academy of Sciences, Budapest, Hungary

(Received: 1998-10-28; accepted: 1998-11-25)

Formaldehyde, as its dimedone adduct, formaldemethone, has been detected and quantified in all species of Pteridophyta examined. The procedure involved the use of an Hypersil C-18 column, methanol-water (60 : 40 v/v) as the mobile phase and an UV detector set at 258 nm. Quantification was based on peak height. Yields varied from 30 µg/g fresh weight for *Polystichum setiferum* to 5370 µg/g fresh weight for *Selaginella viticulosa*.

**Keywords:** Formaldehyde – formaldemethone – HPLC quantitative analysis – ferns – Pteridophyta

### INTRODUCTION

It has become evident in recent years that there is a formaldehyde cycle in biological systems and that there should be analysable amounts of formaldehyde in plant and animal tissues (Tyihák et al. [2] and references quoted therein). This has been demonstrated recently for marine algae. All 41 species tested showed the presence of formaldehyde; quantification of formaldehyde, after conversion to formaldemethone, was achieved using overpressured layer chromatography [3]. As this equipment is not widely available, an alternative method of quantitative analysis was required. An high performance liquid chromatographic procedure has been described by Sárdi and Tyihák [1] and this method has been modified for the routine quantitative analysis of formaldehyde in pteridophytes.

### MATERIALS AND METHODS

#### *Reagents*

Solvents were either of analytical or HPLC grade (Fisher Scientific, U.K., Loughborough, Leicestershire, U.K.). Formaldemethone was synthesised as

\* Presented at the 4th International Conference on the Role of Formaldehyde in Biological Systems, July 1-4, 1998, Budapest, Hungary.

Send offprint requests to: Professor Dr. G. Blunden, School of Pharmacy and Biomedical Sciences, White Swan Road, Portsmouth, Hampshire, PO1 2DT, U.K.



described by Tyihák et al. [2]. Dimedone was purchased from Sigma (Poole, Dorset, U.K.) and ethyl paraben from Aldrich Chemical Co. (Gillingham, Dorset, U.K.).

### *High-performance liquid chromatography (HPLC)*

The apparatus consisted of a LKB 2150 pump (dual piston), a Rheodyne sample injector fitted with a 20 µl loop, an HP 3396 A integrator and a Pye Unicam 4025 UV detector set at 258 nm. An Hypersil C18 column (150 mm × 4.6 mm; 5 µm) was used fitted with a 1 cm C-18 guard cartridge. The mobile phase was methanol-water (60 : 40 v/v) and the flow rate was 1 ml/min; the back pressure was less than 120 bar.

### *Linearity studies*

A standard solution of formaldemethone in methanol-water (60 : 40 v/v) was prepared containing 60 mg/l. From this, 9 ml was mixed with 0.5 ml ethyl paraben solution (20 mg/l) in methanol-water (60 : 40 v/v) and made up to 10 ml with the same solvent mixture. This produced a final solution containing 54 µg/ml formaldemethone. In a similar manner, solutions were prepared containing 48, 42, 36, 30, 24, 18, 12 and 6 µg/ml formaldemethone. The linearity of response was determined by injecting 10 µl of each dilution, in triplicate. Formaldemethone peaks were analysed by measuring their heights.

### *Extraction of plant material*

Fresh plant material of each species, as soon as possible after collection, was frozen and powdered in liquid nitrogen. From this, 500 mg was placed in an Eppendorf tube, mixed with 2 ml 0.2% dimedone solution in methanol and left for 24 hours at room temperature, after which time the supernatant was separated. In the case of *Cyrtomium fortunei*, 1 g frozen and powdered plant material was mixed with 4 ml 0.2% dimedone solution in methanol. Samples of supernatant (0.5 ml) were removed after 30 min and 1, 24, 48 and 72 hours. Control extracts were prepared of each species (500 mg), but with 2 ml methanol instead of dimedone solution. All the supernatants were examined by thin-layer chromatography (TLC) and HPLC.

Prior to examination by HPLC, the supernatants were filtered through a 0.22 µm nylon syringe filter (HPLC Technology, Macclesfield, Cheshire, U.K.). Each filtrate (0.25 ml) was mixed with 0.2 ml ethyl paraben solution (20 mg/l) and made up to 5 ml with methanol-water (60 : 40 v/v). Injection volumes of 10 µl were used for all samples. Formaldemethone peaks were assessed by measuring their heights.

### *Thin-layer chromatography*

The supernatants were examined on silica gel (Merck, TLC grade with fluorescent indicator) layers (250 µm) using chloroform as the development solvent. After development, formaldemethone was observed as a blue spot under ultraviolet light at 254 nm.

## RESULTS AND DISCUSSION

Separation of formaldemethone from dimedone was achieved using the HPLC procedure described and with methanol-water mixtures as the mobile phase. Mixtures of these solvents ranging from 100% methanol to methanol-water (50 : 50) were used. As the percentage of water increased, the retention time of formaldemethone also increased. Optimum separation was achieved using methanol-water (60 : 40) and this mixture was adopted for routine use (Fig. 1). Under these conditions, the development time was always less than 8 min.

A linear response between dimedone concentration and peak height was obtained for the range tested (60–540 ng/ml). Using the regression equation  $y=0.559+0.24 x$ , the value for  $R^2$  was 0.988.

Fresh *Cyrtomium fortunei* was frozen and powdered in liquid nitrogen, and reacted with dimedone solution. Samples were removed after 30 min and 1, 24, 48 and 72

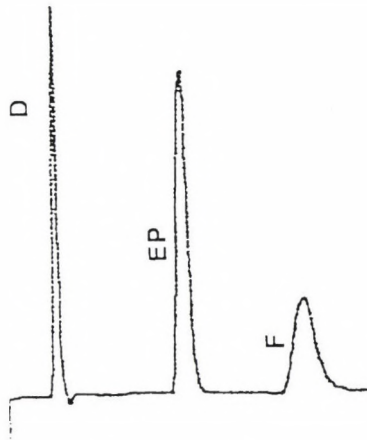


Fig. 1. HPLC Separation of dimedone (D), formaldemethone (F) and ethyl paraben (EP). Retention time : dimedone 1.03 min; ethyl paraben 3.86 min; formaldemethone 6.50 min

Table 1

Formaldehyde contents (as formaldemethone) of *Cyrtomium fortunei* extracts after different reaction times with dimedone

Species	Formaldehyde (as formaldemethone) yield ( $\mu\text{g/g}$ ) after				
	30 min	1 hour	24 hours	48 hours	72 hours
<i>Cyrtomium fortunei</i>	160	180	320	320	330
Sample 2	160	210	430	420	440



*Table 2*  
Formaldehyde contents (as formaldemethone) of Pteridophyta species

Species	Place of collection	Date of collection	Formaldehyde (as Formaldemethone) (µg/g fresh tissue)
FILICOPSIDA			
Adiantaceae			
<i>Adiantum capillus-veneris</i>	Havant, Hampshire U.K. (conservatory)	November 1997	760
Aspidiaceae			
<i>Cyrtomium fortunei</i>	Havant, Hampshire U.K. (conservatory)	December 1997	430
<i>Dryopteris felix-mas</i>	Cambridge University Botanic Garden, U.K.	November 1997	50
<i>Polystichum setiferum</i>	Cambridge University Botanic Garden, U.K.	November 1997	50
Aspleniaceae			
<i>Asplenium trichomanes</i>	Ballyvaughan, Co. Clare, Ireland	March 1998	2130
<i>Ceterach officinarum</i>	Finavarra, Co. Clare Ireland	March 1998	2360
<i>Phyllitis scolopendrium</i>	Near Uppark, W. Sussex, U.K.	December 1997	310
Azollaceae			
* <i>Azolla filiculoides</i>	Romsey, Hampshire, U.K.	January 1998	110
Blechnaceae			
<i>Doodia maxima</i>	Cambridge University Botanic Garden, U.K.	November 1997	80
Hypolepidaceae			
<i>Pteridium aquilinum</i>	Near Veryan, Cornwall, U.K.	April 1998	2540

Species	Place of collection	Date of collection	Formaldehyde (as Formald emethone) (µg/g fresh tissue)
Oleandraceae			
<i>Nephrolepis cordifolia</i>	Cambridge University Botanic Garden, U. K.	November 1997	410
<i>N. exaltata</i>	Havant, Hampshire, U.K. (conservatory)	November 1997	50
Polypodiaceae			
<i>Polypodium vulgare</i>	Finavarra, Co. Clare, Ireland	March 1998	1400
SPHENOPSIDA			
Equisetaceae			
<i>Equisetum telmateia</i>	Near Liss, Hampshire, U.K.	March 1998	2640
LYCOPSIDA			
Lycopodiaceae			
<i>Lycopodium phlegmaria</i>	Cambridge University Botanic Garden, U.K.	April 1998	2330
Selaginellaceae			
<i>Selaginella viticulosa</i>	Cambridge University Botanic Garden, U.K.	April 1998	5370

\* Co-occurs with the cyanobacterium *Anabaena*



hours. The formaldemethone content of the 24 hour sample was noticeably higher than that of the 30 min and 1 hour samples. The results for the 24, 48 and 72 hour samples were very similar (Table 1). These data resulted in the routine use of a 24 hours reaction time. The importance of the concentration of dimedone to optimise formaldemethone production has been reported earlier [2]. All extracts contained excess dimedone.

The extracts of each plant species treated with dimedone solution, when examined by TLC and HPLC, showed the presence of formaldemethone. However, no corresponding spot on TLCs or peak on HPLCs was observed when methanolic extracts of the plants were tested. The formaldehyde contents (as formaldemethone) of sixteen species of Pteridophyta are listed in Table 2. The species investigated included representatives of the Filicopsida, Sphenopsida and Lycopsidea.

The data generated show that the HPLC procedure devised for the analysis of formaldehyde in plant tissues, after capture as formaldemethone, is suitable as a rapid and reliable method for the quantitative estimation of this compound.

#### ACKNOWLEDGEMENTS

We thank the director, University of Cambridge Botanic Garden, for the supply of several of the species. Other species were kindly either supplied or collected by Mr and Mrs A Greenhouse and Mr T M Blunden.

#### REFERENCES

1. Sárdi, É., Tyihák, E. (1994) Simple determination of formaldehyde in dimedone adduct form in biological samples by high performance liquid chromatography. *Biomed. Chromatog.* 8, 313–314.
2. Tyihák, E., Blunden, G., Yang, M-H., Crabb, T. A., Sárdi, E. (1996) Formaldehyde, as its dimedone adduct, from *Ascophyllum nodosum*. *J. Appl. Phycol.* 8, 211–215.
3. Yang, M-H., Blunden, G., Tyihák, E. (1998) Formaldehyde from marine algae. *Biochem. System. Ecol.* 26, 117–123.

## DROUGHT STRESS, PEROXIDASE ACTIVITY AND FORMALDEHYDE METABOLISM IN BEAN PLANTS\*

ÉVA STEFANOVITS-BÁNYAI,<sup>1</sup> ÉVA SÁRDI,<sup>2</sup> SUSAN LAKATOS,<sup>3</sup>  
M. ZAYAN<sup>4</sup> and I. VELICH<sup>2</sup>

<sup>1</sup>Department of Chemistry and Biochemistry, University of Horticulture and Food Industry,  
Budapest, Hungary

<sup>2</sup>Department of Genetics and Plant Breeding, University of Horticulture and Food Industry,  
Budapest, Hungary

<sup>3</sup>Department of Pathophysiology, Institute of Health, HHDF, Budapest, Hungary

<sup>4</sup>Faculty of Agriculture Horticulture Department, Tanta University, Kafr El-Shiekh, Egypt

(Received: 1998-10-28; accepted: 1998-11-25)

In our investigations we have studied the changes of total peroxidase and isozyme activities, peroxidase isozyme pattern and the level of endogenous formaldehyde and trigonelline.

We have examined the effect of drought stress resulted by Carbowax treatment (2, 5, 7, 10%) of two different snap bean (*Phaseolus vulgaris* L.) genotypes [drought tolerant (T) and drought sensitive (S)]. There were no detectable differences in the peroxidase isozyme patterns but the total peroxidase activity was increased. We have found similar steep enhancement in the peroxidase activities of one of three peroxidase fractions while the increase in the other isozyme fractions was not so significant in the two genotypes. Increasing peroxidase activities and changes in the amount of endogenous formaldehyde and trigonelline were detectable with increasing Carbowax treatment in both genotypes, but in different ways.

According to our experiments, the total peroxidase and some isozyme activity correlated with the concentration of endogenous formaldehyde and trigonelline, playing an important role during drought stress.

**Keywords:** Drought stress – formaldehyde – *Phaseolus vulgaris* L. – N-methylated substances – peroxidase

### INTRODUCTION

In spite of its toxic and carcinogenic nature formaldehyde (HCHO) is present in a relatively high concentration in various biological systems and it is a basic and indispensable substance of the biological processes [6, 17]. Endogenous HCHO is produced partly by enzymatic demethylation (demethylases, peroxidases) [5, 8, 9] of different N-, S-, O-methylated compounds, i.e. these compounds can be considered as potential precursors of HCHO [7, 10].

The strong correlation found between stress (abiotic or biotic) and the amount of HCHO can be attributed to an increased activity of demethylases [5] and at the same time stress results in a moderate decrease in the level of the some N-methylated com-

\* Presented at the 4th International Conference on the Role of Formaldehyde in Biological Systems, July 1–4, 1998, Budapest, Hungary.

Send offprint requests to: Dr. Éva Stefanovits-Bányai, Department of Chemistry and Biochemistry, University of Horticulture and Food Industry, H-1502 Budapest, P.O. Box 53, Hungary.



pounds (trigonelline, choline) [18, 19]. The amount of HCHO increases considerably in virus infected tobacco leaves [17]. The high level of HCHO could be attributed to enhanced enzymatic demethylation of L-methionine and S-adenosyl-L-methionine [2] under biotic stress conditions. It can generally be said that naturally occurring quaternary ammonium compounds, which form a structurally heterogeneous class of compounds with the unifying character of a polar, often methylated ammonium head, are the potential metabolic components of stress tolerance [13, 14].

It is established that tolerance of a genotype to drought stress is closely associated with its antioxidant enzyme system. Two wheat genotypes were studied [12] and it was demonstrated that upon drought stress peroxidase activities were increased in both cases. It was found that water stress caused a 200–300% increase in cell wall-associated peroxidase activity in the leaf elongation zone of *Lolium* plants in different drought tolerant soybeans [1]. According to Zheng there is an easily detectable dependence of peroxidase activity upon drought stress [22]. However, Wang could not detect any correlation between peroxidase activity and the extent of drought resistance of maize [20]. It is very difficult to clarify the physiological bases of drought resistance since the rate and kinetics of oxidative burst upon stress depends on the extent of resistance of plant species [21]. Little is known about the relationship if any between drought resistance, antioxidant enzyme activities and the amount of fully N-methylated compounds in different snap bean genotypes.

The aim of this study was to find “biochemical response reactions” which may characterize changes brought about by drought stress in two different snap bean genotypes. Therefore the peroxidase isozyme patterns, the total peroxidase activities, as well as concentrations of HCHO and of the fully N-methylated compound (trigonelline) were compared for bean samples grown under normal and drought stress conditions induced by Carbowax (2, 5, 7 and 10%).

## MATERIALS AND METHODS

### *Plant samples and Carbowax treatment*

We have examined the effects of abiotic stress on two different snap bean genotypes [drought tolerant (T) and drought sensitive (S)] cultivated in commercial compost in a greenhouse. The test plants were treated with Carbowax (2, 5, 7, 10%) and the control ones with an equal volume of distilled water.

### *Sample preparation for OPLC analysis*

The fresh trifoliolate leaves of two different snap bean genotypes were frozen with liquid nitrogen, powdered and treated with dimedone solution (0.05 % dimedone in methanol) (e.g. 0.25 g plant powder/ 0.7 cm<sup>3</sup> of dimedone solution). This suspension was centrifuged at 1500 g for 10 minutes at 4 °C. The clear supernatants were used

for overpressured layer chromatography (OPLC) [4]. Samples were applied with a NANOMAT sample applicator (CAMAG Co., Muttensz, Switzerland).

### *OPLC separations*

The experiments were carried out on OPLC silica gel 80 F 254 precoated chromatoplates using chloroform-methylenechloride (35 : 65, V/V) for formaldemethone determination and i-propanol-methanol-0.1M sodium acetate (20 : 3 : 30, V/V) for the quaternary ammonium compounds. The system was calibrated with a mixture of N<sup>ε</sup>-trimethyl-L-lysine, choline, carnitine, trigonelline and betaine (Merck),  $\lambda = 265$  nm and at  $\lambda = 525$  nm for formaldemethone and for the quaternary ammonium compounds, respectively, using Dragendorff reagent in the latter case. The separations were carried out with an OPLC chromatograph (developed by OPLC-NIT Co., Ltd., Budapest, Hungary). Densitograms were prepared with a Shimadzu CS-930 scanner (Shimadzu Co., Kyoto, Japan).

### *Sample preparation for isoelectric focusing*

Leaves (1 g) were homogenized in 1 ml ice cold extraction buffer: 20 mM Tris-HCl buffer pH 7.8, containing 0.2 mg/ml MgCl<sub>2</sub>, 200 mg/ml saccharose, 3.4 mg/ml potassium metabisulfite, 0.35 mg/ml bovine albumin and 100 mg/ml TritonX-100. The crude extract was centrifuged (1500 g, 4 °C, 15 min) and the supernatants were analyzed.

### *Isoelectric focusing*

This was carried out on a PhastSystem (LKB-Pharmacia, Sweden). In order to develop a pH gradient (pH 3–9) ready-made gels were prerun at 2.5 mA at 10 °C, for 75 Vh, and crude extracts of samples were applied onto the acidic (pH 4.5) end of the gel and run at 2.5 mA at 10 °C, for 700 Vh. Gels were stained for evidence of peroxidase activity with o-dianisidine [15]. Dry gels were scanned and evaluated by an Image Master densitometer (Sharp JX-330).

The total peroxidase activity (U/ml) of snap beans was measured by a spectrophotometric method (Varian DMS 100 UV-Visible Spectrophotometer) [3].

## RESULTS AND DISCUSSION

Figure 1 shows the level of formaldehyde ( $\mu$ g/g fresh matter) in the leaves of two snap bean genotypes grown under different drought stress conditions (Carbowax at 2, 5, 7 and 10%). The formaldehyde level gradually increased with increasing drought stress from 2% to 10%, but in a different way.



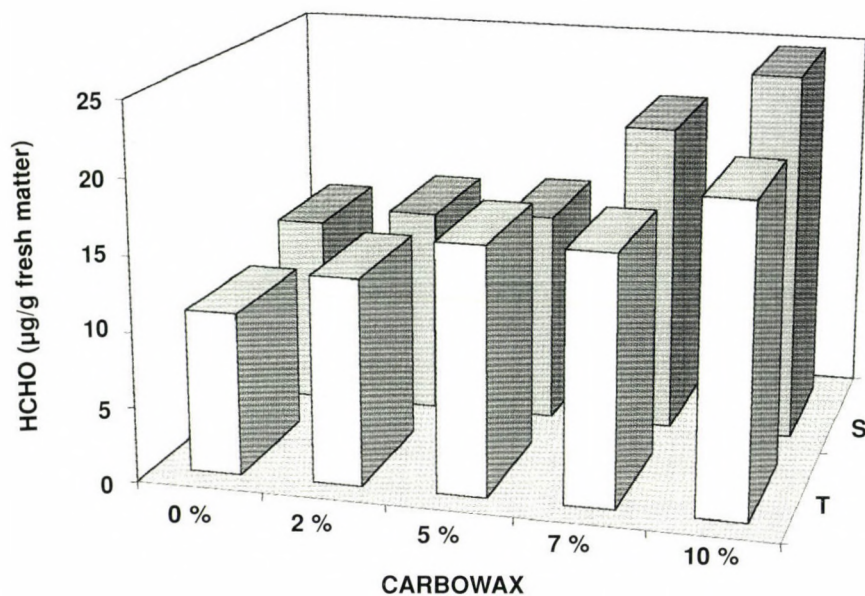


Fig. 1. Effect of Carbowax (2, 5, 7, and 10%) on level of formaldehyde in snap beans [drought tolerant (T), drought sensitive (S)]

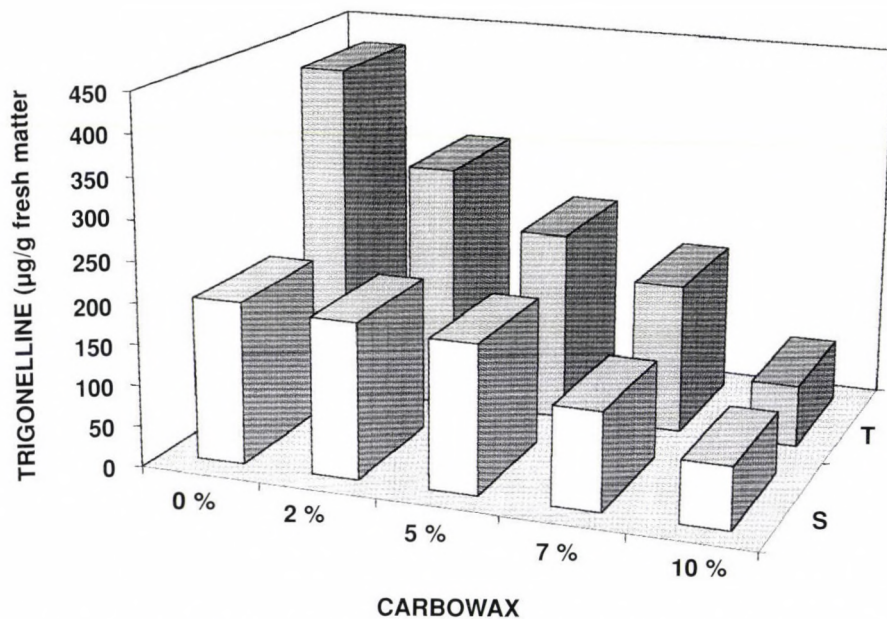


Fig. 2. Effect of Carbowax (2, 5, 7, and 10%) on level of trigonelline in snap beans [drought tolerant (T), drought sensitive (S)]

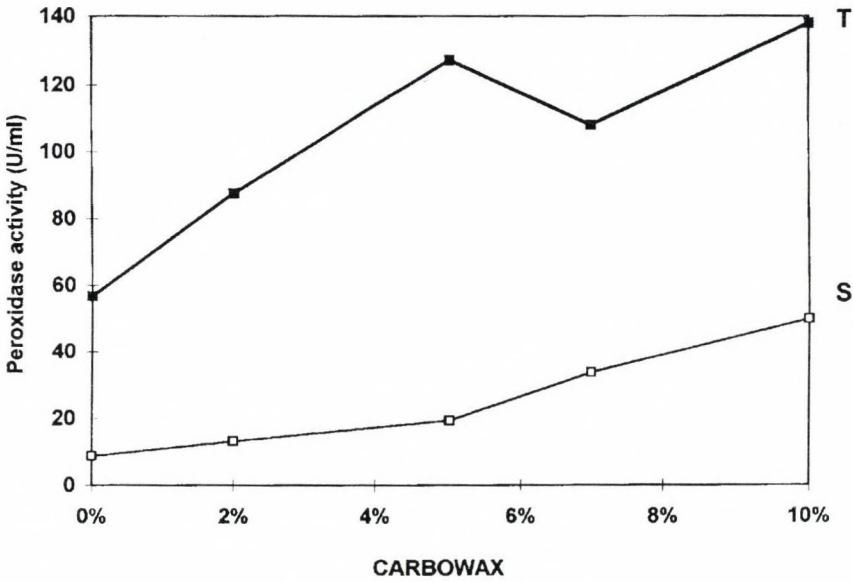


Fig. 3. Effect of Carbowax (2, 5, 7, and 10%) on total peroxidase activity in snap beans [drought tolerant (T), drought sensitive (S)]

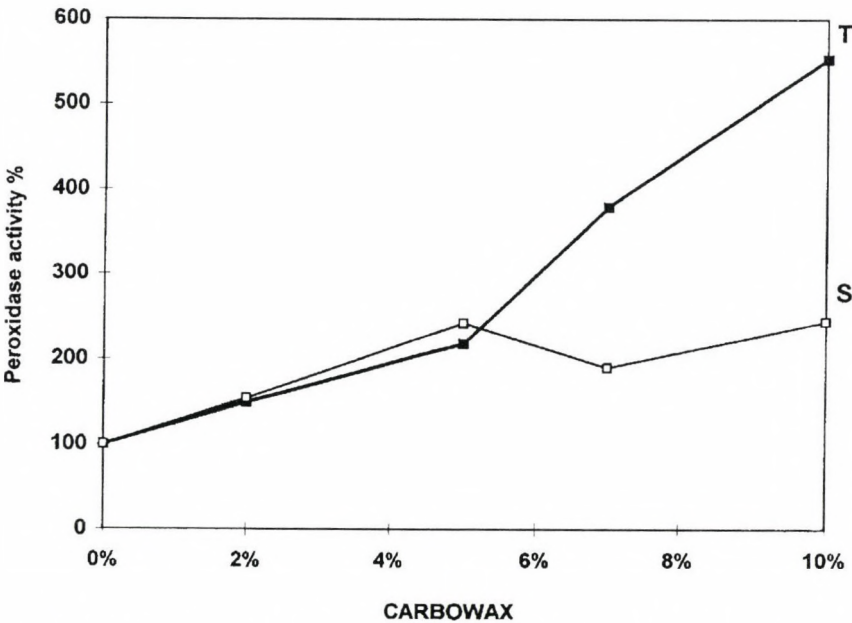


Fig. 4. Effect of Carbowax (2, 5, 7, and 10%) on total peroxidase activity expressed as a percentage of control [drought tolerant (T), drought sensitive (S)]



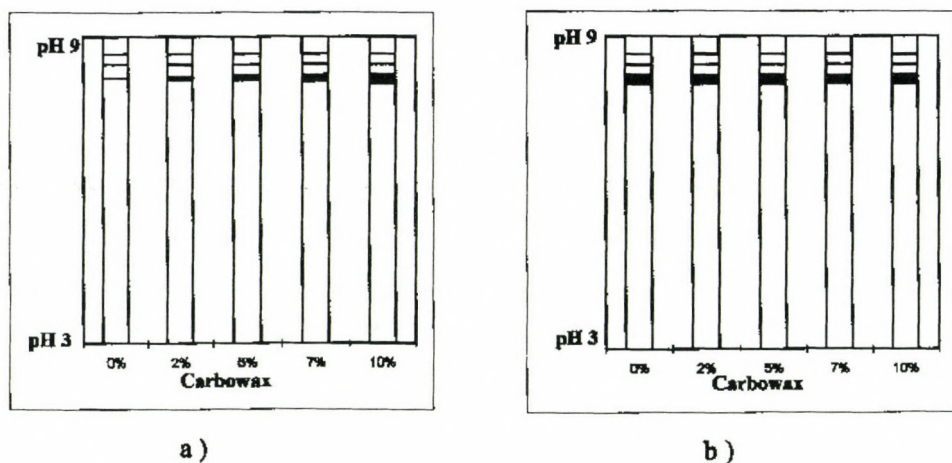


Fig. 5. Peroxidase isozyme patterns of snap beans a) drought tolerant (T), b) drought sensitive (S)

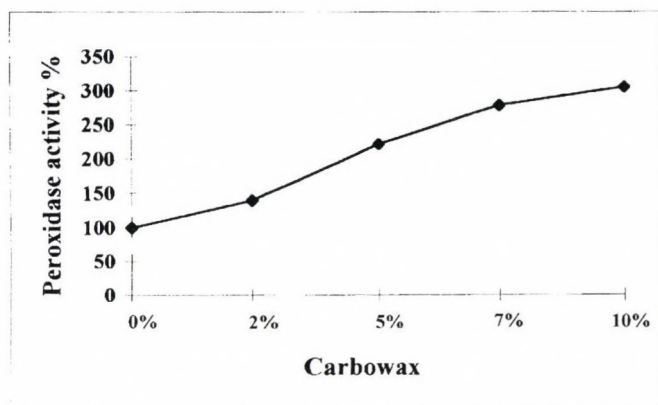
In contrast to formaldehyde, the concentration of trigonelline (Fig. 2) decreased with increasing Carbowax concentration. These changes occurred in both bean samples investigated.

The total peroxidase activity (Fig. 3) increased, although in a different way, with increasing drought stress. However, the percentage of total peroxidase activities increased proportionately with increasing drought stress, as shown in Fig. 4. This quantitative increase of total peroxidase activity may reflect the vital role of these enzymes in protecting plant cells against drought conditions.

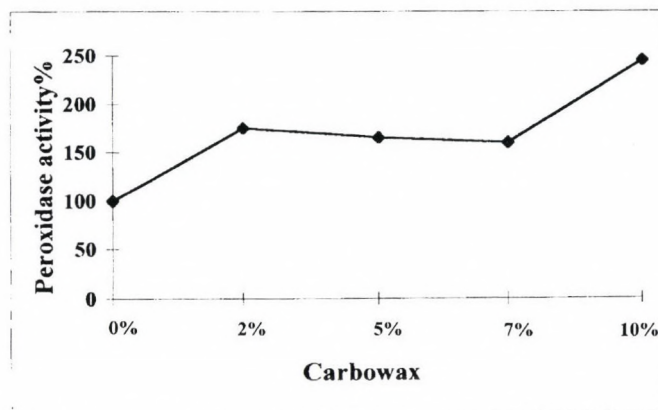
There were no qualitative differences in the peroxidase isozyme patterns, which were composed of three characteristic fractions in the basic pH range in both genotypes (Fig. 5).

Changes in the activities of the isozymes (Fig. 5, band 3) responsible mainly for the changes in total activities are demonstrated in Fig. 6 as a function of drought stress.

The aim of this study was to determine the concentrations of HCHO and trigonelline as well as to ascertain the total peroxidase activity and peroxidase isozyme patterns and activities in the leaves of two different snap bean genotypes grown in a greenhouse under artificial drought stress conditions. Our results show a positive correlation between peroxidase activity and the concentration of endogenous formaldehyde in the leaves of both bean genotypes treated with Carbowax at 2, 5, 7 and 10%. It could be concluded that fully N-methylated compounds plays a positive role as protecting materials in the mechanisms of drought stress. Identification of drought stress induced peroxidase isozyme(s) might serve as a basis of plant selection having the desired characteristics.



a )



b )

Fig. 6. Effect of Carbowax (2, 5, 7, and 10%) on peroxidase isozyme activity a) drought tolerant (T), b) drought sensitive (S)

## REFERENCES

1. Bacon, M. A., Thompson, D. S., Davies, W. J. (1997) Can cell wall peroxidase activity explain the leaf growth response of *Lolium temulentum* L. during drought? *J. Exper. Bot.* 48, 317, 2075–2085.
2. Burgyán, J., Szarvas, T., Tyihák, E. (1982) Increased formaldehyde production from L-methionine-(S-14 CH<sub>3</sub>) by crude enzyme of TMV infected tobacco leaves. *Acta Phytopath. Acad. Sci. Hung.* 17, 11–15.
3. Cseke, E., Vámos-Vigyázó, L. (1991) Peroxidáz. In: Szabolcsi, G. (ed.) *Enzimes analízis*. Akadémiai Kiadó, Budapest.



4. Gersbeck, N., Schönbeck, F., Tyihák, E. (1989) Measurement of formaldehyde and its main generators in *Erysiphe graminis* infected barley plants by planar chromatographic techniques. *J. Planar Chrom.* 2, 86–89.
5. Gullner, G., Tyihák, E. (1987) Hydrogenperoxide dependent N-demethylase activity in the leaves of normal and heat-shocked bean plants. *Plant Sci.* 52, 21–27.
6. Heck, H.d'A., Casanova, N., Starrm, T. B. (1990) Formaldehyde toxicity – new understanding. *Crit. Rev. Toxicol.* 20, 397–426.
7. Kawata, S., Sugiyama, T., Iami, J., Minami, Y., Tarui, S., Okamoto, M., Yamano, T. (1983) Hepatic microsomal cytochrome P-450 dependent N-demethylation of methylguanidine. *Biochem. Pharmacol.* 32, 3723–3728.
8. Kedderis, G. L., Hollenberg, P. F. (1984) Peroxidase-catalyzed N-demethylation reactions. *J. Biol. Chem.* 259, 3663–3638.
9. Mennier, G., Mennier, B. (1985) Peroxidase-catalyzed O-demethylation reactions. *J. Biol. Chem.* 260, 10576–10582.
10. Paik, W., Kim, S. (1980) *Protein Methylation*. Wiley and Sons, New York, pp. 132–136.
11. Sairam, R. K., Deshnukh, P. S., Shukla, D. S. (1997) Tolerance of drought and temperature stress in relation to increased antioxidant enzyme activity in wheat. *J. Agron. Crop. Sci.* 178, 171–177.
12. Sárdi, É., Tyihák, E. (1995) Measurement of formaldehyde cycle in parts of water melon (*Citrullus vulgaris* L.) varieties and F1 hybrids of different *Fusarium* sensitive. *Hort. Sci. Hung.* 27, 66–70.
13. Sárdi, É., Velich, I. (1995) Measurement of formaldehyde and its main potential generators in the leaves of snap bean (*Phaseolus vulgaris* L.) varieties of different biotic stress resistance. *Hort. Sci. Hung.* 27, 99–103.
14. Szarvas, T., János, É., Gáborjányi, R., Tyihák, E. (1982) Increased formaldehyde formation: an early event of TMV infection in hypersensitive host. *Acta Phytopath. Acad. Sci. Hung.* 17, 7–10.
15. Tanksley, S. D., Orton, T. J. (1983) *Isozymes in plant genetics and breeding*. Elsevier Amsterdam Part B. 3–23.
16. Tyihák, E., Balla, J., Gáborjányi, R., Balázs, E. (1978) Increased free formaldehyde level in crude extract of virus infected hypersensitive tobaccos. *Acta Phytopath. Acad. Sci. Hung.* 13, 29–31.
17. Tyihák, E., Király, Z., Gullner, G., Szarvas, T. (1989) Temperature dependent formaldehyde metabolism in bean plants. The heat shock response. *Plant Sci.* 59, 133–139.
18. Tyihák, E., Sarhan, A. R. T., Cong, N. T., Barna, B., Király, Z. (1988) The level of trigonelline and other quaternary compounds in tomato leaves in ratio to the changing nitrogen supply. *Plant and Soil* 109, 285–287.
19. Wang, M. Y., Shao, S. Q., Zhang, J. H., Geng, Q. H. (1995) Effect of water stress upon the activities of protective enzyme systems and the structures of membrane system in maize. *Acta Agr. Boreli Sinica* 10, 2, 43–49.
20. Willekens, H., Inzé, D., Van Montagu, M., Van Camp, W. (1995) Catalases in plants. *Mol. Breed.* 1, 207–228.
21. Zheng, Y. Z., Han, Y. H. (1997) Effect of high temperature and/or drought stress on the activities of SOD and POD of intact leaves in two soybean (*G. max*) cultivars. *Soybean Genetics Newsletter* 24, 39–40.

# THE INCREASE OF FORMALDEHYDE LEVEL IN SOME RARE PATHOLOGICAL CASES OF TEETH DETERMINED WITH THE USE OF QUANTITATIVE TLC\*

T. KATARZYNA RÓŻYŁO,<sup>1</sup> R. SIEMBIDA,<sup>2</sup> ANNA SZYSZKOWSKA<sup>1</sup>  
and ANNA JAMBROŻEK-MAŃKO<sup>2</sup>

<sup>1</sup>Institute of Dentistry, Medical University of Lublin, Lublin, Poland

<sup>2</sup>Faculty of Chemistry, M. Curie-Skłodowska University, Lublin, Poland

(Received: 1998-10-28; accepted: 1998-11-25)

In our previous works we proved that formaldehyde (HCHO) level in hard tissues of teeth could depend on their physiological state. In the current paper we presented the results of HCHO determinations in different dental pathologies, mainly the ones rarely encountered in dental practice, e.g. in the case of reinclusion. The determination of HCHO in the form of dimedone was performed by means of quantitative TLC. The obtained results were compared with HCHO levels in hard tissues of teeth presenting pathological changes. It proved that the highest HCHO level was found in reincluded teeth while it was lower in retained teeth, that is the ones which are not subjected to stress factors present in the mouth. The obtained results can constitute a contribution to the problems of dental pathologies, mainly caries which is a very common problem.

**Keywords:** Formaldehyde – TLC – HCHO in human teeth – rare teeth pathological cases

## INTRODUCTION

Despite intensive prophylaxis of caries and other dental pathologies, for example periodontopathies, this disease is still considered to be a serious problem. Highly sensitive methods of detection of carietic lesions such as for example digital radiography [1, 2] help early treatment, but not prevention. The ethiology of dental pathologies has been discussed in thousands of papers and numerous monographic works [3]. Also many theories of caries origin as well as other dental diseases have been presented, one of which is the chemical approach that is the analysis of composition of hard tissues of teeth [5, 15] and of the changes of their biochemical components [4, 6]. Periodontal disease is one of the most important causes of dental plaque. Many factors accompanying the periodontal diseases have been investigated, including the

\*Presented at the 4th International Conference on the Role of Formaldehyde in Biological Systems, July 1–4, 1998, Budapest, Hungary.

Send offprint requests to: Dr. med. T. Katarzyna Różyło, D. Sc., Institute of Dentistry, Medical University of Lublin, Karmelicka str. 7, 20-081 Lublin, Poland



influence of activators, inhibitors, pH and proteolytic activity of enzymes [8]. Reincluded tooth is a very rarely observed pathologic case in dental practice. This pathology may concern both permanent and deciduous teeth.

In numerous papers [13, 14] an essential role of formaldehyde (HCHO) in biological systems has been underlined. It has been stated that there is as an analyzable amount of HCHO in plant, animal and human tissues. It was also proved that HCHO level in cells of plant, animal and human tissues as well as in body fluids was related to physiological state of a given living organism.

On the basis of these research works, taking under consideration intracellular presence of HCHO, its levels in hard tissues of teeth were determined [7–10]. It was unquestionably proved that mainly in carietic teeth a high level of HCHO was observed. This level of HCHO can differ in relation to various pathologies of teeth. The previous studies of HCHO level as chromatographically measurable indicator of physiological state of teeth tissues were considered in typical cases most often encountered in dental practice.

In the current paper we decided to examine the changes of HCHO levels in rare cases of dental pathologies as well as to compare the collected data with hitherto existing results in this field.

## MATERIALS AND METHODS

### *Investigated cases*

- A tooth with secondary caries under fillings – very often encountered after wrong or careless treatment
- A case of a reincluded tooth (submersion of a tooth in the bone and resorption of its hard tissues)
  - A case of a reincluded deciduous tooth
  - A deciduous tooth with a carietic lesion
  - A tooth extracted due to orthodontic reasons
  - A tooth extracted due to periodontal reasons
  - A retained tooth
  - A carietic tooth

### *The preparation of samples for analysis*

Teeth were thoroughly purified from the remnants of soft tissues, blood and possibly dental fillings. This is crucial as HCHO level in hard tissues of teeth is considerably lower than in soft tissue which could “dilute” pulverized hard tissues of teeth. The analytical procedure of determination of HCHO in hard tissues of teeth is presented in Fig. 1.

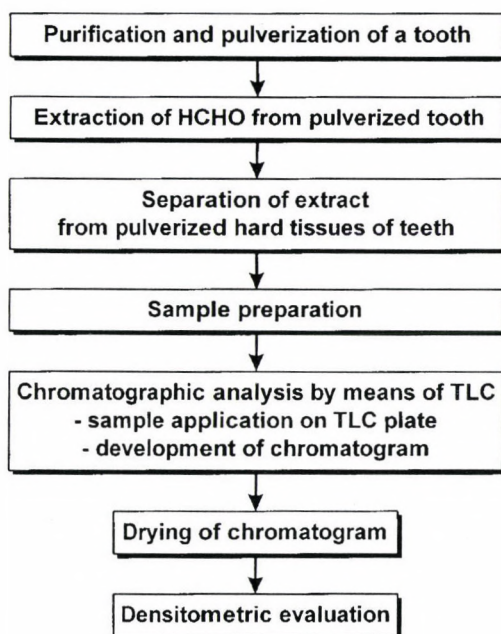


Fig. 1. Scheme of the method for determination of formaldehyde in human teeth

HCHO was then extracted from pulverized samples of teeth by means of methanol solution of dimedone. Later it was centrifuged during 15 minutes. In the same time there was prepared the HCHO-dimedone adduct standard, twice recrystallized from ethanol.

### *Chromatographic analysis of HCHO*

The chromatographic analysis of HCHO as dimedone was carried out by means of adduct by adsorption TLC on silica gel 60 F<sub>254</sub> MERCK plates. The plates were spotted using Applicator AS 30 (DESAGA-Germany) in pure nitrogen atmosphere. It was necessary to minimize contact with laboratory environment in which always a certain amount of HCHO is present which can bind with dimedone. In order to eliminate and determine HCHO derived from laboratory atmosphere, the "blind-sample" of dimedone solution was also applied on the plate. The chromatograms were developed in twin through chambers (CAMAG) at the distance of 100 mm. As the mobile phase there was used chlorophorm-dichloromethane solution (10 : 30 v/v). The details concerning the exact analysis of HCHO by TLC in biological material are presented in the papers [7–11].



## RESULTS AND DISCUSSION

HCHO levels (in the form of dimedone adduct) determined by means of chromatography are shown in Table 1 and on the densitograms of individual teeth samples (Fig. 2) as well as in the diagram which illustrates HCHO content in these samples (Fig. 3).

In the present studies it was resolved to compare the influence of extension of carietic lesions in teeth and the quantity of released HCHO. It proved that in this case relatively higher HCHO level was observed in teeth tissues which deep caries (V) in comparison with HCHO quantity present in case of teeth with secondary caries under restoration (1/R). It testifies the fact that the extension of carietic lesions in teeth influences HCHO level in their tissues. A slightly lower HCHO level was observed in deciduous teeth with caries, however the reason of this observation may be partial resorption of a tooth root (I).

Reclusion of teeth is a process of submersion of a tooth into bone structures of maxilla and its destruction from within. This is a very rare case in dental practice. The ethiology of this pathology is not known so far and there are no methods of treatment of this lesion. This pathology may concern both permanent and deciduous teeth. In our studies so far the highest HCHO level was observed in tissues of teeth affected by reinclusion in permanent (2/R) as well as in deciduous (3/R) teeth. It gives evidence that there exists serious disturbance in metabolism of hard tissues of teeth, considerably greater than in case of teeth affected with caries, even extensive (V) as it is best seen in Fig. 3. Maybe it is caused by prolonged intensive stress situation. It can be clearly seen that these physiological disturbances have their distinct implication in HCHO level of the studied cases of dental pathologies. The explanation of this

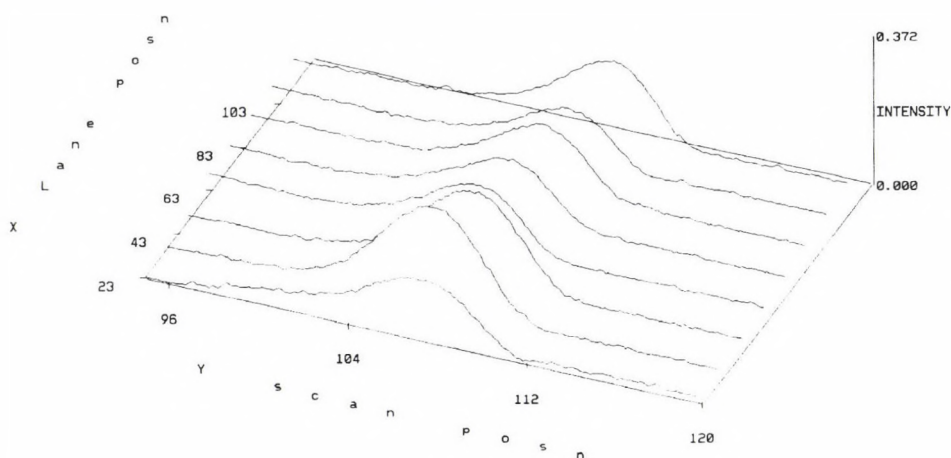


Fig. 2. Densitograms of the formaldehyde of the investigated teeth samples in the order as listed in the part "Materials and methods" and in Fig. 3

Table 1  
Level of formaldehyde (in dimedone adduct form) in different human teeth

A) MASS OF FD [chromatogram] / B) [µgFD IN 20 µl OF EXTRACT]															
1/R		2/R		3/R		I		II		III		IV		V	
a	b	a	b	a	b	a	b	a	b	a	b	a	b	a	b
0.045	0.225	0.070	0.350	0.055	0.275	0.031	0.155	0.028	0.140	0.025	0.125	0.014	0.070	0.049	0.245

phenomenon is possible only after thorough, multidirectional studies, mainly the comparison with the relation of HCHO level to the level of its potential generators. The lowest HCHO level was observed in case of retained teeth (IV). It results from the fact that these teeth are surrounded by bone tissues and are not subjected to such stress as erupted teeth in mouth which results in changes in their metabolism. Relatively low HCHO level was found in teeth extracted due to orthodontic reasons, that is in young people who yet are not affected by dental diseases.

From the presented results it can be concluded that HCHO level in hard tissues of teeth reflects their physiological state and their metabolism. It concerns both healthy teeth and teeth with pathological conditions, also the ones rarely encountered in dental practice.

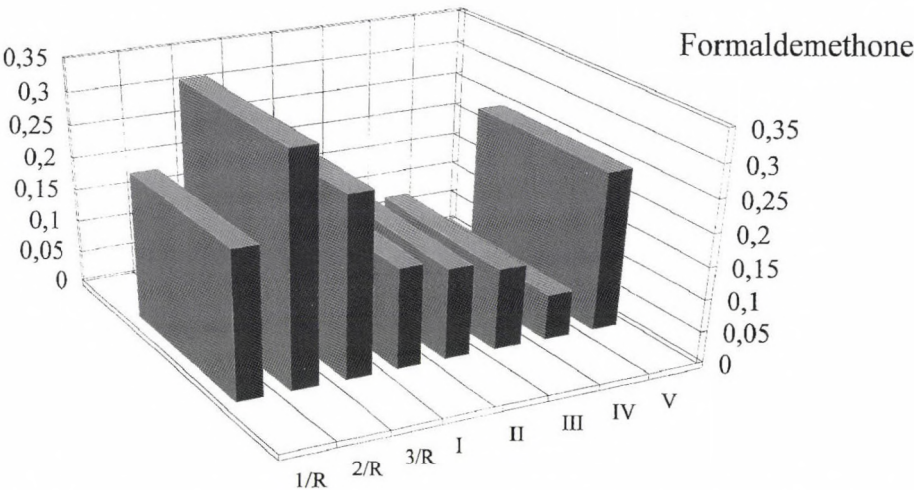


Fig. 3. Diagrams of the level of HCHO as dimedone adduct (µg/20 µl of the extract) in different teeth samples: 1/R – Tooth with secondary caries under fillings, 2/R – A case of reincluded tooth, 3/R – A case of reincluded deciduous tooth, I – A deciduous tooth with a carietic lesion, II – A tooth extracted due to orthodontic reasons, III – A tooth extracted due to periodontal reasons, IV – A retained tooth, V – A carietic tooth



## REFERENCES

1. Benz, C., Mouyen, F. (1989) Radiovisiographie. Ein System zur filmlosen Anfertigung intraoraler Zahnroentgenaufnahmen, *Dtsch. Zahnarztl. Z.* 44, 177–179.
2. Fujita, M., Kadera, Y., Ogawa, M. (1987) Digital image processing of periapical radiographs. *Oral Surg. Oral Med. Oral Path.* 65, 490–494.
3. Hohling, H. J. (1966) *Die Bauelemente von Zahnschmelz und Dentin aus morphologischer, chemischer und struktureller sicht*. Carl Hauser Verlag, Muenchen.
4. Kalasz, H., Kovacs, G. H., Nagy, J., Tyihak, E., Barnes, W. T. (1978) Identification of N-methylated basic amino acids from human adult teeth., *J. Dent. Res.* 57, 128–132.
5. Koenig, K. G. (1987) *Karies und Paradontopathien-Aethiologie und Prophylaxe*. Theme, Stuttgart.
6. Lezovic, J., Ziman, M. (1974) Gel chromatography of proteins from human teeth. *J. Chromatogr.* 96, 258–261.
7. Różyło, T. K. (1996) TLC determination of the presence of formaldehyde in normal and pathological tissues of human teeth. *J. Planar Chromatogr.* 2, 141–143.
8. Różyło, T. K. (1995) Planar chromatography and densitometric determination of formaldehyde in hard tissues of teeth. *Chem. Environ. Res.* 4, 129–134.
9. Różyło, T. K. (1998) Quantitative TLC determination of formaldehyde in hard tissues of teethet, *Biomed. Chromatogr.* 12, 267–270.
10. Różyło, T. K. (1996) The dependence of radiovisiographic image on the level of formaldehyde in tissues of teeth. *Mag. Stom.* 8, 47–50
11. Siembida, R., Różyło, T. K. (1998) The problem of optimal conditions of quantitative determination of HCHO in hard tissues of teeth by TLC. In: *Proc. of the 10th Int. Symp. on Instrumental Planar Chromatography*, Visegrád, Hungary, pp. 223–229.
12. Soder, P. O., Lundblat, G., Linqvist, L. (1966) Proteolytic activity of dental plaque material. *Acta Chem. Scand.* 20, 1504–1512.
13. Tyihak, E. (1987) Overpressured layer chromatographic methods in the study of the formaldehyde cycle in biological systems. *Trends Anal. Chem.* 6, 90–94.
14. Tyihak, E., Balla, J., Gaborjanyi, R., Blazs, E. (1978) Increased free formaldehyde level in crude extract of virus defected hypersensitive tobaccos. *Acta Phytopathol., Acad. Sci. Hung.* 13, 29–31.
15. Veis, A., Spector, A. R., Zamosciany, H. (1972) The isolation of an EDTA-soluble phosphoprotein from mineralizing bovine dentine. *Biochim. Biophys. Acta* 257, 404–413.

## FORMALDEHYDE GENERATORS AND CAPTURERS AS INFLUENCING FACTORS OF MITOTIC AND APOPTOTIC PROCESSES\*

B. SZENDE,<sup>1</sup> E. TYIHÁK,<sup>2</sup> L. TRÉZL,<sup>3</sup> É. SZÖKE,<sup>4</sup> I. LÁSZLÓ,<sup>4</sup> GY. KÁTAY<sup>2</sup>  
and ZS. KIRÁLY-VÉGHÉLY<sup>5</sup>

<sup>1</sup>1st Institute of Pathology and Experimental Cancer Research, Semmelweis University of Medicine and Research Unit for Molecular Pathology, Joint Research Organization of the Hungarian Academy of Sciences, Budapest, Hungary; <sup>2</sup>Plant Protection Institute, Hungarian Academy of Sciences, Budapest, Hungary; <sup>3</sup>Department of Organic Chemical Technology, Technical University of Budapest, Budapest, Hungary; <sup>4</sup>Institute of Pharmacognosy, Semmelweis University of Medicine, Budapest, Hungary; <sup>5</sup>Research Institute for Viticulture and Enology of the Ministry of Agriculture, Experimental Wine Cellar, Budapest, Hungary

(Received: 1998-10-28; accepted: 1998-11-25)

There is a growing amount of evidence pointing to the fact that several endogenous and exogenous methylated compounds are potential formaldehyde generators in their biological reactions. N<sup>ε</sup>-methylated lysines, N<sup>G</sup>-methylated as well as hydroxymethylated arginines, and 1'-methyl-ascorbigen have been examined in this respect. The apoptosis-inducing effect of formaldehyde molecules formed from methyl groups was earlier first published by our group.

Dimedone, an artificial capturer molecule for formaldehyde, has been found to prevent the apoptosis-inducing effect of 1'-methyl-ascorbigen as well as N<sup>G</sup>-hydroxymethylated arginines. More recently resveratrol, present in grapes and wines, has been shown to have cardioprotective and cancer chemopreventive effect. Our group has been successful in demonstrating that this natural formaldehyde capturer molecule can also influence cell proliferation and apoptosis.

The apoptosis-inducing or -preventing effect of formaldehyde generators and capturers seems to be dose-dependent and may be utilized in various disturbances of cell proliferation and active cell death.

**Keywords:** N<sup>G</sup>-hydroxymethylated arginines – 1'-methyl-ascorbigen – resveratrol – dimedone – cell proliferation – apoptosis

### INTRODUCTION

It has recently been demonstrated that formaldehyde (HCHO) is a normal component mainly in the form of hydroxymethyl groups, in all biological systems. It can be formed during enzymatic methylation and demethylation processes [1, 4, 7, 11], as well as from biological oxidation processes [22]. Thus, HCHO can be constantly formed intra- and extracellularly in all cells, and it is obvious that the HCHO path-

\* Presented at the 4th International Conference on the Role of Formaldehyde in Biological Systems, July 1–4, 1998, Budapest, Hungary.

Send offprint requests to: Prof. Dr. B. Szende, 1st Institute of Pathology and Experimental Cancer Research, Semmelweis University of Medicine, H-1085 Budapest, Üllői út 26, Hungary. E-mail: bszende@korkb1.sote.hu.



ways in different tissues may play a crucial role in fundamental biological processes [20].

There is increasing evidence of the presence of a HCHO cycle in biological systems [18], in which formation of the methyl group of L-methionine takes place through HCHO, and the formation of HCHO from the S-methyl group of S-adenosyl-L-methionine (SAM) is linked to different enzymatic transmethylation reactions [7]. The abnormalities of the HCHO cycle can influence cell proliferation and differentiation [14], and HCHO generator and capturer molecules may potentially normalize these abnormal processes.

The present paper aims to summarize the main up-to-date results gained with some HCHO generator and capturer molecules.

## MATERIALS AND METHODS

### *Chemicals*

All chemicals were of analytical purity grade, obtained from Sigma-Aldrich Chemical Co. (Budapest, Hungary) and REANAL Chemical Co. (Budapest, Hungary).

N<sup>G</sup>-hydroxymethylated-L-arginines were prepared according to earlier methods [3].

Synthesis of 1'-methylascorbigen (MeAsc) was in essentials carried out according to methods described previously [13].

### *Biological studies*

PC-3 human prostate carcinoma cells, HT-29 human colon carcinoma cells, SW 620 human colon carcinoma cells, HT-1080 human fibrosarcoma cells and P-388 mouse lymphoma cells were all plated in 6-well Greiner dishes (Nürtingen, Germany). The culture medium was RPMI supplemented with 10% calf serum (Flow, Irvine, Scotland). The dishes were placed into humidified 5% CO<sub>2</sub>, in a 37 °C atmosphere. Cells were plated at 10<sup>4</sup> or 10<sup>5</sup> cells/well. Triplicates were used for each treatment group and time point (control, 1–10–100 µg/ml and 24, 48 and 72 hours after treatment), when cell count was taken after trypsinization, using Buerker's chamber. A series of cultures was fixed 24, 48 and 72 hours after treatment in a 3 : 1 ratio of methanol : 10% acetic acid. Three cover-slips from each treatment group were stained with HE and two of each group were exposed to immunocytochemical reagents using Apop-Tag (Oncor, Gaithersburg, MD, USA), in order to show specifically apoptotic cells. Then the ratio of apoptotic and mitotic cells was determined. Statistical analysis was carried out using the x method.

## RESULTS

Showing dose-dependent inhibition, N<sup>G</sup>-hydroxymethyl-arginines (MAX) in doses of 10 and 100 µg/ml, respectively, significantly decreased the proliferation of HT-29 cells (Fig. 1) and P-388 cells in culture. The cells of the treated cultures showed morphological signs of apoptosis in high percentage (5–15%).

MeAsc inhibited the proliferation of both PC-3 and HT-29 cells, *in vitro*. In case of the HT-29 cell culture, ascorbigen was ineffective, but MeAsc caused significant inhibition (Fig. 2), which was based on a decrease in mitosis and an increase in apoptosis.

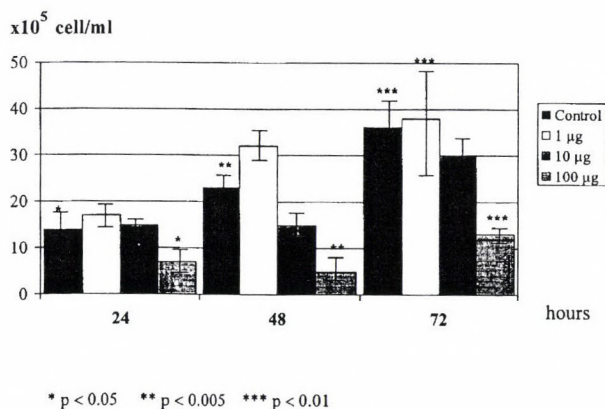


Fig. 1. Effect of MAX on the proliferation of HT-29 cells

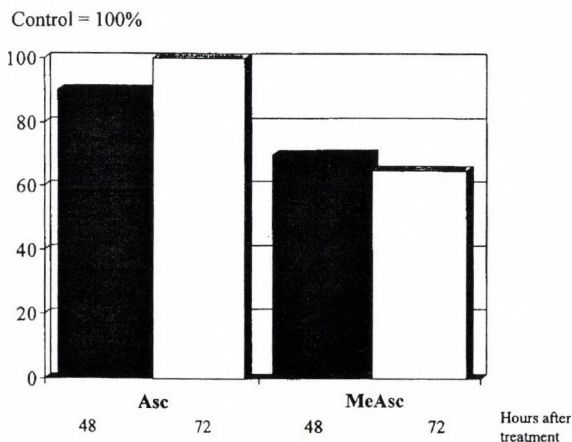


Fig. 2. Effect of 100 µg/ml ascorbigen (ASC) and methyl-ascorbigen (MeAsc) on the number of HT-29 cells in culture



Table 1  
Effect of resveratrol on the apoptotic and mitotic index of HT-1080 cell culture

	Control	100 $\mu\text{g/ml}$	10 $\mu\text{g/ml}$	1 $\mu\text{g/ml}$
24 h A	1	20	2	2
24 h M	4	0	0	2
48 h A	1	80	8	2
48 h M	5	0	1	5

Resveratrol exerted a dose-dependent effect on HT-29, HT-1080 and SW620 cells in culture, i.e. the dose of 100  $\mu\text{g/ml}$  showed significant decrease in cell number and mitosis index, and an increase in the apoptosis index (Table 1).

The dose of 10  $\mu\text{g/ml}$ , however, was ineffective, while 1  $\mu\text{g/ml}$  caused a slight increase in cell number (Fig. 3).

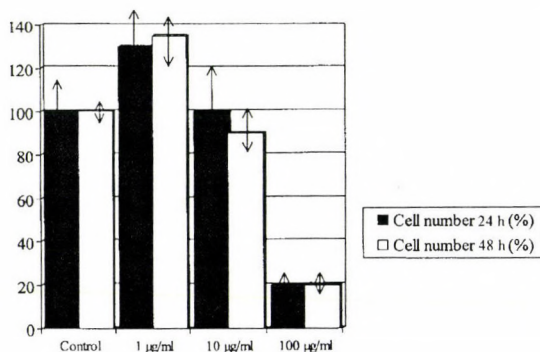


Fig. 3. Effect of resveratrol on SW-620 cells

## DISCUSSION

It has been shown that L-arginine can only be hydroxymethylated by formaldehyde [15]. These  $\text{N}^{\text{G}}$ -hydroxymethylated arginines (e.g.  $\text{N}^{\text{G}}$ -trihydroxymethyl-L-arginine) are relatively stable molecules and can be isolated from the reaction mixture [2, 15]. Such molecules occur in human blood and urine [3] and the hypothesis has been raised that the guanidine group of L-arginine of the enzyme protein could be hydroxymethylated in enzymatic transmethylation reactions [15, 20].

The growth-retarding effect of  $\text{N}^{\text{G}}$ -hydroxymethylated arginines on different animal tumors has been demonstrated in earlier experiments [16, 19]. For example, *in vitro*, a 100  $\mu\text{g/ml}$  mixture of  $\text{N}^{\text{G}}$ -hydroxymethyl-L-arginines (MAX) has been shown to cause total inhibition of proliferation in K-562 cells, while in an *in vivo*

experiment, a daily 400 mg/kg i.p. treatment was found to cause complete inhibition of the growth of Ehrlich ascites tumors. In another experiment, an inhibitory effect of MAX treatment was observable in respect to both metastasis number and average volume of lung nodules [16, 19].

In the present series of experiments, we have been successful in showing the apoptotic effect of these special endogenous substance groups. It is evident that both N<sup>G</sup>-methyl-L-arginines and N<sup>G</sup>-hydroxymethyl-L-arginines are endogenous basic amino acid derivatives [2, 16, 19], however, at the moment we are not in the knowledge of the biogenetic relationship between these two amino acid groups. Although little is known at present about the demethylation of N<sup>G</sup>-methylated arginines, the N<sup>G</sup>-hydroxymethyl-L-arginines generate a direct HCHO-yielding activity which may be responsible for their dramatic apoptotic effect. It also follows from this that while N<sup>G</sup>-methyl-L-arginines are only potential HCHO generators, the N<sup>G</sup>-hydroxymethyl-L-arginines are actual HCHO generators.

In the case of 1'-methyl-ascorbigen (MeAsc) the mitosis- and apoptosis-influencing activity of this compound is also in correlation with the demethylation of the N-methyl group. This means that 1'-methyl-ascorbigen could also be a potential HCHO-generator. Because ascorbigen has no methyl group, it does not generate any antimitotic or apoptotic effect. These investigations repeated by demonstrates that the HCHO formed from the N-methyl group plays a crucial role in the antimitotic and apoptotic effects. Dimedone, a known capturer molecule forming formaldehyde with HCHO, diminished the apoptosis-inducing effect of Me-Asc – when applied simultaneously with Me-Asc in a dose of 10 µg/ml [14].

While dimedone is an unnatural HCHO-capturer molecule, resveratrol – a constituent of grapes, wines, peanuts etc. [8] – has considerable cardioprotective [5, 10], as well as cancer chemopreventive effects [9, 12].

It is especially interesting that the daily consumption of red wine which contains relatively high level of resveratrol, has been found to reduce the susceptibility of plasma and LDL to lipid peroxidation, whereas white wine (low concentration of resveratrol) consumption has been found to show the opposite effect [6]. More recently, synthetic trans-resveratrol has proved to be an effective antioxidant *in vitro* against the hydroxyl radical ( $I = 33 \mu\text{M}$ ), however, resveratrol treatment failed to show any effect on either the lipid profile or Cu<sup>+2</sup>-dependent formation of thiobarbituric-acid-reactive substances (TBARS) from protein-associated lipids [17]. These results suggest that the cardioprotective effect of resveratrol is perhaps not related only to its antioxidant effect.

It is especially important that resveratrol, a phytoalexin as well as a common constituent of the human diet, has been demonstrated to have cancer chemopreventive activity in assays representing three major stages of carcinogenesis as initiation, promotion and progression [9]. This dietary compound has been revealed to inhibit the proliferation of human breast epithelial cells in a dose- and time-dependent manner [12]. Using different tumor cell systems, the results of our group have also managed to support these observations with resveratrol, however, we also demonstrated its considerable apoptotic effect.



According to this preliminary observation, the dose-dependent activity of resveratrol in tumor cell systems is in correlation with its HCHO-cycle influencing effect. It seems that resveratrol can mobilize a special part of the chemically labile bound HCHO forming thereby several resveratrol derivatives with tumor-cell killing activity [21].

## REFERENCES

1. Chelvarajan, R. L., Fannin, F. F., Bush, L. P. (1993) Study of nicotine demethylation in *Nicotiana glauca*. *J. Agric. Food Chem.* 41, 858–862.
2. Csiba, Á., Trézsl, L., Tyihák, E., Graber, H., Vári, É., Téglás, G., Rusznák, I. (1982) Assumed role of L-arginine in mobilization of endogenous formaldehyde. *Acta Physiol. Acad. Sci. Hung.* 59, 35–41.
3. Csiba, Á., Trézsl, L., Tyihák, E., Szarvas, T., Rusznák, I. (1986) N<sup>G</sup>-Hydroxymethyl-L-arginines: new serum and urine components. Their isolation and characterization by ion-exchange TLC. In: *Proc. Int. Symp. TLC with Special Emphasis on OPLC*, Szeged, Hungary, 1984, Tyihák, E. ed., Labor MIM, Budapest.
4. Fannin, F. F., Bush, L. P. (1992) Nicotine demethylation in *Nicotiana*. *Med. Sci. Res.* 20, 867–868.
5. Frankel, E. N., Waterhouse, A. L., Kinsella, J. E. (1993) Inhibition of human LDL oxidation by resveratrol. *The Lancet* 341, 1103–1104.
6. Fuhrman, B., Lavy, A., Aviram, M. (1995) Consumption of red wine with meals reduces the susceptibility of human plasma and low-density lipoprotein to lipid peroxidation. *Am. J. Clin. Nutr.* 61, 49–54.
7. Huszti, S., Tyihák, E. (1986) Formation of formaldehyde from S-adenosyl-L-Methyl-<sup>3</sup>H/methionine during enzymic transmethylation of histamine. *FEBS Letters* 209, 362–366.
8. Ingham, J. L. (1976) 3,5,4'-Trihydroxystilbene as a phytoalexin from groundnuts (*Arachis hypogaea*). *Phytochemistry* 15, 1791–1793.
9. Jang, M. J., Cai, L., Udeani, G. O., Slowing, K. V., Thomas, C. F., Beecher, C. W. W. H. S. S., Farnsworth, N. R., Kinghorn, A. D., Mehta, R. J., Moon, R. C., Pezzuto, J. M. (1997) Cancer chemopreventive activity of resveratrol, a natural product derived from grapes. *Science* 275, 218–220.
10. Kerry, N. L., Abbey, M. (1997) Red wine and fractionated phenolic compounds prepared from red wine inhibit low density lipoprotein oxidation *in vitro*. *Atherosclerosis* 135, 93–102.
11. Kucharczyk, N., Yang, Y. T., Wang, K. K., Sofia, R. D. (1984) The formaldehyde-donating activity of N<sup>5</sup>, N<sup>10</sup>-methylene-tetrahydrofolic acid in xenobiotic biotransformation. *Xenobiotica* 24, 667–676.
12. Mgboneyebi, O. P., Russo, J., Russo, I. H. (1998) Antiproliferative effect of synthetic resveratrol on human breast epithelial cells. *Intern. J. Oncol.* 12, 865–869.
13. Preobrazhenskaya, M. N., Korolev, A. M., Plikhtyak, I. L., Zartseva, I. V., Lazhko, E. I., Aleksandrova, L. G. (1991) Chemistry and biology of ascorbigens. In: Van der Plas, H. C., Simonyi, M. (eds) *Heterocycles in Bio-Organic Chemistry*. The Royal Society of Chemistry, pp. 68–87.
14. Szende, B., Tyihák, E., Szókán, Gy., Kátay, Gy. (1995) Possible role of formaldehyde in the apoptotic and mitotic effect of 1-methyl-ascorbigen. *Path. Oncol. Res.* 1, 38–42.
15. Trézsl, L., Csiba, Á., Rusznák, I., Tyihák, E., Szarvas, T. (1981) L-Arginine as an endogenous formaldehyde carrier in human blood and urine. In: Rosdy, B. (ed.) *Proc. 21st Hung. Ann. Meet. Biochem. Veszprém*, Hungary, Hung. Biochem. Soc. Budapest.
16. Trézsl, L., Szende, B., Csiba, Á., Rusznák, I., Lapis, K. (1986) *In vitro* and *in vivo* inhibition of tumor cell proliferation by N<sup>G</sup>-hydroxymethyl-L-arginines as a natural cell component. Abstr., 14th Int. Cancer Congr., Budapest, Akadémiai Kiadó.
17. Turrens, J. F., Lariccia, J., Nair, G. M. (1997) Resveratrol has no effect on lipoprotein profile and does not prevent peroxidation of serum lipids in normal rats. *Free Rad. Res.* 27, 557–562.

18. Tyihák, E. (1987) Is there a formaldehyde cycle in biological systems? In: Tyihák, E., Gullner, G. (eds) *Proc. 2nd Int. Conf. on the Role of Formaldehyde in Biological Systems*. Keszthely, SOTE Press, Budapest, pp. 155–181.
19. Tyihák, E., Szende, B., Trézl, L. (1990) Biological effects of methylated amino acids. In: Paik, W. K., Kim, S. (eds) *Protein Methylation*. CRC Press, Inc., Boca Raton, FL. pp. 363–388.
20. Tyihák, E., Trézl, L., Szende, B. (1997) Formaldehyde cycle and the phases of stress syndrome. *Ann. N. Y. Acad. Sci.* 851, 259–270.
21. Tyihák, E., Albert, L., Németh, Zs. I., Kátay, Gy., Király-Véghely, Zs., Szende, B. (1998) Formaldehyde cycle and the natural formaldehyde generators and capturers. *Acta Biol. Hung.* 49, 209–218.
22. Yu, P. H. (1998) Increase of formation of methylamine and formaldehyde in vivo after administration of nicotine and the potential cytotoxicity. *Neurochem. Res.* 23, 1205–1210.





# REDUCTION OF APOPTOSIS OF *IN VITRO* CULTURED LYMPHOCYTES OF HIV-POSITIVE PERSONS BY N<sup>G</sup>-HYDROXY-METHYLATED-L-ARGININE AND 1'-METHYL-ASCORBIGEN\*

J. BOCSI,<sup>1</sup> K. NAGY,<sup>3</sup> E. TYIHÁK,<sup>3</sup> L. TRÉZL<sup>4</sup> and B. SZENDE<sup>1</sup>

<sup>1</sup>1st Institute of Pathology and Experimental Cancer Research, Semmelweis University of Medicine, Research Group of Molecular Pathology, Joint Research Organisation, Hungarian Academy of Sciences and Semmelweis University of Medicine, Budapest, <sup>2</sup>National Institute of Dermato-Venereology, Budapest, <sup>3</sup>Research Institute of Plant Protection, Hungarian Academy of Sciences, Budapest, <sup>4</sup>Institute of Organic Chemistry Technology, Technical University, Budapest

(Received: 1998-10-28; accepted: 1998-11-25)

Some formaldehyde generating chemicals due to reduction of apoptosis in lymphocytes may slow down the progress of immune decline of HIV-infected individuals. N<sup>G</sup>-hydroxy-methylated-L-arginine (MAX) and 1'-methyl-ascorbigen (MeAsc) could enter this way the biochemical pathway of cells and affect the apoptotic process.

Separated peripheral blood lymphocytes of five asymptomatic HIV-positive persons were cultured. Unstimulated, IL-2 stimulated and IL-2 stimulated plus 0.1, 1.0, 10.0 µg/ml MAX or MeAsc treated lymphocytes were investigated for apoptosis morphologically (HE) and by flow cytometrical DNA fragmentation method.

IL-2 stimulation lowered the apoptotic rate in lymphocytes of HIV-positive persons related to unstimulated ones. MAX and MeAsc reduced the apoptotic activity of stimulated lymphocytes in the least or the middle doses while in the higher dose did not.

MAX and MeAsc reduced the apoptotic activity of stimulated lymphocytes originated from HIV-positive patients *in vitro*. This compounds may have the same effect *in vivo* and may prolong the symptomless period of HIV-infected patients. The role of methylation and production of formaldehyde in this process is discussed.

**Keywords:** HIV-infection – apoptosis – flow cytometry – N<sup>G</sup>-hydroxy-methylated-L-arginine – 1'-methyl-ascorbigen

## INTRODUCTION

N<sup>G</sup>-hydroxy-methylated-L-arginine (MAX) and 1'-methyl-ascorbigen (MeAsc) are N-methyl compounds (Fig. 1) and it has been shown that they are endogenous formaldehyde (HCHO) generators [10, 13, 14]. HCHO is formed within the cell by demethylation (via demethylases and special peroxidases) and methylation reactions. HCHO, known as a reactive molecule, could react with DNA and proteins, and may

\* Presented at the 4th International Conference on the Role of Formaldehyde in Biological Systems, July 1-4, 1998, Budapest, Hungary.

Send offprint requests to: Prof. Dr. B. Szende, 1st Institute of Pathology and Experimental Cancer Research, Semmelweis University of Medicine, Budapest, H-1085 Üllői út 26, Hungary. E-mail: bszende@korbl.sote.hu.



initiate the degradation of DNA in apoptotic process. Apoptosis is a physiological process in which the dying cell plays an active role in its own destruction; internucleosomal DNA fragmentation is a characterizing step in apoptosis [5]. Previously we demonstrated that N-trimethyl-lysine (the relative molecule of MAX), and MeAsc have immunomodulating activity and protect the animals from bacterial and viral infection [9].

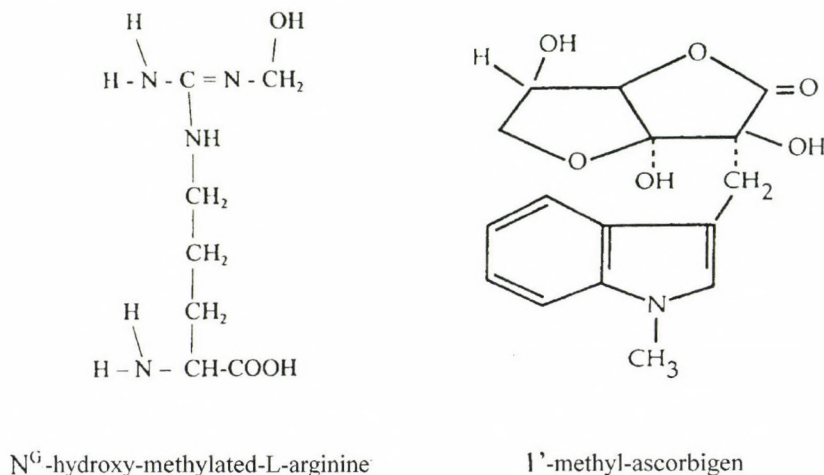


Fig. 1. Chemical structure of MAX and MeAsc

Decreasing cell number of  $\text{CD4}^+$  T lymphocytes often occurs in HIV-infected patients who had not yet developed AIDS. According to some studies [1, 2, 4, 6] apoptosis, associated with lowered T cell reactivity, is responsible for the partial deletion of both  $\text{CD4}^+$  and  $\text{CD8}^+$  cells from HIV-infected individuals. Apoptosis may be initiated by HIV-proteins or by the cytokine regulatory pathways [6].

There is interest to find chemicals which could slow down or arrest immune decline and disease progression at the asymptomatic stage of HIV-infection by maintaining  $\text{CD4}^+$  cells. In this paper we publish the results of *in vitro* studies where the possible regulatory effect of  $\text{N}^G$ -hydroxy-methylated-L-arginine and 1'-methyl-ascorbigen, on apoptosis of *in vitro* cultured lymphocytes of HIV-positive patients was investigated.

## MATERIALS AND METHODS

$3 \times 10^6$ /well separated peripheral blood mononuclear cells from 5 asymptomatic HIV-1-infected patients with  $\text{CD4}^+$  counts  $< 500/\mu\text{l}$  ( $\text{CD4}^+$  T cell number  $\text{CD4}/8$  ratio and beta 2 microglobulin values as well as the time elapsed after the detection of

HIV-infection were known in each case) were plated in 24-well trays (Greiner, Kremsmünster, Austria). The culture medium was RPMI 1640 (Sigma, St. Louis, MO, USA), supplemented with 10% fetal calfserum (Flow, Irvine, UK). For *in vitro* activation/stimulation 20 IU/ml human recombinant IL-2 (Sigma, St. Louis, MO, USA) was used. IL-2 treatment was performed 1 hour after plating. Twenty-four hours after activation MAX and MeAsc (produced in our laboratory) were administered in doses of 0.1, 1.0, 10.0  $\mu\text{g/ml}$ . Forty-eight hours later, progress of apoptosis in the nonstimulated, stimulated, stimulated and treated cultures was evaluated by morphological and flow cytometric DNA fragmentation methods.

### Morphology

Cultured cells were spread on glass specimen holders, fixed with ethanol and stained by HE.

### Flow cytometry

DNA content measurements were performed using a FACStar (Becton-Dickinson, Mountain View, Ca, USA) flow cytometer described by Schuler et al. [8] was applied. Sample preparation was carried out after Gong et al. [3] and Mihalik et al. [7] [briefly: after ethanol fixation internucleosomally fragmented DNA were removed from apoptotic cells by citrate-phosphate buffer (pH = 7.8) supplemented with RNase then DNA content was measured by flow cytometry]. (Figure 2 shows a histogram.)

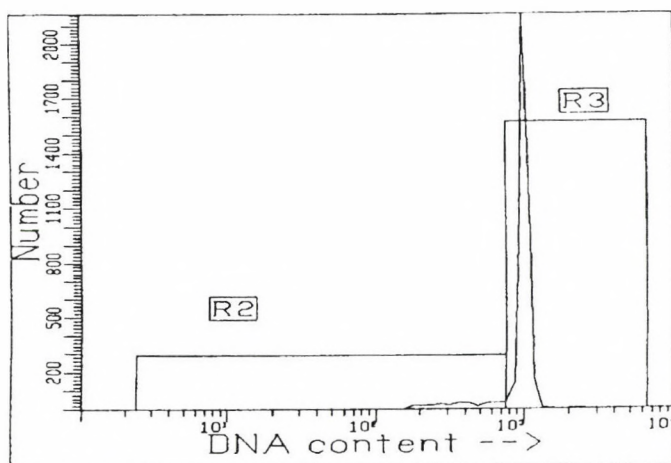


Fig. 2. Flow cytometric DNA histogram of *in vitro* cultured lymphocytes from HIV-positive individuals (apoptotic cell region – R2, normal cell region – R3)



## RESULTS

From all HIV-infected patients samples could be evaluated morphologically and were evaluable by flow cytometry. Apoptotic indices of lymphocytes of the HIV-positive patients measured by flow cytometric studies are shown in Fig. 3 and Fig. 4. Data of hematoxylin-eosin staining are not shown because of fully corroborating trend of flow cytometric data distribution (for the detection of apoptotic figures and the results obtained by these methods were identical). Beside the lymphocytes, other mononuclear cells and granulocytes were also observed in the samples, together with a low amount of cell debris.

The average percentage of apoptotic lymphoid cells of the unstimulated untreated samples was  $9.2 \pm 4.3\%$  in MAX experiment. This value was  $8.6 \pm 3.0\%$  in the case of MeAsc. This difference was not significant calculated for either methods mentioned. These data show an advanced progress of apoptosis in cultured cells of HIV-infected patients. After IL-2 stimulation the apoptotic ratio was diminished ( $6.7 \pm 2.7\%$  and  $6.6 \pm 1.7\%$ , in MAX and MeAsc study, respectively), according to morphological and flow cytometric observations, in all of the samples taken from HIV-positive individuals. Unstimulated ( $9.2 \pm 4.3\%$  and  $8.6 \pm 3.0\%$ ) and stimulated samples ( $6.7 \pm 2.7\%$  and  $6.6 \pm 1.7\%$ ) of MAX and MeAsc are good repetition in this experiment (the same patients, the same conditions), according to both morphological and flow cytometric findings.

Individual differences were seen between the HIV-positive cases regarding the effect of MAX and MeAsc on apoptosis. The apoptotic index altered dose dependently according to our observations. In four of the five HIV-positive cases the apoptotic index decreased by the effect of MAX, the least value of apoptotic index (lower than the IL-2 stimulated cases) was observed either in the  $0.1 \mu\text{g/ml}$  or  $1.0 \mu\text{g/ml}$  treatment (Fig. 3). In one of the five HIV-positive cases the apoptotic index did not change by the effect the least concentration ( $0.1 \mu\text{g/ml}$ ) of MAX. The administration of  $10 \mu\text{g/ml}$  MAX in all patient resulted higher apoptotic ratio (mean =  $9.8 \pm 1.5\%$ ) than stimulated cases (mean =  $6.7 \pm 2.7\%$ ). In MeAsc experiment the  $0.1 \mu\text{g/ml}$  and

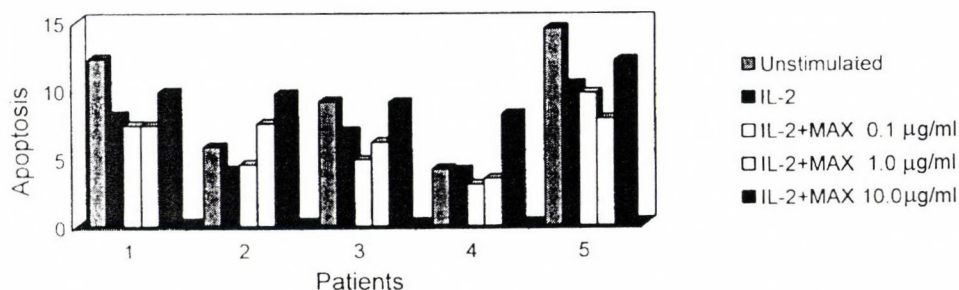


Fig. 3. Effect of  $N^G$ -hydroxymethylated-L-arginine (MAX) on proportion of apoptotic cells among incubated lymphocytes obtained from HIV-infected individuals

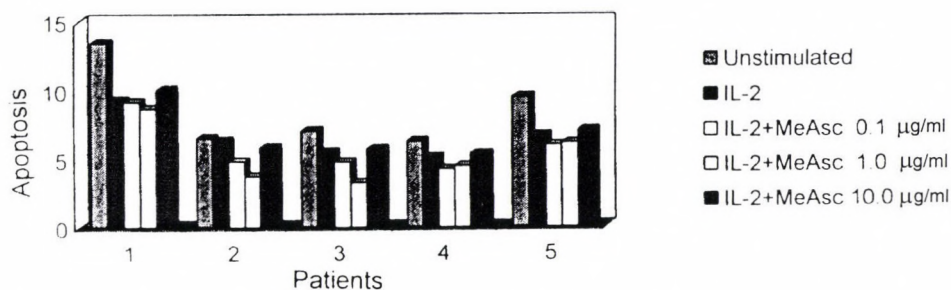


Fig. 4. Effect of 1'-methyl-ascorbigen (MeAsc) on proportion of apoptotic cells among incubated lymphocytes obtained from HIV-infected individuals

the 1.0 µg/ml doses decreased the mean number of apoptotic figures ( $5.8 \pm 2.0\%$  and  $5.3 \pm 2.2\%$ , respectively). The 1.0 µg/ml MeAsc proved to be the most effective dose (Fig. 4). In four of five patients the highest dose resulted the same or higher apoptotic index (mean =  $6.8 \pm 1.9\%$ ) than IL-2 stimulated case.

The absolute number of CD4 positive T lymphocytes, the CD4/CD8 ratio, the beta 2 microglobulin values, the duration of HIV-positivity could not be related to any effect of MAX or MeAsc (data not shown here).

Morphology and flow cytometry pointed out that MAX and MeAsc reduced the apoptotic ratio of stimulated lymphocytes dose dependently and the preventing effect of MAX or MeAsc on programmed cell death in four of the five HIV-positive cases.

## DISCUSSION

Our studies reveal that peripheral blood lymphocytes of HIV-positive individuals show apoptotic activity in cell culture. The stimulation of lymphocytes by IL-2 could not increase the apoptotic ratio in lymphocytes of HIV-positive persons against to our findings published earlier [12].

Data of HE staining were in fully corroborating trend of flow cytometric data distribution (for the detection of apoptotic figures and the results obtained by these methods were identical). This may be explained by the fact that in flow cytometric statistics we distinguish between apoptotic forms of lymphocytes and cell debris. We think that morphological and flow cytometric observations could complete to each other in this experimental design.

According to our findings, MAX and MeAsc dose dependently altered (decreased or increased) the number of apoptosis of cultured peripheral blood lymphocytes of HIV-infected individuals, compared to the IL-2-stimulated samples. The low or middle doses of MAX and MeAsc were the most effective in reducing apoptotic index. It can also be supposed that they may be applied with success *in vivo*, in the treat-



ment of HIV-positive persons. The decrease in number of apoptotic lymphocytes may prolong the symptomless period after HIV-infection.

N<sup>G</sup>-hydroxymethylated-L-arginine (MAX) and 1'-methyl-ascorbigen (MeAsc) are N-methyl compounds, which can be considered endogenous formaldehyde (HCHO) generators [10, 13, 14]. It is unknown how formaldehyde generators influence apoptosis of lymphocytes altered by HIV-infection and stimulated by IL-2. The formation of HCHO from different endogenous and exogenous compounds in the cells is a well known demethylation process. The chemical activity of HCHO is nonspecific and there is a wide variety of possible formaldehyde acceptors, therefore it is difficult to ascertain the actual role of HCHO-producing reactions in the cell. As a reactive molecule HCHO can participate in the degradation of the DNA which could suggest a possible function of formaldehyde in the apoptotic process.

According to the study of Szende et al. [11], HCHO can act as a cell proliferation retardation factor and mediate the apoptotic process of thymic lymphocytes. Other possibilities including the blockade of specific binding sites on the surface of lymphocytes may also be taken into consideration. Previously was demonstrated [9] that N-trimethyl-lysine (the relative molecule of MAX), and MeAsc have immunomodulating activity and protect the animals from bacterial and viral infection. These chemicals due to reduction of apoptosis in lymphocytes may slow down the progress of immune decline of HIV-infected individuals.

#### ACKNOWLEDGEMENT

This work was partly supported by OTKA grants, Nos T 6335 and T 17849.

#### REFERENCES

1. Ameisen, J. C. (1992) Programmed cell death and AIDS: from hypothesis to experiment. *Immunol. Today* 13, 388–391.
2. Conant, M. A., Calabrese, L. H., Thompson, S. E., Poiesz, B. J., Rasheed, S., Hirsch, R. L. et al. (1992) Maintenance of CD4<sup>+</sup> cells by thymopentin in asymptomatic HIV-infected subjects: results of a double-blind, placebo-controlled study. *AIDS* 6, 1335–1339.
3. Gong, J., Traganos, F., Darzynkiewicz, Z. (1994) A selective procedure for DNA extraction from apoptotic cells applicable for gel electrophoresis and flow cytometry. *Anal. Biochem.* 218, 314–319.
4. Gougeon, M. L., Montagnier, L. (1993) Apoptosis in AIDS. *Science* 260, 1269–1270.
5. Kerr, J. F. R., Wyllie, A. H., Currie, A. R. (1972) Apoptosis: a basic biological phenomenon with wide-ranging implication in tissue kinetics. *Br. J. Cancer* 26, 239–257.
6. Meyard, L., Otto, S. A., Jonker, R. R., Mijster, M. J., Keet, R. P. M., Miedema, F. (1992) Programmed death of T cells in HIV-1 infection. *Science* 257, 217–219.
7. Mihalik, R., Kopper, L., Benczur, M. (1995) Modulation of drug-induced apoptosis in a human B-lymphoma cell line (HT58). *Immunol. Letter.* 48, 17–21.
8. Schuler, D., Szende, B., Borsi, J. D., Marton, T., Boesi, J., Magyarosi, E., Koós, R., Csóka, M. L. (1994) Apoptosis as a possible way of destruction of lymphoblasts, after glucocorticoid treatment of children with acute lymphoblastic leukemia. *Pediatric Hematol. Oncol.* 11, 641–649.
9. Stotz, Gy., Szende, B., Lapis, K., Tyihák, E. (1974) The effect of E-N-DL-trimethyl-lysine on human lymphocyte cultures. *Exp. Path.* 9, 317–322.

10. Szende, B., Tyihák, E., Szókán, Gy. (1992) The possible role of formaldehyde in the action of various agents influencing mitosis and apoptosis in vitro. In: *Proceedings of 3rd Int. Conf. Role of Formaldehyde in Biological systems. Methylation and demethylation processes.* pp. 63–68.
11. Szende, B., Tyihák, E., Szókán, Gy., Kátay, Gy. (1995) The possible role of formaldehyde in the apoptotic and mitotic effect of 1'-methyl-ascorbigen. *Pathol. Oncol. Res.* **1**, 38–42.
12. Szende, B., Horváth, A., Nagy, K., Bocsi, J., Kovalszky, I., Barabás, É. (1997) Reduction of apoptosis of *in vitro* cultured peripheral blood lymphocytes of HIV-positive individuals by thymocartin. *Med. Sci. Monitor* **3**, 456–459.
13. Tyihák, E., Szende, B., Lapis, K. (1977) Biological significance of methylated derivatives of lysine and arginine. *Life Sciences* **20**, 385–392.
14. Tyihák, E., Gullner, G., Trézl, L. (1993) Formaldehyde cycle and possibility of formation of singlet oxygen in plant tissues. In: Mózsik, Gy., Emerit, I., Fehér, J., Matkovics, B., Vincze, Á. (eds) *Proceedings Oxygen Free Radicals and Scavengers in the Natural Sciences. Akadémiai Kiadó, Budapest*, pp. 21–28.





## FORMALDEHYDE GENERATION BY N-DEMETHYLATION\*

H. KALÁSZ,<sup>1</sup> MÁRIA BÁTHORI<sup>2</sup> and E. TYIHÁK<sup>3</sup>

<sup>1</sup>Department of Pharmacology, Semmelweis University of Medicine, Budapest

<sup>2</sup>Department of Pharmacognosy, Albert Szent-Györgyi Medical University, Szeged

<sup>3</sup>Plant Protection Institute of the Hungarian Academy of Sciences, Budapest, Hungary

(Received: 1998-10-28; accepted: 1998-11-25)

Microsomal oxidation of exogenic compounds yields efferent metabolites with small molecular size. N-demethylation results in formaldehyde generation in addition to the nor-compound.

Interesting changes in the level of formaldehyde elimination were observed after a single dose of either (–)-deprenyl or (+)-deprenyl. Urine elimination of the generated formaldehyde was determined using thin-layer chromatography after derivatization with dimedone.

**Keywords:** (–)-deprenyl – formaldehyde – *in vivo* formaldehyde – *in situ* formaldehyde – efferent metabolites

### INTRODUCTION

Oxidation plays a major role in the metabolism of exogen and endogen substances. N-methyl compounds are generally subjected to N-demethylation through their biotransformations. Large molecular size products (that is the nor-derivatives) have been widely studied, however, less attention has been paid to the “efferent” metabolites with small molecular size [15]. Although every basic book in pharmacology points out formaldehyde as one constant metabolic product of N-demethylation (and also that of either O-demethylation or S-demethylation) [e.g. 1, 2, 10], quantitative determination of the metabolically generated formaldehyde, and its role, and its topic effects have remained an important and perspective issue for further research.

(–)-Deprenyl that is (R)-(–)-N-methyl-(1-phenyl-2-propyl)-N-propynylamine (also called as Selegiline, Jumex<sup>R</sup>, Eldepryl<sup>R</sup>, etc.) is about 500× more potent inhibitor of monoamine oxidase type B (MAO-B) enzyme than the (+)-form; it has

\* Presented at the 4th International Conference on the Role of Formaldehyde in Biological Systems, July 1–4, 1998, Budapest, Hungary.

Send offprint requests to: Dr. Huba Kalász, Department of Pharmacology, Semmelweis University of Medicine, H-1445 Budapest, P.O. Box 370, Hungary. E-mail: KalHub@net.sote.hu.



reduced toxicity, and less serious side effects (such as hyperthermia and excitation in rats, etc.). (–)-Deprenyl facilitates dopamine release in the brain [5], increasing the activity of *nigro-striatal* dopaminergic neurons, and has protecting effect through the aging process. At the same time, (–)-deprenyl has no effect on the mesolimbic dopaminergic function, i.e., it fails to influence locomotion and rearing activity in rats [16]. MAO-B inhibitory effect of (–)-deprenyl explains its therapeutic effects and wide use in the treatment of Parkinson's disease [4], however, the other important beneficial effects, such as increase of dopamine release [5], inhibition of programmed cell death [11], etc. have mainly remained unexplained.

Drugs are generally subjected to the "first-pass-effect" of liver. At the same time, the majority of other organs also have the ability to metabolize the drugs. In the case of (–)-deprenyl, its substantial portion is subjected to the first pass effect and the majority of metabolites are eliminated with the urine [4].

This paper deals with two basic aspects of formaldehyde generation. How is the bulk amount of the metabolically produced formaldehyde is eliminated, and where can minor but significant formaldehyde generation also be taken into consideration.

## MATERIALS AND METHODS

### *Materials*

Jumex<sup>R</sup> tablets [5 mg of (–)-deprenyl] and (+)-deprenyl were the kind gift of the Chinoin Pharmaceutical Works (Budapest, Hungary). Other chemicals and solvents were purchased from commercial sources in the highest purity grades.

### *Methods*

Healthy male volunteer (about 85 kg of body weight) took a single dose of either 10 mg (–)-deprenyl or 10 mg of (+)-deprenyl, and urine was collected for three times eight hour periods (0–8 hour, 8–16 hour and 16–24 hour). Urine samples were stored at –25 °C until formaldehyde determination.

Formaldehyde content was determined as published earlier [17]. Three parallel determinations were done and the results were within  $\pm 7\%$  of the averages.

## RESULTS

Determination of urinary elimination of formaldehyde after administration of (–)-deprenyl and (+)-deprenyl was done using thin-layer chromatography. The separation was satisfactory and formaldemethone resulted in compact spots. Results are shown in Fig. 1. The control value of formaldehyde elimination was decreased

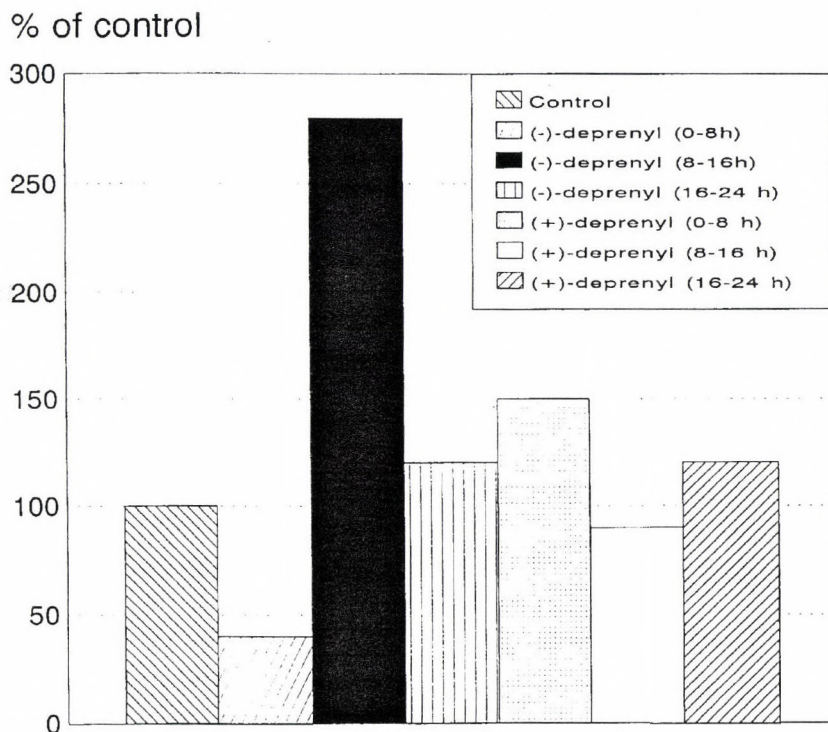


Fig. 1. Urinary elimination of formaldehyde of the subject who did not take any drug (control), after having taken 10 mg of (-)-deprenyl (formaldehyde level in the urine in the 1st, 2nd and 3rd eight hours), and after having taken 10 mg of (+)-deprenyl (formaldehyde level in the urine in the 1st, 2nd and 3rd eight hours)

through the 1st eight hours but highly elevated through the 2nd eight hours following a single daily dose of (-)-deprenyl. Administration of (+)-deprenyl did not cause such a change in the formaldehyde content of the urine.

## DISCUSSION

A great importance in formaldehyde generation is attached to the cycle where S-adenosyl-L-methionine splits to formaldehyde and S-adenosyl-L-homocysteine [17]. Formaldehyde is also formed in the hard tissue of teeth, and it was measured using thin-layer chromatographic determination of formaldemethone [13].

The first pass effect of (-)-deprenyl takes an essential part in its metabolism [4, 18]. In humans, the majority of the administered deprenyl is eliminated with urine in the form of metabolites. Nine metabolites were identified such as desmethyldeprenyl, methamphetamine, amphetamine, norephedrine, norpseudoephedrine,



ephedrine, pseudoephedrine, p-hydroxyamphetamine and p-hydroxymethamphetamine [14]. Although the generation of each of these metabolites is done by one or two steps of N-dealkylation, very little attention has been devoted to the byproducts, the efferent metabolites that are yielded in the course of deprenyl metabolism. At the same time, a study on the metabolism of pargyline (a compound having similar chemical structure to deprenyl, a phenylalkyl amine with both N-methyl and N-propyl substituents) published the formation of formaldehyde, propylaldehyde and the corresponding benzylalkylketone among the metabolites [20]. A recent paper published the occurrence of benzylmethylketone in the human urine after the subject has taken a single dose of Jumex<sup>R</sup> that is (–)-deprenyl.

As one of the major metabolites of deprenyl is amphetamine, N-demethylation procedure has to be taken into consideration. Since the characteristic metabolite profile has already been formed during the first pass process, different preferred metabolic and pharmacokinetic characteristics of the deprenyl enantiomers are postulated. Urinary elimination of (–)-deprenyl and (+)-deprenyl indicates a basic difference in the kinetics of their metabolism. The ratio of (–)-methamphetamine to (–)-amphetamine was well over 1 : 1, in the urine in the first several hours following administration of (–)-deprenyl [9]. The ratio approximates 1:1 from 16 through 24 hours following administration [7]. Similar phenomenon in the cases of (+)-methamphetamine and (+)-amphetamine was not observed, their ratio remained close to 1 : 1, independently of the time of urine collection [7, 9]. However, in any case, the deprenyl metabolism results in amphetamine also, and therefore both the formation and the elimination of formaldehyde have to be considered.

The importance of formaldehyde generation in the course of N-demethylation of an exogenous compound is emphasized by the fact that N-dealkylation procedures may take place in the human brain, where amphetamine was identified in post-mortem Parkinsonian brain after (–)-deprenyl administration [12]. Experiments with rats also indicated the N-dealkylation procedure in the brain itself, as after intracerebroventricular administration of deprenyl, amphetamine and also methamphetamine were identified in the microdialysate [8]. Thereby an *in situ* formaldehyde generation can essentially be supposed which contributes to the protection of the brain from oxidative stress. Oxidative stress is a major source of neurodegenerative processes, protection of the brain from oxidative stress has vital importance.

Positron emission tomography has shown that (–)-deprenyl persists for a much longer period in the brain than (+)-deprenyl [3, 4]. The slowly generated and probably low level of formaldehyde may help eliminating the oxygen free radicals thereby counteracting the damage of the oxidative stress. For the time being, there exists only circumstantial evidence for formaldehyde formation in the brain, while other chemical reactions have also to be considered. *In vitro* reaction between hydrogen peroxide and deprenyl also resulted in the N-dealkylation yielding nordeprenyl, methamphetamine and amphetamine in aqueous solution in a glass test tube [6]. This result gives an alternative possibility for the beneficial effect of (–)-deprenyl either in the treatment or rather in prevention of Parkinson's disease by elimination of hydrogen peroxide for the possible metabolism of (–)-deprenyl.

In addition, recent findings have indicated that (–)-deprenyl is capable of protecting hippocampal neurons in acute cerebral ischemia [19]. However, the mechanism of this effect is unknown.

#### ACKNOWLEDGEMENTS

This work was supported by the grants of T023370 of the OTKA (Budapest, Hungary) and No. 553/1996 of the Ministry of Health and Welfare of Hungary.

#### REFERENCES

1. Benet, L. Z., Kroetz, D. L., Sheiner, L. B. (1995) Pharmacokinetics: The dynamics of drug absorption, distribution, and elimination. In: Hardman, J. G., Libird, L. E., Matinoll, P. B., Ruddon, R. W. (eds) *Goodman and Gilman's The Pharmacological Basis of Therapeutics*. 9th Edition, McGraw-Hill, New York, p. 13.
2. Correia, M. A. (1998) Drug biotransformation. In: Katzung, B. G. (ed.) *Basic and Clinical Pharmacology*, 7th Edition, Appleton and Lange, Stamford, CT, p. 53.
3. Fowler, J. S., MacGregor, R. R., Wolf, A. P. (1987) Mapping human brain monoamine oxidase A and B with  $^{14}\text{C}$ -labelled suicide inactivators and PET. *Science* 235, 481–485.
4. Heinonen, E. H., Antilla, M. I., Lammintausta, R. A. S. (1994) Pharmacokinetic aspects of l-deprenyl (selegiline) and its metabolites. *Clin. Pharmacol. Ther.* 56, 742–749.
5. Kalász, H., Kerecsen, L., Knoll, J., Pucsok, J. (1990) Chromatographic studies on the binding, action and metabolism of (–)-deprenyl. *J. Chromatogr.* 499, 589–599.
6. Kalász, H., Kerecsen, L., Matkovics, B., Hollósi, I. (1986) Decomposition products of (–)-deprenyl reacted by hydrogen peroxide. In: Kalász, H., Ettre, L. S. (eds) *Chromatography '85*. Akadémiai Kiadó, Budapest, pp. 129–134.
7. Kalász, H., Tarjányi, Zs., Hollósi, I., Pucsok, J., Bartók, T., Komoróczy, R., Kiss, J. P., Hennings, E. C. P. (1998) Analysis of deprenyl metabolites using gas chromatography and HPLC-EC-MS (submitted for publication).
8. Lajtha, A., Sershen, H., Cooper, T., Hashim, A., Gaál, J. (1996) Metabolism of (–)-deprenyl and p-fluoro-(–)-deprenyl in brain after central and peripheral administration. *Neurochem. Res.* 21, 1155–1160.
9. Lengyel, J., Magyar, K., Hollósi, I., Bartók, T., Báthori, M., Kalász, H., Fürst, S. (1997) Urinary excretion of deprenyl metabolites. *J. Chromatogr. A* 762, 321–326.
10. Magyar, K. (1998) Fate of the drug in the body, pharmacokinetics. In: Fürst, S. (ed.) *Pharmacology* (Gyógyszertan), Medicina, Budapest, p. 92. (in Hungarian).
11. Magyar, K., Szende, B., Lengyel, J., Tekes, K. (1996) The pharmacology of B-type selective monoamine oxidase inhibitors; milestones in (–)-deprenyl research. *J. Neural Transmission, Suppl.* 48, 29–43.
12. Reynolds, G. P., Riederer, P., Sandler, M., Jellinger, K., Seeman, D. (1978) Amphetamine and 2-phenylethylamine in post-mortem parkinsonian brain after (–)-deprenyl administration. *J. Neural Transmission* 43, 271–277.
13. Rozylo, T. K. (1998) Quantitative TLC determination of formaldehyde in hard tissues of teeth. *Biomed. Chromatogr.* 12, 267–270.
14. Shin, H. S. (1997) Metabolism of selegiline in humans. Identification, excretion, and stereochemistry of urine metabolites. *Drug Metab. and Dispos.* 25, 657–662.
15. Tarjányi, Zs., Kalász, H., Szebeni, Gy., Hollósi, I., Báthori, M., Fürst, S. (1998) Gas-chromatographic study on the stereoselectivity of deprenyl metabolism. *J. Pharm. Biomed. Anal.* 17, 725–731.
16. Timár, J., Gyarmati, Z., Tekes, K., Hársing, G. L., Knoll, J. (1993) Further proof that (–)-deprenyl fails to facilitate mesolimbic dopaminergic activity. *Pharmacol. Biochem. Behav.* 46, 709–714.



17. Tyihák, E., Gullner, G., Trézl, L. (1993) Formaldehyde cycle and possibility of formation of singlet oxygen in plant tissues. In: Mózsik, G., Emerit I., Fehér, J., Matkovics, B., Vincze, Á. (eds) *Oxygen Free Radicals and Scavengers in the Natural Science*. Akadémiai Kiadó, Budapest, pp. 21–28.
18. Yoshida, T., Yamada, Y., Yamamoto, T., Kuroiwa, Y. (1986) Metabolism of deprenyl, a selective monoamine oxidase (MAO-B) inhibitor in rat: relationship of metabolism to MAO-B inhibitory potency. *Xenobiotica* 16, 129–136.
19. Yu, P. H., Davis, B. A., Durden, D. A., Barber, A., Terleckyj, I., Nicklas, W. G., Boulton, A. A. (1994) Neurochemical and neuroprotective effects of some aliphatic propargylamines: new selective non-amphetamine-like monoamine oxidase B inhibitors. *J. Neurochem.* 62, 697–704.
20. Weli, A. M., Hook, B. B., Lindeke, B. (1985) N-dealkylation and N-oxidation of two alpha-methyl-substituted pargyline analogues in rat liver microsomes. *Acta Pharm. Suec.* 22, 249–264.

## FORMALDEHYDE-INDUCED MODIFICATION OF HEMOGLOBIN *IN VITRO*\*

R. FARBISZEWSKI, ELŻBIETA SKRZYDLEWSKA and AGNIESZKA ROSZKOWSKA

Department of Analytical Chemistry, Medical University, Białystok, Poland

(Received: 1998-10-28; accepted: 1998-11-25)

Formaldehyde is known to react with proteins. The purpose of our experiments was to analyse *in vitro* the effect of formaldehyde on the physicochemical and biological properties of hemoglobin molecules. The effect of formaldehyde concentration, reaction time, pH and temperature on hemoglobin free amino groups was estimated. The modified hemoglobin was analysed using electrophoretic, potentiometric and spectrophotometric techniques. Reaction between formaldehyde and hemoglobin was accelerated by increasing concentration of formaldehyde and higher temperature. This reaction was most intensive during the first few hours at pH 7.4 so the amount of free amino groups of hemoglobin was significantly diminished by directly mixing formaldehyde with hemoglobin. The modified protein was characterized by the increase in electrophoretic mobility and the decrease in maximum absorption derived from porphyrin rings. Formaldehyde modified hemoglobin was less susceptible to the action of cathepsin D.

**Keywords:** Formaldehyde – hemoglobin modification – cathepsin D

### INTRODUCTION

Formaldehyde (HCHO) is detectable both in animal and plant cells [25]. It originates mainly from methylation and demethylation reactions [10], but may also occur in animals as a result of intoxication and due to subsequent metabolism of xenobiotics such as methanol [12, 17]. Blood distributes formaldehyde throughout different organs and tissues. It does not normally exist as a free compound, because it easily reacts with many endogenous low molecular compounds such as cysteine, urea and glutathione [3]. Formaldehyde also reacts with functional groups, most often amino and sulfhydryl of many high molecular weight compounds, such as proteins and nucleic acids [3].

Proteins constitute an important part of the organic compounds found in a living cell and play a significant role in multiple cell functions. Among structural proteins,

\* Presented at the 4th International Conference on the Role of Formaldehyde in Biological Systems, July 1-4, 1998, Budapest, Hungary.

Send offprint requests to: Dr. R. Farbiszewski, Department of Analytical Chemistry, Medical University, Białystok, Poland.



a special role is attributed to transport proteins which take part in respiration and photosynthesis. One such protein which may be exposed to the action of formaldehyde is hemoglobin. Such a reaction may result in structural modification of the hemoglobin. Hence, the physicochemical properties and biological function of hemoglobin may get impaired like other proteins [11].

The purpose of this work was to determine the effects of formaldehyde on the physicochemical properties of hemoglobin and its susceptibility to proteolytic enzyme degradation.

## MATERIALS AND METHODS

Formaldehyde, ninhydrin reagent, cathepsin D {Sigma (USA)}; hemoglobin (Difco, USA). The solutions of formaldehyde, hemoglobin and cathepsin D were prepared in 0.04M Britton-Robinson buffer (containing 0.04M phosphate, acetate and borate buffers), pH 3.5 and 7.4.

### *1. The influence of formaldehyde concentration, reaction time, pH and temperature on free amino groups of hemoglobin*

Formaldehyde solution (13, 130 and 1300 mM at pH 3.5 and 7.4) was added to 1% hemoglobin solution, of the same pH, in the proportion 1 : 10 (v/v). The mixture was incubated at 25, 37 and 48 °C. Formaldehyde that was noncovalently linked to hemoglobin was removed by separation on a Sephadex G-25 column both before incubation and after 3, 6, 12, 48, 96 and 192 hours of incubation. Next, the total amount of non linked formaldehyde was spectrophotometrically determined [1]. Control hemoglobin was prepared in the buffer in the absence of formaldehyde. The protein concentration was estimated by the Lowry method [13] and the amount of free amino groups by ninhydrin methods [4].

### *2. Estimation of hemoglobin modification by formaldehyde*

To prepare samples for electrophoretic measurements, the formaldehyde solutions (13, 130 and 1300 mM at pH 7.4) were added to 1% hemoglobin solution. The solutions were incubated for 12 hours at 37 °C and, after removal of formaldehyde, the protein was examined electrophoretically on cellulose acetate at pH 8.6. The samples prepared for electrophoresis were also examined by UV VIS absorption spectroscopy.

The biological properties of hemoglobin were estimated according to the following procedures. The formaldehyde solutions (13, 130 and 1300 mM at pH 3.5 or 7.4) were added to 1% hemoglobin solution of the same pH in the proportion 1 : 10 (v/v) and the solutions were incubated for 0, 6, 12 and 24 hours at 37 °C. After removing

the formaldehyde, the samples were incubated with cathepsin D preparation (4 : 1; v/v) at pH 3.5 for 30 min at 37 °C. Next, the protein was precipitated with 5% TCA. Cathepsin D activity was measured by determination of tyrosine, in the filtrate, using the Folin-Ciocalteu method (2). Furthermore, modified hemoglobin (with 130 mM formaldehyde) was degraded by cathepsin D modified by formaldehyde (13, 130 and 1300 mM). The modification was performed for 1, 2 and 4 hours using the procedure described above.

In all experiments the results were presented as means  $\pm$  S.E.M. For the comparison of mean values, Student's *t*-test for unpaired data was used. The differences were considered as significant at  $p < 0.05$ .

## RESULTS

Formaldehyde reacted with hemoglobin at rates proportional to their concentrations, pH and temperature (Fig. 1). This reaction was most intensive during the first hours of incubation. The protein concentration did not change during the experiment.

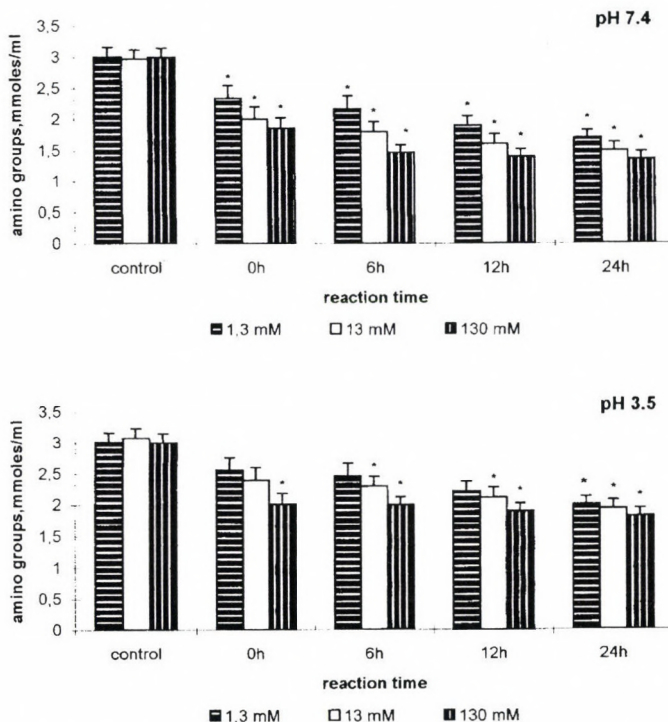


Fig. 1. Effect of different concentrations of formaldehyde and reaction pH on the hemoglobin free amino groups. Data points represent the mean  $\pm$  SEM;  $n = 5$  (\* $p < 0.05$  in comparison to the group where the formaldehyde concentration equals zero)



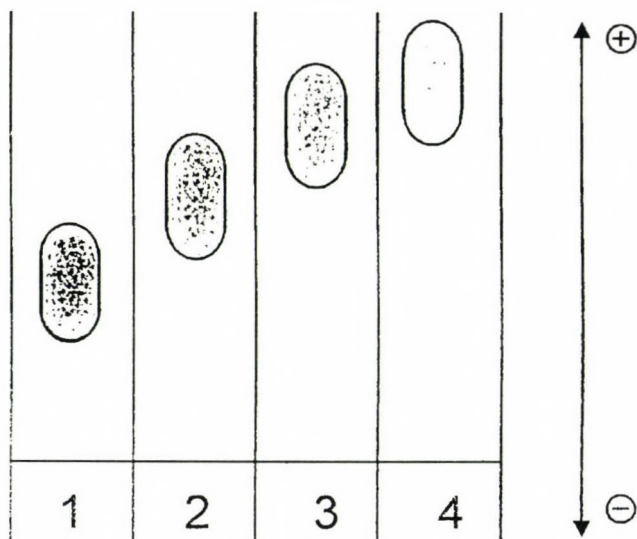


Fig. 2. Effect of different formaldehyde concentrations on electrophoretic mobility of hemoglobin. 1 – native hemoglobin; 2 – hemoglobin modified by 1.3 mM formaldehyde; 3 – hemoglobin modified by 13 mM formaldehyde; 4 – hemoglobin modified by 130 mM formaldehyde

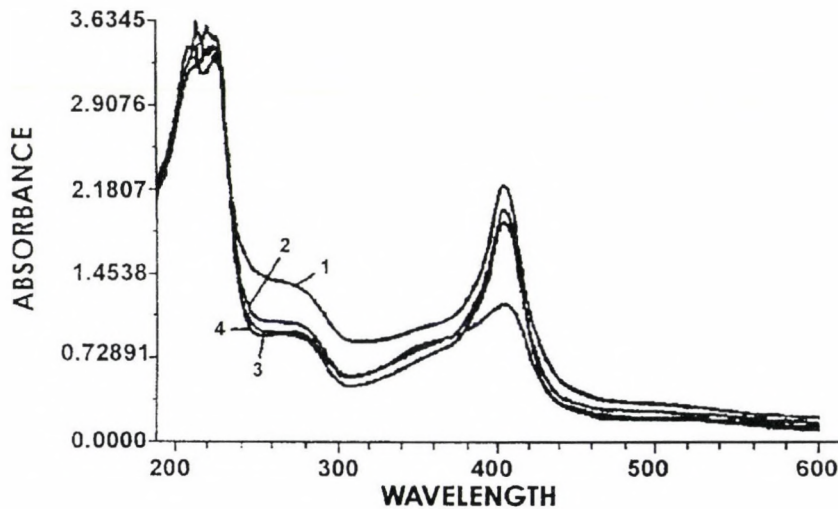


Fig. 3. Effect of different formaldehyde concentrations on UV VIS absorption spectrum of hemoglobin. 1 – native hemoglobin; 2 – hemoglobin modified by 1.3 mM formaldehyde; 3 – hemoglobin modified by 13 mM formaldehyde; 4 – hemoglobin modified by 130 mM formaldehyde

Formaldehyde caused, proportionally to its concentration, decreases in the free amino groups of hemoglobin. The interaction was more intensive at pH 7.4 than 3.5. Temperature proportionally intensified the reaction between formaldehyde and hemoglobin.

Interaction between formaldehyde and amino groups of hemoglobin was confirmed by electrophoresis (Fig. 2). Faster migration of modified hemoglobin to the anode was observed, but these changes were not proportional to the formaldehyde concentration.

The UV VIS absorption spectrum of hemoglobin was also changed after incubation with formaldehyde (Fig. 3). The absorption maxima at 280 and 410 nm were decreased.

Figure 4 shows that modified hemoglobin was less susceptible to proteolytic degradation by cathepsin D. These changes were proportional to formaldehyde concentration, time of reaction and the pH of the mixture. The activity of cathepsin D modified by formaldehyde was also decreased (Fig. 5). The amount of tyrosine released during proteolytic degradation of hemoglobin by modified cathepsin D was smaller than during the proteolytic action of unmodified cathepsin D.

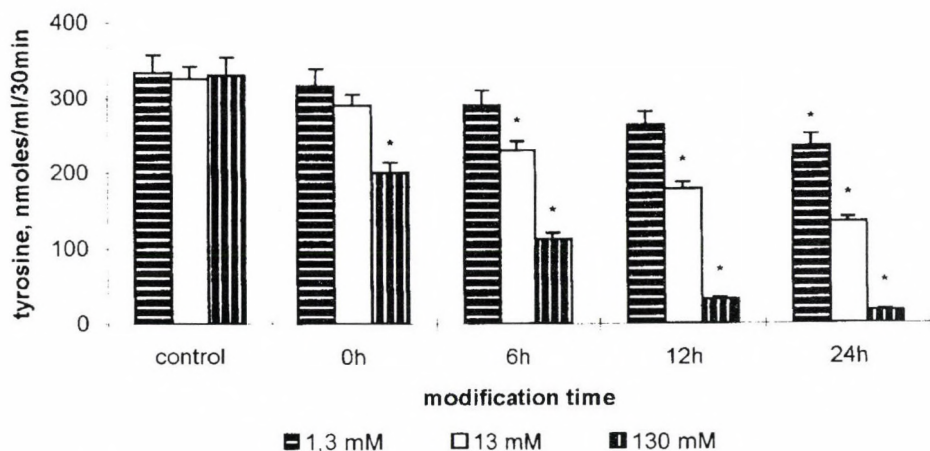


Fig. 4. Effect of different formaldehyde concentrations on hemoglobin susceptibility to degradation by cathepsin D. Data points represent the mean  $\pm$  SEM;  $n = 5$  (\* $p < 0.05$  in comparison to the group where the formaldehyde concentration equals zero)



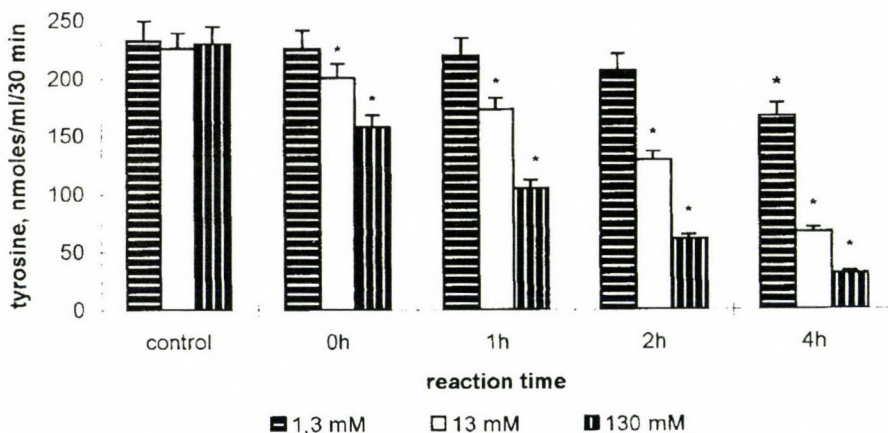


Fig. 5. Effect of different formaldehyde concentrations on hemoglobin susceptibility to degradation by cathepsin D. Data points represent the mean  $\pm$  SEM;  $n = 5$  (\* $p < 0.05$  in comparison to the group where the formaldehyde concentration equals zero)

## DISCUSSION

Reaction of hemoglobin with formaldehyde was found to cause decreases in the amount of total free amino groups. It was shown that formaldehyde molecules react easily with amino groups of hemoglobin and this reaction is more intensive at higher formaldehyde concentration, pH and temperature during the first hours of incubation. These observations were confirmed by electrophoretic studies in which migration of modified hemoglobin was faster than that of unmodified protein. This indicates that the total positive charge of hemoglobin, derived mainly from amino groups, was decreased following this reaction.

Formaldehyde reacts especially easily with the  $\epsilon$ -amino groups of lysine residues of proteins and this reaction is very fast with both structural proteins, such as albumin, and enzymatic ones, for example chymotrypsin [14, 19]. The formaldehyde interaction with hemoglobin is more effective at basic pH. This is due to the fact that formaldehyde molecules react with uncharged amino groups [8]. Such a condition was observed for collagen during the leather tanning process [8]. Furthermore, formaldehyde reacts also with cysteine, tryptophan, tyrosine, serine, asparagine, glutamine residues, amino groups of N-terminal amino acids and with peptide bonds [5, 8, 20, 22], but the course of these reactions is slower. Reaction of formaldehyde with aromatic amino acid residues of hemoglobin was confirmed by the decrease in the UV maximum absorption at 280 nm, but not before 12 hours of incubation.

The first step in the formaldehyde reaction with proteins is the formation of reversible hydroxymethyl compounds with reactive groups in the polypeptide chain. Mono- and dihydroxymethyl derivatives can be formed by reaction with  $\alpha$ -amino

groups [15], whose formation depends on reaction conditions, e.g. one imidazole ring nitrogen atom of histidine reacts with formaldehyde in a basic medium, whereas both nitrogen atoms react in a strongly basic medium yielding the N-hydroxymethyl derivatives [5]. Some hydroxymethyl groups react with nucleophilic groups of protein molecules, yielding methylene bridges. Mainly lysyl and cysteinyl, and to a lesser degree, arginyl, asparaginyl and glutaminyl residues are active in the formation of such bridges [6, 7, 21]. Additionally, the hydroxymethyl groups of lysyl residues react with the phenyl ring of tyrosine, the indole ring of tryptophan and the imidazole ring of histidine [6, 7, 16]. As a result, intra- and intermolecular bonds are formed [6], which cause changes in the structural and physico-chemical properties of proteins such as polymerization with resultant increases in their molecular weight [9]. In this situation the rate of hemoglobin migration in the electric field is not proportional to the increase in formaldehyde concentration.

On the other hand, the cross-bindings protect the proteins against other destructive agents, e.g. high temperature and proteolytic enzymes [9, 19]. Cathepsin D (cellular protease) hydrolyses peptide bonds formed by tyrosine [2], the aromatic amino acid which is probably modified by formaldehyde. Moreover, it was shown that the isolated reaction products of formaldehyde with albumin, tetanus and diphtheria toxins contained bridges between lysine and tyrosine [9, 20]. In this situation, the hydrolytic action of cathepsin D on modified hemoglobin is significantly less. A similar situation was observed in the peptide mapping of formaldehyde-modified hemoglobin, after degradation of this protein by trypsin (unpublished data). Moreover, formaldehyde reacts with biologically-active proteins which leads to a decrease in their activities. This applies particularly to the enzymes whose catalytic action depends on free amino groups, such as ribonuclease [11]. Although cathepsin D is a carboxyl protease, it is also modified by formaldehyde (unpublished data). Probably formaldehyde does not change the carboxyl active centre of this protease, but modifies the structural conformation of the polypeptide chain near this centre and thereby decreases the protease activity. A similar situation was observed after alpha-1-antitrypsin modification by formaldehyde [18].

The hydroxymethyl derivatives and imines (the Schiff bases) formed in small amounts following reactions between formaldehyde and hemoglobin, can undergo reduction to methyl derivatives. This concerns particularly lysyl residues transformed into methyllysyl or formyllysyl residues [20, 23, 24]. Changes in the potentiometric curve above pH 6 indicate a raise in the dissociation constants of some basic amino acids after formaldehyde modification (unpublished data). It is known that dimethylamines are weaker bases than amines [15].

Significant changes were observed in the VIS absorption spectrum at 410 nm, especially in the Soret band characteristic of the porphyrin ring, existing due to the ring system connection. These systems are formed during colourless porphyrin oxidation. Formaldehyde may directly react with methylenide bridges or indirectly affect amino groups which results in partial reduction of methylenide to methylene bridges. As a consequence, the Soret band absorption is significantly decreased.



## REFERENCES

1. Ahmed, N., Furth, A. J. (1991) A microassay for protein glucation based on the periodate method. *Anal. Biochem.* 192, 109–111.
2. Barrett, A. J. (1977) Cathepsin D and other carboxyl proteinases. In: Barrett A. J. (eds) *Proteinases in mammalian cells and tissues*. North-Holland Pub. Co., Amsterdam, New York, Oxford.
3. Bolt, H. M. (1987) Experimental toxicology of formaldehyde. *J. Cancer Res. Clin. Oncol.* 113, 305.
4. Devenyi, T., Gergely, J. (1968) *Analytische Methoden zur Untersuchung von Aminosäuren. Peptiden und Proteinen*. Akadémiai Kiadó, Budapest.
5. Dunlop, P., Marini, M., Fales, H. M., Sokoloski, E., Martin, C. (1973) NMR studies of the reaction of FA with the imidazole side chain of histidine, a reactive amino acids in enzyme catalysis. *J. Bioorg. Chem.* 2, 235–247.
6. Fraenkel-Conrat, H., Olcott H. S. (1948) The reaction of formaldehyde with proteins. V. Cross-linking between amino and primary or guanidyl groups. *J. Am. Chem. Soc.* 70, 2673–2684.
7. Fraenkel-Conrat, H., Olcott H. S. (1948) Reaction of formaldehyde with proteins. VI. Cross-linking of amino groups with phenol, imidazole, or indole groups. *J. Biol. Chem.* 174, 827–843.
8. French, L., Edsall J. T. (1945) The reactions of formaldehyde with amino acids and proteins. *Adv. Protein Chem.* 2, 277–335.
9. Galembeck, F., Ryan, J. R., Feeney, R. E. (1977) Reaction of proteins with formaldehyde in the presence and absence of sodium borohydride. *J. Agric. Food Chem.* 25, 238–245.
10. Huszti, Z., Tyihák, E. (1986) Formation of formaldehyde from S-adenosyl-L-(methyl-<sup>3</sup>H) methionine during enzymatic transmethylation of histamine. *FEBS Lett.* 209, 362–366.
11. Jentof, J. E., Jentof, N., Gerken, T. A., Dearbon D. G. (1979) <sup>13</sup>C NMR studies of ribonuclease A methylated with [<sup>13</sup>C] formaldehyde. *J. Biol. Chem.* 254, 4366–4370.
12. Liesivuori, J., Savolainen, H. (1991) Methanol and formic acid toxicity: biochemical mechanisms. *Pharmacol. Toxicol.* 69, 157–163.
13. Lowry, O. H., Rosenbrought, N. J., Farr, A. L., Randal, R. J. (1951) Protein measurement with Folin phenol reagent. *J. Biol. Chem.* 153, 265–275.
14. Martin, C. J., Oza, N. B. (1972) Formaldehyde as an active site label of alpha-chymotrypsin. *Can. J. Biochem.* 50, 1114–1121.
15. Means, G. E., Feeney R. E. (1968) Reductive alkylation of amino groups in proteins. *Biochemistry* 7, 2192–2201.
16. Naulet, N., Tome, D., Martin G. J. (1983) <sup>15</sup>N NMR studies of amino acids and their reaction products with formaldehyde. *Org. Magn. Reson.* 21, 564–566.
17. Restani, P., Galli, C. L. (1991) Oral toxicity of formaldehyde and its derivatives. *Crit. Rev. Toxicol.* 21, 315–328.
18. Skrzydlewska, E., Mielczarska, J. (1997) Influence of methanol and its metabolites on the activity of  $\alpha_1$ -antitrypsin. *Alcohol* 14, 295–299.
19. Tome, D., Bertrand, D., Viroben, G., Delort-Laval, J. (1979) Tanage par le formol des aliments proteiques du ruminant. I. Etude preliminaire du mode d'action du formol sur un substrat proteique modele. *Ann. Technol. Agric.* 29, 299–318.
20. Tome, D., Kozlowski, A., Mabon, F. (1985) Carbon-13 NMR study on the combination of formaldehyde with bovine serum albumin. *J. Agric. Food Chem.* 33, 449–455.
21. Tome, D., Naulet, N., Kozlowski, A. (1985) <sup>13</sup>C-n.m.r. characterization of formaldehyde bonds in model mixtures and proteins containing lysine. *Int. J. Peptide Protein Res.* 25, 258–266.
22. Tome, D., Naulet, N., Martin, G. J. (1982) Application de la RMN a l'étude des reactions du formaldehyde avec les fonctions amines de la alanine et de la lysine en fonction du pH du milieu. *J. Chim. Phys.* 79, 361–366.
23. Trézl, L., Rusnak, I., Tyihák, E., Szarvas, T., Szende, B. (1983) Spontaneous N-methylation and N-formylation reactions between L-lysine and formaldehyde inhibited by L-ascorbic acid. *Biochem. J.* 214, 289–292.
24. Tyihák, E., Trézl, L., Rusznák, I. (1980) Spontaneous N<sup>ε</sup>-methylation of L-lysine by formaldehyde. *Pharmazie* 35, 18–20.
25. Tyihák, E., Trézl, L., Szende, B. (1998) Formaldehyde cycle and the phases of stress syndrome. *Ann. NY Acad. Sci.* 851, 259–270.

## CHANGE OF BIOTRANSFORMATION STEPS OF FORMALDEHYDE CYCLE IN WATER-MELON PLANTS AFTER INFECTION WITH *FUSARIUM OXYSPORUM*\*

ÉVA SÁRDI<sup>1</sup> and E. TYIHÁK<sup>2</sup>

<sup>1</sup>Department of Genetics and Plant Breeding, University of Horticulture and Food Industry,  
Budapest, Hungary

<sup>2</sup>Plant Protection Institute, Hungarian Academy of Sciences, Budapest, Hungary

(Received: 1998-10-28; accepted: 1998-11-25)

Recent experiments indicate that the measurable formaldehyde (HCHO) level is considerably elevated in the parts of water-melon plants immediately after a nonlethal infection with *Fusarium oxysporum* f. sp. *niveum*. At the same time the level of some quaternary ammonium compounds (N<sup>ε</sup>-trimethyl-L-lysine, choline) as potential HCHO generators (gene products) is considerably decreased. That is probably due to the fact that the alarm reaction phase of this biotic stress syndrome includes an intensive demethylation process. It has been proved that HCHO may play a role in dynamic methylation-demethylation processes that also may include the methylation of biotic stress proteins.

In this paper we report on qualitative and quantitative changes in the biotransformation steps of the formaldehyde cycle in different parts of the water-melon plant after nonlethal infection (biotic stress) with *Fusarium*.

In consequence of the infection identical quantitative changes, but to a different degree, of the compounds examined are observable in both varieties. The connections resulting from the depiction of the time-dependent quantitative changes of the measured methylated compounds due to infection show a picture similar to that of Selye's stress syndrome model.

**Keywords:** Biotic stress – methylation – demethylation – formaldehyde – quaternary ammonium compounds

### INTRODUCTION

According to the results of experiments conducted during the last few years, a detectable amount of formaldehyde (HCHO), using a special isolation procedure, can be found in biological systems [5, 12, 19]. This endogenous HCHO can originate from both methylation [6] and demethylation [7, 9] processes. Recently, the S-CH<sub>3</sub>-<sup>3</sup>H of S-adenosyl-L-methionine (SAM) in the course of the enzymatic conversion of histamine to N<sup>ε</sup>-methylhistamine in the presence of dimedone as a HCHO capture molecule suggested that the formation of HCHO is probably linked to the enzymatic

\* Presented at the 4th International Conference on the Role of Formaldehyde in Biological Systems, July 1-4, 1998, Budapest, Hungary.

Send offprint requests to: Dr. Éva Sárdi, Department of Genetics and Plant Breeding, University of Horticulture and Food Industry, H-1502 Budapest, P.O. Box 53, Hungary.



transmethylation of histamine [6]. It also follows from these results that the high level of HCHO and at the same time the accumulation of N-methylated substances during the early development stages and in rapidly dividing cells originate from intensive transmethylation reactions [22].

With regard to the production of endogenous HCHO, the important formation pathways are the demethylation reactions of different N-, S- and O-methylated compounds [3, 8]; these compounds can, therefore, be considered as potential precursors of HCHO.

A correlation exists between the external temperature and measurable amount of HCHO in Pinto bean leaf tissues. The level of some potential HCHO generators, such as choline, trigonelline and N<sup>ε</sup>-trimethyl-L-lysine (TML), moderately decreased with heat shock in comparison to normal room temperature. In the presence of dimedone the amount of these HCHO generators further decreased at all temperatures [21]. It can generally be said that naturally occurring quaternary ammonium compounds (choline, glycinebetaine, trigonelline etc.), which form a structurally heterogeneous class of compounds with the unifying character of a polar, often methylated ammonium head, are the potential metabolic components of stress tolerance [1].

There are also observations on the role of demethylation in biotic stress situations. The amount of HCHO increases considerably in virus infected tobacco leaves [18] until the appearance of lesions, thereupon, the level decreases to that of control leaves [17]. The higher level of HCHO is probably the result of enhanced enzymatic demethylation of L-methionine and SAM [2].

Trigonelline, the fully N-methylated derivative of nicotinic acid, and choline were accumulated in tomato plants with an increasing NO<sub>3</sub>-nitrogen supply (salt stress) [20]. It can generally be said that naturally occurring quaternary ammonium compounds are the potential metabolic components of the stress tolerance. Choline and glycine betaine in wheat germ extract stimulate *Fusarium gramineum in vitro* [16]. The increased resistance of tomato plants against *Fusarium* wilt, induced by a high NO<sub>3</sub>-nitrogen supply in the nutrient solution, is associated with an increased juvenility of the tissue [10].

A correlation exists between *Fusarium* tolerance of different water-melon varieties and the amount of HCHO and level of fully N-methylated compounds measurable in water-melon seeds [13].

Results of comparative examinations have shown a relationship between the level of HCHO and some quaternary ammonium compounds measured in leaf tissues of different snap bean genotypes and their natural disease resistance (to *Pseudomonas*) [12].

It follows from these new results that there is an analyzable amount of HCHO in different biological systems and that HCHO is not a side product, but a basic and indispensable substance of the biological processes. There is a HCHO cycle in biological systems, that is, the enzymatic methylation reactions take place through HCHO and at the same time all methyl groups are potential HCHO precursors. There exists a number of quick HCHO pathways through the methylol groups of different binding force [19, 22].

## MATERIALS AND METHODS

### *Plants and pathogen culture*

We have examined the effect of biotic stress on two varieties of water-melon plant (*Citrullus vulgaris* L); the *Fusarium*-tolerant Charleston and the sensitive Sugar Baby, which were cultivated in commercial compost in a greenhouse. The seeds were collected from field experiments (1993) according to the practice of the Department of Genetics and Plant Breeding (University of Horticulture and Food Industry).

The inoculum used for the infection had been produced by the multiplication (on potato dextrose culture medium) of *Fusarium* isolated from infected water-melon plants. The density of spore suspension was  $10^7$ – $10^8$  cell/cm<sup>3</sup>. Before infection, the soil was scratched with a sharp scalpel between the lines in order to injure the roots thus promoting the rapid introduction of the pathogen. The same procedure was applied to the control plants to secure identical conditions. The spore suspension of 30–30 cm<sup>3</sup> was applied to every furrow between the lines of plants. The control plants were treated with an equal volume of distilled water.

We observed the biochemical changes due to *Fusarium* infection by examining three groups of plants grown at different times but under identical conditions and treated in identical ways. Sampling took place 1, 3 and 6 hours after the infection on the same day and at 24 hour intervals after that. Each sample consisted of 15 plants or parts of these plants.

### *Synthesis of formaldemethone*

Formaldemethone, as an adduct of dimedone, was prepared for identification purposes by adding HCHO solutions (20 cm<sup>3</sup> of 40% solution) to a solution of dimedone (5 g) in hot ethanol (30 cm<sup>3</sup>) and water (5 cm<sup>3</sup>). The white precipitate which separated was filtered and recrystallised from aqueous ethanol, m.p. 191 °C [15].

All other chemicals and solvents used were of analytical grade and were purchased from REANAL Co. (Budapest, Hungary) and Merck Co. (Darmstadt, Germany).

### *Chemical preparation of plant samples*

The fresh parts of plants were frozen with liquid nitrogen, powdered and treated with dimedone solution (0.02% dimedone in methanol) (e.g. 0.25 g plant powder/0.7 cm<sup>3</sup> of dimedone solution). This suspension was centrifuged at 1500 g for 10 minutes at 4 °C. The clear supernatants were used for overpressured layer chromatographic (OPLC) examination [4] and, after dilution, for HPLC separations [11].



## EQUIPMENTS

*OPLC separations*

The separations were carried out with a CHROMPRES 25 OPLC chromatograph (Factory of Laboratory Instruments Co., Ltd., Budapest, Hungary). Densitograms were taken with a Shimadzu CS-930 scanner (Shimadzu Co., Kyoto, Japan). Samples were applied with a NANOMAT sample applicator (CAMAG Co., Muttenz, Switzerland).

The separations were carried out on OPLC silica gel 80 F 254 precoated chromatoplate using chloroform-methylenechloride (35 : 65, V/V) for formaldemethone determination and i-propanol-methanol-0.1M sodium acetate (20 : 3 : 30, V/V) for quaternary ammonium compounds. Calibration curves were made by means of authentic substances (at  $\lambda = 265$  nm for formaldemethone and at  $\lambda = 525$  nm for quaternary ammonium compounds using in this case Dragendorff reagent) [4].

*HPLC separation*

A Liquochrom Mode 2010 liquid chromatograph equipped with a UV 308 detector (Factory of Laboratory Instruments Co. Ltd., Budapest, Hungary), a OH-814 recorder (RADELKIS Co., Budapest, Hungary), Digint-180 Integrator (Servintern Co., Budapest, Hungary) and a 20  $\mu$ l loop were used.

Formaldemethone was eluted with methanol at a flow-rate of 0.7 cm<sup>3</sup>/min and with UV detection ( $\lambda = 260$  nm) using a BST Si-100-S-C-18 column (250 mm  $\times$  4 mm I.D., 10  $\mu$ m) (BioSeparation Technical Cooperative, Budapest, Hungary) [11].

## RESULTS

Table 1 displays the resistance to *Fusarium oxysporum* f. sp. *niveum* infections, known from cultivation experience, of the examined water-melon varieties.

Table 1

The resistance of varieties of water-melon plants to *Fusarium oxysporum* f. sp. *niveum* infections from cultivation experience

Water-melon varieties	The order of varieties on the basis of their resistance to <i>Fusarium</i>
<b>Charleston</b>	<b>Resistant</b>
Crimson	Resistant
Gömb FU-TO	Tolerant
Hevesi FU-TO	Tolerant
Szigetcsépi 51	Sensitive
<b>Sugar Baby</b>	<b>Sensitive</b>

The phases of Selye’s stress syndrome model are shown in Fig. 1 [14].

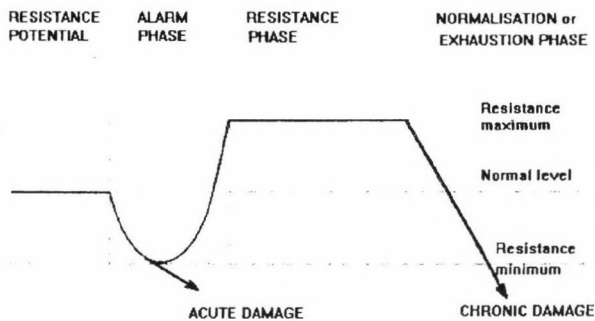


Fig. 1. The phases of Selye’s stress syndrome model

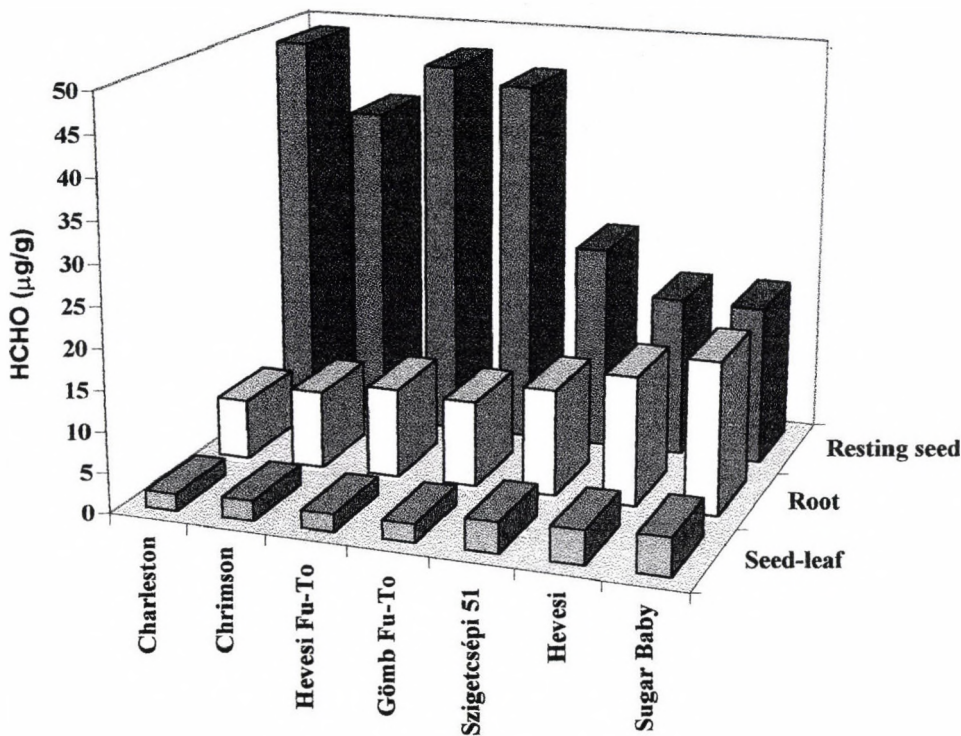


Fig. 2. Amount of HCHO in the parts of water-melon varieties with different resistance levels

Figure 2 demonstrates the amount of HCHO in the parts of water-melon varieties with different resistance levels. In the case of water-melon plants, first of all the higher concentration of N<sup>ε</sup>-trimethyl-L-lysine (TML) and choline is related to the resis-



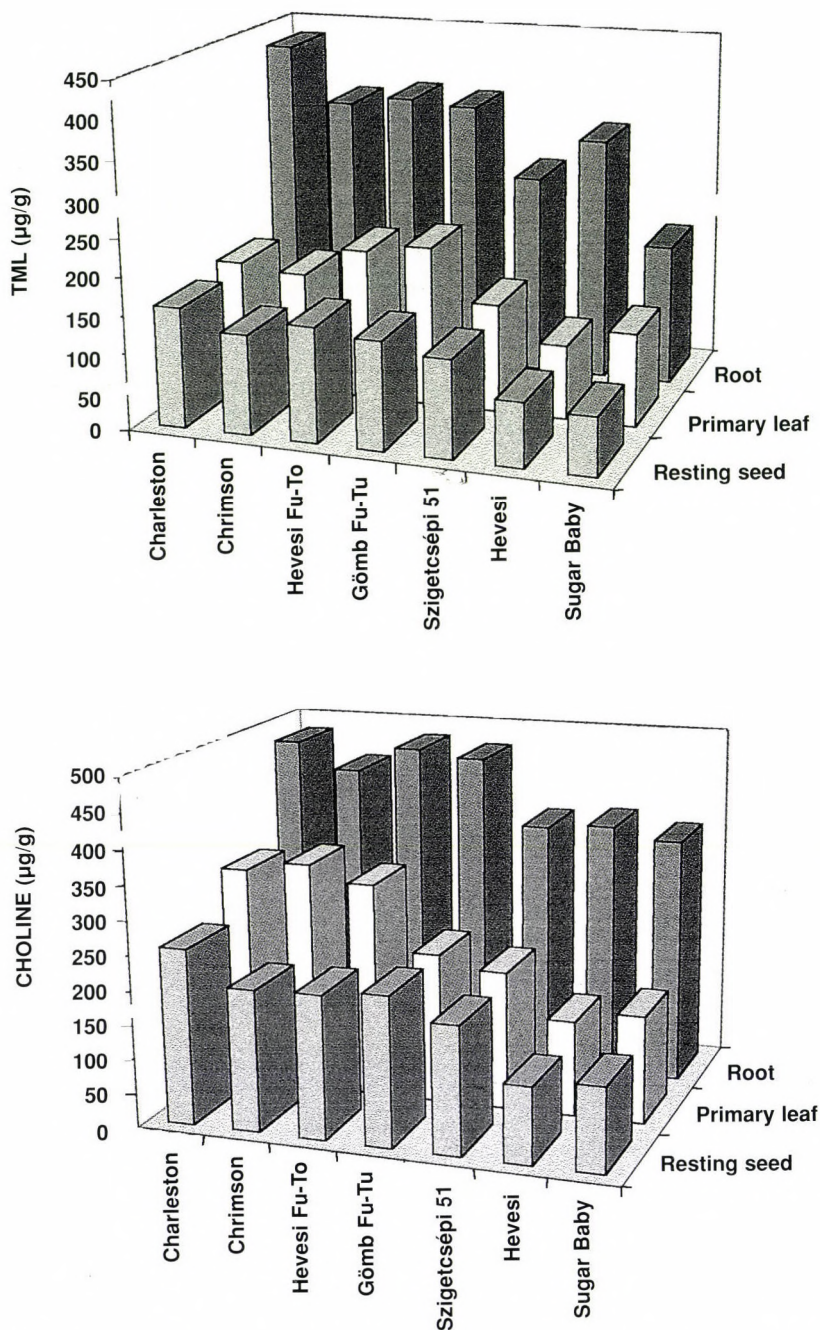


Fig. 3. Amount of TML and CHOLINE in the plant tissues of water-melon varieties of different resistance levels

tance against *Fusarium*. The relationships between the amount of the fully N-methylated compounds and the natural disease resistance (to *Fusarium oxysporum* f. sp. *niveum*) of the varieties are shown in the first place by the results of the examination of the root and the resting seeds (Fig. 3).

The effect of *Fusarium* infection, based on the results of the root examination of a sensitive water-melon variety (Sugar Baby) can be seen in Fig. 4.

Figure 5 shows the time-dependent concentration changes due to the infection of a resistant water-melon variety (Charleston).

Figures 4–5 show that an increased level of HCHO is measurable for both varieties and in all the examined plants parts as soon as 1 or 2 hours after the infection. The biggest increase can be observed in the roots, that is where the plant is attacked by the pathogen through the injured surface. After that, from a certain time (e.g. in the case of root from 24 h) the level of measurable HCHO was decreased.

The figures illustrate clearly that in parallel with the increase of HCHO the level of some fully N-methylated substances such as choline and TML is decreased in the aftermath of infection. It is obvious that this decrease of fully N-methylated (quaternary ammonium) substances belongs to the alarm phase of the stress syndrome.

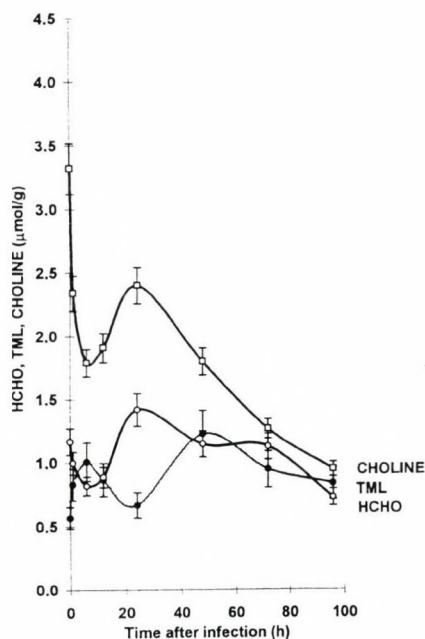


Fig. 4. Effect of *Fusarium* infection on the level of measured compounds in the root of a sensitive water-melon variety (Sugar Baby)

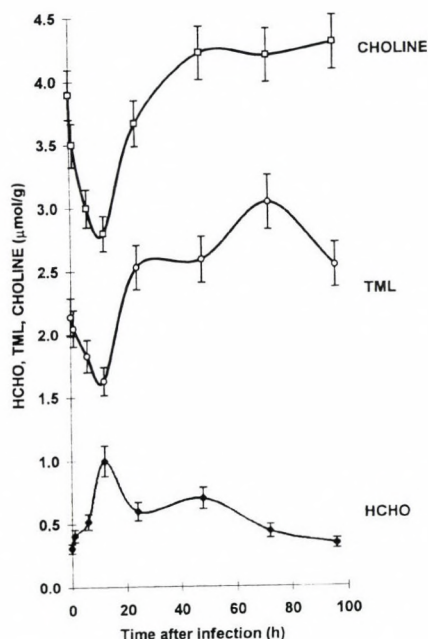


Fig. 5. Effect of *Fusarium* infection on the level of measured compounds in the root of a resistant water-melon variety (Charleston)



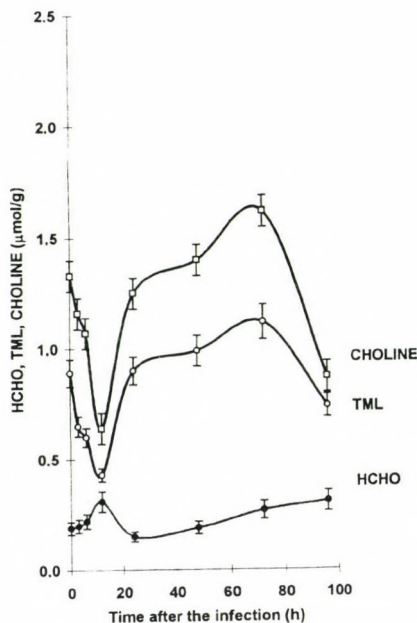


Fig. 6. Effect of *Fusarium* infection on the level of measured compounds in the stem of a sensitive water-melon variety (Sugar Baby)

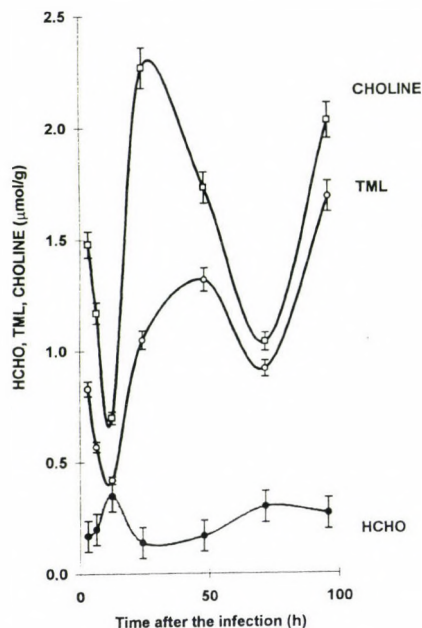


Fig. 7. Effect of *Fusarium* infection on the level of measured compounds in the stem of a resistant water-melon variety (Charleston)

From a certain time there is a significant increase in the fully N-methylated substances practically in all plant parts as the aftermath of the normalization process of the stress syndrome (Figs 4–5). The levels of HCHO measured on the 4th day after infection are higher than the original values for the root tissues of both examined varieties. However, there are differences between the varieties. After the normalization process (stabilization phase) the level of HCHO is similar to its original level in the *Fusarium*-tolerant variety, but it is higher in the *Fusarium*-sensitive variety. The levels of the TML and choline are higher in the tolerant variety and lower in the *Fusarium*-sensitive variety than the original values.

The effects of *Fusarium* infection, based on the results of the stem examination of a sensitive water-melon variety (Sugar Baby) can be seen in Fig. 6.

Figure 7 shows the time-dependent concentration changes due to the infection of a resistant water-melon variety (Charleston).

## DISCUSSION

We identified HCHO in dimedone adduct form by UV spectra and mass spectrometry in water-melon plant tissues. At that time we developed an efficient liquid chromatographic method (HPLC) for the measurement of HCHO in dimedone adduct form [11].

It is obvious that there is a given level of HCHO and fully N-methylated substances in the normal state of plants. The level of these molecules determines partly the resistance potential (natural disease resistance) of the plant tissues. Figure 3 illustrates that there is a relationship between the level of fully N-methylated compounds (as HCHO precursors) measured in young parts of plants and the natural disease resistance of the various varieties of water-melon. This relationship is especially attractive in the case of root and resting seed.

Comparison of the starting points of Figures 4–5 and 6–7 shows the differences between the *Fusarium*-resistant and -sensitive varieties: The resistant variety is characterized by a higher methylated level in the stressfree condition (homeostasis).

On the basis of the concentration of fully N-methylated compounds, it can be supported that the disease resistance of the resistant variety was increased, while the variety sensitive to fungus infection was not able to restore its original methylated level after the stabilization phase. That conclusion is further supported by the fact that the infected plants of the *Fusarium*-sensitive variety are totally destroyed within 2 or 3 weeks, while the resistant variety survives this period.

## CONCLUSIONS

1. Infection with *Fusarium* (biotic stress) decreased the amount of fully N-methylated compounds while the level of endogenous HCHO simultaneously was increased during the alarm phase of the stress syndrome.

2. The HCHO molecules originating from the methyl groups during the demethylation processes can take part in reactions which may cover the stress sensitive points (enzyme proteins, nucleic acids) of the biological system through methylation.

3. Comparing the concentrations measured in the normalization phase, we found a dramatic increase of level of fully N-methylated substances in the case of the resistant variety and a significant decrease in the case of the sensitive one.

4. On the basis of our experiments, it seems that the endogenous HCHO and certain fully N-methylated compounds generally play an important role during stress-reactions: varieties with a higher methylated level have a potentially higher resistance.

5. As a consequence, we can suppose that the formation mechanism of methyl-groups or the endogenous transmethylation processes are involved in the phases of the stress syndrome.



## REFERENCES

1. Anthoni, U., Christophersen, C., Hougaard, L., Nielsen, P. H. (1991) Quaternary ammonium compounds in the biosphere – an example of a versatile adaptive strategy. *Comp. Biochem. Physiol.* 99B, 1–8.
2. Burgyán, J., Szarvas, T., Tyihák, E. (1982) Increased formaldehyde production from L-methionine-(S-<sup>14</sup>CH<sub>3</sub>) by crude enzyme of TMV infected tobacco leaves. *Acta Phytopathol. Acad. Sci. Hung.* 17, 11–15.
3. Fannin, F. F., Bush, L. P. (1992) Nicotine demethylation in *Nicotiana*. *Med. Sci. Res.* 20, 867–868.
4. Gersbeck, N., Schönbeck, F., Tyihák, E. (1989) Measurement of formaldehyde and its main generators in *Erysiphe graminis* infected barley plants by planar chromatographic techniques. *J. Planar Chromatogr.* 2, 86–89.
5. Heck, H. d'A., Casanova-Schmitz, M. (1984) Biochemical toxicology of formaldehyde. *Rev. Biochem. Toxicol.* 6, 155–189.
6. Huszti, Z., Tyihák, E. (1986) Formation of formaldehyde from S-adenosyl-L-(methyl-<sup>3</sup>H) methionine during enzymatic transmethylation of histamine. *FEBS Letters* 209, 362–366.
7. Kawata, S., Sugiyama, T., Iami, J., Minami, Y., Tarui, S., Okamoto, M., Yamano, T. (1983) Hepatic microsomal cytochrome P-450 dependent N-demethylation of methylguanidine. *Biochem. Pharmacol.* 32, 3723–3728.
8. Kedderis, G. L., Hollenberg, P. F. (1984) Peroxidase-catalyzed N-demethylation reactions. *J. Biol. Chem.* 259, 3663–3668.
9. Paik, W. K., Kim, S. (1980) *Protein Methylation*. Wiley and Sons, New York, 132–136.
10. Sarhan, A. R. T., Barna, B., Király, Z. (1982) Effect of nitrogen nutrition on *Fusarium* wilt of tomato plants. *Ann. Appl. Biol.* 101, 245–250.
11. Sárdi, É., Tyihák, E. (1994) Simple determination of formaldehyde in dimedone adduct form in biological samples by high performance liquid chromatography. *Biomed Chromatogr.* 8, 313–314.
12. Sárdi, É., Tyihák, E., Velich, I. (1994) Occurrence of endogenous formaldehyde and its main potential generators in the leaves of snap beans (*Phaseolus vulgaris* L.). *Annual Rep. Bean Impr. Coop. Fort Collins USA.* 38, 101–102.
13. Sárdi, É., Tyihák, E. (1995) Measurement of formaldehyde and its main potential generators in the seeds of water-melon (*Citrullus vulgaris* L.) varieties and F1 hybrids of different *Fusarium* sensitivity. *Hort. Sci. Hung.* 27, 66–70.
14. Selye, J. (1964) *Életünk és a stressz*. (Our life and the stress) Akadémiai Kiadó, Budapest.
15. Spencer, D., Henshall, T. (1955) The kinetics and mechanisms of the reaction of formaldehyde with dimedone (Part I). *J. Am. Chem. Soc.* 77, 1943–1948.
16. Strange, R. N., Mayer, J. R., Smith, H. (1974) The isolation and identification of choline and betaine as the two major components in anthers and wheat germ that stimulate *Fusarium graminearum* in vitro. *Physiol. Plant Path.* 4, 277–290.
17. Szarvas, T., János, É., Gáborjányi, R., Tyihák, E. (1982) Increased formaldehyde formation: an early event of TMV infection in hypersensitive host. *Acta Phytopathol. Acad. Sci. Hung.* 17, 7–10.
18. Tyihák, E., Balla, J., Gáborjányi, R., Balázs, E. (1978) Increased free formaldehyde level in crude extract of virus infected hypersensitive tobaccos. *Acta Phytopathol. Acad. Sci. Hung.* 13, 29–31.
19. Tyihák, E. (1987) Is there a formaldehyde cycle in biological systems? In: Tyihák, E., Gullner, G. (eds) *Proc. 2nd Intern. Conf. on the Role of Formaldehyde in Biological Systems*. Keszthely, Hungary, SOTE Press. Budapest, pp. 137–144.
20. Tyihák, E., Sarhan, A. R. T., Cong, N. T., Barna, B., Király, Z. (1988) The level of trigonelline and other quaternary ammonium compounds in tomato leaves in vitro to the changing nitrogen supply. *Plant and Soil* 109, 285–287.
21. Tyihák, E., Király, Z., Gullner, G., Szarvas, T. (1989) Temperature-dependent formaldehyde metabolism in bean plants. The heat shock response. *Plant. Sci.* 59, 133–139.
22. Tyihák, E., Rozsnyay, Zs., Sárdi, É., Szőke, É. (1992) Formaldehyde cycle and the cell proliferation. Plant Tissue as a Model. In: Tyihák, E. (ed.) *Proc. 3rd Intern. Conf. on the Role of Formaldehyde in Biological Systems*, Sopron, Hung. Biochem. Soc., Budapest, pp. 139–144.

## THE EFFECT OF HEAT SHOCK ON THE FORMALDEHYDE CYCLE IN GERMINATING ACORNS OF EUROPEAN TURKEY OAK\*

L. ALBERT,<sup>1</sup> ZS. I. NÉMETH<sup>1</sup> and SZ. VARGA<sup>2</sup>

<sup>1</sup>Institute for Chemistry and

<sup>2</sup>Department of Silviculture, University of Sopron, Hungary

(Received: 1998-10-28; accepted: 1998-11-25)

The effect of heat shock (40 °C) on the formaldehyde cycle has been studied in European Turkey oak (*Quercus cerris* L.) acorns germinated to a 10% increase in mass. Hydroxy-methyl groups bonded to sulfur, oxygen and nitrogen atoms were made to react with dimedone and the derivative obtained (formaldehyde-methone), which represented the endogenous formaldehyde level, was determined by high performance liquid chromatography. Qualitative alterations of methyl donors and acceptors in the response of acorns to the heat shock have been mapped by MALDI (matrix assisted laser desorption-ionization) mass analysis. In the first experiment the acorns were prevented from withering by wrapping them in aluminium foil and in the second they were not. The relatively high temperature of the acorns wrapped in aluminium foil was the dominant stress effect and the role of withering was subsidiary. Alteration of the endogenous formaldehyde level in the seed-leaves reflected the phases of the stress syndrome. If the withering were not hindered, two local minima in the alteration of endogenous formaldehyde level were found. First, the increase in temperature decreased the endogenous formaldehyde level and after a local maximum a repeated local minimum was observed as a delayed response. It is presumed that the second minimum was induced by the decreasing water amount becoming more and more significant in the seed-leaves.

**Keywords:** Formaldehyde – formaldehyde-methone – high performance liquid chromatography – matrix assisted laser desorption/ionization mass spectrometry – heat stress – *Quercus cerris* L.

### INTRODUCTION

Of the forest areas in Hungary 33.3% are oakenshaws. The European Turkey oak (*Quercus cerris* L.) accounts for 11.3% of the oak forests since it has a wide ecological niche [4]. The oak-trees having economic significance (pedunculate oak, robur oak, etc.) periodically bear acorns every 2nd to 5th year. Thus, it is an important task to store the acorns without damaging their quality for growing seedlings as well as for forest regeneration between two crops. The classification of the stored acorns demands the development of methods which can supply some information about

\* Presented at the 4th International Conference on the Role of Formaldehyde in Biological Systems, July 1–4, 1998, Budapest, Hungary.

Send offprint requests to: Dr. L. Albert, Institute for Chemistry, University of Sopron, H-9400 Sopron, P.O. Box 132, Hungary.



their biological condition. We have investigated endogenous formaldehyde and its generators as marker compounds for the biological characterization of the stored and germinating acorns [1]. It has been established that these substances (for example: formaldehyde, methylated compounds) reflect the developmental stages and the characteristic periods of the response given to cold shock [2]. In this work the quantitative alteration of marker compounds playing a key role in heat shock was studied.

## MATERIALS AND METHODS

Fresh acorns of European Turkey oak (*Quercus cerris* L.) were gathered from Hungarian trees (Vitnyéd, Hungary).

After removing the shells of the acorns the seeds, with about 1.27 g/cm<sup>3</sup> density and no mould growth were picked out for germination. A hundred seeds were half buried in a bed of wet sterile perlite (P2 perlite, Baumit Ltd., Hungary). The masses and densities of the imbibing seeds were measured each day. Seeds with approximately the same density showing about a 10% increase in mass were selected and divided into two groups. Two experiments were carried out. In one of them the acorns were wrapped in aluminum foil and in the other not. The acorns with and without aluminum foil were put into a drying chamber at 40 °C. After storing the seeds for different times the seedleaves of the acorns were broken into small pieces in the presence of liquid nitrogen. The 0.25 g masses of powdered seedleaves were suspended in 0.7 cm<sup>3</sup> methanol containing dimedone in 0.01% concentration. The suspensions were stored at 22 °C at atmospheric pressure for seven days. The determination of the endogenous formaldehyde level was based on the separation of the derivative compound (formaldemethone) originating from the reaction between dimedone and hydroxy-methyl groups bound to O-, S- and N- atoms [5]. For the chromatographic separation by HPLC and the MALDI analysis the concentrated methanolic extracts were diluted with methanol in a ratio 1 : 11.

After dilution with methanol, the supernatant (0.5 µl) was mixed with 0.5 µl α-cyano-4-hydroxy cinnamic acid (ACH) matrix (2 mg/cm<sup>3</sup> in 60% methanol/40% water) directly on the disposable sample slide. The droplet was allowed to dry naturally for MALDI MS analysis. Preparing a sample of the authentic formaldemethone was carried out by described earlier, but the diluted supernatant was substituted for the standard solution ( $2 \cdot 10^{-5}$  M).

### Chemicals

The solvents for the separation by HPLC were obtained from Merck Chemical Co. (Germany) and Reanal Chemical Co. (Hungary). The matrix material, α-cyano-4-hydroxy cinnamic acid (ACH) for the MALDI analysis and the methyl donor and acceptor compounds (trigonelline, γ-amino-butyric acid betaine and γ-amino-butyric

acid) were bought from Sigma Chemical Co. (USA). Formaldemethone (1,1',3,3'-tetraketo-5,5,5',5'-tetramethyl-2,2'-dicyclohexylmethane) was prepared for identification purposes by adding formaldehyde solution (20 ml of 38% solution) to a solution of dimedone (5 g) in hot ethanol (30 ml) and water (5 ml). The white precipitate was filtered and recrystallized from aqueous ethanol, m.p. 191 °C [3]. The suspension was centrifuged at 1000 g for 10 minutes at 20 °C. The clear supernatants were used for MALDI analysis, as well as for HPLC separation.

### Equipment

The mass spectrometer used in this work was a Finnigan LASERMAT 2000 (Finnigan MAT Ltd., Hemel Hempstead, UK). The HPLC equipment consisted of a Gynkotek M 480 pump, a TOSOH 6040 UV detector (260 nm), and a Rheodyne 8125 injector with a 20 µl loop. The column used was a ChromSpher C-18 (150 × 4.6 mm; 5 µm). The chromatograms were recorded through an EF 2102 ADDA converter (Elektroflex GM, Szeged, Hungary) by a personal computer. The applied mobile phase was methanol – 0.01 M HCl (76 : 24, v/v; pH = 2.63) [1].

## RESULTS

The endogenous formaldehyde levels versus the duration of the heat effect (40 °C) are depicted in Fig. 1 in the case of acorns without their shells as well as for acorns peeled and wrapped in aluminum foil.

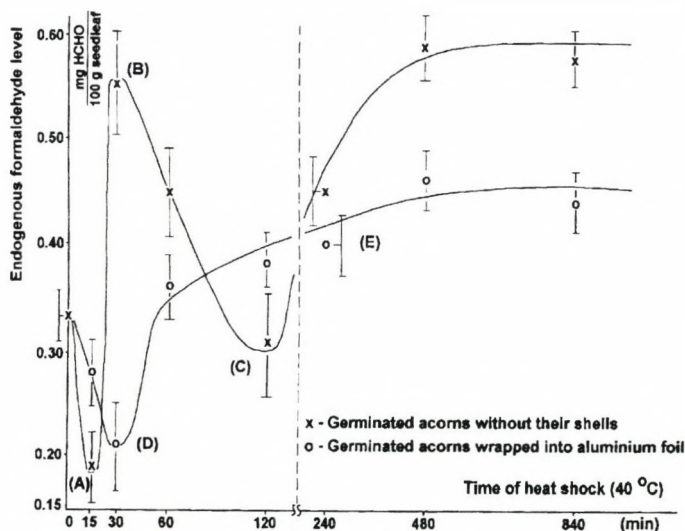


Fig. 1. The alteration of endogenous formaldehyde level in germinated acorns during the heat shock



The results of the two investigated groups differ from each other. The endogenous formaldehyde level of wrapped acorns shows only one minimum (D) while the second has two local minima (A, C). There is also a considerable difference in the formaldehyde contents of the resistance range. The MALDI spectra in Fig. 2, belong-

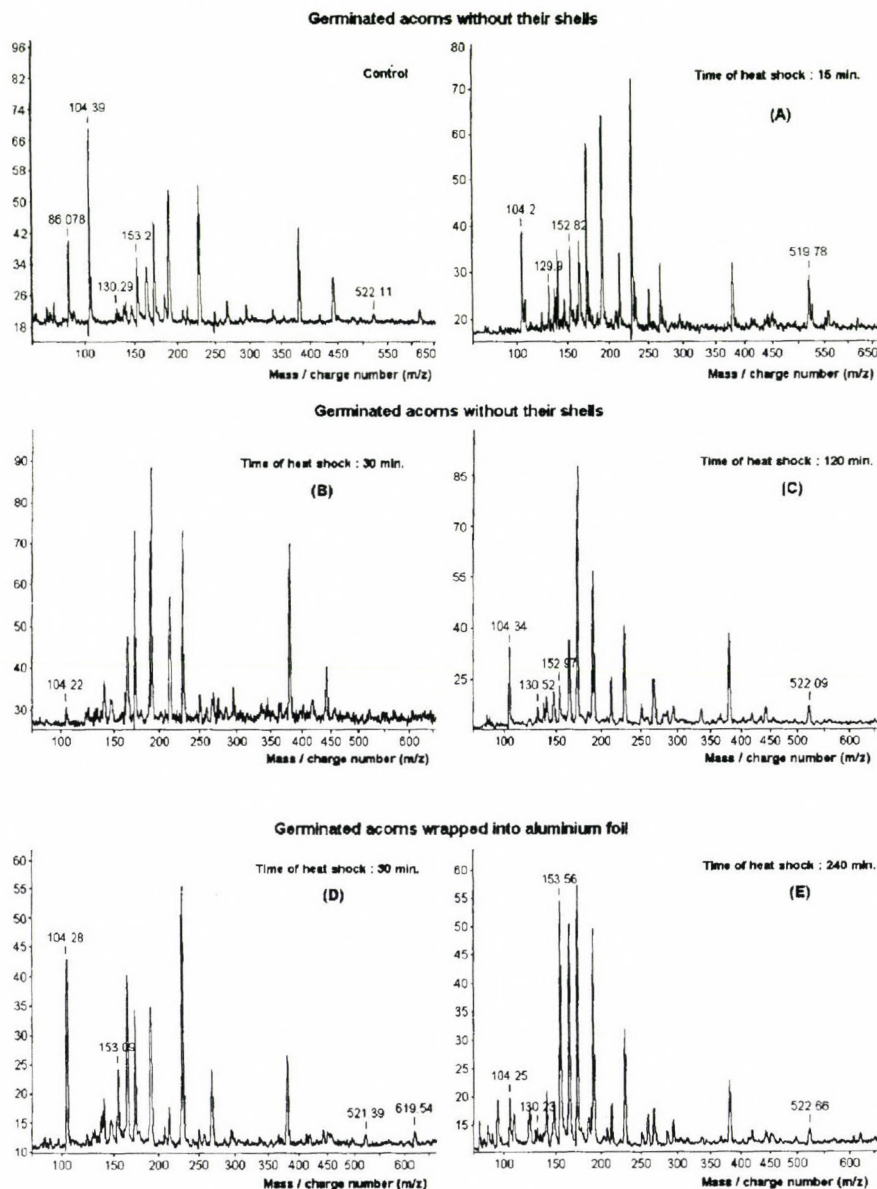


Fig. 2. MALDI spectra of the extracts from germinated acorns exposed to the heat shock

ing to the characteristic stages of the heat shock response, indicate various compounds extracted from acorn seedleaves in the small molecular mass range (0–650 D).

It can be seen that there are significant differences in the signal intensities and constituents of the spectra. Among the signals the one at  $m/z$  104 (molecular mass/charge number value), which can be found in all spectra, derives from  $\gamma$ -amino-butyric acid. The signal unidentified up till now at  $m/z$  86 appears in the control state but not in the other spectra. This was also experienced in the cold shock investigation in one of our earlier works [2].

The other signals in the spectra are also unidentified and alterations and relations among them have not yet been found.

## DISCUSSION

Germinated acorns without their shells respond to heat shock by an alarm phase having two local minima (A–C) and nearly double the amount of endogenous formaldehyde in the resistance range than that of the control acorns. After removing the acorn shells and soaking, some acorns were wrapped in aluminum foil so as to model the role of the shell in stress condition. The heat shock responses of the wrapped acorns and the ones without shells are different from each other. The wrapped acorns is characterized by only one local minimum (D) and, although, they have also a higher endogenous formaldehyde level than the control ones, their values are lower than those of the acorns without shells.

When shells are removed it is supposed that the two local minima are the result of increasing the temperature and, afterwards, the withering which becomes more and more significant during the stress effect.

The heat shock response shown in the endogenous formaldehyde level is reflected also in the MALDI spectra.

The signal intensities of MALDI spectra belonging to the various stress phases differ from each other significantly. The compound ( $m/z$  86), which has not been identified yet and which is present in the germinating acorns, disappears after the heat shock. A high amount of  $\gamma$ -amino-butyric acid ( $m/z$  104) is associated with low endogenous formaldehyde levels (A–C–D) while high formaldehyde levels involve small  $\gamma$ -amino-butyric acid signals (B–E).

## ACKNOWLEDGEMENT

This work was supported by a grant from the National Forest Service of Hungary, Kecskemét, Hungary.



## REFERENCES

1. Albert, L., Németh, Zs. I., Barna, T., Varga, Sz., Tyihák, E. (1998) Measurement of endogenous formaldehyde in the early developmental stages of European Turkey oak (*Quercus cerris* L.). *Phytochem. Anal.* 9, 227–231.
2. Németh, Zs. I., Albert, L., Varga, Sz. (1998) Changes in formaldehyde contents of germinating acorns of *Quercus cerris* L. under low temperature stress conditions. *Acta Biologica Hungarica* 49, 369–374.
3. Spencer, D., Henshall, T. (1955) The kinetics and mechanism of the reaction of formaldehyde with dimedone. Part 1. *J. Am. Chem. Soc.* 77, 1943–1948.
4. Szabó, P., Csóka, P., Czirok, I., Fejes, L., Jancsó, Gy., Madas, K., Szepesi, A. (1997) *Magyarország erdőállományainak főbb adatai 1996*. Állami Erdészeti Szolgálat, Budapest.
5. Tyihák, E., Blunden, G., Yang, M., Crabb, T. A., Sárdi, É. (1996) Formaldehyde, as its dimedone adduct, from *Ascophyllum nodosum*. *J. Applied Phycology* 8, 211–215.

# CHANGES IN FORMALDEHYDE CONTENTS OF GERMINATING ACORNS OF *QUERCUS CERRIS* L. UNDER LOW TEMPERATURE STRESS CONDITIONS\*

ZS. I. NÉMETH,<sup>1</sup> L. ALBERT<sup>1</sup> and SZ. VARGA<sup>2</sup>

<sup>1</sup>Institute for Chemistry and

<sup>2</sup>Department of Silviculture, University of Sopron, Hungary

(Received: 1998-10-28; accepted: 1998-11-25)

Acorns of *Quercus cerris* L., after saturation with water and storage at -20 °C, were studied for changes in their contents of endogenous formaldehyde and its potential precursor and generator compounds. For the measurement of formaldehyde, after conversion to formaldemethone and some methyl acceptor and donor substances, high performance liquid chromatography (HPLC) were used. First, the amount of formaldehyde was drastically decreased. Having reached a minimum value within three to five days of the beginning of low temperature storage, a higher steady-state than the control acorns was recorded.

Trigonelline and  $\gamma$ -amino-butyric acid in seedleaf extracts were identified by matrix assisted laser desorption-ionization mass spectrometry (MALDI-MS).

**Keywords:** Formaldehyde – formaldemethone – high performance liquid chromatography – matrix assisted laser desorption/ionization mass spectrometry – *Quercus cerris* L.

## INTRODUCTION

Methyl groups linked to O-, S- and N-atoms, after oxidation into hydroxy-methyl groups, are involved via formaldehyde, in enzymatic transmethylation of S-adenosyl-L-methionine (SAM) [4, 5, 9]. The rate of these transformations is significantly altered when environmental conditions alter. Such changes can be attributed to stress in both animal and plant species.

The endogenous formaldehyde level in virus-infected tobacco leaves (biotic stress) has been shown to increase considerably [7]. The extract from tobacco leaves in the early stage of the infection in the presence of L-methionine and SAM indicated increased demethylase activity [2].

A strong correlation also exists between external temperatures and the amount of measurable formaldehyde in Pinto bean leaf tissues [8]. Moreover, high levels were detected after heat shock treatment of the leaves, which led to the levels of three

\* Presented at the 4th International Conference on the Role of Formaldehyde in Biological Systems, July 1-4, 1998, Budapest, Hungary.

Send offprint requests to: Dr. Zs. I. Németh, Institute for Chemistry, University of Sopron, H-9400, Sopron, P.O. Box 132, Hungary.



potential formaldehyde generators (trigonelline, choline and laminine) being decreased moderately. The higher activities of demethylase at elevated temperatures, including heat shock, is the cause of higher amounts of formaldehyde being detected (abiotic stress) [3].

On the basis of the citations mentioned above it was assumed that the formaldehyde cycle of germinating acorns from the European Turkey oak (*Quercus cerris* L.) would show sensitive responses to stress effects.

Based on knowledge of the formaldehyde levels of European Turkey oak seedlings in their early stages of development [1], we have studied the changes in the formaldehyde contents of the seedleaves after the acorns had absorbed water to about 10% of their original mass and exposure to a temperature of  $-20^{\circ}\text{C}$ . These changes have been tracked by HPLC and both the methyl donor and acceptor compounds associated with the cold shock have been mapped by MALDI-MS.

## MATERIALS AND METHODS

Fresh acorns of the European Turkey oak were gathered from Hungarian trees (Vitnyéd, Hungary).

After removing the shells, seeds with a density of about  $1.27\text{ g/cm}^3$  and shown no signs of fungal attack were picked out for germination. A hundred seeds, standing upwards, were planted into a wet, sterile perlite (P2 perlite, Baumit Ltd., Hungary) bed as far as their half volumes. The masses and densities of the planted seeds were measured daily. Seeds of similar density, showing an increase in weight of about 10%, were wrapped in aluminum foil and put into a refrigerator set at  $-20^{\circ}\text{C}$ . After storing the seeds for different times, the seedleaves were powdered in liquid nitrogen. The powder (0.25 g) was suspended in  $0.7\text{ cm}^3$  of 0.01% dimedone solution in methanol and stored at  $22^{\circ}\text{C}$  at atmospheric pressure for seven days. Determination of the endogenous formaldehyde level was based on the separation of the derivative compound (formaldemethone) originating from the reaction between dimedone and hydroxy-methyl groups bound to O-, S- and N- atoms [10]. For HPLC separation and MALDI-MS analysis the concentrated methanolic extracts were diluted with methanol (1 : 11).

After dilution the supernatant ( $0.5\text{ }\mu\text{l}$ ) was mixed with  $0.5\text{ }\mu\text{l}$   $\alpha$ -cyano-4-hydroxy cinnamic acid (ACH) matrix ( $2\text{ mg/cm}^3$  in 60% methanol/40% water) directly on the disposable sample slide. The droplet was allowed to dry naturally for MALDI MS analysis.

### Chemicals

The HPLC solvents were obtained from Merck Chemical Co. (Germany) and Reanal Chemical Co. (Hungary). The matrix material,  $\alpha$ -cyano-4-hydroxy cinnamic acid (ACH) for the MALDI analysis and the methyl donor and acceptor compounds

(trigonelline,  $\gamma$ -amino-butyric acid) were bought from Sigma Chemical Co. (USA). Formaldemethone (1,1',3,3'-tetraketo-5,5,5',5'-tetramethyl-2,2'-dicyclohexylmethane) for identification purposes, was prepared by adding formaldehyde solution (20 ml of 38% solution) to a solution of dimedone (5 g) in hot ethanol (30 ml) and water (5 ml). The white precipitate was filtered and recrystallized from aqueous ethanol, m.p. 191 °C [6]. The suspension was centrifugated at 1000 g for 10 minutes at 20 °C. The clear supernatants were used for MALDI analysis, as well as for HPLC separation.

## EQUIPMENT

The mass spectrometer used was a Finnigan LASERMAT 2000 (Finnigan MAT Ltd., Hemel Hempstead, UK). The HPLC equipment consisted of a Gynkotek M 480 pump, a TOSOH 6040 UV detector (260 nm), a Rheodyne 8125 injector with a 20  $\mu$ l loop. The column used was ChromSpher C-18 (150  $\times$  4.6 mm; 5  $\mu$ m). The chromatograms were recorded through an EF 2102 ADDA converter (Elektroflex GM, Szeged, Hungary) by a personal computer. The applied mobile phase was methanol – 0.01 M HCl (76 : 24, v/v; pH = 2.63).

## RESULTS

For determination of endogenous formaldehyde levels of seedleaf extracts, the chromatogram of a typical separation is shown in Fig. 1. The chromatogram depicted with the peak of authentic formaldemethone indicates that the formaldemethone sig-

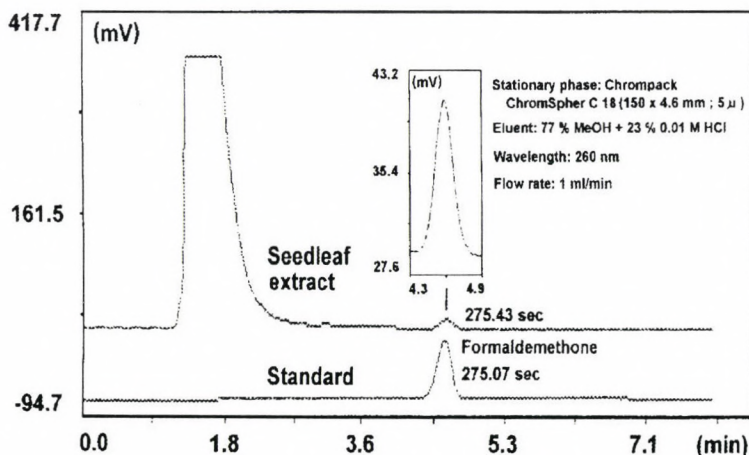


Fig. 1. A typical HPLC chromatogram of seedleaf extracts



nal in the sample appears as a single peak without overlapping. This made the reproduction of serial separations possible.

The endogenous formaldehyde contents, with their confidence intervals ( $P = 0.05$ ), of the seedleaves stored for different times at  $-20\text{ }^{\circ}\text{C}$  are depicted in Fig. 2. The amount of formaldehyde was drastically decreased for the first three hours. However, having reached a minimum value within three to five days of the beginning of low temperature storage, a higher steady-state than the control acorns was recorded.

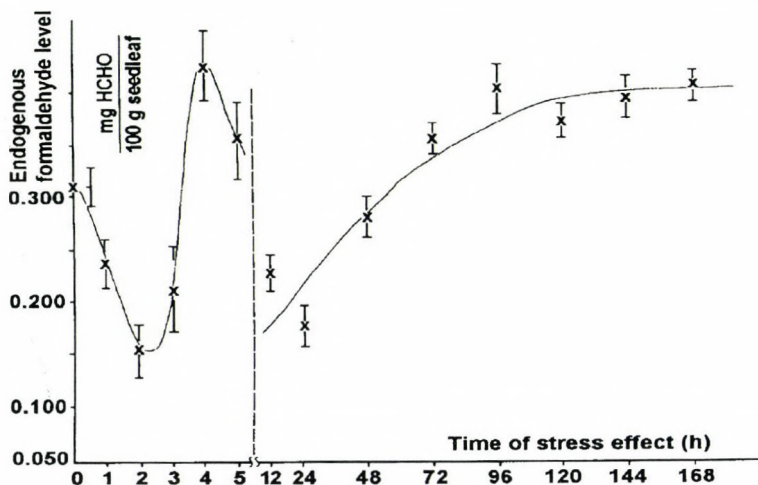


Fig. 2. The alteration of endogenous formaldehyde in germinating acorns stored at low temperature ( $-20\text{ }^{\circ}\text{C}$ )

The MALDI spectra of the extracts of frozen acorns exhibited significant differences between the control and alarm phases. The spectra of the resistance range have been shown to be very similar to those of the alarm phase.

$\gamma$ -amino-butyric acid, identified as a methyl acceptor compound, and trigonelline as a methyl donor, were present in all samples. The intensities of their signals did not differ significantly from each other.

The MALDI spectra of control and alarm phases can be seen in Fig. 3. The spectrum belonging to the control state contains two characteristic peaks at  $m/z$  86 and 153 which are absent from the spectrum of the seedleaves subjected to cold shock. However, the latter contains a signal, of high intensity, at  $m/z$  130. The identification of these three substances is progress. It is hypothesised that the compound at  $m/z$  86 is a methyl acceptor substance whose methylated and hydroxyl-methylated derivatives are responsible for the compound with  $m/z$  130. If this supposition was successfully proved then it would show that the acorns can respond to cold shock by methylating compounds with a small molecule mass.

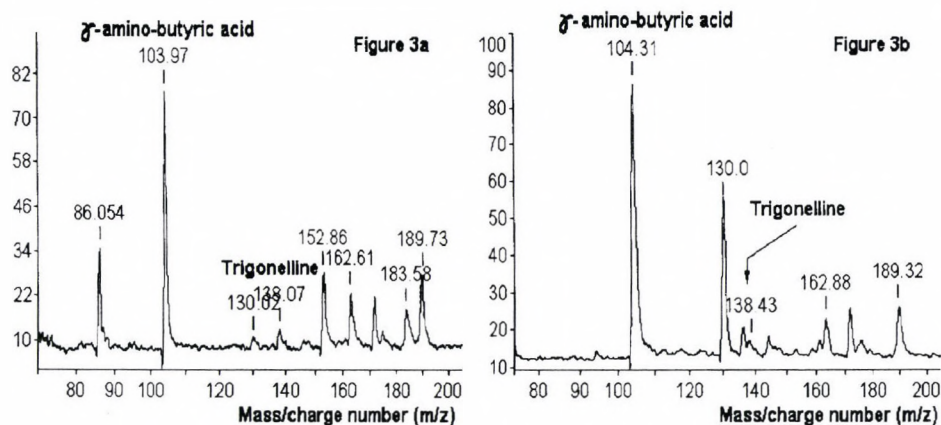


Fig. 3. The MALDI spectra of germinating acorns under control and cold shock conditions. (3a – control; 3b – alarm phase, time of stress effect: two hours)

## DISCUSSION

The formaldehyde cycle in seedleaf tissue of germinating acorns can react to low-temperature stress in a short time. The change in formaldehyde content after cold shock follows the phases of the stress syndrome. It is possible to infer that the alteration of resistance potential from the measured values belongs to the stress phases. It has been shown that MALDI analysis can give a comprehensive picture of small molecular weight compounds and that this analytical technique is of value in showing changes brought about by stress.

## ACKNOWLEDGEMENT

This work was supported by a grant from the National Forest Service of Hungary, Kecske-mét, Hungary.

## REFERENCES

1. Albert, L., Németh, Zs. I., Barna, T., Varga, Sz., Tyihák, E. (1998) Measurement of endogenous formaldehyde in the early developmental stages of European Turkey oak (*Quercus cerris* L.). *Phytochem. Anal.* 9, 227–231.
2. Burgyán, J., Szarvas, T., Tyihák, E. (1982) Increased formaldehyde production from L-methionine (S-<sup>14</sup>CH<sub>3</sub>) by crude enzyme of TMV infected tobacco leaves. *Acta Phytopathol. Acad. Sci. Hung.* 17, 11–15.
3. Gullner, G., Tyihák, E. (1987) Hydrogen peroxide dependent N-demethylase activity in the leaves of normal and heat-shocked bean plants. *Plant. Sci.* 52, 21–27.
4. Huszti, Z., Tyihák, E. (1986) Formation of formaldehyde from S-adenosyl-L-(methyl-<sup>3</sup>H)methionine during enzymatic transmethylation of histamine. *FEBS Letters* 209, 362–336.



5. Kedderis, G. L., Hollenberg, P. F. (1983) Peroxidase-catalysed N-demethylation reactions. *J. biol. Chem.* 259, 663–668.
6. Spencer, D., Henshall, T. (1955) The kinetics and mechanism of the reaction of formaldehyde with dimedone. Part 1. *J. Am. Chem. Soc.* 77, 1943–1948.
7. Tyihák, E., Balla, J., Gáborjányi, R., Balázs, E. (1978) Increased free formaldehyde level in crude extract of virus infected hypersensitive tobaccos. *Acta Phytopathol. Acad. Sci. Hung.* 13, 29–31.
8. Tyihák, E., Király, Z., Gullner, G., Szarvas, T. (1989) Temperature-dependent formaldehyde metabolism in bean plants. The heat shock response. *Plant. Sci.* 59, 138–139.
9. Tyihák, E., Rozsnyai, Z., Sárdi, É., Szőke, É. (1992) Formaldehyde cycle and the cell proliferation: Plant tissue as a model. In: Tyihák, E. (ed.) *Proc. 3rd Intern. Conf. on the Role of Formaldehyde in Biological Systems*. Hungarian Biochem. Soc., Budapest.
10. Tyihák, E., Blunden, G., Yang, M., Crabb, T. A., Sárdi, É. (1996) Formaldehyde, as its dimedone adduct, from *Ascomyllum nodosum*. *J. Applied Phycology*. 8, 211–215.

## ALTERATION OF ENDOGENOUS FORMALDEHYDE LEVEL FOLLOWING MERCURY ACCUMULATION IN DIFFERENT PIG TISSUES\*

T. RÉTFALVI,<sup>1</sup> Zs. I. NÉMETH,<sup>2</sup> I. SARUDI<sup>1</sup> and L. ALBERT<sup>2</sup>

<sup>1</sup>Department of Chemistry and Biochemistry, Pannon Agricultural University Faculty of Animal Science, Kaposvár, Hungary

<sup>2</sup>Institute for Chemistry, University of Sopron, Sopron, Hungary

(Received: 1998-10-28; accepted: 1998-11-25)

The effect of mercury accumulation on the formaldehyde cycle of different pig tissues resulted by a single dose of mercury (0.4 mg mercury in Hg(II)-chloride form, 500 kBq Hg-203/animal) has been studied. Daily mercury excretion was tracked, and having reached the steady-state mercury level of the body (10th day), samples were taken from the liver, kidney and muscle (*musculus longissimus dorsi*). After reaction with dimedone the endogenous formaldehyde levels in the samples were measured by high performance liquid chromatography.

Our results show that the endogenous formaldehyde level decreased by more than 50% in the liver and the kidney, where the average mercury accumulation was the highest (1017 Bq/100 g and 625 Bq/100 g, respectively). In contrast, the muscle tissues, with a low mercury level (139 Bq/100 g), responded to the stress effect by about a 30% increase in their endogenous formaldehyde level.

**Keywords:** Mercury accumulation – formaldehyde – stress – pig

### INTRODUCTION

The mercury level of feed supplements (e.g. fish meal) used in pig feed can reach 2 mg/kg [3], part of which accumulates in the organs of the animals. The amount accumulated varies from 0.01 to 0.1 mg/kg, depending on the organ [7].

It is well known that mercury forms coordination complexes with compounds, including those with sulphur atoms [5], and thus changes their biological activities. A number of compounds containing sulphur take part in the formaldehyde cycle of cells. Of these compounds S-adenosyl-L-methionine (SAM) has a key role in transmethylation [2]. The mercury attached to thiol groups (-SH) can decrease the amount of methyl acceptor compounds, which will influence both the intensity and the direction of methylation-demethylation processes.

\* Presented at the 4th International Conference on the Role of Formaldehyde in Biological Systems, July 1–4, 1998, Budapest, Hungary.

Send offprint requests to: Dr. T. Rétfalvi, Department of Chemistry and Biochemistry, Pannon Agricultural University Faculty of Animal Science, H-7400, Kaposvár, P.O. Box 16, Hungary.



The effect on the formaldehyde cycles of various organs has been studied resulting from the addition of a single dose of mercury.

For the optimalization of the single mercury dose, two aspects were taken into consideration. The first was not to overdose the animals. The tolerable weekly rate for mercury intake for humans set by the WHO is 0.3 mg. On the other hand, the dose given had to lead to a significant increase in the mercury content of the tissues. As a result, the dose chosen was 0.4 mg mercury.

For establishing the additionally accumulated amount of mercury excretional investigations were carried out and alterations in endogenous formaldehyde levels in some tissues were studied. The additional accumulated mercury was tracked using a radiometric analytical technique which was sensitive to the mercury intake, excretion and additional accumulation.

Endogenous formaldehyde levels in different tissues were measured as the derivative compound, formaldemethone, which originates from the reaction of dimedone with hydroxy-methyl groups bound to O-, N- and S-atoms [6]. The separation of formaldemethone from extracts of pig tissues was achieved by high performance liquid chromatography (HPLC) [1].

## MATERIAL AND METHODS

The experiment was carried out on 6 male Hungarian Large White  $\times$  Pietrain pigs (16–18 kg body weight). The animals were housed in cages with variable basic areas which made it possible to collect separately faeces and urine. The animals were fed *ad libitum* with MT-10 standard diet produced by Dél-Dunántúli Grain Co. (Pécs, Hungary) and consumed common tap water *ad libitum*. The animals were divided into two groups each of three animals. After a three day acclimatization period, the control (Group I) and trial groups (Group II) consumed 0 and 500 kBq activity (0.4 mg of mercury content) contaminating substance, respectively, in one dose. The contaminating substance was mercury(II)-chloride labelled with  $^{203}\text{Hg}$  isotope (half-life:  $T_{1/2} = 46.8$  d;  $\gamma$ -energy:  $E_{\text{max}} = 279$  keV).

The specific activity of faeces and urine were measured daily, and thus the mercury excretion was followed.

The nuclear measuring system consisted of the following units: ND-321 measuring head equipped with a scintillation detecting crystal in a NZ-138 measuring set (GAMMA Co., Hungary) and a NK-370 adapter (GAMMA Co., Hungary), which includes a 256-channel amplitude-analyzer and a personal computer. In order that the radioactive decay should not affect the results, the specific activities measured have been calculated from the time of mercury intake (so-called zero time).

Within 10 days of the mercury intake the daily mercury excretion had decreased to below the detectable level and at this stage samples were taken from the liver, kidney and muscle (*musculus longissimus dorsi*). The specific activity and formaldehyde level of the samples were measured.

### Sample preparation

Samples (0.25 g) were suspended in 1 ml 0.01% dimedone in methanol and stored at 22 °C at atmospheric pressure. After seven days the formaldehyde content of the suspensions was determined by High Performance Liquid Chromatography (HPLC).

The HPLC equipment consisted of a Gynkotek M 480 pump, a TOSOH 6040 UV detector (260 nm), and a Rheodyne 8125 injector with a 20 µl loop. A ChromSpher C-18 (150 × 4.6 mm; 5 µm) column was used. The chromatograms were recorded through an EF 2102 ADDA converter (Elektroflex GM, Szeged, Hungary) by a personal computer. The applied mobile phase was methanol – 0.01 M HCl (76 : 24, v/v; pH = 2.63) at 1 ml/min flow rate. The injected amount was 20 µL.

## RESULTS AND DISCUSSION

The cumulative excretion curve (Fig. 1) shows that more mercury was excreted via faeces than urine. The maximum daily excretion was recorded on the second day after intake, and the majority occurred during the first 5 days. Of the mercury ingested, 70% was excreted during the first 10 days. The excretion curve could be characterized by an exponential curve. The highest accumulation of mercury was in the liver followed by the kidney and muscle (Table 1). This is in accordance with our former experiments [4].

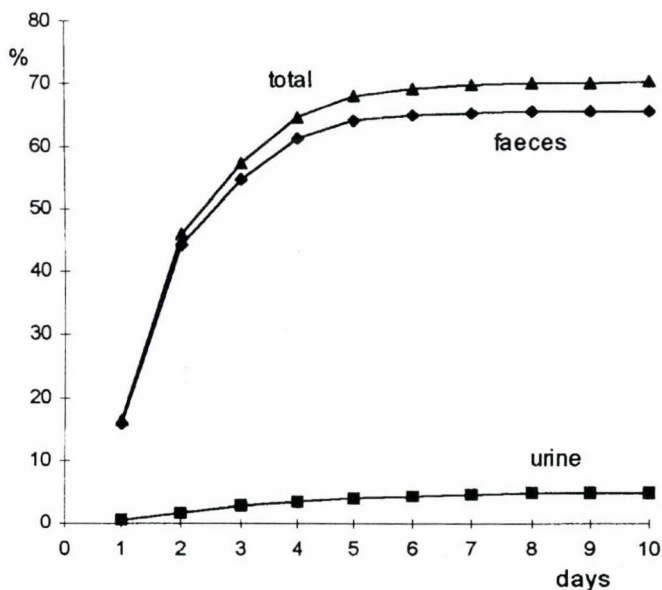


Fig. 1. The cumulative excretion of Hg-203 in Group II



*Table 1*  
The relative Hg-203 activity and concentration of pig organs

	Liver		Kidney		Muscle	
	kBq/kg	µg/kg	kBq/kg	µg/kg	kBq/kg	µg/kg
Group II $\bar{X}$	<b>10.17</b>	<b>8.14</b>	<b>6.25</b>	<b>5.0</b>	<b>1.39</b>	<b>1.11</b>
SD	2.68	2.14	0.90	0.72	0.26	0.21

*Table 2*  
The formaldehyde level of pig tissues

		Content of formaldehyde (mg/100 g)		
		liver	kidney	muscle
Group I	$\bar{X}$	<b>1.180<sup>a</sup></b>	<b>0.875<sup>a</sup></b>	<b>0.624<sup>a</sup></b>
	SD	0.017	0.028	0.012
Group II	$\bar{X}$	<b>0.698<sup>b</sup></b>	<b>0.397<sup>b</sup></b>	<b>0.817<sup>b</sup></b>
	SD	0.027	0.003	0.005

In the same column, figures followed by different letters are significantly different ( $P < 0.05$ )

The formaldehyde level of each tissue altered significantly as a result of the additional mercury intake, although the nature of the changes has not yet been interpreted (Table 2). While the formaldehyde concentrations in the liver and kidney decreased by half, increases were observed in the muscle.

Of the inorganic mercury ingested, 70% was excreted during the first ten days, the majority via faeces. The 0.4 mg additional mercury intake, as a stress factor, caused significant alteration in the endogenous formaldehyde levels of the liver, kidney and muscle. The direction and extent of the alteration presumably depends on the amount of mercury accumulated. The applied analytical process proved to be competent to indicate the abiotic stress effect caused by mercury.

## REFERENCES

1. Albert, L., Németh, Zs. I., Barna, T., Varga, Zs., Tyihák, E. (1998) Measurement of endogenous formaldehyde in the early developmental stages of European turkey oak (*Quercus cerris* L.). *Phytochem. Anal.* 9, 1–5.
2. Huszti, Z., Tyihák, E. (1986) Formation of formaldehyde from S-adenosyl-L-(methyl-<sup>3</sup>H) methionine during enzymatic transmethylation of histamine. *FEBS Letters* 209, 362–366.
3. Palusova, O., Ursinyova, M. (1983) Quecksilber als Kontaminant der Umwelt. In: Anke, M. (ed.) *Proc. 4. Spurenelement Symposium*. Leipzig.
4. Sarudi, I., Lassu-Merényi, Zs., Kelemen, J., Sarudi, I. P., Rétfalvi, T. (1996) Suppression of absorption of radioactive strontium for pig gut by protective materials. In: Pais, I. (ed.) *Proc. 7. International Trace Element Symposium*. Budapest.
5. Siggia S. (1972) *Instrumental Methods of Organic Functional Group Analysis*. Wiley-Interscience, New York.
6. Tyihák, E., Blunden, G., Yang, M., Crabb, T. A., Sárdi, É. (1996) Formaldehyde, as its dimedone adduct, from *Ascophyllum nodosum*. *J. Applied Phycology* 8, 211–215.
7. Vogt, H., Uebersvhär, K. H., Matthes, S. (1986) Einfluss von Methylquecksilber-chloridzusätzen zum Legehennenfutter. In: Anke, M. (ed.) *Proc. 5. Spurenelement Symposium*. Leipzig.





## INVESTIGATION OF SOME METHYLATED COMPOUNDS AND PEROXIDASE ACTIVITY DURING PLANT ONTOGENESIS IN SNAP BEAN\*

ÉVA SÁRDI<sup>1</sup> and ÉVA STEFANOVITS-BÁNYAI<sup>2</sup>

<sup>1</sup>Department of Genetics and Plant Breeding, University of Horticulture and Food Industry, Budapest, Hungary

<sup>2</sup>Department of Chemistry and Biochemistry, University of Horticulture and Food Industry, Budapest, Hungary

(Received: 1998-10-28; accepted: 1998-11-25)

Changes in the level of endogenous formaldehyde (HCHO) and some N-methylated compounds were investigated in the leaves of snap bean (*Phaseolus vulgaris* L.) during ontogenesis. In addition, the activity and isozyme pattern of peroxidase enzymes were also examined. HCHO, as dimedone adduct, and fully N-methylated compounds were determined by overpressured layer chromatography in different development stages of snap bean plant. Peroxidase activities were measured by spectrophotometry and isozyme patterns were examined by isoelectric focusing. HCHO level decreased until blooming with aging of the plant being the highest in the youngest leaves all the time, but then increased again in old leaf tissues. At the same time the concentration of choline and trigonelline as potential HCHO generators (marker molecules or gene products) decreased considerably while peroxidase activity increased with aging of plants.

**Keywords:** Demethylation – fully N-methylated compounds – methylation – ontogenesis – peroxidase activity – snap bean

### INTRODUCTION

According to earlier reports, formaldehyde (HCHO) can be found in human bodies [19] and animals [8] as well as in plant tissues [21].

The endogenous HCHO can be produced by both methylation and demethylation processes catalyzed by demethylases and peroxidases [9, 10, 12].

Since the endogenous transmethylation processes occur via HCHO [9], this compound can be considered as one of the basic constituents of biological systems. Analysis of different plant samples has shown that a correlation exists between the amount of endogenous HCHO and the amount of endogenous fully N-methylated compounds and the natural disease resistance and/or stress tolerance of the given plant [14, 16, 17].

\* Presented at the 4th International Conference on the Role of Formaldehyde in Biological Systems, July 1–4, 1998, Budapest, Hungary.

Send offprint requests to: Dr. Éva Sárdi, Department of Genetics and Plant Breeding, University of Horticulture and Food Industry, H-1502 Budapest, P.O. Box 53, Hungary.



Peroxidases play roles not only in demethylation processes but they are indicators of different stress reactions and they are important in the identification of different genotypes [1, 4]. Attempts have been made to use leaf peroxidase activity as a marker of ontogenetic age of plant, too [13].

In our previous studies relationships have been found between the amount of quaternary ammonium compounds (choline, trigonelline) and the biotic stress tolerance of some varieties of snap bean having known resistance genes. *Pseudomonas*, *Colletotrichum* and virus resistant varieties especially in their young trifoliates have higher concentrations of these quaternary ammonium compounds than other genotypes [17].

The differentiation of various developmental stages (primary leaf-trifoliolate leaf) is particularly important with regard to the stress response of plants. It is a well known phenomenon that plants at different developmental stages show different reactions to pathogen infections. In *Phaseolus vulgaris* L. – *Pseudomonas syringae* pv. *phaseolicola* host – pathogen relationship the primordial leaf is sensitive to the pathogen in spite of the presence of the recessive *plr* resistance gene [18].

The aim of this study was to reveal relationships between the amount of HCHO, some quaternary ammonium compounds (choline, trigonelline) and the activity and isozyme patterns of peroxidase enzymes in primary and trifoliolate leaves of snap bean at different developmental stages.

## MATERIALS AND METHODS

The snap bean plants were cultivated in commercial compost in a greenhouse. Leaf samples were collected at different phenophases, following the stages of ontogenesis from the semideveloped primary leaf stage to the appearance of young pods (Table 1). In our experiments we have studied the seed-leaf, the different developmental stages of primary leaves (the leaf primordium, half grown, fully developed) and the leaf primordium of the first trifoliolate leaf, too.

### *Preparation of plant samples for chromatographic analyses*

Leaf tissues were frozen with liquid nitrogen, powdered and suspended in dimedone solution (0.05% dimedone in methanol) (e.g. 0.25 g plant powder/0.7 ml of 0.05% dimedone solution). This suspension was centrifuged at 1500 g for 10 minutes at 4 °C. The clear supernatants were used to overpressured layer chromatographic (OPLC) [7] and HPLC separations [15].

### *OPLC separation*

OPLC separations were carried out on OPLC silica gel 80 F 254 precoated chromatoplates using a chloroform-methylenechloride mixture (35 : 65, V/V) for formal-

demethone determination and an i-propanol-methanol-0.1 M sodium acetate mixture (20 : 3 : 30, V/V) for quaternary ammonium compounds. Calibration curves were made by means of authentic substances (at  $\lambda = 265$  nm for formaldemethone and at  $\lambda = 525$  nm for quaternary ammonium compounds which were detected by Dragendorff reagent) [7].

The separations were carried out with OPLC chromatograph (developed by OPLC-NIT Co., Ltd., Budapest, Hungary). Densitograms were taken with a Shimadzu CS-930 scanner (Shimadzu Co., Kyoto, Japan). Samples were applied with a NANOMAT sample applicator (CAMAG Co., Muttenz, Switzerland).

### *HPLC separation*

Separations were carried out with a Liquochrom Mode 2010 liquid chromatograph equipped with UV 308 detector (Factory of Laboratory Instruments Co. Ltd., Budapest, Hungary), OH-814 recorder (RADELKIS Co., Budapest, Hungary), Digint-180 Integrator (Servintern Co., Budapest, Hungary) and a 20  $\mu$ l loop.

Formaldemethone was the eluted with methanol at a flow-rate of 0.7 cm<sup>3</sup>/min using a BST Si-100-S-C-18 column (250 mm  $\times$  4 mm I.D., 10  $\mu$ m) (BioSeparation Technical Cooperative, Budapest, Hungary) and determined with UV spectrophotometry ( $\lambda = 260$  nm) [15].

### *Sample preparation for isoelectric focusing*

Leaves (1 g) were homogenized in 1 ml ice cold 20 mM Tris-HCl extraction buffer (pH = 7.8), containing 0.2 mg/ml MgCl<sub>2</sub>, 10 mg/ml polyvinylpyrrolidone, 200 mg/ml sucrose, 3.4 mg/ml potassium metabisulfite, 0.35 mg/ml bovine albumin, 100 mg/ml Triton X-100. The crude extracts were centrifuged with 1500 g at 4 °C for 15 minutes and the supernatants were analyzed.

Isoelectric focusing was carried out on a PhastSystem (LKB-Pharmacia, Sweden). In order to develop pH gradient (pH 3–9) ready-made gels were prerun by 2.5 mA at 10 °C, for 75 Vh, and crude extracts of samples were applied onto the acidic (pH 4.5) end of the gel and run by 2.5 mA at 10 °C, for 700 Vh. Gels were stained for peroxidase activity with o-dianisidine [20]. Dry gels were evaluated by Image Master densitometer (Sharp JX-330).

The total peroxidase activity (U/ml) was measured by a spectrophotometric method at  $\lambda = 460$  nm (by a Varian DMS 100 UV-Visible Spectrophotometer) [3].

## RESULTS

We have determined the concentration of HCHO and some quaternary ammonium compounds and the activity of peroxidase enzymes in the seed leaf, primary leaves and trifoliates in different developmental stages of snap bean plant (Table 1).



Table 1

Leaf samples were collected at different phenophases, following stages of ontogenesis from the semi-developed primary leaf stage to the appearance of young pods


Phenophases	Ageing of plant 					
	I	II	III	IV	V	VI
Primary leaves	middle developed	developed, young	developed	developed, old	the oldest, yellowing	
First trifoliates		middle developed	developed, young	developed	developed, old	
Second trifoliates			the youngest	developed, young	developed	
Third trifoliates (blooming)				the youngest	developed, young	
Fourth trifoliolate (pods)					the youngest	the youngest, upper leaf
Pods					the youngest	2 cm long

Figure 1 shows the concentration of HCHO measured in the primary and trifoliolate leaf tissues of different ages. These results clearly show that the amount of endogenous HCHO decreased with aging of plant tissues until blooming, but increased again in old leaf tissues of old plants. The relatively high level of HCHO can be produced by demethylation processes of the methylated substances catalyzed by peroxidases and/or demethylases in the old leaf tissues of old plants.

Figures 2 and 3 summarize the changes of the concentration of trigonelline and choline in different phenophases in the snap bean leaves. The figures clearly show that in parallel with the development of leaf and/or the aging of plants the concentration of trigonelline, choline was decreased.

In parallel with the determination of endogenous fully N-methylated compounds peroxidase activity was also analyzed in the same samples. Figure 4 shows the relationship between the level of fully N-methylated compounds and the activity of peroxidase enzymes in a given developmental stage. The peroxidase activity was increased with the ageing of leaves, reversely the concentrations of choline and trigonelline were decreased from the youngest leaves to the oldest ones in a given developmental stage of the plant. The same tendencies were observed during the senescence of a given leaf, too. A possible explanation for these result is that the methylation processes are more intensive in the rapidly proliferating cells (semi-developed and the youngest leaves).

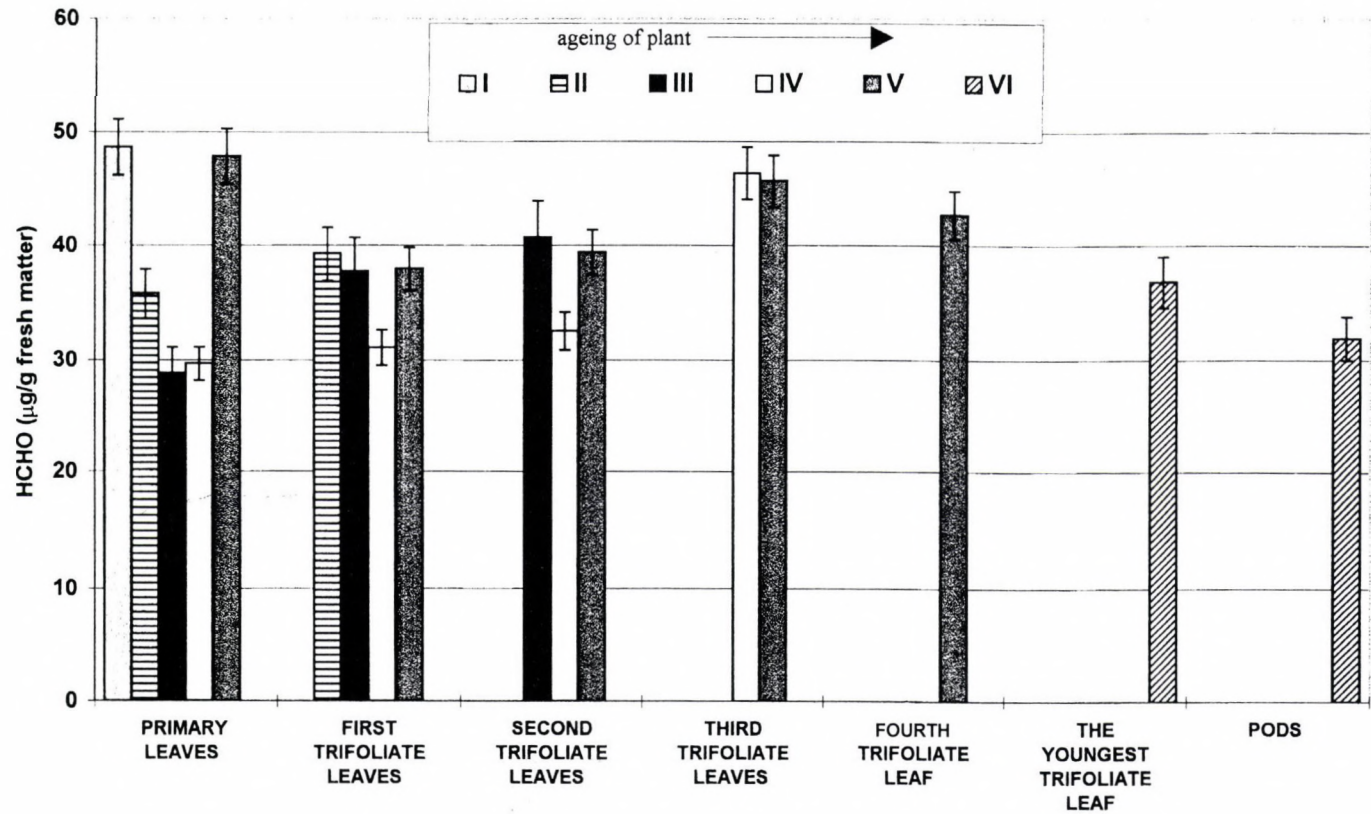


Fig. 1. Change of formaldehyde level in the different phenophases



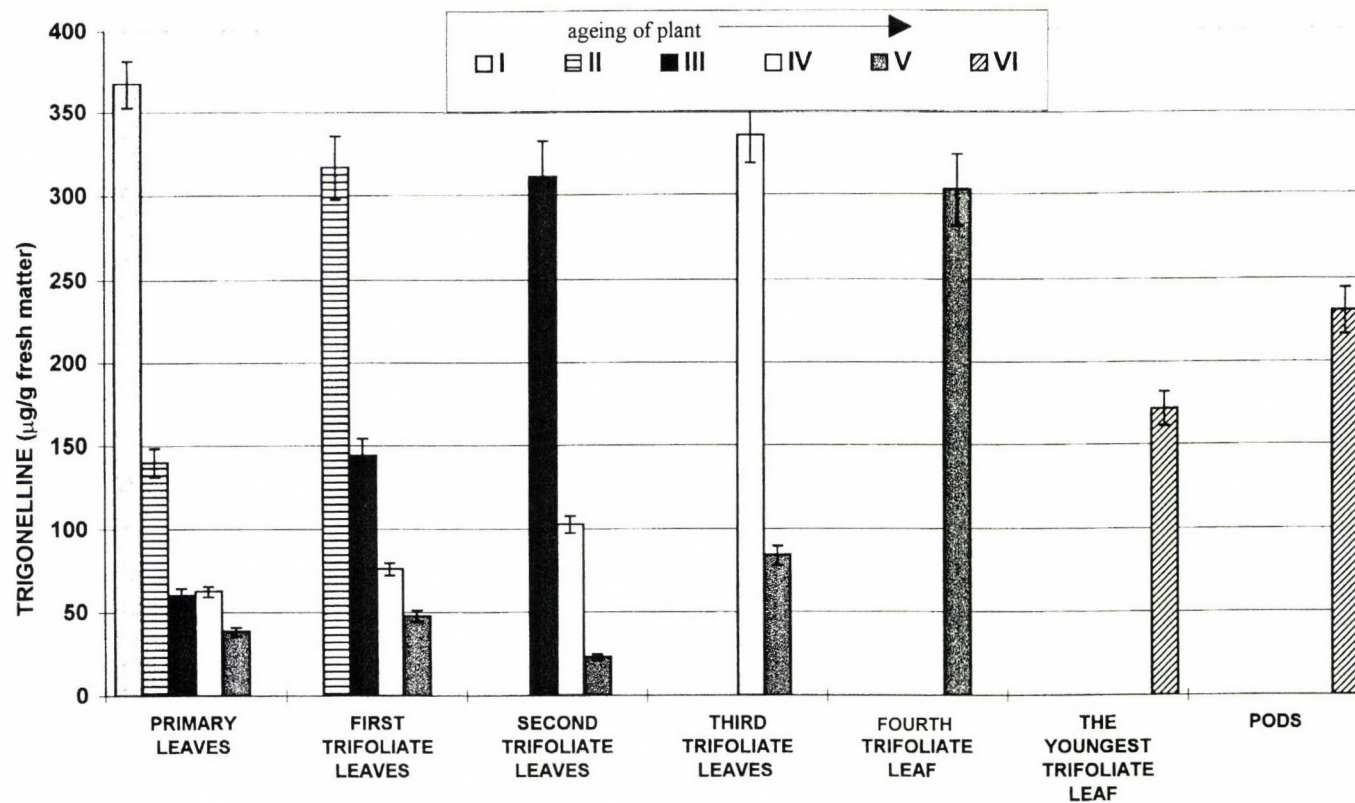


Fig. 2. Change of trigonelline concentration in the different phenophases

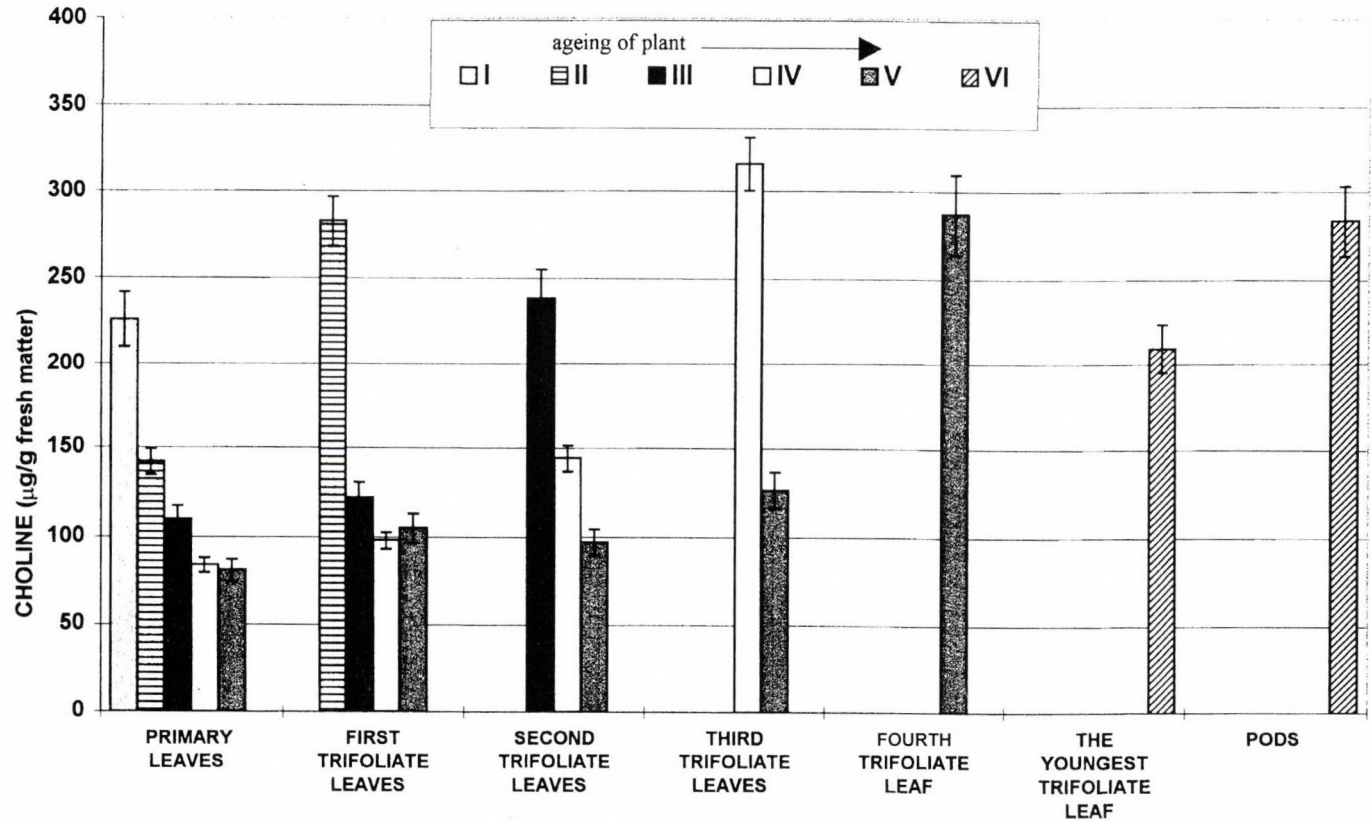


Fig. 3. Change of choline concentration in the different phenophases



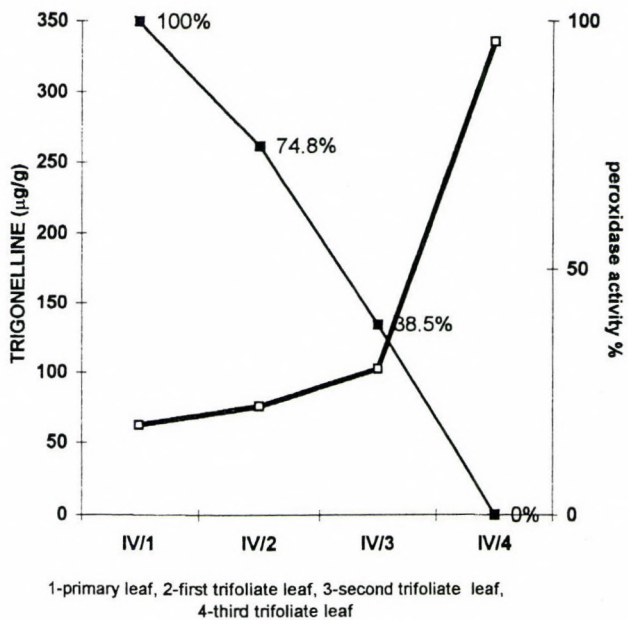
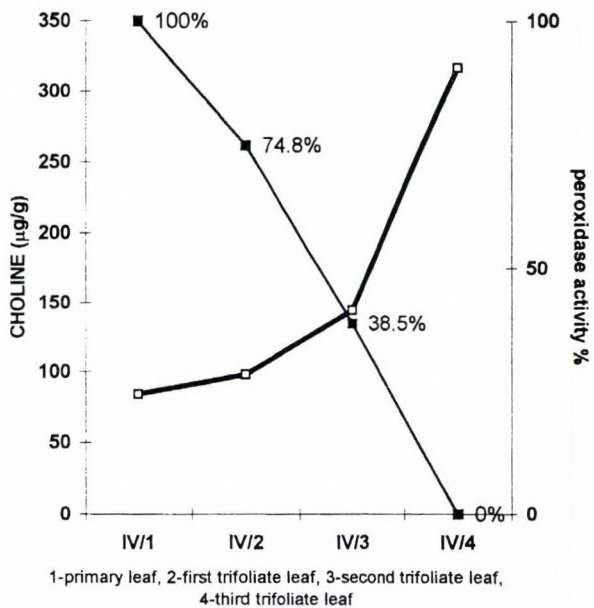


Fig. 4. The relationship between the level of fully N-methylated compounds and the activity of peroxidase enzymes

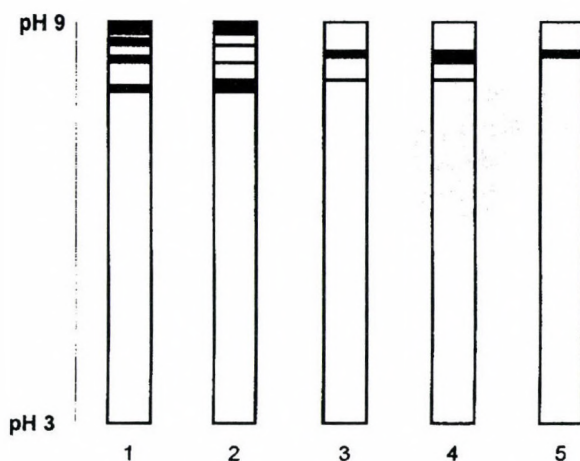


Fig. 5. The peroxidase isozyme patterns (1 – seed leaf, 2 – leaf primordium of primary leaf, 3 – primary leaf half grown, 4 – primary leaf fully developed, 5 – leaf primordium of the first trifoliate)

Considerable differences could be indicated in the peroxidase isozyme patterns in the various phenological phases of ontogenesis. We have found well-detectable peroxidase isozyme bands in the basic pH range but there were differences both in number of bands and isozymes activities during the development of bean plants (Fig. 5).

At the seed leaf stage we obtained four isozyme bands (Fig. 5, band 1). and at the next stage of development only one fraction could be seen. Results of isozyme activity indicated that with the ageing of the plant the activity of isozymes increased in the primary leaves (Fig. 5, bands 2, 3, 4) but at the trifoliate stage (Fig. 5, band 5) the activity was lower.

## DISCUSSION

The high level of HCHO in young leaf tissues observed in our studies appeared to originate from methylation processes [24]. The level of choline and trigonelline decreased with ageing of the plant and during the development of a leaf. The content of HCHO also decreased with ageing of bean plants [6], but increased again in old leaf tissues of old plants. The relatively high level of HCHO in old tissues can be originated from demethylation processes of the methylated substances catalyzed by peroxidases and/or demethylases. It is known that peroxidase enzymes participate in hydrogen peroxide-dependent demethylation processes [5]. It is supposed that the elevated peroxidase activity observed in old tissues contributed to the accumulation of HCHO in these tissues.

The phenophase dependence of relative peroxidase activities in snap bean plants shows a continuous decrease in activities from old leaves to younger ones [6].



A possible explanation for the observed time dependence of HCHO concentration is that in young proliferating cells methylation processes are dominant over demethylation [24] while in the old leaves the oxidative demethylation – in which beside demethylases, peroxidases play crucial role – overwhelms methylation [24].

The decrease of fully N-methylated compounds during ontogenesis as well as an increase in peroxidase activity support the idea that not only demethylases but peroxidases can be involved in oxidative demethylation [11].

It could be concluded that peroxidase activities and level of fully N-methylated compounds showed close connection with plant development and its senescence stage. The increase of peroxidase activity which is in connection with development of primary leaves showed similar tendencies with the changes of peroxidase activities measured in plants having leaves of different ages and stages of development.

#### REFERENCES

1. Bachmann, O. (1994) Peroxidase isoenzyme patterns in Vitaceae. *Vitis* 33, 3. 151–156.
2. Burgyán, J., Szarvas, T., Tyihák, E. (1982) Increased formaldehyde production from L-methionine- $(S-^{14}CH_3)$  by crude enzyme of TMV infected tobacco leaves. *Acta Phytopathol. Acad. Sci. Hung.* 17, 11–15.
3. Cseke, E., Vámos-Vigyázó, L. (1991) Peroxidáz. In: Szabolcsi, G. (ed.) *Enzimes analízis*. Akadémiai Kiadó, Budapest.
4. Fransz, P. F., Ruijter, N. C. A., Schell, J. H. N. (198) Isoenzyme as biochemical and cytochemical markers in embryogenic callus cultures of maize (*Zea mays* L.). *Plant Cell Reports* 8, 67–70.
5. Gullner, G., Tyihák, E. (1987) Hydrogen peroxide dependent N-demethylase activity in the leaves of normal and heat-shocked bean plants. *Plant Sci.* 52, 21–27.
6. Gullner, G., Tyihák, E. (1991) Measurement of formaldehyde, hydrogen peroxide and non-protein thiols in tobacco leaves during ageing. *Biochem. Physiol. Pflanzen* 187, 131–138.
7. Gersbeck, N., Schönbeck, F., Tyihák, E. (1989) Measurement of formaldehyde and its main generators in *Erysiphe graminis* infected barley plants by planar chromatographic techniques. *J. Planar Chromatogr.* 2, 86–89.
8. Heck, H. d'A., Casanova, M., Starm, T. B. (1990) Formaldehyde toxicity – new understanding. *Crit. Rev. Toxicol.* 20, 397–42.
9. Huszti, Z., Tyihák, E. (1986) Formation of formaldehyde from S-adenosyl-L-(methyl- $^3H$ )methionine during enzymatic transmethylation of histamine. *FEBS Letters* 209, 362–366.
10. Kawata, S., Sugiyama, T., Iami, J., Minami, Y., Tarui, S., Okamoto, M., Yamano, T. (1983) Hepatic microsomal cytochrome P-450 dependent N-demethylation of methylguanidine. *Biochem. Pharmacol.* 32, 3723–3728.
11. Kedderis, G. L., Hollenberg, P. F. (1983) Peroxidase-catalysed N-demethylation reactions. *J. Biol. Chem.* 259, 663–668.
12. Paik, W. K., Kim, S. (1980) *Protein Methylation*. Wiley and Sons, New York, pp. 132–136.
13. Sanchez-Romero, C., Garcia-Gomez, M. L., Pliego-Alfaro, F., Heredia, A. (1993) Peroxidase activities and isoenzyme profiles associated with development of avocado leaves at different ontogenetic stages. *J. Plant Growth Reg.* 12:2, 95–100.
14. Sárdi, É., Tyihák, E. (1992) Effect of Fusarium infection on the formaldehyde cycle in parts of water melon (*Citrullus vulgaris* L.) plants. In: E. Tyihák (ed.), *Proceedings of 3rd International Conference on Role of Formaldehyde in Biological Systems*. Sopron, 1992. Hung. Biochem. Soc., Budapestpp. 145–149.
15. Sárdi, É., Tyihák, E. (1994) Measurement of formaldehyde in dimedone adduct form in biological samples by high performance liquid chromatography. *Biomed. Chromatogr.* 8, 313–314.

16. Sárdi, É., Tyihák E. (1995) Measurement of formaldehyde and its main potential generators in the seeds of water-melon (*Citrullus vulgaris* L.) varieties and F1 hybrids of different Fusarium sensitive. *Hort. Sci. Hung.* 27, 66–70.
17. Sárdi, É., Velich, I. (1995) Measurement of formaldehyde and its main potential generators in the leaves of snap bean (*Phaseolus vulgaris* L.) varieties of different biotic stress resistance. *Hort. Sci. Hung.* 27, 99–103.
18. Szarka, J., Velich, I. (1983) Testing of the epidemiological performance of *Pseudomonas phaseolicola* isolates with different aggressivity on the susceptible bean variety, Cherokee. *Ann. Rep. BIC Geneva, N.Y.* 26, 99–100.
19. Szarvas, T., Szatlóczky, E., Volford, J., Trézl, L., Tyihák, E., Rusznák, I. (1986) Determination of endogenous formaldehyde level in human blood and urine by dimedone-<sup>14</sup>C radiometric method. *J. Radioanal. Nucl. Chem. Lett.* 106, 357–367.
20. Tanksley, S. D., Orton, T. J. (1983) *Isozymes in Plant Genetics and Breeding*. Elsevier Amsterdam, Part B., pp. 3–23.
21. Tyihák, E., Balla, J., Gáborjányi, R., Balázs, E. (1978) Increased free formaldehyde level in crude extract of virus infected hypersensitive tobaccos. *Acta Phytopathol. Acad. Sci. Hung.* 13, 29–31.
22. Tyihák, E., Szarvas, T., Trézl, L., Király, Z. (1984) Possibility of spontaneous formylation reaction by endogenous formaldehyde after heat shock in plants. *Acta Biochim. Biophys. Acad. Sci. Hung.* 19, 136.
23. Tyihák, E., Rozsnyay, Zs., Sárdi, É., Gullner, G., Trézl, L., Gáborjányi, R. (1994) Possibility of formation of excited formaldehyde and singlet oxygen in biotic and abiotic stress situations. *Acta Biol. Acad. Sci. Hung.* 45, 3–10.
24. Tyihák, E., Rozsnyay, Zs., Sárdi, É., Szőke, É. (1992) Formaldehyde cycle and the cell proliferation: plant tissue as a model. In: Tyihák, E. (ed.) *Proc. of 3rd Intern. Conf. on Role of Formaldehyde in Biological Systems*. Hungary Biochem. Soc., Budapest, pp. 139–144.
25. Vallejos, C. E. (1983) Enzyme activity staining. In: Tanksley, S. D., Orton, T. J. (eds), *Isoenzymes in Plant Genetics and Breeding*, Part A., Elsevier, Amsterdam, pp. 469–516.





## FORMALDEHYDE AS A PROOF AND RESPONSE TO VARIOUS KIND OF STRESS IN SOME *BASIDIOMYCETES*\*

ANNA JAROSZ-WILKOŁAZKA, MONIKA FINK-BOOTS, ELŻBIETA MALARCZYK  
and A. LEONOWICZ

Department of Biochemistry, Maria Curie-Skłodowska University, Lublin, Poland

(Received: 1998-10-28; accepted: 1998-11-25)

The influence of cadmium chloride and/or high temperature on the level of selected parameters were examined in both medium and mycelium of some *Basidiomycetes* belonging to white-rot fungi: *Abortiporus biennis*, *Trametes versicolor* and *Cerrena unicolor*. We investigated changes in the formaldehyde (FA) level and in the level of superoxide radical anions (SR). Accordingly, the capacity of three enzymes was also studied: two enzymes of the cellular antioxidative system – superoxide dismutase (SOD; EC 1.15.1.1), and catalase (CAT; EC 1.11.1.6), and laccase (LAC; EC 1.10.3.2) – the main lignin-modifying enzyme, which is produced by white-rot fungi. During the first 24 hours after application of separate stressors, or jointly with two stressors to 10-day-old cultivation, changes in all selected parameters were observed. Moreover, we found significant changes in the levels of extracellular SR, FA and extra- and intracellular activity of LAC. Simultaneous action of two stressors in the fungal cultures decreased the extracellular LAC level, intracellular CAT activity and the level of SR in the medium compared to the control values, while using the two stress factors separately would strongly make these values increase. Stressful conditions brought a rapid increase in the level of FA in all fungal species. The results of our study, carried out on selected strains of *Basidiomycetes*, seem to have shown that: (1) LAC, the lignin-modifying enzyme, may have an important application in fungal stress response, and take part in the cross-protection between responses to heat shock and cadmium resistance; (2) the oxidative burst as a result of cadmium and high temperature treatment is an additional factor to damage fungal cells; (3) FA may be a determining factor in the phases of fungal stress syndrome.

**Keywords:** *Basidiomycetes* – cadmium – heat shock – cross-protection – formaldehyde

### INTRODUCTION

In response to various stressors, a complex of cellular adaptations commonly called “stress response” is triggered so as to assure the survival of fungi [3, 23, 30]. Different stress conditions may prompt a general stress response by creating the same

\* Presented at the 4th International Conference on the Role of Formaldehyde in Biological Systems, July 1–4, 1998, Budapest, Hungary.

Send offprint requests to: Dr. Anna Jarosz-Wilkołazka, Department of Biochemistry, Maria Curie-Skłodowska University, Lublin, Poland.

Abbreviations: CAT – catalase; Cd – cadmium; FA – formaldehyde; SOD – superoxide dismutase; SR – superoxide radicals.

intracellular signals, such as: abnormal and denatured proteins [9, 18], internal acidification [27], alterations in cytoskeletal structures [8], changes in the level of intracellular cyclic AMP [7, 28], or overproduction of reactive oxygen species [5, 29].

Based upon the recent literature, production of formaldehyde from its potential generators can also be considered as an initial response. Endogenous N-, S- and O-methylated substances are potential formaldehyde generators in enzymatic demethylation [15] and transmethylation processes [16]. The measurable level of formaldehyde was dramatically elevated as a result of disease stress, e.g. in infected tobacco leaves [6] or in *Citrullus vulgaris* after a nonlethal infection with *Fusarium oxysporum* [31]. The same result was found in the case of changes in temperature, or after application of different exogenous substances, e.g. in pinto bean leaves after heat shock, or in *Quercus cerris* after cold shock treatment [2, 32]. As a result of the action of these biotic and abiotic stress factors, levels of potential formaldehyde generators were considerably decreased [33].

## MATERIALS AND METHODS

### *Fungal material and growth conditions*

*Abortiporus biennis* (Bull. ex Fr), *Cerrena unicolor* (Bull. ex Fr) and *Trametes versicolor* (L. ex Fr) Pil. were obtained from the culture collection of the Department of Biochemistry, University of Lublin, Poland. Selected strains were incubated at 25 °C for 10 days in 25 ml Erlenmayer flasks containing 10 ml medium according to Lindeberg (for *A. biennis* and *C. unicolor*) or Fahreus (for *T. versicolor*) [10, 21]. After that time they were treated with either separate stressors [cadmium chloride ( $\text{CdCl}_2 \times 2.5 \text{ H}_2\text{O}$ ) and/or high temperature], or jointly with both. The temperature and concentration of  $\text{CdCl}_2$  were established experimentally for each kind of fungus on the basis of extracellular laccase activity, the main lignin-modifying enzyme. The following values were obtained: for *A. biennis* 10 mg l<sup>-1</sup>  $\text{CdCl}_2$  and/or 90 min at 55 °C; for *C. unicolor* 25 mg l<sup>-1</sup>  $\text{CdCl}_2$  and/or 90 min at 45 °C; and for *T. versicolor* 25 mg l<sup>-1</sup>  $\text{CdCl}_2$  and/or 60 min at 45 °C [12, 24]. After treatment with the stressors the cultures were kept for five days.

### *Preparation of the mycelium for all determinations*

The mycelia from three vials (1 g wet weight) were harvested and homogenized at a low temperature in a motor-driven Potter's homogenizer, in 2 ml of 0.005 M Naphosphate buffer pH 7.0. The homogenates were then centrifuged for 10 min (10 000 g at 4 °C) and the clear supernatant fluids obtained were used for enzyme activity determination and as superoxide radical sources.



### Determination of protein, superoxide radicals and formaldehyde

Protein determinations were performed according to the dye-binding method of Bradford using bovine serum albumin as a standard [4]. Relative concentrations of the superoxide radicals (SR) were assessed spectrophotometrically in the alkaline medium by detection of the superoxide-dependent formation of formazone from nitrotetrazolium blue (NBT). The reaction was carried out in 3 ml 0.05 M NaOH containing 0.5  $\mu$ M NBT and 0.1 ml of sample. After incubation at 25 °C for 30 minutes, the absorbance was monitored at 560 nm. In the above-mentioned conditions the precipitation of dark-blue formazone was avoided. The level of formaldehyde (FA) was determined using the 4-amino-3-hydrazino-5-mercapto-1,2,4-triazol method of MERCK (Darmstadt, Germany).

### Enzyme assays

Laccase (LAC) activity was measured spectrophotometrically with syringaldazine (2.5  $\mu$ M) as a substrate using 0.1 M citrate-phosphate buffer pH 5.2 [20]. The activity of superoxide dismutase (SOD) was calculated on a percentage basis by the autoxidation inhibition of pyrogallol (one unit = 50% inhibition) [25]. Briefly, 0.1–0.2 ml of each sample was mixed with 0.1 ml 5 mM pyrogallol and adjusted to a final volume of 3 ml with 50 mM Tris-HCl buffer (pH 8.5), containing 0.1 mM EDTA. The autoxidation rate of pyrogallol was measured as absorbance changes at 320 nm. The catalase activity (CAT) was examined by the modified Aebi method [1], by monitoring the disappearance of H<sub>2</sub>O<sub>2</sub> at 240 nm. Samples (0.01–0.02 ml) were mixed for a short time with 0.1 M Na-citrate buffer (pH 5.2) containing 3  $\mu$ M H<sub>2</sub>O<sub>2</sub>.

## RESULTS

Having measured the activity of the extracellular LAC during the first five days (Fig. 1), we found that treating with both stress factors alone distinctly increased the LAC activity, while simultaneous treatment with both stressors made its level decrease almost to the control value. This was particularly noticeable in the medium of *C. unicolor* and *T. versicolor*. Meanwhile in the mycelium of all the studied strains we observed an increase in the level of intracellular LAC after the onset of stress.

During the first 24 hours following the shock treatment, we noted an increased level of SR as compared to the control values in the medium and that of all the examined strains (Fig. 2). When using the two stress factors jointly, we observed a decrease in the level of SR in the medium, to a value almost similar to that of the control.

Increased activities of both SOD and CAT were found after application of CdCl<sub>2</sub> and/or high temperature, except that the supply of CdCl<sub>2</sub> to *A. biennis* strain decreased the activity of intracellular SOD (Fig. 3). After using the two stressors jointly on *A. biennis* and *C. unicolor*, slight inductions of activities of CAT were established.



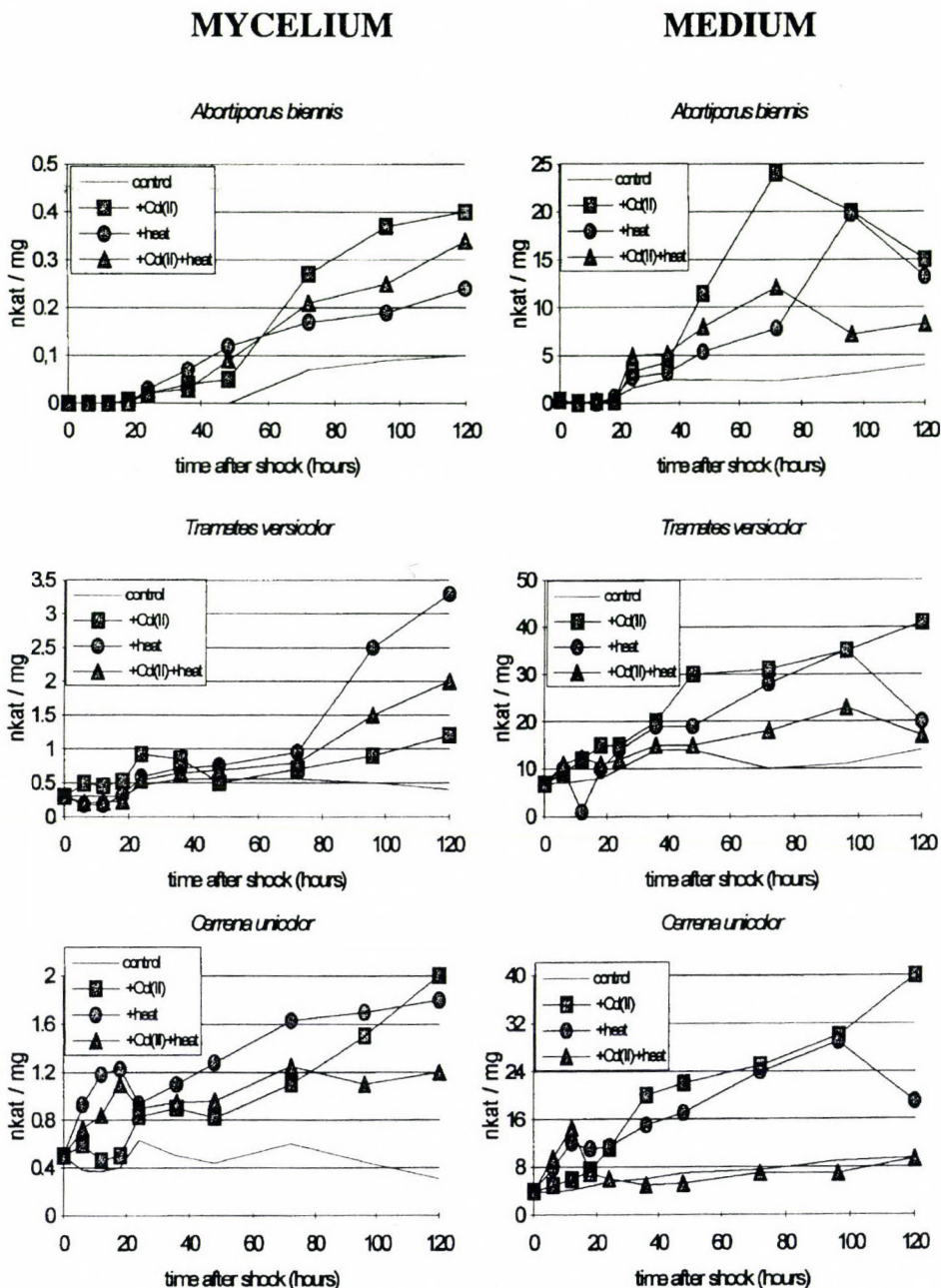


Fig. 1. Changes in laccase activity (nkat/mg of protein) in the mycelium and medium after stress influence ( $\text{CdCl}_2$  and/or high temperature) on 10-day-old cultures

# MYCELIUM

# MEDIUM

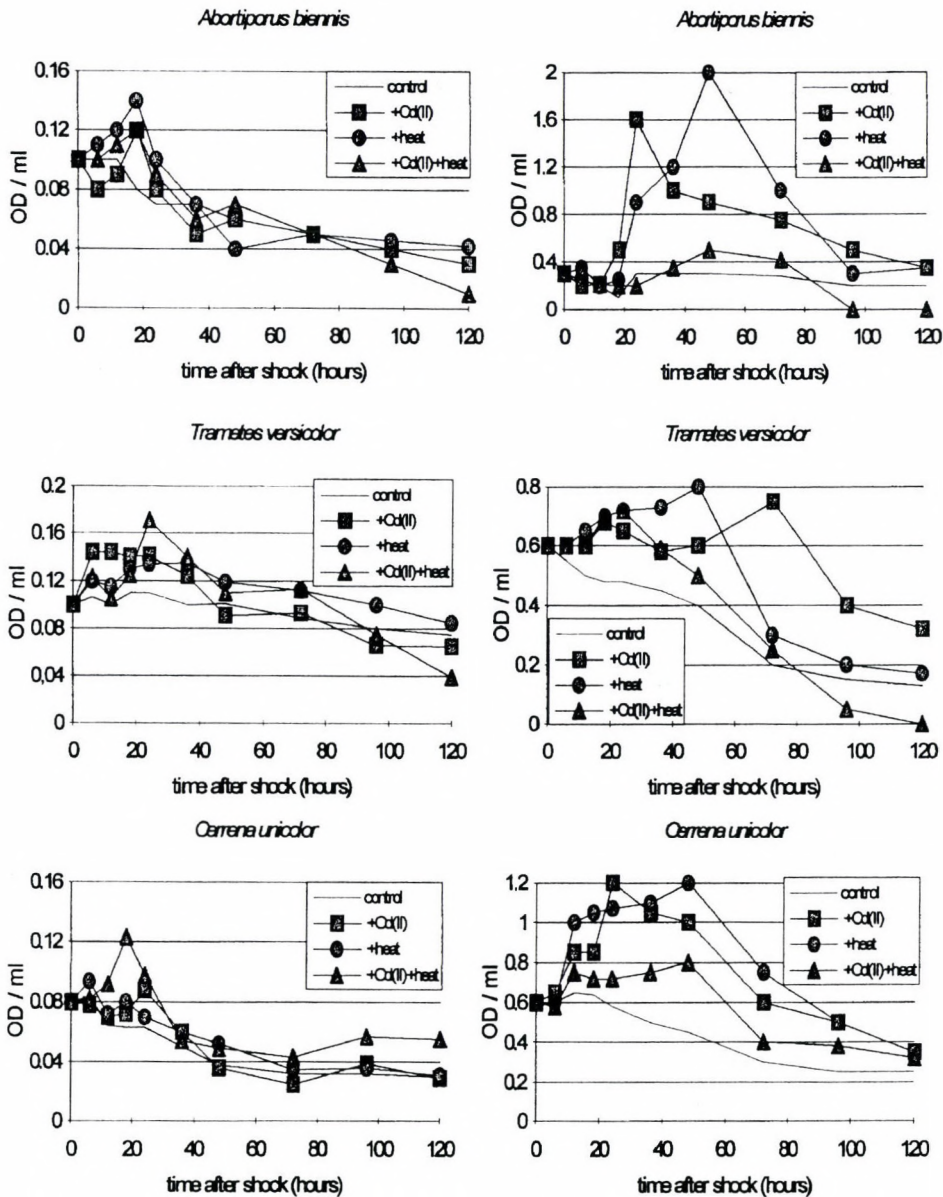


Fig. 2. Level of superoxide radicals in the mycelium and medium after stress influence ( $\text{CdCl}_2$  and/or high temperature) on 10-day-old cultures of *Basidiomycetes*

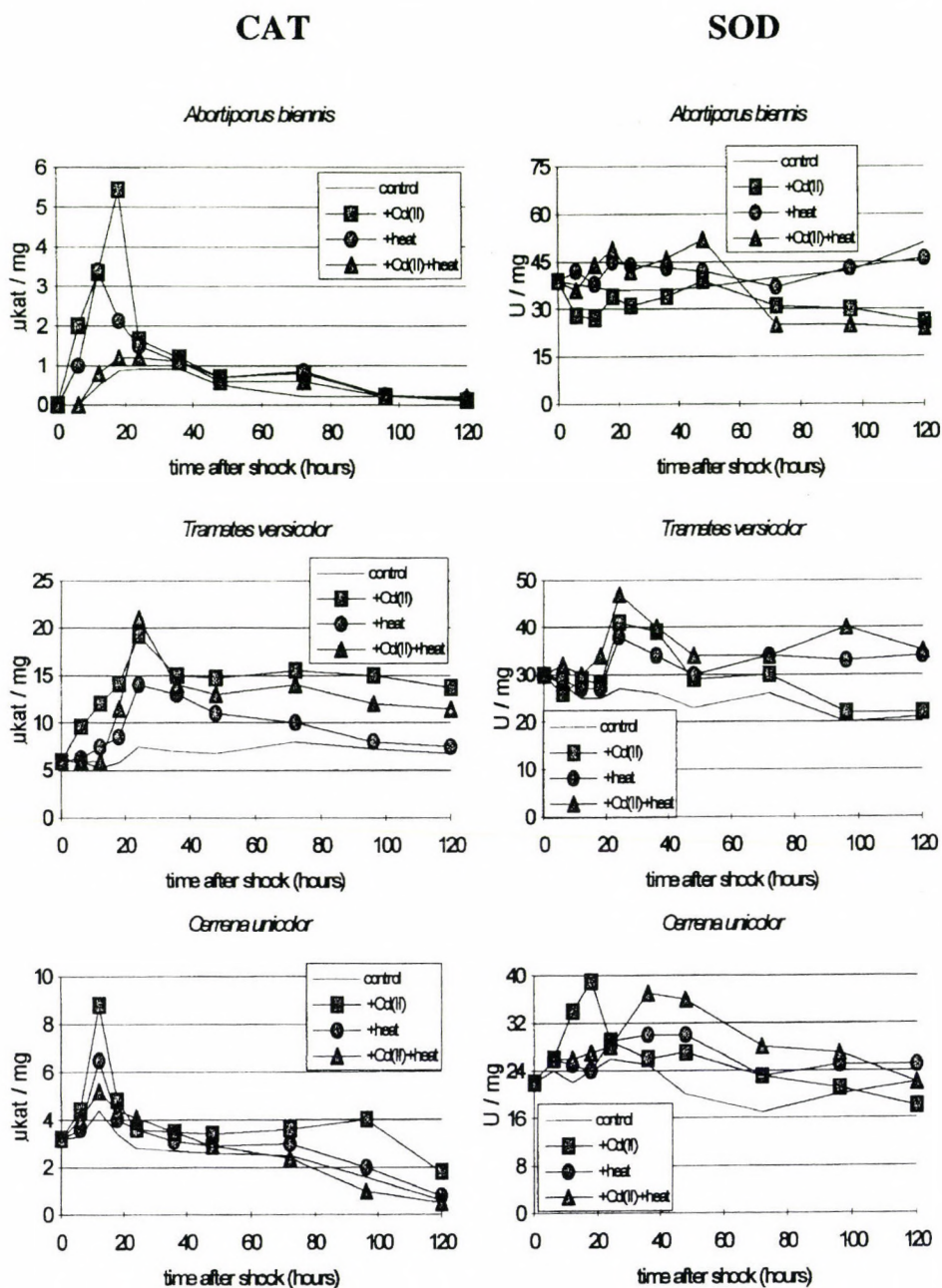


Fig. 3. Intracellular activities of superoxide dismutase (SOD; U/mg of protein) and intracellular catalase (CAT; µkat/mg of protein) after stress influence ( $\text{CdCl}_2$  and/or high temperature) on 10-day-old cultures of *Basidiomycetes*



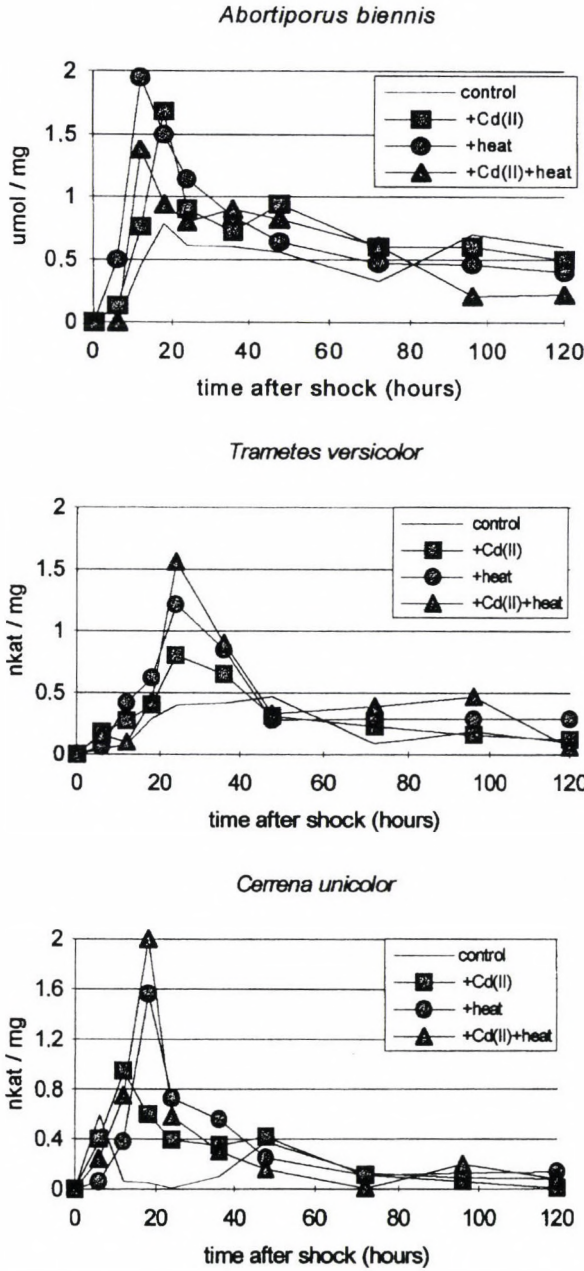


Fig. 4. Level of intracellular formaldehyde ( $\mu\text{mol/mg}$  of protein) after stress influence ( $\text{CdCl}_2$  and/or high temperature) on 10-day-old cultures of *Basidiomycetes*

Stressful conditions caused a rapid increase in the FA level of all the fungal species (Fig. 4). The observed changes occurred during the first 24 hours following the treatment with high temperature and  $\text{CdCl}_2$  separately. FA production under stressful conditions was several times higher in comparison with the control cultures. After using these two stress factors jointly, we also observed a rapid increase in the FA level.

## DISCUSSION

The results of our investigation suggested a link between the activities of LAC, CAT and SOD, and the relative SR and FA levels in fungal cultures as a response to a single stress condition, such as the addition of abundant  $\text{Cd}^{2+}$  or subjection to high temperature. It was also observed that the simultaneous action of both stressors significantly changed the resultant levels of tested biochemical parameters. There was a decrease in LAC activity and SR level in the culture medium of all three investigated fungal strains during the 5 days following the simultaneous application of both stress factors. Moreover, the level of CAT activity was changed drastically when determined in the mycelium of *A. biennis* and *C. unicolor* after twenty hours of stress duration, yet when both stressors were applied the activity of CAT fell to that of the control.

Contrary to the examined enzymes, the level of FA increased as soon as the stress was initiated and showed a tendency to accumulate in the mycelium of the cultures. The same tendency was observed for SOD activity and SR, when determined in the mycelium. Various types of environmental stress, such as changes in temperature, heavy metal concentration, and fluctuations in osmotic and humidity conditions affect fungal metabolism. Stress factors induce resistance and develop toleration for other kinds of stress, a mechanism known as cross-protection or cross-resistance.

There are many reports of cross-protection among bacteria and plants [14, 22]. According to Ferienc et al., cadmium induced general stress protection and activated the global stress mechanisms in *E. coli* [11]. Cadmium-stressed cells were found to be cross protected against subsequent cadmium and oxidation stresses, osmotic and heat shock, and exposure to ethanol [11]. Exposure to cadmium and heat shock induced broad protection against other environmental stress in the cells of *Vibrio parahaemolyticus* [19].

To our knowledge, the literature provides little information about changes in FA level under various stress conditions. The FA level was drastically elevated in virus infected tissues of *Citrullus vulgaris* after a nonlethal infection with *Fusarium oxysporum* [31]. The same result was found in the case of various abiotic stress factors, for example in pinto bean leaves after heat shock and in *Quercus cerris* after cold shock treatment [2, 32].

It has been recently documented that some shock proteins, already present in cells not preexposed to stress conditions, are activated by stress signals to initiate a cascade of e.g. protein kinases [23, 30]. This early response provides a minimal protec-



tion against sudden stress, initiating a delayed response and synthesis of heat shock proteins, enzymes scavenging toxic oxygen radicals, or nonenzymatic defense systems, such as glutathione and ascorbic acid [17, 26]. These last protect cells more permanently and effectively by allowing an adaptation to another stress.

Our investigation showed that the FA level estimated in the fungus culture mycelium after two simultaneous shocks approximates to the sum of the two individual stress values. This is particularly noticeable for *T. versicolor* and *C. unicolor* cultures; these two are high-laccase strains of *Basidiomycetes* and are very active in the process of lignin destruction. They are very tolerant of various stress conditions, such as high  $\text{Cd}^{2+}$  levels [12, 13, 24]. The third fungus, *A. biennis*, is not so resistant to high concentrations of  $\text{Cd}^{2+}$  and not so active in lignin destruction. For this strain, the accumulated FA level remained at the same level as that for each individual stress condition. This result showed that FA production was proportional to the ligninolytic fungal condition and for this reason, it may be taken into consideration as a determining factor in the phases of fungal stress syndrome.

On the other hand, LAC and CAT, the lignin-modifying enzymes, may have an important application in fungal stress response and take part in the cross-protection between responses to heat shock and Cd resistance [13]. The enhanced LAC activity under stressful conditions also suggests its important role in the fungal adaptation process, but its biosynthesis seems to be regulated at the molecular level when the stress conditions are competitive to each other for activation of LAC genes. Though molecular aspects of these cross-reactions are not clear yet, our results show a distinct correlation between LAC and CAT activity, FA production and the pool of SR and SOD activity in the reaction medium, which is likely to damage fungal cells. Physiological amounts of FA could assume a protective role against the damaging activity of stress conditions in fungal organisms because of its very reactive character and its possibility to take part in methylation processes.

#### ACKNOWLEDGEMENT

This work was supported in part by KBN Grant no. 5P064 099 14.

#### REFERENCES

1. Aebi, H. (1984) Catalase in vitro. *Meth. Enzymol.* 105, 121–124.
2. Albert, L., Németh, Zs. I., Varga, Z., Barna, T. (1997) The cold shock in the early stage of european turkey oak (*Quercus cerris* L.). In: *Abst. Intern. Cong. Stress of Life. Stress and Adaptation from Molecules to Man*. Budapest, p. 180.
3. Banuett, F. (1998) Signalling in the yeasts: An informational cascade with links to the filamentous fungi. *Microbiol. Mol. Biol. Rev.* 62, 249–274.
4. Bradford, M. M. (1976) A rapid method for the quantification of microgram quantities of protein utilizing the principle of the protein-dye binding. *Anal. Biochem.* 72, 248–254.
5. Brennan, R. J., Schiestel, R. H. (1996) Cadmium is an inducer of oxidative stress in yeast. *Mut. Res.* 356, 171–178.



6. Burgyán, J., Szarvas, T., Tyihák, E. (1982) Increased formaldehyde production from L-methionine- $(S-^{14}CH_3)$  by crude enzyme of TMV-infected tobacco. *Acta Phytopath. Acad. Sci. Hung.* 17, 11–15.
7. Burnett, K. G. (1997) Evaluating intracellular signaling pathways as biomarkers for environmental contamination exposures. *Amer. Zool.* 37, 585–594.
8. Chowdhury, S., Smith, K. W., Gustin, M. C. (1992) Osmotic stress and the yeast cytoskeleton: phenotype-specific suppression of an actin mutation. *J. Cell Biol.* 118, 561–571.
9. Craig, E. A., Gross, C. A. (1991) Is hsp the cellular thermometer? *Trends Biochem. Sci.* 16, 135–140.
10. Fahreus, G., Reinhammar, B. (1967) Large scale production and purification of laccase of the fungus *Polyporus versicolor* and some properties of laccase A. *Acta Chem. Scand.* 21, 2367–2378.
11. Ferianc, P., Farewell, A., Nyström, T. (1998) The cadmium-stress stimulation of *Escherichia coli* K-12. *Microbiology* 144, 1045–1050.
12. Fink-Boots, M. D., Jaszek, M., Leonowicz, A. (1997) Heat shock stimulation of laccase in *Abortiporus biennis* and *Cerrena unicolor*. In: *Proc. of 2nd TAPPI Biological Sciences Symposium*, San Francisco, pp. 395–396.
13. Fink-Boots, M., Wilkołazka, A., Malarczyk, E., Leonowicz, A. (1998) Changes in sets of laccase isoforms under stress conditions in *Cerrena unicolor*. In: *Proc. of 7th Int. Con. on Biotechnology in the Pulp and Paper Industry*, Vancouver, B179.
14. Gutea-Dahan, Y., Yaniv, Z., Zilinskas, B. A., Ben-Hayim, G. (1997) Salt and oxidative stress: similar and specific responses and their relation to salt tolerance in Citrus. *Planta* 203, 460–469.
15. Gullner, G., Tyihák, E. (1987) Hydrogen peroxide dependent N-demethylase activity in the leaves of normal and heat-shocked bean plants. *Plant Sci.* 52, 21–27.
16. Huszti, S., Tyihák, E. (1986) Formation of formaldehyde from S-adenosyl-L-(methyl- $^3H$ ) methionine during enzymic transmethylation of histamine. *FEBS Lett.* 209, 362–366.
17. Jamieson, D. J. (1995) The effect of oxidative stress on *Saccharomyces cerevisiae*. *Redox Report.* 1, 89–95.
18. Jungmann, J., Reins, H.-A., Schobert, C., Jentsch, S. (1993) Resistance to cadmium mediated by ubiquitin-dependent proteolysis. *Nature* 361, 369–371.
19. Koga, T., Takumi, K. (1995) Comparison or cross-protection against some environmental stresses between cadmium-adapted and heat-adapted cells of *Vibrio parahaemolyticus*. *J. Gen. Appl. Microbiol.* 41, 263–268.
20. Leonowicz, A., Grzywnowicz, A. (1981) Quantitative estimation of laccase forms in some white-rot fungi using syringaldazine as substrate. *Enzyme Microbiol. Technol.* 3, 55–58.
21. Lindeberg, G., Holm, G. (1952) Occurrence of tyrosinase and laccase in fruit bodies of mycelia of some *Hymenomycetes*. *Physiol. Plant.* 5, 100–114.
22. Lou, Y., Yousef, A. E. (1997) Adaptation to sublethal environmental stresses protects *Listeria monocytogenes* against lethal preservation factors. *Appl. Environ. Microbiol.* 63, 1252–1255.
23. Mager, W. H., de Kruijff, A. J. J. (1995) Stress-induced transcriptional activation. *Microbiol. Rev.* 59, 506–531.
24. Malarczyk, E., Wilkołazka, A. (1997) Affection of laccase but not superoxide dismutase activity in cadmium enriched cultures of some white-rot fungi. In: *Abst. Intern. Cong. Stress of Life. Stress and Adaptation from Molecules to Man*. Budapest, p. 176.
25. Marklund, S., Marklund, C. (1974) Involvement of the superoxide anion radical in the autoxidation of pyrogallol and a convenient assay for superoxide dismutase. *Eur. J. Biochem.* 47, 469–474.
26. Moradas-Ferreira, P., Costa, V., Piper, P., Mager, W. (1996) The molecular defences against reactive oxygen species in yeast. *Mol. Microbiol.* 19, 651–658.
27. O'Sullivan, E., Condon, S. (1997) Intracellular pH is a major factor in the induction of tolerance to acid and other stresses in *Lactococcus lactis*. *Appl. Environ. Microbiol.* 63, 4210–4215.
28. Piper, P. W. (1993) Molecular events associated with acquisition of heat tolerance by the yeast *Saccharomyces cerevisiae*. *FEMS Microbiol. Rev.* 11, 339–355.
29. Richards, K. D., Schott, E. J., Sharma, Y. K., Davis, K. R., Gardner, R. C. (1998) Aluminum induces oxidative stress genes in *Arabidopsis thaliana*. *Plant Physiol.* 116, 409–418.
30. Ruis, H., Schller, C. (1995) Stress signaling in yeast. *Bioessays* 17, 959–965.

31. Sárdi, É., Balla, J. (1997) Effect of *Fusarium* infection on the formaldehyde cycle in *Citrullus vulgaris* L. In: *Abst. Intern. Cong. Stress of Life. Stress and Adaptation from Molecules to Man*. Budapest, p. 180.
32. Tyihák, E., Király-Véghely, Zs., Gullner, G., Szarvas, T. (1989) Temperature-dependent formaldehyde metabolism in bean plants. The heat shock response. *Plant Sci.* 59, 133–139.
33. Tyihák, E., Szöke, É. (1992) Measurement of formaldehyde and some fukky N-methylated substances in tissue cultures of *Datura innoxia*. *Plant Growth Reg.* 20, 317–320.
34. Tyihák, E., Rozsnaya, Z., Sárdi, É., Szöke, É. (1992) Formaldehyde cycle and the cell proliferation: Plant tissue as a model. In: Tyihák, E. (ed.) *Proc. 3rd Intern. Conf. on the Role of Formaldehyde in Biological Systems*. Hungarian Biochemical Society, Budapest, pp. 139–144.





## RELATIONSHIPS BETWEEN DEMETHYLASE ACTIVITY, FORMALDEHYDE AND OXYGEN DURING INCUBATION OF *RHODOCOCCLUS ERYTHROPOLIS* WITH VERATRATE\*

MARZANNA PAŹDZIOCH-CZOCZRA and ELŻBIETA MALARCZYK

Department of Biochemistry, Maria Curie-Skłodowska University, Lublin, Poland

(Received: 1998-10-28; accepted: 1998-11-25)

Relationships between demethylase activity, formaldehyde and oxygen were investigated. Demethylase activity was measured against the following substrates: veratric, vanillic, and isovanillic acids, as well as in the presence of guaiacol. The influence of ATP and GTP on demethylase activity was also checked. Demethylase activity was found to be dependent on the capability of the cells for endogenous oxygen uptake. In some cases ATP produced the opposite effect: instead of being taken up, oxygen was released, which suggested a reversibility of the demethylation reaction. Curiously enough, GTP demonstrated the same effect. Changes in enzyme activity were correlated with those occurring in the level of formaldehyde. The latter increased after addition of ATP, but decreased after addition of GTP.

**Keywords:** Demethylation – demethylase – formaldehyde – *Rhodococcus erythropolis* – veratric acid

### INTRODUCTION

All biological systems have HCHO-yielding potentials, which can originate from demethylation and methylation processes [12]. Enzymatic methylation reactions proceed with formaldehyde release, and all methyl groups generate formaldehyde [11].

Participation of formaldehyde in the demethylation reaction of veratric acid was proved by Ribbons [9, 10] in his research on *Pseudomonas aeruginosa* and *P. testosteroni*. He showed that the reaction needed 4 atoms of oxygen, and that this process was not stoichiometric, as more than one mole of formaldehyde per one methoxyl group ( $-\text{OCH}_3$ ) was released in the reaction. These results made it possible to develop a scheme of demethylation of methoxyphenolic compounds. According to this scheme, oxidative demethylation proceeds with the participation of demethylating

\* Presented at the 4th International Conference on the Role of Formaldehyde in Biological Systems, July 1-4, 1998, Budapest, Hungary.

Send offprint requests to: Dr. Marzanna Paździoch-Czochra, Department of Biochemistry, Maria Curie-Skłodowska University, Lublin, Poland.

Abbreviations: VER – veratric acid, VAN – vanillic acid, IVA – isovanillic acid, GU – guaiacol, ATP – adenosine triphosphate, GTP – guanosine triphosphate.

monooxygenase (demethylase) and simultaneously, formaldehyde production [9, 10]. A similar enzyme was found by Bernhardt et al. [1, 2] in *Pseudomonas putida*. It was a multienzymatic membrane complex, responsible for monooxygenase activity.

*Nocardia* and *Rhodococcus* strains are able to decompose methoxyphenolic compounds in the demethylation reaction. Veratric acid (two methoxyl groups) was degraded by the above strains of *Acitnomycetes* to vanillic and isovanillic acids, both resulting from partial demethylation of veratrate and protocatechuic acid-product of the total demethylation of veratrate under the effect of 3-O and 4-O-demethylases [3, 4, 6]. Each reaction followed the scheme proposed by Ribbons [9, 10], which meant that it was accompanied by oxygen uptake, and formaldehyde was released in the process. Guaiacol (the result of decarboxylation of vanillic acids) and catechol (the result of decarboxylation of protocatechuic acid) also appeared among the products of degradation of veratrate [8]. Investigation of the properties of demethylases has shown a constitutive character for 4-O-demethylase and an inducible one for 3-O-demethylase [7]. The demethylation reaction of veratrate may be reversible, although no unequivocal evidence has been obtained so far. It was illustrated only by using formaldehyde- $^{14}\text{C}$ , which can be incorporated into the methoxyl group. Formaldehyde may be a bearer of the methoxyl group in the methylation/demethylation reaction and thus become a main regulator in these processes [5, 7]. Demethylation of veratrate – a substrate for the two demethylases – is accompanied by oscillatory changes in the level of endogenous oxygen uptake, that is consequently a substrate for inducible monooxygenases [6, 8].

In our earlier research we proved that cells of *Rhodococcus erythropolis* showed different reactions at the maximum and minimum oxygen uptakes in the presence of effectors. This paper demonstrates relations between demethylase activity, formaldehyde and oxygen uptake, at different stages of oxygen uptake.

## MATERIALS AND METHODS

### *Biological material*

*Rhodococcus erythropolis* (*Nocardia* DSM 1069) was subcultured on agar medium supplemented with 0.04% guaiacol, prepared according to Malarczyk [4]. The strain grown in this medium grew less intensively than that on the standard medium, but it adapted to the metabolism of methoxyphenolic compounds.

### *Cultures of Rhodococcus erythropolis*

The cells were transferred from agar slants to the liquid medium without the guaiacol described above. Cultures were grown in 250 ml conical flasks filled with 100 ml of liquid medium on a rotary shaker (150 rpm/min) at 30 °C until the middle-loga-



rhythmic phase of their growth was reached. Finally the cells were collected by centrifugation at  $10^4 \times g$ , and a suspension of optical density  $A_{660} = 1$ , prepared with an adequate portion of 0.06 M phosphate buffer, pH 7.4.

### Induction experiments

Veratric acid (0.02%) in the form of Na-vertrate was added to this suspension as an inducer, and incubation was continued on a rotary shaker at 30 °C in the dark. The determination of oxygen uptake by *Rhodococcus erythropolis* cells started with the addition of vertrate and was measured with a biological oxygen monitor (YSI model 5300) in 3 mL incubation suspension. The cells were collected separately at the start of incubation, during the maximum and minimum oxygen uptake, as well as between the two stages (intermediate) (Fig. 1).

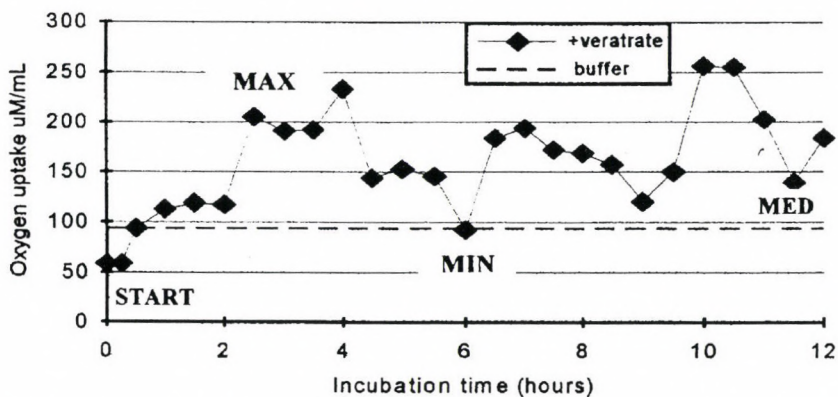


Fig. 1. Changes in oxygen level during incubation of *Rhodococcus erythropolis* cells with veratric acid (0.02%)

### Enzyme assay

The measurements of biological oxygen uptake were carried out according to Malarczyk [6]. Similarly the influence of ATP and GTP on demethylase activity was examined. We added an extra  $3.34 \times 10^{-3} \%$  ATP and GTP before and after adding phenolic substrates.

### Formaldehyde assay

The formaldehyde concentration, after assaying demethylase activity, was determined spectrophotometrically with the Merck test (Darmstadt, Germany). The formaldehyde test was also made on phenolic compounds alone and the values obtained taken into consideration is the determinations of formaldehyde.



## RESULTS

Our results showed that the oxygen uptake was dependent on the stage of the cells, in the presence of phenolic compounds (MF). Oxygen release (values below 0) was observed for cells at the start in the presence of guaiacol, and at the intermediate stage in the presence of veratric acid. In the other cases only oxygen uptake was noticed. The greatest differentiation in the oxygen level was observed in the presence of veratrate, vanillate and guaiacol.

In further investigations, the influence of ATP on oxygen uptake and the level of HCHO was examined (Fig. 2). ATP added after MF compounds brought oxygen release for all stages in the presence of veratric acid, vanillic acid (except cells at the start), and at the initial and intermediate stages in the presence of isovanillic acid. Guaiacol combined with ATP also released oxygen in the cells at the start. At the maximum stage ATP showed the opposite effect in the presence of vanillic and isovanillic acids, which might be due to the different position of the methoxyl group in these compounds.

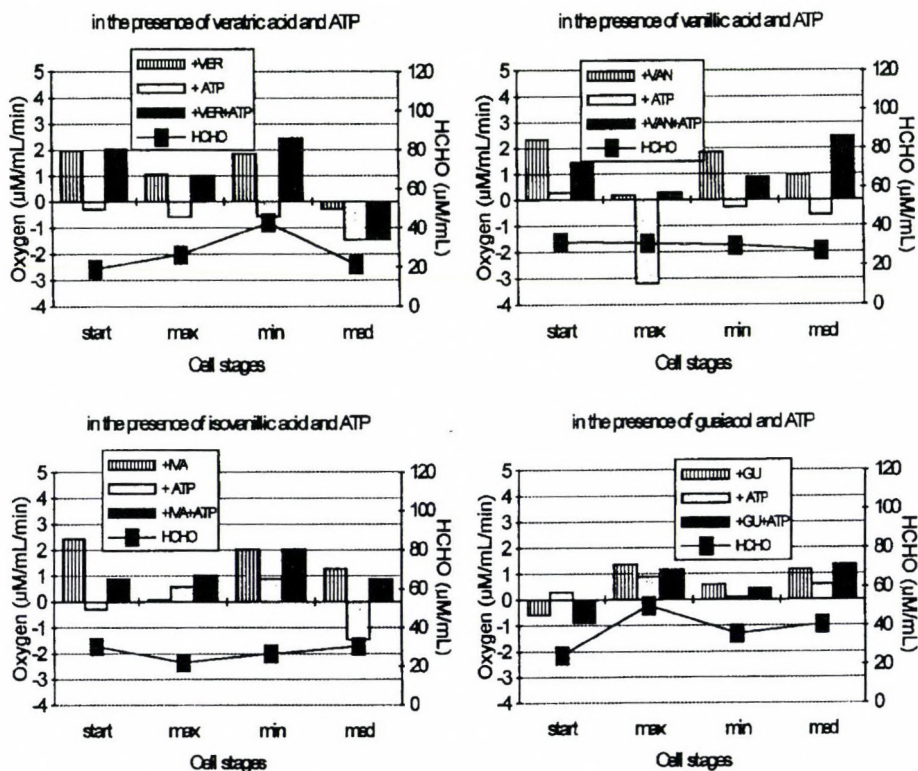


Fig. 2. Changes in oxygen uptake and concentration of HCHO in the presence of MF compounds and ATP (added after the addition of MF). Columns denote oxygen uptake, and the line HCHO concentrations

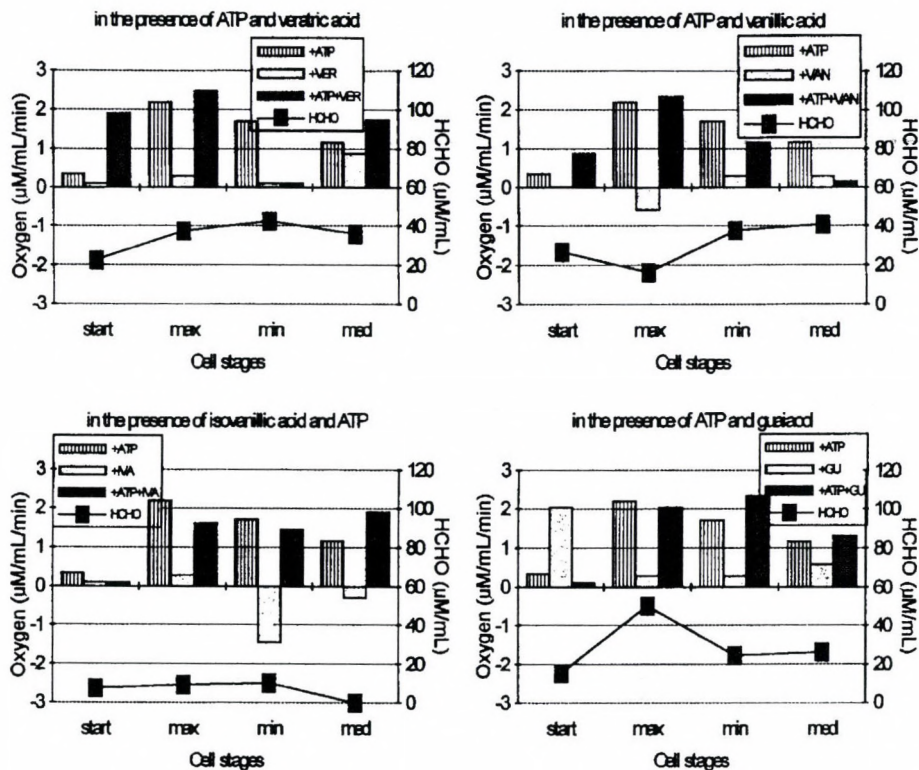


Fig. 3. Changes in oxygen uptake and concentration of HCHO in the presence of MF compounds and ATP (added before the addition of MF). Columns denote oxygen uptake, and the line HCHO concentrations

Addition of ATP before MF compounds inhibited oxygen release in the presence of veratrate (Fig. 3), which was observed when ATP was added after a MF compound. Added ATP demonstrated the opposite behavior in the presence of vanillic and isovanillic acids. ATP made oxygen release at the maximum in the presence of vanillate and at the minimum in the presence of isovanillate, but the minimum oxygen uptake was noted in the presence of vanillate, and the maximum one in the presence of isovanillate. Consequently the influence of GTP was also checked. Addition of GTP after MF compounds decreased the oxygen uptake, which was observed for MF compounds alone (Fig. 4). Thus GTP emphasized a different behavior of the cells in the presence of vanillate and isovanillate, because at the maximum oxygen release for vanillate and oxygen uptake for isovanillate was observed. GTP decreased the HCHO level in comparison with that observed for ATP. The highest HCHO concentration was demonstrated in the presence of guaiacol. Adding GTP before MF compounds decreased the effect of phenolic compounds (Fig. 5). At the minimum oxygen uptake, GTP resulted in oxygen release, but a subsequent addition of MF compounds effected oxygen uptake.



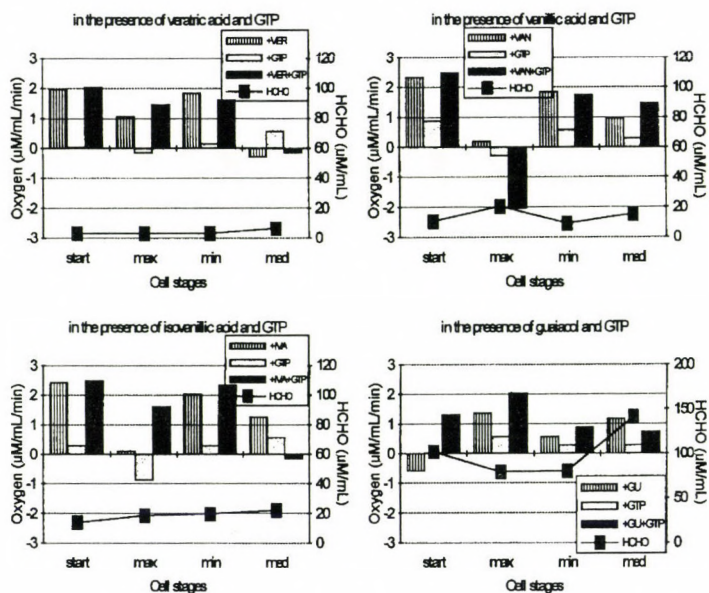


Fig. 4. Changes in oxygen uptake and concentration of HCHO in the presence of MF compounds and GTP (added after the addition of MF). Columns denote oxygen uptake, and the line HCHO concentrations

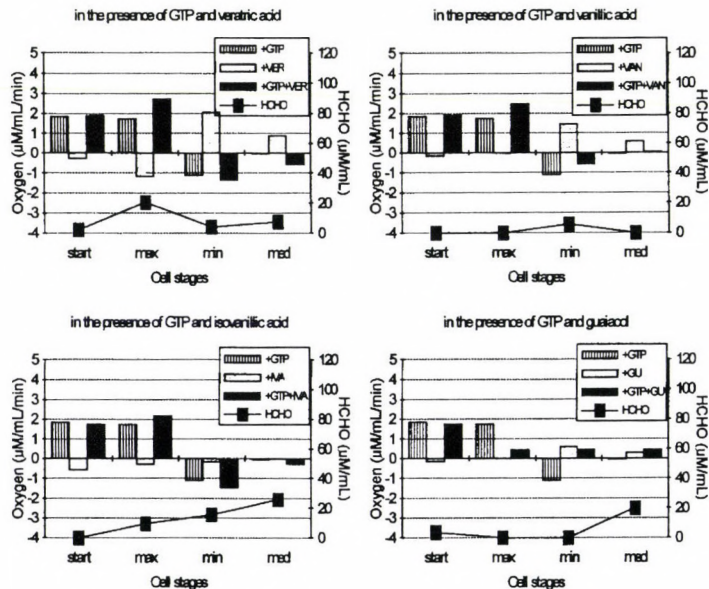


Fig. 5. Changes in oxygen uptake and concentration of HCHO in the presence of MF compounds and GTP (added before the addition of MF). Columns denote oxygen uptake, and the line HCHO concentrations



At the other stages we observed oxygen uptake in the presence of GTP, which turned in most cases into oxygen release after addition of phenolic compounds: at the start for all phenolic compounds, at the maximum for veratric, vanillic and isovanillic acids, at the minimum for isovanillic acid. We observed no HCHO in the presence of vanillic acid at the initial, maximum and intermediate stages; in the presence of isovanillic acid at the start, and for guaiacol at the maximum and minimum stage.

## DISCUSSION

*Rhodococcus erythropolis* cells incubated with veratric acid showed a varied capability of endogenous oxygen uptake. They also revealed different respiratory properties, which depended on the level of oxygen uptake. During experiments, we distinguished 4 oxidative cell stages, designated as start, maximum, minimum and medium (Fig. 1). For each group of cells, belonging to separate stages, changes in oxygen uptake were determined in the presence of methoxyphenolic compounds. These were veratric (VER), vanillic (VAN), and isovanillic (IVA) acids, and guaiacol (GU), as products of partial demethylation of veratric acid. Having completed the measurements of oxygen uptake, the level of formaldehyde was determined in the reaction medium. The same determinations were repeated in the presence of ATP and GTP, taking account of double sequence of additions of nucleotides, adding them before and after MF compounds. Indeed, addition of high-energetic compounds influenced oxygen uptake in all measurements, turning the process of oxygen uptake into that of oxygen release. The greatest differences in oxygen level always occurred at the maximum and minimum stages. The type of MF compounds, and the type and sequence of addition of nucleotides distinctly differentiated the investigated cell material. It was observed that smaller differences occurred in the oxygen level after addition of GTP, whereas the highest concentration of HCHO was present in the medium. This indicated a higher efficiency of the demethylation process. GTP stabilized the oxygen uptake, if added after MF substrate. When GTP was added before the substrate, addition of substrate distinctly decreased the oxygen uptake and HCHO production. These correlations appeared distinctly in the presence of guaiacol. ATP added at the beginning of measurements, before adding the substrate, inhibited HCHO production, as was seen in the presence of isovanillic acid. When ATP was added as secondary effector, the production of HCHO increased 3 times.

These observations indicated the essential participation of phosphorylating factors in the demethylation process of methoxyphenols. These last seem to compete with the appropriate MF substrate, causing strong modifications in the direction of oxygen transformations from oxygen uptake into oxygen release. According to the reaction of Ribbons [9, 10], it would be an effect of reversibility of the directions of reaction, when a high oxygen level is accompanied by a low HCHO level and vice versa.

## ACKNOWLEDGEMENT

This work was supported by a grant from the Polish Committee of Scientific Research, no. 5P06A 01414.

## REFERENCES

1. Bernhardt, F.-H., Staudinger, H., Ulrich, V. (1970) The properties of p-anisate O-demethylase in cell-free extracts of *Pseudomonas* sp. (German). *Z. Physiol. Chem.* 351, 467–478.
2. Bernhardt, F.-H., Pachowsky, H., Staudinger, H. (1975) A 4-methoxybenzoate O-demethylase from *Pseudomonas putida*. A new type of monooxygenase system. *Europ. J. Biochem.* 57, 241–256.
3. Eggeling, L., Sahm, H. (1980) Degradation of coniferyl alcohol and other lignin-related aromatic compounds by *Nocardia* sp. DSM 1069. *Arch. Microbiol.* 126, 141–148.
4. Malarczyk, E. (1984) Substrate induction of veratric acid O-demethylase in *Nocardia* sp. *Acta Biochim. Polon.* 31, 383–395.
5. Malarczyk, E., Rogalski, J., Kochmańska-Rdest, J., Leonowicz, A. (1987) Formaldehyde as the possible substrate in formation and methylation of aromatic ring. In: *Proc. II Formaldehyde Conference*, Keszthely, Budapest, Sote Press, pp. 184–188.
6. Malarczyk, E. (1989) Transformation of phenolic acids by *Nocardia*. *Acta Microbiol. Polon.* 38, 45–53.
7. Malarczyk, E. (1991) The role of formaldehyde in regulation of 3- and 4-O-demethylase systems in *Nocardia*. *ABC 1*, 9–14.
8. Malarczyk, E., Kochmańska-Rdest, J. (1990) New aspects of cor-regulation of decarboxylation and demethylation activities in *Nocardia*. *Acta Biochim. Polon.* 34, 145–148.
9. Ribbons, D. W. (1970) Stoichiometry of O-demethylase activity in *Pseudomonas aeruginosa*. *FEBS Letters* 8, 101–104.
10. Ribbons, D. W. (1971) Requirement of two protein fractions for O-demethylase activity in *Pseudomonas testosteroni*. *FEBS Letters* 12, 161–165.
11. Tyihák, E. (1987) Is there a formaldehyde cycle in biological systems? In: *Proc. II Formaldehyde Conference*, Keszthely, Budapest, Sote Press, pp. 137–144.
12. Tyihák, E., Szőke, É. (1996) Measurement of formaldehyde and some fully N-methylated substances in tissue cultures of *Datura innoxia*. *Plant Growth Reg.* 20, 317–320.



# COMPARATIVE QUANTITATIVE CHROMATOGRAPHIC DETERMINATION OF FORMALDEHYDE IN DIFFERENT GROUPS OF PHYSIOLOGICAL AND PATHOLOGICAL HARD TISSUES OF TEETH\*

T. KATARZYNA RÓŻYŁO<sup>1</sup> and R. SIEMBIDA<sup>2</sup>

<sup>1</sup>Institute of Dentistry, Medical University of Lublin, Lublin, Poland

<sup>2</sup>Faculty of Chemistry, M. Curie-Skłodowska University, Lublin, Poland

(Received: 1998-10-28; accepted: 1998-11-25)

Taking into consideration that HCHO level in cells of plant, animal and human tissues as well as in body fluids depends from physiological state of an organism in the current study it was decided to find out if there are changes of HCHO level in different physiological and pathological hard tissues of teeth. The obtained results showed in all 4 groups of teeth separately analysed that there were some regularities in the level of HCHO as far as similar physiological or pathological states are concerned. This was best seen when comparing the obtained results with mean HCHO level of the studied groups of teeth.

**Keywords:** Formaldehyde – quantitative TLC – stress in human tissues – HCHO in human teeth

## INTRODUCTION

Nowadays the issue of oral pathology and in particular of dental pathology is not only a morbidity problem but an important social problem as well. During recent years more and more attention has been paid to studies of human teeth and their state (physiological and pathological). Various analytical methods were used in these studies but chromatography proved to be one of the most efficient for this purpose. So far it is generally believed that pathological changes of hard tissues of teeth and in periodontal tissues are mainly the result of deficit of microelements such as fluorine. The studies of composition of proteins of human teeth and particularly of their basic component – collagen (90% of organic matter of teeth) were described [3], while the content of many other substances in teeth-proteins among other – has also been described [18]. The relationships between physical and chemical properties of hard tissues of teeth and their biochemical components were extensively studied in

\* Presented at the 4th International Conference on the Role of Formaldehyde in Biological Systems, July 1-4, 1998, Budapest, Hungary.

Send offprint requests to: Dr. med. T. Katarzyna Różyło, D. Sc., Department of Dentistry, Medical University of Lublin, Karmelicka str. 7, 20-081 Lublin, Poland.



[4, 6–8]. The role of aminoacids in tissues of living organisms as well as tissues of oral cavity was also examined [1]. Despite numerous considerable achievements the hitherto existing studies did not give clear answer concerning the relation between physiological state of teeth and their chemical content.

Lately the importance of formaldehyde (HCHO) in biological systems came to light. It was proved [8, 9] that HCHO was not a by-product in these systems but rather their basic and indispensable component. HCHO is formed inside plant cells, animal and human tissues. It is formed intracellularly in the course of enzymatic transmethylation of histamine. Biochemical research using radioactive isotopes and experimental data presented by other authors suggest presence of so-called HCHO cycle [16, 17]. The formaldehyde reacts with the amino group of an amino acid forming a methyloprotein complex. The hydroxymethyl ( $-\text{CH}_2\text{OH}$ ) group of this complex is labile and can be transferred to an acceptor molecule [12]. On the basis of the papers [1, 9–13] it was proved that in tissues of human teeth there were analysable amounts of HCHO. Thus they confirmed the information [2, 5] on possibilities of analysis of HCHO levels in human tissues.

In our previous works we demonstrated that there exists a relation between HCHO level and physiological state of hard tissues of teeth. We found that the higher level of HCHO was observed in the case of carietic teeth. The current study was aimed to find out if the observed changes in HCHO levels in different physiological and pathological hard tissues of teeth show characteristic regularities. We concentrated on studying the problem if there are observed regularities in HCHO level in hard tissues of healthy and pathologic teeth.

## MATERIALS AND METHODS

Four groups of teeth (5 teeth in each group) were used in the study:

- I. deciduous teeth
- II. orthodontic teeth
- III. periodontal teeth
- IV. retained teeth
- V. carietic teeth.

### *Preparation of teeth for analysis*

After mechanical purification and drying the studied teeth were preliminarily brought up in order to obtain the particles of 0.5–1 mm. Then they were individually pulverised by means of the vibrational mortar Pulverisette (Fritsch, Germany) during 1 hour. The pulverised teeth from each group were mixed and homogenized.

## Quantitative chromatographic determination of HCHO in teeth

### HCHO extraction

0.25 g of the pulverised sample was weighed and placed in polyethylene container for centrifugation of eppendorf type of 1.5 cm<sup>3</sup> volume. 0.4 dm<sup>3</sup>F of methanole solution of dimedone, as capture molecule of HCHO was added. The extraction was carried out during 1 hour in a mechanical shaker. After the extraction the mixture was centrifuged during 6 min in order to separate the precipitate. The optimum dimedone concentration for extraction was chosen in experimental way –100 g/cm<sup>3</sup>. During the analysis it was attempted to minimise air access to solutions containing dimedone due to possibility presence of trace amounts of HCHO in laboratory atmosphere.

### Synthesis of HCHO-dimedone adduct standard

Less than stochiometric amount of HCHO (10 cm<sup>3</sup> of 37% HCHO solution) was added to hot alcohol solution of dimedone (2.5 g of dimedone + 15 cm<sup>3</sup> of ethanol + 2.5 cm<sup>3</sup> of water). The obtained adduct was crystallised and purified by means of repeated crystallisation with ethanol.

### Chromatographic analysis

The analysis was carried out on Silica Gel F<sub>254</sub> plates on aluminum foil (Merck). Twenty µl of studied extracts were applied on the plates with the use of TLC Applicator AS 30 of Desaga (Germany) in nitrogen atmosphere. The blind sample was the dimedone solution used for extraction as well as 5 µl of methanol solutions of HCHO-dimedone adduct standard in concentration range from 0.05 to 0.50 mg/cm<sup>3</sup>. In order to limit air access after application of the following samples the application sites were covered with a glass plate. The chromatogram was developed immediately after application. As the mobile phase there were used the chloroform-dichloromethane solutions (10 : 30 v/v). The development of chromatogram was carried out in US chamber. After the development the adduct reaches RF of about 0.4–0.5 (the spot is visible in UV light at 254 nm wave length). The quantitative analysis was carried out using CS-9001 PC Shimadzu densitometer at the 275 nm wave length.

## RESULTS AND DISCUSSION

The HCHO level determined in the form of the dimedone adduct formaldemethone is presented in Table 1, as densitograms of particular investigated samples (Figs 1–4) and in the form of diagrams in Fig. 5. In Table 1 in two cases in the samples 3 and 4 there are no data concerning the group of teeth number III due to difficulties in collecting sufficient amount of comparative material. However, a general tendency can

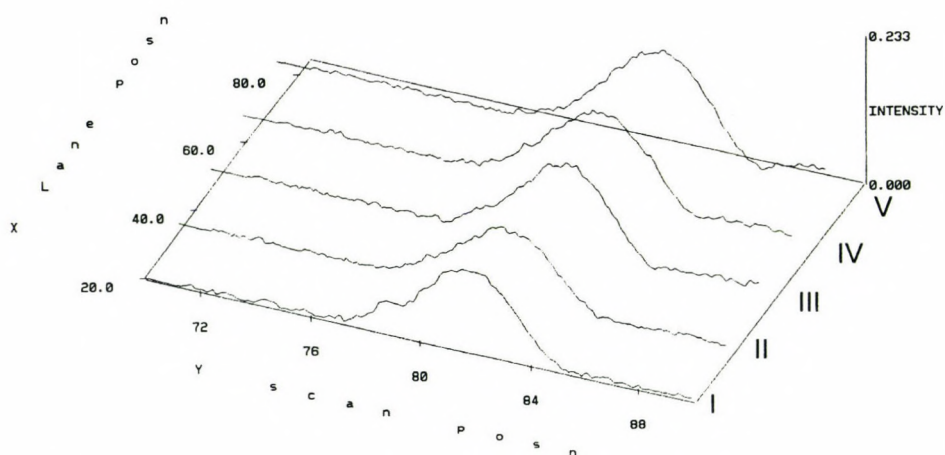


Fig. 1. Densitograms of formaldehyde in samples of teeth in the experiment 1. I – deciduous teeth; II – orthodontic teeth; III – periodontal teeth; IV – retained teeth; V – carietic teeth

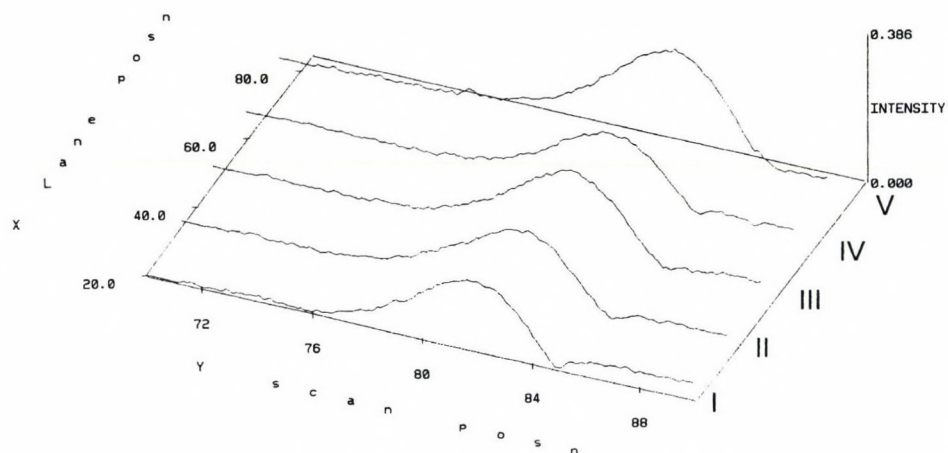


Fig. 2. Densitograms of formaldehyde in samples of teeth in the experiment 2. For details see Fig. 1

be observed that quantitative values of formaldehyde are similar in different samples within the same groups of teeth. So the highest formaldehyde level is observed in the case of carietic teeth in all samples. In one case (sample I, 1) relatively high HCHO level provides evidence that deciduous teeth were also carietic.



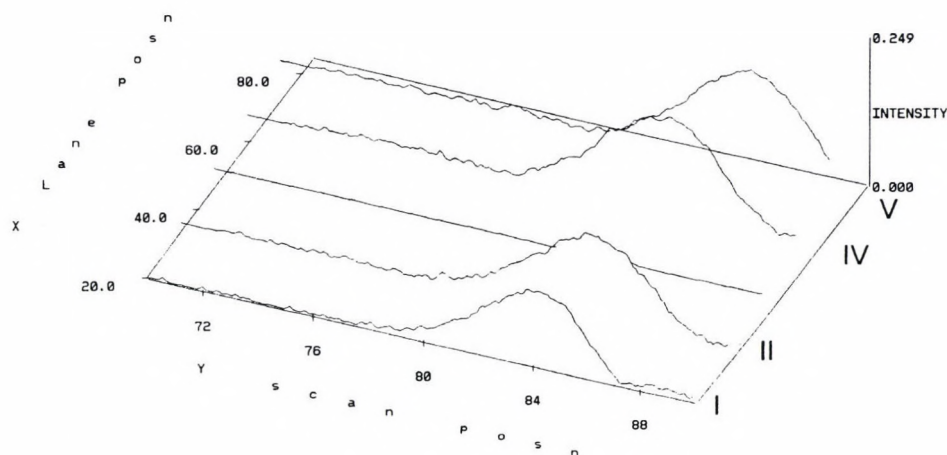


Fig. 3. Densitograms of formaldemethone in samples of teeth in the experiment 3. For details see Fig. 1

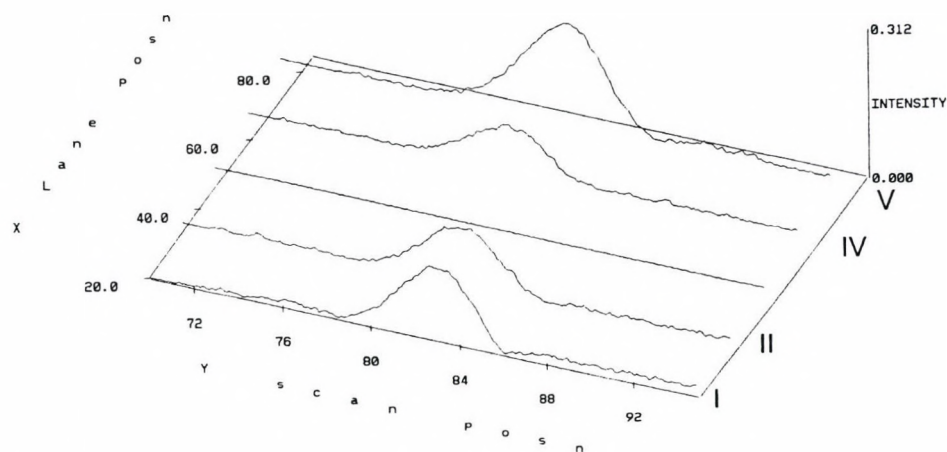


Fig. 4. Densitograms of formaldemethone in samples of teeth in the experiment 4. For details see Fig. 1

Relatively low HCHO level is detected in teeth extracted due to orthodontic reasons because these teeth are sound teeth. Similar HCHO levels are found in periodontal teeth that is ones where pathological process is limited to periodontal tissues while the tooth itself is healthy. Considerable differences in HCHO levels were observed in

retained teeth. These teeth, apart from being retained, are affected also by concomitant pathological changes such as for instance inflammatory changes in periodontal tissue.

On the basis of these more extensive studies it can be generally concluded that undoubtedly there exist regularities concerning HCHO level in hard tissues of teeth.

*Table 1*  
Level of formaldehyde (in dimedone adduct form) in different human teeth

Sample	Group		a) Mass of FD [chromatogram] / b) [µgFD in 20 µl of extract]									
			I		II		III		IV		V	
	a	b	a	b	a	b	a	b	a	b	a	b
1	0.024	<b>0.120</b>	0.015	<b>0.075</b>	0.029	<b>0.145</b>	0.029	<b>0.145</b>	0.050	<b>0.250</b>		
2	0.031	<b>0.155</b>	0.028	<b>0.140</b>	0.025	<b>0.125</b>	0.013	<b>0.065</b>	0.049	<b>0.245</b>		
3	0.019	<b>0.095</b>	0.030	<b>0.150</b>	—		0.045	<b>0.255</b>	0.045	<b>0.225</b>		
4	0.051	<b>0.255</b>	0.032	<b>0.160</b>	—		0.021	<b>0.105</b>	0.059	<b>0.295</b>		
Average value	0.0312	<b>0.156</b>	0.0263	<b>0.131</b>	0.027	<b>0.135</b>	0.0285	<b>0.1425</b>	0.0508	<b>0.2538</b>		

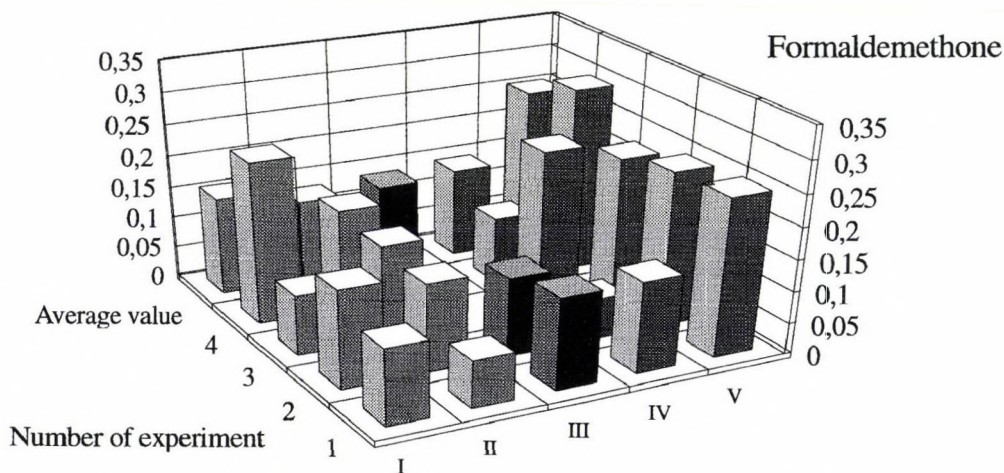


*Fig. 5.* Diagram of the amount of formaldehyde as dimedone adduct (formaldemethone) in different samples of teeth (µg/20 µl of the extract). 1, 2, 3, 4 – numbers of particular experiments. I – deciduous teeth, II – orthodontic teeth, III – periodontic teeth, IV – retained teeth, V – carietic teeth

It is most clearly visible on the diagram containing average HCHO values (in the form of formaldemethone) from 4 independent experiments (diagrams 5 in Figures 1–5). At present the connection between these values and metabolism in cells of hard tissues of teeth should be established. In order to do this it is necessary to compare HCHO levels in tissues of teeth with levels of its potential generators, but such investigations would exceed the boundaries of the present paper.

## REFERENCES

1. Eastoe, J. E. (1963) The amino acid composition of proteins from oral tissues. *Arch. Oral. Biol.* 8, 633–652.
2. Heck, E., d'A. Casanova, M., Star, T. B. (1990) Formaldehyde toxicity – new understanding. *Crit. Rev. Toxicol.* 20, 397–426.
3. Hohling, H. J. (1966) *Die Bauelemente von Zahnschmelz und Dentin aus morphologischer, chemischer und struktureller sicht*. Hauser, München.
4. Kalász, H., Kovács, G. H., Nagy, J., Tyihák, E., Barnes, W. T. (1978) Identification of N-methylated basic amino acids from human adult teeth. *J. Dent. Res.* 57, 128–132.
5. Kucharczyk, N., Yang, J. T., Wong, K. K., Sofia, R. D. (1984) The formaldehyde donating activity of N<sup>5</sup>, N<sup>10</sup>-methylene tetrahydrofolic acid in xenobiotic biotransformation. *Xenobiotica*, 14, 667–676.
6. Lezovic, Y., Ziman, M., Hochman, G. (1974) Gel chromatography of proteins from human teeth. *J. Chromatogr.* 96, 258–261.
7. Mechanić, G. L., Katz, E. P., Glimcher, M. J. (1966) The sephadex gel filtration characteristics of the neutral soluble proteins of embryonic bovine enamel. *Biochim. Biophys. Acta*, 133, 97–113.
8. Nord, C. E. (1970) Fractionation of hyaluronidases from dental plaque material by ion-exchange chromatography and gel filtration. *Acta Odont. Scand.* 28, 223–232.
9. Rózyło, T. K. (1996) Planar chromatography and densitometric determination of formaldehyde in hard tissues of teeth. *J. Planar Chromatogr.* 9, 141–143.
10. Rózyło, T. K. (1995) Planar chromatography and densitometric determination of formaldehyde in hard tissues of teeth. *Chem. Environ. Res.* 4, 129–134.
11. Rózyło, T. K. (1998) Quantitative TLC determination of formaldehyde in hard tissues of teeth. *Biomed. Chromatogr.* 12, 1–4.
12. Siembida, R., Rózyło, T. K. (1998) The problem of optimal conditions of quantitative determination of HCHO in hard tissues of teeth by TLC. In: *Proc. Int. Symposium on Instrumental Planar Chromatography*, Visegrád (Hung.), pp. 223–228.
13. Siembida, R., Rózyło, T. K., Jamrózek-Mańko, A. (1998) The dependence of optimal conditions of quantitative determination of formaldehyde in hard tissues of teeth on different analytical factors. In: *Abstracts 4th Int. Conference on Role of Formaldehyde in Biological Systems*. Budapest, p. 54.
14. Szende, B., Tyihák, E., Szokan, G., Kátay, G. (1995) Possible role of formaldehyde in the apoptotic and mitotic effect of 1-methyl-ascorbigen. *Path. Oncol. Res.* 1, 38–42.
15. Tyihák, E., Huszti, S. (1986) Formation of formaldehyde from S-adenosyl-L-(methyl-<sup>3</sup>H)methionine during enzymatic transmethylation of histamine. *FEBS Letter* 209, 362–366.
16. Tyihák, E., Szőke, E. (1996) Measurement of formaldehyde and some N-methylated substances in tissue cultures of *Datura innoxia*. *Plant Growth Res.* 20, 317–320.
17. Tyihák, E. (1977) Study of formaldehyde cycle in budding and apoptosis of trees by personal OPLC. In: Kaiser, O. et al. (eds) *Chromatography*. InCom Sonderband, Düsseldorf, Germany, pp. 333–342.
18. Veis, A., Spector, A. R. (1972) The isolation of an EDTA-soluble phosphoprotein from mineralizing bovine dentine. *Biochim. Biophys. Acta*, 257, 404–413.





# ARE THE REDUCTIONS IN NEMATODE ATTACK ON PLANTS TREATED WITH SEAWEED EXTRACTS THE RESULT OF STIMULATION OF THE FORMALDEHYDE CYCLE?\*

T. JENKINS,<sup>1</sup> G. BLUNDEN,<sup>2</sup> YUE WU,<sup>2</sup> S. D. HANKINS<sup>3</sup> and B. O. GABRIELSEN<sup>4</sup>

<sup>1</sup>School of Biological Sciences and <sup>2</sup>School of Pharmacy and Biomedical Sciences, University of Portsmouth, Portsmouth, U.K.; <sup>3</sup>Maxicrop International Ltd., Corby, Northamptonshire, U.K.;

<sup>4</sup>Hydro Research Centre, Porsgrunn, Norway

(Received: 1998-10-28; accepted: 1998-11-25)

Soil application to the roots of tomato plants (*Lycopersicon esculentum*) of a commercially-available alkaline extract of the brown alga, *Ascophyllum nodosum*, resulted in a significant reduction in the number of second-stage juveniles of both *Meloidogyne javanica* and *M. incognita* invading the roots, compared to those of plants treated with water alone. Egg recovery from the seaweed extract treated plants was also significantly lower. The three major betaines found in the seaweed extract ( $\gamma$ -aminobutyric acid betaine,  $\delta$ -aminovaleric acid betaine and glycinebetaine) also led to significant reductions in both the nematode invasion profile and egg recovery when applied at concentrations equivalent to those present in the extract. This led to the conclusion that the betaines present in the seaweed extract play a major role in bringing about the observed effects.

Treatment of *Arabidopsis thaliana* plants with seaweed extract also resulted in a significant decrease in the number of females of *M. javanica* which developed in the roots. Significant reductions in egg recovery were also achieved from plants treated with the seaweed extract and similar effects were produced with the betaines found in the seaweed extract. As the experiments were conducted under monoxenic conditions, it can be concluded that the results obtained with the application of either the seaweed extract or betaines are not dependent on microorganisms associated with the rhizosphere.

**Keywords:** Seaweed extract – root-knot nematode – *Meloidogyne* species – betaines – formaldehyde cycle

## INTRODUCTION

Extracts of marine brown algae are used in agriculture and many economically-useful results have been recorded after application of these products [1]. The alga most commonly used for the production of the commercial extracts in Europe and North America is *Ascophyllum nodosum* (L.) Le Jol. One of the benefits claimed for the

\* Presented at the 4th International Conference on the Role of Formaldehyde in Biological Systems, July 1-4, 1998, Budapest, Hungary.

Send offprint requests to: Dr. T. Jenkins, School of Biological Sciences, University of Portsmouth, King Henry 1st Street, Portsmouth, PO1 2DY, U.K.

extracts is that treated plants have increased resistance to pathogen attack [1]. In particular, there are several reports which show that application of seaweed extracts to plants resulted in decreased levels of nematode attack [11]. The effects on root-knot nematodes (*Meloidogyne* species) have been studied using products derived from *Ecklonia maxima* (Osbeck) Papenfuss [3, 4], and *A. nodosum* [5, 11, 12]. In all cases, application of the seaweed products resulted in reduced root-knot nematode infection of the plants.

The compounds in the seaweed extract responsible for increasing the resistance of treated plants to root-knot nematode attack have not been determined, although it has been suggested [4] that the effects could be due to cytokinins present in the seaweed extracts. However, the role of betaines in the extracts could also be of importance. The *A. nodosum* extracts used contain  $\gamma$ -aminobutyric acid betaine,  $\delta$ -aminovaleric acid betaine and glycinebetaine [2]. When applied at low concentrations, betaines have been demonstrated to increase the resistance of plants to attack by fungi [6, 7, 10]. It was decided, therefore, to determine the possible involvement of the betaines present in the *A. nodosum* extracts in conferring resistance to root-knot nematode attack by plants treated with the extracts.

## MATERIALS AND METHODS

### *Seaweed extract*

The seaweed extract used was an aqueous alkaline extract of the brown marine alga *Ascophyllum nodosum*. This is marketed as Maxicrop Original (Maxicrop International Ltd.) and contains approximately 8% dissolved solids. When assayed for betaines [2], the extract used in the tomato trials was shown to contain  $\gamma$ -aminobutyric acid betaine (52 mg/L),  $\delta$ -aminovaleric acid betaine (15 mg/L) and glycinebetaine (4 mg/L), while the extract used in the *Arabidopsis* trial contained  $\gamma$ -aminobutyric acid betaine (62 mg/L),  $\delta$ -aminovaleric acid betaine (21 mg / L) and glycinebetaine (18 mg/L).

### *Nematodes*

For the tomato trials, *Meloidogyne javanica* and *M. incognita* were obtained from stock cultures maintained on tomato plants (*Lycopersicon esculentum* cv. Ailsa Craig). The eggs harvested from the entire root ball were hatched to release infective second stage juveniles (J2s) over 7 days at 25 °C in water [11].

For the *Arabidopsis* trial, eggs of *M. javanica* were obtained from egg sacs dissected from stock cultures maintained on tomato plants (cv. Tiny Tim). These eggs were hatched to release J2s over 2 days at 25 °C in water.



## Inoculation and treatment

### Tomato trials

In each experiment, a sample of 60 tomato plants (cv. Ailsa Craig), all at the 4-leaf stage and planted in approximately 450 cm<sup>3</sup> John Innes No. 1 compost, was divided into 2 groups of 6 experimental sets containing 5 plants per set, all arranged randomly. One set of 6 was used to determine invasion profiles, and the second set of 6 for egg recovery. The experimental sets were treated with 30 ml per plant of one of the following: (i) water, as a control; (ii) Maxicrop Original (36 ml diluted to 1 L), (iii)  $\gamma$ -aminobutyric acid betaine solution; (iv)  $\delta$ -aminovaleric acid betaine solution; (v) glycinebetaine solution (each betaine being applied in the same quantity as that present in the 3.6% Maxicrop Original solution); and (vi) a mixture of the three betaines in the concentrations applied in (iii), (iv) and (v).

Two plastic pipette tips with additional perforations were pushed into the soil to a depth of 2 cm on either side of the tomato stem. The inoculum (750 J2s of either *M. javanica* or *M. incognita*) was applied through the pipettes. Plants were inoculated 2 days after treatment and were watered every day. The plants were maintained under glasshouse conditions at 20 °C  $\pm$  4 °C.

### *Arabidopsis* trials

*A. thaliana* was grown in Gamborg's B5 medium (pH 6.4, 1.5% sucrose) containing 0.8% agar. The test solution was prepared by replacing the water of the medium with either 0.075% Maxicrop Original or a solution of betaines containing the same concentrations as those in the 0.075% Maxicrop Original solution. Approximately 10 ml medium, previously sterilized by autoclaving at 121 °C for 15 min, was used for each 9 cm i.d. plastic Petri dish, just to cover the base of the dish.

*A. thaliana* (Landsberg erecta) seeds were soaked for 1 min in 70% ethanol followed by 5 min in 1.05% sodium hypochlorite solution and 0.05% Tween 20. The surface-sterilized seeds were then washed 5 times in sterile water before being transferred to an agar plate (1 seed per plate). There were 15 replicates of each treatment. The plates were sealed with Parafilm and kept at 23 °C with a 16 : 8 h light : dark cycle.

A suspension of freshly hatched J2s of *M. javanica* was centrifuged at 1000 rpm for 2.5 min. The pellet of J2s was taken up in 4.5 ml water to which 0.5 ml 0.1% HgCl<sub>2</sub> solution was added. The tube was covered with Parafilm, the contents were mixed gently and then centrifuged at 100 rpm for 2.5 min. Most of the supernatant was removed with a sterile glass pipette, except for about 200  $\mu$ l, which contained the J2s. The surface-sterilized juveniles were washed 5 times, by replacing the supernatant with sterile water, followed by centrifugation, as described above. After the final wash, the J2 concentration was adjusted to 10 J2/ $\mu$ l. Ten days post-germination, each *A. thaliana* seedling was inoculated with 100 J2s, which were placed in the centre of the agar plate about 1 cm from the main root tip.

## Counting juveniles and eggs

### Tomato trials

Fourteen days post-inoculation, the roots of each plant were washed free from soil, bleached, stained with acid fuchsin and the number of juveniles in the root tissues counted [9].

After one generation, at 49 (*M. javanica*) and 63 (*M. incognita*) days post-inoculation, the egg sacs from each plant in each experimental set were removed using 1% sodium hypochlorite solution and the total numbers of eggs recovered from the egg sacs were counted under a microscope [9].

### Arabidopsis trials

At 45 days post-inoculation, the number of *M. javanica* females and eggs were counted under a microscope [10]. For the egg count, the plants were removed from the plates and the eggs extracted with 10 ml 1.05% sodium hypochlorite solution.

For both tomato and *Arabidopsis* trials, means and standard errors of the mean were calculated using *t*-test comparisons for significance. All statistical calculations utilized 'Minitab' computer programmes.

## RESULTS

Application of a 3.6% solution of an alkaline extract of *Ascophyllum nodosum* as a soil drench to tomato plants resulted in a significant reduction ( $P < 0.05$ ), compared to water-treated controls, in the number of second-stage juveniles of *Meloidogyne incognita* and *M. javanica* invading the roots (Table 1). Significant reductions ( $P < 0.05$ ) also resulted when  $\gamma$ -aminobutyric acid betaine,  $\delta$ -aminovaleric acid betaine and glycinebetaine were used in the same amounts as those applied in the seaweed extract. A mixture of these betaines also produced significant reductions (Table 1).

The soil drench treatment with the seaweed extract also led to a significant ( $P < 0.05$ ) reduction in egg recovery from plants infected with *M. incognita* and *M. javanica* after one generation (49 and 63 days, respectively, post-inoculation; Table 2). Similar significant reductions were achieved with the use of  $\gamma$ -aminobutyric acid betaine,  $\delta$ -aminovaleric acid betaine, glycinebetaine and a mixture of all three betaines, when used in the same quantities as those when the seaweed extract was used (Table 2).

Growing *Arabidopsis thaliana* plants under monoxenic conditions in the presence of the *A. nodosum* extract resulted in a significant ( $P = 0.05$ ) decrease in the number of *M. javanica* females found in the roots at 45 days post inoculation (Table 3). Similar results were obtained when the plants were grown in the presence of the mixture of  $\gamma$ -aminobutyric acid betaine,  $\delta$ -aminovaleric acid betaine and glycinebetaine



Table 1

Mean number ( $\pm$  standard error) of second stage juveniles (J2s) of *Meloidogyne incognita* and *M. javanica* per tomato plant 14 days post-inoculation

Nematode species	Mean number of J2s per plant					
	Control	Seaweed extract	GABAB	DAVAB	GB	Betaine mixture
<i>M. incognita</i>	106.2 $\pm$ 15.0	10.4 $\pm$ 6.4 P < 0.001	21.6 $\pm$ 5.7 P < 0.01	4.8 $\pm$ 3.6 P < 0.01	17.2 $\pm$ 7.4 P < 0.01	23.4 $\pm$ 4.9 P < 0.01
<i>M. javanica</i>	89.2 $\pm$ 11.0	9.6 $\pm$ 3.5 P < 0.01	55.6 $\pm$ 12.0 P < 0.05	52.2 $\pm$ 13.0 P < 0.05	19.4 $\pm$ 6.1 P < 0.001	68.0 $\pm$ 9.2 P = 0.096

GABAB =  $\gamma$ -aminobutyric acid betaine; DAVAB =  $\delta$ -aminovaleric acid betaine; GB = glycinebetaine; P = probability.

Table 2

Mean number ( $\pm$  standard error) of eggs of *Meloidogyne incognita* and *M. javanica* per tomato plant 63 and 49 days post-inoculation, respectively

Nematode species	Mean number of eggs per plant					
	Control	Seaweed extract	GABAB	DAVAB	GB	Betaine mixture
<i>M. incognita</i>	11400 $\pm$ 1800	660 $\pm$ 157 P < 0.05	1040 $\pm$ 225 P < 0.05	1320 $\pm$ 206 P < 0.05	940 $\pm$ 112 P < 0.05	1460 $\pm$ 448 P < 0.05
<i>M. javanica</i>	18540 $\pm$ 1569	4600 $\pm$ 899 P < 0.001	2940 $\pm$ 730 P < 0.001	6400 $\pm$ 1994 P < 0.001	3660 $\pm$ 453 P < 0.001	3260 $\pm$ 733 P < 0.001

GABAB =  $\gamma$ -aminobutyric acid betaine; DAVAB =  $\delta$ -aminovaleric acid betaine; GB = glycinebetaine; P = probability.

Table 3

Numbers of *Meloidogyne javanica* females observed in, and egg recovery from, *Arabidopsis thaliana* plants grown in a control medium and in a medium containing either seaweed extract or a mixture of betaines (45 days post-inoculation)

Treatment	Number of females per plant			Egg recovery per plant		
	mean	S.E.	P	mean	S.E.	P
Control	5.2	0.99	—	1011	202	—
Seaweed extract	3.0	0.86	0.05	590	123	<0.05
Betaine mixture	3.4	0.51	0.06	559	179	0.05

S.E. = standard error; P = probability.



in quantities equal to those present in the medium containing the seaweed extract. Significant reductions in egg recovery were recorded for the plants grown in media containing the seaweed extract and betaines (Table 3).

## DISCUSSION

The reduction in the numbers of eggs of both *Meloidogyne javanica* and *M. incognita* recovered from the roots of tomato plants after treatment with seaweed extract are consistent with earlier findings [11]. The seaweed extract treatment also resulted in significant reductions in the numbers of second stage juveniles of both nematode species which successfully invaded the roots. Similar results were obtained with the plants treated with the betaines found in the seaweed extract, either when applied separately or as a mixture. These data indicate clearly the major role played by the betaines present in the seaweed extract in reducing both the numbers of J2s invading the roots of tomato plants and the number of eggs recovered after one generation. However, the mode of action of the betaines is not obvious. One proposition is that the active constituents of the seaweed extract are absorbed by the plant and then undergo transformation, leading to the formation of compounds which are responsible for the reduction in root invasion by the nematodes. However, the seaweed extract may stimulate the growth of microorganisms in the rhizosphere, which could lead to the results observed. It was to resolve this problem that the experiments with *Arabidopsis thaliana* were undertaken as this is an established model host for developmental studies of plant parasitic nematodes under monoxenic conditions [8].

When *A. thaliana* was challenged with *M. javanica* under monoxenic conditions, the inclusion of seaweed extract in the growth medium resulted in significant reductions, both in numbers of females in the roots and in the numbers of eggs recovered 45 days after inoculation. Similar results were obtained when the betaines were incorporated into the growth medium. Seaweed extracts and betaines may have effects on soil microorganisms and may stimulate the growth of some which affect the level of nematode invasion. However, this work shows that the seaweed extract and its constituent betaines produce their effects independent of soil microorganisms.

The role of betaines and other quaternary ammonium compounds in increasing plant resistance to fungal attack has been reported [10]; this work linked the resistance of tomato plants to *Fusarium oxysporum* to their content of trigonelline, glycinebetaine and choline. Trigonelline has also been shown to be a potential resistance inducer in plants against obligate biotrophic fungi [6].

A formaldehyde cycle has been postulated for biological systems. All methyl groups are potential precursors and hence betaines are potential sources of formaldehyde. It has also been proposed that the formation of this compound is linked to the induction of disease resistance [7]. Our results are consistent with these findings. It is probable that the betaines in the seaweed extract are a major contributor to the

increased resistance shown by the plants treated with the seaweed extract, although other methylated compounds may be present in the extract which could potentially also contribute to the overall effect.

## REFERENCES

1. Blunden, G. (1991) Agricultural uses of seaweeds and seaweed products. In: Guiry, M. D., Blunden, G. (eds) *Seaweed Resources in Europe. Uses and Potential*. J. Wiley & Sons, Chichester, pp. 65–81.
2. Blunden, G., Cripps, A. L., Gordon, S. M., Mason, T. G., Turner, C. H. (1986) The characterisation and quantitative estimation of betaines in commercial seaweed extracts. *Bot. mar.* 29, 155–160.
3. Crouch, I. J., van Staden, J. (1993) Effect of seaweed concentrate from *Ecklonia maxima* (Osbeck) Papenfuss on *Meloidogyne incognita* infection on tomato. *J. appl. Phycol.* 5, 37–43.
4. Featonby-Smith, B. C., van Staden, J. (1983) The effect of seaweed concentrate on the growth of tomato plants in nematode infested soil. *Scientia Hortic.* 20, 137–147.
5. Gabrielsen, B. O., Chinnasri, B., Marwoto, B. (1998) *Seaweed extract against root-knot nematodes*. Presented at the 16th International Seaweed Symposium.
6. Kraska, T., Schönbeck, F. (1992) Resistance induction in plants by trigonelline and possible mechanisms. In: Tyihák, E. (ed.) *Proceedings of 3rd International Conference on Role of Formaldehyde in Biological Systems: Methylation and Demethylation Processes*. Hungarian Biochemical Society, Budapest, pp. 136–168.
7. Manninger, K., Csösz, M., Tyihák, E. (1992) Biochemical immunization of wheat plants to biotrophic fungi by endogenous, fully N-methylated compounds. In: Tyihák, E. (ed.) *Proceedings of 3rd International Conference on Role of Formaldehyde in Biological Systems: Methylation and Demethylation Processes*. Hungarian Biochemical Society, Budapest, pp. 157–162.
8. Sijmons, P. C., Grundler, F. M. W., von Mende, N., Burrows, P. R., Wyss, U. (1991) *Arabidopsis thaliana* as a new model host for plant parasitic nematodes. *The Plant J.* 1, 245–254.
9. Southey, J. F. (1986) *Laboratory Methods for Work with Plant and Soil Nematodes*. Ministry of Agriculture, Fisheries and Food. London, pp. 202.
10. Tyihák, E., Sarhan, A. R. T., Cong, N. T., Barna, B., Király, Z. (1988) The level of trigonelline and other quaternary ammonium compounds in tomato leaves in ratio to the changing nitrogen supply. *Plant and Soil* 109, 285–287.
11. Whapham, C. A., Jenkins, T., Blunden, G., Hankins, S. D. (1994) The role of seaweed extracts, *Ascophyllum nodosum*, in the reduction in fecundity of *Meloidogyne javanica*. *Fundam. appl. Nematol.* 17, 181–183.
12. Wu, Y., Jenkins, T., Blunden, G., Whapham, C., Hankins, S. D. (1997) The role of betaines in alkaline extracts of *Ascophyllum nodosum* in the reduction of *Meloidogyne javanica* and *M. incognita* infestations of tomato plants. *Fundam. appl. Nematol.* 20, 99–102.





## EFFECT OF 1'-METHYLASCORBIGEN ON THE RESISTANCE POTENTIAL OF PLANTS TO PATHOGENS\*

GY. KÁTAY and E. TYIHÁK

Plant Protection Institute, Hungarian Academy of Sciences, Budapest, Hungary

(Received: 1998-10-28; accepted: 1998-11-25)

We have studied the effect of 1'-methylascorbigen, an immunostimulating substance in animal systems on the resistance potential of barley, bean and wheat plants to the fungal pathogens *Erysiphe graminis*, *Uromyces phaseoli* and *Puccinia recondita*, respectively.

The effectiveness of protection depends – as in the case of other endogenous, N-methylated compounds – on the dosage of applied 1'-methylascorbigen and on the time interval between the chemical pretreatment and inoculation.

The time- and dose-dependent double immune response was clearly demonstrated in case of the barley – *Erysiphe graminis* and bean – *Uromyces phaseoli* host-parasite relationships while in case of the wheat – *Puccinia recondita* relationship the relatively long-time interval between pretreatment and inoculation allowed manifestation of only a single immune response.

**Keywords:** Biochemical immunization – double immune response – formaldehyde cycle – formaldehyde generator – 1'-methylascorbigen

### INTRODUCTION

According to Schönbeck et al. [13] all plants possess a genotype-dependent resistance potential which can be activated by inducers. Therefore, this type of disease resistance is not a static but rather an elastic feature of plants [7, 18, 19]. Induced resistance means the improvement of the natural resistance of plants without alteration of their genome [14]. Schönbeck et al. [14] proposed the following criteria for the verification of induced resistance: absence of toxic effects of the inducer on the parasite, necessity of a time interval between application of the inducer and the onset of effects in the plant, suppression of the induced resistance by specific inhibitors affecting the gene expression of the plant, and absence of a significant dose-response correlation.

\* Presented at the 4th International Conference on the Role of Formaldehyde in Biological Systems, July 1–4, 1998, Budapest, Hungary.

Send offprint requests to: Dr. Gy. Kátay, Plant Protection Institute, Hungarian Academy of Sciences, H-1022 Budapest, Herman Ottó út 15, Hungary.

An important component of the disease resistance repertoire of plants is systemic acquired resistance (SAR) which is characterized by durability and a systemic type of resistance response, a broad spectrum of disease control and an associated coordinate expression of a set of genes (SAR genes) [3, 4, 12]. The SAR defence pathway is activated by pathogens that cause a necrotic reaction originating from a hypersensitive reaction or from a disease lesion, as well as by chemical treatment of plants (e.g. salicylic acid (SA), benzo(1,2,3)thiadiazole-7-carbothioic acid S-methylester (BTH)) [3, 4, 12].

Another type of induced resistance concerns the application of endogenous N-, O- and S-methylated compounds (e.g. betaines) for the induction of disease resistance in the host by pretreatment of plants with the inducer before inoculation [7, 16, 17–20]. Tyihák et al. [16] were the first to report on the induction of disease resistance in bean plants to *Uromyces phaseoli* by N<sup>ε</sup>-trimethyl-L-lysine (TML). They observed a special “immune response” of the system: infection rate at  $10^{-3}$  and  $10^{-9}$  mol/l concentrations of applied TML in case of an induction time of 6 days was low. From these preliminary experimental data it can be established that TML as an inducer significantly decreased disease severity at the concentration values mentioned.

On the basis of numerous experiments it can be concluded that the inducers act within two concentration ranges characterized by low infection rates. In case of a short induction time (2 days) these ranges are around  $10^{-5}$  and  $10^{-12}$  mol/l concentration values, respectively, of the applied substance. It seems that there is a “pharmacological dose-dependent” (high concentration) and a “physiological dose-dependent” (very low concentration) induced resistance [7, 18, 21]. Between these “active” ranges there is an “inactive” range (5–7 dilutions) characterized in general by a high rate of infection. This phenomenon is called the double immune response [7, 19, 21].

The degree of protection also depends on the time interval between pretreatment and inoculation of plants [7, 16, 17, 21]. The time-dependence of the double immune response which is manifested by the shift of the two active concentration values so that the inactive range between them remains the same, may be due to continuous metabolism of methylated substances in the host plant [7, 16, 21].

It is evident that the mechanism of interaction between the pathogen and the chemical agent has to be indirect, involving a characteristic change in host plant metabolism [7]. The successive demethylation of the inducer by the host plants and the participation of formaldehyde (HCHO) formed in different reactions may be the basic phenomenon underlying this mechanism [19]. It follows from this that the chemically labile bound forms of HCHO (mainly in the form of a -CH<sub>2</sub>OH group) and its potential generators constitute a part of the resistance potential of plants [21].

The type of induced disease resistance in which the HCHO cycle plays a determining role with the contribution of dynamic, enzymatic methylation-demethylation processes, is called biochemical immunization (BI) [16, 17, 19]. However, the mechanism by which different types of methylated substances manifest their immunization effects is not clear at present.



Ascorbigen (ASC; 2-C[(indol-3-yl)methyl]- $\alpha$ -L-threo-D,L-glycero-3-hexulofuranosonic acid 1,4-lactone; Fig. 4) is a natural, indole ring containing derivative of L-ascorbic acid (AA). The biological evaluation of ASC and its synthetic derivatives showed that the most active substance is 1'-methylascorbigen (MeASC, Fig. 4): it inhibited the growth of different types of tumors in animals, protected animals from certain bacterial and viral infections, and manifested an immunomodulating activity [1, 2, 10, 11]. Recently it was proved that MeASC has a pronounced apoptotic effect *in vitro*. It was concluded that HCHO formed *in situ* from the methyl group of the MeASC molecule plays a determining role in its apoptotic effect [15]. It is assumed that MeASC, a potential HCHO generator and immunomodulating substance in animal test systems, can be used for BI of plants in a similar way as other methylated substances. MeASC was first used for the induction of disease resistance in plants against pathogens in case of the barley – *Erysiphe graminis* relationship. Preliminary results showed that MeASC has an immunostimulating effect on barley plants in response to this parasite [5].

The aim of this work was to study the effect of MeASC on the resistance potential of barley, bean and wheat plants to the fungal pathogens *Erysiphe graminis*, *Uromyces phaseoli* and *Puccinia recondita*, respectively.

## MATERIALS AND METHODS

Authentic MeASC was synthesized essentially as previously described [6, 8–10, 22].

Plants and pathogens: barley (*Hordeum vulgare* cv. GK-Omega), bean (*Phaseolus vulgaris* L., cv. Inka), and wheat (*Triticum vulgare* cv. Yubileynaya) plants were cultivated in commercial compost in the greenhouse. *Erysiphe graminis*, *Uromyces phaseoli* and *Puccinia recondita* were maintained on barley, bean and wheat plants, respectively, in the greenhouse.

Biochemical immunization: aqueous solutions of MeASC with concentrations of  $10^{-2}$ – $10^{-14}$  mol/l were used. The solutions were sprayed onto the leaf surface in case of wheat and barley plants and onto the abaxial leaf surface in case of bean plants. Plants treated with water were used as controls.

Inoculations: plants were inoculated with an aqueous spore suspension of the pathogens 2, 4, and 6 days after treatment with the inducer solution and then incubated at 22 °C for 24 hours.

Evaluation of data: pustule densities were assessed 7 days after inoculation and disease severity (infection rate) was expressed as pustules  $\times$  cm<sup>-2</sup> in case of bean plants (using a special, home-made pattern) and as the average number of pustules on a leaf in case of wheat and barley plants. These characteristics were reported to the corresponding values of the control plants to obtain relative (expressed in percents) data.

In order to study the effect of MeASC on the resistance potential of these plants, the dependence of infection rate on the concentration of MeASC administered (expressed in logarithmic scale) was examined.



## RESULTS

Figure 1 illustrates the effect of MeASC on the disease resistance of barley plants to *Erysiphe graminis* after an induction time of 2 days. The characteristic, dose-dependent double immune response of the biosystem is manifested at  $10^{-5}$  mol/l and  $10^{-10}$  mol/l concentration values which correspond to two minima of the infection rate: 46% and 47% of control, respectively.

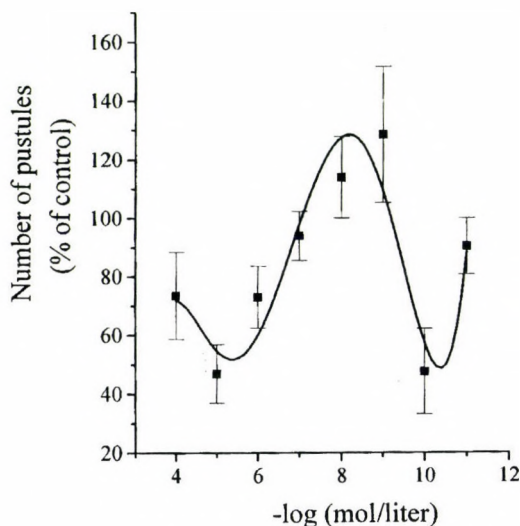


Fig. 1. Effect of MeASC on the resistance potential of barley plants against *Erysiphe graminis*. Induction time: 2 days. Fifth degree polynomial regression:  $Y = -4509.4909 + 3917.6892 - 1284.9758X^2 + 201.2825X^3 - 15.0529X^4 + 0.4313X^5$ ,  $R = 0.9225$ ,  $R^2 = 0.851$ ,  $SD = 21.0630$

The effect of MeASC on the resistance potential of bean plants to *Uromyces phaseoli* is shown in Fig. 2. In this case the induction time was 4 days. Two concentration values ( $10^{-3}$  mol/l and  $10^{-10}$  mol/l) correspond to significantly decreased rates of infection (28% and 32% of control).

Figure 3 shows the induction of resistance in wheat plants to *Puccinia recondita* by exogenous administration of MeASC with an induction time of 6 days. In this case the existence of two resistance values corresponding to two different inducer concentrations could not be clearly demonstrated. The minimum infection rate (10% of the control) occurred in response to  $10^{-7}$  mol/l MeASC.

The inactive range in each experiment is characterized by a high rate of infection: 129% of control for the barley – *Erysiphe graminis*, 102% of control for the wheat – *Puccinia recondita* and 88% of control for the bean – *Uromyces phaseoli* relationships, respectively.

In case of all three host-parasite relationships investigated the statistical evaluation of data showed a strong functional correlation (polynomial regression) between the infection rate and concentration of MeASC.

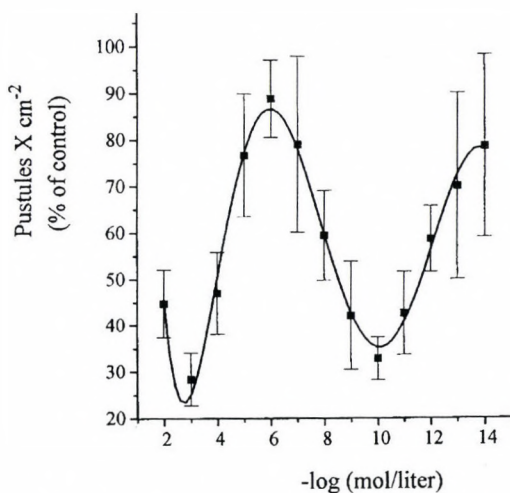


Fig. 2. Effect of MeASC on the resistance potential of bean plants against *Uromyces phaseoli*. Induction time: 4 days. Fifth degree polynomial regression:  $Y = 408.0771 - 376.3698X + 131.4627X^2 - 19.6716X^3 + 1.3128X^4 - 0.0321X^5$ ,  $R = 0.9839$ ,  $R^2 = 0.9680$ ,  $SD = 4.5911$

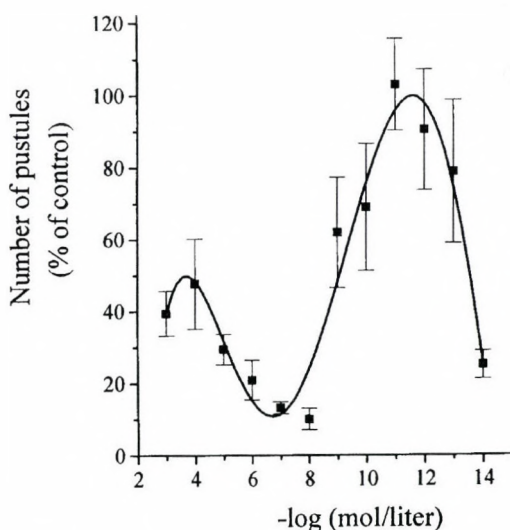


Fig. 3. Effect of MeASC on the resistance potential of wheat plants against *Puccinia recondita*. Induction time: 6 days. Fifth degree polynomial regression:  $Y = -647.0965 + 542.36517X - 152.8956X^2 + 19.1448X^3 - 1.6757X^5$ ,  $R = 0.9721$ ,  $R^2 = 0.9450$ ,  $SD = 9.9067$

## DISCUSSION

Results of the present study indicate that MeASC conferred an immunostimulating effect on barley, bean and wheat plants in response to infections by *Erysiphe graminis*, *Uromyces phaseoli* and *Puccinia recondita*, respectively. Pretreatment with MeASC generated a characteristic double immune response in case of the barley – *Erysiphe graminis* and bean – *Uromyces phaseoli* host-pathogen relationships while in case of the wheat – *Puccinia recondita* relationship the relatively long-time interval (6 days) between pretreatment and inoculation allowed manifestation of only a single immune response. The results of this latter case can be interpreted considering the time-dependence of the double immune response. During a longer induction time a larger amount of the inducer is metabolised in the host plant (it is supposed that MeASC is demethylated in plant tissues due to the effect of demethylases and/or peroxidases according to Fig. 4), so its effective concentration in the plant should correspond to a higher dosage value. The occurrence of the second minimum of infection rate shifted from the ca.  $10^{-11}$  mol/l inducer concentration to the  $10^{-7}$  mol/l, while the first minimum from the ca.  $10^{-5}$  mol/l value to about  $10^{-1}$  mol/l. This means that the first immune response could not be “caught” in this experiment and the minimum of the infection rate corresponds practically to the second immune response.

It is an important fact that ASC, an unmethylated substance, has no immunostimulating activity.

Also, it must be pointed out that in accordance to the above described and other numerous experimental results, there is a significant dose-response correlation in the case of BI.

It is interesting that TML, a fully N-methylated substance which promotes animal tumor cell proliferation in an earlier study [18], generated an immunostimulating activity on the plant systems [16]. In this experiment we demonstrated that MeASC which is a tumor cell proliferation retarding factor [15], had also an immunostimu-

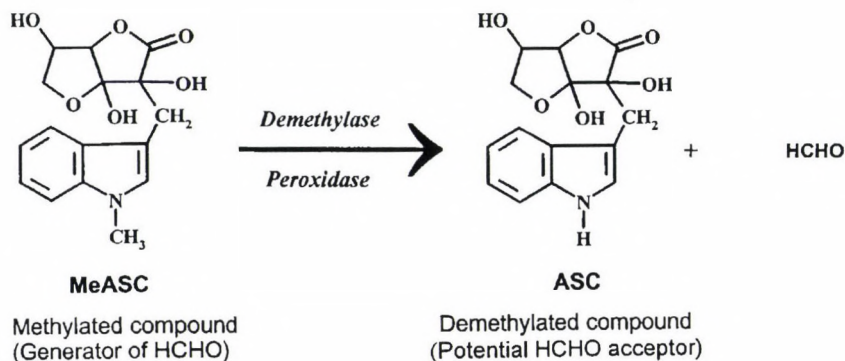


Fig. 4. Enzymatic demethylation supposed of MeASC



lating activity in different plant systems. TML and MeASC have a common feature: both are natural methylated compounds, that is, they are potential endogenous HCHO generators. However, the exact mechanism of their action is unclear.

## REFERENCES

1. Beresina, L. K., Posevaya, T. A., Barinsky, I. F., Korolev, A. M., Zakharov, V. E., Preobrazhenskaya, M. N. (1993) Antiviral activity of 1'-methylascorbigen at experimental arboviral infections. *Chem. Pharmac. Zhurnal* 27, 125–129. (In Russian)
2. Efimov, S. (1989) Study of immunomodulating activities of 1'-methyl- and 1'-ethylascorbigenes. *Antibiot. Khimioter* 34, 125–129. (In Russian)
3. Friedrich, L., Lawton, K., Ruess, W., Masner, P., Specker, N., Gut Rella, M., Meier, B., Dincher, S., Staub, Th., Uknes, S., Métraux, J.-P., Kessman, H., Ryals, J. (1996) A benzothiadiazole derivative induces systemic acquired resistance in tobacco. *The Plant Journal* 10, 61–70.
4. Görlach, J., Volrath, S., Knauf-Beiter, G., Hengy, G., Beckhove, U., Kogel, K.-H., Oostendorp, M., Staub, Th., Ward, E., Kessman, H., Ryals, J. (1996) Benzthiadiazole, a novel class of inducers of systemic acquired resistance, activates gene expression and disease resistance in wheat. *The Plant Cell* 8, 629–643.
5. Kátay, Gy., Manninger, K., Tyihák, E. (1997) Biochemical immunization of plants to pathogens by N-methylascorbigen. In: *Abstracts Intern. Cong. Stress of Life. Stress and Adaptation from Molecules to Man*. Budapest, Hungary, p. 187.
6. Kiss, G., Neukom, H. (1966) Über die Struktur des Ascorbigens. *Helv. Chim. Acta* 49, 989–992.
7. Manninger, K., Csősz, M., Tyihák, E. (1992) Biochemical immunization of wheat plants to biotrophic fungi by endogenous, fully N-methylated compounds. In: Tyihák, E. (ed.) *Proc. of 3rd Intern. Conf. on Role of Formaldehyde in Biological Systems. Methylation and Demethylation Processes*. Sopron, Hungary, pp. 157–162.
8. Mukhanov, V. I., Yartseva, I. V., Kibot, B. S., Volodin, Y. Y., Kustova, I. L., Lesnaya, N. A., Sofina, Z. P., Ermakova, N. P., Preobrazhenskaya, M. N. (1984) Investigation of ascorbigen and its derivatives. *Bioorg. Khim.* 10, 544–559. (In Russian)
9. Plikhtyak, I. L., Yartseva, I. V., Aleksandrova, L. G., Podhalusina, N. Y., Preobrazhenskaya, M. N. (1991) 3-Hydroxymethylindoles and synthesis of ascorbigens. *Khim. Pharm. Zh.* 25, 57–59. (In Russian)
10. Preobrazhenskaya, M. N., Korolev, A. M., Plikhtyak, I. L., Yartseva, I. V., Lazhko, E. I., Aleksandrova, L. G. (1991) Chemistry and biology of ascorbigens. In: Bergman, J., Van der Plas, H. C., Simonyi, M. (eds) *Heterocycles in Bio-Organic Chemistry*. The Royal Society of Chemistry, Cambridge, p. 68–87.
11. Preobrazhenskaya, M. N., Bukhman, V. M., Korolev, A. M., Efimov, S. (1994) Ascorbigen and other indole-derived compounds from Brassica vegetables and their analogs as anticarcinogenic and immunomodulating agents. *Pharmac. Ther.* 60, 301–313.
12. Ryals, J. A., Neuenschwander, U. H., Willits, M. G., Molina, A., Steiner, H.-Y., Hunt, M. D. (1996) Systemic acquired resistance. *The Plant Cell* 8, 1809–1819.
13. Schönbeck, F., Dehne, H.-W., Beicht, W. (1980) Untersuchungen zur Aktivierung unspezifischer Resistenz-mechanismen in Pflanzen. *Z. PflKrankh. PflSchutz* 87, 654–666.
14. Schönbeck, F., Steiner, U., Kraska, T. (1993) Induzierte Resistenz: Kriterien, Mechanismen, Anwendung und Bewertung. *Z. PflKrankh. PflSchutz* 100, 541–557.
15. Szende, B., Tyihák, E., Szókán, Gy., Kátay, Gy. (1995) Possible role of formaldehyde in the apoptotic and mitotic effect of 1-methyl-ascorbigen. *Path. Oncol. Res.* 1, 38–42.
16. Tyihák, E., Steiner, U., Schönbeck, F. (1989) Induction of disease resistance by N<sup>ε</sup>-trimethyl-L-lysine in bean plants against *Uromyces phaseoli*. *J. Phytopath.* 126, 253–256.

17. Tyihák, E., Steiner, U., Manninger, K., Schönbeck, F. (1990) Biochemical immunization of plants. In: FEBS Publication committee (ed.) *Abstracts 20th Meeting of the Federation of European Biochemical Societies*, Budapest, Hungary, p. 339.
18. Tyihák, E., Szende, B., Trézl, L. (1990) Biological effects of methylated amino acids. In: Paik, W. K., Kim, S. (eds) *Protein Methylation*. CRC Press, Inc. Boca Raton, Florida, pp. 363–388.
19. Tyihák, E., Manninger, K., Csősz, M. (1995) Formaldehyde cycle, “double immune response” and biochemical immunization of plants. In: Manka, M. (ed.) *Environmental Biotic Factors in Integrated Plant Disease Control*. The Polish Phytopath. Soc., Poznan, Poland, pp. 571–574.
20. Tyihák, E., Manninger, K., Csősz, M., Sárdi, É., Trézl, L., Blunden, G. (1997) Formaldehyde cycle and stress syndrome. In: *Abstracts Intern. Cong. Stress of Life. Stress and Adaptation from Molecules to Man*. Budapest, Hungary, p. 186.
21. Tyihák, E., Trézl, L., Szende, B. (1998) Formaldehyde cycle and the phases of stress syndrome. *Ann. N. Y. Acad. of Sci.* 851, 259–270.
22. Virtanen, A. I., Kiesvaara, M. (1963) On the purity of ascorbigen preparation and their antiscorbutic effect. *Acta Chim. Scand.* 17, 848–853.

## ANALOGIES AND DIFFERENCES IN THE EXCITED REACTIONS OF FORMALDEHYDE AND D-GLUCOSE\*

L. TRÉZL,<sup>1</sup> L. HULLÁN,<sup>2</sup> T. SZARVAS,<sup>3</sup> A. CSIBA<sup>4</sup> and J. PIPEK<sup>5</sup>

<sup>1</sup>Department of Organic Chemical Technology, Technical University of Budapest, Budapest, Hungary

<sup>2</sup>Department of Biochemistry, National Institute of Oncology, Budapest, Hungary

<sup>3</sup>Institute of Isotopes Co. Ltd., Budapest, Hungary

<sup>4</sup>Veterinary and Food Control Station, Budapest, Hungary

<sup>5</sup>Technical University of Budapest, Institute of Physics, Quantum Theory Group, Budapest, Hungary

(Received: 1998-10-28; accepted: 1998-11-25)

The investigations proved that D-glucose (as reducing sugar) can easily be activated in a ternary system (L-lysine : D-glucose : H<sub>2</sub>O<sub>2</sub>) similarly to formaldehyde at 20 °C, in pH = 7.4 forming chemiluminescence (CL) and singlet oxygen. The kinetic investigation showed that : CL lasted many hours (permanent emission) and had no bell-shaped curve differently from other aldehydes e.g. formaldehyde. The reason of the effect is that D-glucose exists mainly in ring form in water solution (Haworth ring form) and the open form (the aldehyde group) is slowly liberated during the excited reaction. These excited reactions may be important in human organism, because D-glucose and lysyl residues of proteins occur permanently in human body and endogenous formaldehyde and H<sub>2</sub>O<sub>2</sub> may be liberated there, too.

**Keywords:** L-lysine – formaldehyde – D-glucose – hydrogen peroxyde – chemiluminescence emission

### INTRODUCTION

Szent-Györgyi drew the attention first for the specific reaction between L-lysine (casein) and methyl-glyoxal forming excited molecules already at room temperature proved by ESR investigation [6]. Similar reaction can take place between L-lysine and other unsaturated aldehydes and ketones : acrolein, malondialdehyde, 4-hydroxy-nonenal, dihydroxy-acetone (the last compound induced skin-browning) etc. It was proved that this type of excited reaction requires dissolved oxygen since it does not occur in N<sub>2</sub> or Ar atmosphere [13]. Saturated aldehydes e.g. formaldehyde, acetaldehyde, propionaldehyde, benzaldehyde could be activated only in the presence of L-lysine and hydrogen peroxyde. The L-lysine mediated ternary system (L-lysine : aldehyde : H<sub>2</sub>O<sub>2</sub>) showed excited reactions forming burst of chemiluminescence emission (CL), excited aldehyde and singlet oxygen [8, 9, 10, 11]. The excited reaction was investigated in detail for formaldehyde. The reaction mecha-

\* Presented at the 4th International Conference on the Role of Formaldehyde in Biological Systems, July 1–4, 1998, Budapest, Hungary.

Send offprint requests to: Dr. L. Trézl, Department of Organic Chemical Technology, Technical University of Budapest, H-1521 Budapest, Műegyetem rkp. 3, Hungary.



nism has been solved. We can explain how singlet oxygen and excited formaldehyde are formed. The investigations were extended to biological objects (liver S9-mix, plants) [11, 14, 15] and to formaldehyde precursors (dimethyl-nitrosamine, N-methyl-hydrazine etc.) [7].

It is known that in Maillard browning reaction between L-lysine and various reducing sugars CL and singlet oxygen could be formed at 100 °C, or higher temperature [5, 16]. Low oxygen level inhibited CL and no CL was produced in nitrogen purged solution [5]. The reaction parameters and the reaction mechanism of the excited Maillard reaction ( $\geq 100$  °C) are well determined in the literature. The reaction conditions ( $\geq 100$  °C) could not adapt to living organisms because D-glucose was supposed to be non-activable at room temperature (20 °C).

As in D-glucose which has a hidden aldehyde group (in Haworth ring form), similar reactions were supposed between L-lysine : D-glucose :  $\text{H}_2\text{O}_2$  at 20 °C and physiological pH as in the case of formaldehyde has been found in the appropriate ternary system [11]. The open form is in very low concentration in water solution (0.0026% at 25 °C) [3]. The excited reaction took place permanently, therefore, the aldehyde group had to be liberated slowly according to the equilibrium during the reaction. The ternary system may be present in human body because there are D-glucose and a lot of lysyl side chains in proteins and endogenous  $\text{H}_2\text{O}_2$  may be liberated.

We found analogies and differences between the reactions of formaldehyde and D-glucose in the appropriate ternary systems.

## MATERIALS AND METHODS

### *Chemiluminescence (CL) emission measurements*

Reaction condition : 0.1 M phosphate buffer (pH = 7.4), 25 °C. CL emission measurement was carried out in Packard TriCarb LSC using coincidence operating mode on  $^3\text{H}$  channel.

*Light emission analysis.* The chemiluminescence (CL) spectral distribution was analysed by the spectrometer model VG-05 developed at the Central Research Institute for Chemistry of Hungarian Academy of Sciences in Budapest. Transmitting CL radiation through a series of colored glass filters having different cut-off wavelength characteristics enabled the spectral profile of the emission to be calculated thus pinpointing the emitter even in complex situations (Fig. 2.) [8, 9].

### *HPLC investigations for formaldehyde determination (Waters HPLC system)*

The prepared samples were injected through a 20  $\mu\text{l}$  loop (Rheodyne, USA) for analysis on a reversed-phase silica column (LiChrosorb-7-RP-18 250  $\times$  3.9 mm I.D., Merck, Darmstadt, Germany) at 30 °C temperature. The mobile phase (pH = 4.5) was

30% acetonitrile in 0.05 M  $\text{KH}_2\text{PO}_4$  pumped by a Waters Model 501 HPLC pump at a flow-rate of  $1.0 \text{ ml} \times \text{min}^{-1}$ . Detection was carried out using a Waters 470 type spectrofluorimetric detector at 237 nm (excitation) and above 370 nm (emission) wavelengths. The amplification of the detector was hundredfold.

Reaction mixtures:

– 100 mM D-glucose + 30 mM L-lysine  $\times$  HCl in 0.1 M phosphate buffer pH = 7.4.

– 100 mM D-glucose + 30 mM L-lysine  $\times$  HCl + 30 mM  $\text{H}_2\text{O}_2$  in 0.1 M phosphate buffer pH = 7.4.

– 100 mM D-glucose + 30 mM L-lysine  $\times$  HCl + 30 mM  $\text{H}_2\text{O}_2$  + 3.0 mM  $\text{K}_4[\text{Fe}(\text{CN})_6]$  in 0.1 M phosphate buffer pH = 7.4.

Reaction mixtures were held at 37 °C for 8 hours, then were diluted 100 fold with distilled water. 4.0 ml hydrazine hydrochloride (HP-HCl) reagent (10 mg in 100 ml 0.2 M  $\text{KH}_2\text{PO}_4$ ) was added to 4.0 ml reaction mixture. It was heated on a boiling water bath for 15 minutes then 20  $\mu\text{l}$  aliquotes of reaction mixtures were injected directly into the HPLC apparatus. The concentration of formaldehyde in the samples was determined by interpolation from calibration curve constructed by plotting the peak areas of triazolo (3,4- $\alpha$ ) phthalazine (formaldehyde adduct) versus the concentration of formaldehyde.

### *Investigations with labelled compound*

L-Lysine : D-glucose( $^{14}\text{C}$ ) :  $\text{H}_2\text{O}_2$  (molar ratio = 1 : 3 : 1) were reacted in phosphate buffer (pH = 7.4) at 37 °C for 1 hour. The specific radioactivity of D-glucose-( $^{14}\text{C}$ ) was 187.2 MBq/mmol, 12.8 mCi/mmol. TLC analysis was carried out on Kieselgel  $\text{HF}_{254}$  sheet. Running solution was n-buthanol-acetic acid-water = 8 : 1 : 1 (see Fig. 4). Experiments were carried out using L-lysine-6( $^3\text{H}$ ) (187.2 MBq/mmol, 5.06 mCi/mmol), unlabelled D-glucose and  $\text{H}_2\text{O}_2$  for the identification of L-lysine-glucose adduct in the same molar ratio as before.

## RESULTS AND DISCUSSION

CL emissions were similar in several aspects for the formaldehyde and D-glucose reactions in the appropriate ternary systems (Table 1). Both compounds were activated in the presence of  $\text{H}_2\text{O}_2$  if the pH of the system was higher than 10. However, at physiological pH both compounds could be activated in the presence of L-lysine and  $\text{H}_2\text{O}_2$ .

The investigation of CL emission as a function of time showed considerable differences between the CL emissions emerged in the reactions of D-glucose and the other investigated aldehydes (Fig. 1). The durations of excited reactions are relatively short in case of formaldehyde and methyl-glyoxal (about 0.5–1 hour), but the intensity of CL emission is very high in both case. The intensity of CL emission is



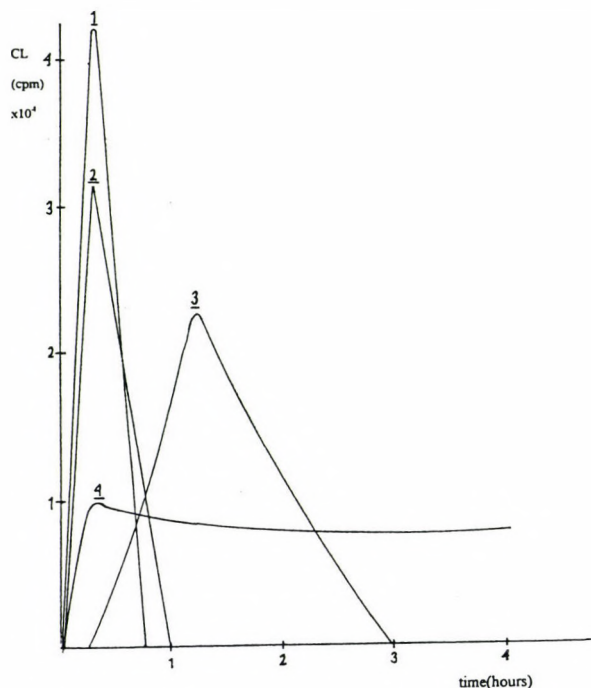


Fig. 1. Chemiluminescence emission curves of different ternary systems versus time. **1** 1 mM L-lysine : 1 mM methyl-glyoxal : 1 mM  $\text{H}_2\text{O}_2$  (pH = 7.4, 20 °C); **2** 1 mM L-lysine : 1 mM  $\text{CH}_2\text{O}$  : 1 mM  $\text{H}_2\text{O}_2$  (20 °C, pH = 7.4); **3** 1 mM L-lysine : 3 mM D-glucose (+ dissolved oxygen in water, Maillard browning reaction, 100 °C) **4** 1 mM L-lysine : 3 mM D-glucose : 1 mM  $\text{H}_2\text{O}_2$  (20 °C, pH = 7.4, permanent emission)

much lower in the case of D-glucose, however, the excited state lasted many hours (10–20 hours). The CL emission of D-glucose reaction did not show a bell-shaped curve as in the case of formaldehyde and methyl-glyoxal were because the D-glucose containing ternary system produced a permanent long-term life emission. It is known from the literature an excited reaction between D-glucose and L-lysine (Maillard reaction) if the temperature is  $\geq 100$  °C. The CL emission of the Maillard reaction takes much longer than the CL emission of aldehydes investigated on 20 °C (Fig. 1).

The light emission analysis at different wavelength indicates that at the excited reaction e.g. in the case of formaldehyde (Fig. 2) excited aldehyde (430 nm) and singlet oxygen (633 nm, 705 nm) could be formed and in the reaction mixture a significant amount of N<sup>ε</sup>-formyl-lysine was detected [11]. Similar reaction was proved with radiochemical method in the case of D-glucose.

Radiochemical analysis with labelled D-glucose (Fig. 3) showed that in the ternary system (L-lysine : D-glucose- $^{14}\text{C}$  :  $\text{H}_2\text{O}_2$ ) glucose radical could be formed at 20 °C and this radical can react with oxygen and lysine radical and CL and singlet oxygen



Table 1  
Chemiluminescence emission (CL) investigation

Reaction mixture	Temperature (pH = 7.4)	CL
L-lysine + CH <sub>2</sub> O	20 °C	–
L-lysine + H <sub>2</sub> O <sub>2</sub>	20 °C	–
CH <sub>2</sub> O + H <sub>2</sub> O <sub>2</sub>	20 °C	very weak
CH <sub>2</sub> O + H <sub>2</sub> O <sub>2</sub>	20 °C, pH > 10	+++ burst
L-lysine + D-glucose	20 °C	–
D-glucose + H <sub>2</sub> O <sub>2</sub>	20 °C	–
D-glucose + H <sub>2</sub> O <sub>2</sub>	20 °C, pH >10	+++
L-lysine + CH <sub>2</sub> O + H <sub>2</sub> O <sub>2</sub>	20 °C	+++ (burst)
L-lisine + D-glucose + H <sub>2</sub> O <sub>2</sub>	20 °C	+++ (long life emission)
L-lysine + D-glucose + O <sub>2</sub> (dissolved oxygen in water)	>100 °C	++ (Maillard browning reaction)

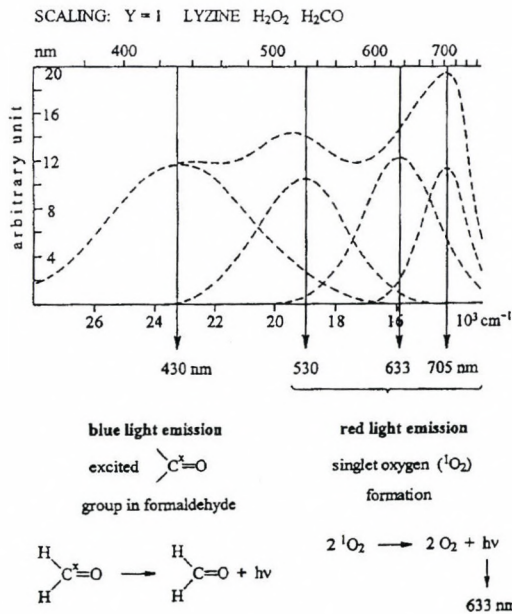


Fig. 2. Light emission analysis at different wavelength in a mixture including L-lysine : CH<sub>2</sub>O : H<sub>2</sub>O<sub>2</sub>, molar ratio: 1 : 1 : 1 mM, at 25 °C in 0.1 M Sörensen buffer, pH 7.4 (8)

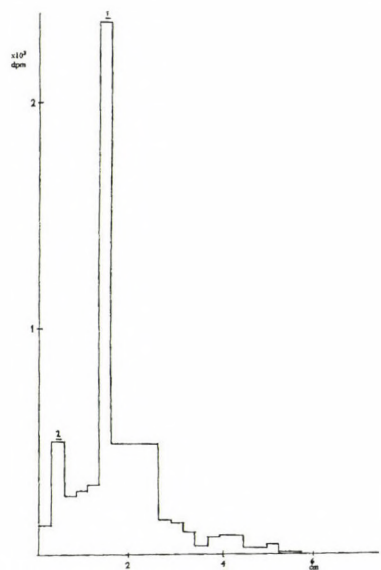


Fig. 3. Radiochromatogram of the reaction between 1 mM L-lysine : 3 mM D-glucose-U-(<sup>14</sup>C) : 1 mM H<sub>2</sub>O<sub>2</sub>. 1 D-glucose-U-(<sup>14</sup>C) 2 L-lysine-D-glucose-U-(<sup>14</sup>C)

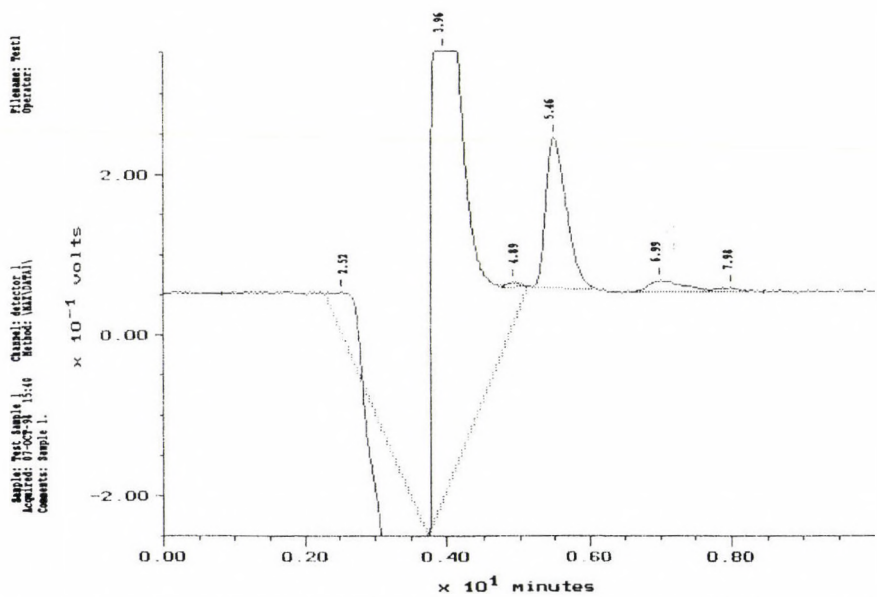


Fig. 4. HPLC chromatogram of reaction mixture: D-glucose, L-lysine and H<sub>2</sub>O<sub>2</sub> (37 °C, 8 h). Peaks: 2.52 min (unknown), 3.96 min hydralazine reagent, 4.89 min (unknown), 5.46 min hydralazine – D-glucose adduct, 6.99 min hydralazine-formaldehyde adduct (formaldehyde concentration 0.065 mM), 7.98 min (unknown)

could be formed in the reaction (see later the reaction mechanism). Formation of L-lysine-D-glucose adduct (Fig. 3, peak 2) could be identified and confirmed using L-lysine-6( $^3\text{H}$ ) in the investigation. Radiochemical experiments proved, that similar excited reaction cannot take place between L-lysine and D-glucose-( $^{14}\text{C}$ ) at 20 °C without  $\text{H}_2\text{O}_2$ . The situation is very similar in the case of formaldehyde, where large amounts of N $^{\epsilon}$ -formyl-L-lysine could be formed in the ternary system simultaneously with singlet oxygen liberation. Between L-lysine and formaldehyde do not exist CL and  $^1\text{O}_2$  liberation.

There is another very interesting result in the ternary system: L-lysine : D-glucose :  $\text{H}_2\text{O}_2$ . We supposed from theoretical considerations that in the ternary system formaldehyde could be liberated from D-glucose. HPLC investigations brought confirmatory evidence that formaldehyde was liberated in the reaction of the ternary system (Figs 4, 5). The result may be significant in biological systems especially in human body because without L-lysine does not liberate formaldehyde from D-glucose and  $\text{H}_2\text{O}_2$  at 20 °C and 37 °C. L-lysine is a catalyst in this reaction. What is the biochemical pathway of the liberated formaldehyde, will it take place in excited reactions or not, may it be harmful or not, it is not known up to date.

What is the main difference between D-glucose and other aldehydes in the excited reactions? *The main difference is:* D-glucose exists mainly in ring form in aqueous solution (Haworth ring form) and the open form is liberated slowly in the excit-

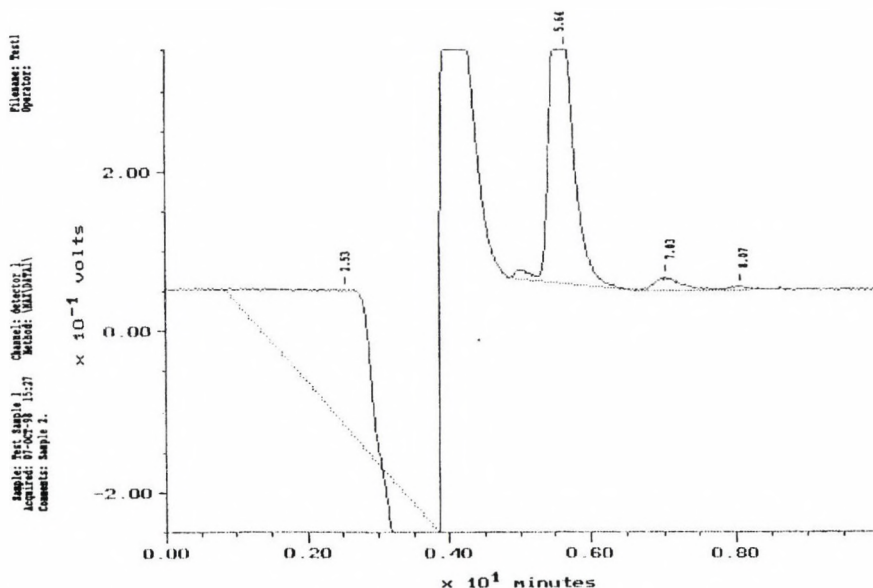


Fig. 5. HPLC chromatogram of reaction mixture: D-glucose, L-lysine,  $\text{H}_2\text{O}_2$  and  $\text{K}_4[\text{Fe}(\text{CN})_6]$ . 2.53 min (unknown), 5.64 min hydralazine-glucose adduct, 7.03 min formaldehyde-hydralazine adduct (formaldehyde concentration 0.077 mM), 8.07 min (unknown)



ed reaction (L-lysine : D-glucose :  $\text{H}_2\text{O}_2$ ). The equilibrium will be shifted slowly for the open form (Fig. 6) forming permanently D-glucose. D-glucose has very low carbonyl concentration in aqueous solution (open form 0.0026% at 25 °C) [3]. Other aldehydes are in open form or in hydrated form (e.g. formaldehyde) in aqueous solution.

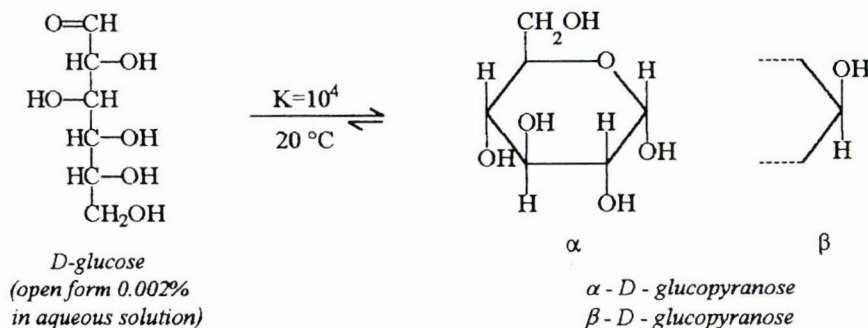


Fig. 6

According to the reaction mechanism only the open form can react with excited lysine radical forming excited glucose radical molecule and the equilibrium will be shifted to the left side.

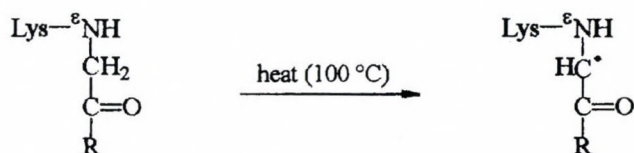
Kurosaki et al. [5] suggested a reaction mechanism for the excited reaction (CL and  $^1\text{O}_2$  formation) between L-lysine and D-glucose when the temperature was  $\geq 100\text{ }^\circ\text{C}$ . First in the reaction an Amadori compound could be formed from lysine and glucose then radical compounds were formed by heat from Amadori compound (Fig. 7).

In our ternary system at  $20\text{ }^\circ\text{C}$  Amadori compound could not be formed, therefore, it has to be supposed that D-glucose may be activated by lysine radical (Fig. 8).

The reaction mechanism is validated by CL emission and singlet oxygen liberation (supported by light emission analysis, radiochemical investigations and the quenching of reaction by  $\text{NaN}_3$ ).

The excited reactions may be important in the human organism, because D-glucose and lysyl residues of proteins occur permanently in human body and endogenous formaldehyde and  $\text{H}_2\text{O}_2$  may be liberated there too. The elevated D-glucose level in patients with diabetes may be especially harmful due to the consequences of the excited reactions.

The excited formaldehyde and glucose molecules are very reactive and can attack proteins, DNA and RNA, while the formed singlet oxygen can attack DNA at guanosine forming 8-hydroxy-guanosine and DNA may be degraded [1, 4].



Amadori compound: substituted  
1-amino-1-deoxy-2 ketose

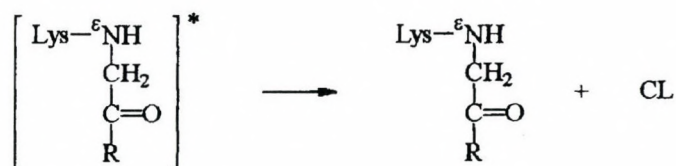
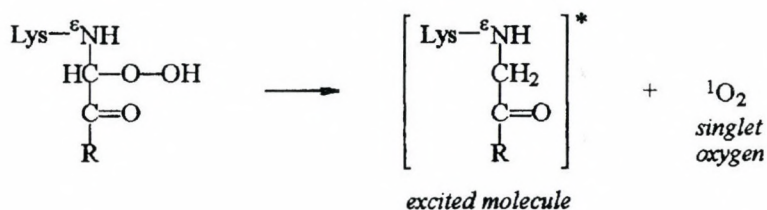
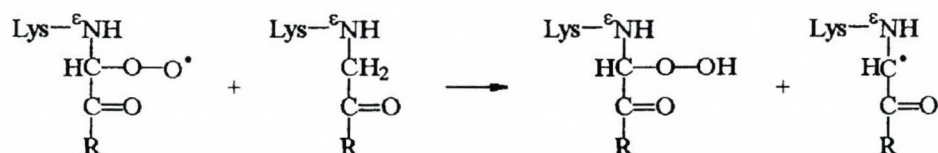
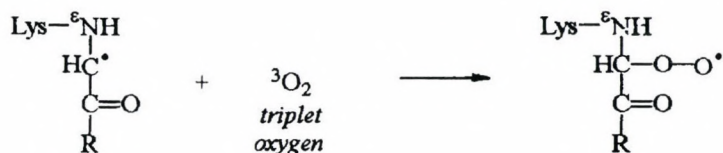


Fig. 7. Proposed reaction mechanism for generation of chemiluminescence (CL) and singlet oxygen in Lysine : D-glucose Maillard browning reaction (100 °C), according to [5]

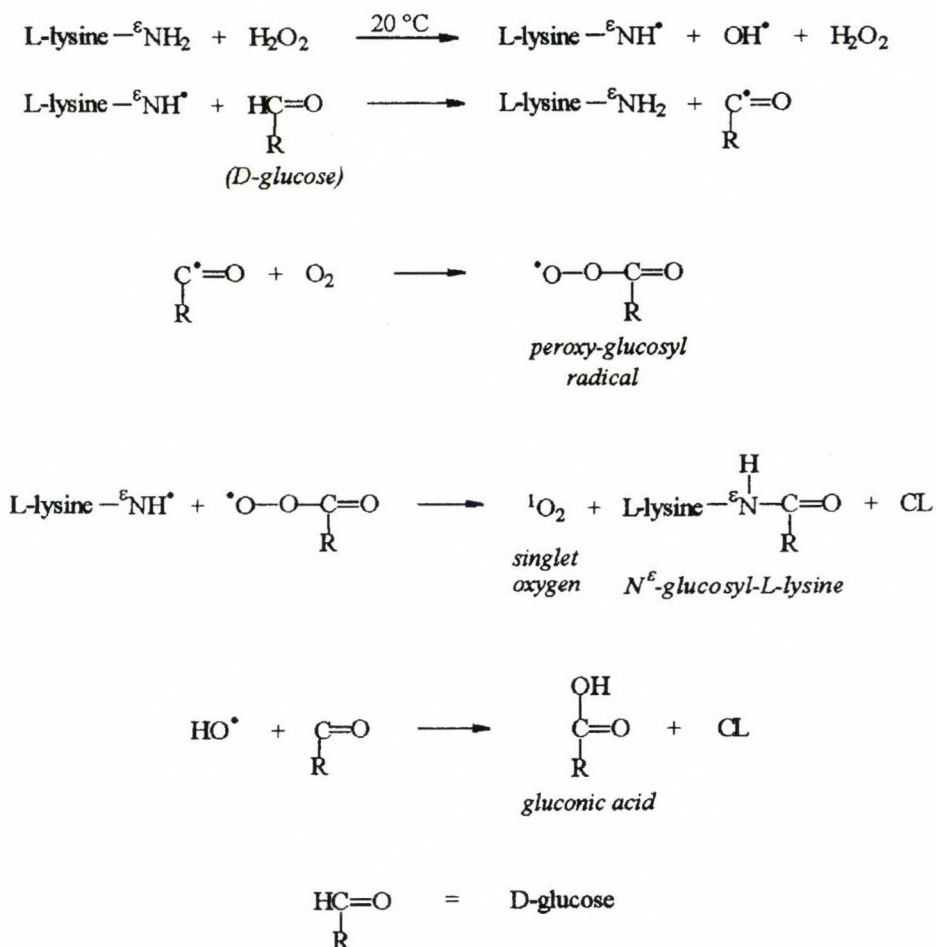


Fig. 8. Proposed reaction mechanism for generation of chemiluminescence (CL) and singlet oxygen ( $^1\text{O}_2$ ) in L-lysine : D-glucose :  $\text{H}_2\text{O}_2$  ternary system at 20 °C (pH = 7.4), according to authors



## REFERENCES

1. Devasagayam, T., Steenken, S., Obendorf, M. S., Schulz, W. A., Sies, H. (1991) Formation of 8-hydroxy(deoxy) guanosine and generation of strand breaks at guanine residues in DNA by singlet oxygen. *Biochemistry* 30, 6283–6289.
2. Griffin, B. W., Ting, P. L. (1978) Mechanism of N-demethylation of aminopyrine by hydrogen peroxide catalysed by horse radish peroxidase, metmyoglobin, and prothemin. *Biochemistry* 17, 2206–2211.
3. Hayward, L. D. (1977) A symmetry rule for the circular dichroism of reducing sugars, and the proportion of carbonyl forms in aqueous solutions thereof. *Carbohydr. Res.* 53, 13–20.
4. Khan, A.V., Wilson, T. (1995) Reactive oxygen species as cellular messengers. *Chemistry and Biology* 2, 437–445.
5. Kurosaki, Y., Sato, H., Mizugaki, M. (1989) Extra-weak chemiluminescence of drugs. VIII. Extra-weak chemiluminescence arising from the amino-carbonyl reaction. *J. Biolumin. Chemilumin.* 3, 13–19.
6. Pethig, R., Szent-Györgyi, A. (1977) Electronic properties of the casein-methylglyoxal complex. *Proc. Natl. Acad. Sci. USA* 74, 226–228.
7. Trézl, L., Rusznák, I., Tyihák, E., Szarvas, T., Szende, B. (1983) Spontaneous N<sup>ε</sup>-methylation and N<sup>ε</sup>-formylation reactions between L-lysine and formaldehyde inhibited by L-ascorbic acid. *Biochem. J.* 214, 289–292.
8. Trézl, L., Pipek, J. (1988) Formation of excited formaldehyde in model reactions simulating real biological systems *J. Mol. Struct. (Theochem)* 170, 213–223.
9. Trézl, L., Ludányi, A., Rusznák, I., Horváth, V., Szarvas, T., Vasvári, G., Tyihák, E. (1989) Enforcing effect of basic terminal group of L-lysine in the reactions between formaldehyde and hydrogen peroxide. *Magyar Kém. Folyóirat* 95, 131–139. (In Hungarian)
10. Trézl, L., Pipek, J. (1991) Quantum chemical interpretation of the reaction between L-ascorbic acid and formaldehyde and its biological significance. *Period. Polytech.* 35, 207–219.
11. Trézl, L., Török, G., Vasvári, G., Pipek, J., Hullán, L. (1992) Formation of burst chemiluminescence, excited aldehydes and singlet oxygen in model reactions and from carcinogenic compounds in rat liver S9 fractions. *Period. Polytech.* 36, 239–347.
12. Trézl, L., Csiba, A., Juhász, S., Szentgyörgyi, M., Lombai, G., Hullán, L. (1997) Endogenous formaldehyde level of foods and its biological significance. *Z. Lebensm. Unters. Forsch. A.* 205, 300–304.
13. Trézl, L., Hullán, L., Szarvas, T., Csiba, A., Pipek, J. (1998) Analogies and differences in the excited reactions of formaldehyde and reducing sugars (e.g. D-glucose). In: Abstract 4th Int. Conf. The Role of Formaldehyde in Biological Systems, Methylation, Demethylation Processes. Budapest, July 1–4, 1998.
14. Tyihák, E., Rozsnyai, S., Sárdi, É., Gullner, G., Trézl, L., Gáborjányi, R. (1994) Possibility of formation of excited formaldehyde and singlet oxygen in biotic and abiotic stress situations. *Acta Biol. Hung.* 45, 3–10.
15. Tyihák, E., Trézl, L., Szende, B. (1998) Formaldehyde cycle and phases of stress syndrome. *Annals of N.Y. Acad. Sci.* 851, 259–270.
16. Wondrak, G., Pier, T., Tressl, R. (1995) Light from Maillard reaction: Photon counting, emission spectrum, photography and visual perception. *J. Biolumin. Chemilumin.* 10, 277–284.



## MICROBIAL UREA-FORMALDEHYDE DEGRADATION INVOLVES A NEW ENZYME, METHYLENEDIUREASE\*

T. JAHNS, ROSWITHA SCHEPP, C. SIERSDORFER and H. KALTWASSER

Fachrichtung 13.3 Mikrobiologie, Universität des Saarlandes, Saarbrücken, Germany

(Received: 1998-10-28; accepted: 1998-11-25)

The enzymic mechanism of metabolism of urea-formaldehyde condensation products (methylenureas; MU) and the fate of the degradation products ammonium, urea and formaldehyde were studied in bacteria isolated from garden soil, which were able to use methylenureas as the sole source of nitrogen for growth. An organism identified as *Ochrobactrum anthropi* completely degraded methylenediurea (MDU) and dimethylenetriurea (DMTU) to urea, ammonia, formaldehyde and carbon dioxide. An enzyme designated as methylenediurease (methylenediurea deiminase; MDUase) was responsible for the degradation of both MDU and DMTU as well as higher polymerized MU. Growth on MU as the nitrogen source specifically induced the synthesis of this enzyme, which seems to be located in the periplasm of the bacterium. Under these growth conditions, urease as well as NAD-specific formaldehyde and formate dehydrogenase were expressed to high levels, efficiently using the products of MU degradation, and high-affinity transport systems for urea and ammonia were synthesized scavenging the environment for these products.

**Keywords:** Methylenurea – urea-formaldehyde – degradation – ammonification

### INTRODUCTION

Urea-formaldehyde compounds (methylenureas; MU) are widely used as a slow release fertilizer on greens, lawns and in greenhouses [2] and have been employed to improve the nitrogen status of forest soils [1]. These compounds are condensation products of urea and formaldehyde, their degree of polymerization largely depending on the ratio of urea and formaldehyde during the condensation process. With formaldehyde in excess, high-molecular resinous polymeres are produced which are used as plastics, insulating materials and adhesives. At a molar ratio of urea and formaldehyde between 1.2–1.5 to 1, condensates suitable for the use as a slow-release fertilizer are formed, consisting of a mixture of MU polymers having a shorter

\* Presented at the 4th International Conference on the Role of Formaldehyde in Biological Systems, July 1–4, 1998, Budapest, Hungary.

Send offprint requests to: Dr. T. Jahns, Fachrichtung 13.3 Mikrobiologie, Universität des Saarlandes, Postfach 15150, D-66041 Saarbrücken, Germany. E-mail: toja@rz.uni-sb.de.



chain length, e.g. methylenediurea (diureidomethane), dimethylenetriurea, trimethylenetetraurea (MDU, DMTU, TMTU) etc. MU are known to be mineralized by microbial activity [5], but nothing was known regarding the mechanism of their degradation until recently, when an enzyme from a strain of *Ochrobactrum anthropi* was isolated and purified [8]. It was shown that MU degradation is a result of both biotic and abiotic reactions, with in a first step the hydrolytic release of a terminal amino group from these compounds. In the present study, the fate of the products of microbial degradation of MU, i.e., ammonia, urea and formaldehyde, was studied in more detail, and it is shown that they are efficiently used by *O. anthropi* as a source of energy and nitrogen for growth.

## MATERIALS AND METHODS

*Ochrobactrum anthropi* was grown to the early stationary growth phase in a mineral medium as previously described [8] with 0.2% (w/v) glucose as the carbon source and the nitrogen sources indicated in the experiments, harvested by centrifugation ( $10\,000 \times g$  for 20 min at 4 °C) and washed twice in 50 mM Na<sub>2</sub>HPO<sub>4</sub>, pH 7.5, 3 mM mercaptoethanol. Cell-free extracts used for the enzyme assays were prepared as described previously [8]. Osmotic shock was carried out as described by Nossal and Heppel [11]. All enzyme and transport activities were measured as described before [3, 6, 7, 8, 9, 10]. The activity of alkaline phosphatase was determined in 1 M diethanolamine, 10 mM p-nitrophenylphosphate, 0.25 mM MgCl<sub>2</sub> and shock fluid/cell-free extracts in appropriate amounts at pH 9.8; absorbance was read at 410 nm after 20, 40 and 60 min of incubation at 30 °C.

## RESULTS AND DISCUSSION

In a previous study, a bacterium able to use MU as the sole source of fixed nitrogen for growth has been isolated and identified as a strain of *Ochrobactrum anthropi* [8]. The MU metabolizing enzyme from this organism was designated as methylenediurease (MDUase) and has been shown to be specifically induced by MDU and fractions of ureaform of different water solubility to activities of up to 26 nmol ammonium released from MDU per min and mg protein [8]. In the present study even higher activities are observed when the cells were grown with unfractionated methyleneureas (Table 1), and the aim of our work was to investigate the fate of the products released during the degradation of MU.

Products released in the breakdown of MU are further metabolized by *O. anthropi* through a series of different enzyme and uptake systems. While a number of enzymes responsible for the assimilation of ammonium are expressed at similar levels at growth with both ammonium and MU as nitrogen source (glutamine synthetase, alanine dehydrogenase, glutamate-pyruvate transaminase), the transport systems for urea and ammonium as well as enzymes responsible for the further metabolism of

Table 1  
Transport and enzyme activities in *O. anthropi* after growth with ammonium and methyleneureas as a nitrogen source

Nitrogen source	20 mM NH <sub>4</sub> Cl	0.6 g/l methyleneureas
MDUase	0.4	970
Urease	90	471
Formaldehyd-DH	2.2	99
Formiat-DH	0.2	45
NH <sub>4</sub> <sup>+</sup> transport	0.1	4.0
Urea transport	0.2	14
Gln Synthetase	139	138
GOGAT	nd	nd
Glu-Pyr Transaminase	49	41
Ala-DH (NAD)	154	118
Glu-DH (NAD/NADP)	nd	nd

All activities are given in nmol product formed/substrate metabolized or transported/min × mg protein  
nd = not detected

the products of MU degradation (urease, formaldehyde and formiate dehydrogenase) are induced or derepressed at growth with MU (Table 1). A remarkable finding is the absence of a glutamate dehydrogenase in *O. anthropi*. Instead, ammonium is metabolized to amino acids via glutamine synthetase, an NAD-dependent alanine dehydrogenase (AlaDH) and specific transaminases. Formaldehyde is oxidized via formiate to CO<sub>2</sub> by NAD-dependent formaldehyde and formiate dehydrogenase, thereby using these compounds as a source of energy. No evidence was found for an assimilation of formaldehyde as a carbon source for growth in *O. anthropi*.

The molecular mechanism of degradation of MU was studied with MDUase from cells grown with MU as the sole source of nitrogen, which was purified by a procedure consisting of heat treatment and a series of chromatographical methods including HIC, SEC and IEC, as described before [8]. Using this purified enzyme preparation, a complete degradation of MDU, DMTU and TMTU was observed. These compounds were hydrolysed to ammonium, formaldehyde and urea in a molar ratio of 2 : 1 : 1 (MDU), 4 : 2 : 1 (DMTU) and 6 : 3 : 1 (TMTU). The proposed pathway of the degradation of MDU by the MDUase is shown in Fig. 1. The degradation of DMTU (TMTU) is catalysed by the same enzyme and may occur by the same route. In the first step ammonium and carbon dioxide are formed as well as an aminated methyl-MDU (methyl-DMTU), which hydrolyses to ammonium and N-hydroxymethyl-MDU (N-hydroxymethyl-DMTU). The latter compound subsequently

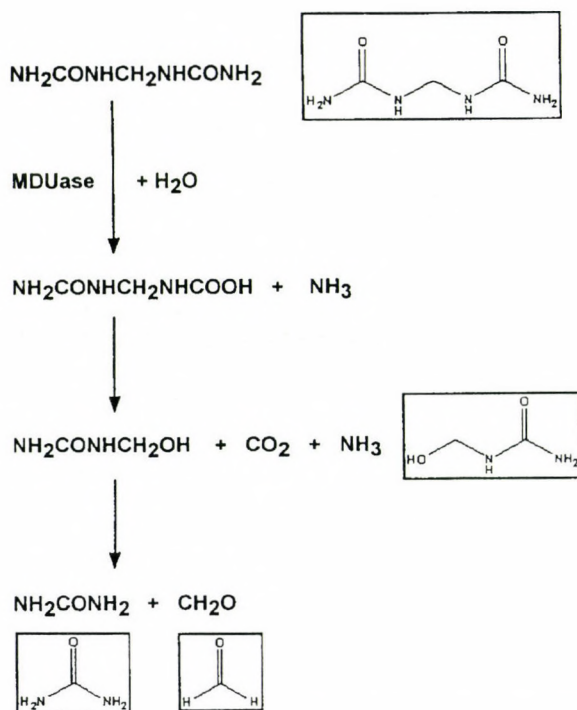


Fig. 1. Pathway of MDU degradation by *O. anthropi*. See text for further explanation

decomposes to formaldehyde and MDU (DMTU), which is then degraded via the route described above. An identification of the postulated intermediates is restrained by their instability.

Table 2  
Localization of methylenediurease in *O. anthropi*

Enzyme	Percent volume activity in the shock fluid
MDUase	7.7
Urease	0.4
Ala-DH (NAD)	0.0
Alkaline phosphatase	6.7

Total enzyme activities of both extract and shock fluid were determined, and the percentage of enzyme activities in the shock fluid was calculated.



Highly condensed methyleneureas are large molecules, and the cytoplasmic membrane of the cells is expected to act as a permeability barrier for the uptake of these compounds. Therefore, transport systems would be needed in order to allow sufficiently fast translocation of MU through the membrane and their subsequent degradation. Another possibility would be an extracellular localization of the MDUase, i.e. a secretion of the enzyme into the periplasm or into the culture supernatant. Since MDUase activity was not observed in the culture fluid at any phase of growth of the organism, attempts to detect the enzyme in the periplasm were carried out using sphaeroplasts and osmotically shocked cells. *O. anthropi* turned out to be highly resistant to lysozyme, even in the presence of high concentrations of EDTA (results not shown), and no sphaeroplasts could be obtained in order to test the hypothesis of a localization of the enzyme in the periplasm by this approach. Furthermore, the cells were comparably resistant to osmotic shock treatment, and only low amounts of protein were released from the cells during this procedure; these findings are in accordance to the high resistance of this organism to a range of antibiotics, which may be due to an extraordinarily 'tight' cell surface [4]. However, significant activities of methylenediurease and alkaline phosphatase (known as a marker for periplasmic enzymes) were detected in the shock fluid, while urease and alanine dehydrogenase were virtually absent (Table 2). Furthermore, the metabolism of methylenediurea by whole cells was not inhibited by the uncoupler carbonyl-

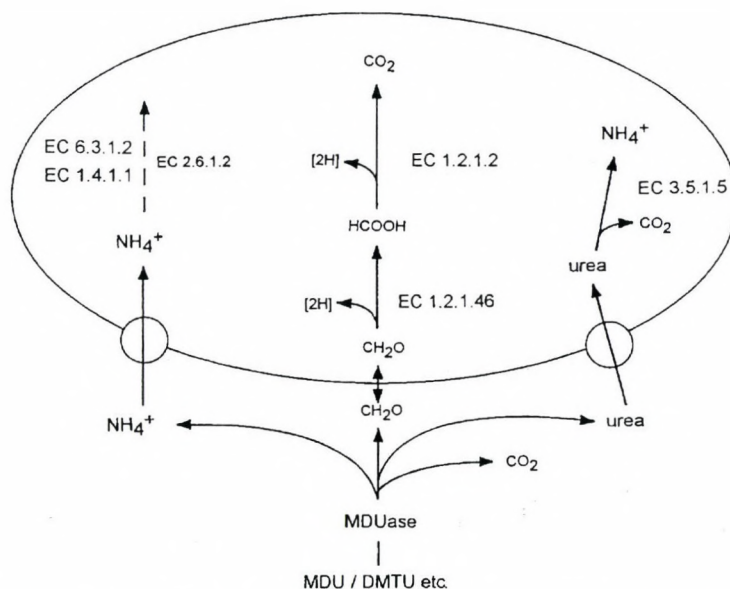


Fig. 2. Current model for MU degradation in *O. anthropi*. EC 1.2.1.2 = formiate dehydrogenase; EC 1.2.1.46 = formaldehyde dehydrogenase; EC 1.4.1.1 = alanine dehydrogenase; EC 2.6.1.2 = glutamate-pyruvate aminotransferase; EC 3.5.1.5 = urease; EC 6.3.1.2 = glutamine synthetase

cyanide-m-chlorophenylhydrazone known to inhibit energy-dependent membrane transport systems (results not shown); if active transport processes were involved in the translocation of MU through the bacterial cytoplasmic membrane, an inhibition would have been expected. Both findings suggest that methylenediurease may be a periplasmic enzyme, and our current model for the degradation of MU in *O. anthropi* is depicted in Fig. 2.

Further studies are required in order to determine whether higher condensated urea-formaldehyde compounds as they occur in MU used as fertilizers (tetramethylenepentaurea, pentamethylenehexaurea, etc.) are also degraded by the enzyme. Until now, such studies are hampered by the very low solubility of these condensates and both the lack of pure substances and suitable analytical techniques. However, a slow but continuous release of ammonium was observed from hot-water insoluble methyleneurea incubated with purified MDUase. Since this MU-fraction does not contain significant amounts of urea, MDU, DMTU and TMTU, this indicates that methyleneureas with a higher degree of polymerization may also be metabolized by this enzyme.

#### REFERENCES

1. Aarnio, T., McCullough, K., Trofymow, J. A. (1996) Fate of urea and ureaformaldehyde nitrogen in a one-year laboratory incubation with Douglas-fir forest floor. *Soil Biol. Biochem.* 28, 1407–1415.
2. Alexander, A., Helm, H.-U. (1990) Ureaform as a slow-release fertilizer: a review. *Z. Pflanzenernähr. Bodenk.* 153, 249–255.
3. Bender, R. A., Jannsen, K. A., Resnick, A. D., Blumenberg, M., Foor, F., Magasanik, B. (1977) Biochemical parameters of glutamine synthetase from *Klebsiella aerogenes*. *J. Bacteriol.* 129, 1001–1009.
4. Bizet, C., Bizet, J. (1995) Comparative susceptibility of *Ochrobactrum anthropi*, *Agrobacterium tumefaciens*, *Alcaligenes faecalis*, *Alcaligenes denitrificans* subsp. *denitrificans*, *Alcaligenes denitrificans* subsp. *xyloisidans* and *Bordetella bronchiseptica* against 35 antibiotics including 17 beta-lactams. *Pathol. Biol. (Paris)* 43, 258–263.
5. Fuller, W. H., Clark, K. G. (1947) Microbiological studies on urea-formaldehyde preparations. *Soil Sci. Soc. Amer. Proc.* 12, 198–202.
6. Heinz, F. (1984) Formaldehyde (methanal). In: Bergmeyer, H. U. (ed.) *Methods of Enzymatic Analysis*. 3rd ed. vol VI. Verlag Chemie, Weinheim, pp. 657–661.
7. Jahns, T. (1992) Occurrence of cold-labile NAD-specific glutamate dehydrogenase in *Bacillus* species. *FEMS Microbiol. Lett.* 96, 187–192.
8. Jahns, T., Schepp, R., Kaltwasser, H. (1997) Purification and characterization of an enzyme from a strain of *Ochrobactrum anthropi* that degrades condensation products of urea and formaldehyde (ureaform). *Can. J. Microbiol.* 43, 1111–1117.
9. Jahns, T., Zobel, A., Kleiner, D., Kaltwasser, H. (1988) Evidence for carrier-mediated, energy-dependent uptake of urea in some bacteria. *Arch. Microbiol.* 149, 377–383.
10. Nason, A., Little, H. N. (1955) Formic dehydrogenase from peas. In: Colowick, S. P., Kaplan, N. O. (eds) *Meth Enzymology*. Vol. I. Academic Press Inc, New York, pp. 536–539.
11. Nossal, N. G., Heppel, L. A. (1966) The release of enzymes by osmotic shock from *Escherichia coli* in exponential growth phase. *J. biol. Chem.* 241, 3055–3062.



## DIFFERENTIAL DETECTION OF *N*-HETEROCYCLIC COMPOUNDS AND THEIR *N*-METHYLATED DERIVATIVES BY IMMUNOANALYSIS\*

HONG M. LE, GYÖNGYVÉR HEGEDŰS and A. SZÉKÁCS

Plant Protection Institute of the Hungarian Academy of Sciences, Budapest, Hungary

(Received: 1998-10-28; accepted: 1998-11-25)

Competitive enzyme-linked immunosorbent assay (ELISA) systems are proposed for the indirect monitoring of formaldehyde by the parallel detection of its *N*-methylated precursors and the corresponding demethylated compounds. As an example for such immunoanalytical differentiation between an *N*-heterocyclic compound and its *N*-methylated derivative, the quantitative detection of the systemic triazole fungicide, myclobutanil, is discussed. Antibodies recognizing the non-zwitterionic structure of 2-(4-chlorophenyl)-2-[(1,2,4-triazol-1-yl)-methyl]-hexanonitrile (myclobutanil) showed only minor binding to corresponding *N*-alkylated derivatives of myclobutanil. And *vice versa*, literature data indicate that antibodies raised against the pyridinium ionic structure of the herbicide paraquat, displayed only mediocre reactivity towards the corresponding dealkylated derivatives. Thus, both experimental and literature data suggest that immunoanalytical methods for differential detection of *N*-methylated heterocycles (potentially including formaldehyde precursors) and their non-methylated counterparts are possible to develop.

**Keywords:** ELISA – immunoassay – cross-reactivity – myclobutanil – paraquat

### INTRODUCTION

As the significance of biological methylation/demethylation processes is revealed, differential quantitative detection of various *N*-compounds (amines or heterocycles) and their *N*-methylated counterparts becomes of increasing importance. This applies particularly to studies when generation of formaldehyde or the kinetics of its precursors are examined.

Enzymatic demethylation of *N*- or *S*-methyl compounds have been proposed to result in the generation of formaldehyde [6, 7]. Moreover, endogenous formaldehyde has been hypothesized to be generated through methylation processes as well [4]. Putative key intermediates in formaldehyde generating demethylation processes are

\* Presented at the 4th International Conference on the Role of Formaldehyde in Biological Systems, July 1–4, 1998, Budapest, Hungary.

Send offprint requests to: Dr. A. Székács, Plant Protection Institute of the Hungarian Academy of Sciences, H-1525 Budapest, P.O.Box 102, Hungary.



quaternary *N*-methyl derivatives. Although the majority of stress-related physiological *N*-methylated compounds (including presumed formaldehyde precursors) includes quaternary derivatives of aliphatic amines (e.g., glycine betaine, choline, *N*<sup>ε</sup>-trimethyl-*L*-lysine, *L*-carnithine, etc.), several quaternary heterocyclic formaldehyde precursors (trigonelline, stachydrine) are also assumed. Trigonelline (3-carboxy-1-methylpyridinium hydroxide inner salt, nicotinic acid *N*-methylbetaine, caffeine, gynesine) has been long known to occur in coffee beans, as well as in seeds of various plants including *Trigonella foenumgraecum* L. (*Leguminosae*), *Strophanthus* spp. (*Apocynaceae*), *Cannabis sativa* L. (*Moraceae*) and many other species [5, 9, 20, 23]. Stachydrine (2-carboxy-1,1-dimethylpyrrolidinium hydroxide inner salt, methyl hydrate betaine, hygric acid methylbetaine) also occurs widely in nature, especially in alfalfa, *Chrysanthemum*, *Citrus* and *Stachys* species [22]. Both of these compounds are quaternary ammonium salts (trigonelline is a monomethyl derivative of an aromatic *N*-heterocycle, while stachydrine is a dimethyl derivative of a cycloaliphatic *N*-heterocycle).

It is important to note, however, not only quaternary ("fully alkylated") *N*-alkyl ammonium compounds can act as formaldehyde precursors. *N*-methyl-ascorbigen, an indolyl derivative of ascorbic acid, is also suspected to generate formaldehyde. This compound, formed in methylation of ascorbigen and isolated from cruciferous vegetable tissues, has been proven to exert strong biological activity including immunomodulating and antitumoral effects. Previous studies suggested that these beneficial effects are related to formaldehyde generation [10]. In addition to *N*-methyl-ascorbigen, several other, not "fully alkylated" compounds containing no quaternary ammonium moieties have been suspected as formaldehyde generators, including epinephrine, ethylmorphine, nicotine or nicomorphine [24].

Formaldehyde is readily detected by instrumental analytical chromatographic methods e.g., HPLC, OPLC or TLC, nonetheless, it is often monitored indirectly by measuring the concentration of certain formaldehyde scavengers (e.g., dimedone) or the level of the formaldehyde precursor *N*-methyl compounds and their demethylated derivatives. An interesting novel possibility of such indirect detection is offered by the use of immunoanalytical methods. Recent developments in the field of immunodetection of small molecules have proven that immunoassays serve as facile, time- and cost-effective alternatives to instrumental analysis [2, 3]. Enzyme-linked immunosorbent assays (ELISAs) are particularly applicable in environmental monitoring, where large numbers of – mostly aqueous – samples are analyzed [3, 19].

As an example to illustrate characteristic differences in antibody affinity as a function of *N*-alkylation of the antigen, cross-reactivity patterns of our antibodies against a triazole fungicide, myclobutanil (2-(4-chlorophenyl)-2-[(1,2,4-triazol-1-yl)-methyl]-hexanonitrile) [11, 13] is discussed with respect of differential sensitivity to alkylated and non-alkylated triazole derivatives. In addition, literature data for differences in immunorecognition of the pyridylum herbicide, paraquat and its *N*-demethylated derivatives [16–18] are cited. These data together suggest the possibility of immunoanalytical distinction between methylated and demethylated forms of putative formaldehyde precursors as well.

## MATERIALS AND METHODS

### *Hapten synthesis, conjugation and verification*

Haptenic compounds and immunogenic conjugates were prepared as described by Székács and Hammock [13]. 2-(4-chlorophenyl)-2-[(1,2,4-triazol-1-yl)-methyl]-hexanoic amide (**II**) was prepared by the partial hydrolysis of myclobutanil (**I**) under phase transfer conditions, while 2-(4-chlorophenyl)-2-[(1,2,4-triazol-1-yl)-methyl]-hexanoic acid (**III**) was prepared by the nitrosation of **II**. The products were purified and characterized by IR,  $^1\text{H}$  NMR,  $^{13}\text{C}$  NMR and mass spectroscopy. Spectral data are listed in Székács and Hammock [13]. The hapten (**III**) was conjugated to carrier proteins, i.e. conalbumin (CONA) and bovine serum albumin (BSA), *via* amide bonds by the DCC method [15].

### *Immunization, serum collection and enzyme-linked immunosorbent assay (ELISA)*

New Zealand white rabbits were immunized intradermally with the immunogen **III**-CONA (CONA conjugate). The immunoglobulin fraction of the serum was collected by sodium-sulfate precipitation.

ELISA determinations were performed in 96-well microplates following the basic solid phase immunoassay principle of Voller [21]. BSA conjugates were used as plate coating antigens. Bound antibodies were exposed to anti-rabbit IgG (1 : 2500 dilution in phosphate buffer) conjugated to horseradish peroxidase (HRP) and enzymatic activity was measured using hydrogen-peroxide as a substrate and *o*-phenylenediamine (OPD) as a chromophore. Analyte concentrations were measured indirectly by competition with the coating antigen for antibody binding sites.

## RESULTS AND DISCUSSION

### *Hapten synthesis and conjugation*

In order to obtain and utilize antibodies, immunoanalytical methods require the synthesis of analogs of the target analytes (haptens) containing functional groups for coupling to larger molecules. These small and immunologically inactive compounds are rendered immunogenic by being coupled to carrier proteins. A haptenic derivative (**III**) of myclobutanil (**I**) (Fig. 1) was conjugated to proteins (CONA, BSA). The quantity of the hapten coupled to the protein was determined by the back-titration of the free amino groups available on the protein before and after conjugation, and was found to be 0.19 and 0.23 mmol hapten/g protein for the CONA and the BSA conjugate, respectively. An additional hapten with a quarternary nitrogen atom in the triazole ring (**V**) was prepared by alkylation of the parent compound.



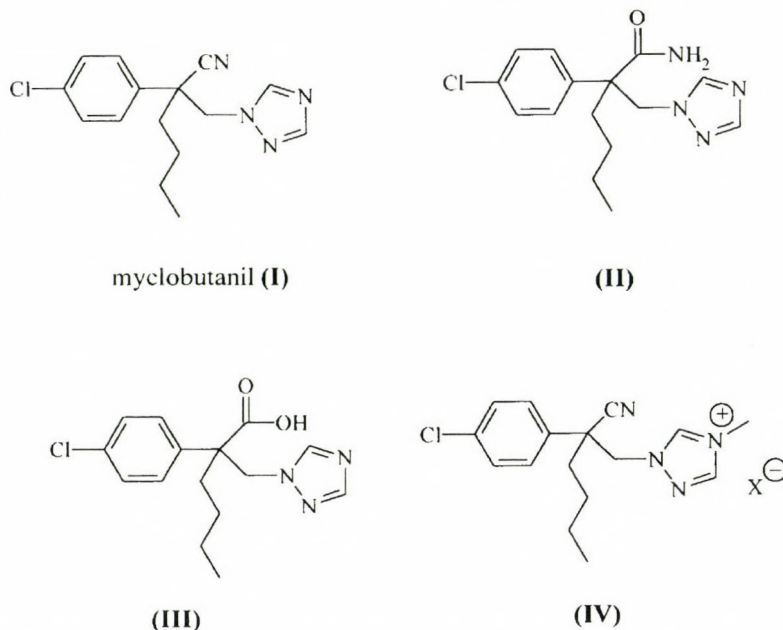


Fig. 1. Chemical structure of myclobutanil and its haptenic and quarternary alkylated derivatives

### *Immunoassay development and characterization*

Enzyme-linked immunosorbent assays (ELISAs) detect given target compounds by their characteristic binding to target-specific antibodies. *N*-methylation or demethylation results in outstanding differences in molecular features of the given compounds: water solubility is highly increased by quaternary salt formation, moreover, the electron distribution within the molecule is also greatly modified. These differences are expected to result in expressed alterations of antigenic properties and immunogenicity. Therefore, antibodies specific for given *N*-methylated compounds are likely to recognize the corresponding demethylated derivatives with a characteristic difference, and *vice versa*. This differential sensitivity of the above-mentioned antibodies makes immunoanalysis an applicable and facile method in monitoring of putative formaldehyde precursors, and therefore in the indirect monitoring of formaldehyde.

In this study, an immobilized antigen based, competitive indirect immunoassay was utilized, where binding of the antiserum to an immobilized macromolecular antigen is suppressed by the target analyte in solution. The assay is therefore based on a competition between the target analyte in solution and the hapten immobilized on the solid surface as a protein conjugate. The influence of the following factors were tested on assay performance: pH (4.9–9.4), incubation temperatures (4 °C, room tem-



perature and 37 °C), the amount of the coating antigen (1 µg/mL to 20 µg/mL), as well as the addition of surfactants. Comparative competitive inhibition experiments were carried out under optimized conditions.

Inhibition by myclobutanil appeared to be in the micromolar range that is close to the sensitivity of similar immunoassays reported [1, 8]. Competitive inhibition tests with the purified antiserum were run in at least three replicates with a coefficient of variation of less than 7%, under optimized conditions. The minimum detectable concentration of myclobutanil was 0.2 mg/mL. The  $I_{50}$  values of myclobutanil (**I**) and intermediates **II** and **III** were found to be 4.9, 1.4 and 2.4 mg/mL, respectively.

Utilization of the present ELISA system has been discussed elsewhere [11, 14]. Nonetheless, it is a particularly interesting feature of the antibody that it shows characteristically low binding to *N*-alkylated derivatives of the parent compound. This is seen particularly from cross-reactivity values. [Cross-reactivity of a given compound is defined as a percentage ratio of the  $IC_{50}$  value of the reference compound (myclobutanil) and that of the given compound.] Cross-reactivities with various triazole derivatives ranged between 0–15%. The assay, however, was not inhibited by *N*-alkylated triazoles. One analog of this kind, *N*-alkylated on the triazole ring by a 5-carboxypentyl moiety (**V**) was prepared intended to be used as an additional immunogen. Antibodies raised against the conjugate of intermediate **III** did not appear to bind to this analog.

Literature results indicate that antibodies are possible to be formed against *N*-alkylated quaternary compounds [16–18]. One example is the herbicide paraquat (**VI**) (Fig. 2), where antibodies of good affinity were obtained against the parent compound containing two quaternary pyrimidinium nitrogen atoms. The same antibodies, however, showed highly reduced binding to the partially or fully demethylated analogs (**VIII**, **IX**) (Table 1).

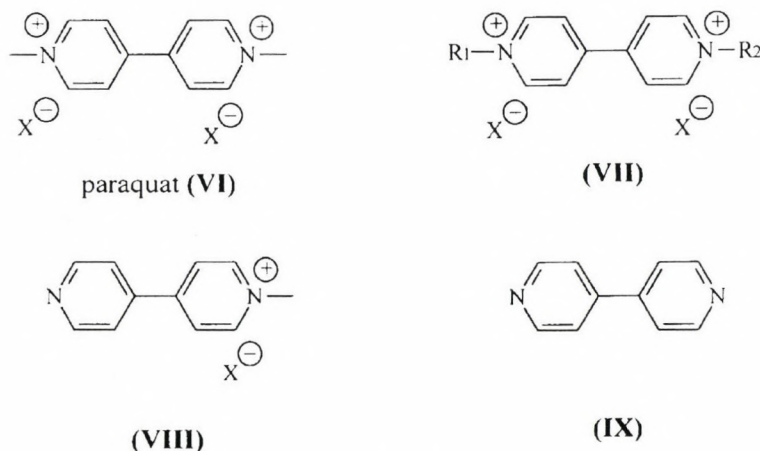


Fig. 2. Chemical structure of paraquat and its haptenic derivatives

Table 1

Cross-reactivities of (A) polyclonal antibodies raised against a haptenic derivative (III) of myclobutanil (I) with various related compounds (B) polyclonal antibodies raised against a quarternary alkylated haptenic derivative of paraquat (VI) with various related compounds. Data on paraquat and its derivatives are cited from Van Emon et al. [22]

Compound	Cross-reactivity <sup>a</sup>	Compound	Cross-reactivity <sup>a</sup>
(A)		(B)	
Myclobutanil (I)	100 (IC <sub>50</sub> = 4.9 ± 0.5 µg/ml)	Paraquat (VI)	100 (IC <sub>50</sub> = cca. 1 ng/ml)
2-(4-chlorophenyl)-2-[(1,2,4-hexanoic amide (II)	354	Alkyl paraquat derivatives (VII)	
2-(4-chlorophenyl)-2-[(1,2,4-triazol-1-yl)-methyl ]-hexanoic acid (III)	204	R <sub>1</sub> = Et, R <sub>2</sub> = Et	89
N-methyl-myclobutanil (IV)	2.1	R <sub>1</sub> = Me, R <sub>2</sub> = Pr	100
N-(5-carboxypentyl)-myclobutanil (V)	4.6	R <sub>1</sub> = Pr, R <sub>2</sub> = Pr	94
		R <sub>1</sub> = Hex, R <sub>2</sub> = Hex	42
		R <sub>1</sub> = Oct, R <sub>2</sub> = Oct	32
		R <sub>1</sub> = <i>t</i> Bu, R <sub>2</sub> = <i>t</i> Bu	18
		R <sub>1</sub> = Bz, R <sub>2</sub> = Bz	45
		Monodesmethyl paraquat (monoquat) (VIII)	31
		Didesmethyl paraquat (4,4'-bipyrididyl) (IX)	14

<sup>a</sup>Cross-reactivities are defined as the percentage ratio of the IC<sub>50</sub> value (the concentration which inhibits the assay by 50%) of the reference compound (myclobutanil or paraquat) and of the given compound. IC<sub>50</sub> values were calculated from four-parameter fit, and were not determined above 1 mg/mL concentration.

## CONCLUSION

In conclusion, literature data and our laboratory results indicate that antibodies, in certain cases, sharply distinguish between *N*-alkylated and non-alkylated counterparts of *N*-containing heterocycles. A prerequisite for this differentiation is that the antibody recognizes at least one of these chemical types of molecules. A small *N*-heterocycle, 1,2,4-triazole was found not being immunogenic of sufficient affinity to bind to antibodies raised against various triazole derivatives [1, 12, 14, 19]. Other *N*-heterocycles e.g., triazines appear highly immunogenic [3]. In two such cases, highly different immunoaffinity is seen towards derivatives of different alkylation rates on the ring nitrogen atom(s). Could antibodies of sufficient affinity be raised against putative formaldehyde precursors, the ratio of their methylated and non-methylated forms may be detected, and therefore, immunoassays may offer a means of indirect monitoring of minute levels of formaldehyde generated.

## ACKNOWLEDGMENT

This work was supported by EC INCO-COPERNICUS Grant ERBIC15CT960802. A. Sz. is a Bolyai János Research Scholar of the Hungarian Academy of Sciences, 1998–2001.

## REFERENCES

1. Forlani, F., Arnoldi, A., Pagani, S. (1992) Development of an enzyme-linked immunosorbent assay for triazole fungicides. *J. Agric. Food Chem.* 40, 328–331.
2. Hall, J. C., Deschamps, R. J. A., McDermott, M. R. (1990) Immunoassays to detect and quantitate herbicides in the environment. *Weed Technol.* 4, 226–234.
3. Hammock, B. D., Gee, S. J., Harrison, R. O., Jung, F., Goodrow, M. H., Li, Q. X., Lucas, A., Székács, A., Sundaram, A. (1990) Immunochemical Technology in environmental analysis: Addressing critical problems. In: Van Emon, J., Mumma, R. (eds) *Immunochemical Methods for Environmental Analysis. ACS Symp. Ser.* 442, 112–139.
4. Huszti, S., Tyihák, E. (1986) Formation of formaldehyde from *S*-adenosyl-*L*-(methyl-<sup>3</sup>H) methionine during enzymic transmethylation of histamine. *FEBS Lett.* 209, 362–366.
5. Jahns, E. (1896) Vorkommen von Stachydrin in den Blättern von *Citrus vulgaris*. *Chem. Ber.* 29, 2065.
6. Kapoor, M., Lewis, J. (1987) Heat shock induces peroxidase activity in *Neutospora crassa* and confers tolerance toward oxidative stress. *Biochem. Biophys. Res. Commun.* 147, 904–910.
7. Kedderin, G. L., Hollenberg, P. F. (1983) Steady state kinetics of chloroperoxidase-catalyzed *N*-demethylation reactions. *J. Biol. Chem.* 258, 12413–12419.
8. Newsome, W. H. (1986) Development of an enzyme-linked immunosorbent assay for triadimefon in foods. *Bull. Environ. Contam. Toxicol.* 36, 9–14.
9. Planta, A., Schulze, E. (1893) Über Stachydrin. *Chem. Ber.* 26, 939.
10. Szende, B., Tyihák, E., Szókán, Gy., Kátay, Gy. (1995) Possible role of formaldehyde in the apoptotic and mitotic effect of 1-methyl-ascorbigen. *Pathol. Oncol. Res.* 1, 38–42.
11. Székács, A. (1994) Development of enzyme-linked immunosorbent assay (ELISA) systems for environmental monitoring. *Acta Biologica Hungarica* 45, 77–80.



12. Székács, A., Jung, F., Hammock, B. D. (1995) Chemical modification of haptens – Selective amino group protection by chromophores for an immunoassay for aminotriazoles. In: Kurtz, D. A., Skerritt, J. H., Stanker, L. (eds) *New Frontiers in Agrochemical Immunoanalysis*. Am. Org. Anal. Chem., Washington DC., pp. 65–75.
13. Székács, A., Hammock, B. D. (1995) Development of an enzyme-linked immunosorbent assay for the detection of the triazole fungicide myclobutanil. *J. Agric. Food Chem.* 43, 2083–2091.
14. Székács, A., Cairolì, S., Le, H. M., Pagani, S. (1996) Comparative studies on enzyme-immunoassays (ELISA) for the triazole fungicides tetraconazole and myclobutanil. *Acta Phytopathologica et Entomologica Hungarica* 31, 293–301.
15. Tijssen, P. (1985) *Practice and Theory of Enzyme Immunoassay*. Elsevier: Amsterdam, The Netherlands.
16. Van Emon, J. M., Seiber, J. N., Hammock, B. D. (1985) Applications of immunoassay to Paraquat and other pesticides. In: Hedin, P. A. (ed.) *Bioregulators for Pest Control. ACS Symp. Ser.* 276, 308–316.
17. Van Emon, J. M., Hammock, B. D., Seiber, J. N. (1986) Enzyme-linked immunosorbent assay for Paraquat and its application to exposure analysis. *Anal. Chem.* 58, 1866–1873.
18. Van Emon, J. M., Seiber, J. N., Hammock, B. D. (1987) Application of an enzyme-linked immunosorbent assay (ELISA) to determine paraquat residues in milk, beef and potatoes. *Bull. Environ. Contam. Toxicol.* 39, 490–497.
19. Vanderlaan, M., Watkins, B. E., Stanker, L. (1988) Environmental monitoring by immunoassay. *Environ. Sci. Technol.* 22, 247–254.
20. Vickery, H. B. (1924) Some nitrogen constituents of the juice of the alfa plant. *J. Biol. Chem.* 61, 117–127.
21. Voller, A. (1976) Enzyme Immunoassay in Diagnostic Medicine: Theory and Practice. *Bull. W.H.O.* 53, 55–65.
22. Windholz, M., Budavari, S., Blumetti, R. F., Otterbein, E. S. (eds) (1983) *The Merck Index* 10th Edition. Merck & Co., Inc., Rahway, NJ, USA.
23. Yoshimura, K. (1913) Über die Verbreitung organischer Basen, insbesondere von Adenin und Cholin im Pflanzenreich. *Z. Physiol. Chem.* 88, 334.
24. Yu, P. H. (1998) Increase of formation of methylamine and formaldehyde in vivo after administration of nicotine and the potential cytotoxicity. *Neurochem. Res.* 23, 1205.

## UREA-FORMALDEHYDE RESINS AND FREE FORMALDEHYDE CONTENT\*

VIKTÓRIA VARGHA

Department of Plastics, Rubber and Fibre Technology  
Technical University of Budapest, Budapest, Hungary

(Received: 1998-10-28; accepted: 1998-11-25)

Specifications of wood adhesives must be in correlation with the requirements for the corresponding wood products, for which they will be used. Formaldehyde emission of wood products bonded with urea-formaldehyde resin based adhesives is strictly regulated by standards and there is a compromise between formaldehyde emission and performance, such as strength, or water resistance. Since values of formaldehyde emission depend on the test method used, in Europe urea-formaldehyde resins for adhesives may generally be classified according to HCHO emission in the particleboard rating of Emission 0 to Emission 1 class (E–O to E–1). According to DIN EN 120, particleboard quality E1 emits <6.5 mg/100 g dry article determined with the perforator method. Although a great number of factors effect the formaldehyde emission of the cured products, such as the hardener system, the type of wood etc., the emission of formaldehyde is in strict correlation with the free formaldehyde content of the resin before the curing process. E1 emission class can be achieved, if the free formaldehyde content of the resin is lower than 0.2% by mass. Urea-formaldehyde resins containing higher than 0.5% free formaldehyde by mass exceed emission class E2, and are not accepted. Since the free formaldehyde content of the urea-formaldehyde resin effects the emission of formaldehyde in the cured product, low formaldehyde content must be ensured during resin synthesis. This can be achieved by properly selecting synthesis conditions as well as raw materials. The quality of raw materials is an essential and determining factor for the synthesis of urea formaldehyde resins. The principal changes which may take place in the formaldehyde solution on storage are the polymerization and precipitation of the polymer, Cannizzaro reaction, methylation formation, oxydation to formic acid, condensation to hydroxyaldehydes and sugars. Any of these reactions are detrimental to product quality. The state of formaldehyde is also an essential factor, since the reaction of poly(methylene glycol)s with urea leads to methylene ether linkages resulting in emission of formaldehyde during storage and later on during the process of curing. Hydrolysis, isomerisation and decomposition of urea may take place simultaneously during improper storage conditions, such as high humidity, high temperatures, industrial atmosphere. The side products formed affect the reaction with formaldehyde during the synthesis resulting in high free formaldehyde content of urea-formaldehyde resins. The relation between synthesis conditions, free formaldehyde content and performance of urea-formaldehyde resins are discussed in detail.

**Keywords:** Urea – formaldehyde – emission –  $^{13}\text{C}$ -NMR-spectroscopy – wood – adhesives

\* Presented at the 4th International Conference on the Role of Formaldehyde in Biological Systems, July 1–4, 1998, Budapest, Hungary.

Send offprint requests to: Dr. Viktória Vargha, Institute of Chemistry, Chemical Research Center, Hungarian Academy of Sciences, H-1525 Budapest, P.O. Box 17, Hungary; E-mail: [vargha.mua@chem.bme.hu](mailto:vargha.mua@chem.bme.hu)



## INTRODUCTION

Hazardous properties of exogenous formaldehyde are very well known, although formaldehyde-based resins still make a considerable part of synthetic resins overall. The most important representatives of formaldehyde-based products are the phenoplastics and aminoplastics, the first synthetic thermosetting plastic materials. Precursors of phenoplastics are the phenol-formaldehyde resins, whereas the most important precursors of aminoplastics are urea-formaldehyde and melamine-formaldehyde resins. Due to their excellent performance, durability, ease of synthesis, and relatively low price, all these thermosetting resins still have a widespread application all over the world. This may only be possible, if these materials meet the international requirements of environmental protection. This refers to the free formaldehyde content of these resins, which is in strict correlation with the formaldehyde emission of the cured product.

Urea-formaldehyde resins are excellent adhesives for wood products and are widely used even nowadays as wood adhesives [1]. In spite of their advantageous properties, i.e. excellent adhesion to lignocellulosics, excellent intrinsic cohesion, ease of handling and application, lack of colour in the finished product and low cost, urea-formaldehyde resins have two main drawbacks. They do not resist weather and water and emit formaldehyde vapours during the use of wood products bonded with them. While the lack of weather resistance is a drawback, which can be tolerated when these adhesives are used for interior wood products, formaldehyde emission is especially harmful because of environmental reasons. Application of these products is possible only if the free formaldehyde content is reduced to a minimum level. Efforts are made all over the world to decrease formaldehyde emission, which may be achieved on one side by using urea-formaldehyde resins of very low free formaldehyde content. This paper reveals the factors, which influence and determine the free formaldehyde content of urea-formaldehyde resins. These factors include the state and reactions of raw materials during improper storage, state of formaldehyde before and during synthesis, side reactions of monomers, and the effects of synthesis conditions on the free formaldehyde content of the resin. A short survey is given on the requirements described by the international standards on free formaldehyde content of the resins and formaldehyde emission of the final products, and the ways, how to achieve these requirements, are discussed.

## FORMALDEHYDE EMISSION

### *Methods for determination of formaldehyde emission*

Formaldehyde emission of wood products may be determined by different methods. The *perforator or extraction method* is given by the European standard EN 120:1992. The principle of this method is that formaldehyde in test samples is extracted with boiling toluene, absorbed in distilled or deionized water, and deter-



mined photometrically by using acetylacetone as reagent. The value of formaldehyde emission is given in mg/100 g dry board. *The gas analysis method* is described in EN 717-2:1994. The principle of this method is the following: test sample of known surface and thickness is inserted in a tempered vessel and air is flown through the vessel with a constant rate. The eliminating formaldehyde will be carried by the flowing air and is absorbed into distilled water. The analysis is carried out photometrically by using acetylacetone as reagent. The quantity of formaldehyde is given in mg/m<sup>2</sup>h. *The evaluation chamber method* is given by EN 717-1. The principle of the chamber test is that the test sample is placed in a closed chamber, which is ventilated according to a strictly given program. The equilibrium concentration of formaldehyde in ppm is measured. Any of these methods may be carried out in Hungary by the Wood Quality Control and Consulting Ltd., Budapest (Faipari Minőségellenőrző és Tanácsadó Kft., Budapest).

### *Classification of wood products according to formaldehyde emission*

Wood products, such as chipboard, fibreboard or plywood, are classified according to formaldehyde emission, i.e. according to the expectable concentration of formaldehyde in the air of rooms, where they are used. The German Committee for Uniform Technical Building Regulations (Ausschuß für Einheitliche Technische Baubestimmungen – ETB) published in April 1980 the Regulations for the Application of Wood Panels relating to the Restriction of Formaldehyde Concentration in Closed Area. The limits of formaldehyde emission and the referring classes of wood products were established on the emission values determined by the perforator method [earlier described by DIN 68763-1989]. As there are some other methods for determining formaldehyde emission, different from the perforator method, such as the gas analysis method [earlier by DIN 52368-1984] or the chamber test method [2], which was standardized later in CEN-Norm pr EN 717-1, it is rather difficult to draw a correlation between the values gained by the use of these different methods. The Regulations for the Application of Wood Panels relating to the Restriction of Formaldehyde Concentration in closed Area published first in April 1980 have been continuously surveyed and were republished in October 1991 by the German Institute for Building Technic (Deutsches Institut für Bautechnik – DIBt) with the new title “Regulations on the Classification and Control of Wood Panels relating to Formaldehyde Emission”. In the last publication of these Regulations in June 1994 [3] the following classes of wood products are distinguished according to value of formaldehyde emission of the wood product (Table 1).

### *Factors effecting formaldehyde emission*

Formaldehyde emission of wood products depends on a rather great number of factors. One of these is the *free formaldehyde content of urea-formaldehyde resin*. There

is an experimental relation between free formaldehyde content of urea-formaldehyde resins and formaldehyde emission of wood products bonded with those resins. According to this for E1 class wood product the free formaldehyde content of the resin should not exceed 0.2%. This, however, may not definitely guarantees low emission of formaldehyde, corresponding to class E1, if the *structure of the resin* allows methylene ether linkages. Kim and Amos [4] revealed the relation between formaldehyde to urea molar ratio and methylene linkages in urea-formaldehyde resins on the base of  $^{13}\text{C}$ -NMR-spectroscopy. Ferg, Pizzi, and Levendis apply model equations relating peak intensities assigned to  $^{13}\text{C}$ -NMR resonance of the possible functional groups in urea-formaldehyde resins with molar ratio of formaldehyde to urea in the corresponding resin, and with the help of these equations the release of formaldehyde during storage and application may be predicted [5]. This means that the presence of methylene ether linkages in the resin structure results in elimination of formaldehyde in a later stage. The other important factor contributing to formaldehyde emission is the *latent formaldehyde in wood* itself. The different procedures for determining formaldehyde emission take into consideration the elimination of formaldehyde deriving from wood. *Storage conditions*, such as temperature and humidity, also effect formaldehyde emission.

### *Free formaldehyde content of urea-formaldehyde resins, and the influencing factors*

In order to reduce formaldehyde emission, the free formaldehyde content of urea-formaldehyde resins should be restricted to a minimum, i.e. for E1 class resin to under 0.2%, and the formation of methylene ether linkages should be eliminated from the structure as much as possible. Free formaldehyde content of urea-formaldehyde resins is mostly effected by the quality of raw materials and by the conditions of resin synthesis.

### *Raw materials*

Raw materials must definitely meet standard specifications, and proper storage conditions must be maintained.

### *Reactions of urea during storage*

Specifications for urea for industrial uses are given by MSZ 3437-81. Urea is stable only in solid form at ambient temperature and dry conditions. It undergoes a number of reactions on heating above its melting point (m.p. 132.7 °C). At 150–160 °C, it decomposes to yield ammonia, ammonium cyanate ( $\text{NH}_4\text{OCN}$ ) and biuret ( $\text{HN}(\text{CONH}_2)_2$ ). As the temperature is raised further, other products including the cyclic compounds of cyanuric acid,  $\text{C}_3\text{N}_3(\text{OH})_3$ , and ammelide,  $\text{NH}_2\text{C}_3(\text{OH})_2$ , are



formed [6]. In the absence of microorganisms neutral solutions of urea are hydrolyzed very slowly to ammonia and carbon dioxide. Hydrolysis is accelerated by higher temperatures, addition of either acids or bases, presence of the enzyme urease, or increase in the concentration of urea [6]. Urea undergoes oxidation to form carbon dioxide, nitrogen and water in the presence of oxidizing agents such as hypochlorite. Hydrolysis, isomerisation and decomposition may take place simultaneously during improper storage conditions, such as high humidity, high temperatures, industrial atmosphere. The side products formed affect the reaction with formaldehyde during the synthesis of urea-formaldehyde resins.

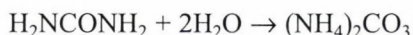
#### Reactions caused by impurities in urea during urea-formaldehyde resin synthesis

*Reactions caused by product of isomerization* Ammoniumcyanate,  $\text{NH}_4\text{OCN}$ , is a product resulting from the isomerisation of urea [7]. It reacts with formaldehyde to form cyanic acid:



The formation of cyanic acid results in decrease of pH during the dissolution of urea in neutralized formaldehyde solution. Decrease in pH results in an increasing rate of polycondensation of urea and formaldehyde before completion of methylol formation. This leads to resin precipitation and high free formaldehyde content.

*Reactions caused by product of hydrolysis* As a result of improper storage (e.g. under high humidity) urea contains ammonium carbonate,  $(\text{NH}_4)_2\text{CO}_3$ , as a hydrolysis product:



Formaldehyde reacts with ammonium carbonate to form urotropin according to the equation:



The above reaction results in the loss of formaldehyde from the reaction mixture. Consequently the degree of methylolation and solubility of condensed resin decreases leading to resin precipitation. Wirpsza [7] deals also with the effect of some impurities in urea which may form during its production.

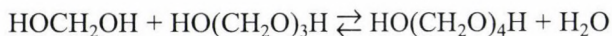
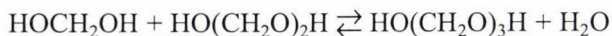
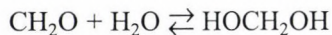
#### Reactions during storage of commercial formaldehyde solution

Formaldehyde for industrial use is marketed mostly in the form of aqueous solutions of 37% inhibited with 10–11% methanol to prevent precipitation of solid poly-



mer. Storage conditions depend on methanol content, formaldehyde concentration and temperature. Specifications of commercial formaldehyde solution used for urea-formaldehyde resin synthesis are given in MSZ 2337-83. The principal changes which may take place in formaldehyde solution on storage are the followings [8, 9]: Polymerization and precipitation of polymer, Cannizzaro reaction, methylal formation, oxydation to formic acid, condensation to hydroxylaldehydes and sugars. All of these reactions are detrimental to product quality but may be avoided or kept at a minimum by maintainance of proper storage conditions. Proper storage in general involves the avoidance of temperature extremes and the use of lined containers or storage tanks constructed of materials, i.e. aluminum or stainless steel, which are substantially inert to corrosion by the mildly acidic solution. The temperature of storage depends on formaldehyde concentration and on type and concentration of stabiliser. For a 37 per cent formaldehyde solution in water, stabilized with 11 per cent methanol, a range of 10–25 °C is recommended. The above reactions except polymerization result in loss of formaldehyde, polymerization, however, may lead to the formation of methylene ether linkages in the resin structure. Therefore poly-(oxymethylene glycol) formation will be discussed in detail.

*Polymerization and precipitation of polymer* Formaldehyde dissolved in water exists in hydrated form. At ordinary temperatures these hydrates have a relatively high degree of stability, and precipitation occurs at relatively high concentrations. Dissolved formaldehyde is present principally in the form of monohydrate, i.e. methylene glycol,  $\text{CH}_2(\text{OH})_2$ , and a series of low molecular mass polymeric hydrates or poly(oxymethylene glycol)s of the general formula  $\text{HO}(\text{CH}_2\text{O})_n\text{H}$ . A small concentration of monomeric formaldehyde is also present but its concentration is well under 0.1 per cent even in concentrated solutions. Low formaldehyde concentrations favor methylene glycol and high concentrations favor the poly(oxymethylene glycol)s. The concentration of poly(oxymethylene glycol)s and their average degree of polymerization increase progressively with increase of the total concentration of dissolved formaldehyde. Poly(oxymethylene glycol)s decrease in solubility with increase of molecular mass and precipitate from solution when their concentration exceeds their solubility in the solution media at the prevailing temperature and concentration. Solubility increases with temperature, which also favors a somewhat increased methylene glycol content and a somewhat decreased poly(oxymethylene glycol)s content. Solution composition may be represented by the following sequence of reversible reactions:



etc. The major factors which determine the precipitation of polymer are formaldehyde concentration, temperature, hydrogen ion concentration, concentration and type of solution stabilizers, and storage time. Dilution favors depolymerization of polymeric formaldehyde hydrate. Table 2 shows the number average molecular mass of formaldehyde in aqueous solutions at different concentrations determined with the cryoscopic method [8]. Table 3 shows the fraction of formaldehyde as methylene glycol at different temperatures [8].

According to the data in Table 2 the number-average molecular mass increases with increasing formaldehyde concentration and even at 5% formaldehyde concentration there is polymer formation. The values of the degree of polymerization at different concentrations support the above statement [8]. A solution of 5% formaldehyde contains overall 82.2% formaldehyde in the form of methyleneglycol, whereas in a solution of 35% formaldehyde the methyleneglycol content is only 31.2% [8]. These values refer to the temperature of 35 °C, although temperature was found to have much less effect on the magnitude of methylene glycol fraction than formaldehyde concentration (Table 3) [8]. It must be noted that this statement refers to formaldehyde solutions where no pH adjustment was made, i.e. in the pH range of 2.6–4.5. As it was shown above the state of equilibrium between mono- and polymeric formaldehyde hydrates is determined by the temperature and concentration of the formaldehyde solution. On dilution, the polymeric hydrates depolymerize and a new state of equilibrium is attained. The third factor effecting the state of equilibrium between formaldehyde monohydrate and polymeric hydrates is the hydrogen ion concentration. The rate of depolymerization is at minimum in the pH range 2.6 to 4.8 and increases rapidly with higher or lower pH values. The lowest rate of depolymerization was found by Iliceto at ice water temperature and at pH 4.75 [8]. Magnetic susceptibility measurements confirmed that high pH values favor the monomeric methylene glycol [8]. The effect of hydroxyl ion was found to be  $10^7$  times stronger than that of the hydrogen ion. In general, solutions having a pH in the range 2.6 to 4.8 are the most stable with respect to polymer precipitation since both polymerization and hydrolysis proceed at minimal rates in this range. Solutions in which polymer has precipitated can be clarified by warming if exposure to unfavourable temperatures has been short; after long exposure, clarification is practically impossible. Methylene glycol is not stable at high temperatures, although hydrolysis of polyoxymethylene glycols is extremely slow at 0 °C. The state of formaldehyde during resin synthesis significantly effects the structure of the forming resin and indirectly effects the formaldehyde emission of wood products bonded with that resin during storage and application. In respect to urea-formaldehyde resin synthesis most of dissolved formaldehyde should be in the form of methylene glycol. Methylene glycol formation is favoured by low concentration of formaldehyde, i.e. high dilution, pH value in the range of 8.0–8.5 and in the temperature range of 30–50 °C. All these factors must be considered during urea-formaldehyde resin synthesis.



### *Synthesis conditions*

Proper selection of reaction parameters including pH, temperature and molar ratio of the components is essential for synthesizing urea-formaldehyde resins of low free formaldehyde content. The basic relationships between reaction conditions and product properties have already been elucidated, and a great number of monographs discuss the subject in detail [6, 10, 11]. It is worthwhile, however, to report on the latest results of investigations on this field considering present environmental requirements. Dunky [12] investigated the effect of molar ratio on the properties of urea-formaldehyde-based adhesives and the obtainable bond strength in gluing of plywood. Six formaldehyde-urea copolymer adhesives having HCHO-urea molar ratios of 0.86–1.85 were prepared. Decrease of the molar ratio resulted in a decrease of the free and methylol formaldehyde, which was responsible for longer gelation times at 20 and 100 °C. Viscosity and density decreased, although the adhesives had the same solid contents measured after 2 h at 120 °C. The water-soluble content increased with higher HCHO content. Plywood bond strength was independent of molar ratios at  $>1.2$ , whereas a strong decrease occurred at ratios  $<1.2$ . Tomas [13] investigated the effect of the molar HCHO-urea ratio (R) and MeOH content in the initial polymerization mixture on the quality of urea-formaldehyde resins. The free HCHO content and the amount of splitted off HCHO increased with increasing HCHO-urea ratio but decreased (at HCHO-urea ratio = 1.5) with increasing condensation degree and methanol content. The content of methylol groups increased with increasing HCHO-urea ratio but decreased with increasing condensation degree and methanol content. The condensation time at 100 °C decreased with increasing HCHO-urea ratio. Absence of methanol improved the reactivity of formaldehyde-urea copolymer with low HCHO-urea ratio. The adhesive bond strength was insufficient at HCHO-urea ratio = 1, but increased significantly with increasing HCHO-urea ratio. Serantes et al. [14] determined the limit of HCHO concentration in a urea-HCHO resin adhesive formulation to minimize free HCHO in the final product. The authors found that resins with a HCHO to urea molar ratio of  $>1.3$  were highly reactive and had a high concentration of free HCHO. The amount of free HCHO in the resin to obtain particleboard of quality E2 according to the German standard DIN 68763 was 0.4–0.5%. The resin manufacturing parameters, which must be maintained to produce urea-formaldehyde resins for low – formaldehyde – emission particleboards of class E1 are presented and discussed by Pizzi et al. [15]. At laboratory level, even formulations of HCHO-urea molar ratio as low as 0.7 gave an acceptable balance of results, while industrially the optimum balance of properties appeared to be reached in the molar ratio range of 0.9 to 1.0 but particularly at around 0.96. E1 emission levels of 5 mg/100 g board and lower (by perforator test) were achieved with ease according to the authors. Hse et al. [16] studied the effect of catalysts used for adjusting reaction pH on properties and performance of urea-formaldehyde resins. Based on the bond strength and HCHO emission data, the weak acid catalysts seemed to provide the best compromise between the strong acid and the conventional catalyst system



currently used for formulating aminoplast wood adhesives. Ph control of resin structure and of formaldehyde emission of urea-formaldehyde resins are discussed by Szesztay et al. [17].

## MATERIALS AND METHODS

For  $^{13}\text{C}$ -NMR-spectroscopy measurements formaldehyde solution of analytical grade supplied by Reanal Rt. (Budapest) was used. The raw materials, urea and formaldehyde, used for the synthesis were commercial products, the catalysts, sodium hydroxide and formic acid, were of analytical grade. Specifications for formaldehyde are given in MSZ 2337-83, for urea in MSZ 3437-81.

Free formaldehyde content was determined according to the sodium sulphite method by MSZ 7757-86.

For pH measurements a Radelkis OP-274 Microproc pH/ion meter was used.

For  $^{13}\text{C}$ -NMR-spectroscopy a Bruker DRX-500 instrument was used. The samples were dissolved in  $\text{DMSO-d}_6$ .

Gelation time was determined according to MSZ 7757-86.

Plywood Adhesion Strength in normal state and after warm water treatment was determined according to MSZ 775786 on lauan veneer of 0.6 mm thickness. Tensile shear strength measurements were carried out by using a Zwick 1445 mechanical testing instrument with a rate of 50 mm/min.

## RESULTS AND DISCUSSION

### *State of formaldehyde before methylol formation*

The effect of pH and temperature on the state of formaldehyde have been investigated by  $^{13}\text{C}$ -NMR-spectroscopy.  $^{13}\text{C}$ -NMR-spectra of formaldehyde solution before pH adjustment (at pH 3.18) at room temperature (at 30 °C, 303 K) and at 80 °C (353 K), as well as after pH adjustment to pH 8 at 30 °C (303 K) and at 80 °C (353 K) were taken. The results are represented as intensities of resonance peaks corresponding to the carbon atoms in methylenehydroxide in methylene glycol, dimethylene glycol and in poly(oxymethylene glycol)s in Table 4.

The data in Table 4 show that in formaldehyde solution monomeric methylene glycol and five oligomers up to hexamer could be detected by  $^{13}\text{C}$ -NMR-spectroscopy. Increase in pH from 3.18 to 8.01 did not significantly effect depolymerization of oligomers at 30 °C. Increase of temperature from 30 °C to 80 °C for one hour at pH 3.18 did not effect the state of formaldehyde in solution. If the temperature of formaldehyde solution at pH 8.01 was increased from 30 °C to 80 °C for 1 hour, significant depolymerization could be detected, although the pH decreased to 6.39 after thermal treatment. The concentration of monomeric formaldehyde, i.e. methylene glycol, increased, while the hexamer disappeared from the solution. Since all of these

reactions are equilibrium reactions, it must be considered before and during the syntheses of urea-formaldehyde resins, that simultaneous effect of pH and temperature is needed for depolymerizing poly(oxyethylene glycol)s in formaldehyde solution.

### *Syntheses*

Urea-formaldehyde resins of low formaldehyde content on the other hand have to meet the following requirements: good dispersion stability, adequate curing time, adhesion strength, adequate hydrolytic stability and low formaldehyde emission of the cured product. On the base of literature results and preliminary experiments the syntheses have been carried out in the following stages:

- Depolymerization of formaldehyde at 70 °C and at  $p_H$ 8
- Methylol formation at 70 °C and at  $p_H$ 8
- First stage of polycondensation at 90 °C and at  $p_H$ 5
- Second stage of polycondensation at 90 °C and at  $p_H$ 5
- $p_H$  adjustment to pH 8.0

The characteristics of the synthesized resins are summarized in Table 5. The structure of the resins have been evaluated by  $^{13}\text{C}$ -NMR-spectroscopy.

By properly selecting syntheses conditions including the treatment of formaldehyde solution before the addition of urea, in order to promote depolymerization of poly(oxyethylene glycol)s, the requirements could be met for a urea-formaldehyde resin as a matrix resin for wood adhesive. Table 5 shows that the equilibrium content of free formaldehyde is below 0.2% m/m if final formaldehyde to urea molar ratio is 1.2. This ensures adequate strength of adhesion and water resistance of the adhesive. Formulations 3–7 may ensure low formaldehyde emission, since the intensity of methylene ether bridges, detected by  $^{13}\text{C}$ -NMR-spectroscopy at 75, 78.9 and 79.1 ppm is negligible. Free formaldehyde present in the resin is in the form of methylene glycol, detected at 65.00 and 71.56 ppm. Methylene linkages could be detected at 47.24 ppm and in the range of 65.30–63.71 ppm. By one-stage polycondensation, however (Resin No3), separation of the resin from the water phase occurs, and the adhesive bond is not resistant to water. This may be due to lack of polydispersity.

*Table 1*  
Classification of wood products according to formaldehyde emission determined by different methods [3]

No.	Coloumn No.	1	2	3a	3b	4a	4b
	MATERIAL	CLASS	FORMALDEHYDE EMISSION				
			ppm (Chamber test) CEN-Norm pr EN 717-1	mg/100 g dry board (Perforator test) <sup>1</sup> EN 120: 1992		mg/m <sup>2</sup> h (Gas analysis) EN 717-2: 1994	
				average value <sup>2</sup>	spare value <sup>2</sup>	average value <sup>2</sup>	spare value <sup>2</sup>
1	Uncoated chipboard	E1	≤0.1	≤6.5	≤8.0	–	–
2	Uncoated chipboard	E1	≤0.1	≤7.0	≤8.0	–	–
3	Uncoated plywood, laminated wood and veneer	E1	≤0.1	–	–	≤5.0 <sup>3</sup> ≤2.5 <sup>4</sup>	≤6.0 <sup>3</sup> ≤3.5 <sup>4</sup>
4	Coated chipboard and fibreboard coated plywood	E1	≤0.1	–	≤10 <sup>5</sup> ≤3.5 <sup>6</sup>	–	≤3.5 ≤3.5
5	Chipboard and fibreboard to be coated <sup>7</sup>	E1b	(≤0.1) <sup>8</sup>	–	≤10	–	–

<sup>1</sup>The values refer to a state of material of 6.5% moisture content

<sup>2</sup>The average value is determined as gliding half year value

<sup>3</sup>Quick test: max. 3 days after preparation

<sup>4</sup>Tested 4 weeks after preparation (storage at 20 °C and 65% relative humidity)

<sup>5</sup>Perforator value of the vehicle plate before coating max. 10 mg/100 g; Perforator value after grinding the coating off max 12 mg/100 g.

<sup>6</sup>Values of gas analysis of the vehicle board such as the spare values in line 3 column 4b

<sup>7</sup>Raw panels with perforator values >8 and ≤10 mg HCOH/100 g dry board must be tradd only with the following remark, according to CEN-Norm pr. EN 717-1: "It may be used only if coated. The suitable coating must be proven"

<sup>8</sup>After coating



*Table 2*  
Number-average molecular mass of formaldehyde in aqueous solutions [8]

Formaldehyde concentration (% m/m)	$\overline{M}_n$ 0 °C	$\overline{M}_n$ 35 °C
5		33.6
10		37.5
15	42.5	41.3
20		45.1
25	50.7	48.8
30		52.6
35		56.4
40		60.9
45		66.3

*Table 3*  
Fraction of dissolved formaldehyde as methylene glycol at different temperatures [8]

Formaldehyde concentration (% m/m)	Fraction of methylene glycol		
	0 °C	35 °C	100 °C
5		0.82	0.78
10		0.67	0.63
15	0.49	0.55	0.55
20		0.46	0.48
25	0.36	0.41	0.43
30		0.36	0.40
35		0.31	0.36
40		0.27	0.33
45			0.29
50			0.25

Table 4

Assignment and intensity of  $^{13}\text{C}$ -NMR-resonances of hydroxymethylene carbon atoms of formaldehyde solution at different pH and temperatures

Components	pH 3.18				pH 8.01			
	30 °C (303 K)		80 °C (353 k)*		30 °C (303 K)		80 °C (353 k)*	
	chem. shift (ppm)	intensity	chem. shift (ppm)	intensity	chem. shift (ppm)	intensity	chem. shift (ppm)	intensity
Monomer $\text{HO}-\text{CH}_2\text{OH}$	81.90	12.13	82.26	11.91	81.86	11.52	82.27	11.79
Dimer $\text{HO}-(\text{CH}_2\text{O})_2\text{H}$	85.36	11.83	85.94	11.44	85.31	11.92	85.95	10.43
Trimer $\text{HO}-(\text{CH}_2\text{O})_3\text{H}$	85.75	2.74	86.28	2.46	85.71	2.69	86.29	2.28
Tetramer $\text{HO}-(\text{CH}_2\text{O})_4\text{H}$	85.90	4.59	86.45	4.51	85.85	4.32	86.46	3.57
Pentamer $\text{HO}-(\text{CH}_2\text{O})_5\text{H}$	86.07	1.14	86.56	1.01	86.03	0.98	86.65	2.50
Hexamer $\text{HO}-(\text{CH}_2\text{O})_6\text{H}$	86.15	2.59	86.64	2.58	86.11	2.37	—	—

\*Thermal treatment at 80 °C took place for 1 hour and  $^{13}\text{C}$ -NMR-spectra were taken before thermal treatment, and after thermal treatment. At pH 3.18 the pH of formaldehyde solution did not change, at pH 8.01 the pH decreased to 6.39 after 1 hour at 80 °C

*Table 5*  
Characteristics of the synthesized urea-formaldehyde resins

Resin No.	F/U molar ratio Free HCOH content (% m/m)			Equilibril HCOH (% m/m)	Time of gelation (s)	Strength of adhesion (MPa)	
	1. stage	2. stage	3. stage			normal state	after water treatment
1	1.5 –	1.2 0.95	–	0.40	120	1.00 ± 0.08	0.56 ± 0.14
2	2 4.00	1.2 1.93	–	1.07	60	–	1.25 ± 0.20
3	1.2 0.75	–	–	0.20	110	1.06 ± 0.14	–
4	2 3.56	1.38 0.99	1.2 0.44	0.17	105	1.53 ± 0.02	0.91 ± 0.21
5	2 2.58	1.38 0.65	1.2 0.19	0.13	150	1.13 ± 0.24	0.77 ± 0.05
6	2 –	1.38 1.04	1.2 0.42	0.20	110	0.95 ± 0.20	0.64 ± 0.21
7	2 4.00	1.38 1.12	1.3 0.53	0.22	110	0.89 ± 0.21	0.73 ± 0.23



## ACKNOWLEDGEMENTS

Thanks are due to Dr. Áron Szöllösy (Department of General and Analytical Chemistry, Technical University of Budapest) for the NMR-spectra. Supported by the Hungarian Scientific Research Fund (OTKA), grant No. T 025589.

## REFERENCES

1. Pizzi, A. (1994) Urea-formaldehyde adhesives. In: Pizzi, A., Mittal, K. L. (eds) *Handbook of Adhesive Technology*. Marcel Dekker, Inc., New York, pp. 381–392.
2. *Bundesgesundheitsblatt* (1991) 10, 488–489.
3. *Mitteilungen DIBt* (1994) 6, 203–207.
4. Kim, M. G., Amos, L. W. (1990) Quantitative carbon-<sup>13</sup>NMR study of urea-formaldehyde resins in relation to the formaldehyde emission levels. *Ind. Eng. Chem. Res.* 29, 208–212.
5. Ferg, E. E., Pizzi, A., Levendis, D. C. (1993) <sup>13</sup>CNMR Analysis method for urea-formaldehyde resin strength and formaldehyde emission. *J. Appl. Pol. Sci.* 50, 907–915.
6. Wolff, F. A. (1955) Urea and urea derivatives. In: Kirk, R. E., Othmer, D. F. (eds) *Encyclopedia of Chemical Technology*. Vol. 14, The Interscience Encyclopedia, Inc., New York, pp. 458–472.
7. Wirpsza, Z. (1970) The effect of some side products on the reaction between urea and formaldehyde. *Polymery – Tworzywa Wielkocząsteczkowe*, 15, 275–276.
8. Walker, J. F. (1953) State of dissolved formaldehyde. In: *Formaldehyde*. Reinhold Publishing Corporation, New York, pp. 46–64.
9. Walker, J. F. (1953) Commercial formaldehyde solutions. In: *Formaldehyde*. Reinhold Publishing Corporation, New York, pp. 65–85.
10. Mark, H. F., Gaylord, N. G., Bikales, N. M. (1965) *Encyclopedia of Polymer Science and Technology*. Vol. 2, John Wiley & Sons Inc., New York, pp. 1–94.
11. Wegler, R. (1963) Polyadditions- und Polykondensationsprodukte von Carbonyl- und Thiokarbonylverbindungen mit Harnstoffen, Melaminen, Urethanen, Carbonsäureamiden, Dicyandiamid, Guanidin, Sulfurylamid, Sulfonsäureamiden, Nitrilen, Ammoniak, aliphatischen Aminen und Phosphin. In: Houben-Weyl K. (ed.) *Methoden der Organischen Chemie*, Band 14/2, Georg Thieme Verlag, Stuttgart, pp. 319–413.
12. Dunky, M. (1985) Harnstoff-Formaldehyd Leime Einfluß des Molverhältnisses auf die Eigenschaften der Leime und die erreichbaren Bindefestigkeiten bei Sperrholzverleimungen. *Holzforsch.* Holzverwert. 37, 75–82.
13. Tomas, M. (1986) Effect of some factors on the quality of urea-formaldehyde resins prepared under different conditions. *Drev. Vysk.* 110, 69–81.
14. Serantes, M., Martinez, O., Almarales, G., Morales, A. (1989) Study of free formaldehyde in urea-formaldehyde resins for production of bagasse particle boards. *Sobre Deriv. Cana Azucar* 23, 26–29.
15. Pizzi, A., Lipschitz, L., Valenzuela, J. (1994) Theory and practice of the preparation of low formaldehyde emission UF adhesives. *Holzforschung* 48, 254–261.
16. Hse, C.-Y., Xia, Z.-Y., Tomita, B. (1994) Effects of reaction pH on properties and performance of urea-formaldehyde Resins. *Holzforschung* 48, 527–532.
17. Szesztay, M., László-Hedvig, Zs., Takács, C., Gács-Baitz, E., Nagy, P., Tüdös, F. (1994) pH control of the condensation reaction and its effect on the properties of formaldehyde/urea resins. *Angew. Makromol. Chem.* 215, 79–91.

MAGYAR  
TUDOMÁNYOS AKADÉMIA  
KÖNYVTÁRA

## ANNOUNCEMENT

In order to expand the international character of *Acta Biologica Hungarica*, starting from the next 50th Volume, some changes will occur in the composition of the Editorial Board. Four leading scientists, three of them foreign members of the Hungarian Academy of Sciences, B. Gulyás (Stokholm, neuroscience) Éva Klein (Stocholm, cell biology), D. F. Roberts (Newcastle-upon-Tyne, human biology) and D. A. Sakharov (Moscow, developmental biology) agreed upon to join our scientific board. They will take part in reviewing manuscripts and contribute to keep the high standard of the journal.

At the same time, a distribution of the editorial work will be performed by nominating Prof. K. Elekes as Editor, while Prof. J. Salánki will function as Editor-in-Chief. Manuscripts can be sent to either of them, to the address given in the Instructions.

Editorial Board





# ACTA BIOLOGICA HUNGARICA

Volume 49, 1998

## INDEX

### Number 1

Editorial J. SALÁNKI .....	1
Reflections. P. KÁSA .....	3
Biological activities of amyloid precursor protein. K. GULYA .....	7
The olfactory bulb in Alzheimer's disease. I. KOVÁCS, I. TÖRÖK, J. ZOMBORI, H. YAMAGUCHI .....	29
Effects of beta-amyloid on cholinergic, cholinceptive and GABAergic neurons. MAGDOLNA PÁKÁSKI, HENRIETTA PAPP, MÓNKA FORGON, P. KÁSA JR., B. PENKE .....	43
Cholinesterase in Alzheimer's disease and cholinesterase inhibitors in Alzheimer therapy. Z. RAKONCZAY, I. KOVÁCS .....	55
Aged synthetic human amyloid $\beta$ -peptide 1-42 and related fragments induce direct acetylcholine release from rat basal forebrain tissue slices. MÓNKA FORGON, Z. FARKAS, MAGDOLNA PÁKÁSKI, MÁRTA ZARÁNDI, B. PENKE .....	71
Investigation of 2,6-dimethoxy-benzoquinone in eight tree species grown in Hungary. RITA TÖMÖSKÖZI FARKAS, M. HIDVÉGI, R. LÁSZTITY .....	79
DNA technology and its application in forensic medicine. A. LÁSZIK, A. FALUS, L. KERESZTURY, P. SOMOGYI .....	89
RAS-dependence of nerve growth factor-induced inhibition of proliferation of PC12 cells. KATALIN KISS, B. BARTEK, NÓRA NUSSE, J. SZEBERÉNYI .....	97
Evaluation of genotoxic, mutagenic and antitumor properties of 2-amino-2-thiazoline, L-thio-proline and 2-amino-2-thiazoline $\epsilon$ -formylaminocaproate. VITALIJA ŠIMKEVIČIENĖ, J. STRAUKAS, LARISA CHAUSTOVA .....	103
Growth hormone inhibits the interleukine-6 induced junB protooncogene and fibrinogen expression in HepG2 human hepatoma cells. P. IGÁZ, BEÁTA DÉRFALVI, SÁRA TÓTH, A. FALUS .....	113
Homoplasmic A12,753G mitochondrial DNA mutation in a Hungarian family. ANDREA KIS, A. MATOLCSY, L. VÉCSEI, G. KOSZTOLÁNYI, K. MÉHES, B. MELEGH .....	119
Colormapping: a non-matemathical procedure for genetic mapping. G. B. KISS, A. KERESZT, P. KISS, GABRIELLA ENDRE .....	125
Effects of administration of cyproterone acetate on seminal vesicle and testicular activity, and serum testosterone and estradiol-17 $\beta$ levels in the catfish <i>Clarias batrachus</i> . M. S. SINGH, K. P. JOY .....	143
Body perception and consciousness. Contributions of interoception research. R. HÖLZL, A. MÖLTNER, C. NEDIG .....	155

## Numbers 2–4

Preface .....	165
An evolutionary role of formaldehyde. M. P. KALAPOŠ .....	167
Related <sup>15</sup> N- and <sup>14</sup> N-methyltransferases methylate the large and small subunits of Rubisco. Z. YING, R. M. MULLIGAN, N. JANNEY, M. ROYER, R. L. HOUTZ .....	173
Methylation and gene mutation in eukaryotic DNA. C.-Q. LIU, J.-F. HUANG, YING WANG, W.-B. LIU .....	185
Role of formaldehyde in direct formation of glycine and serine in bean leaves. Á. NOSTICZIUS .....	193
Effect of methionine enrichment on the biological activities of food proteins. GYÖNGYI HAJÓS, SZ. FARKAS, EMŐKE SZERDAHELYI, MARIANNE POLGÁR .....	201
L-carnitine as essential methylated compound in animal metabolism. An overview. M. SZILÁGYI .....	209
Addition of CH <sub>2</sub> O to arginine – a theoretical study by <i>ab initio</i> method. CORNELIA KOZMUTZA, E. M. EVLETH, L. UDVARDI, J. PIPEK .....	219
Formaldehyde cycle and the natural formaldehyde generators and capturers. E. TYIHÁK, L. ALBERT, ZS. I. NÉMETH, GY. KÁTAY, ZS. KIRÁLY-VÉGHÉLY, B. SZENDE .....	225
Formaldehyde in the plant kingdom. G. BLUNDEN, B. G. CARPENTER, MARICELLA ADRIAN- ROMERO, M.-H. YANG, E. TYIHÁK .....	239
Plant tissue culture as a model for study of diversity in formaldehyde binding. I. LÁSZLÓ, ÉVA SZŐKE, ZS. NÉMETH, L. ALBERT .....	247
Determination of endogenous formaldehyde in plants (fruits) bound to L-arginine and its rela- tion to the folate cycle, photosynthesis and apoptosis. L. TRÉZL, L. HULLÁN, T. SZARVAS, A. CSIBA, B. SZENDE .....	253
The hydrazine derivative aminoguanidine inhibits the reaction of tetrahydrofolic acid with hydroxymethylarginine biomolecule. L. HULLÁN, L. TRÉZL, T. SZARVAS, A. CSIBA .....	265
Induction of resistance of wheat plants to pathogens by pretreatment with N-methylated sub- stances. KLÁRA MANNINGER, MÁRIA CSÓSZ, E. TYIHÁK .....	275
Identification and measurement of resveratrol and formaldehyde in parts of white and blue grape berries. ZSUZSA KIRÁLY-VÉGHÉLY, E. TYIHÁK, L. ALBERT, ZS. I. NÉMETH, GY. KÁTAY .....	281
Relationship between dimedone concentration and formaldehyde captured in plant tissues. ÉVA SÁRDI, E. TYIHÁK .....	291
The use of HPLC for the detection and quantification of formaldehyde in the Pteridophyta. MARICELA ADRIAN-ROMERO, G. BLUNDEN, B. G. CARPENTER, SHEILA LUCAS, E. TYIHÁK .....	303
Drought stress, peroxidase activity and formaldehyde metabolism in bean plants. ÉVA STEFANOVITS-BÁNYAI, ÉVA SÁRDI, SUSAN LAKATOS, M. ZAYAN, I. VELICH .....	309
The increase of formaldehyde level in some rare pathological cases of teeth determined with the use of quantitative TLC. T. KATARZYNA RÓŻYŁO, R. SIEMBIDA, ANNA SZYSZKOWSKA, ANNA JAMBROŻEK-MAŃKO .....	317
Formaldehyde generators and capturers as influencing factors of mitotic and apoptotic processes. B. SZENDE, E. TYIHÁK, L. TRÉZL, ÉVA SZŐKE, I. LÁSZLÓ, GY. KÁTAY, ZS. KIRÁLY-VÉGHÉLY .....	323
Reduction of apoptosis of <i>in vitro</i> cultured lymphocytes of HIV-positive persons by N <sup>G</sup> - hydroxy-methylated-L-arginine and 1'-methyl-ascorbigen. J. BOCSI, K. NAGY, E. TYIHÁK, L. TRÉZL, B. SZENDE .....	331
Formaldehyde generation by N-demethylation. H. KALÁSZ, MÁRIA BÁTHORI, E. TYIHÁK .....	339
Formaldehyde-induced modification of hemoglobin <i>in vitro</i> . R. FARBISZEWSKI, ELŻBIETA SKRZYDLEWSKA, AGNIESZKA ROSZKOWSKA .....	345



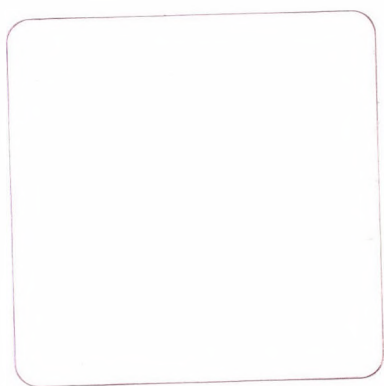
Change of biotransformation steps of formaldehyde cycle in water-melon plants after infection with <i>Fusarium oxysporum</i> . ÉVA SÁRDI, E. TYIHÁK .....	353
The effect of heat shock on the formaldehyde cycle in germinating acorns of European turkey oak. L. ALBERT, Zs. I. NÉMETH, SZ. VARGA .....	363
Changes in formaldehyde contents of germinating acorns of <i>Quercus cerris</i> L. under low temperature stress conditions. Zs. I. NÉMETH, L. ALBERT, SZ. VARGA .....	369
Alteration of endogenous formaldehyde level following mercury accumulation in different pig tissues. T. RÉTFALVI, Zs. I. NÉMETH, I. SARUDI, L. ALBERT .....	375
Investigation of some methylated compounds and peroxidase activity during plant ontogenesis in snap bean. ÉVA SÁRDI, ÉVA STEFANOVITS-BÁNYAI .....	381
Formaldehyde as a proof and response to various kind of stress in some <i>Basidiomycetes</i> . ANNA JAROSZ-WILKOŁAZKA, MONIKA FINK-BOOTS, ELŻBIETA MALARCZYK, A. LEONOWICZ .....	393
Relationships between demethylase activity, formaldehyde and oxygen during incubation of <i>Rhodococcus erythropolis</i> with veratrate. MARZANNA PAŹDZIOCH-CZOCZRA, ELŻBIETA MALARCZYK .....	405
Comparative quantitative chromatographic determination of formaldehyde in different groups of physiological and pathological hard tissues of teeth. T. KATARZYNA RÓŻYŁO, R. SIEMBIDA .....	413
Are the reductions in nematode attack on plants treated with seaweed extracts the result of stimulation of the formaldehyde cycle? T. JENKINS, G. BLUNDEN, YUE WU, S. D. HANKINS, B. O. GABRIELSEN .....	421
Effect of 1'-methylascorbigen on the resistance potential of plants to pathogens. GY. KÁTAY, E. TYIHÁK .....	429
Analogies and differences in the excited reactions of formaldehyde and D-glucose. L. TRÉZL, L. HULLÁN, T. SZARVAS, A. CSIBA, J. PIPEK .....	437
Microbial urea-formaldehyde degradation involves a new enzyme, methylenediurease. T. JAHNS, ROSWITHA SCHEPP, C. SIERSDORFER, H. KALTWASSER .....	449
Differential detection of <i>N</i> -heterocyclic compounds and their <i>N</i> -methylated derivatives by immunoanalysis. HONG M. LE, GYÖNGYVÉR HEGEDŰS, A. SZÉKÁCS .....	455
Urea-formaldehyde resins and free formaldehyde content. VIKTÓRIA VARGHA .....	463



PRINTED IN HUNGARY

Akadémiai Nyomda, Martonvásár





## DIRECTIONS TO CONTRIBUTORS

ACTA BIOLOGICA HUNGARICA publishes original works in the field of experimental biology.

Manuscripts should be addressed to DR. JÁNOS SALÁNKI, Editor, *Acta Biologica Hungarica*, H-8237 Tihany, Hungary.

Only original papers will be published and a copy of the Publishing Agreement will be sent to the authors of papers accepted for publication. Manuscripts will be processed only after receiving the signed copy of the agreement.

The manuscripts should not exceed 16 typed pages in general. The manuscripts should be typed double-spaced, on one side of the paper. In order to assure rapid publication, contributors are requested to submit two copies of the manuscript including an abstract (max. 200 words), tables and figures. An electronic version of the manuscript (including the figures, except the micrographs) should also be submitted on a 3.5" diskette, using Word for Windows 6.0, 2.0 or (Rich Text Format) wordprocessor package in Microsoft Windows '95 or Windows 3.1 system. Each table should be typed on a separate sheet, numbered and provided with a title. All figures, either photographs or drawings or graphs, should be numbered consecutively. Figure legends should be typed in sequence on a separate sheet. Color plates (micrographs and drawings) will be charged to the authors (in 1998 US\$ 280 per page).

Papers should be headed with the title of the paper, the names of the authors (male authors use initials, female authors use one given name in full), department, institute and town where the work was performed. A running title, not to exceed 50 letter spaces, should be included on a separate sheet and immediately following the summary 5 keywords must be supplied.

The *full paper* should be divided into the following parts in the order indicated:

1. *Abstracts*
2. *Introduction*
3. *Materials and Methods*
4. *Results*
5. *Discussion*
6. *References*. Papers – the essential ones only – cited in the manuscript should be listed on a separate sheet in alphabetical order according to the first author's surname. The references should be numbered so that each may be referred to in the text by its number only.

Examples:

1. Boas, N. F. (1953) Method for determination of hexosamine in tissue. *J. Biol. Chem.* 204, 553–563.
2. De Duve, C. (1959) Lysosomes, a new group of cytoplasmic particles. In: Hayashi, T. (ed.) *Sub-cellular Particles*. Ronald Press, New York, pp. 1–72.
3. Umbreit, W. E., Burris, R. H., Stauffer, I. F. (1957) *Manometric Techniques*. Burgess Publishing Co., Minneapolis.

*Short communication*. Manuscripts should not exceed 1000 words (4 types pages), including references. The text of manuscripts containing tables and/or figures must be correspondingly shorter. Accepted short communications will be published within six months after submission of manuscripts. In order to speed up publication, no proof will be sent to authors.

Authors will be furnished, free of charge, with 25 reprints. Additional reprints may be obtained at cost.

